Analytical Studies of the Behaviour of Semi-rigid Non-sway Frames with Tubular Columns

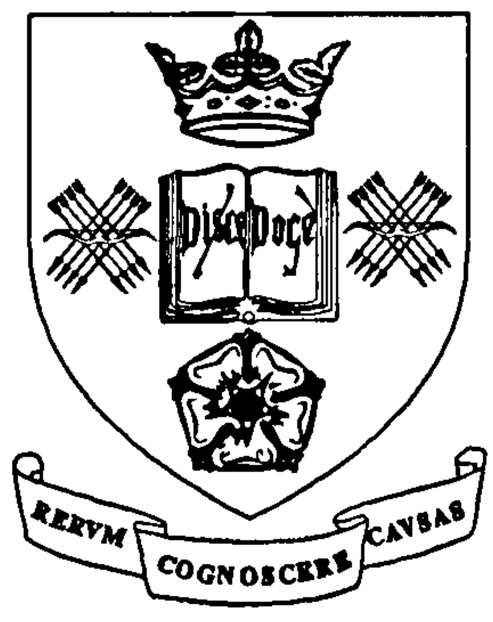

by

Ahmad Baharuddin Abd-Rahman

B.Eng. (Hons.), M.Sc.

A thesis submitted in partial fulfilment of the requirements for the Degree of

Doctor of Philosophy

Department of Civil and Structural Engineering

University of Sheffield

February 1999

List of Contents

List of Tables

Chapter 7

List of Figures

Acknowledgements

I am indebted to my supervisor, Dr. Patrick Kirby who has provided valuable guidance, motivation, suggestion and encouragement throughout this project. Furthermore, his understanding and willingness to help is very much appreciated.

Appreciation is also due to Universiti Teknologi Malaysia for providing the financial support of my study. Also, I would like to thank S. Mohammad for his guidance in understanding the code of the computer program. In addition, I would like to extend my thanks to the lecturers and staff in the Department of Civil and Structural Engineering for their helpful cooperation.

I am also indebted to my parents for their understanding and patience. Finally, I am grateful to my wife, Nor Azizah; my daughters, Nabihah and Nadrah and my son Ahmad Nazmi for their support and understanding during the period of my study in Sheffield.

Declaration

I hereby declare that the work in this thesis is the result of my own investigations except where specific reference has been made to the work of others.

No part of this thesis has been submitted to any University or other educational establishment for a degree, Diploma or other qualification.

Ahmad Baharuddin Abd-Rahman

Summary

This thesis reports the research investigation on the behaviour of non-sway frames with SHS columns taking into consideration the influence of semi-rigid flowdrill connections. The aim of the studies was to investigate the behaviour of the non-sway frames in the elastic and inelastic ranges, the acceptability of the flowdrill connections for low-rise non-sway frames and to develop a simplified semi-rigid design that is suitable for daily design routine.

The analytical studies were conducted using an existing finite element program which was modified to work with frames employing tubular columns. The program is able to simulate the response in the elastic and inelastic ranges taking into account the semi-rigid connections, the geometrical and material nonlinearities and the development of spread yield. The program has been validated against the experimental results and can reasonably predict the true frame behaviour.

The results of the parametric studies show several important observations; one of which is the phenomenon of moment shedding. This phenomenon causes the relaxation of the detrimental moment at the column top end which in turn causes the moment redistribution to the neighbouring members. Eventually, the detrimental column moment diminishes and sometimes acts as restraining moments. As a consequence, at ultimate load, the columns behave in the general form of axially loaded compression members and the beams as simply supported with a certain degree of end restraint.

Knowing that restrained beam-columns can be treated as axially loaded, extensive parametric studies on different frame configurations were conducted to determine the ultimate strength of beam-columns. The studies were conducted on low rise multi-storey non-sway frames. The principal parameters varied are the column slenderness, connection types and the magnitude of beam loads. The values of ultimate strength of restrained beam-columns are compared directly against the strength of pin ended columns as specified by the BS 5950 and EC3 codes. The results

show that in many cases, the ultimate strength of restrained beam-columns are in excess to the strength of axially loaded pin ended column as specified by BS 5950 and EC3.

Based on the results of the parametric studies, a simplified design for simple, semi-rigid and rigid frames is developed. The columns are designed as axially loaded compression members without any consideration of eccentricity or partial fixity moments. The beams for simple construction are designed as simply supported with pin ends; whereas, the beams for semi-rigid and rigid construction are designed as simply supported with a certain amount of end restraint moment to take into account the effect of semi-rigid and rigid connections. The design of strength for beams and columns can be carried out individually and is not dependent on the stiffnesses of the M-ϕ of the connections, beams and columns.

Finally, general conclusions and recommendations for further work are also included.

Notation

A	Cross sectional area of a member
A_{yield}	Yielded cross sectional area of a member
C_{j1}, C_{j2}	Connection stiffnesses at nodes 1 and 2 respectively
D	Column depth
e	Eccentricity between column centre-line and column face
e_o	Initial geometrical imperfection of a column
E	Modulus of elasticity
E_t	Tangent modulus
EA	Axial stiffness
EI	Flexural stiffness
F	Axial force
h	Column height
I	Second moment of area of a section
I_{xx}	Second moment of area of a section about x-x axis
I_{yy}	Second moment of area of a section about y-y axis
k_1, k_2, k_3	Rotational stiffness in a trilinearised representation of the connection
K	Effective length factor
L	Member length
L_e	Effective length of a member
M	Moment
M_a	Moment at the end of a beam
M_b	Moment at the midspan of a beam
M_{axial}	Column top end moment due to column axial load only
M_{beam}	Column top end moment due to beam load only
M_c	Column top end moment
M_e	Eccentricity moment
M_p	Plastic moment capacity of a beam
M_{sr}	Beam end moment for semi-rigid frame
M_{rigid}	Beam end moment for rigid frame
N_1 to N_6	Shape functions for the semi-rigid element
$\overline{N}_1$ to $\overline{N}_6$	Shape functions for the rigid element
P	Applied vertical point load
P_1, P_2, P_3	Column axial loads at higher load levels in which the columns behave as axially loaded compression members
P_{pin}	Column strength with pin ended restraint

$P_{pin\ BS\ 5950}$	Column strength with pin ended restraint as specified by BS 5950
$P_{pin\ EC3}$	Column strength with pin ended restraint as specified by EC3
P_{sq}	Squash load
P_{sr}	Predicted analytical column strength with semi-rigid connections
P_y	Column axial load at first yield
p_y	Design strength
R	Beam reaction
r	Radius of gyration
w	Intensity of uniformly distributed load

Greek Symbols

α	Angle between the centre-line of a beam to the centre-line of a column located at the underside of the beam
α_{pin}	Alpha-pin ratio = P_{sr} / P_{pin}
δ	Deflection of a member
δ_{pin}	Beam midspan deflection with pinned connections
δ_{sr}	Beam midspan deflection with semi-rigid connections
δ_{rigid}	Beam midspan deflection with rigid connections
Δ	Global deflection of a frame
ε	Strain
ε_y	Yield strain
ε_{st}	Strain hardening strain
ϕ, $\phi_{connection}$	Connection rotation
ϕ_{beam}	Beam rotation
ϕ_{column}	Column rotation
ϕ_{pin}	End rotation of simply supported beam
ϕ_1, ϕ_2, ϕ_3	Connection rotations in a trilinearised representation of the connection
γ	Load factor
γ_{ult}	Collapse load factor
λ	Column slenderness
λ_{pin}	Pinned column slenderness
λ_{sr}	Restrained column slenderness
θ_o	Initial lean angle for global imperfection in a frame
θ_p	Plastic rotation = $(M_p)_{beam} / (EI/L)_{beam}$

σ	Stress
σ_y	Yield strength
μ	Dimensionless factor = M_{sr} / M_{rigid}

Abbreviations

DL	Dead load
LL	Live load
WL	Wind load
PDEP	Partial depth end plate
FEP	Flush end plate
EEP	Extended end plate
UB	Universal beam
SHS	Square hollow section
cm	Centimetre
m	Meter
kN	Kilonewton
kip	1000 pounds = 4.4482 kN
millirad	Milliradian = 0.0573 degree

Matrices and Vectors

$[B]$	Strain displacement matrix
$[B_O]$	Small strain displacement matrix
$[B_L]$	Large strain displacement matrix
$[D]$	Modulus of material matrix
$[K_E]$	Elastic stiffness matrix based on small deflection theory
$[K_G]$	Geometrical stiffness matrix
$[K_L]$	Large displacement stiffness matrix
$[K_T]$	Tangential stiffness matrix
$[N]$	Shape function matrix

Chapter 1

Introduction

1.1 Introduction

The structural system of steel frames in multi-storey buildings consists of main components beams and columns and connections. The latter play an important role in joining the beams and columns and it is well known that the connections show a variation of behaviour in terms of stiffness and strength. This in turn affects the frame behaviour and the way in which the frames are designed.

In traditional methods of design, the connections are normally assumed as either perfectly pinned or perfectly rigid. The assumption of pinned connections implies no rotational continuity within the frame; in other words, no moment is transmitted from the beam to the column, see Figure 1.1(a). The connections which are normally assumed as pinned are flexible connections such partial depth end plate, web cleat and flange cleat types. The assumption of perfectly pinned connections as normally adopted in non-sway frames may lead to:

- over-estimation of beam moments, resulting in larger, heavier beams
- over-estimation of service deflections in beams
- under-estimation of column end moments.

On the other hand, the assumption of perfectly rigid connections implies full moment continuity. Hence a 100% of beam end moment will be transmitted to the column as shown in Figure 1.1(b). Connections which are normally assumed as rigid are stiffened extended end plate and full welded connection types. The assumption of perfectly rigid connections may lead to:

- over-estimation of column end moment, resulting in larger, heavier columns
- over-estimation of connection moments, resulting in more complex connections which normally require the use of stiffeners at the column web.

The two assumptions described above are merely based on idealistic conditions. In reality, the results of experimental studies show that the connections which are normally assumed as pinned actually possess some rotational stiffness, while connections assumed as rigid often display some flexibility [1-1], [1-2]. With this regard, all connections are more correctly to be described as semi-rigid which covers the full spectrum between the two extreme pin and rigid conditions.

The real semi-rigid connections lead to partial continuity meaning that only a partial amount of beam fixed end moment is transmitted to the column as illustrated in Figure 1.1(c). The amount of moment transmitted depends on the stiffness of connections and on the stiffness of the connected beams and columns. The benefits of considering the real semi-rigid characteristics are:

- A more rational design method based on realistic action of the connections.
- A more economical design. Research on beam economies shows that the use of double web angles, flush end plates and extended end plates resulted in beam weight saving of the order of 6%, 22% and 29% respectively [1-3]. Other results show that an overall cost saving for a non-sway planar frame of 5.5% can be achieved if semi-rigid design is adopted instead of simple design [1-4]. In the case of sway frames, about 20% of saving of the total cost of the frame can be achieved [1-5].

Numerous investigations have been undertaken to study the influence of semi-rigid connections on the performance of individual members and global frames for the past 60 years. However a comprehensive semi-rigid design method is not yet readily available in any leading design code. Although, Clause 2.1.2.4(b) BS 5950 [1-6] has provided a simplified semi-rigid design method, the provisions are somewhat arbitrary and do not realise the full potential offered by semi-rigid design. On the other hand, the methods proposed by various researchers are too complicated for hand calculations and hence are not suitable for routine daily design. Most of the rigorous design methods require the information of M-ϕ curves of the connections which can only be obtained from experimental tests or alternatively by using complex analytical models although work on databanks of both experimental tests and analytical models are being developed [1-7]. Moreover, researchers realised that the translation of the research information correspond to semi-rigid connections into straightforward design procedures is arguably a more challenging task [1-8]. Hence, the design methods based on the idealistic assumption as either pin or rigid continue to dominate the way the structures are being designed because of their simplicity.

Most of the studies on semi-rigid connections and global frame behaviour are associated with the use of open section columns. The popularity of the open section columns may be attributed to the availability of simple connections such as web cleats, flange cleats and flush end plates which are simple to fabricate, less expensive and easy to install. With these types of connections, the problem of access for installing bolts at both side is not present.

The availability of a new blind bolting system known as a flowdrill connection has made the connection between open section beams and closed section columns much simpler. In view of this development, the use of tubular columns as compression members in normal storey height of frames is increasingly accepted because of their structural efficiency. This is due to the fact that tubular columns such as square hollow sections and circular hollow sections have symmetrical properties and equal resistance of buckling in both axes. Hence, more investigations are required to identify the benefit and the influence of the flowdrill connections to the behaviour of frames with tubular columns.

1.2 Objectives of the Research

The main aim of the research presented in this thesis is to investigate the influence of semi-rigid joints using flowdrill connectors on the global behaviour of frames with tubular columns. Consequently, by taking advantage of this behaviour, a more realistic simplified design method may be suggested. The emphasis is being directed towards the behaviour of non-sway frames.

Several objectives to achieve the main aim can be described as follows:

- to modify an existing finite element program to work with tubular columns both in non-sway and sway frame cases
- to study the influence of connection restraint on the behaviour of tubular columns in non-sway frames
- to investigate the ultimate strength of tubular columns with flowdrill semi-rigid connections
- to develop a simplified design method of frames with semi-rigid restraints.

1.3 Scope of the Thesis

The scope of the thesis is as follows:

- Chapter 2 represents the review of previous work carried out by other researchers. The overview discusses the strength of columns as influenced by connection restraints and detrimental moments.
- In chapter 3, the basic formulation of the amended program has been presented.
- Chapter 4 demonstrates the ability of the program to predict the real behaviour of full-scale frames.
- Chapter 5 discusses the behaviour of beam-columns with semi-rigid end restraints. The phenomenon of moment shedding which occurs as the ultimate load level of column is neared is discussed. Consequently, the behaviour of beam-columns

observed in these studies has been adopted as the basis of the simplified design method.

- In chapter 6, the results of ultimate strength of beam-columns with semi-rigid connections are presented in terms of the strength of equivalent pin ended column capacities. This has resulted in the development of beam-column strength curves as compared directly with the design strength curves of BS 5950 [1-6] and EC3 [1-9]. The results of the investigations have been adopted for the development of a simplified design of non-sway frames.

- In chapter 7, the simplified design of non-sway frames based on the above approach has been discussed.

- Finally, chapter 8 summarises the overall conclusions of the research and in order to facilitate further research, some recommendations for further work are also included.

1.4 References

[1-1] Jones, S.W., Kirby, P.A. and Nethercot, D.A., 'The analysis of frames with semi-rigid connections - A state-of-the-art report', Journal of Constructional Steel Research: Vol. 3, No. 2: 1983, pp. 1-13.

[1-2] Davison, J.B., Kirby, P.A. and Nethercot, D.A., 'Column behaviour in PR construction: experimental behaviour', Journal of Structural Engineering, Vol. 113, No. 9, September, 1987, pp. 2032-2050.

[1-3] Nethercot, D.A., Davison, J.B. and Kirby, P.A., 'Connection flexibility and beam design in non-sway frames', Engineering Journal, American Institute of Steel Construction, Third quarter, 1988, pp. 99-108.

[1-4] Anderson, D. and Tahir, M.M., 'Economic comparisons between simple and partial-strength design of braced steel frames', in Connection in steel structures III, Behaviour, strength and design, ed. Bjorhovde, R., Colson, A., Zandonini, R., Italy, 1995, pp. 527-533.

[1-5] Bjorhovde R. and Colson, A., 'Economy of semi-rigid frame design', in Connection in steel structures II, Behaviour, strength and design, ed. Bjorhovde, R., Haaijer, G. and Stark, J.W.B., Chicago, 1992, pp. 418-430.

[1-6] BS 5950: Part 1: 1990, 'Structural use of steelwork in building', Part 1. Code of practice for design in simple and continuos construction : hot rolled sections, British Standards Institution.

[1-7] Weynand, K., Huter, M., Kirby, P., Simoes da Silva, L.A.P. and Cruz, P.J.S., 'SERICON - A databank for tests on semi-rigid joints', COST1, Liege, September, 1998.

[1-8] Nethercot, D.A., 'Behaviour of semi-rigid connections and implementation in frame design', in Connections in steel structures II, Behaviour, strength and design, ed. Bjorhovde, R., Haaijer, G. and Stark, J.W.B., Chicago, 1992, pp. 360-369.

[1-9] Eurocode 3, 'Design of steel structures - Part 1.1: General rules and rules for buildings', ENV 1993-1-1.

[1-10] Kulak, G.L., Fisher, J.W. and Struik, J.H.A., 'Guide to design criteria for bolted and riveted joints', John Wiley & Sons, USA, 2nd. edition, 1987.

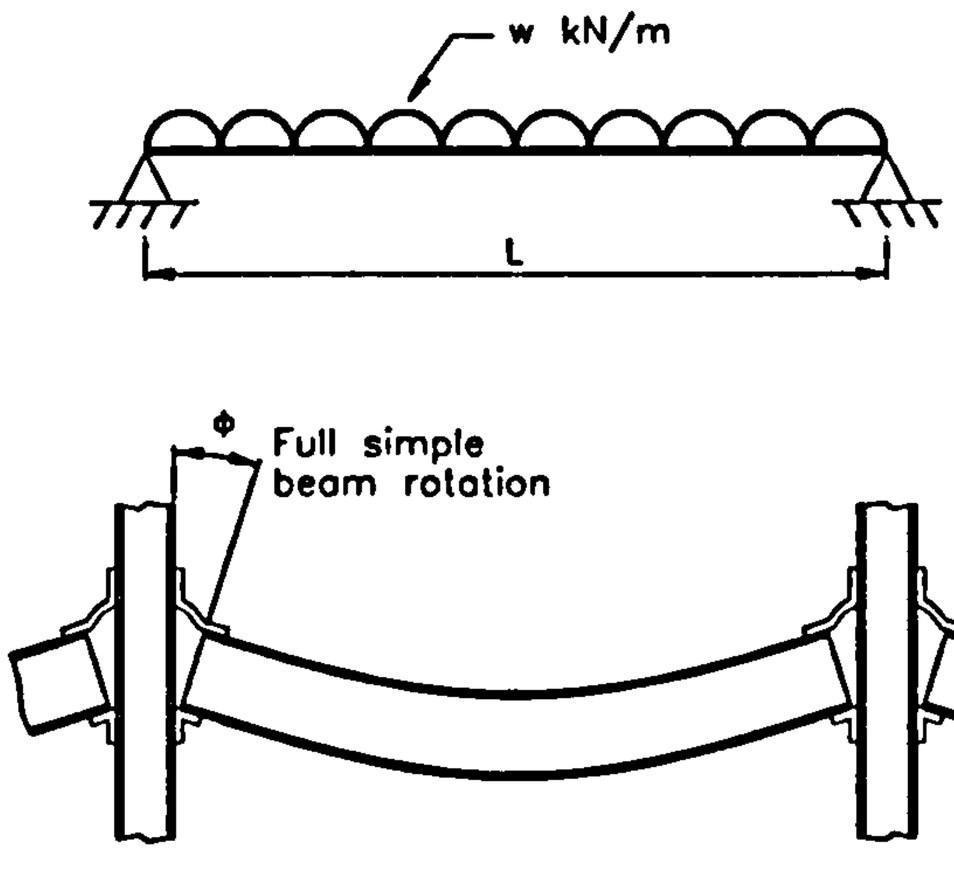

(a). Flexible (pinned) connection

(b). Rigid connection

(c). Semi-rigid connection

Figure 1.1 Classes of beam-column connections

Chapter 2

Review of Previous Work

2.1 Introduction

Semi-rigid connections and their potential benefits to multi-storey steel frame structures have been the focus of many investigations for the past 60 years. Numerous investigations into the global behaviour of steel frames as influenced by the presence of semi-rigid connections have been reported by many researchers. The studies were mainly focused on steel frames utilising open section columns and open section beams. Lately, however, the use of tubular columns with open section beams coupled with an innovative bolting system has become an alternative for the construction of multi-storey buildings.

This chapter presents a brief overview of the main areas that have contributed to the understanding the behaviour of semi-rigid connections, columns and frames. The related main subject areas are:

- semi-rigid connections
- the application of tubular columns in multi-storey buildings
- connections between open beam sections and SHS columns
- analysis of frames with semi-rigid connections

- axially loaded columns with pin ends and axially loaded columns with semi-rigid ends
- beam-columns with end restraints
- phenomenon of moment shedding in beam-columns.

2.2 The Characteristics of Semi-rigid Connections

The behaviour of a semi-rigid connection is very complex and can be best described by its fundamental characteristic of the M-ϕ relationship. This is the relation between the moment, M, transmitted through the connection and the relative connection rotation, ϕ, as measured between the column centre-line to the beam centre-line. Figure 2.1 shows the relation between moment and rotation of a semi-rigid connection. From the M-ϕ curve characteristics, the degree of stiffness and strength of the connection can be determined. The stiffness of the connection is associated with the slope of the M-ϕ curve and the value of this indicates the ability of the connection to develop restraint. The strength of the connection (moment capacity) is associated with the peak value on the M-ϕ curve which is a measure of the ability of the connections to transfer the anticipated loads.

Figure 2.2 shows variation of M-ϕ curves with respect to different types of connections. As can be seen from this figure, the general response of M-ϕ curve is non-linear. Curve *(f)* represents the perfectly pinned connection where moment is always zero for all values of rotations. Curve *(g)* represents the perfectly rigid connections where rotation is always zero for all values of moment. Real connections, as represented by curves *(a)* to *(e)*, will have their M-ϕ curves located between the two extremes pinned and rigid conditions. This reflects that practical connections are neither pinned nor rigid and instead show the semi-rigid characteristics. It can be said that all connections possess some degree of rotational stiffness (rigidity) that permit some amount of connection rotation to develop.

A prior knowledge of M-ϕ characteristics is regarded as essential in order to employ them in the analysis of frames with semi-rigid actions. The understanding of the real

interaction between connections and the adjoining members may result in more realistic predictions of frame behaviour and eventually more realistic design method for semi-rigid frames.

The effect of semi-rigid connections is very complicated. One complexity is that the connection plays a dual role in column response [2-1]. In the first role, the semi-rigid connection transfers beam end moment which causes a detrimental effect to the column axial load capacity; whilst in the second role, the connection provides a restraining effect which can enhance the column axial load capacity. Experimental results showed that even if a small amount of rotational stiffness in simple connections is considered, more economical and competitive column design can be achieved [2-2], [2-3]. Hence, due to such a complexity, more studies are still underway to improve the understanding on how the connections influence the behaviour of columns and complete frames.

2.3 The Application of Tubular Columns in Multi-storey Buildings

The use of tubular columns in multi-storey buildings is gaining more popularity with architects, engineers and the public. Structures employing tubular members can be more visible and display an elegant aesthetic appearance, and provide more internal space with little intrusion. There are various types of tubular sections suitable for applications as structural members in multi-storey buildings such as circular hollow section (CHS), square hollow sections (SHS) and rectangular hollow section (RHS). This thesis, however, only concerned on the subject areas related to SHS columns in multi-storey buildings as illustrated in Figure 2.3.

From a structural point of view, SHS columns have been regarded as efficient in carrying axial compressive loads and have been effectively used as columns in low to medium rise buildings [2-4]. Other benefits of SHS columns as opposed to open sections columns are :

- column sizes can be set to be uniform with increasing storey heights by varying the section thicknesses
- equal flexural stiffnesses in both axes
- high strength to weight ratio.

The design of SHS columns follows the same procedures as designing open section columns as specified by BS 5950 [2-5]. In terms of local buckling, the problem can be avoided by satisfying the limitations of web and flange slenderness ratios specified by Table 7 of BS 5950. The limitations will restrict the use of very thin walled columns which may cause local buckling failure prior to failure by general yielding. McGuire [2-6] suggested that where tubular columns are used in ordinary bridges and buildings, they are usually of the type for which regular column design procedures apply and the special problems of shell buckling need not be considered.

The main obstacle to the use of SHS columns is the cost and complexity of the connection systems. As compared to open sections, tubular columns are more difficult to manufacture and hence a little more expensive weight for weight. Additionally, traditional connection systems require welding to the column wall which contributes to further difficulty in the fabrication work.

However, realising the many benefits of SHS columns, many research investigations are currently underway to improve:

(i). the connection systems. The studies to improve the connection systems to be used in multi-storey frames have been underway and the reviews are explained in section 2.4.

(ii). the column strength by concrete filling [2-7]. The results show that the concrete filling can improve the properties of the section, gaining a higher compressive strength, associated with good ductility and large energy absorption.

2.4 Connections Between Open Section Beams and SHS Columns

White and Fang [2-8] conducted one of the earliest experimental studies on connections between open sections and SHS columns in the mid 1960s. The connection types suggested were mainly welded. At that time, welding was the only practical method because of the closed cross section of the tube. Figure 2.4(a) shows the connections using plate and tees angles as part of the connections tested by White & Fang. Researchers such as Shanmugam et al. [2-9] extended the scope of the investigations by providing external stiffeners between open beams and SHS columns. Such connections are still very expensive and not ideal for actual constructions. Overall, early developments on open beam to SHS columns were mainly concentrated on welded connection types. The complex fabrication of a welded connection has made its use in practice limited and restricted, more probably due to difficulty in site welding or joints have to be made twice, first in the factory and second on site.

The problem with SHS sections is lack of access to the inside of the tube for the nut, if traditional bolting system is to be employed. A major development to overcome this problem is the use of blind bolting system. A hole may be cut into the hollow section to give access for the blind bolts. This system then allows the installation of bolts from one side only in which nuts are not required as normally used in the traditional bolting.

Tanaka et al. [2-10] conducted investigations on a new method combining the SHS column with blind bolts. The column wall at the connection zone has larger thickness as compared to other part of the column. The objective is to prevent excessive out-of-plane deformation and to increase the bolt contact length. The thicker wall is obtained by first heating the required wall area to a pre-defined temperature at which the column material can deform plastically. This is then followed by applying compressive forces at a specific speed at both column ends. This caused the heated column to swell. Figure 2.4(b) shows the special connection developed by

Tanaka et al. The connection is developed for moment resisting frames of low and medium storeys. The blind bolting system employs special mechanical bolts.

Figure 2.4(c) shows the blind bolting system without the need to increase the column wall thickness. The installation is made possible with the use of special mechanical bolts. Korol & Ghobarah [2-11] and Mourad et al. [2-4] investigated the performance of two types of blind fasteners namely blind oversized mechanically locked fastener (BOM) and High strength blind bolts (HSBB) (see Figures 2.5(a) and 2.5(b)). The performance of BOM and HSSB in connecting open beams and SHS columns has been investigated. The results show that the HSBB system can provide effective moment connections in steel frame structures. Whereas, the BOM connections are more suitable for applications which are dominantly controlled by shearing action. The installation of HSBB requires the use of a special electrical hydraulic device.

The blind bolting system described above is a mechanical system which uses expensive components and requires the use of oversized holes. The system also needs special installation equipment which can be more expensive and cumbersome. In contrast, the simplest form of blind bolting system is the flowdrill connection.

2.4.1 Flowdrill Connections

When sections with high wall thicknesses are used, threads may be tapped directly into the column wall but for many SHS sections wall thickness are too small for tapped holes to provide adequate thread length. In this case, flowdrilling can be utilised. In the past, the flowdrill system is used in car production, metal furniture and household electrical appliances [2-12]. Currently, the technique has been used in the structural steelwork joints due to the development of a new tungsten carbide drill bit that can be used for hard material.

Flowdrilling is a process which consists of forming a hole using a plain tapered cone which simultaneously increases the wall thickness of the SHS section locally. Figure 2.6 (a) shows the process and the procedures are described as follows:

1st. stage:

(i). A special tungsten carbide drill bit which operates at very high speed is forced into the material.

(ii). When the drill comes into contact to the column wall, it produces high heat and consequently softens the SHS section locally.

(iii). The drill bit is then forced through the steel section to produce a hole.

(iv). The softened material displaced by the drill bit will form a conical extension mainly on the inside of the tubular section and finally increases the tube thickness locally by extrusion. The material forming an upstand on the exterior of the tube is removed by a cutter on the first tool to leave a flush surface.

(v). The completed hole is a truncated cone shape with sufficient depth to permit an adequate thread to be tapped for standard bolt application.

2nd. stage:

(i). The thread in the hole is made in a cold formed process by using a different tool.

Figure 2.6(b) shows a three dimensional view of the flowdrill holes. Currently, the wall thickness of the SHS columns that is suitable for the flowdrill connection system is in the range of 6mm up to 12.5mm [2-13], [2-14]. The connections can be site bolted without special machines or skilled workers. The bolts can be fastened from the outside of the columns without access to the internal hollow sections. Beams with conventional end plates can be bolted to the SHS columns easily using Grade 8.8 bolts. Figure 2.6(c) shows the installation of the flowdrill connections as viewed from the cross section.

Yeomans [2-15] investigated the performance of the flowdrill connection components for possible use in structural steelwork joints. The results show that the connections are suitable to be used with SHS columns.

Ballerini et al. [2-12] conducted tests to study the performance of the connections in both shear and tension. They concluded that flowdrill connections are suitable for the jointing of tubular columns and suggested that the system is a solution for the bolted

connections of steel hollow section members. They later suggested that full scale beam-to-column joint tests should be undertaken.

The University of Sheffield, in collaboration with British Steel, have conducted numerous full scale beam-to-column joint tests involving flowdrill connections and SHS columns. The objective is to study the performance of flowdrill connections for possible use in low rise non-sway and sway frames. France [2-13] conducted a total of 25 beam-to-column flowdrill joint tests comprising three major connection types namely partial depth end-plate, flush end plate and extended end plate connections. The joints were subjected to realistic loadings as expected in real buildings. The test results showed that the flowdrill connections exhibited no unexpected failures and that they behave as semi-rigid. Thus, the connections are able to transfer moment between the beams and the columns but simultaneously permit some relative rotations between the connected members. These results are in accordance with other types of conventional steel connections such as connections between H-columns and open beams which also show semi-rigid behaviour. The results of experimental work have provided an understanding of the behaviour of flowdrill connections which can be exploited further in analytical studies of global frames.

2.5 Analysis of Frames with Semi-rigid Connections

This section reviews some of the analytical programs developed by different researchers to study the influence of semi-rigid connections on the behaviour of global frames. Apart from the semi-rigid connections, modern programs also include the effects of geometrical and material nonlinearities. With all these parameters taken into consideration, a more accurate prediction of the true frame behaviour can be obtained. This is useful as the development of current limit states design methods needs a more realistic evaluation of the true behaviour of structures particularly the behaviour at ultimate load levels.

Jones [2-16] developed a finite element program to investigate the effect of end restraints on a limited individual column model. The parameters of the column such as residual stresses and initial out-of-straightness can be varied in order to study the influence of such parameters to the column behaviour. The connection M-ϕ characteristics are modelled using B-spline technique. His study has provided some insights on the important aspects of connection restraints which influence the behaviour and performance of columns. The program has been modified further by other researchers at the University of Sheffield [2-17], [2-18], [2-19].

Poggi and Zandonini [2-20] developed the SERVAR program for the nonlinear analysis of flexibly connected steel frames based on the finite element method. The program employed three types of elements. The first element is the central beam-column element. The second element is the spring element representing the connection, whereas, the third element is the rigid element representing the finite dimensions of the joint which is normally taken as equal to $D/2$, where D is the depth of the column. The spring element is located between the rigid and central elements at each beam end. The connection M-ϕ characteristics are incorporated in the spring elements as a series of piecewise linear segments. The program is capable of analysing plane frame structures with columns buckled about their major axes only. The geometrical imperfections can be incorporated in the analysis by specifying the deformed co-ordinates of the columns.

Foley and Vinnakota [2-21] developed a finite element program for inelastic second-order analysis of partially and fully restrained planar steel frames. The cross section of each element is discretised into "fibers" in which the strains and stresses are monitored. As a result, spread of plastification can be traced within the cross section and along the member length. The connections are modelled using non-linear spring elements located at beam ends. The M-ϕ characteristics of the connections are included as a series of quadrilinear curves (four linear segments). According to Foley and Vinnakota, this connection model is easy to implement in the computer program as it can prevent numerical instability during the analysis.

The availability of the analytical tools as described above has enabled the studies on columns and frames with semi-rigid connections to be carried out.

2.6 Axially Loaded Columns with Pin Ended Connections

The buckling load of a column was first derived by Euler in 1759 as

$$P_{cr} = \frac{\pi^2 EI}{L^2} \tag{2.1}$$

where EI is the elastic flexural stiffness and L is the length of the column.

The limitation of the Euler buckling load is that it is based on assumptions namely; the material is perfectly elastic, the column is perfectly straight and the applied column load is perfectly axially loaded.

In reality, many practical columns are not perfect due to the presence of imperfections such as initial out-of-straightness and residual stresses. Furthermore, columns with intermediate slenderness ratio fail due to a combination of elastic and plastic effects. The effects of imperfections and elastic-plastic behaviour reduce the ultimate strength of the columns below the Euler load. Hence, in the case of practical columns, the Euler buckling load gives an upper bound to the buckling load. In relation to these aspects, the behaviour of pin ended column with different slenderness ratios is discussed further in section 6.2.

The understanding of the behaviour of the axially loaded pin ended column is widely accepted and, as a result, the pin ended column has become the basic reference point to which the strength and behaviour of columns with various degree of end restraints is compared.

2.7 Axially Loaded Columns with End Restraints

The influence of semi-rigid end connections on the strength and behaviour of columns has been studied by many researchers. The incorporation of semi-rigid connections has called for the concept of effective lengths in which it is defined as the length of member which when pin ended behaves as the real member with its actual end constraints [2-22]. Consequently, the strength of the restrained columns can be determined by reference to the effective length of the columns.

Jones et al. [2-23] conducted analytical investigations on the ultimate strength of isolated axially loaded columns with semi-rigid end restraints (see Figure 2.7(a)). The results showed that the strength of axially loaded columns with semi-rigid connections was much higher than that the strength of axially loaded column with pin ended conditions with equal lengths. Figure 2.7(b) shows the comparison of strength curves between the axially loaded end restraint columns and the axially loaded pin ended columns. It can be observed that the stiffer connections contribute to higher column strength. They further discovered that even if detrimental effects such as residual stresses and initial out-of-straightness were included, the strength of a restrained column was seen to be higher than the strength of the same column with pin ended conditions. In view of this, they suggested the reduced effective length factor, *K*, to be used in column design to obtain more economical columns. For example, they suggested the reduced effective length factors of 0.75 for simple cleat connections and 0.55 for fairly substantial end plate connections which represented a significant increase in economy relative to the generally adopted values of *K* - probably 0.75, 0.85 or 1.00.

Lui and Chen [2-24] conducted analytical investigations on the strength and behaviour of axially loaded wide-flange steel column with end restraints. Their study also showed that the maximum strength of the end-restrained column was higher than that of the pinned ended column. The influence of connection end restraints in increasing the column strength is more obvious in columns with higher slenderness ratios. They suggested that the effective length factor, *K* of an axially loaded column with end restraints can be calculated as

$$K = 1 - 0.017\alpha \tag{2.2}$$

$$\alpha = C/M_{pc} \tag{2.3}$$

where

α is the coefficient of end restraint

C is the initial connection stiffness

M_{pc} is the plastic moment capacity of the column

Bjorhovde [2-25] proposed a comprehensive method for determining the effective length factor of columns with semi-rigid end restraints. He introduced a significant modification to the SSRC G-factor [2-26] that is amended for rigid frames. In order to include the effect of semi-rigid connections he suggested that the G factor is to be evaluated as

$$G_r = \frac{\sum\left(\frac{EI_c}{L_c}\right)}{C^*} \tag{2.4}$$

instead of

$$G = \frac{\sum\left(\frac{EI_c}{L_c}\right)}{\sum\left(\frac{EI_b}{L_b}\right)} \tag{2.5}$$

where

G is the stiffness distribution factor

G_r is the stiffness distribution factor for a joint restraint

E is the modulus elasticity

I_c is the column moment inertia

I_b is the beam moment of inertia

L_c is the column length

L_b is the beam length

C^* is the effective stiffness of a connection

Hence, by knowing the G_r factors at the top and bottom joints of a column, the effective length factor, K, can then be obtained by using the alignment chart given in the AISC specifications [2-27]. Consequently, the strength of axially loaded column with end restraints can be evaluated.

2.8 Beam-columns with End Restraints

The studies described in sections 2.6 and 2.7 only concentrated on columns carrying axial loads without any consideration of moments. Hence, in investigating the column strength, only the beneficial effect due to connection restraints is considered. In reality, however, the columns have to carry both axial loads and moments as transferred by the beams. In this case, columns carrying axial loads and moments are also known as beam-columns. The presence of this acting moment may cause detrimental effects to the beam-columns.

In view of the above, this section discusses some of the tests in which beam-columns were loaded up to failure in the presence of an acting moment. The objective is to highlight the response and the ultimate strength of beam-columns as observed in the tests.

2.8.1 Beam-columns with Rigid Connections

In 1938, the studies on the behaviour of beam-columns with rigid connections in a small scale sub-frame were conducted by Baker [2-28]. The sub-frame used by Baker was a two dimensional type as shown in Figure 2.8. In this study, the beams were loaded to induce detrimental moment prior to loading the column to collapse. The investigations showed that the application of heavy beam loads had little effect on the axial load at collapse. He concluded that the ability of the column to sustain high axial loads before collapse was attributed by the rigid restraints at the column ends.

In 1969, Gent and Milner [2-29], [2-30], [2-31] conducted several tests on a small scale three dimensional sub-frames with rigid joints (see Figure 2.9). The beams were loaded first to produce a severe column bending followed by loading the column to failure. The results of the investigations showed that most of the column failure loads were close to the squash loads. The reason for this is discussed in section 2.9.

The Joint Committee on Fully-rigid Multi-storey Welded Steel Frames [2-32] proposed a simplified design method for rigid frames. During the period of 1964-1970, two types of full scale three storey rigid frames designed by the Joint Committee's method were tested [2-32], [2-33], [2-34]. The objective was to establish the accuracy of the simplified design method that the committee had proposed and consequently to produce economical design for rigid frames. In this test, the beam loads were applied first and then followed by loading the selected columns to failure. The results of the tests showed that the actual failure loads of the beam-columns were higher by about 20% than those predicted by the Joint Committee method [2-32]. This implies the conservatism of the proposed design method.

2.8.2 Beam-columns with Semi-rigid Connections

The tests described in section 2.8.1 were mainly associated to beam-columns with rigid connections. In reality, however, all connections show semi-rigid behaviour. In view of this, in the period of 1980s to 1990s, the Sheffield University team conducted a series of tests involving full scale sub-frames, full scale plane frames and full scale three dimensional frames to investigate the strength and behaviour of beam-columns with semi-rigid connections.

Davison [2-35] conducted a series of ten two dimensional tests on sub-frames to test columns with semi-rigid ends. The tests were conducted on 152 x 152 UC 23 columns, 6.5 m in length and connected to very short beams. The sub-frame is as shown in Figure 2.10. Various types of connections were employed namely web cleats, bottom flange and web cleats, flange cleats, flush end plate and extended end plate. The objective was to investigate experimentally the effect of semi-rigid connections to the stability of the columns. The results of the investigations showed that the failure loads of the columns in the presence of practical beam loads were considerably higher than the suggested capacity as predicted by the interaction equation specified in AISC LRFD specifications [2-27]. Furthermore, Davison confirmed the presence of inflection points within the column length even when

employing 'simple connections' such as web cleats. This implies that even if a small amount of restraint is provided at the column ends, a considerable contribution of end restraint to the columns can be achieved.

Gibbons et al. [2-2], [2-36] conducted ten three dimensional subassemblage tests on columns with different semi-rigid connection types. There were two types of subassemblages used in this test, one of them is as shown in Figure 2.11. Two types of connections were utilised namely web cleat and flange cleat connections. The beam loads were applied prior to loading the columns to failure. They then compared the column failure loads obtained from the tests against the predicted design method specified by BS 5950 in clause 4.8.3.3.1 [2-5] which is given as

$$\frac{F}{A_g . p_c} + \frac{m . M_x}{M_b} + \frac{m . M_y}{p_y . Z_y} \leq 1 \qquad (2.6)$$

where

F is the compressive force

p_c is the compressive strength

A_g is the gross cross-sectional area

m is the equivalent uniform moment

M_x is the nominal moment about the major axis

M_y is the nominal moment about the minor axis

M_b is the buckling resistance moment capacity about major axis

Z_y is the elastic modulus about the minor axis

p_y is the design strength

The comparisons showed that, in all the ten cases considered, the actual collapse loads were higher than that predicted by the interaction equation given in Equation (2.6). They suggested that the large reserve strength attributed to the connection restraints was still present in the columns. It is also concluded from these findings that the higher collapse loads of the columns are associated with the beneficial effects offered by the connections. The detrimental effect of the "acting" moment has been outweighed by the beneficial restraint effects from the connections. They also found that the presence of even the most simple connections can have significant influence on the column strength.

Two full scale semi-rigid plane frames tests were conducted by the Sheffield University group as part of a collaboration between BRE and Hatfield Polytechnic in which 5 frames were tested [2-35]. A description of the frames is shown in Figure 2.12. The connections were of the flange cleat type which in reality possess semi-rigid characteristics but in design are normally assumed to be pinned connections. The beams were loaded first prior to loading the columns to failure. The results showed that even with modest restraint offered by the connections, the column failure loads were still higher than the predicted design loads suggested by the interaction equation given in clause 4.8.3.3 BS 5950 [2-21], (see Equation (2.6) of this chapter). Again, the results showed the conservatism of the BS 5950 specifications.

In 1990, Gibbons [2-36] conducted two full scale three-dimensional semi-rigid frame tests. Each test was associated with columns bent about minor and major axes. Only the frame with columns bent in minor axes is discussed in this section and is shown in Figure 2.13. The $2\frac{1}{2}$ storeys and 2 bays frame was constructed using 152 x 152 UC 23 for the columns and 254 x 102 UB 22 for the beams. The connections were of the flush end plate type. The beams were loaded first followed by loading the columns to failure. Interestingly, the results showed that the column failure loads were close to the squash loads. Gibbons reported that the high failure loads in the columns were attributed by the beneficial effect of the connection restraints and the presence of minor axis moment reversal. He also pointed out that, at the point of ultimate load, there exist an interaction between the adjacent members and the columns.

2.8.3 Conclusions of the Beam-column Tests

Overall, it is evident that even with the presence of detrimental moments from beam loads, the restrained columns are still capable of sustaining high axial loads. More interestingly the failure loads are significantly higher than the predicted design strengths as proposed by the BS 5950 [2-5] and AISC [2-27] codes.

2.9 Phenomenon of Moment Shedding in Beam-columns

The experimental results explained above have shown that in many cases the ultimate loads of the beam-columns are larger than those predicted by the interaction equations specified by many design codes. It has been mentioned that the increase in beam-column strength is due to the connection restraints. However, one significant observation by Gent and Milner [2-29], [2-30] also indicates that this response may be described as moment shedding.

Moment shedding is a phenomenon in which the moment at column top end is progressively shed as the column starts to undergo failure. In multi-storey buildings, this kind of phenomenon has been seen in many tests either in small scale or full scale frames [2-2], [2-28], [2-29], [2-30], [2-34], [2-37]. The effect has also been observed in offshore structures [2-38].

2.9.1 Moment Shedding in Beam-columns With Rigid Connections

The early tests which can be associated with the moment shedding phenomenon were mainly in frames with rigid connections [2-28], [2-29], [2-30], [2-34]. Baker et al. [2-28] observed the effect of decreasing moment at the top end of beam-column with increasing axial load (see Figure 2.14). The corresponding beam-column is as shown in Figure 2.8.

Gent and Milner [2-29], [2-30] observed the behaviour of moment shed away from the column and then act as restraining moment as the column is approaching failure (see Figure 2.15). The corresponding beam-column is as shown in Figure 2.9. Based on this behaviour, the first use of the term moment shedding was then introduced by Gent & Milner. They also realised that the shedding of end moments was another factor contributing to the increased in the ultimate column strength. As a result of moment

shedding, they proposed a simplified method of designing beam-columns with rigid joints as axially loaded only.

The two full scale rigid frame tests conducted by the Joint Committee on Fully-rigid Multi-storey Welded Steel Frames that was described in section 2.8.1 also showed the phenomenon of moment shedding [2-33], [2-34]. The committee reported that the relaxation of beam support moments acting at the column will generally be beneficial to column performance.

Wood [2-39] studied extensively the variations of end moments and maximum moments within the column length with increasing axial loads. He noted that one important characteristic in the buckling of restrained columns is the rapid change of detrimental minor axis moments to restraining moments. As a result of this investigation, he then developed a more realistic simplified design method of columns with rigid ends. He introduced the concept of vanishing stiffness and showed great interest in the phenomenon of moment shedding.

2.9.2 Moment Shedding in Beam-columns With Semi-rigid Connections

The investigations carried out at the University of Sheffield that were discussed in section 2.8.2 showed that the moment shedding phenomenon also occurred in beam-columns with semi-rigid connections. Davison [2-35] identified the complex variation of beam and column moments as the columns approach its ultimate load. He then suggested that the higher column loads above the AISC LRFD design interaction were due to the relaxation of column end moments. Gibbons et al. [2-2], [2-36] observed that as the column approaches failure, the applied column end moments reduced to zero and then became restraining moments (see Figure 2.16). The corresponding beam-column as part of the three dimensional subassemblage is shown in Figure 2.11. As the moment shedding occurred, the columns continued to sustain additional loads. These phenomenon occurred in all the column tests.

Finally, the even more convincing evidence is that the phenomenon of moment shedding was also seen in the full scale semi-rigid plane frame [2-37] and three dimensional frame tests [2-36]. As reported in reference [2-37], one significant observation was the shedding of moment away from the collapsing columns. Figures 2.17 and 2.18 show the development of moment shedding at the top end of columns in the plane frame and three-dimensional frame tests respectively. The corresponding beam-columns are shown in Figures 2.12 and 2.13 respectively.

Nethercot [2-40] stressed the important of moment shedding phenomenon. He suggested that such response can have important implications in terms of the correct member forces for which the column can be designed. In relation to this, Kirby et al. [2-41] proposed a simplified design method of designing beam-columns as axially loaded columns only. The design method is known as the α_{pin} approach and is discussed further in section 6.6.2 of Chapter 6.

Numerous full scale frame test results on sub-frames and plane frames suggest that the moment shedding occurred due to the interaction of internal forces between beams and columns. The study on individual columns as carried out by Jones [2-16] had not seen the effect of moment shedding as the beam action was not present. Hence, to study the effect of moment shedding, it is justified to employ a plane frame model where full interaction and continuity between beams and columns are present.

2.10 Conclusions

A review of previous work related to the studies of steel frames has been presented. Important subject areas focusing on semi-rigid connections, new connections between open section beams and tubular columns were discussed. In addition, the phenomenon of moment shedding which is vital for understanding the interaction of members at ultimate load levels has been highlighted.

Several important conclusions from the review may be outlined as follows:

- Separate independent frame tests have been performed on columns with both semi-rigid or rigid connections. The results clearly demonstrate that, irrespective of connection types employed, the actual column failure loads are always higher than that predicted by the proposed design methods suggested by the Joint Committee [2-32] or the codes [2-5], [2-27]. It should be mentioned that these design methods are based on the interaction equations. This suggests a conservatism in the design methods although the interaction equations have incorporated all the required parameters such as beam moments and connection restraints (as defined by using reduced effective length factors). In view of this, a solution for economical column design needs to be sought.

- The phenomenon of moment shedding is seen to have a very significant effect on the behaviour of structures particularly at the ultimate load levels. On the other aspect, previous investigations showed that moment shedding can contribute to additional column strength.

In realising all these aspects, the phenomenon of moment shedding in frames with tubular columns needs to be investigated. There is also a need to investigate the strength of SHS columns using flowdrill connections. In addition, the observations made in experiments still require more rigorous explanations which are only possible by the use of analytical methods.

2.10 References

[2-1] Kirby, P.A. and Davison, J.B., 'Full scale testing of semi-rigid response in non-sway steel frames', in Structural Assessment: The Role of Large and Full Scale Testing, Joint IStructE/City University International Seminar, City University, London, 1-3 July 1996, pp. 77.1-77.8.

[2-2] Gibbons, C. Kirby, P.A. and Nethercot, D.A., 'Experimental behaviour of 3-D column subassemblages with semi-rigid joint', Journal of Constructional Steel Research, Vol. 19, 1991, pp. 235-246.

[2-3] Davison, J.B., Kirby, P.A. and Nethercot, D.A., 'Column behaviour in PR construction: experimental behaviour', Journal of Structural Engineering, Vol. 113, No. 9, September, 1987, pp. 2032-2050.

[2-4] Mourad, S., Korol, R.M. and Ghobarah, A., 'Design of extended end plate connections for hollow section columns', Canadian Journal of Civil Engineering, 23, 1996, pp. 277-286.

[2-5] BS 5950: Part 1: 1990, 'Structural use of steelwork in building', Part 1. Code of practice for design in simple and continuous construction : hot rolled sections, British Standard Institution.

[2-6] McGuire, W. , 'Steel structures', Prentice-Hall,1968.

[2-7] Zhang, J.Q. and Brahmachari, K., 'Flexural behaviour of rectangular tubular sections filled with fibrous high strength concrete', Tubular Structures VI, ed. Grundy, Holgate & Wong, Balkema, Rotterdam, 1994, pp. 247-254.

[2-8] White, R. N. and Fang, P.J., 'Framing connections for square structural tubing', Journal of the Structural Division, Proceedings of the American Society of Civil Engineers, ST2, April, 1966, pp. 175-194.

[2-9] Shanmugam, N.E., Ting, L.C. and Lee, S.L., 'Static behaviour of I-beam to box-column connections with external stiffeners', The Structural Engineer, Volume 71, No. 15/3, August, 1993, pp. 269-275.

[2-10] Tanaka T., Tabuchi, M., Furumi, K., et al., 'Experimental study on end-plate to SHS column connections reinforced by increasing wall thickness with one side bolts', Tubular Structures VII in Proceedings Seventh International Symposium on Tubular Structures', ed. Farkas & Jarmai, Balkerma, Rotterdam, 1996, pp. 253-260.

[2-11] Korol, R.M., Ghobarah, A. and Mourad, S., 'Blind bolting W-shape beams to HSS columns', Journal of Structural Engineering, Vol. 119, No. 12, December, 1993, pp. 3463-3481.

[2-12] Ballerini, M., Piazza, M., Bozzo., E, et al., 'Shear capacity of blind bolted connections for RHS steel structural elements', Tubular Structures VII, ed. Farkas , Jarmai, Balkema, Rotterdam, 1996, pp. 99-106.

[2-13] France, J.E., 'Bolted connections between open section beams and box columns', Ph.D. Thesis, Department of Civil & Structural Engineering, University of Sheffield, U.K., January, 1997.

[2-14] Ballerini, Bozzo, E. and M. Piazza, 'The flowdrill system for the bolted connection of steel hollow sections. Part 1: the drilling process and the technological aspects', Costruzioni Metalliche, N.4, August, 1995.

[2-15] Yeomans, N.F., 'I-beam/rectangular hollow section column connections using the flowdrill system', Tubular Structures VI, ed. Grundy, Holgate & Wong, Balkema, Rotterdam, 1994, pp. 381-388.

[2-16] Jones, S.W., 'Semi-rigid connections and their influence on steel column behaviour', Ph.D. Thesis, Department of Civil and Structural Engineering, University of Sheffield, U.K., June, 1980.

[2-17] Rifai, A.M., 'Behaviour of columns in sub-frames with semi-rigid joints', Ph.D. Thesis, Department of Civil and Structural Engineering, University of Sheffield, U.K., June,1987.

[2-18] Ahmed, I., 'Semi-rigid action in steel frames', Ph.D. Thesis, Department of Civil and Structural Engineering, University of Sheffield, U.K., June, 1992.

[2-19] Mohammad, S., Ph.D. Thesis, to be submitted, Department of Civil and Structural Engineering, University of Sheffield.

[2-20] Poggi C. and Zandonini, R., 'Behaviour and strength of steel frames with semi-rigid connections', in Connection Flexibility and Steel Frames, ed. Chen, W.F., American Society of Civil Engineers, New York, 1985, pp. 57-76.

[2-21] Foley, C.M and Vinnakota S., 'Inelastic behaviour of multi-story partially restrained steel frames - Part 1', Journal of Structural Engineering, ASCE, still in press, 1998.

[2-22] Kirby, P.A., 'Continuous multi-storey frames', in Introduction to steelwork design to BS 5950: Part 1, The Steel Construction Institute, 1998, pp. 15-1,15-8.

[2-23] Jones, S.W., Nethercot, D.A. and Kirby, P.A., 'Influence of connection stiffness on column strength', The Structural Engineer, Volume 65A, No. 11, November, 1987, pp. 399-405.

[2-24] Lui, E.M. and Chen, W.F., 'Strength of H-columns with small end restraints', The Structural Engineer, Volume 61B, No. 1, March, 1981, pp. 17-26.

[2-25] Bjorhovde, R., 'Effect of end restraint on column strength - practical applications', Engineering Journal, AISC, 1st. quarter, Vol. 21, No. 1, 1984, pp. 1-13.

[2-26] SSRC, 'Guide to stability design criteria for metal structures', Johnston, B.G. ed., 3rd. edition, Wiley-Interscience, New York, 1976.

[2-27] AISC, 'Manual of steel construction', American Institute of Steel Construction, Inc., 7th. edition, 1970, New York.

[2-28] Baker J.F., Horne, M.R. and Heyman J., 'The steel skeleton', Cambridge University Press, Vol. 2, 1956.

[2-29] Gent, A.R. and Milner H.R., 'The ultimate load capacity of elastically restrained H-columns under biaxial bending', Proceedings, Institution of Civil Engineers, Vol. 41, December, 1968, pp. 685-704.

[2-30] Gent, A.R., 'Elastic-plastic column stability and the design of no-sway frames', Proceedings, Institution of Civil Engineers, Vol. 34, June, 1966, pp. 129-152.

[2-31] Milner, H.R and Gent, A.R., 'Ultimate load calculations for restrained H-columns under biaxial bending', The Institution of Engineers, Australia, Civil Engineering Transaction, April, 1971, pp. 35-44.

[2-32] Joint Committee Report, 'Fully-rigid multi-storey welded steel frames', Institution of Structural Engineers, UK, December, 1964.

[2-33] Wood, R.H., Needham F.H. and Smith, R.F., 'Test of a multi-storey rigid steel frames', The Structural Engineer, April, 1968, No. 4, Volume 46, pp. 107-119.

[2-34] Smith, R.F. and Roberts, E.H., 'Test of a fully continuous multi-storey frame of high yield steel', The Structural Engineer, Vol. 49, No. 10, October, 1971, pp. 451-466.

[2-35] Davison, J.B, 'Strength of beam-columns in frames with semi-rigid connections', Ph.D. Thesis, Department of Civil & Structural Engineering, University of Sheffield, U.K., June, 1987.

[2-36] Gibbons, C., 'The strength of biaxially loaded columns in flexibly connected steel frames', Ph.D. Thesis, Department of Civil and Structural Engineering, University of Sheffield, December, 1990.

[2-37] Moore, D.B., Nethercot, D.A. and Kirby, P.A., 'Testing steel frames at full scale', The Structural Engineer, Vol. 71, Nos. 23 & 24/7, December, 1993, pp. 418-427.

[2-38] International Union of Theoretical and Applied Mechanics, 'Collapse : the buckling of structures in theory and practice: symposium' , University College London, 31 August to 3 September, 1982, edited by J.M.T. Thompson, G.W. Hunt, Cambridge University Press, 1983.

[2-39] Wood R.H., 'A new approach to column design', Department of the Environment Building Research Establishment, Her Majesty's Stationery Office, 1974.

[2-40] Nethercot, D.A., 'Frame analysis and the link between connection behaviour and frame performance', in Frame and slab structures, ed. Armer, G.T, Moore, D.B., Butterworths, London,1988, pp. 57- 74.

[2-41] Kirby P.A., Bitar, S.S. and Gibbons, C., 'Design of columns in non-sway semi-rigidly connected frames', First World Conference on Constructional Steel Design', Acapulco, Mexico, December, 1992, pp. 54-63.

[2-42] Davison, J.B., 'Overview of connection behaviour', in Structural connections - Stability and strength, ed. Narayanan, R., Elsevier Applied Science, London, 1989, pp. 1-22.

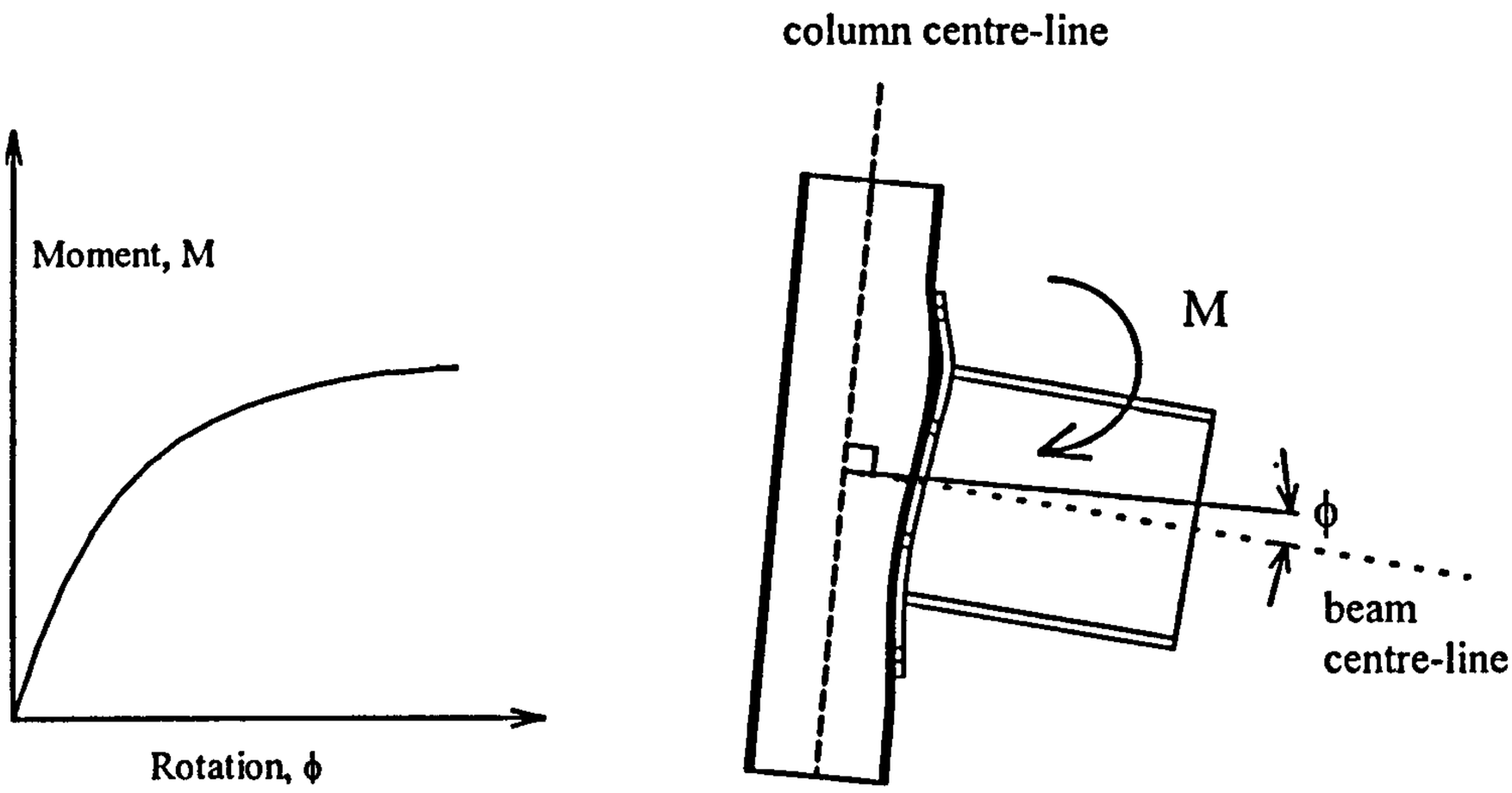

Figure 2.1 Connection M-ϕ relationship

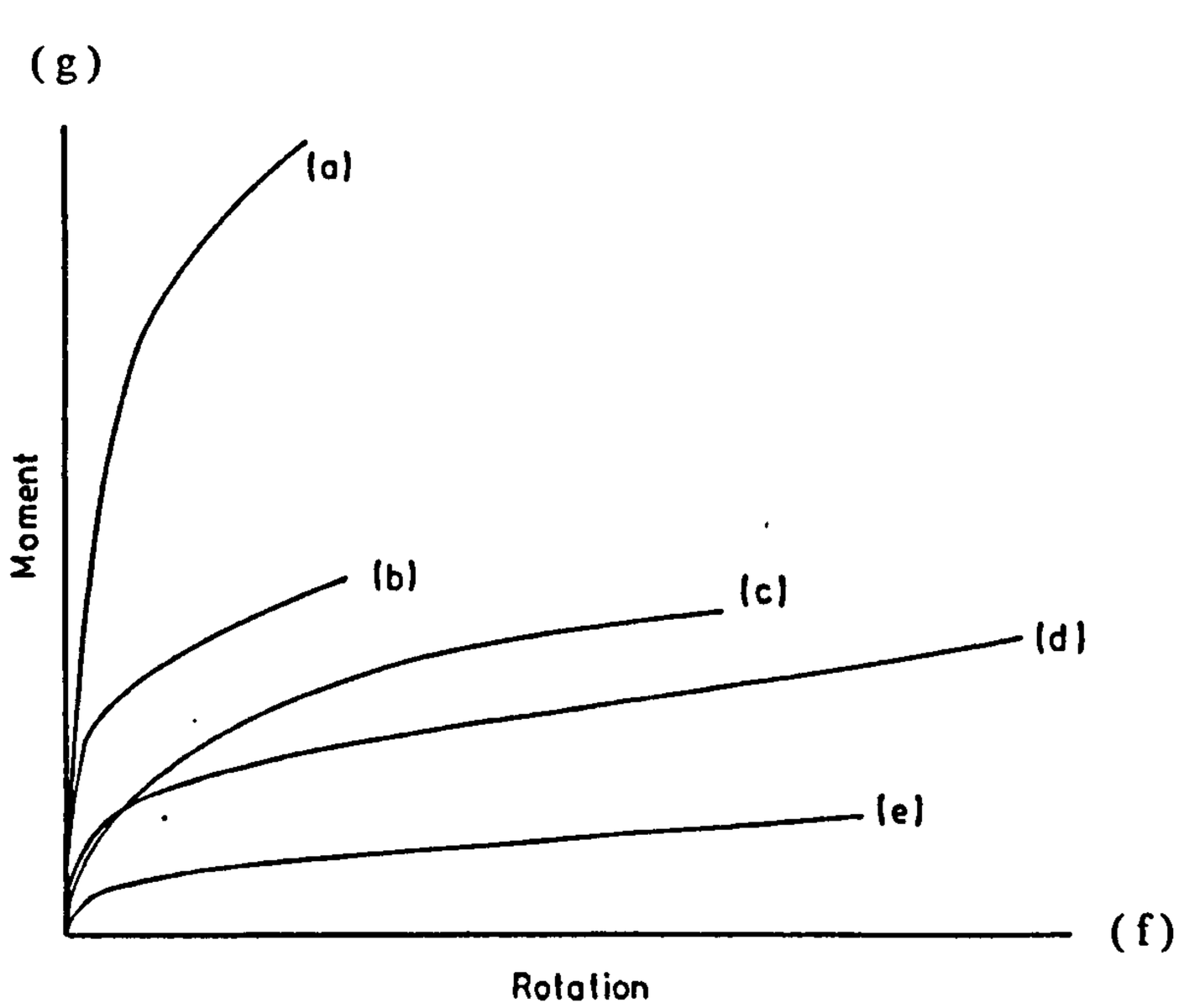

Figure 2.2 M-ϕ response for a range of semi-rigid connection types [2-42]
(a) extended end plate; (b) flush end plate;
(c) seat and web cleats; (d) flange cleats; (e) web cleats;
(f). perfectly pinned ; (g). perfectly rigid.

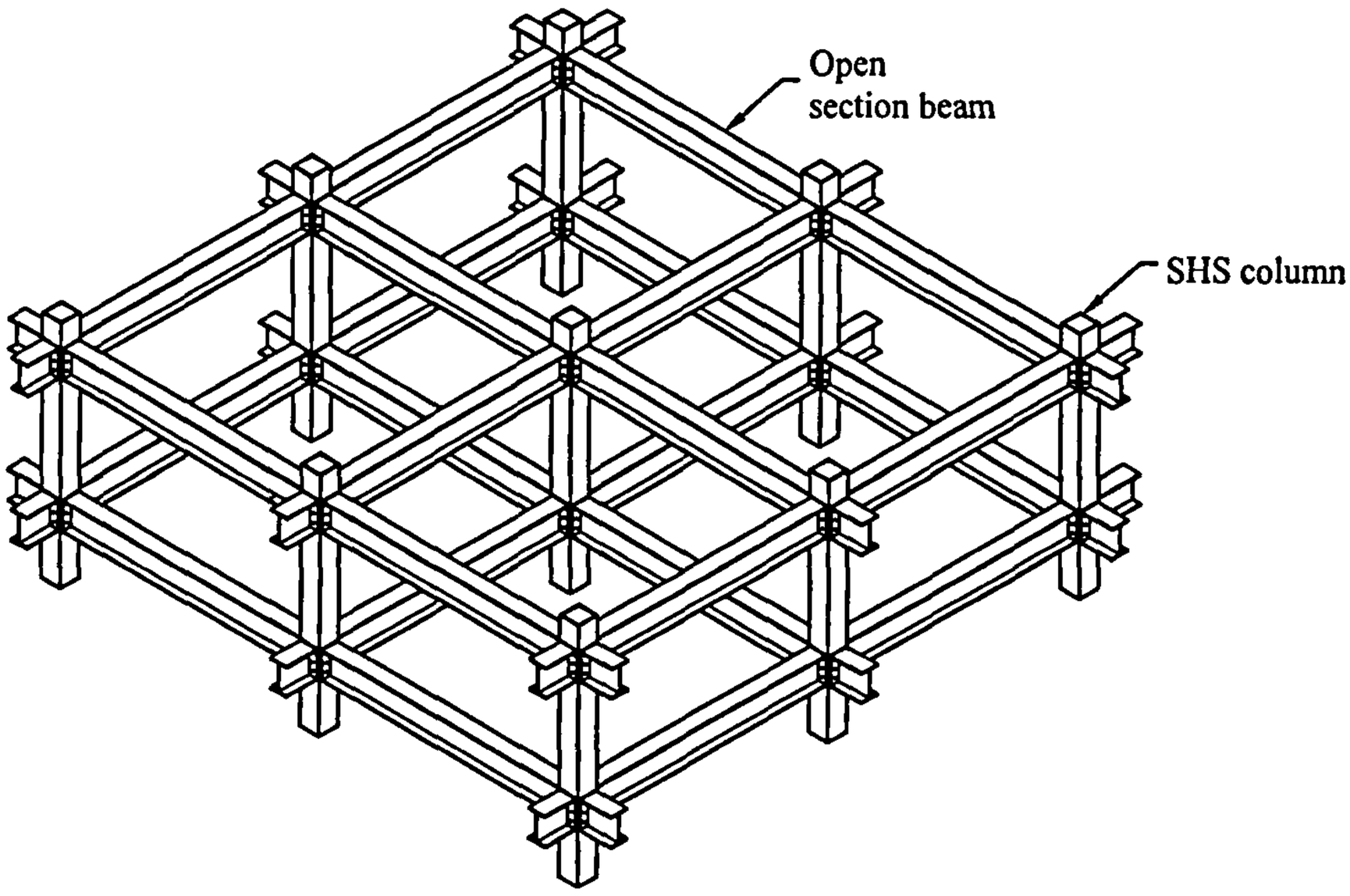

Figure 2.3 Typical structural system of multi-storey frames with open section beams and SHS columns

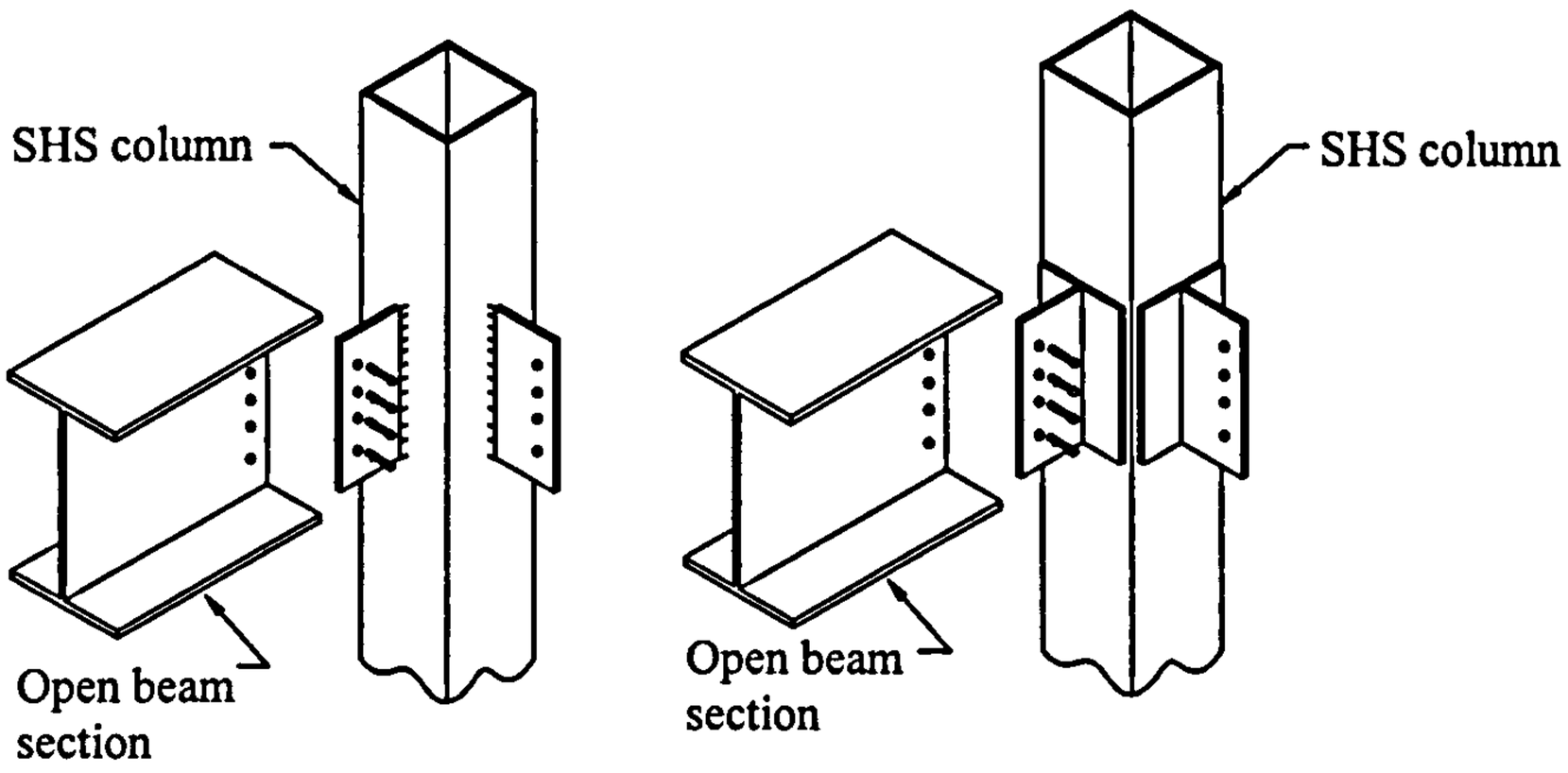

(a). Traditional connections with welding to column walls

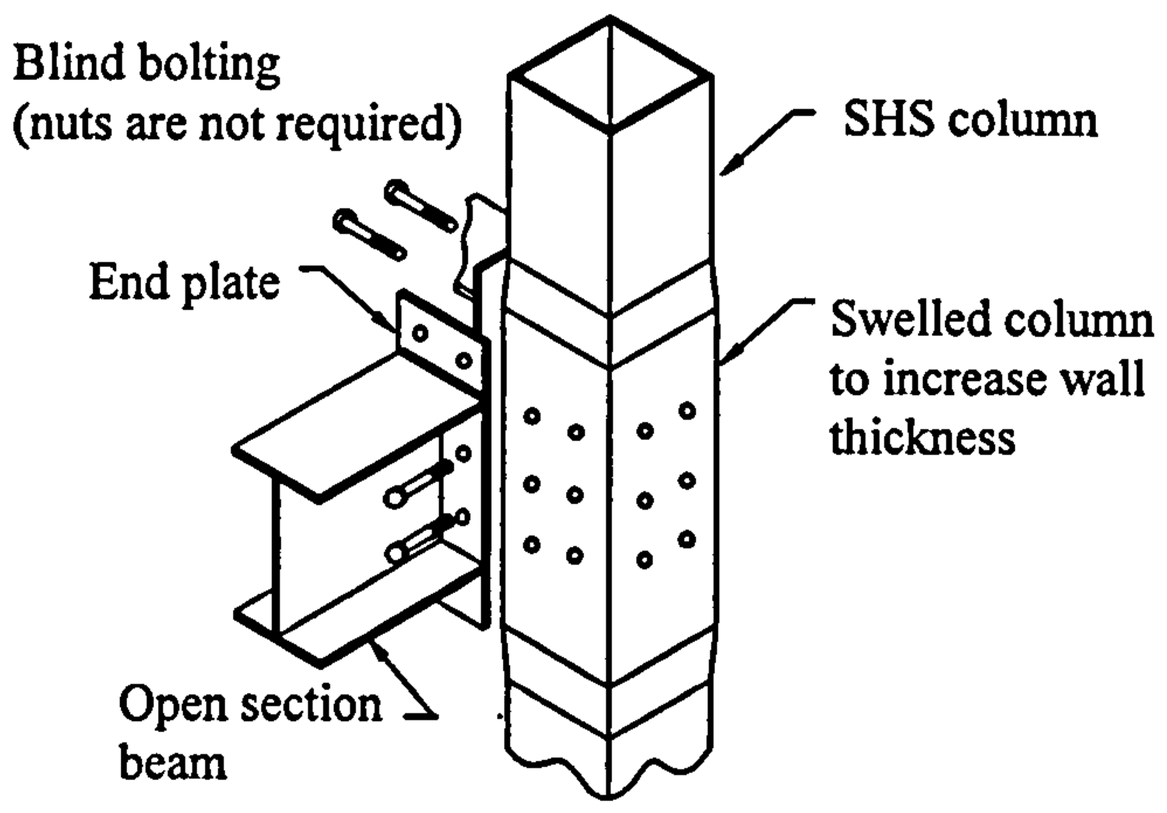

(b). Special connection with welding and bolting to column walls

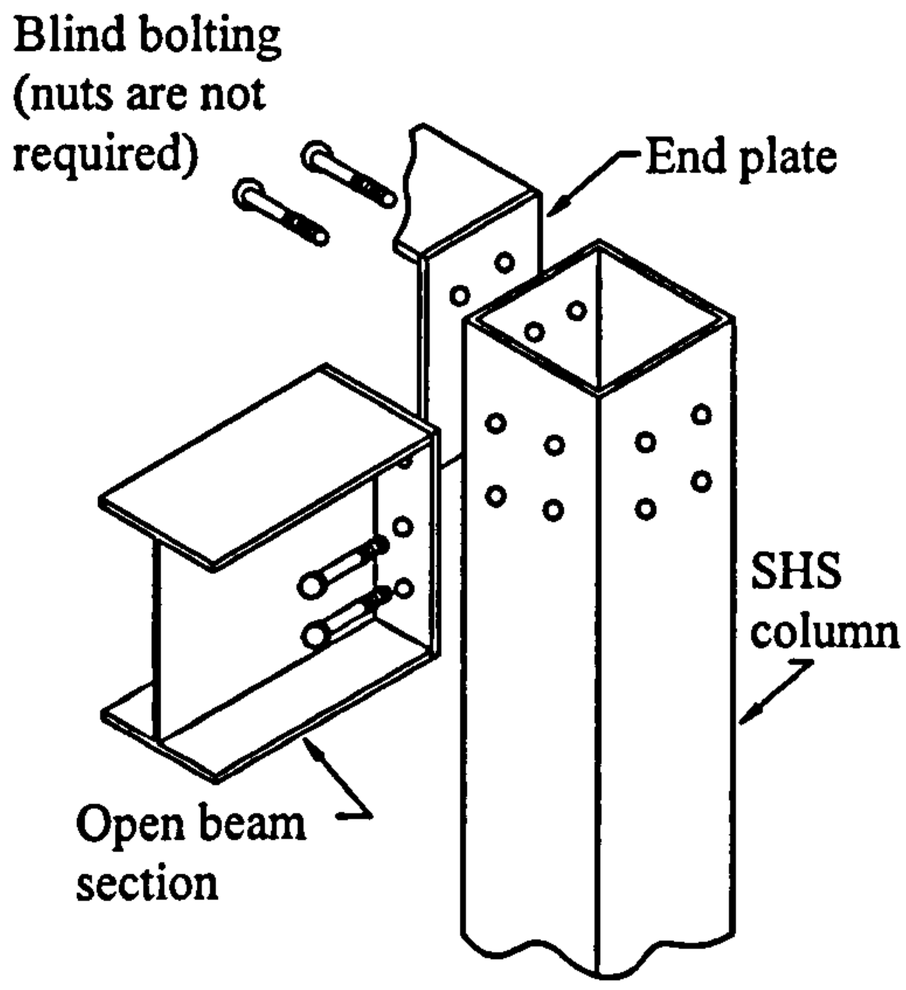

(c). Blind bolting to column walls

Figure 2.4 Types of connections between open section beams and SHS columns

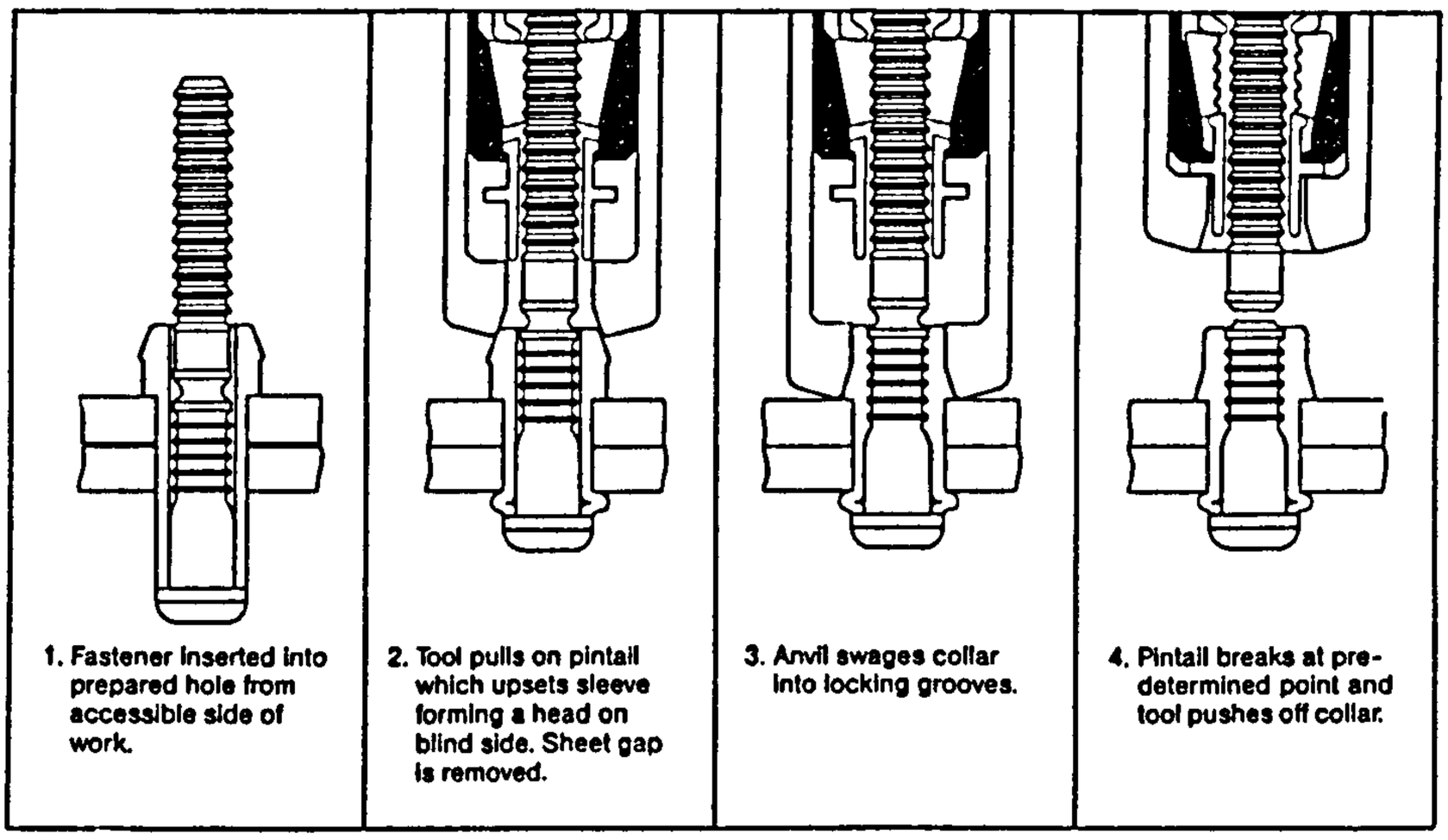

Installation Sequence for BOM Bolts (Courtesy Huck International Inc.)

(a). Blind oversized mechanically locked fasteners [2-11]

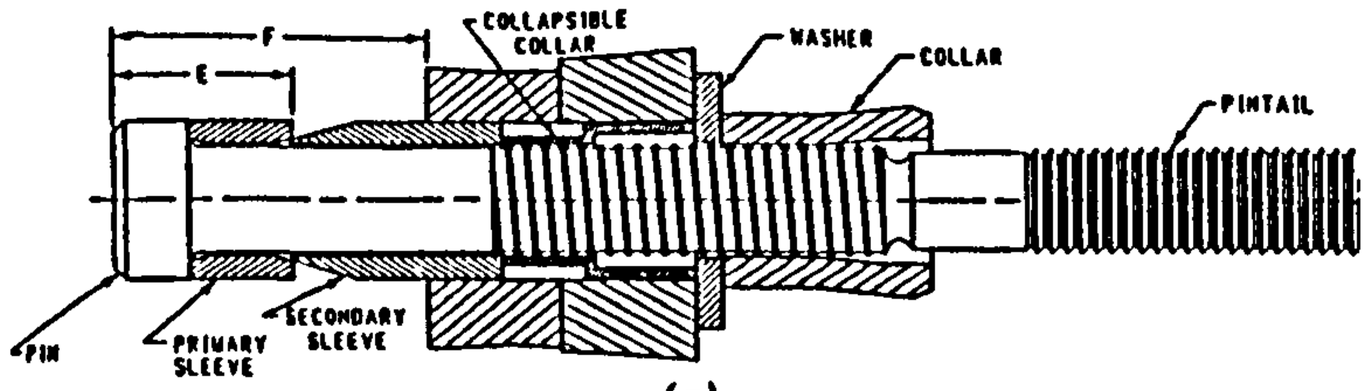

(a)

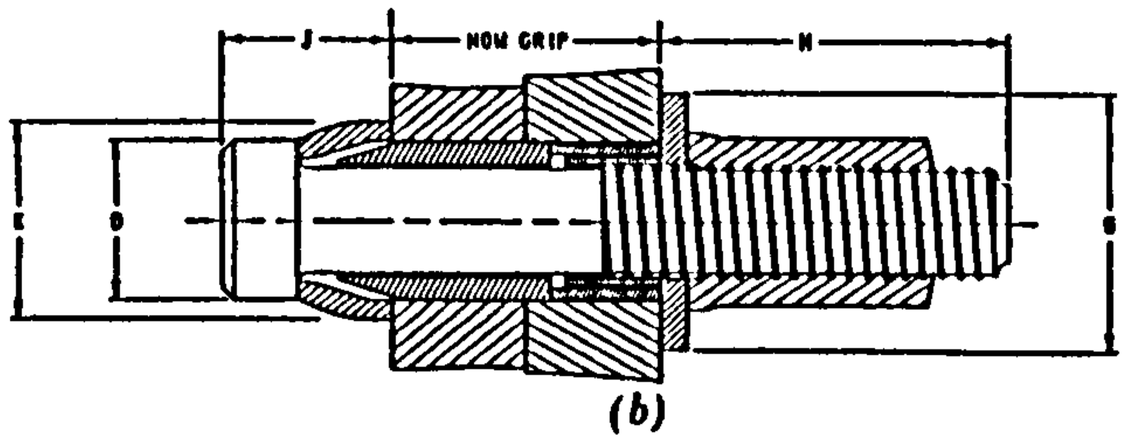

(b)

HSBB before and after installation: (*a*) before installation; and (*b*) after installation (Courtesy Huck International Inc.)

(b). High strength blind bolts [2-11]

Figure 2.5

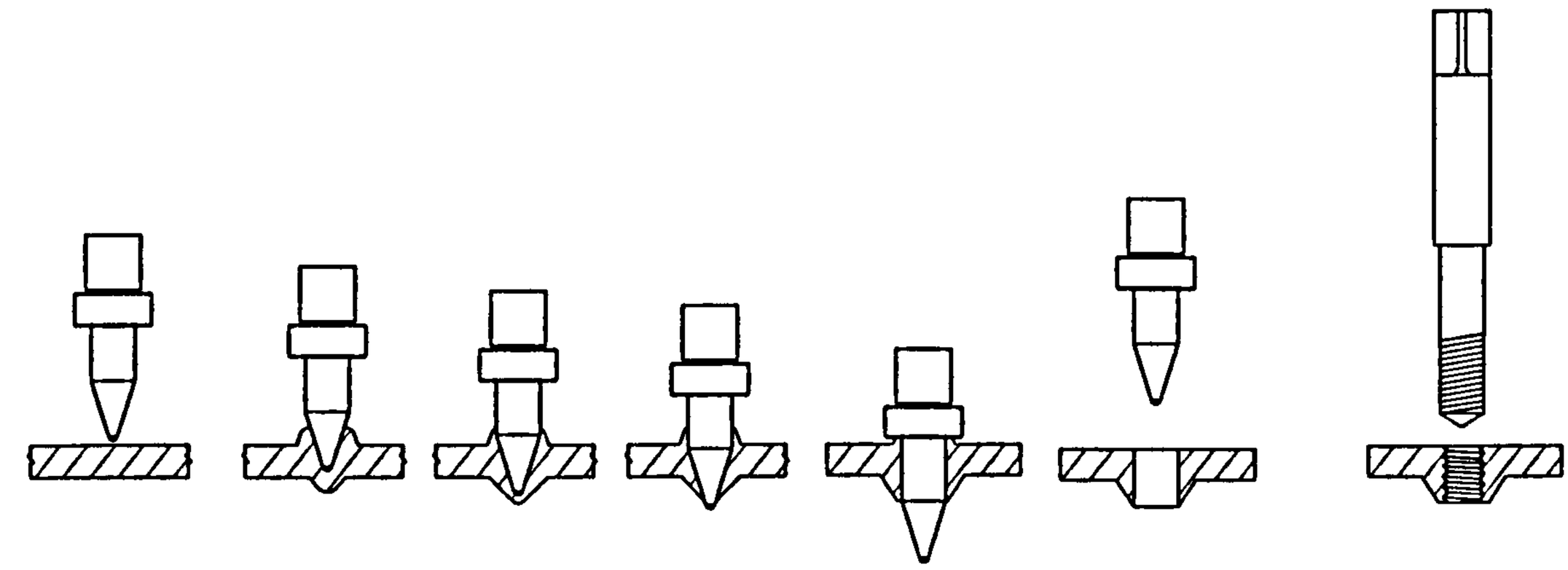

1st stage

2nd stage

(a). Flowdrilling process

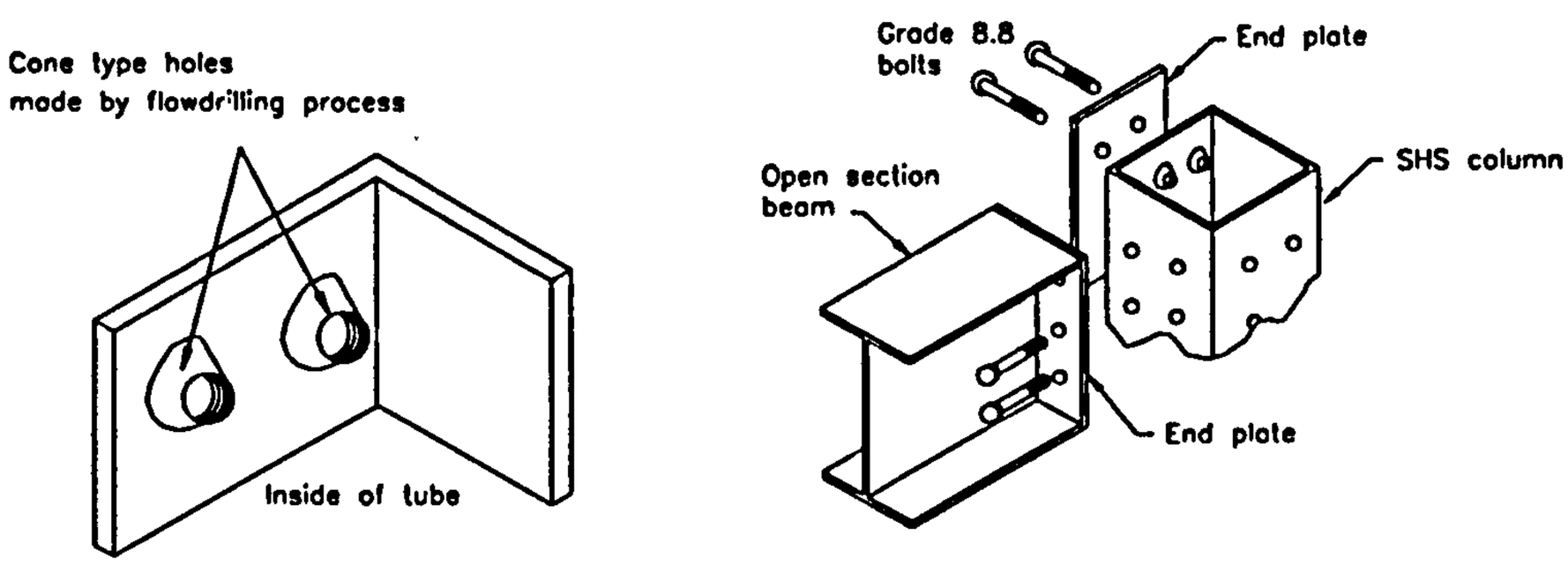

(b). Three dimensional view

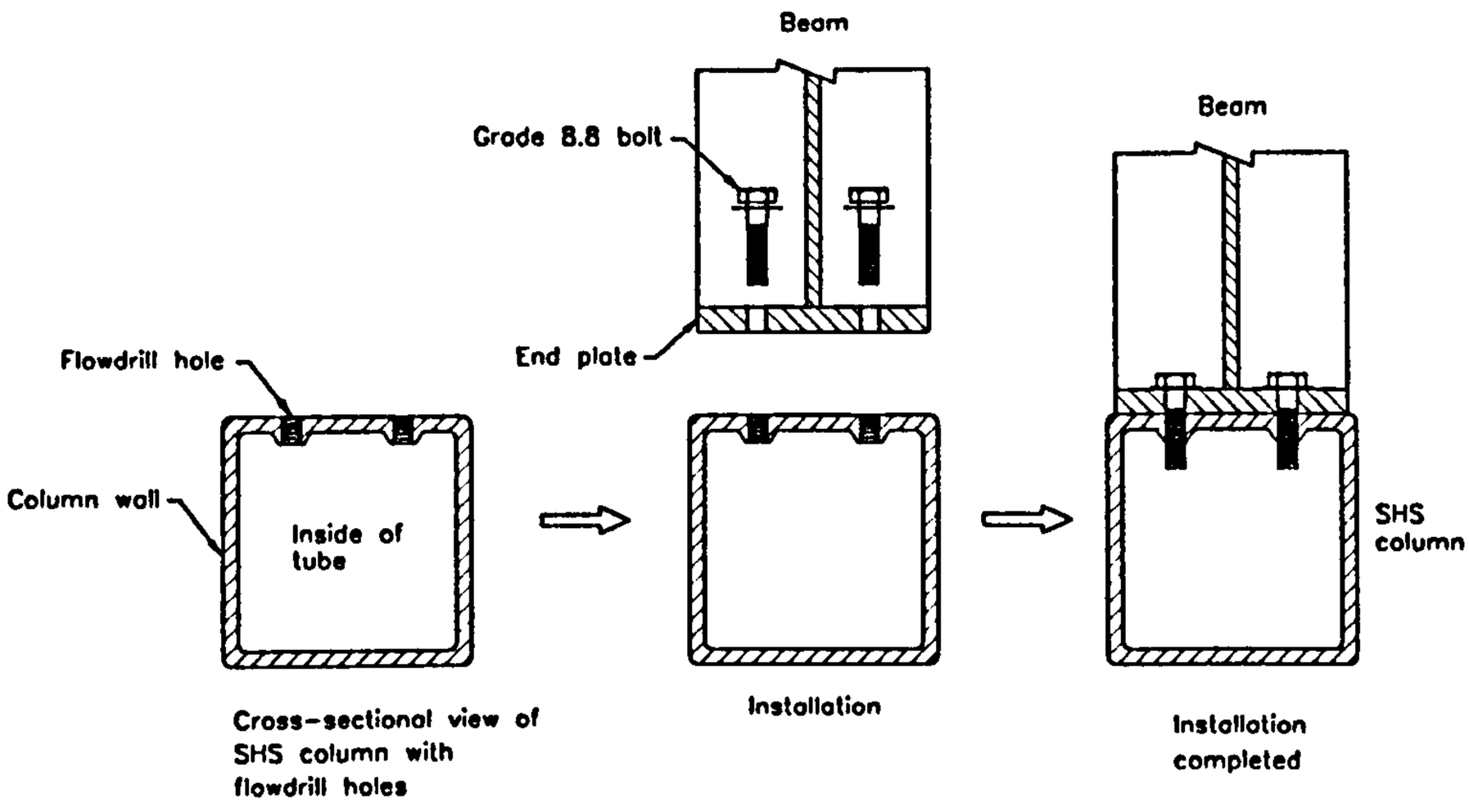

(c). Installation of flowdrill connections – cross sectional view

Figure 2.6

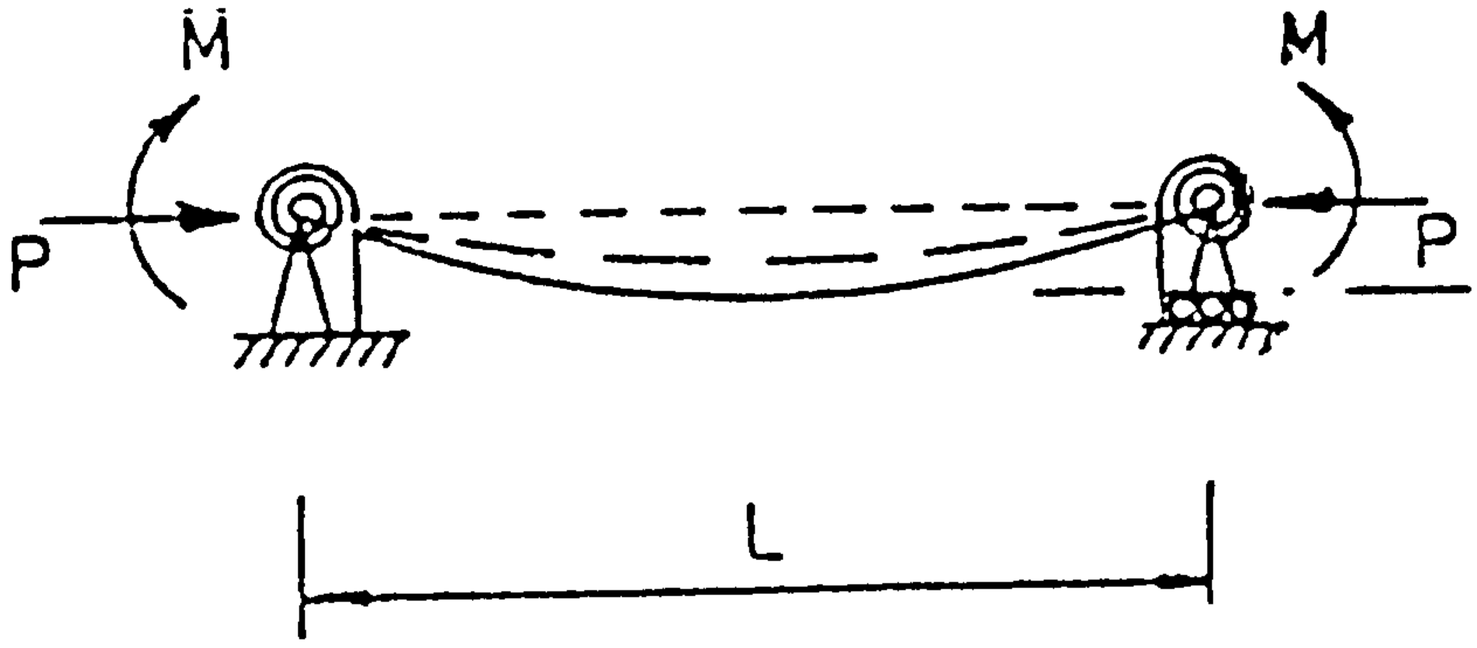

where P = axial load, M = moment, L = column length

(a). Axially loaded column with end restraint [2-23]

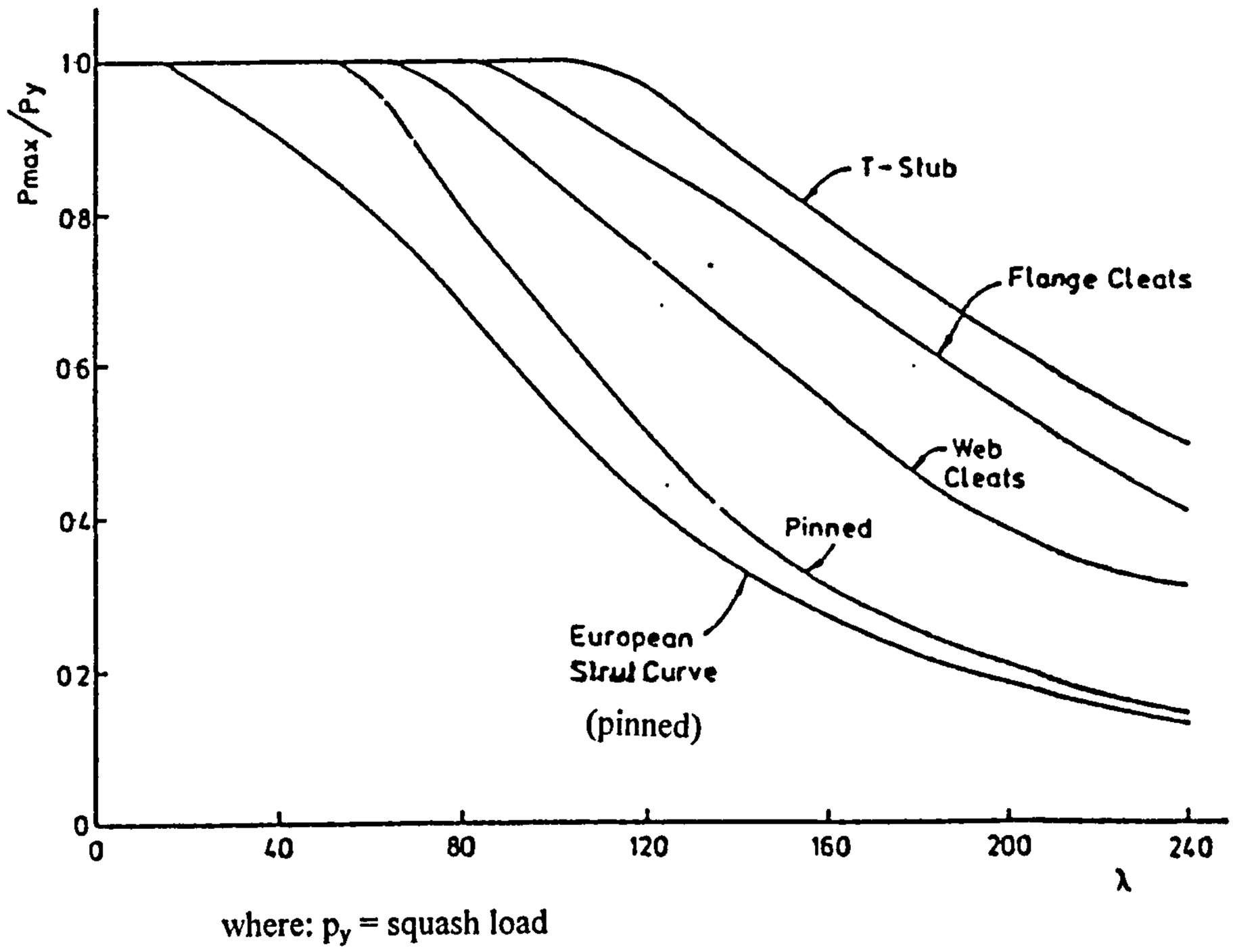

where: p_y = squash load

(b). Influence of connection types on the strength of axially loaded columns [2-23]

Figure 2.7

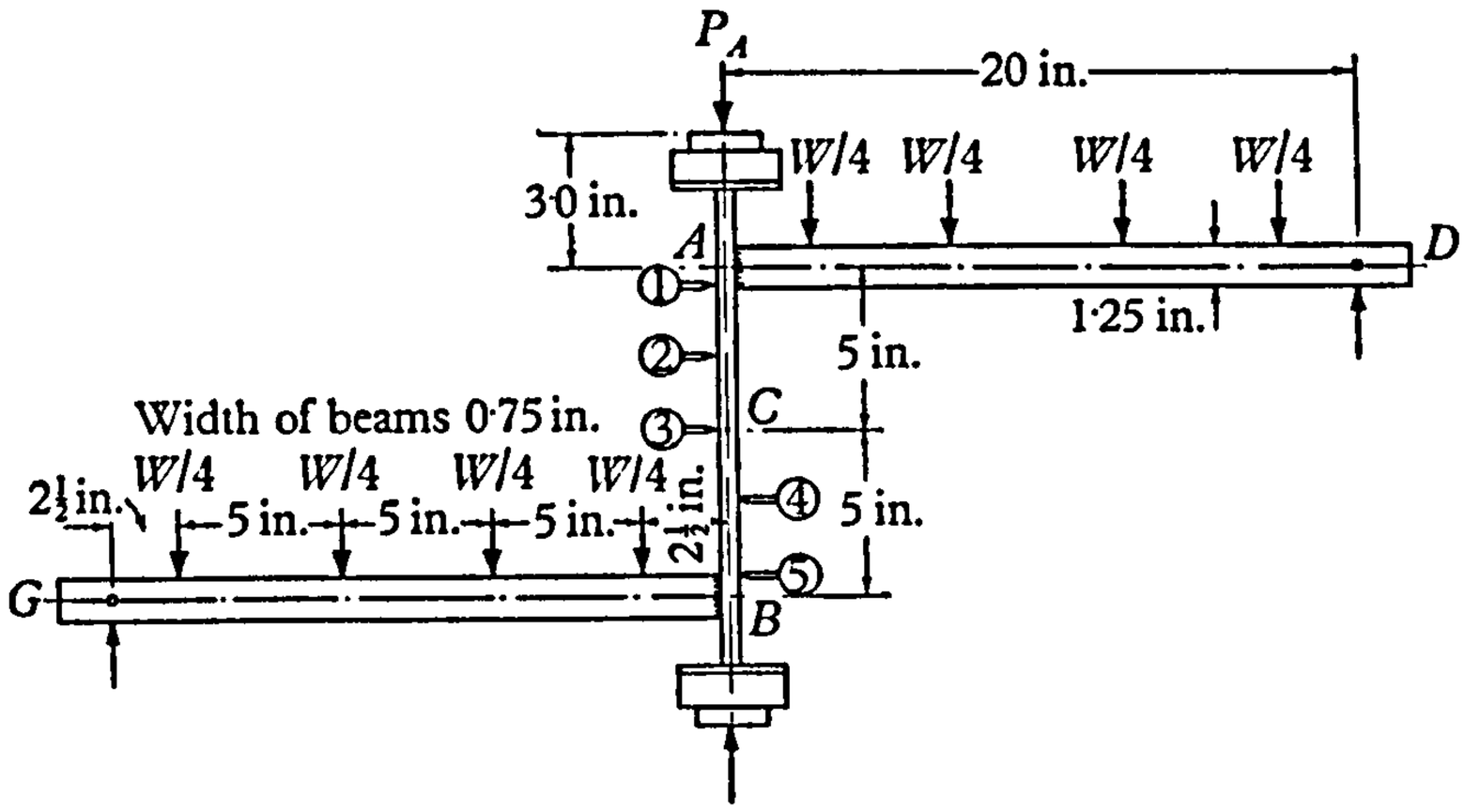

Figure 2.8 Beam-column with rigid joints in Baker's small scale plane sub-frame model [2-28]

Figure 2.9 Beam-column with rigid joints in Gents and Milners' small scale three dimensional sub-frame model [2-31]

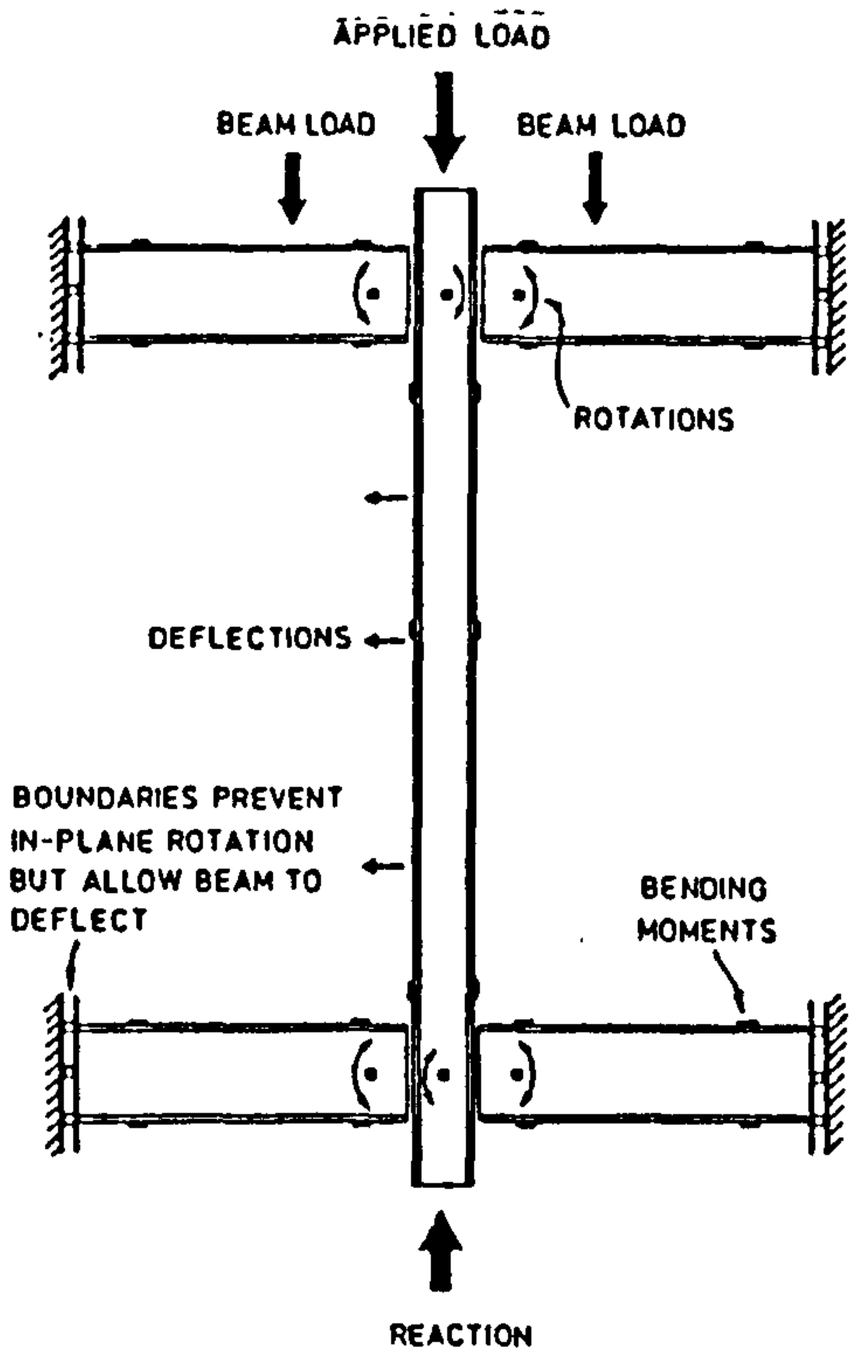

Figure 2.10 Beam-column with semi-rigid connections in Davison's full scale two dimensional sub-frame model [2-35], [2-3]

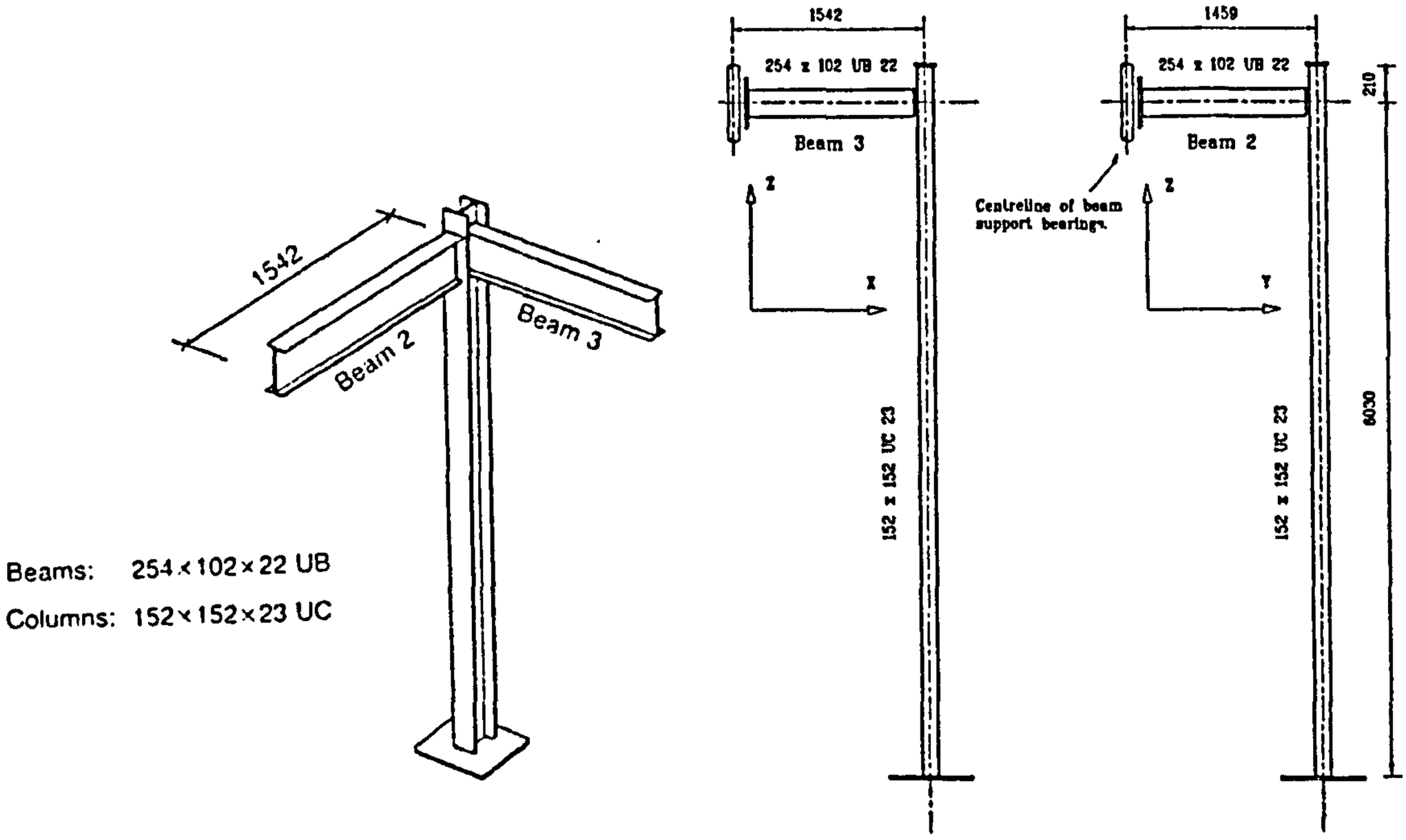

Figure 2.11 Beam-column with semi-rigid connections in Gibbons's full scale three dimensional subassemblage model [2-36]

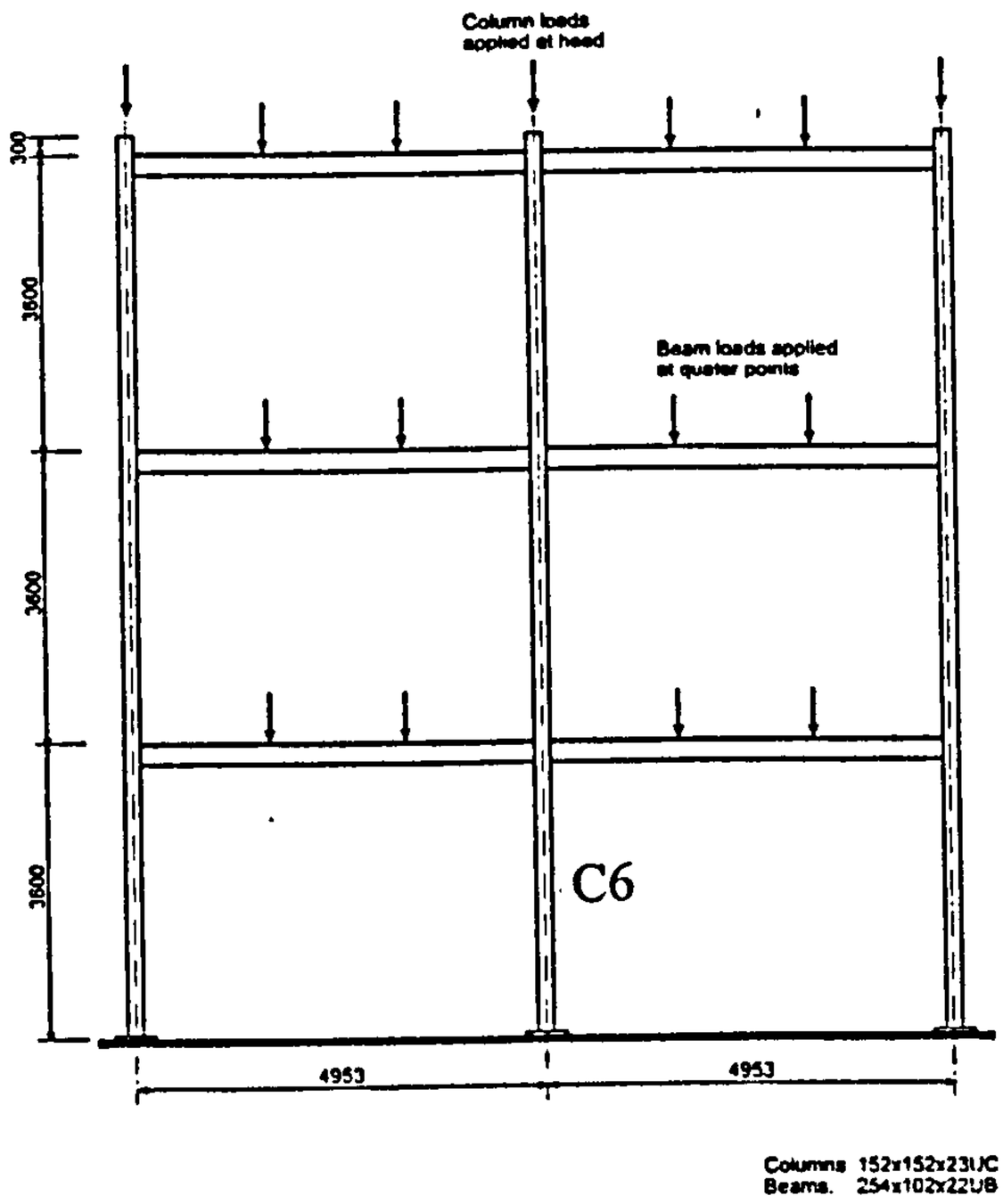

Figure 2.12 Beam-columns with semi-rigid connections in full scale plane frame tests [2-1], [2-35],[2-38]

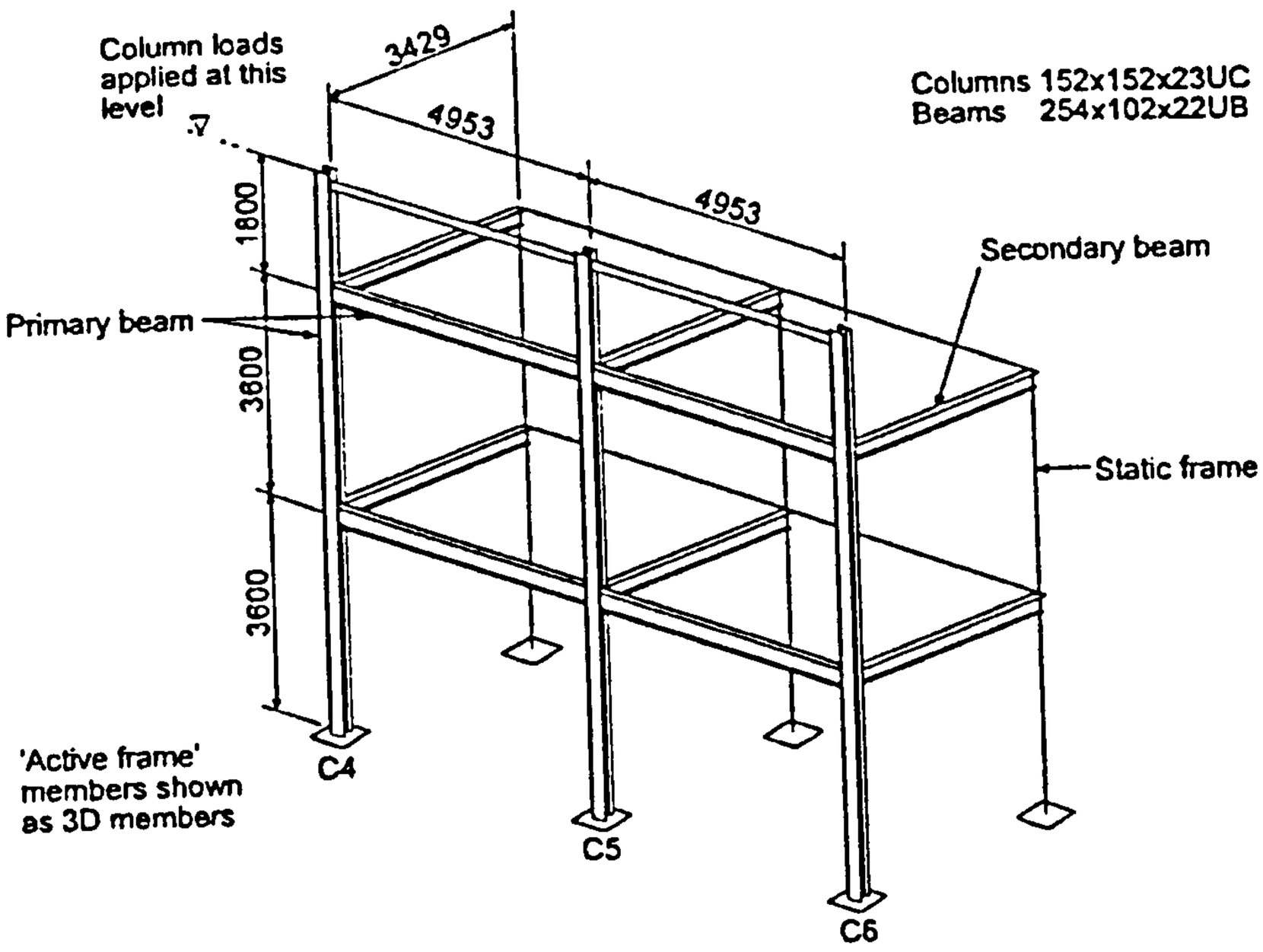

Figure 2.13 Beam-columns with semi-rigid connections in full scale three dimensional frame tests [2-1], [2-36]

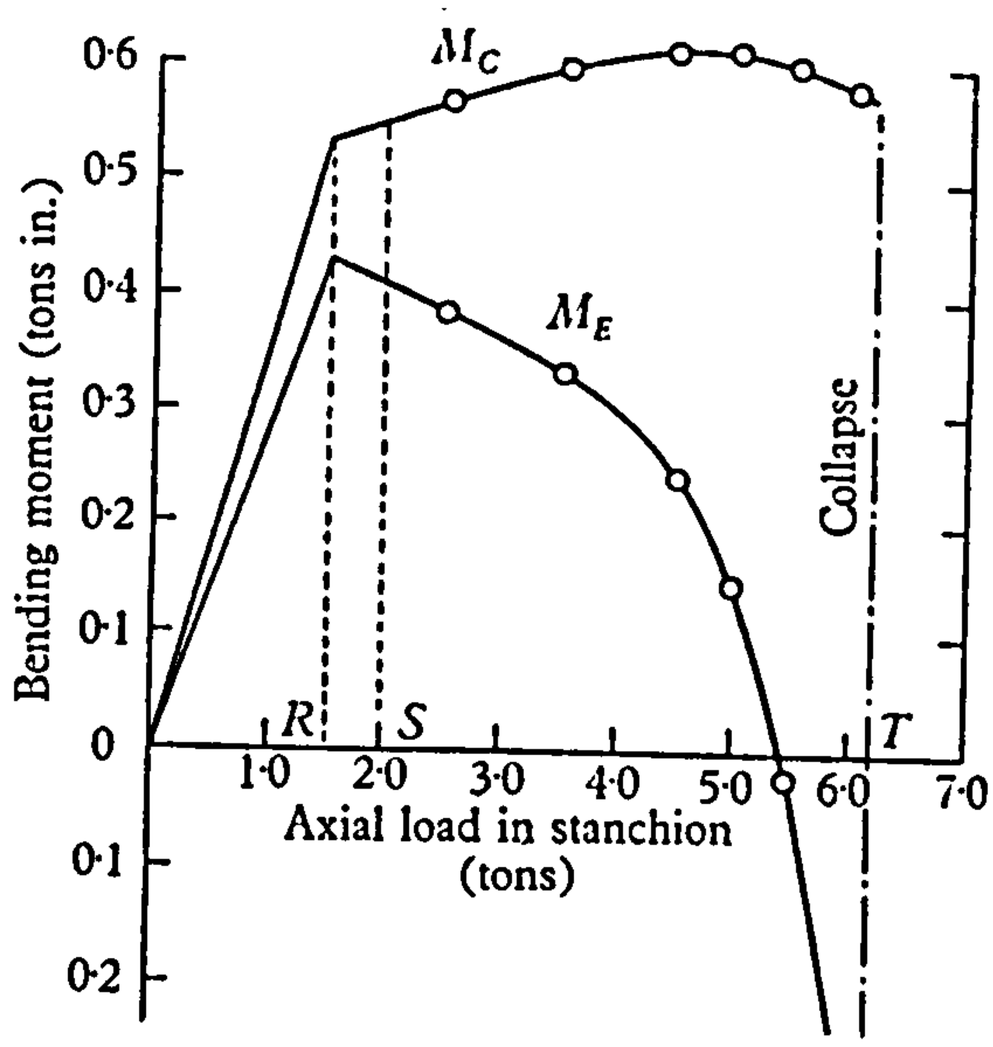

where: M_E = Moment at column top end
M_C = Moment at column mid-height

Figure 2.14 Reduction of moment at top end of beam-column as observed by Baker for the small scale sub-frame of Figure 2.8 [2-28]

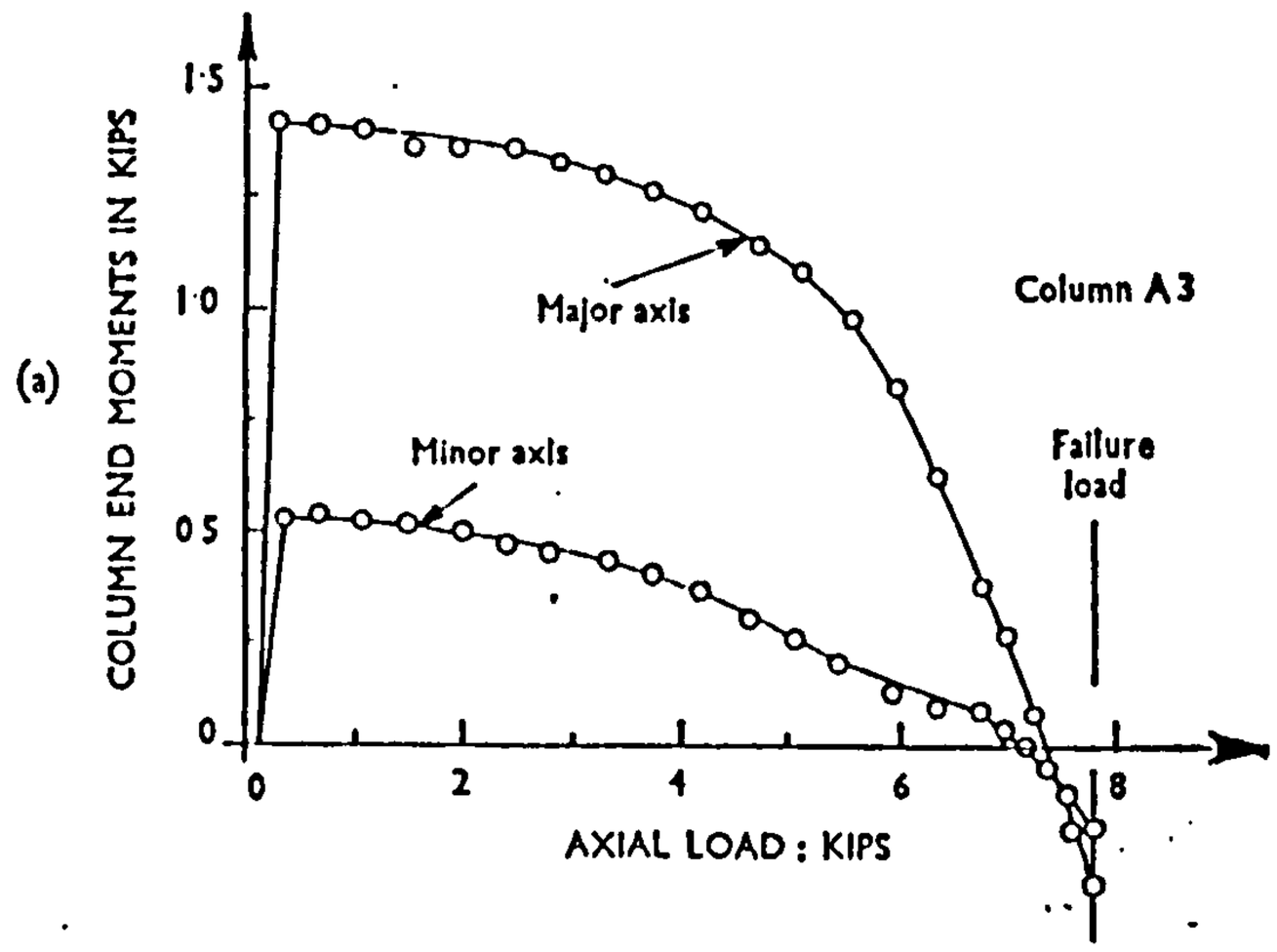

where: column A3 is 1" x 1" H section,
flange thickness=0.1", web thickness=0.06"

Figure 2.15 Moment shedding at top end of beam-column as observed by Gent & Milner for the small scale sub-frame of Figure 2.9 [2-29]

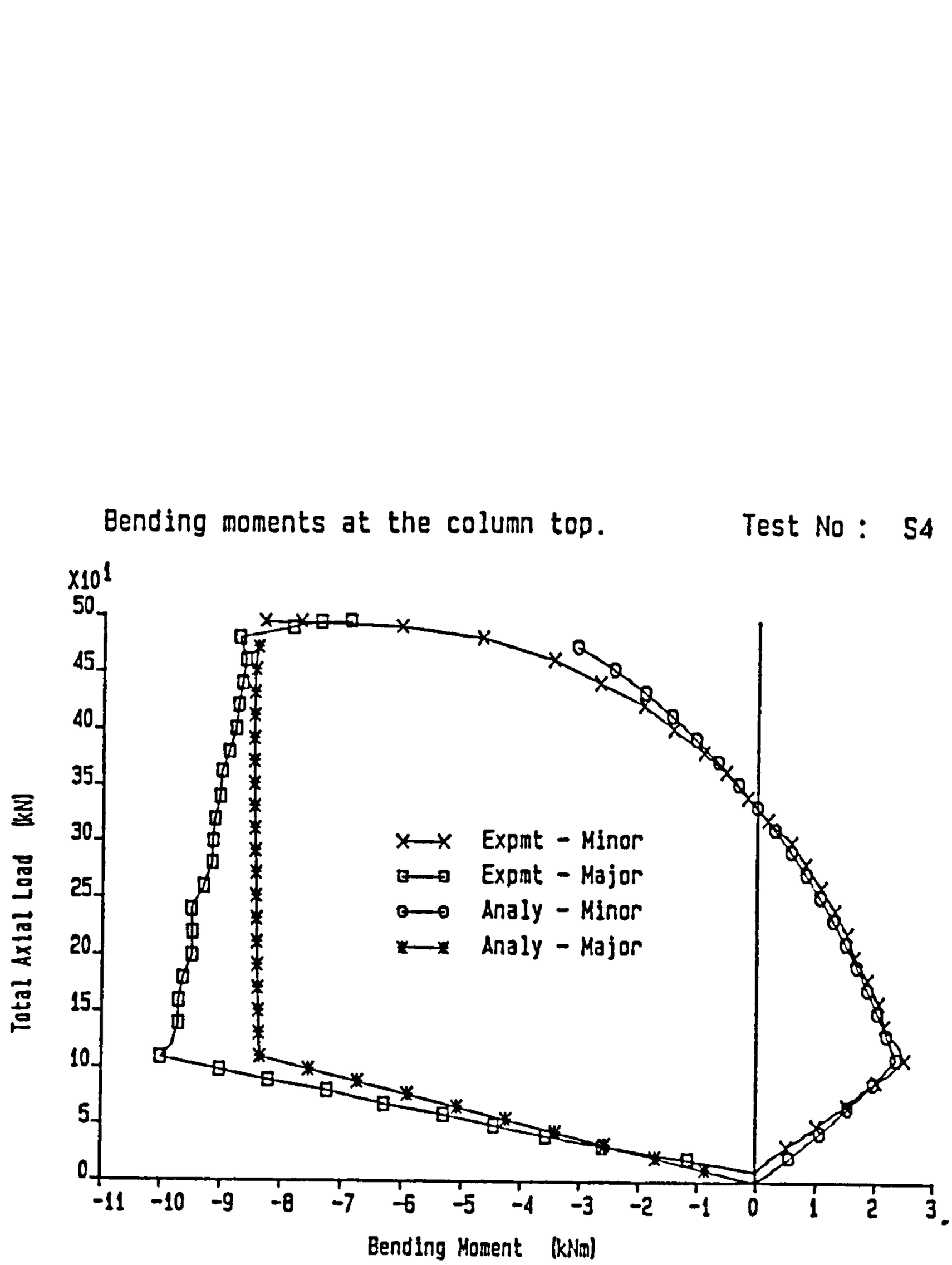

Figure 2.16 Moment shedding at top end of beam-column as observed in three-dimensional subassemblage of Figure 2.11 [2-36]

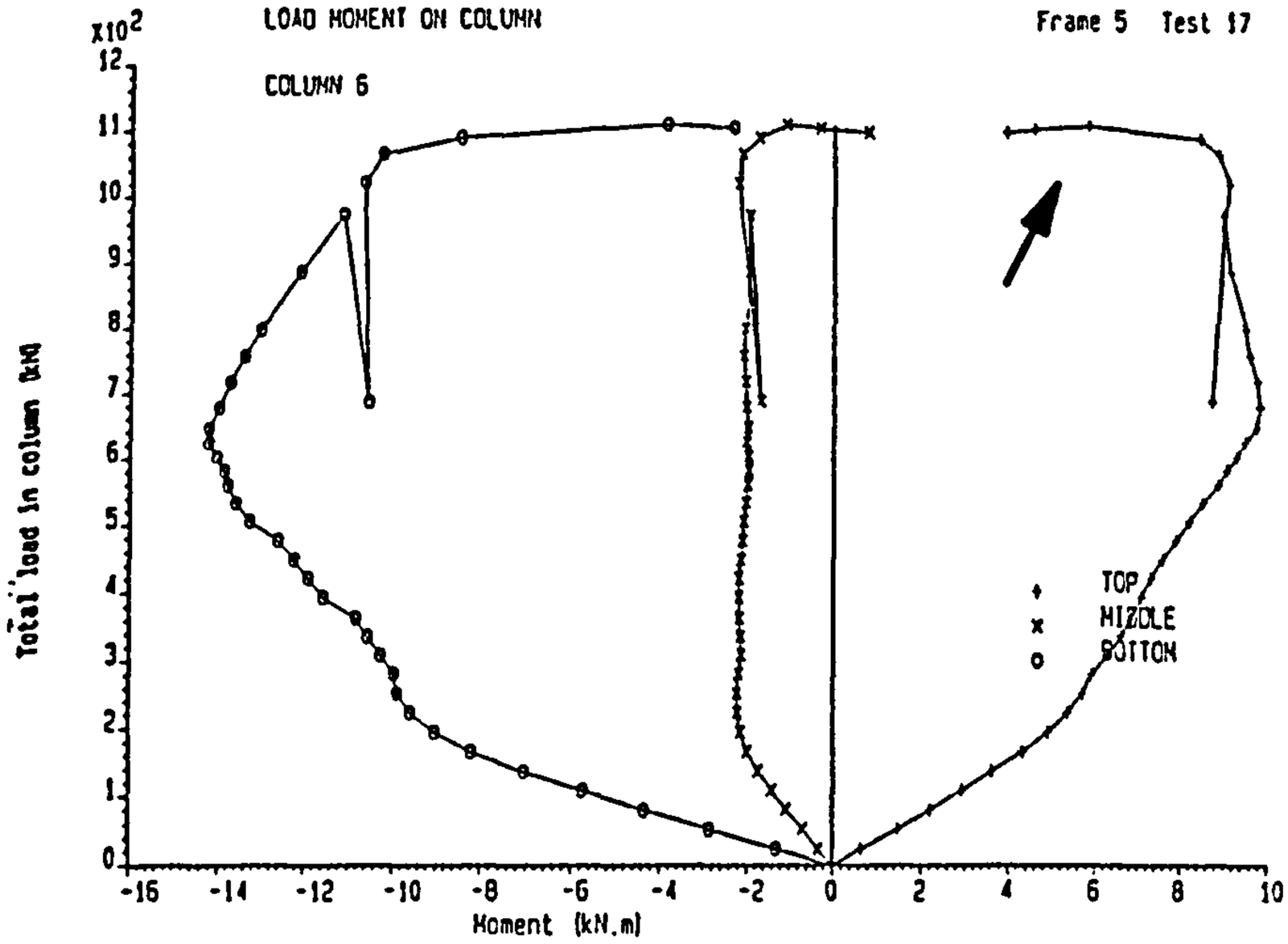

Figure 2.17 Moment shedding at top end of beam-column 6 as observed in full scale plane frame tests of Figure 2.12 [2-35]

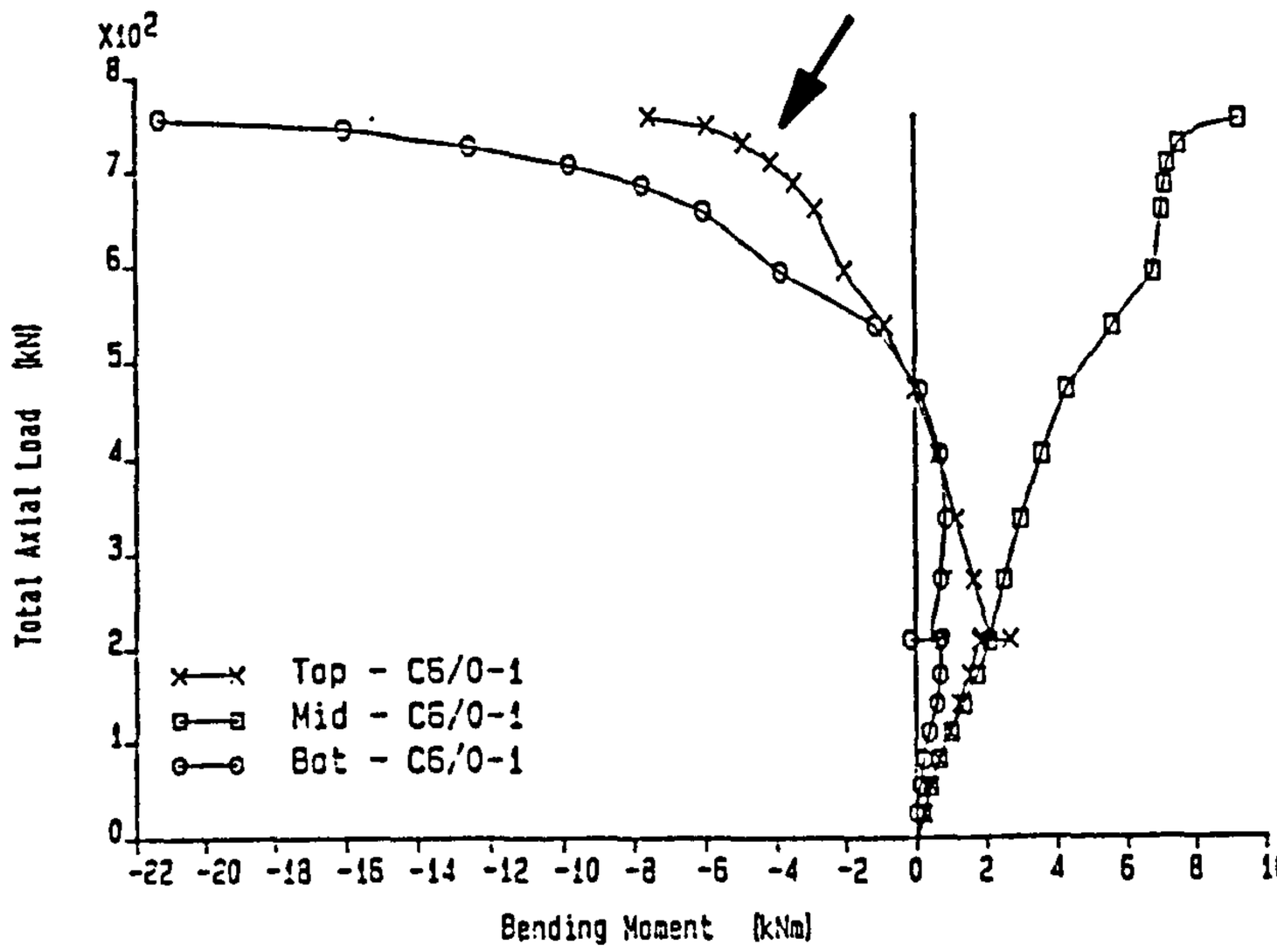

Figure 2.18 Moment shedding at top end of beam-column C6 as observed in full scale three dimensional frame tests of Figure 2.13 [2-36]

Chapter 3

Nonlinear Inelastic Analysis of Semi-rigid Plane Frames Using Finite Element Method : Formulation and the Computer Program

3.1 Introduction

The nonlinear finite element analysis of plane frame steel structures has become a useful research tool to study the response of real structures. Important aspects such as the effects of semi-rigid connections, geometrical and the material nonlinearities that are present in real frames can now be incorporated into the finite element programs. The inclusion of these characteristics can capture the actual response of real frames both in the elastic and inelastic ranges. Informative results obtained from this range of behaviour will be useful in predicting the strength of both individual members and complete frames at both service and ultimate load levels.

The program used in this study has incorporated all the characteristics mentioned above. The program has been continuously developed by researchers at the University of Sheffield since 1980 using the finite element method. It started with Jones [3-1] who developed the program for analysing a single column element with semi-rigid connections as shown in the model of Figure 3.1(a). The limitation of this program is that the column ends are connected by the semi-rigid end-restraint to rigid supports and hence any frame action due beam end rotations from beam bending is neglected.

Davison et al. [3-2] suggested that the analytical studies on the column performance should consider the column acting as part of a frame rather than as an isolated member. In view of this, the following development was made by Rifai [3-3] who modified the individual column model into a sub-frame subassemblage model which is shown in Figure 3.1(b). This model includes the effect of beam bending and considers the column as part of a frame. The results of a parametric study carried out using this subassemblage model show that the program can provide a good estimate of the force distribution but cannot provide accurate predictions at ultimate load condition [3-4].

In view of the above, further developments to modify the subassemblage model into a plane frame model as shown in Figure 3.1(c) were carried out by Ahmed [3-5] in order to overcome the limitations found in the previous programs. The plane frame program was modified further by Mohammad [3-6] to incorporate the actual behaviour of internal forces in the members, evaluation of section properties at Gauss points, refinement of strain formulation as well as the incorporation of loading and unloading behaviour of semi-rigid connections under slow cyclic loadings. This program is now known as SERIFA (Semi Rigid Finite Element Analysis).

Further developments on the SERIFA computer program have been made by the author. These modifications include the incorporation of higher order strain terms for large deflections, geometrical imperfections, a square hollow section model in the section properties and the modelling of the eccentricity moment at column ends. In addition, an improvement on the analysis of results involving the percentage of yield spreading across the sections as well as along the elements is included. Furthermore,

the true response of the structures when the section is fully yielded and has reached the plastic moment capacity has also been included. As a result, the program can predict the real response at ultimate load levels.

Although the program was formulated using semi-rigid connection characteristics, it can be employed for analysing semi-rigid, pinned and rigid plane frames. The following section will discuss the finite element formulation and the features of the program which then leads to the nonlinear analysis of semi-rigid steel frames.

3.2 Beam-column Element

The plane frame members are idealised as a finite number of elements. Each element is modelled as a 2-node element. These elements are beam-column elements as they are formulated for both beam and column members. Figure 3.2 shows the model of the beam-column element with its properties of modulus elasticity, E, cross sectional area, A, second moment of area, I, and length, L . The types of sections to be used for this beam-column elements are explained in section 3.7.1. Each element has six degrees of freedom of displacement namely $\{u_1, v_1, \theta_1, u_2, v_2, \theta_2\}^T$ which are located at node 1 and node 2 respectively. Each node has two translations and one rotation which means that the node can displace in three directions namely u, v and θ. The associated vector of forces with respect to the degree of freedom of the displacement is $\{F_1, V_1, M_1, F_2, V_2, M_2\}^T$.

The influence of semi-rigid connections can be incorporated in the structures. One of the common methods is by treating the connection as an independent spring element connecting the beam to column elements [3-7]. The second (preferred) method is by incorporating the connection characteristics into the formulation of the existing beam-column elements. The other method which is also of interest is by treating the connection as an independent short-rigid beam element [3-8].

The SERIFA program incorporates the connection characteristics by employing the second method. This reduces the degrees of freedoms in the structures and hence can

increase the efficiency of the numerical calculations. The idealisation of the semi-rigid connections as part of a beam-column element is shown in Figure 3.3. The connection characteristics are entered into the formulation in two ways. The first, is through the formulation of the shape functions of the beam-column elements and the second is through the formulation of the element stiffness. The following sections will discuss these formulations.

3.3 Shape Functions

As explained in section 3.2, the nodes of the elements can displace in either three directions. As the displacements between the nodes are always not similar, this will result in the deformations of the elements between the two nodes. This can be illustrated in Figures 3.4 and 3.5, where the elements can deform appreciably in different shapes due to the action of external forces.

Figure 3.5 shows a state of a deformed element due to nodal forces shown in Figure 3.2. Referring to Figure 3.5, the effect of semi-rigid connections in influencing the deformed shape of the elements can be explained. Considering node 1, if θ_1 is the beam rotation and $\overline{\theta}_1$ is the column rotation, then the difference between the two rotations is the connection rotation θ_{j1} with θ_{j1} being defined as $\theta_{j1} = \theta_1 - \overline{\theta_1}$. This implies that the rotation of the beam which governed the element deformed shape is influenced by the flexibility of the connections. Similarly, the same effect will be present in node 2. The relationship between the element deformation and the semi-rigid connections is needed and can be obtained by the use of shape functions.

Shape functions are equations that describe the possible deformed shapes of an element due to applied loads. The shape functions of a 2-node beam-column element employed in this finite element computer program consist of six functions which are associated with the six possible different deformed modes.

Figure 3.6 shows the shape functions and the corresponding deformed shapes of elements with both rigid and semi-rigid connections. The shape functions for a beam-column element with rigid connections at its nodes are defined as

$$\overline{N_1} = 1 - \frac{x}{L} \tag{3.1}$$

$$\overline{N_2} = \frac{x}{L} \tag{3.2}$$

$$\overline{N_3} = 1 - 3\left(\frac{x}{L}\right)^2 + 2\left(\frac{x}{L}\right)^3 \tag{3.3}$$

$$\overline{N_4} = L\left[\frac{x}{L} - 2\left(\frac{x}{L}\right)^2 + \left(\frac{x}{L}\right)^3\right] \tag{3.4}$$

$$\overline{N_5} = \left[3\left(\frac{x}{L}\right)^2 - 2\left(\frac{x}{L}\right)^3\right] \tag{3.5}$$

$$\overline{N_6} = \frac{x}{L}\left[-\left(\frac{x}{L}\right)^2 + \left(\frac{x}{L}\right)^3\right] \tag{3.6}$$

The shape functions for the rigid elements are then modified to incorporate the semi-rigid connections at its nodes and are denoted as follows [3-3], [3-9] :

$$N_1 = \overline{N}_1 \tag{3.7}$$

$$N_2 = \overline{N}_2 \tag{3.8}$$

$$N_3 = \overline{N}_3 - \theta_{31}\overline{N}_4 - \theta_{j32}\overline{N}_6 \tag{3.9}$$

$$N_4 = \left[\overline{N}_4\left(1 - \theta_{j41}\right) - \overline{N}_6\theta_{j42}\right] \tag{3.10}$$

$$N_5 = \left(\overline{N}_5 + \overline{N}_4\theta_{j51} + \overline{N}_6\theta_{j52}\right) \tag{3.11}$$

$$N_6 = \left[\overline{N}_6\left(1 - \theta_{j62}\right) - \overline{N}_4\theta_{j61}\right] \tag{3.12}$$

Referring to mode shape 3 of Figure 3.6, the slope deflection equations are written as [3-5]:

$$M_1 = \frac{2EI}{L}\left(-2\theta_{j31} - \theta_{j32} + \frac{3}{L}\right) = C_{j1}\theta_{j31} \tag{3.13}$$

$$M_2 = \frac{2EI}{L}\left(-\theta_{j31} - 2\theta_{j32} + \frac{3}{L}\right) = C_{j2}\theta_{j32} \tag{3.14}$$

where

C_{j1} , C_{j2} = connection stiffnesses at nodes 1 and 2 respectively

M_1 , M_2 = moments at nodes 1 and 2 respectively

$\frac{EI}{L}$ = flexural stiffness of the element

Solving Equations (3.13) and (3.14) for θ_{j1} and θ_{j2} result in the following:

$$\theta_{j31} = \frac{A_1 B_1}{H} \tag{3.15}$$

$$\theta_{j32} = \frac{A_1 B_2}{H} \tag{3.16}$$

Similar solutions are implemented for mode shapes 4, 5 and 6 which result in the following:

$$\theta_{j41} = \frac{A_2 B_3}{H} \tag{3.17}$$

$$\theta_{j42} = \frac{A_2 C_{j1}}{2H} \tag{3.18}$$

$$\theta_{j51} = \theta_{j31} \tag{3.19}$$

$$\theta_{j52} = \theta_{j32} \tag{3.20}$$

$$\theta_{j61} = \frac{A_2 C_{j2}}{2H} \tag{3.21}$$

$$\theta_{j62} = \frac{A_2 B_4}{H} \tag{3.22}$$

where

$$A_1 = \frac{6EI}{L^2} \qquad A_2 = \frac{4EI}{L^2}$$

$$B_1 = \frac{2EI}{L} + C_{j2} \qquad B_2 = \frac{2EI}{L} + C_{j1}$$

$$B_3 = \frac{3EI}{L} + C_{j2} \qquad B_4 = \frac{3EI}{L} + C_{j1}$$

$$H = \frac{L}{2} A_1 A_2 + A_2 (C_{j1} + C_{j2}) + C_{j1} C_{j2}$$

As can be observed from Equations (3.9) to (3.12) and Equations (3.15) to (3.22), the functions for N_3, N_4, N_5 and N_6 are dependent on the connection stiffness C_j. Referring to these four shape functions shown in Figure 3.6, if any end of the nodes is rigid then the corresponding value of C_j at that node is infinity. In this program the value of C_j for rigid node is taken as equal to 1.0E20 kNcm/rad. In the case that the nodes at any end of the element is semi-rigid than the corresponding value of C_j is equal to the stiffness of the semi-rigid connection given in the moment rotation M-ϕ data. If the connection is pinned C_j is taken as a very small value equal to 1.0E-20 kNcm/rad.

Comparison of mode shapes between the rigid and semi-rigid elements shows that the mode shapes of rigid elements have zero rotations θ_{ji} at the nodes whereas the semi-rigid elements have finite rotations at both left and right nodes. This indicates that the presence of these rotations that contribute to the difference between the rigid and semi-rigid shape functions.

3.4 Strain-displacement Relationship

The shape functions will later be utilised to obtain the relationship between strains and displacements in a finite element. The strain formulation has been modified to include the large displacement effects. The strain, ε, at any point along the element is usually obtained using the following relation:

$$\varepsilon = \varepsilon_1 + \varepsilon_2 + \varepsilon_3 \tag{3.23}$$

$$\varepsilon = \frac{\partial u}{\partial x} + \frac{1}{2}\left(\frac{\partial u}{\partial x}\right)^2 + \frac{1}{2}\left(\frac{\partial v}{\partial x}\right)^2 \tag{3.24}$$

where

$\varepsilon_1 = \frac{\partial u}{\partial x}$ is the linear strain due to axial displacement

$\varepsilon_2 = \frac{1}{2}\left(\frac{\partial u}{\partial x}\right)^2$ is the nonlinear strain due to axial displacement

$\varepsilon_3 = \frac{1}{2}\left(\frac{\partial v}{\partial x}\right)^2$ is the nonlinear strain due elongation of the element induced by deflection v

However Equation 3.24 neglects the strain due to curvature, ε_4. Hence, the total strain equation can be written as

$$\varepsilon = \varepsilon_1 + \varepsilon_2 + \varepsilon_3 + \varepsilon_4$$

$$\varepsilon = \frac{\partial u}{\partial x} + \frac{1}{2}\left(\frac{\partial u}{\partial x}\right)^2 + \frac{1}{2}\left(\frac{\partial v}{\partial x}\right)^2 - y\left(\frac{\partial^2 v}{\partial x^2}\right) \tag{3.25}$$

where $\varepsilon_4 = -y\left(\frac{\partial^2 v}{\partial x^2}\right)$ is the curvature strain

The strain components given in Equation (3.25) can be separated into two parts. First is the linear strain ε_O and secondly is the nonlinear strain ε_L. Hence,

$$\varepsilon = \varepsilon_O + \varepsilon_L \tag{3.26}$$

in which

$$\varepsilon_O = \left\{ \frac{\partial u}{\partial x},\ 0,\ \frac{\partial^2 v}{\partial x^2} \right\}^T \tag{3.27}$$

$$\varepsilon_L = \left\{ \frac{1}{2}\left(\frac{\partial u}{\partial x}\right)^2,\ \frac{1}{2}\left(\frac{\partial v}{\partial x}\right)^2,\ 0 \right\}^T \tag{3.28}$$

or

$$\varepsilon = \begin{Bmatrix} \frac{\partial u}{\partial x} \\ 0 \\ \frac{\partial^2 v}{\partial x^2} \end{Bmatrix} + \begin{Bmatrix} \frac{1}{2}\left(\frac{\partial u}{\partial x}\right)^2 \\ \frac{1}{2}\left(\frac{\partial v}{\partial x}\right)^2 \\ 0 \end{Bmatrix} \tag{3.29}$$

From Equation (3.29), differentiating ε with respect to $d\delta$ will result in a relationship between the incremental strain $d\varepsilon$ and the incremental nodal displacements $d\delta$ which may be written as

$$d\{\varepsilon\} = d\{\varepsilon_o\} + d\{\varepsilon_L\}$$

$$\{d\varepsilon\} = -\left[\begin{bmatrix} \frac{\partial N_1}{\partial x} & 0 & 0 & \frac{\partial N_2}{\partial x} & 0 & 0 \\ 0 & \frac{\partial^2 N_3}{\partial x^2} & \frac{\partial^2 N_4}{\partial x^2} & 0 & \frac{\partial^2 N_5}{\partial x^2} & \frac{\partial^2 N_6}{\partial x^2} \end{bmatrix}\right.$$

$$\left. + \left(\frac{\partial v}{\partial x}\right)\begin{bmatrix} \frac{\partial N_1}{\partial x} & \frac{\partial N_3}{\partial x} & \frac{\partial N_4}{\partial x} & \frac{\partial N_2}{\partial x} & \frac{\partial N_5}{\partial x} & \frac{\partial N_6}{\partial x} \\ 0 & 0 & 0 & 0 & 0 & 0 \end{bmatrix}\right] \{d\delta\} \tag{3.30}$$

Equation (3.30) which is described in terms of the derivatives of the shape functions may be written symbolically as

$$\{d\varepsilon\} = (\ [B_O] + [B_L]\ ) \cdot \{d\delta\} \tag{3.31}$$

where

$$[B_O] = \begin{bmatrix} \frac{\partial N_1}{\partial x} & 0 & 0 & \frac{\partial N_2}{\partial x} & 0 & 0 \\ 0 & \frac{\partial^2 N_3}{\partial x^2} & \frac{\partial^2 N_4}{\partial x^2} & 0 & \frac{\partial^2 N_5}{\partial x^2} & \frac{\partial^2 N_6}{\partial x^2} \end{bmatrix} \tag{3.32}$$

$$[B_L] = \left(\frac{\partial v}{\partial x}\right)\begin{bmatrix} \frac{\partial N_1}{\partial x} & \frac{\partial N_3}{\partial x} & \frac{\partial N_4}{\partial x} & \frac{\partial N_2}{\partial x} & \frac{\partial N_5}{\partial x} & \frac{\partial N_6}{\partial x} \\ 0 & 0 & 0 & 0 & 0 & 0 \end{bmatrix} \tag{3.33}$$

in which $[B_O]$ is the small strain-displacement matrix which is associated with the linear strains and $[B_L]$ is the large strain-displacement matrix which is associated with the nonlinear strains.

The overall strain-displacement matrix, $[B]$ which consist of both the linear and nonlinear terms can be expressed as

$$[B] = [B_O] + [B_L] \tag{3.34}$$

Hence, Equation (3.30) can be written symbolically as

$$\{d\varepsilon\} = [B] \cdot \{d\delta\} \tag{3.35}$$

3.5 Formulation of Element Stiffness Matrix

The tangential stiffness matrix for a beam-column element with semi-rigid connections has been derived by Rifai [3-3] following the procedure described by Zienkiewicz [3-10] and using the principle of virtual work. The stiffness matrix that was developed for an open section beam-column element is also applicable for a tubular column based on the assumption that local buckling is not considered in the analysis. This, however, does not limit the use of the program because in normal design procedures of hollow sections, the local buckling is controlled by checking the ratios of D/t and B/t for the webs and flanges where D is the depth, B is the width and t is the thickness of the section. By ensuring that the section classifies as plastic, local buckling in the flanges and webs can be avoided.

In order to derive the element tangential stiffness matrix, consider a beam-column element with semi-rigid connections at the ends. This element is subjected to imposed virtual displacement instead of external forces in order to induce element deformations. As the element is deformed and reaches equilibrium, it will yield an expression of the general form of virtual work principle which can be written as follows:

$$W_{\text{int}} - W_{ext} = 0 \tag{3.36}$$

where

W_{int} = total internal work done due to virtual displacement

W_{ext} = total external work done due to virtual displacement

If the applied virtual displacement is denoted as $d\delta$ then the external work done is the external loads $\{F\}$ multiplied by the displacements $\{d\delta\}$ and can be written as

$$W_{ext} = \{d\delta\}^T \{F\} \tag{3.37}$$

where

$\{F\}$ = vector of external forces due to the virtual displacement

Hence, the associated nodal displacements and nodal forces at each degree of freedom can be written as

$$W_{ext} = \begin{bmatrix} du_1 & dv_1 & d\theta 1 & du_2 & dv_2 & d\theta_2 \end{bmatrix} \begin{Bmatrix} F_1 \\ V_1 \\ M_1 \\ F_2 \\ V_2 \\ M_2 \end{Bmatrix} \tag{3.38}$$

The external work is absorbed by the element in two ways. The first is through the stress $\{\sigma\}$ multiplied by the strain $\{d\varepsilon\}$ which can be written as

$$W_{\text{int}1} = \int_0^L \{d\varepsilon\}^T \{\sigma\} dx \tag{3.39}$$

$$\{\varepsilon\} = [B]\{\delta\} \tag{3.40}$$

$$d\varepsilon = [B]\{d\delta\} \tag{3.41}$$

$$W_{\text{int}1} = \int_0^L \{d\delta\}^T [B]^T \{\sigma\} dx \tag{3.42}$$

The second is through the moment M_j multiplied by the rotation $d\theta$ at the two nodes which can be written as

$$W_{\text{int}2} = d\theta_{j1} M_{j1} + d\theta_{j2} M_{j2} \tag{3.43}$$

The detailed derivation of $W_{\text{int}2}$ by Rifai [3-3] which relates the joint rotations with the semi-rigid connections has resulted in the following equation,

$$W_{\text{int}2} = d\delta^T \left(N_{j1}{}^T C_{j1} N_{j1} + N_{j2}{}^T C_{j2} N_{j2} \right) \delta \tag{3.44}$$

where

$$N_{j1} = \left[0 \quad \frac{\partial N_3}{\partial X} \quad -1 + \frac{\partial N_4}{\partial X} \quad 0 \quad \frac{\partial N_5}{\partial X} \quad \frac{\partial N_6}{\partial X} \right] \tag{3.45}$$

$$N_{j2} = \left[0 \quad \frac{\partial N_3}{\partial X} \quad \frac{\partial N_4}{\partial X} \quad 0 \quad \frac{\partial N_5}{\partial X} \quad -1 + \frac{\partial N_6}{\partial X} \right] \tag{3.46}$$

C_{j1} = connection stiffness at node 1

C_{j2} = connection stiffness at node 2

It can be observed from Equation (3.44) that the effect of semi-rigid connections has been entered into the formulation.

The total internal work done can now be defined as the summation of Equations (3.42) and (3.44) and may be written as

$$\begin{aligned} W_{int} &= (W_{int\,1} + W_{int\,2}) \\ &= d\delta^T \left(\int B^T \sigma . dx + \left[{N_{j1}}^T C_{j1} N_{j1} + {N_{j2}}^T C_{j2} N_{j2} \right] d\delta \right) \end{aligned} \tag{3.47}$$

Equating Equations (3.37) and (3.47) results in the following,

$$\{d\delta\}^T \{F\} = d\delta^T \left(\int B^T \sigma . dx + \left[{N_{j1}}^T C_{j1} N_{j1} + {N_{j2}}^T C_{j2} N_{j2} \right] d\delta \right) \tag{3.48}$$

$$\{F\} = \left(\int B^T \sigma . dx + \left[{N_{j1}}^T C_{j1} N_{j1} + {N_{j2}}^T C_{j2} N_{j2} \right] \right) d\delta \tag{3.49}$$

Equation (3.49) can be written as

$$\psi = \left(\int B^T \sigma . dx + \left[{N_{j1}}^T C_{j1} N_{j1} + {N_{j2}}^T C_{j2} N_{j2} \right] d\delta \right) - F \tag{3.50}$$

Differentiation of ψ with respect to δ will result in the tangential stiffness,

$$K_T = \frac{d\psi}{d\delta} = \int_0^L B^T \frac{d\sigma}{d\delta} dx + \int_0^L \frac{dB^T}{d\delta} \sigma . dx + \left[{N_{j1}}^T C_{j1} N_{j1} + {N_{j2}}^T C_{j2} N_{j2} \right] \tag{3.51}$$

From Equation (3.51) it can be observed that the effect of connection stiffness C_{ji} has increased the value of tangential stiffness, K_T.

The relation between stress and strain can be expressed as

$$\sigma = D\,\varepsilon \tag{3.52}$$

where D = modulus of material

From Equations (3.35) and (3.52) the following relationship is then obtained,

$$\frac{d\sigma}{d\delta} = D\frac{d\varepsilon}{d\delta} = D \cdot B \tag{3.53}$$

Substituting Equation (3.53) into Equation (3.51) gives,

$$K_T = \int_0^L B^T D \cdot B \cdot dx + \int_0^L \frac{dB^T}{d\delta}\sigma . dx + \left[{N_{j1}}^T C_{j1} N_{j1} + {N_{j2}}^T C_{j2} N_{j2} \right] \tag{3.54}$$

Consequently Equation (3.54) can be written symbolically in matrix forms as

$$[K_T]^e = [K_E]^e + [K_G]^e + [K_L]^e \tag{3.55}$$

where (using Equation 3.34 for the expression of $B = B_O + B_L$)

$$[K_E]^e = \int_0^L {B_o}^T D \cdot B_o \cdot dx + \left[{N_{j1}}^T C_{j1} N_{j1} + {N_{j2}}^T C_{j2} N_{j2} \right] \tag{3.56}$$

$$[K_L]^e = \int_0^L \left[{B_o}^T D B_L + {B_L}^T D B_o + {B_L}^T D B_L \right] dx \tag{3.57}$$

$$[K_G]^e = \int_0^L \frac{dB^T}{d\delta}\sigma . dx \tag{3.58}$$

where $[K_E]$ is the small displacement stiffness matrix, $[K_L]$ is the large displacement stiffness matrix and $[K_G]$ is the geometric stiffness matrix. The superscript e indicates the stiffness of the element.

The tangential stiffness matrix $[K^T]$ is formulated based on the current state of displacements, semi-rigid connection stiffness and the section properties.

3.6 Internal Forces

The formulation of the internal forces has been incorporated in the SERIFA program by Mohammad [3-6] based on the formulation procedure in the INSTAF program [3-7]. Figure 3.7 shows the displacements u and v of an arbitrary point 'O' on the beam cross-section which can be defined in terms of the displacement at the neutral axis. This in turn results in the nonlinear strain-displacement relationship at any point on the cross section as described by El-Zanaty [3-7] in which Equation (3.25) can be written as

$$\varepsilon = u_o' + \frac{1}{2}(u_o') + \frac{1}{2}(v_o')^2 - yv_o'' \qquad (3.59)$$

where $u_o' = \frac{\partial u}{\partial x}$, $v_o' = \frac{\partial v}{\partial x}$ and $v_o'' = \frac{\partial^2 v}{\partial x^2}$

The differentiation of Equation (3.59) gives,

$$\delta\varepsilon = \delta u_o' + u_o' \delta u_o' + v_o' \delta v_o' - y\delta v_o'' \qquad (3.60)$$

Equations (3.37) and (3.39) give

$$\delta W = \int_V \{\sigma\}\{\delta\varepsilon\} dV - \{F\}\{d\delta\} \qquad (3.61)$$

Equations (3.60) and (3.61) give

$$\delta W = \int_L \sigma\left[\{1 + uo'\}\delta uo' + \{vo'\}\delta vo' - y\delta vo''\right] dA.dx - \{F\}\{d\delta\} \qquad (3.62)$$

The stress resultants are defined as

$$n = \int_A \sigma.dA \qquad = \text{internal axial force} \qquad (3.63)$$

$$m = \int_A \sigma . y . dA \ = \text{internal moment} \tag{3.64}$$

Differentiating Equation (3.62) with respect to $\partial\delta$ gives,

$$\{\psi(\delta)\} = \int_L \left(a_1 \frac{\partial u_o'}{\partial \delta} + a_2 \frac{\partial v_o'}{\partial \delta} + a_3 \frac{\partial v_o''}{\partial \delta} \right) dx - \{F\} \tag{3.65}$$

where $\{\psi\}$ is a vector of nodal unbalanced forces and the values of a_1, a_2 and a_3 are given in Equations (3.73), (3.74) and (3.75) respectively.

It can be seen that $\{\psi\}$ is dependent upon the displacement vector $\{\delta\}$ and its derivatives. The value of ψ with an increment of $\{\Delta\delta\}$ can be expressed in terms of Taylor series and may be written as

$$\psi(\delta_i + \Delta\delta i) = \psi(\delta i) + \left[\frac{\partial \psi}{\partial \delta} \right] \Delta\delta i + \cdots\cdots = 0 \tag{3.66}$$

The higher order terms are ignored and Equation (3.66) can be written as

$$\psi(\delta i) + \left[\frac{\partial \psi}{\partial \delta} \right] \Delta\delta i + \cdots\cdots = 0 \tag{3.67}$$

$$-\psi(\delta i) = \left[\frac{\partial \psi}{\partial \delta} \right] \Delta\delta_i \tag{3.68}$$

Knowing that $\frac{\partial \psi}{\partial \delta}$ is the tangential stiffness then Equation (3.68) can be written as

$$K_T . \Delta\delta = -\psi \tag{3.69}$$

Substituting Equation (3.65) into (3.69) gives,

$$K_T . \Delta\delta = \{F\} - \int_L \left(a_1 \frac{\partial u_o'}{\partial \delta} + a_2 \frac{\partial v_o'}{\partial \delta} + a_3 \frac{\partial v_o''}{\partial \delta} \right) dx \tag{3.70}$$

Hence Equation 3.70 can be written as

$$\{\Delta F\} = \{F\} - \int_L \left[a_1 \frac{\partial u_o'}{d\delta} + a_2 \frac{\partial v_o'}{d\delta} + a_3 \frac{\partial v_o''}{\partial \delta} \right] dx \qquad (3.71)$$

where

$\{\Delta F\}$ = vector of out-of-balance forces

$\{F\}$ = vector of external forces

From Equation (3.71) the internal forces is written as

$$\text{internal forces} = \int_L \left[a_1 \frac{\partial u_o'}{d\delta} + a_2 \frac{\partial v_o'}{d\delta} + a_3 \frac{\partial v_o''}{\partial \delta} \right] dx \qquad (3.72)$$

where

$$a_1 = \int_A \sigma_z . dA \quad = \text{n} \qquad (3.73)$$

$$a_2 = \int_A \sigma_z . dA . v_o' = n v_o' \qquad (3.74)$$

$$a_3 = -\int_A \sigma_z . y . dA = -m \qquad (3.75)$$

The values of n and m are defined in Equations (3.63) and (3.64) respectively. It can be seen that the internal forces given in Equation (3.72) are a function of displacements and stress resultants of n and m.

When the cross section is fully yielded, the stress resultant m is kept constant and Equation (3.75) may be written as [3-11]

$$a_3 = -\int \sigma_y . y . dA_p = -m_p \qquad (3.76)$$

A

where

σ_y = yield strength

A_p = yielded area

m_p = plastic moment

Finally, Equation (3.70) can be symbolically written in matrix forms as

$$[K_T].\{\Delta D\} = \{\Delta F\} \tag{3.77}$$

where $[K_T]$ and $\{\Delta F\}$ are evaluated from Equations (3.55) and (3.71) respectively.

In the case of solving for nodal displacements, Equation (3.77) can be expressed as

$$\{\Delta D\} = [K_T]^{-1}\{\Delta F\} \tag{3.78}$$

The tangential stiffness $[K_T]$ depends on the unknown displacements and their associated derivatives. Similarly the vector of internal forces $\{\Delta F\}$ depends on the stress resultants and the displacement derivatives. Thus, Equation (3.78) which contains the nonlinear terms $[K_T]$ and $\{\Delta F\}$ can only be solved by using iteration methods [3-12] in which the solution is achieved when $\{\Delta F\}$ is sufficiently small. In this relationship, $\{\Delta F\}$ is the vector of unbalanced forces which caused the inequilibrium in the deformed structures. If the values of $\{\Delta F\}$ are sufficiently small and within the tolerance limit then the structure is said to be in equilibrium.

3.7 Properties of the Cross-section

The tangential stiffness matrices of the elements $[K_T]$ are affected by the properties of the beam-column elements which in turn depend on the properties of the element cross sections. Thus, it is necessary to evaluate the section properties first prior to the evaluation of the element stiffness matrices.

The cross section properties are evaluated at four sampling points along the element. The points, which are also known as the Gauss points, are shown in Figure 3.8. The availability of the properties at the Gauss points will enable the evaluation of the overall properties of the beam-column element. In addition, the properties at the two element nodes are also evaluated in the computer program.

3.7.1 Discretisation of cross-section

The properties of the cross sections are evaluated by first discretising the cross sections into sub-elements. The types of cross sections of beam-column elements that can be employed in this program are UB and SHS sections as shown in Figures 3.9(a) and 3.9(b) respectively. As shown in these figures the cross sections are first divided into several plates. Three plates for UB sections and four plates for SHS sections. Each of the plates is further discretised into small sub-elements. The centroid of each sub-element will become a sampling point for evaluating the strain ε in the sub-element. Each sub-element will have area ΔA and lever arm y from the centroid.

There are two properties that need to be evaluated at each cross section namely the material and geometrical properties.

3.7.2 Material Properties (σ–ε relationship)

The strength characteristic of the material is described in terms of the relationship between stress σ and strain ε. Knowing the total strain ε at any sampling point in the sub-elements will enable the stress σ to be evaluated.

In the stress-strain relationship shown in Figure 3.10 the material modulus, E, in the elastic range is taken as between 200 and 210 kN/mm^2 and in the plastic range, $E = 0$. As can be seen from this figure, the relationship between stress and strain is no longer linear when the sub-element strain, ε, exceeds the yield strain, ε_y. When this occurs, the effect of material nonlinearity is incorporated in the analysis.

3.7.3 Geometrical Properties

A diagrammatic relationship between the strain and stress distributions in the sub-elements and the corresponding condition of the section is shown in Figure 3.11. When the sub-element strain, ε, exceeds the yield strain, ε_y, the stress becomes

constant and the sub-element becomes yielded (plastic). The discretised sub-elements allow the process of yielding to spread gradually over the cross sections. Thus, accurate prediction of the effective values of flexural stiffness, *EI,* and axial stiffness, *EA,* with respect to any change in the cross section properties due to a partially yielded section can be evaluated accordingly.

The cross sectional area of the sub-element is calculated as (see Figure 3.9)

$$\Delta A = \Delta x \times \Delta y \tag{3.79}$$

This is followed by calculating the lever arm, y from the centroid of the sub element to the centroidal axis of the section.

Subsequently, the important properties of *EA* and *EI* of the cross sections can be evaluated as follows:

$$EA = \int_A E \cdot dA \tag{3.80}$$

$$EI = \int_A E \cdot y^2 \cdot dA \tag{3.81}$$

In the case of inelastic section the properties of *EI* need to be re-evaluated as

$$\overline{EI} = EI - \bar{y}^2 \int_A dA \tag{3.82}$$

where

$$\bar{y} = \frac{\int_A y \cdot E_{eff} \cdot dA}{\int E_{eff} \cdot dA} \tag{3.83}$$

In this program, the above integration equations are performed numerically and can be re-written as

$$EA = \sum_{i=1}^{n} (E_{eff})_i \cdot \Delta A_i \tag{3.84}$$

$$EI = \sum_{i=1}^{n} (E_{eff})_i \cdot y_i^{\,2} \cdot \Delta A_i \tag{3.85}$$

In the case of an inelastic section the properties of *EI* need to be evaluated as

$$EI = \sum_{i=1}^{n} (E_{eff})_i \cdot y_i^{\,2} \cdot \Delta A_i - \bar{y}^{2} \cdot A_{eff} \tag{3.86}$$

where

$$\bar{y} = \frac{\sum y_i \cdot (E_{eff})_i \cdot \Delta A_i}{\sum (E_{eff})_i \cdot \Delta A_i} \tag{3.87}$$

A_{eff} = remaining elastic area of the cross section

ΔA = sub-element area as defined by Equation (3.79)

E_{eff} = effective modulus of elasticity which depends on the strain in the material

3.7.4 The Effect of Yielded Element to the Properties of the Sections

The yielding in the sub-elements will change their material properties and may affect the structure in the following ways:

1. The stress in the yielded sub-elements will be $\sigma = \sigma_y$. This implies that the yielded sub-elements will provide their maximum strength capacity. In the case that all the sub-elements in the cross section become yielded then the section is said to be in a fully plastic condition. This will result in the section to provide a maximum squash load carrying capacity or maximum moment capacity for pure axial or pure moment conditions.

2. The elastic modulus of the sub-elements will be *E=0*, and hence the corresponding values of the axial stiffness, *EA,* and flexural stiffness, *EI,* will become zero. This

implies that the yielded sub-elements have lost their contribution to the stiffness of the section. This, in turn, will reduce the stiffness of the structure.

3.8 Properties of the Beam-column Elements

Once the properties of the cross sections at the four Gauss points are known, a second numerical integration along the element can be implemented to obtain the overall properties of the beam-column elements. The corresponding properties are the element stiffnesses and the nodal internal forces which are obtained by performing numerical integration along the element.

The difference in the degree of yield between sub-elements reflects the contribution of the material nonlinearity to the global structure properties. Knowing the gradual penetration of yield spreading across the section at the four Gauss points will enable the gradual yield spreading along the element to be investigated.

3.9 Evaluation Of Stress Resultants

Stress resultants which include axial load and moment can be obtained by knowing the properties of the section. These stress resultants are expressed as

Axial force, $F = \int \sigma \cdot dA$ (3.88)

Moment, $M = \int \sigma \cdot y \cdot dA$ (3.89)

The integration of the above equations are performed numerically as follows:

Axial force , $F = \sum_{i=1}^{i=n} \sigma_i . \Delta A_i$ (3.90)

Moment , $$M = \sum_{i=1}^{i=n} \sigma_i . y_i . \Delta A_i \qquad (3.91)$$

where i = no. of sub-elements

n = total no. of sub-elements

3.10 Evaluation of Element Stiffness

The program evaluates the section properties followed by the evaluation of the local element stiffness matrices. The stiffness matrices are the elastic stiffness matrix $[K_E]$, geometric stiffness matrix $[K_G]$ and the stiffness matrix due to axial load $[K_L]$. These stiffness matrices are combined to obtain the element tangential stiffness matrix $[K_T]$ which is

$$[K_T]^e = [K_E]^e + [K_G]^e + [K_L]^e \qquad (3.92)$$

The element stiffness matrix $[K_T]^e$ is formulated based on the local co-ordinate system. Figure 3.12(a) shows the local and global co-ordinate axes of the elements in a structure. The local element tangential stiffness $[K_T]^e$ must be transformed into the global co-ordinates system to form the global element tangential stiffness matrix $[K_T]^g$. The transformation is implemented by using the matrix multiplication given below,

$$[K_T]^g = [T]^T [K_T]^e [T] \qquad (3.93)$$

The transformation matrix $[T]$ is given as

$$[T] = \begin{bmatrix} cos\varphi & sin\varphi & 0 & 0 & 0 & 0 \\ -sin\varphi & cos\varphi & 0 & 0 & 0 & 0 \\ 0 & 0 & 1 & 0 & 0 & 0 \\ 0 & 0 & 0 & cos\varphi & sin\varphi & 0 \\ 0 & 0 & 0 & -sin\varphi & cos\varphi & 0 \\ 0 & 0 & 0 & 0 & 0 & 1 \end{bmatrix} \qquad (3.94)$$

where φ is the angle of transformation from the local axis to the global axis which is shown in Figure 3.12(b).

Once the global element tangential stiffness matrix $[K_T]^g$ in the global axis has been determined for each element then the assembly of the individual beam-column stiffness matrices to obtain the structure stiffness matrix $[K_T]$ is performed. When the assembling of $[K_T]$ is completed , the solution of equilibrium equation $\{F\}=[K_T]\ \{D\}$ is sought.

3.11 Numerical Integration

The values of cross section properties of E , A and I are not constant along the element length. To compute the overall stiffness matrix of an element, a numerical integration of the properties along the element needs to be performed. In the finite element method this integration is performed numerically by using the Gauss Quadrature method which is explained in many finite element books such as reference [3-13]. The contribution of the section properties at the four Gauss points with the corresponding weight factors in one element will give an accurate prediction of the overall stiffness of that element.

3.12 Modelling the Semi-rigid Connections

Numerous forms of semi-rigid connection models which can be employed for analytical studies are discussed in detail by Jones et al. [3-14]. The B-Spline model occupies a large amount of computer storage. On the other hand the polynomial models can sometimes cause a negative stiffness which the program cannot accommodate [3-15].

In the study of non-sway frames carried out in the University of Sheffield [3-1],[3-16], it is observed that, when the individual column model is employed, a small variation

in M-ϕ curves can cause a significant different in the behaviour of the structure [3-1]. However as the portal or multi-storey plane frame model is adopted, it is seen that the variation of ±20% in the M-ϕ curves does not cause any significant effect to the column behaviour. This implies that the precise form of M-ϕ model is less important [3-16] if a frame is analysed.

In view of the above mentioned aspects, the multi-linear model is used in the current analysis of plane frame structures. Figure 3.13(a) shows the typical characteristics of the connections described in terms of moment, M, and connection rotation ϕ. The M-ϕ curve can be approximated by a series of linear curves as shown in Figure 3.13(b). This model is simpler to incorporate into the program than other methods such as the B-Spline, exponential, cubic and power models.

Input data for the trilinear model includes the connection rotations ϕ_1, ϕ_2 and ϕ_3 as well as the associated connection stifnesses k_1, k_2 and k_3 respectively.

The stiffness of the connection is evaluated from the data file based on the value of current connection rotation calculated in the program. It is then used in the evaluation of the beam-column element stiffness matrix and the shape functions in which the effects of semi-rigid are incorporated.

The loading and unloading of the connection are determined by checking the values of moments at every load steps in all connections. Any increase in moment indicates loading and any decrease in moment indicates unloading. Tests indicate that unloading occurs with a stiffness which is close to the initial elastic loading value.

3.12.1 Connection Offset

In the finite element model, the connection can be idealised as located at a concentrated point which may be taken as the intersection between beam-to-column centroid. If this model is adopted the associated forces from beams are transferred directly to columns and the problem of load eccentricity is not present. However, in

reality, the connection is made to the column flange and hence the connection can be modelled more accurately as located at an offset from the column centre-line. The presence of this connection offset between the column centre-line and the actual connection location can induce eccentricity moment which may cause significant effects to the column.

In view of this problem, a simplified model to include the effect of connection offset is shown in Figure 3.14. A nodal moment equal to the eccentricity moment $M = R \times e$ is applied at the intersection of beam and column centrelines, where R is the beam reaction and e is the eccentricity between column centre-line and column face. The inclusion of this moment will incorporate the offset effect.

3.13 Spread of Yield

A short computer program has been written in the section properties subroutine to evaluate the spread of yield over the cross section at every Gauss points. The spread of yield is calculated as the percentage of the yielded section as compared to the gross sectional area of the element. When the percentage of the yielded sections at every Gauss points is known, the approximate development of yield spreading along the element can also be quantified.

3.14 Inclusion of Geometrical Imperfection

The shear formulation in this program has been modified to include the effects of P-δ and P-Δ in a column (see Figure 3.15). This method has been adopted by Nair [3-17], Springfield and Adam [3-18] and Chen [3-19] in order to analyse the second order effects in multi-storey frames. Generally, the shear forces due to secondary effects can be obtained by the following equations [3-20] :

$$V = -\left(\frac{M_{ab} + M_{ba}}{L}\right) + \frac{P\delta}{L} \quad \text{or} \tag{3.95}$$

$$V = -\left(\frac{M_{ab} + M_{ba}}{L}\right) + \frac{P\Delta}{L} \tag{3.96}$$

where

M_{ab} , M_{ba} = internal moments in an element

P = member load

L = is the length of the element

The result of this modification is shown in Figure 3.16. The larger deflections and the nonlinear response resulted from the inclusion of P-δ and P-Δ effects are observed. It shows how these secondary effects can influence the response of lateral deflections, in which deflections are important for checking serviceability limit state of a structure.

As a result of modifying the shear formulation above, a further modification has been made to incorporate initial out-of-straightness in columns. Initial work on the program required the application of imaginary lateral loads to induce the initial column shape, which requires several trial and error analyses in order to obtain the required imperfection [3-1], [3-3], [3-5]. The purpose of applying the lateral forces is to increase lateral deflections as column bending increases due to axial loads acting through the initial out-of-straightness [3-1]. This method, however, can be replaced by the new method which only requires the co-ordinates of the initial column shape associated with the imperfection δ or Δ.

The co-ordinates of the deformed shape of the column can be defined by using a sine wave equation defined as

$$y = e_o \cdot \sin(\pi x) / L \tag{3.97}$$

where e_o is the initial central deflection, L is the column length and y is the initial deformed shape at a distance x along the column. The value of e_o for SHS tubular columns as investigated by Davison and Birkemoe [3-21] is approximately L/6000.

On the other hand, the mean value of e_o is reported as L/6384 [3-22], [3-23]. These values show that the initial out-of-straightness in tubular columns is very small.

The presence of the δ or Δ imperfections in a column, in combination with the axial load, has the effect of introducing additional moments, $P\delta$ and $P\Delta$ respectively. Consequently, additional shear forces $\frac{P\delta}{L}$ and $\frac{P\Delta}{L}$ will develop which will induce additional deflections. Eventually, this will give the same effects as imposing lateral forces as employed by Jones [3-1] , Rifai [3-3] and Ahmed [3-5].

Figures 3.17(a) to 3.17(c) show the possible types of geometrical imperfections that can be incorporated in the program. Figure 3.17(a) shows the local geometrical imperfection which normally occurs due to initial out-of-straightness of the column; whereas Figure 3.17(b) shows the global geometrical imperfections as a result of out-of-plumb within the erection tolerance limit. Further explanations on global imperfections can be found in section 5.2.4.3 of EC3 [3-24]. If both local and global imperfections exist then the type of imperfection is illustrated in Figure 3.17(c).

3.15 Treatment of Applied Forces

In finite element method, applied loads are treated as nodal loads (see Figure 3.18). This is in concurrence with the associated degree of freedoms shown in Figure 3.2. In this program, four types of applied loads are acceptable which are:

1. A vertical point load acting at a node (see Figure 3.18(a)).
2. A horizontal point load acting at a node (see Figure 3.18(b)).
3. A uniformly distributed load which is applied as a total uniform load acting along an element. In the program this load is simplified into a series of point loads acting at the nodes as shown in Figure 3.18(c).
4. A concentrated moment acting at the top end of column element. This moment is also used to model an eccentricity moment due to connection offset (see Figure 3.14(b)).

3.16 Nonlinear Analysis

The formulation of the program has been explained in the above sections. This section will demonstrate the basic procedure of executing the nonlinear analysis in a plane frame structure using the SERIFA program. The nonlinear analysis involves the procedure of solving the nonlinear equations given in Equation (3.78) at various load steps. The main response as a result of this analysis is the load-displacement characteristics. In addition, other important parameters such as the magnitude of collapse loads, the distribution of internal forces, the development of yield spreading and the evaluation of stiffness loss in the structure can also be quantified.

In general, the investigation on the behaviour of structures based on the nonlinear analyses requires that the loadings in the analyses must be applied starting from zero loads and continued up to the collapse loads. Such history of loadings will include the application of incremental applied loads. Consequently, at every load step, the problem of equilibrium is to be solved prior to the next load increment using the Newton Raphson iteration method.

Once a position of equilibrium is achieved, the next load increments can be applied to check for the next load level that can be sustained by the structure. The similar Newton-Raphson iteration processes are performed to obtain the corresponding equilibrium points. The repeated process of the load increments and the solution for equilibrium points will result in the complete load-displacement curve as illustrated in Figure 3.19(a). In this figure only four load steps are shown for simplicity and clarity of the diagram. In reality more load steps are required to give the true nonlinear load-deflection response. This procedure is also known as the incremental-iterative Newton-Raphson due to the incremental loads and the iterative iterations at every load step.

Figure 3.19(b) shows an example of the real frame response which can be associated with the Newton-Raphson iteration method presented in Figure 3.19(a). The figure illustrates a series of diagrammatic equilibrium deformed shapes of the plane frame due to a constant lateral load and incremental column loads up to collapse.

In the procedure of this program, the nonlinear analysis is completed when the applied load has reached the maximum load carrying capacity of the structure for which the equilibrium condition must be satisfied. The maximum load carrying capacity is known as the collapse load. Any further load increment beyond the collapse load will cause the collapse of the structure in which the structure is no longer in equilibrium. Finer load increments in the higher load level will give a more accurate prediction of the collapse loads.

3.16.1 Process of Newton-Raphson Iteration

This section will explain the process of iteration using the incremental-iterative Newton Raphson method. This iteration technique is adopted to solve the nonlinear equation $\{D\}=[K_T]^{-1}\{F\}$ to obtain the global displacements $\{D\}$ in the equilibrium deformed configuration. The term $[K_T]$ used in this explanation represents the stiffness matrix of the whole structure in the global co-ordinate system. The solution to this equation is achieved when the unbalanced forces in the vector $\{\Delta F\}$ have converged to significantly small values. Subsequently, at all nodes, the nodal external forces are almost equal to the nodal internal forces. When the solution is achieved, the structure is said to be in equilibrium in its deformed configuration.

Figure 3.20 shows the first stage of the load step with the associated iterations corresponding to the complete load-deflection curve shown in Figure 3.19(a). The detailed process of the iterations to obtain convergence in the first load step is described as follows:

1. At zero applied forces evaluate the initial section properties E , A and I of the elements.

2. Evaluate the initial tangential stiffness matrix of the structure, $K_{T\,1}$ based on the section properties calculated in step 1.

3. Apply the vector of the external forces, $\{F\}_1$

4. Based on $[K_T]_1$ and $\{F\}_1$ calculate the values of the incremental displacements at all available nodes in the structure using Equation (3.78), that is $\{\Delta D\}_1 = [K_T]_1^{-1}\{\Delta F\}_1$.

5. Calculate the incremental strains using Equation (3.30) based on the incremental displacements, $\{\Delta D\}_1$. The incremental strains are added to the previous total strains to give the current total strain. Similarly, incremental displacements $\{\Delta D\}_1$ are added to the previous total displacement to give the current total displacements, $\{D\}_1$.

6. Based on these total strains, evaluate the corresponding stresses (see section 3.7.2). Subsequently, update the section properties E, A and I of the elements. Any yielded sub-element will change the section properties.

7. Evaluate the internal forces $\{F_{int1}\}_1$ based on the updated section properties as calculated in step 6.

8. Update the structure stiffness matrix $[K_T]_2$ based on the current section properties. This updated stiffness will be used in the following iteration.

9. Knowing the external forces $\{F_1\}$ and the internal forces $\{F_{int}\}_1$, the unbalanced forces $\{\Delta F\}_2$ can be determined as $\{\Delta F\}_2 = \{F\}_1 - \{F_{int}\}_1$.

10. Check convergence criteria at point P.

11. In this example, the convergence is still not satisfied at point P. The structure is still not in equilibrium due to the existence of vector of unbalanced forces $\{\Delta F\}_2$. Thus, based on the updated properties, namely $[K_T]_2$ and $\{\Delta F\}_2$, a second iteration is performed to calculate the next incremental displacements $\{\Delta D\}_2$ due to the vector of unbalanced forces $\{\Delta F_2\}$, that is by solving $\{\Delta D_2\} = [K_{T2}]^{-1}\{\Delta F_2\}$.

12. Check the convergence criterion at point Q to determine whether the remaining out-of-balanced forces and the incremental displacements have reduced to sufficiently small values less than the specified tolerances. If this is not satisfied

repeat steps 5 to 11 for the subsequent iterations. The process of iterations continues until the unbalanced forces dissipate and have little effects on the deformation of the structure.

13. The convergence and the associated equilibrium state are achieved at point S. At this point, all the internal forces at the nodes are considered to be in equilibrium with the external forces. The corresponding results of the analysis such as the axial forces, shear forces, moments, deflections, rotations and the properties of *EI* and *EA* of the elements can be printed in the output files.

14. The iteration process in any load step terminates when acceptable convergence is achieved. The stiffness of the connection is updated at the start of each load increment. Further load increments can be applied and a similar process of iterations as described above is repeated to obtain another convergence. The load can be increased until the structure becomes unstable.

3.16.2 Convergence Criteria

In reality, it is impossible to obtain zero values of vector of unbalanced forces at all nodes in the structure. Hence, a criterion to minimise the vector of the unbalanced forces to a required accuracy can be obtained by specifying the convergence criterion.

The two convergence factors to be evaluated in order to achieve equilibrium in the structures are as follows:

(1). The load convergence factor is given as

$$\sqrt{\frac{\sum_{i=1}^{n}\{\Delta Fi\}^2}{\sum_{i=1}^{n}\{Fi\}^2}} \times 100 \leq Tolerance \qquad (3.98)$$

(2). The displacement convergence factor is given as

$$\sqrt{\frac{\sum_{i=1}^{n}\{\Delta Di\}^2}{\sum_{i=1}^{n}\{Di\}^2}} \times 100 \leq Tolerance \qquad (3.99)$$

where

$\{\Delta Fi\}$ = vector of unbalanced forces

$\{Fi\}$ = vector of total applied forces

$\{\Delta Di\}$ = vector of incremental nodal displacements

$\{Di\}$ = vector of total nodal displacements

The convergence is said to be accomplished when both the convergence factors are equal to or smaller than the specified tolerances. In the case of this study, the tolerance of 0.001 was specified in the program for both the load and the displacement convergence factors. The specified tolerance ensures the convergence of the equilibrium Equation (3.77). Consequently an accurate point of equilibrium is obtained in which internal forces and external forces are in a balanced condition and hence resulting accurate prediction of load-deflection response. A smaller tolerance may be employed and will give more accurate analysis results. However this will require more iterations for each load step which eventually requires a longer computing time. If larger tolerances are used fewer iterations are involved but less accurate results are obtained. Therefore the appropriate tolerances suggested by other researchers should be considered [3-25].

3.16.3 Failure Criteria

Instability occurs when the vector of displacements $\{D\}$ in Equation $\{D\}=[K_T]^{-1}\{F\}$ becomes very large. This occurs when the tangential stiffness $[K_T]$ is infinitely small which in turn results in a infinitely large inverse stiffness matrix $[K_T]^{-1}$. The corresponding determinant stiffness matrix $[K_T]$ becomes zero or negative indefinite. A zero determinant indicates the exact collapse load whilst a negative determinant indicates that the collapse load of the structure has been exceeded. At this stage the Newton-Raphson iteration process fails to converge which implies that the internal

forces can no longer be in equilibrium with the external forces. Structurally, the structure has lost its stiffness and consequently has lost its equilibrium and can no longer sustain additional loads. It is then not possible to increase the load increments and the program is terminated.

The terms of collapse load and collapse of structures used in this study are in accordance with Moy [3-26]. According to Moy, the greatest load at which equilibrium can be maintained is the collapse load. In other words, the collapse load is defined as the maximum load the structure can sustain just before the structure collapses. At the collapse load level the structure is in a state of deformed equilibrium. Analysis results such internal forces, moments and displacements are available.

3.16.4 Layout of the Program

The SERIFA plane frame program is written in Salford Fortran 77. The program runs on a minimum 486 IBM compatible portable computer system. The program can be used to analyse a portal or a multi-storey frame with either pin, rigid or semi-rigid connections. Any combination of different connection types can be included in the frame models.

The general procedure of the program in performing the nonlinear analysis is discussed as follows:

1. *Reading data files*. There are three data files employed by this program. First, the program will read DATA1 to obtain information on nodal co-ordinates of the frame geometry, boundary conditions, connection and element connectivity, initial imperfections, level of accuracy in the analysis, values of loadings and the types of load increments. Secondly, the program will read DATA2 to obtain the stress-strain characteristics, initial properties of the cross section such as the area A and the second moment of area I. Two types of second moment of area namely I_{xx} and I_{yy} can be chosen to incorporate bending about either major or minor axis respectively. Finally, in DATA3, the program will read the information of connection types and the M-ϕ characteristics.

2. *Applying external loads*. All types of applied loads are converted into forces acting at the nodes only.

3. *Evaluating the element stiffness matrix*. The program will evaluate the initial stiffness matrix of each element. The element stiffness matrices are transformed into global element stiffness matrices followed by the assembling process to obtain the global structure stiffness matrix.

4. *Specifying the boundary conditions*. The restrained degree of freedom is initialised as having zero displacements.

5. *Checking the stability*. The stability is checked at every iteration and at every load increments by evaluating the determinant of the global structure stiffness matrix. A zero or negative determinant indicates that the structure is unstable.

6. *Solving the nonlinear equation*. The nonlinear equilibrium equation is solved to obtain the unknown displacements. Iterations are required to obtain the convergence and hence the solution of the analysis.

7. *Printing the results*. At every equilibrium point corresponding to each load increment, the analysis results are printed out in the files. There are four types of output files to print various forms of analysis results, that is:

(i). *The main analysis result*. The program will print the nodal shear forces, moments and axial loads acting at the two nodes in each element. In addition, results of nodal displacements of u,v and θ are also included. From these results, the bending moment diagram and the deformed shape of the structures can be plotted. The program also prints the variation in the values of EA and EI in order to trace the level of loss of stiffness in the element.

(ii). *The summary results*. The program will only print deflections and internal forces at any required node at each load increment. This output file is useful for plotting various responses such as load-deflection using a spreadsheet program.

(iii). *The connection response results.* This file will provide the information on the response of the connections which includes the level of connection rotations, stiffnesses, the loading and unloading history and the moment applied to the connections.

(iv). *Spread of yield results.* This is an optional file which can trace the development of yield spreading across the cross-sections as well as along the elements. This output file, if activated in the analysis, will cause the computing process to become very slow and furthermore occupies a large amount of file storage.

3.17 Conclusions

A formulation of the nonlinear analysis program based on the finite element method has been presented in this chapter. The formulations in the program include the incorporation of semi-rigid connections, P-delta effects, initial geometrical imperfection and the effects of geometrical and material nonlinearities.

In the formulation, the cross-section of the beam-column element is discretised into small areas of sub-elements. The discretised cross section at specified Gauss points allow the yield to spread gradually across the cross-section as well as along the element. Eventually, the effective values of *EA* and *EI* which influence the stiffness of structures are evaluated accurately. The effect of semi-rigid connections is incorporated in the analysis by including the semi-rigid characteristics in the formulations of shape functions and the element stiffness matrices.

An iterative-incremental Newton Raphson method is employed to obtain the solution of the nonlinear equilibrium equation. The program can trace the load-deflection curves of a structure beyond the elastic range up to collapse. This enables the behaviour of structures at ultimate limit states to be studied. The ability of the program to simulate the actual behaviour of the frame will be presented in Chapter 4.

3.18 References

[3-1] Jones, S.W., 'Semi-rigid connections and their influence on steel column behaviour', Ph.D. Thesis, Department of Civil and Structural Engineering, University of Sheffield, U.K., June, 1980.

[3-2] Davison, J.B., 'Strength of beam-columns in frames with semi-rigid connections', Ph.D. Thesis, Department of Civil & Structural Engineering, University of Sheffield, U.K., June, 1987.

[3-3] Rifai, A.M., 'Behaviour of columns in sub-frames with semi-rigid joints', Ph.D. Thesis, Department of Civil and Structural Engineering, University of Sheffield, U.K., June, 1987.

[3-4] Nethercot, D.A., 'Frame analysis and the link between connection behaviour and frame performance', in Frame and Slab Structures, edited by Armer, G.S.T. and Moore, D.B., Butterworth, London, 1989, pp. 57-71.

[3-5] Ahmed, I., 'Semi-rigid action in steel frames', Ph.D. Thesis, Department of Civil and Structural Engineering, University of Sheffield, U.K., June, 1992.

[3-6] Mohammad, S., Ph.D. Thesis, to be submitted, Department of Civil and Structural Engineering, University of Sheffield.

[3-7] El-Zanaty M.H., Murray D.W. and Bjorhovde R., 'Inelastic behaviour of multistory frames', Ph.D. Thesis, Department of Civil Engineering, University of Alberta, USA, April, 1980.

[3-8] Poggi, C. and Zandonini, R., 'Behaviour and strength of steel frames with semi-rigid connections', in Connection Flexibility and Steel Frames, ed. Chen W.F., American Society of Civil Engineers, New York, October, 1985, pp. 57-76.

[3-9] Nethercot, D.A., Kirby, P.A. and Rifai, A.M., 'Columns in partially restrained construction: analytical studies', Canadian Journal of Civil Engineering, Vol. 14, 1987, pp. 485-497.

[3-10] Zienkiewicz, O.C. and Taylor, R.L., 'The finite element method', Volume 2, 4th. edition, McGraw Hill, London, 1991.

[3-11] Foley C.M. and Vinnakota, F., 'Inelastic behaviour of multi-story partially restrained steel frames - Part 1', Journal of Structural Engineering, still in press, 1998.

[3-12] Chajes, A. and Churchill, J.E., 'Nonlinear frame analysis by finite element methods', Journal of Structural Engineering, Vol. 113, No. 6, June, 1987, pp. 1221-1235.

[3-13] Cook, R.D., Malkus, D.S. and Plesha M.E., 'Concepts and applications of finite element analysis', 3rd. edition, John Wiley & Sons, New York, 1989.

[3-14] Jones, S.W., Kirby, P.A. and Nethercot, D.A., 'The analysis of frames with semi-rigid connections : A state-of-the-art report', Department of Civil & Structural Engineering, University of Sheffield, U.K., 1982.

[3-15] Nadjai, A., 'The behaviour of steel frames with semi-rigid joints containing unreinforced infill panels', Ph.D. Thesis, Department of Civil and Structural Engineering, U.K., April, 1993.

[3-16] Lau S.M., 'The response of non-sway steel framed structures with semi-rigid connections', Ph.D. Thesis, Department of Civil & Structural Engineering, University of Sheffield, U.K., December, 1993.

[3-17] Nair, R.S., 'Overall elastic stability of multistory buildings', Journal of the Structural Division, Proceedings of the American Society of Civil Engineers, Vol. 101, No. ST9, September, 1975, pp. 2487-2503.

[3-18] Springfield, J. and Adams, P.F., 'Aspects of column design in tall steel buildings', Journal of the Structural Division, Proceedings of the American Society of Civil Engineers, Vol. 98, No. ST 5, May, 1972, pp. 1069-1083.

[3-19] Chen, W.F., 'Stability design of steel frames', CRC Press, Boca Raton, Florida, 1991.

[3-20] Kirby, P.A. and Nethercot, D.A, 'Design for structural stability', Crosby Lockwood Staples, London, 1979.

[3-21] Davison, T.A. and Birkemoe, P.C., 'Column behaviour of cold-formed hollow structural steel shapes', Canadian Journal of Civil Engineering, 10, 1983, pp. 125-141.

[3-22] Bjorhovde, R. and Birkemoe, P.C., 'Limit states design of HSS columns', Canadian Journal of Civil Engineering, 6, 1979, pp. 276-291.

[3-23] Kato, B. 'Cold-formed welded steel tubular members', in Axial Compressed Structures : Stability and Strength, ed. R. Narayanan, Applied Science Publisher, London, 1982, pp. 149-180.

[3-24] Eurocode 3, 'Design of steel structures - Part 1.1: General rules and rules for buildings', ENV 1993-1-1.

[3-25] Owen, D.R.J. and Hinton, E., 'Finite element in plasticity: Theory and practice', Pineridge Press, Swansea, U.K., 1980.

[3-26] Moy, S.S.J., 'Plastic methods for steel and concrete structures', Macmillan, 2nd. edition, 1996.

[3-27] Structures Laboratory Instructions, 'Plastic collapse of a portal framework', Department of Civil and Structural Engineering, University of Sheffield.

[3-28] Torkamani M.A.M., Sonmez, M. and Cao J., 'Second-order elastic plane-frame analysis using finite-element method', Journal of Structural Engineering, Vol. 123, No. 9, September, 1997, pp. 1225-1235.

(a). Jone's individual column model

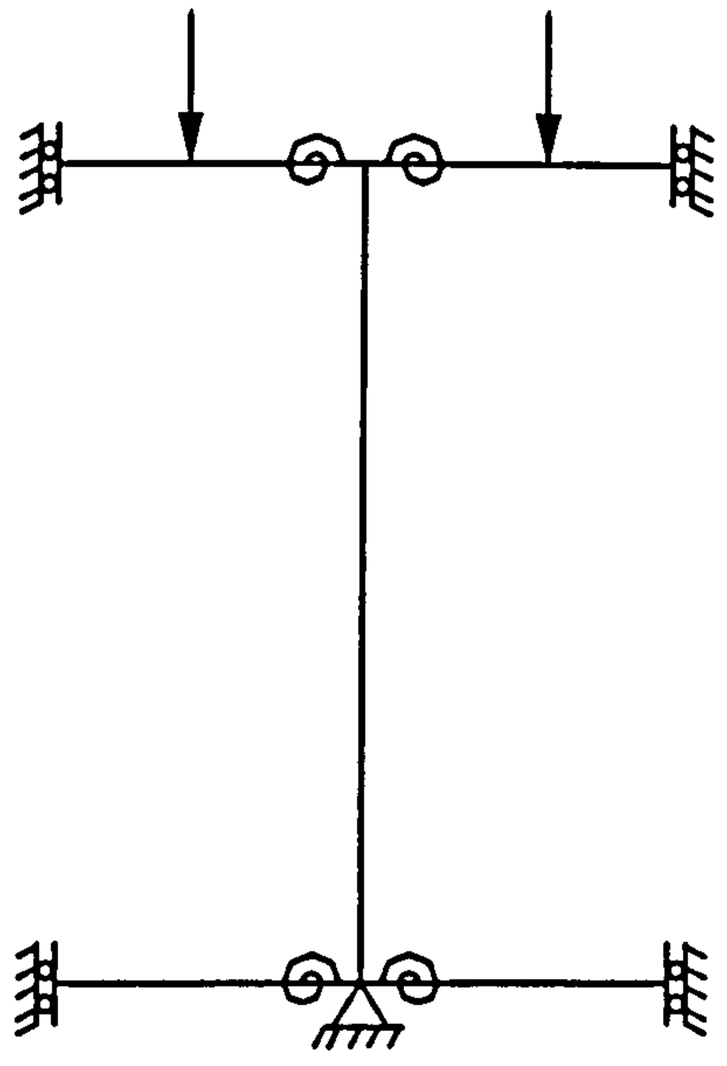

(b). Rifai's sub-assemblage frame model

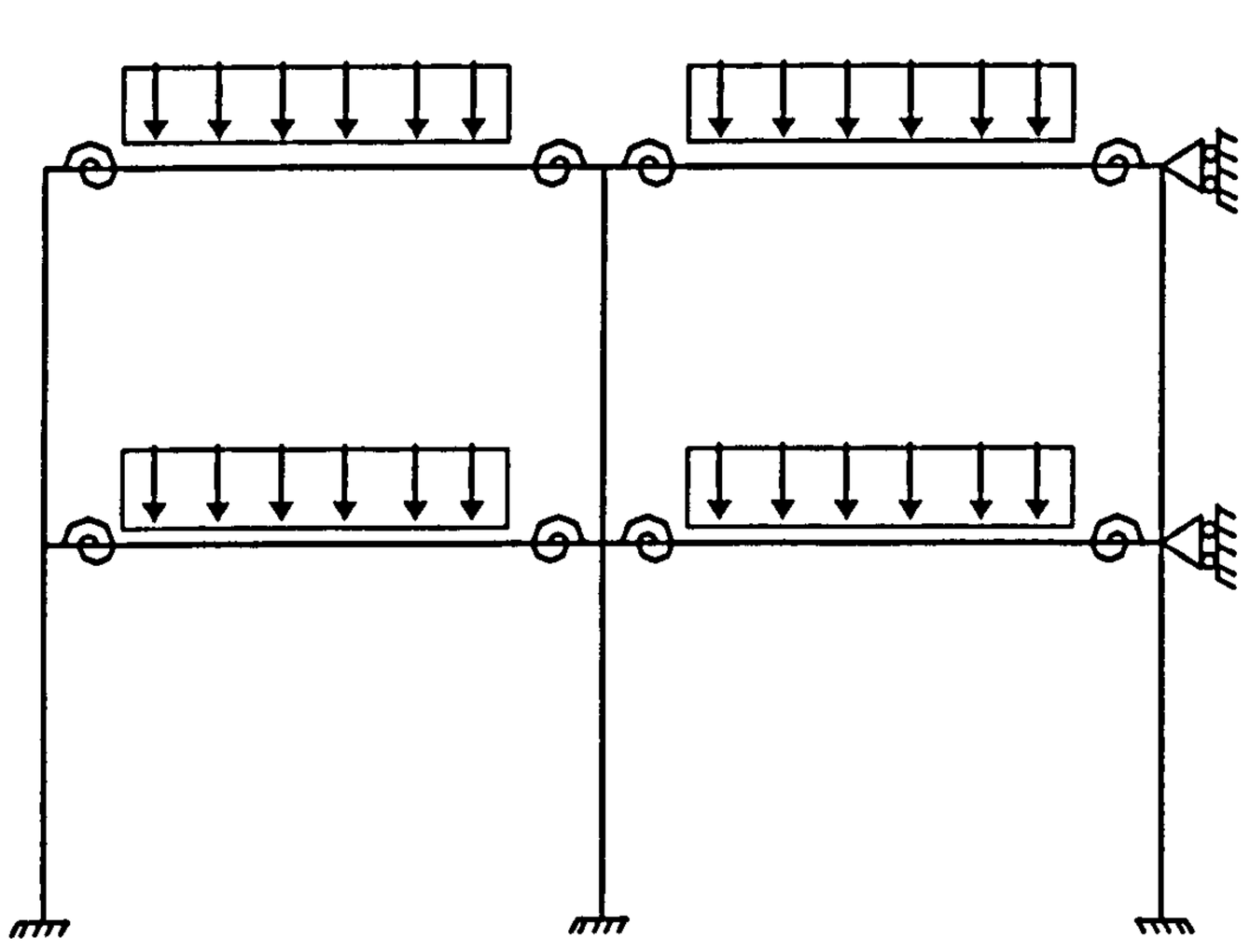

(c). Plane frame model for the current SERIFA program

Figure 3.1 The development of finite element models used in the SERIFA program

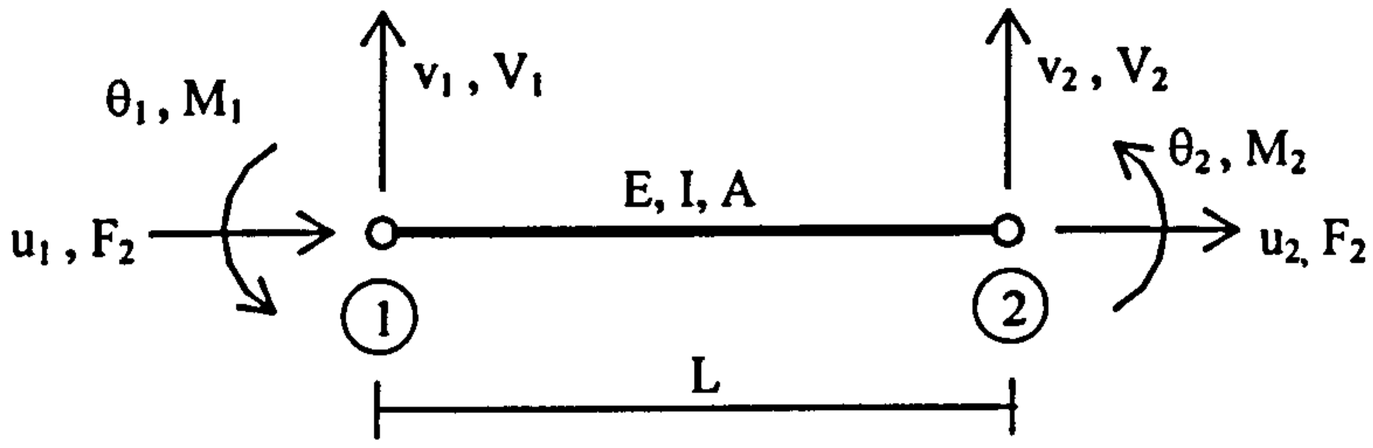

Figure 3.2 Local beam-column element with six degree of freedoms

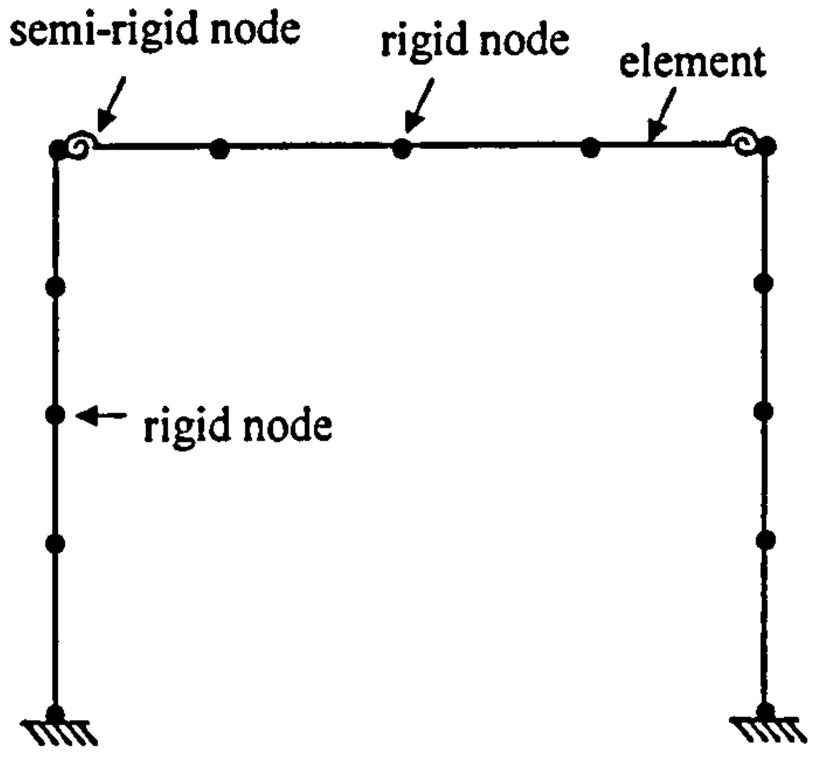

Figure 3.3 Idealisation of plane frame

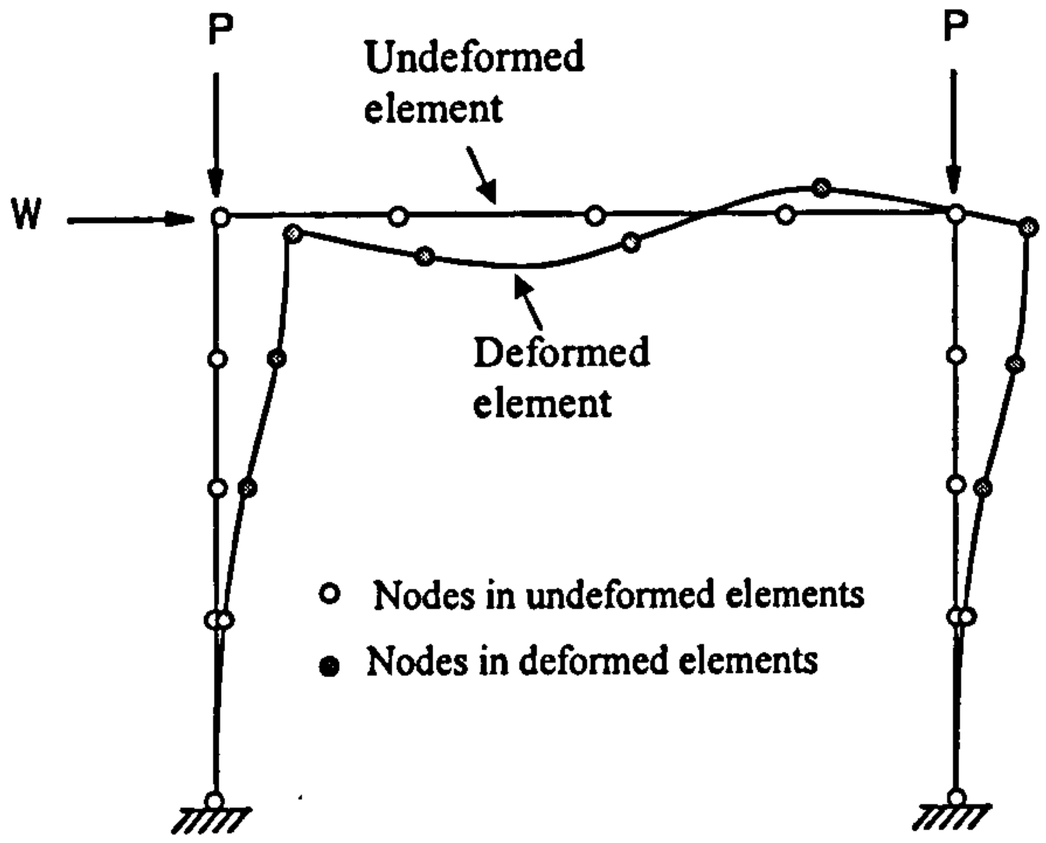

Figure 3.4 Plane frame deformation due to applied loads

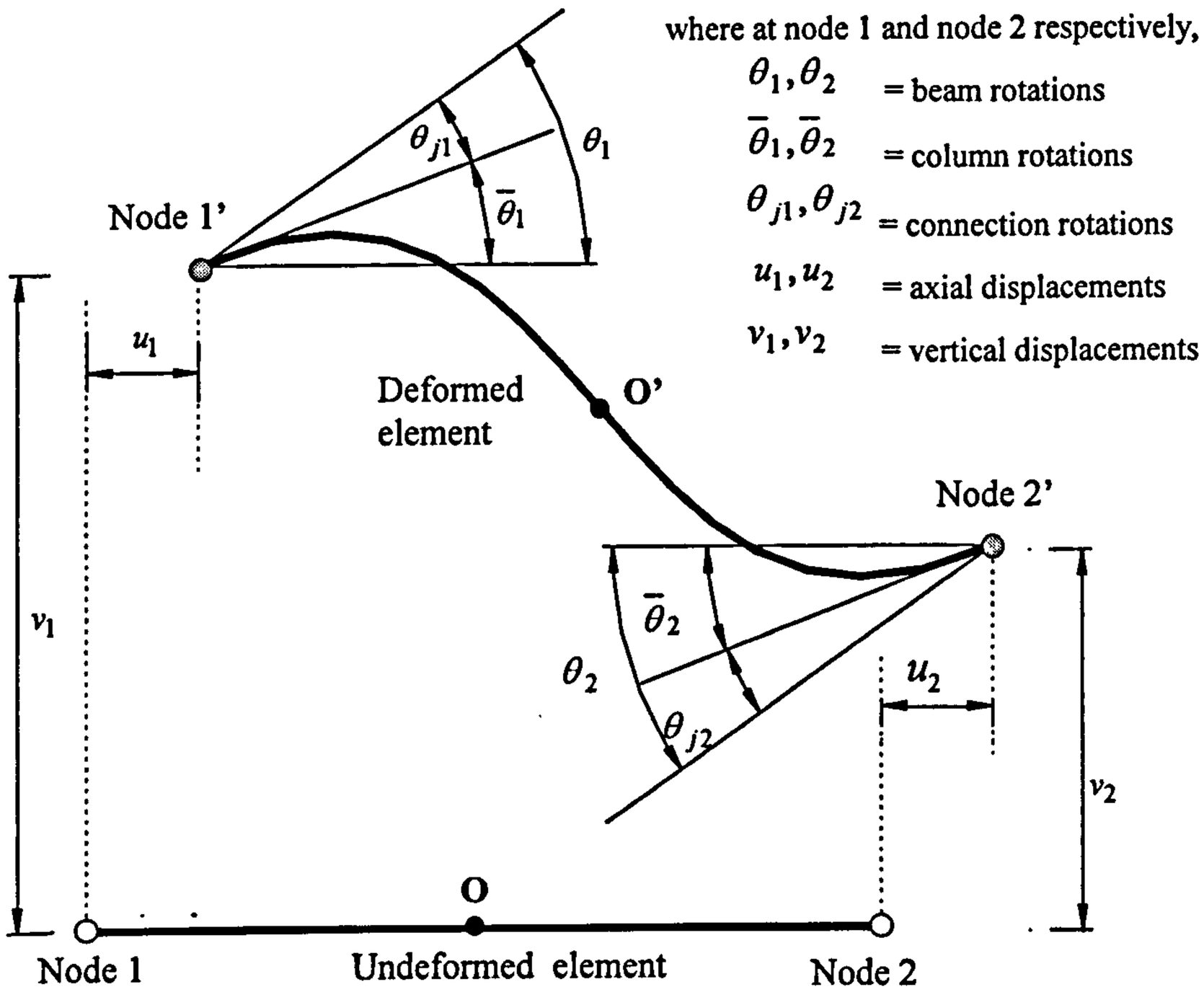

Figure 3.5 Undeformed and deformed shapes of beam-column elements with semi-rigid connections

Mode Shape	Element with rigid nodes	Element with semi-rigid nodes
1	 $\overline{N}_1 = 1-r$	 $N_1 = \overline{N}_1$
2	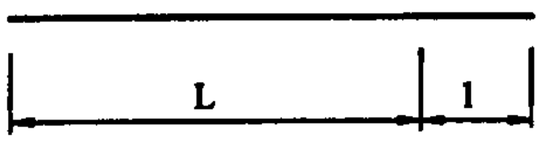 $\overline{N}_2 = r$	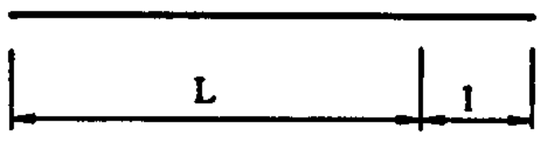 $N_2 = \overline{N}_2$
3	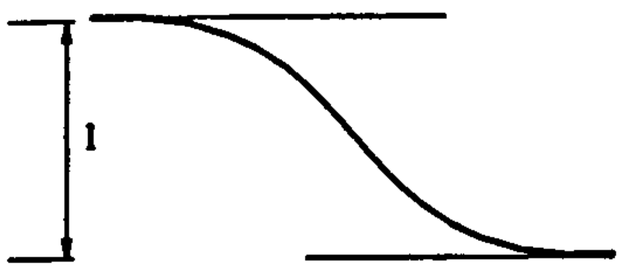 $\overline{N}_3 = 1-3r^2+2r^3$	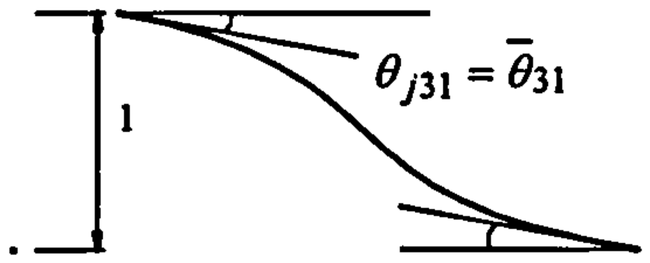 $N_3 = \overline{N}_3 - \theta_{j31}\overline{N}_4 - \theta_{j32}\overline{N}_6$
4	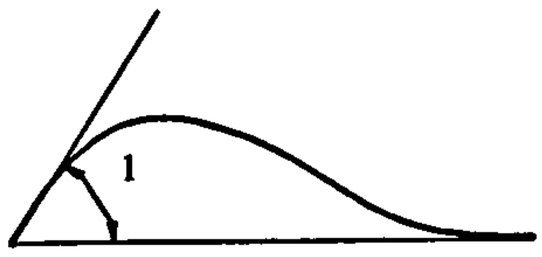 $\overline{N}_4 = L(r-2r^2+r^3)$	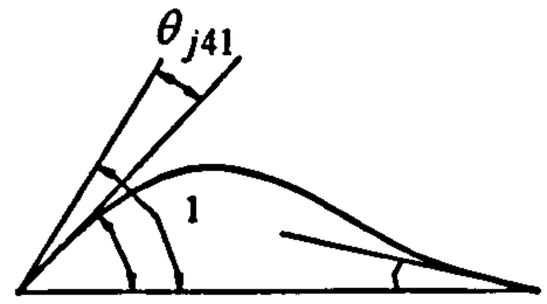 $\overline{\theta}_{41} = (1-\theta_{j41})$ $\theta_{j42} = \overline{\theta}_{42}$ $N_4 = (\overline{N}_4(1-\theta_{j41}) - \overline{N}_6\theta_{j42})$
5	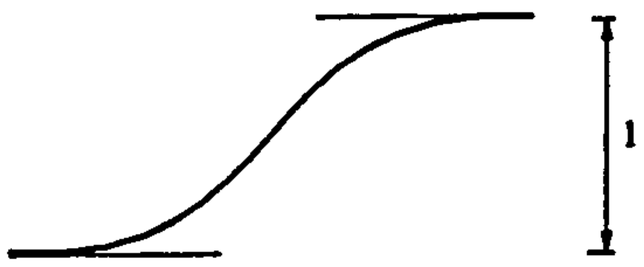 $\overline{N}_5 = 3r^2-2r^3$	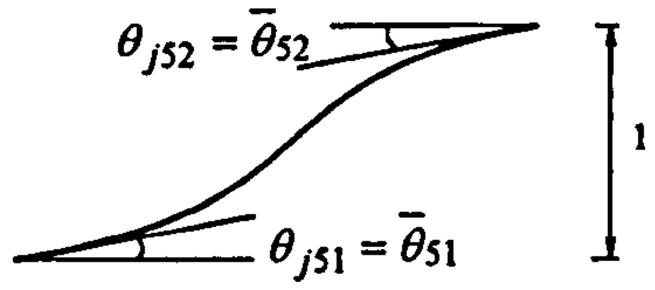 $N_5 = (\overline{N}_5 + \overline{N}_4\theta_{j51} + \overline{N}_6\theta_{j52})$
6	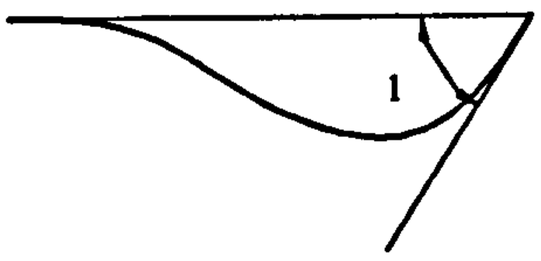 $\overline{N}_6 = L(-r^2+r^3)$	$\theta_{j61} = \overline{\theta}_{61}$ $\overline{\theta}_{62} = (1-\theta_{j62})$ 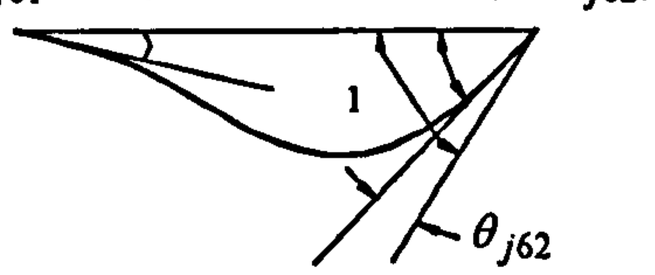 $N6 = (\overline{N}_6(1-\theta_{j62}) - \overline{N}_4\theta_{61})$

where : r = x/L , L = element length

θ_{jab} = joint rotation at end *b* due to displacement *a*

$\overline{\theta}_{ab}$ = member rotation at end *b* due to displacement *a*

$\overline{N}_1,..,\overline{N}_6$ = rigid shape functions

$N_1,..,N_6$ = semi-rigid shape functions

Figure 3.6 Mode shapes and shape functions of beam-column elements with rigid and semi-rigid nodes

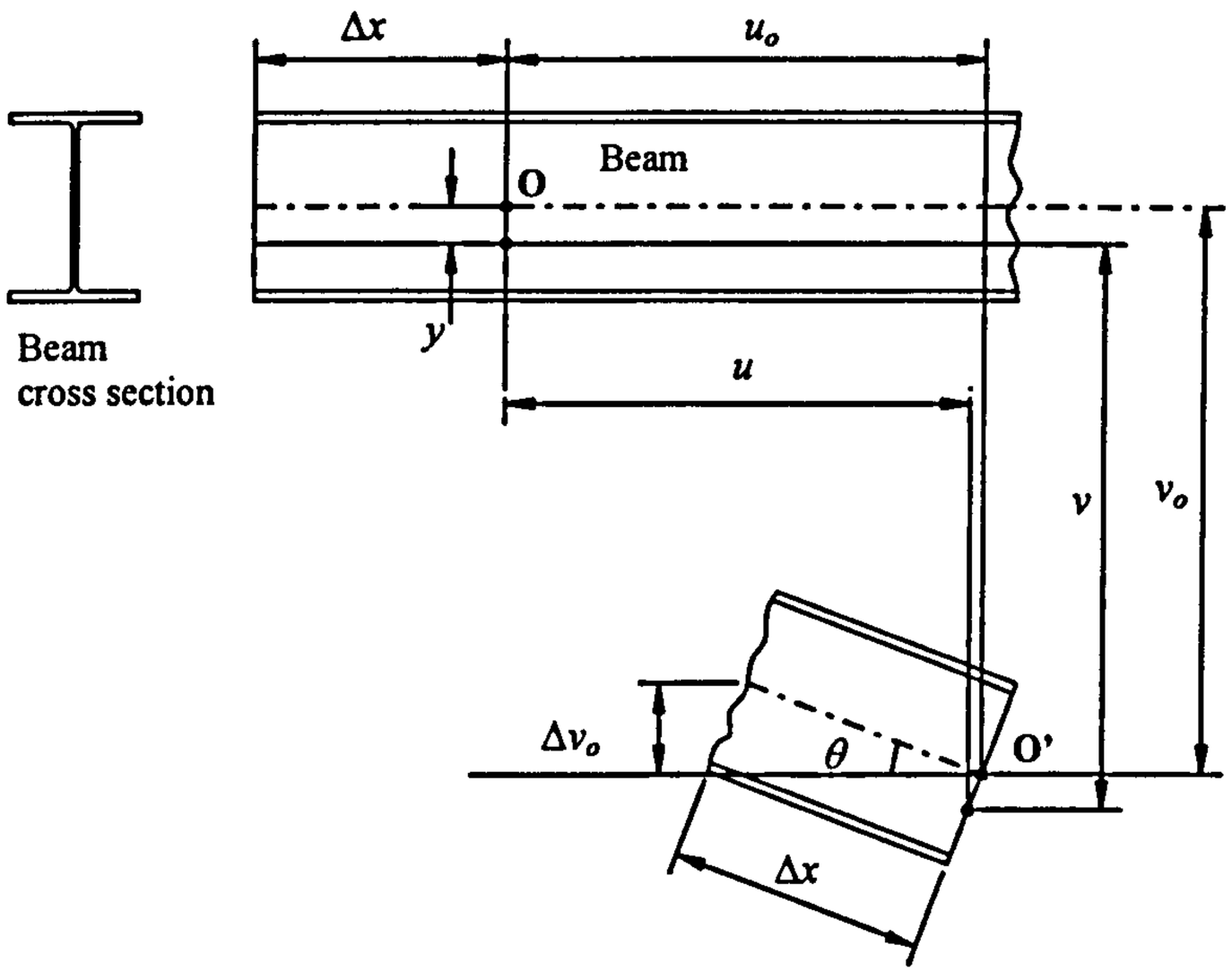

Figure 3.7 Element deformation

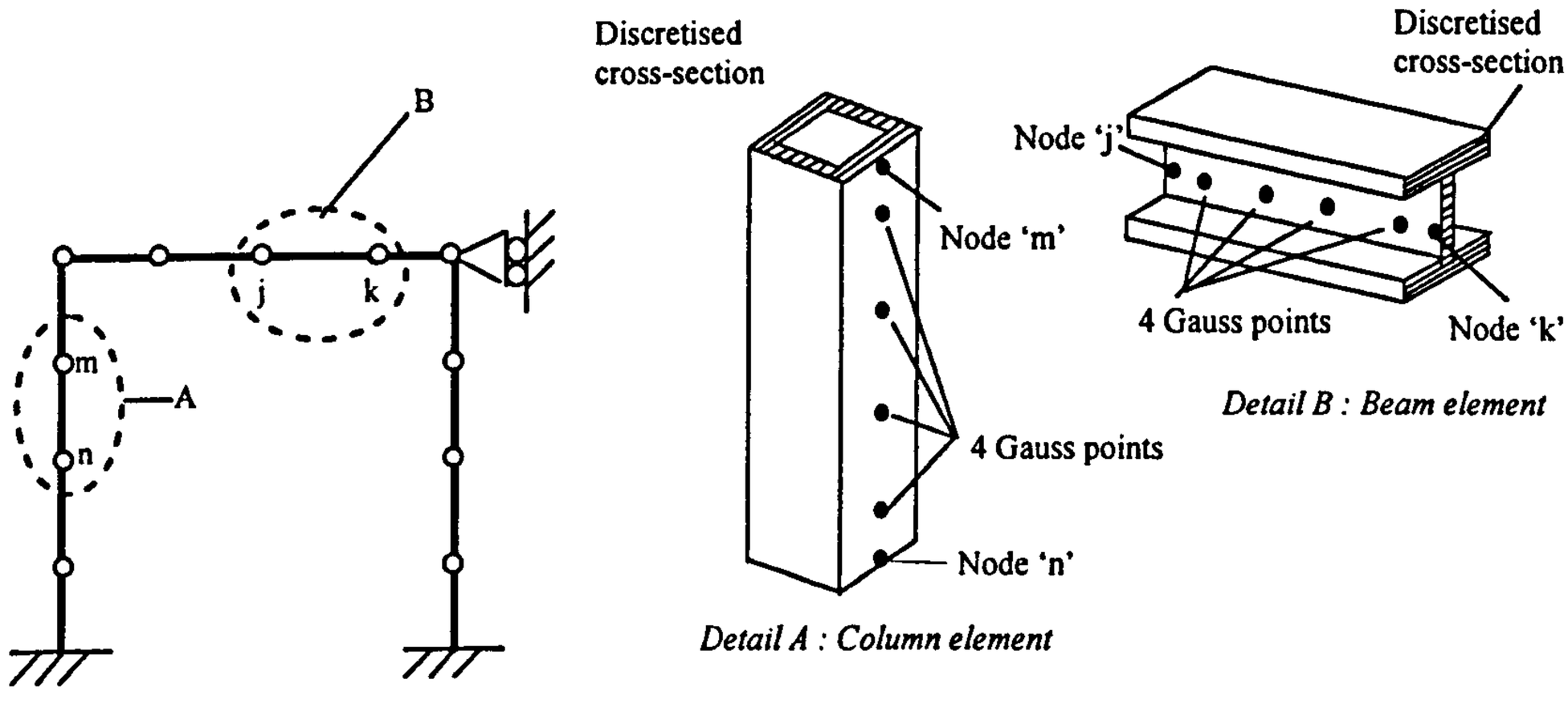

Figure 3.8 Locations of Gauss points along the length of a beam-column element

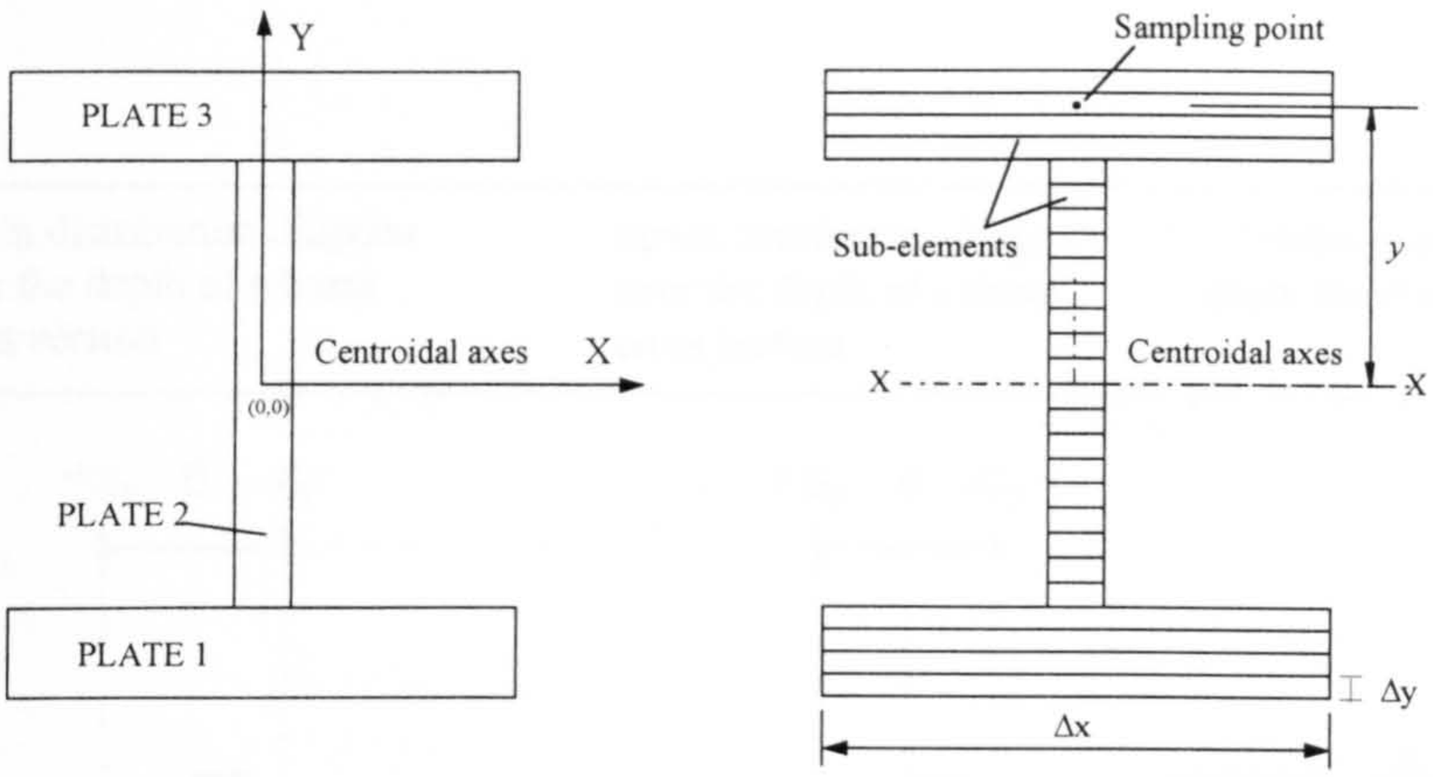

(a)

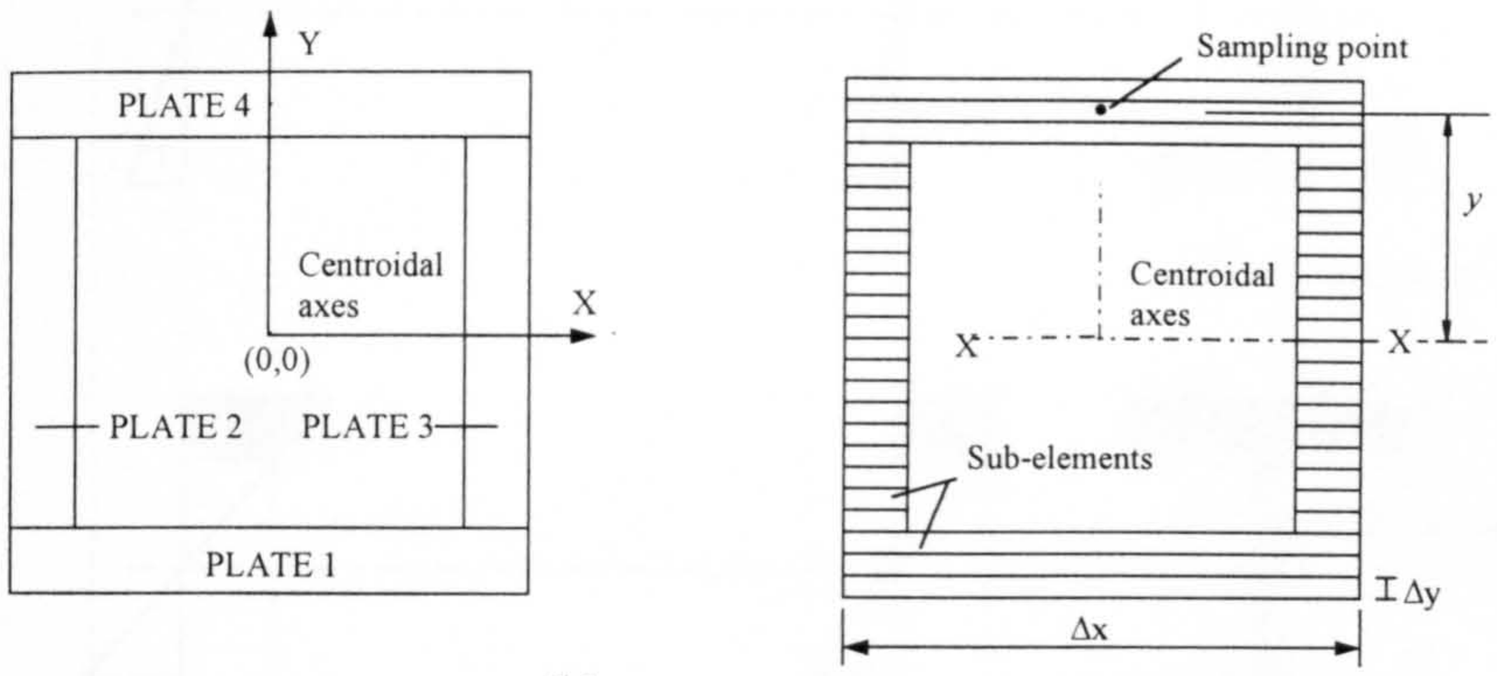

(b)

Figure 3.9 Discretised of cross section into plates and sub-elements for
(a) Universal section
(b) SHS cross section

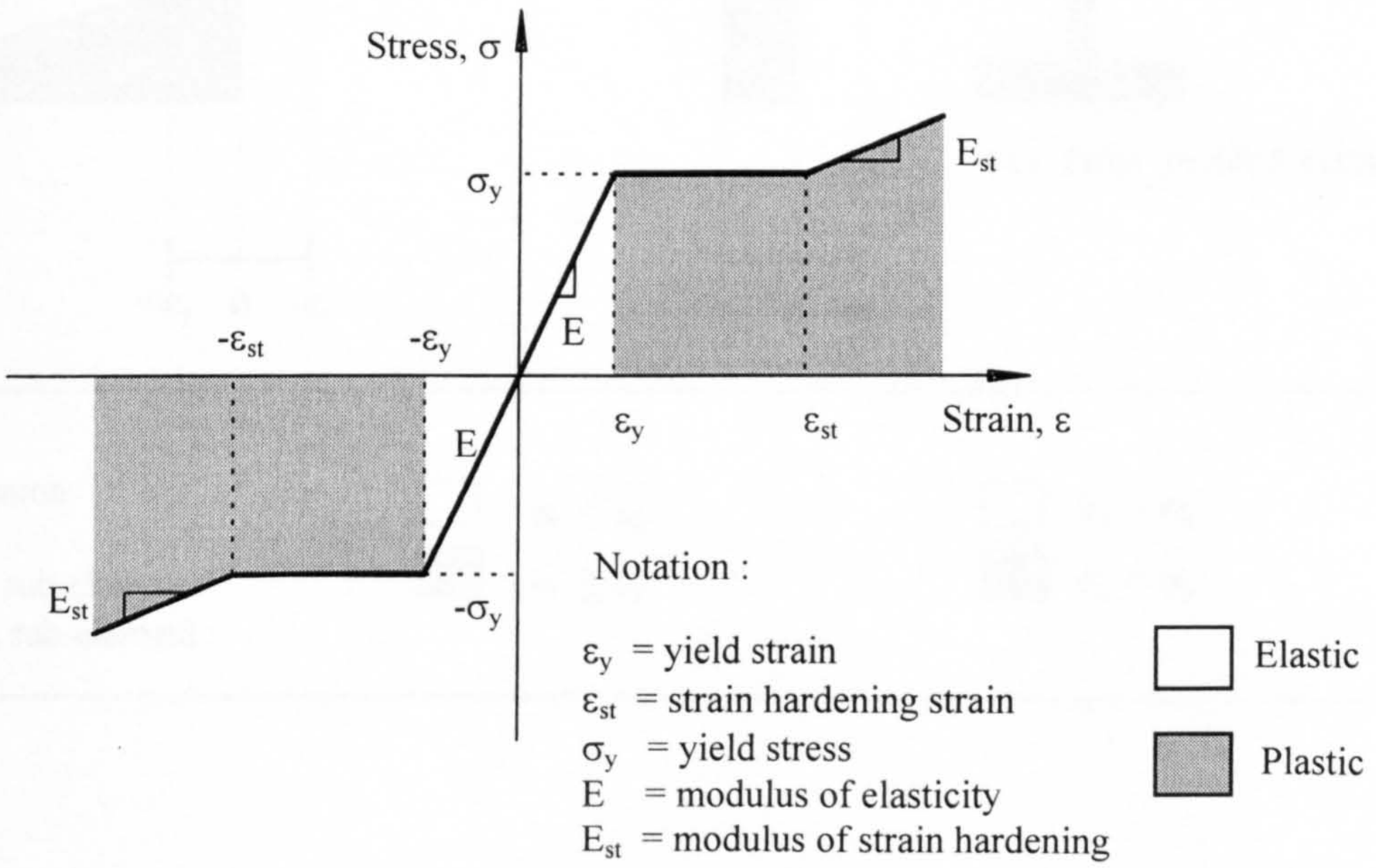

Figure 3.10 Idealised stress-strain characteristics of the steel material

Strain distribution diagram over the depth of a beam cross section	Stress distribution diagram over the depth of a beam cross section	Condition of beam cross section

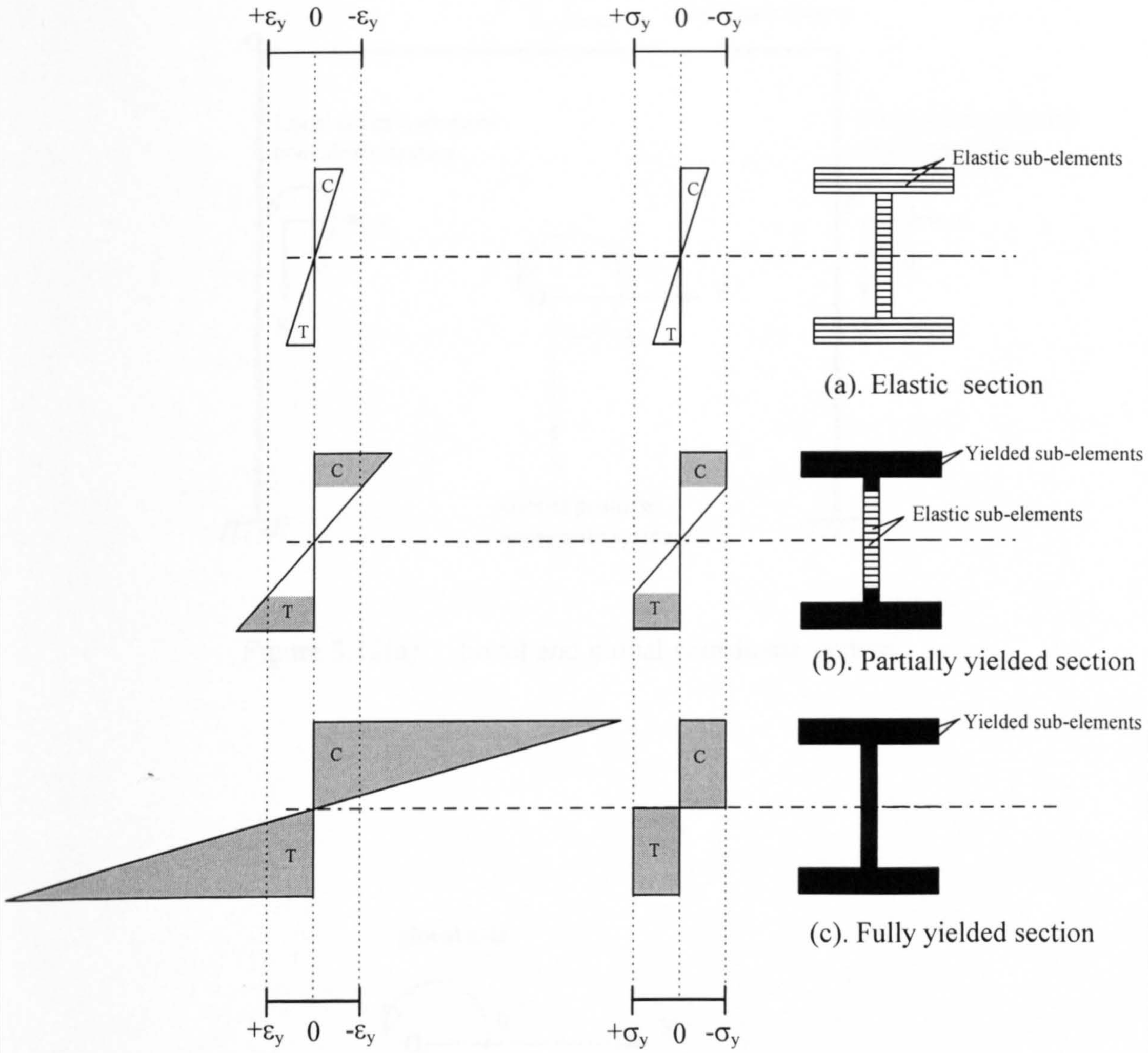

Notation :
C = compression
T = tension
ε_i = strain in sub-element
σ_i = stress in sub-element

$\varepsilon_i < \varepsilon_y$
$\varepsilon_i \geqq \varepsilon_y$
$\sigma_i < \sigma_y$
$\sigma_i = \sigma_y$

Figure 3.11 Strain and stress distribution diagrams and the condition of the element cross section

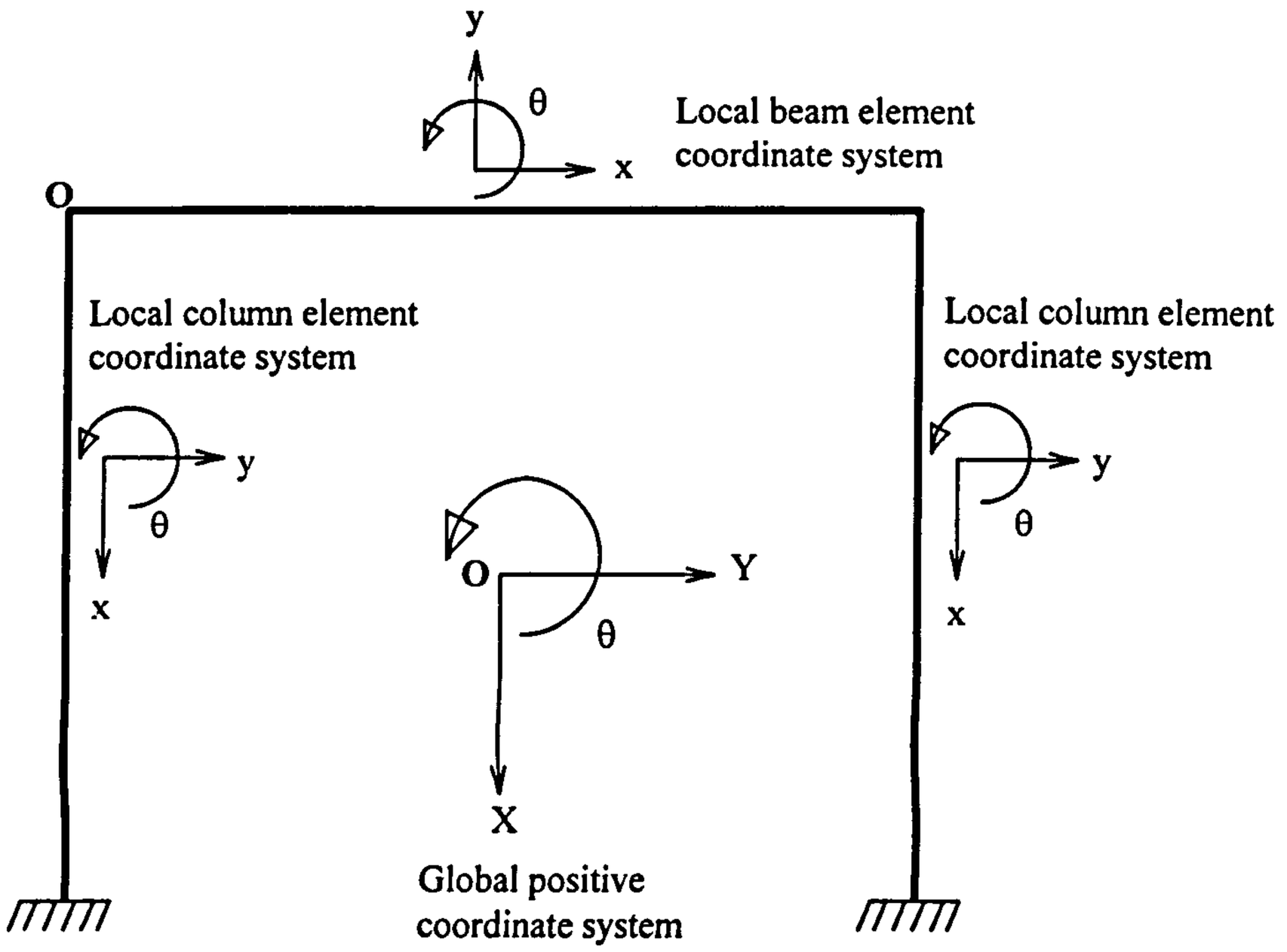

Figure 3.12(a) Local and global coordinate system

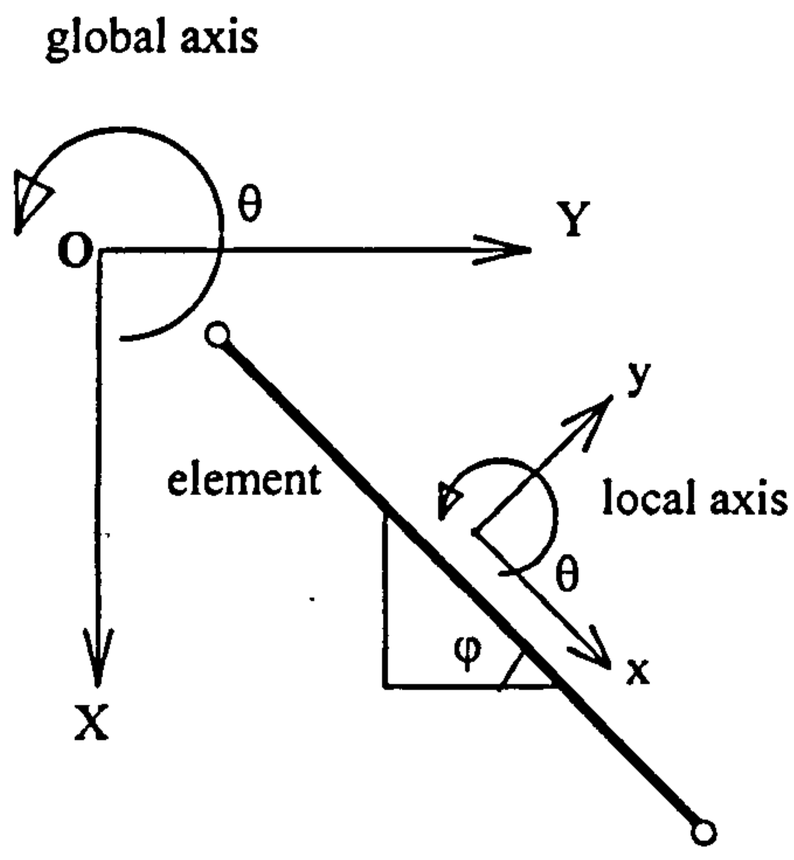

Figure 3.12(b) Axis of transformation of an element

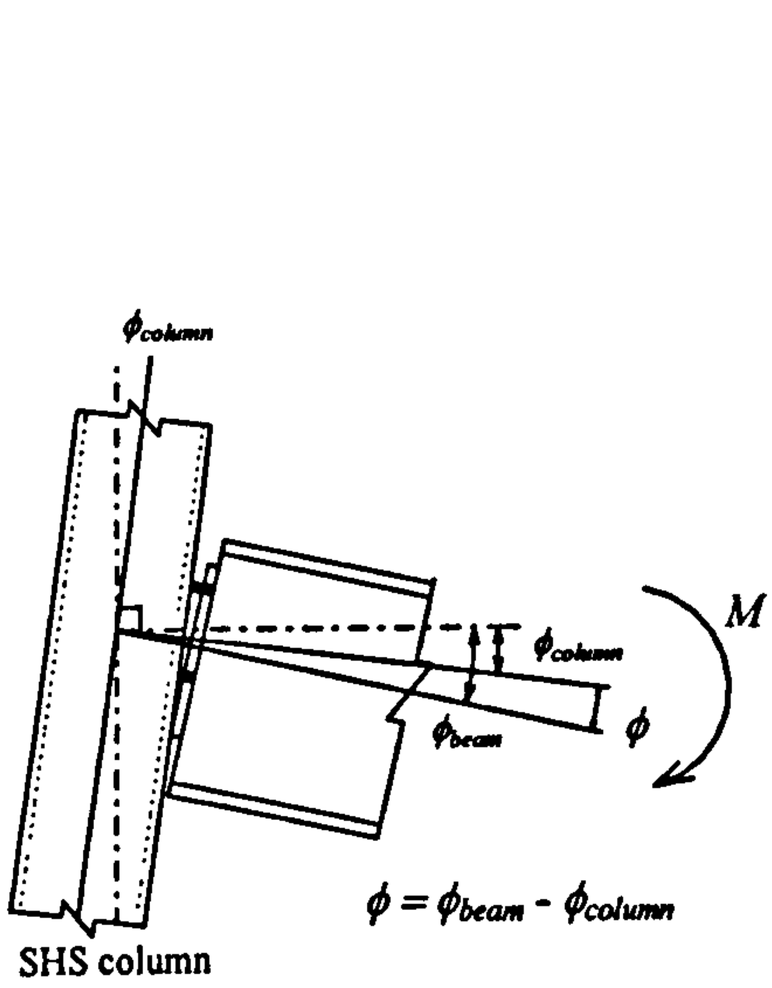

(a). Moment-rotation of a connection

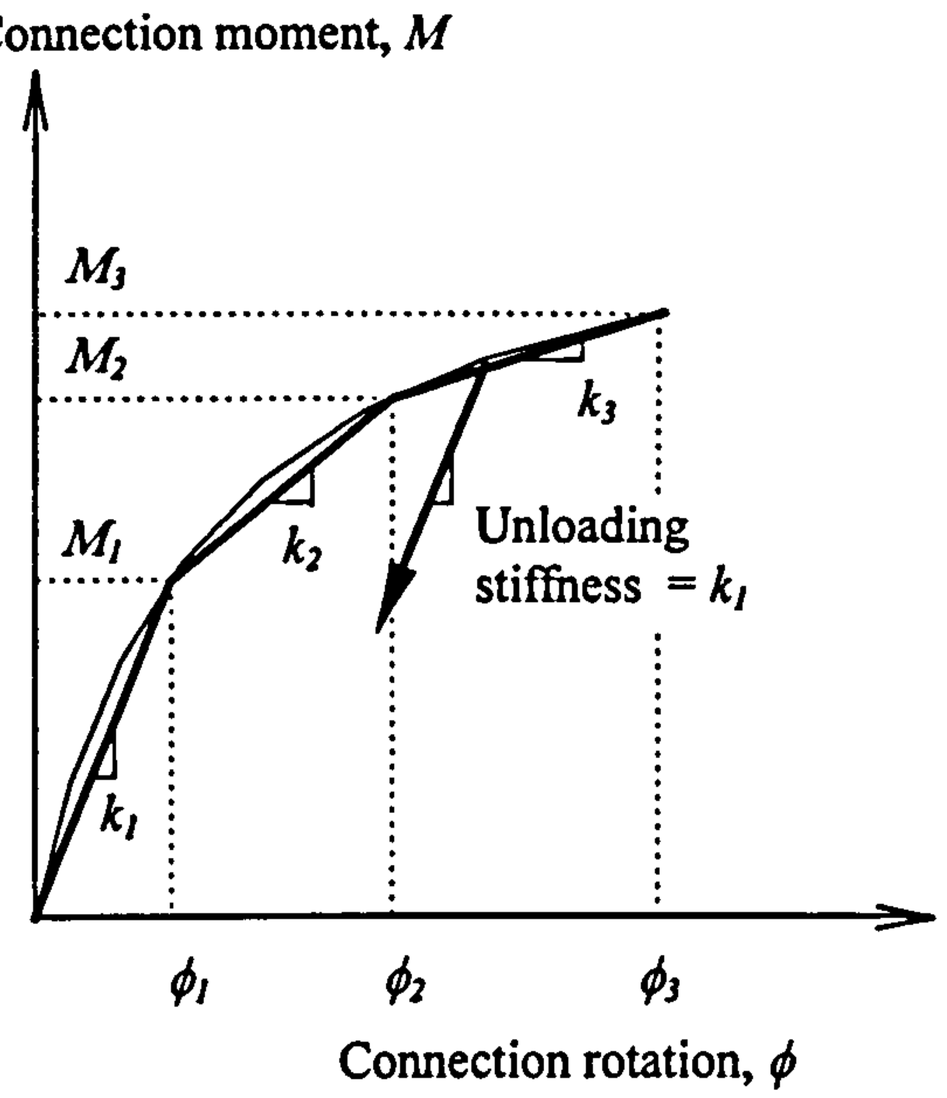

(b). Trilinear M-ϕ curve model of semi-rigid connection

Figure 3.13

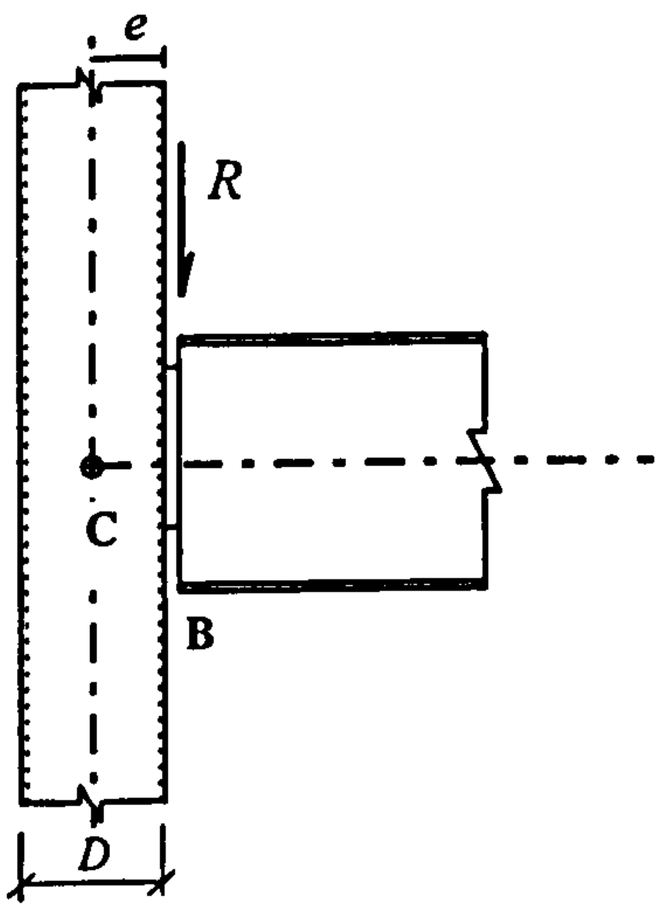

(a).

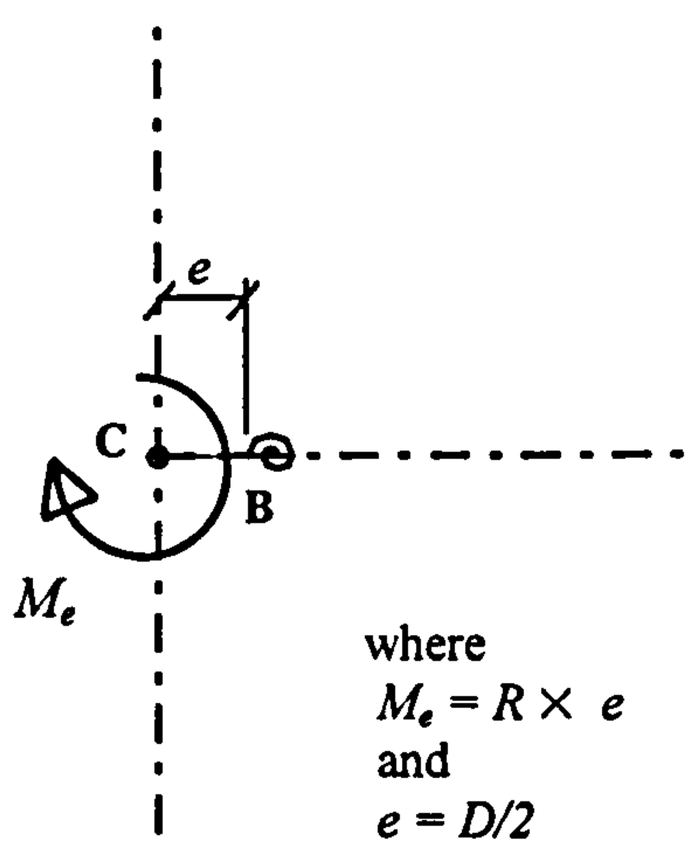

(b).

Figure 3.14 Modelling the connection offset :
(a). Actual connection location with reaction load acting at column face
(b). Model to include the effect of connection offset

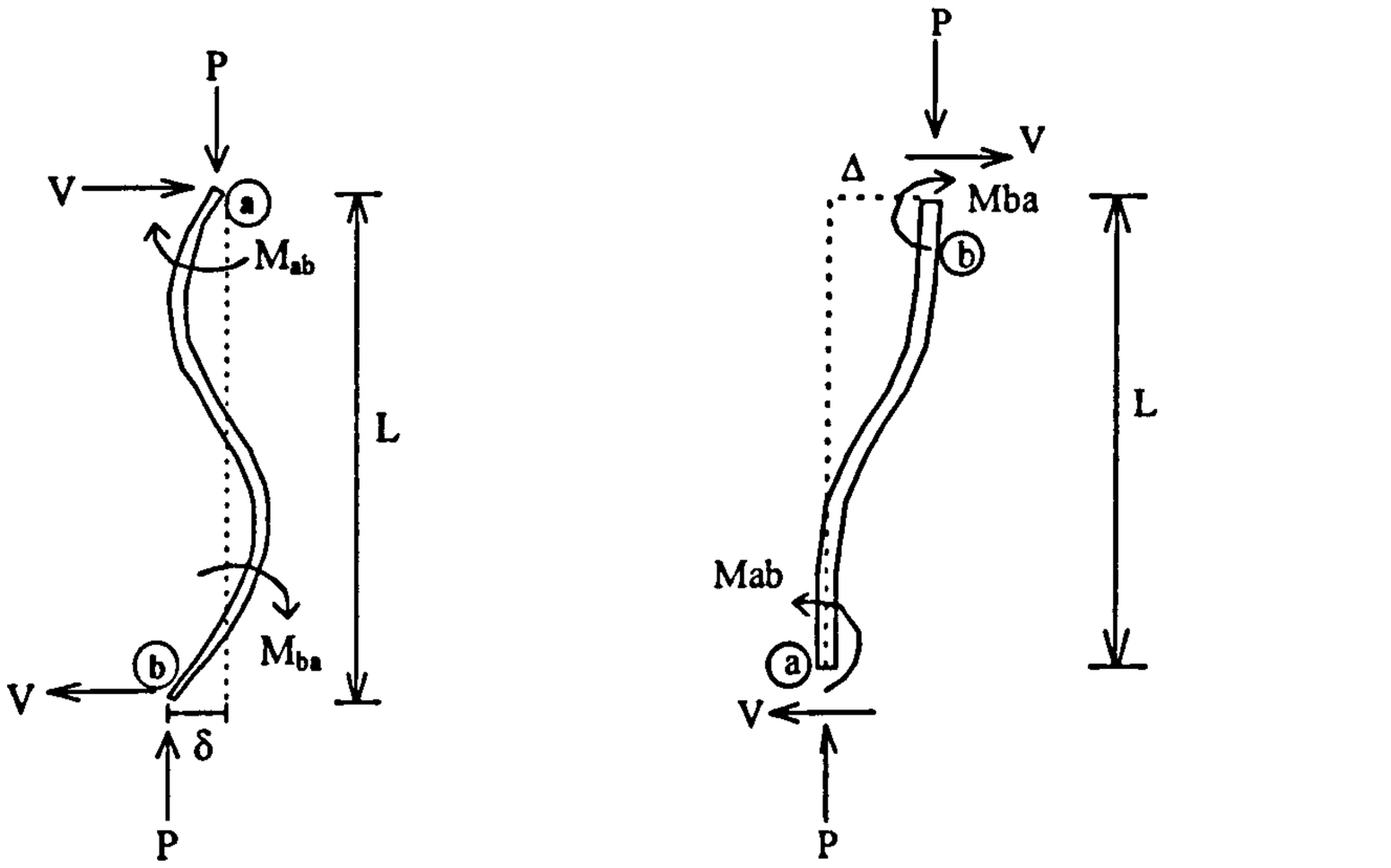

Figure 3.15 Possible *P-δ* and *P-Δ* effects in an element

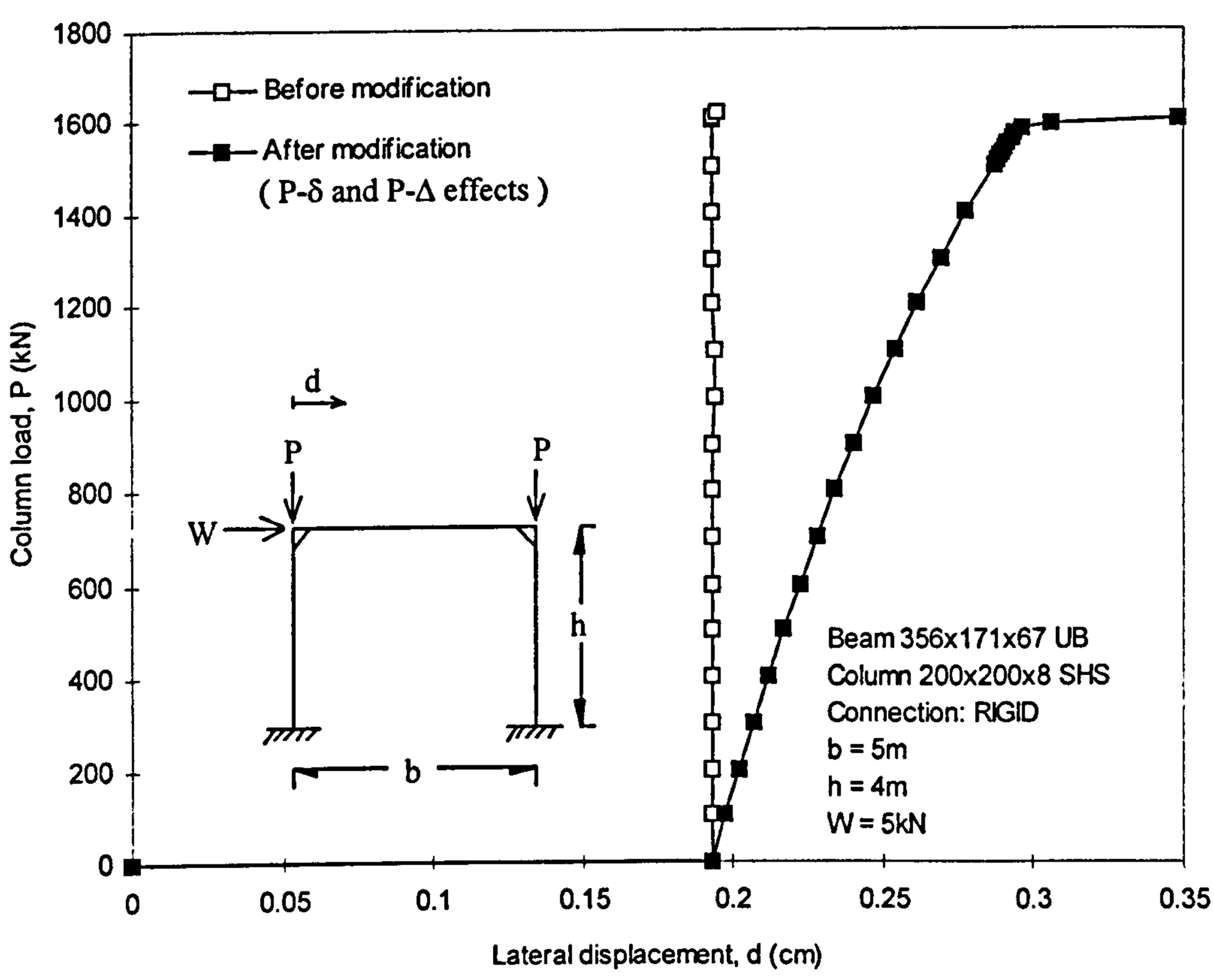

Figure 3.16 Comparison of load-deflection response

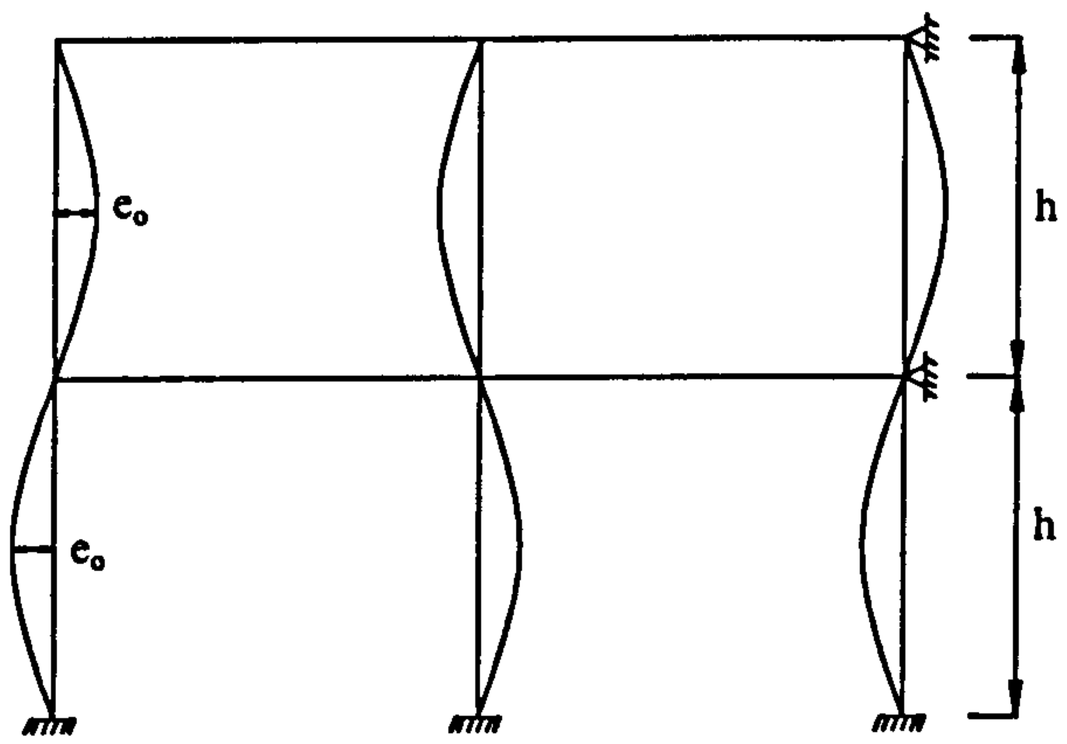

(a). Local geometrical imperfections

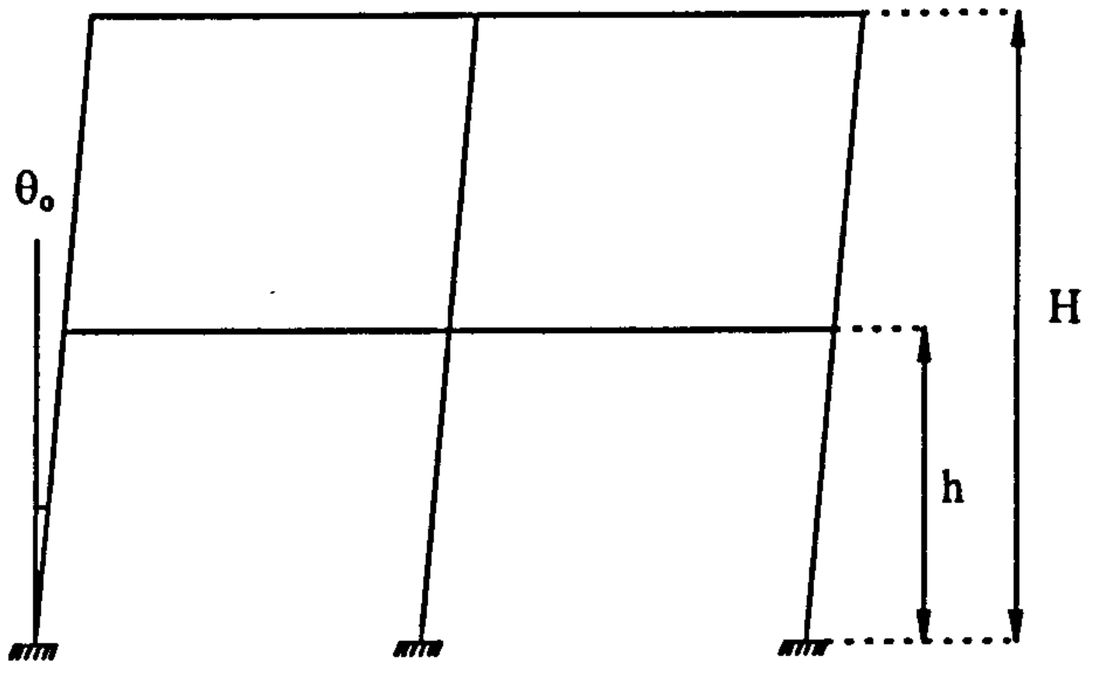

Note:
e_o = initial imperfection
θ_o = lean angle
h = storey height
H = frame height

(b). Global geometrical imperfections

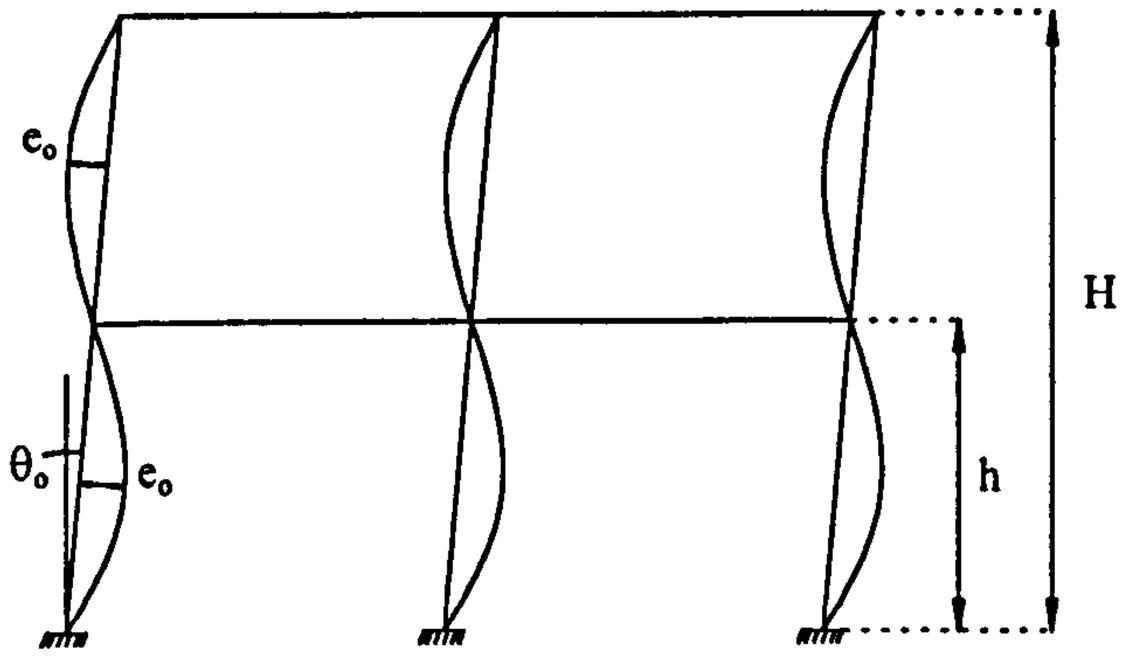

(c). Local and global geometrical imperfections.

Figure 3.17 Types of geometrical imperfections in frames

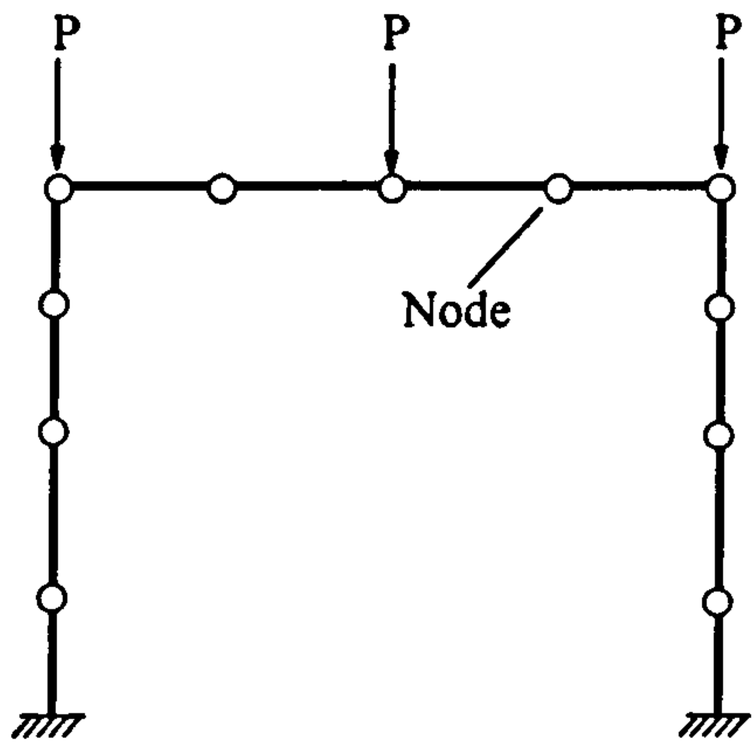

(a). Vertical point loads

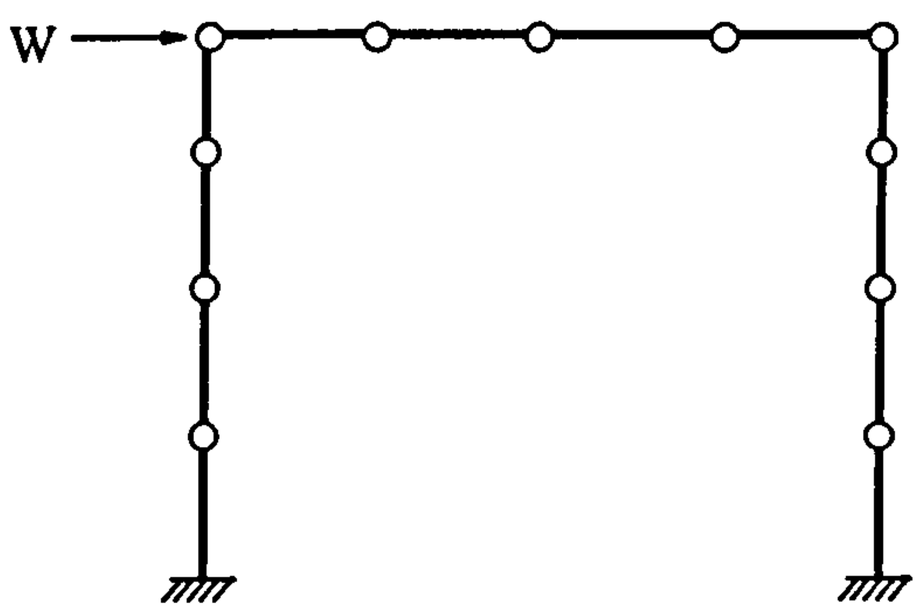

(b). Horizontal point load

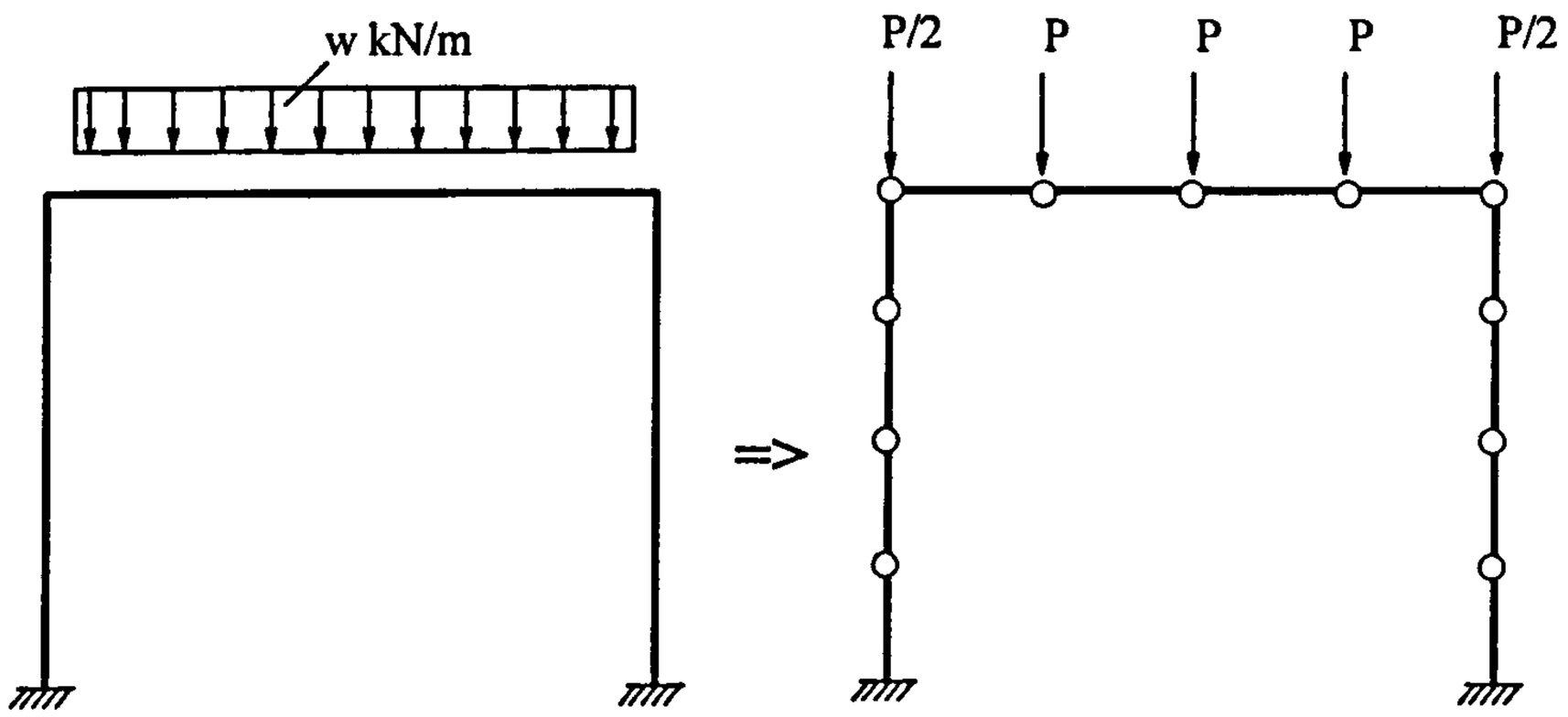

(c). Uniform distributed loads modelled as a series of vertical point loads

Figure 3.18 Treatment of applied loads

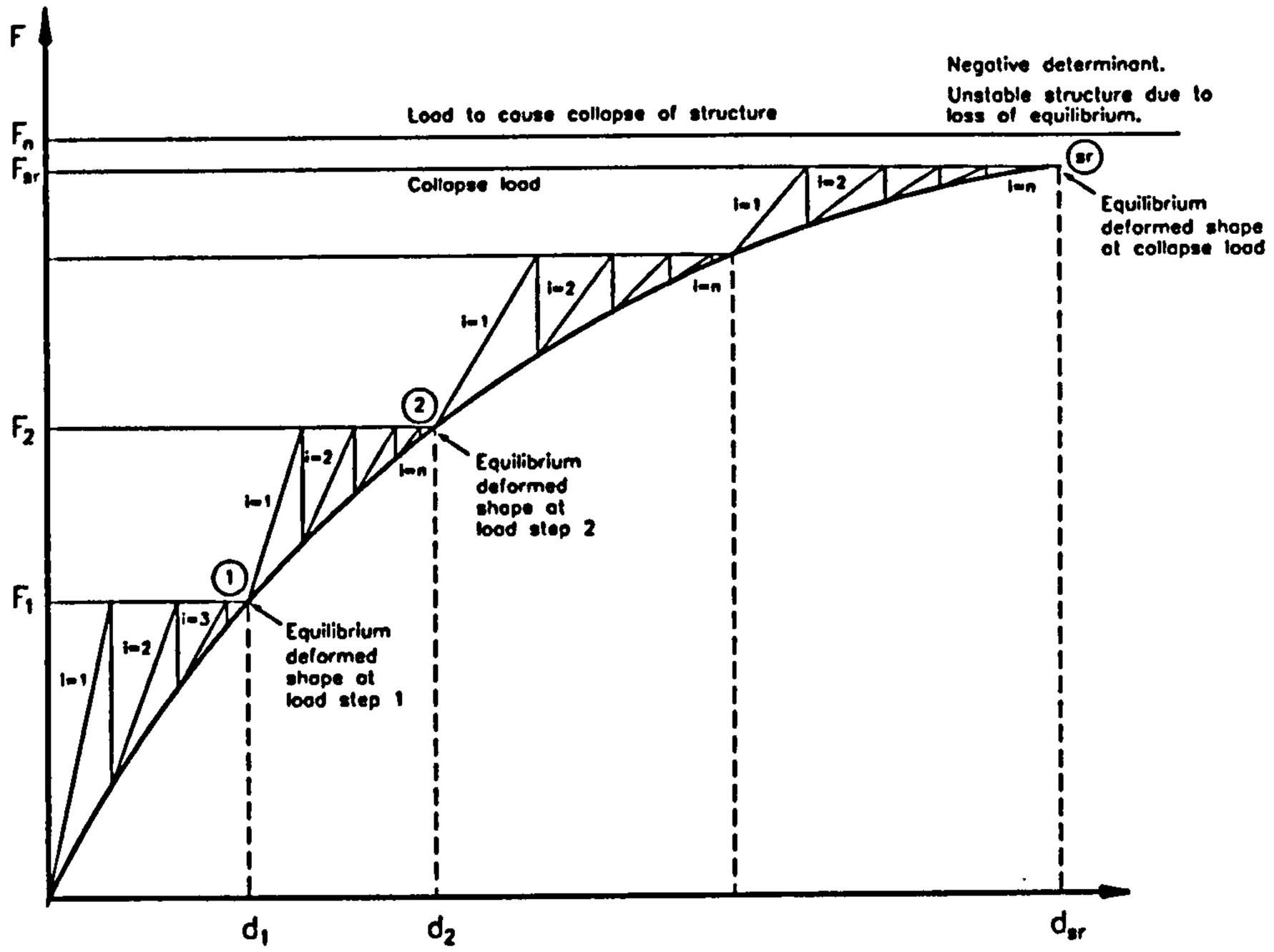

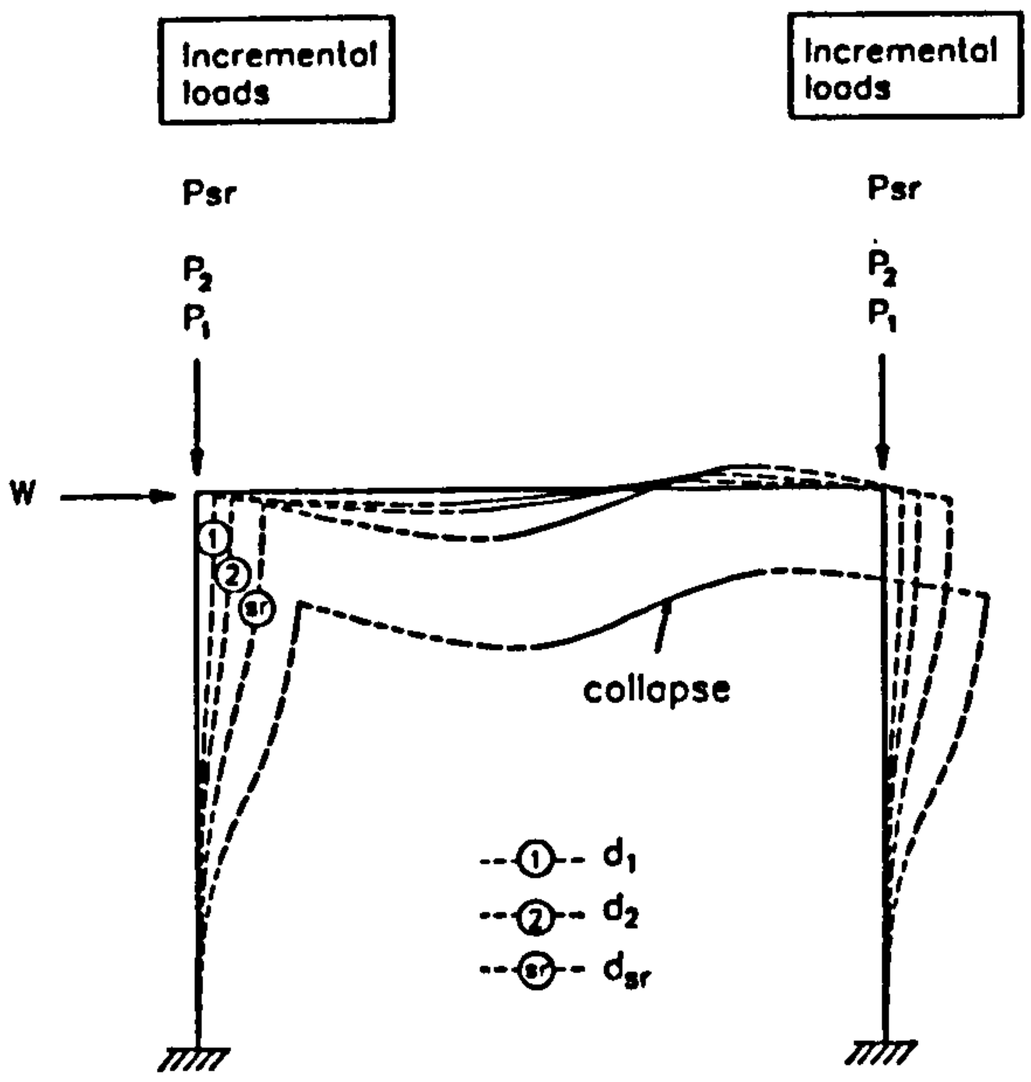

Load step	Applied forces in Figure 3.19(b)	Associated vector of forces in Figure 3.19(a)
1	W . P_1	F_1
2	W . P_2	F_2
:	:	:
sr	W . P_{sr}	F_{sr}

Notes:
Loads W & P are associated with load vector F
i = iteration

Figure 3.19 Analysis of structure up to collapse

(a). Graphical representation of incremental–iterative Newton–Raphson method in solving the nonlinear analysis

(b). Equilibrium deformed frames as related to explanations in Figure 3.19(a)

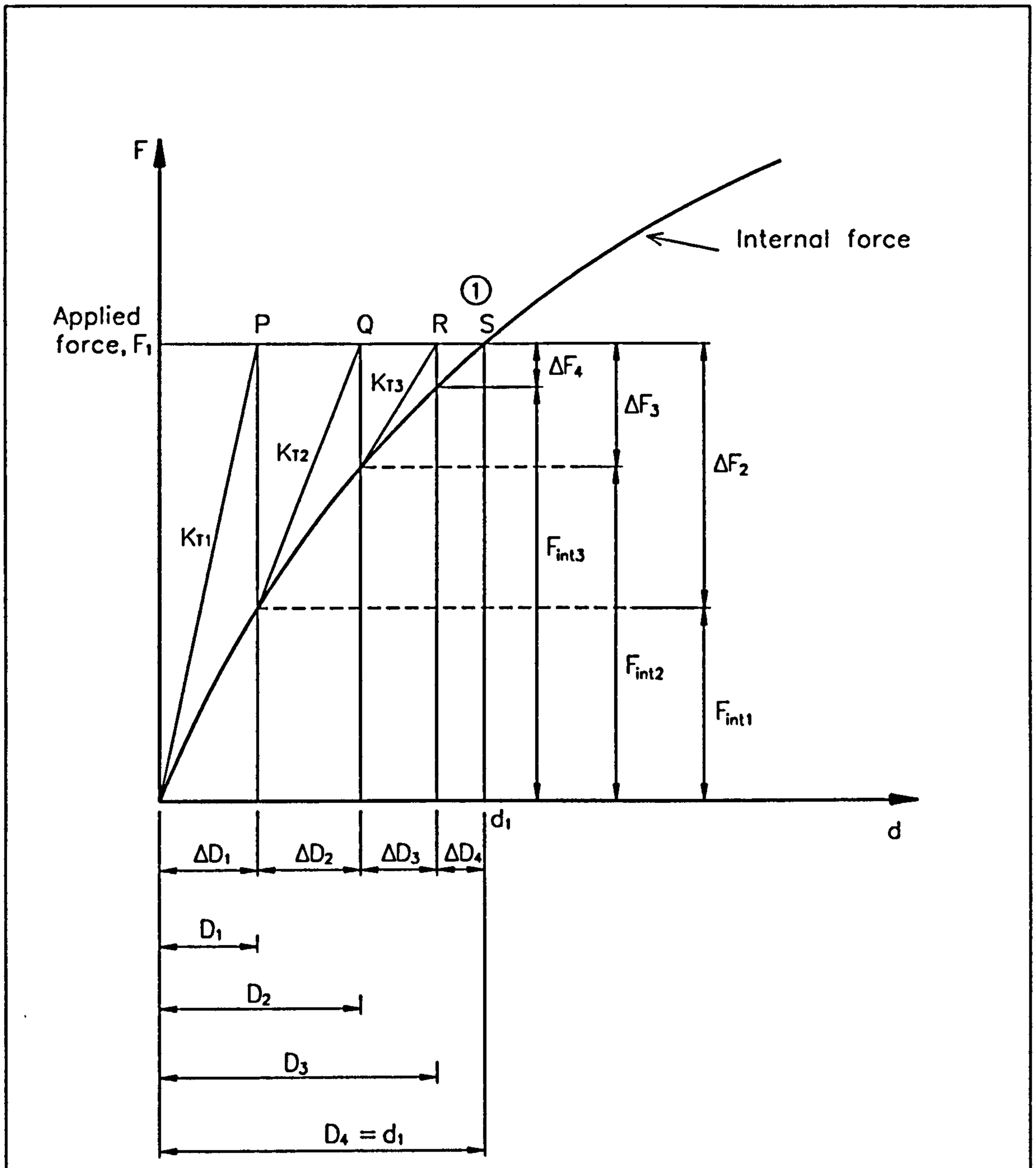

Notes:

ΔD_i = inequilibrium displacement due to unbalance force at iteration 'i'

D_i = inequilibrium total displacement at iteration 'i'

ΔF_i = out-of-balance forces which caused the inequilibrium at iteration 'i'

K_{Ti} = tangential stiffness at iteration 'i'

d_1 = equilibrium displacement due to load F_1

$Fint_i$ = internal force

Figure 3.20 Newton-Raphson Iteration

Chapter 4

Verification of Semi-rigid Frame Response in Non-sway and Sway Modes

4.1 Introduction

The plane frame program for the analysis of semi-rigid frames described in Chapter 3 needed to be verified against the real semi-rigid frame response in order to check its accuracy before being used to carry out the parametric studies in chapters 5 and 6. This was performed by comparing the analytical results against the experimental test results. The ability of the program to simulate the actual frame response confirmed its validity and then can be employed to perform further analytical studies on various plane frame problems.

4.2 Verification in Non-sway Modes

The purpose of this section is to describe this validation process for the behaviour of non-sway frames.

4.2.1 Description of the Test Frames

In order to validate the non-sway frame response, direct comparisons were made against full scale non-sway frame tests.

Under a joint collaboration among Building Research Establishment (BRE), University of Sheffield and Hatfield Polytechnic, a total of five full scale non-sway plane frames employing semi-rigid connections was tested. Two of the five frames were designed and tested by the University of Sheffield group [4-1] and were identified in this thesis as frames 1 and 2 accordingly. Each of the frames was basically a three-storey and two-bay structure with the overall dimension of 10m wide × 11m high and was fully supported by fixed bases. The frames were braced against lateral sway by tying the frame to the rigid balcony. Each beam was braced and fully restrained to avoid the lateral torsional instability. The columns were prevented from the out-of-plane buckling by employing bracing members which were located at the column mid-height. Further information of the tests can be found in references [4-1], [4-2], [4-3].

For the purpose of this study, the experimental results of frames 1 and 2 were chosen to verify the SERIFA program. Frame 1 was tested with the columns bent about their major axes whereas frame 2 was tested with the columns bent about their minor axes.

Figures 4.1(a) and 4.1(b) show the geometrical dimensions of test frames 1 and 2 respectively. The bay widths and the storey heights of both frames were taken as 4.953m and 3.600m respectively. The orientations of the columns to allow buckling about major axes in frame 1 and about minor axes in frame 2 are also shown in the

respective figures. The sizes of the main structural members employed in the frames were 254 × 102 × UB 22 for beams and 152 × 152 × UC 23 for columns.

The actual values of the yield strength, σ_y as measured from the test varied very widely [4-1], [4-3], [4-4]. In the case of beams, the values of σ_y varied from 244 N/mm^2 to 313 N/mm^2. Whereas, in the case of columns, the value of σ_y varied from 222 N/mm^2 to 303 N/mm^2.

Despite the large variation as mentioned above, the yield strength of the steel sections was assumed as 285 N/mm^2. In addition, analyses using different yield stress values of 265 N/mm^2 and 275 N/mm^2 were also included. The modulus elasticity was taken as 210 kN/mm^2.

4.2.2 Analytical Models of the Test Frames

Figures 4.2(a) and 4.2(b) show the finite element models of frames 1 and 2 respectively. The frames were modelled with four elements for each beam and four elements for each column. The bases were modelled as fixed. The frames were prevented against any lateral movement by restraining the degrees of freedom in the lateral directions by means of the vertical roller supports as shown in the figures.

4.2.3 Initial Imperfections

The values of initial out-of-straightness of frames 1 and 2 as measured from the tests are given in Figures 4.3(a) and 4.3(b) respectively. It should be mentioned that the initial out-of-straightness was incorporated in the SERIFA program by defining the co-ordinates at the nodes of the deformed columns.

It was also observed that the various types of imperfections such as the wide range of residual stress values, variation in geometrical section properties and the eccentricity of column load were also present in the test frames [4-3]. For example, in the case of

imperfection due to load eccentricity, experimental studies by Davison [4-1] showed that, as the beam loads were fully applied to a pre-defined level, deformation at the column head was produced thus giving load eccentricity. As axial loads were increased at the column head, the effect of the eccentricity contributed to larger bending moments in the column which then reduced the column capacity.

In view of the above, the presence of the complex imperfections as mentioned above was approximated and incorporated in the verification analysis by adopting a larger initial out-of-straightness. As shown in Figure 4.3(b), the values of the imperfections shown in brackets are associated with this larger initial out-of-straightness model. In this verification, however, only frame 2 was involved with the larger initial out-of-straightness model.

4.2.4 Loading

The loadings of both frame tests involved the following loading sequences:

1. Beam loading phase.

2. Column loading phase.

In the first loading phase, the beams were loaded and then kept constant, whilst in the second loading phase, the selected columns were loaded individually until failure of the individual columns with the beam loads remain unchanged. According to Moore et al. [4-2], the reason of employing this loading scheme was that under initial beam loadings, the connections would undergo significant rotations which would result in a large portion of the M-ϕ curve being consumed and consequently the location of M-ϕ response is away from the initial stiffness. As a result, the effects of a change in using different connection types can obviously be seen.

It should be mentioned that during the test, the applied beam loads were not exactly the same values throughout. Therefore, in this analysis, the loading pattern was modelled to be as close as possible to that adopted in the test.

In frame 1, the beam loads were first applied at the quarter and three quarter points of all beams as shown in Figure 4.4(a). In this analysis, during the beam loading phase, beam B5 was loaded up to the total unfactored dead load of 60 kN and the other beams B2, B3, B4 and B6 were loaded up to the total factored dead and imposed load of 120 kN. The beam loads were then kept constant followed by the column loading phase. In the first phase of the column loading, columns in positions 2 and 3 were subjected to incremental axial loads of 0 kN to 250 kN in five equal increments. In the second phase of the column loading, the axial load at column in position 3 was kept constant at 250 kN as the load at column in position 2 was increased up to the failure.

In frame 2 (see Figure 4.4(b)), the beam loads were applied in a similar fashion as in frame 1. The beam loads were then kept constant, followed by the column loading. In the first phase of the column loading, all columns in positions 1, 2 and 3 were subjected to axial loads of 150 kN. In the second phase of the column loading, column loads at positions 2 and 3 were kept constant at 150 kN as the load at position 1 was increased up to the failure. Finally, once the external column (column in position 1) was brought to failure, the internal column in position 2 was loaded incrementally in similar fashion up to the failure.

4.2.5 Connection Types

Test frames 1 and 2 employed semi-rigid connections consisting of top and bottom flange cleats as shown in Figures 4.5(a) and 4.5(b) respectively. Separate cruciform tests to determine the connection characteristics using nominally identical joints were conducted by Davison [4-1]. The results of the investigations showed that the response of the connections in the full scale cruciform tests and in the full scale plane frame tests were seen to be similar. Studies by Lau [4-3] showed that the use of M-ϕ curves as that obtained from the cruciform joint tests and the use of M-ϕ curves as that obtained from the plane frame tests did not give any significant difference in the results of analysis. He further concluded that a small variation in M-ϕ curves does not significantly affect the ultimate capacity of the structural members.

In view of the above, for the purpose of this verification, the M-ϕ curves obtained from the cruciform joint tests as tested by Davison were used in the analysis. Figures 4.6(a) and 4.6(b), respectively, show the experimental cruciform M-ϕ curves and the corresponding trilinear M-ϕ curve models used in the analysis.

4.2.6 Comparisons of the Analytical Predictions with the Experimental Results

The test frame models have been analysed by the SERIFA program considering all the characteristics of the real frames as were described in sections 4.2.1 to 4.2.5. The results of the analysis are compared directly with the experimental results.

4.2.6.1 Response of Semi-rigid Frame with Columns Bent about the Major Axes - Response of Frame 1

The response of beams and columns as part of semi-rigid frames with the columns bent about the major axes is presented in Figures 4.7 to 4.8 and Table 4.1.

Response of Beams

Figures 4.7(a) to 4.7(c) show the progression of load-deflection responses of beams B2, B4 and B6 during the beam loading phase. The responses were obtained using the design strength of σ_y = 285 N/mm^2. The load deflection curves are plotted based on the quarter point load versus mid-span deflection of each beam. The comparisons at different beam locations show that the predicted load-deflection responses as obtained from the analysis are in good agreement with the experimental results. This implies that the program is able to provide good predictions of realistic behaviour of beams with semi-rigid connections.

Response of Column C4

Column C4 was chosen to predict the column response as part of a semi-rigid frame. In the case of verifying the response of column C4, the following two models were employed:

1. The model using $\sigma_y = 285$ N/mm^2.

2. The model using $\sigma_y = 275$ N/mm^2.

Both models had the initial out-of-straightness as measured from the test which is shown in Figure 4.3(a). The results of the column response for the first and second models in terms of the load-deflection relationship of column C4 are shown in Figures 4.8(a) and 4.8(b) respectively. The curves are obtained by plotting the internal axial column load against the mid-height column deflection of the column considered. It can be seen in both figures that the analytical models have successfully traced the experimental load-deflection response very closely. Furthermore, it can be seen from the latter figure that by employing lower value of σ_y has resulted a softer load-deflection response and a lower value of the ultimate capacity of the column.

Table 4.1 gives the corresponding comparison of the ultimate loads of column C4 between the analytical and experimental results. As can be seen from the table, the experimental failure load is 560 kN. The predicted collapse loads of the first and second models are 609 kN and 560 kN respectively. In this case, the second model gives the failure load similar to the test failure load. This coincidence may be due to the fact that using a lower value of yield stress has caused the column to undergo early yielding and early loss of stiffness. Hence, reduced the failure load from 609 kN to 560 kN accordingly.

4.2.6.2 Response of Semi-rigid Frames with Columns Bent about the Minor Axes - Response of Frame 2

The response of beams and columns as part of semi-rigid frames with the columns bent about the minor axes is reported here.

Response of Beams

Figures 4.9(a) to 4.9(f) show the progression of the predicted and the experimental load-deflection responses of beams B1, B2, B3, B4, B5 and B6 with increasing beam load. The responses were obtained using the design strength of σ_y = 285 N/mm^2. The actual initial out-of-straightness as measured from the test was employed in the model. The comparisons of the analytical and the experimental results show that the predicted responses for all the beams shown in the figures are in good agreement with the test results.

Response of Column C2

Column C2 was chosen to verify the column response as part of a semi-rigid frame. In the case of verifying the response of column C2, the following two models were employed:

1. The model using σ_y = 285 N/mm^2 and the actual initial out-of-straightness as measured from the test, i.e. using the values given without brackets as shown in Figure 4.3(b).

2. The model using σ_y = 265 N/mm^2 and the larger initial out-of-straightness, i.e. using the values in bracket as shown in Figure 4.3(b). If the values of imperfection in brackets are not given then the values of actual initial imperfection as measured from the test are used.

Figure 4.10(a) shows the load-deflection response of column C2 based on the first model. It can be seen from the figure that the analytical result quite closely traced the load-deflection path of the real column and showed the same form of response. A very close prediction is observed at the early loading stages up to 350 kN. However, at the

higher load levels, it is observed that the paths separate with the analytical column having a stiffer response.

On the other hand, Figure 4.10(b) shows the load-deflection response of column C2 based on the second model. It can be seen now that the use of the lower yield strength, σ_y and the larger initial out-of-straightness model has resulted a softer response of the analytical column at the higher load levels. As a result, the predicted load-deflection response compared favourably with the experimental result.

Table 4.2 presents the corresponding experimental and the analytical failure loads of column C2. The experimental failure load is 590 kN. The analytical prediction based on the first model has resulted the ultimate load of 666 kN. However when the second model is adopted, the lower value of ultimate load of 591 kN is obtained. Hence, comparing the failure load of the second model of 591 kN with the test result of 590 kN appears to be very satisfactory. This indicates that the response of the frame is sensitive to yield stress and that the predicted collapse load agrees well with the experimental failure load when adjusted imperfections are incorporated in the model.

Response of Column C5

In the case of verifying the response of column C5, the following two models were employed:

1. The model using σ_y = 285 N/mm^2 and the actual initial out-of-straightness as measured from the test.

2. The model using σ_y = 285 N/mm^2 and the larger initial out-of-straightness (see Figure 4.3(b)).

Figure 4.11(a) shows the load-deflection response of column C5 based on the first model. As can be seen from the figure, the analytical response is much stiffer than the response of the test result.

Figure 4.11(b) shows the load-deflection response of column C5 based on the second model. It can be seen now that the softer response of the analytical result is achieved.

Hence, the result of the analysis is greatly improved and accurately simulates the real response when the larger initial out-of-straightness is included. Consequently, a significantly improved prediction of the load-deflection path and the ultimate load is obtained.

Table 4.3 presents the corresponding experimental and the analytical failure loads of column C5. The experimental failure load of the column is 620 kN. The predicted failure loads based on the first and second models are 705 kN and 632 kN respectively. It is seen that the use of the second model, i.e. with the larger initial out-of-straightness has resulted in good prediction of the test failure load.

The above results indicate that the proper model of incorporating the complex imperfections could result in the improved analytical predictions. It is therefore, acceptable to conclude that the analytical predictions are able to closely simulate the observed experimental responses in terms of the load-deflection and the ultimate load.

4.2.7 Discussion of Results

4.2.7.1 Parameters that are Difficult to Model

The comparison of results between the analysis and the experiment is seen to have some limitations. As highlighted by Davison [4-1], it is not possible to obtain an exact correlation between tests and analysis for all different cases due to the complexity of the full scale frames; variation in residual stresses, variation in yield strength, the influence of experimental errors and the effect of friction which may be present in the experiments and are difficult to take into account in the analysis.

Furthermore, during the actual tests, as reported by Davison [4-1] the load was actually acting at an eccentricity from the column centre-line due to rotation of the column stub above top beam level. This eccentricity induced extra moment at the column head and had caused lower values of the test failure load.

Another factor that may contribute to the differences of response between the analytical predictions and the test results is that the section geometry of the beams and columns which were measured in the tests varied widely from one cross section to another. This has contributed to the variation in the second moment area, I and the cross sectional area, A which will then influence the column response.

Based on this limited parametric study, it is seen that the following parameters influence the column ultimate loads and the load-deflection responses:

- material yield strength, σ_y
- initial out-of-straightness of the columns
- the second moment area, I and cross sectional area, A of the columns.

In addition, it is also seen that the column response is not to sensitive to the following parameter:

- precise M-ϕ curves of the connections.

4.2.7.2 Improved Model

In this study, it was decided that the complex imperfections discussed in section 4.2.7.1 were approximated and taken into account in the analysis by incorporating the larger initial out-of-straightness model. In addition, further analyses employing different values of yield strength were also carried out.

The results show that the use of larger initial out-of-straightness model and different values of yield strength has led to good correlation of the predicted response with the experimental results. It is also seen that the responses in terms of the ultimate load and load-deflection are improved further with the use of lower yield strength.

Another important aspect obtained from this verification is that the program permits accurate predictions of the frame behaviour from the start of the loading up to collapse. This enables analytical investigations to be performed in both elastic and inelastic ranges.

Overall, considering the complexity of the full scale frames, it is concluded that the analytical results compared favourably with the experimental results. This implies that the analysis results obtain from the SERIFA program is acceptable and reasonably gives accurate prediction of the true response of non-sway frames.

4.3 Verification in Sway Mode

The purpose of this section is to describe the validation process for the behaviour of sway frames.

4.3.1 Comparisons of the SERIFA Predictions with the Experimental Results

4.3.1.1 Description of the Test Frames

In order to verify the sway frame response, direct comparisons are made against the full scale sway frame tests. A two-storey and one-bay semi-rigid sway frame as tested by Stelmack et al. [4-5] was chosen by the author to verify the SERIFA program against the actual frame response in sway mode. The test frame was a half scale model.

The description of the frame is shown in Figure 4.12. The test frame employed wide flange sections of W5 × 16 for both beams and columns. The steel grade was A36 and the value of the yield strength was given as 248 N/mm^2 (36 ksi) with an elastic modulus of 200 kN/mm^2. The flexural rigidity of the structural members was computed as $EI = 1755 \times 104$ kN/cm^2 and the gross sectional area as $A = 30.19$ cm^2. The columns were connected to pinned bases and were oriented to bend about their strong axes.

4.3.1.2 Analytical Model of the Test Frames

Figure 4.13 shows the finite element model of the sway frame. In this model, the beam elements are connected to the column elements at the concentrated point of the intersection between the beam and column centre-lines. The material characteristic was modelled as elastic-perfectly plastic.

4.3.1.3 Loading

Figure 4.14 shows the corresponding loads applied to the frame. The sway frame was subjected to gravity point loads of 10.68 kN at the first storey beam at a distance of 914.3 mm from the left and right connections respectively. The gravity loads were kept constant and then followed by the application of increasing lateral load. The lateral load at the first storey was applied incrementally at a level which was twice than that at the second storey. A detailed description of the loadings is available in reference [4-5].

4.3.1.4 Connection Types

The column-to-base connections were designed to act as pinned bases (see Figure 4.15). To enable the column web to be fixed between the two steel plate, the column flanges near the base were removed. A bolt of 1.25 inches nominal diameter was employed to join the column web to the two plates to form the pinned end condition.

The beam-to-column connections consisted of top and bottom seat angle connections (see Figure 4.16). The size of the angles were 4 inches by 4 inches with the thickness of 1/2 inch. Standard holes with a nominal diameter of 1/16 inch greater than the bolt diameter were employed at the column flanges, beam flanges and angles. The top and seat angles were all bolted to the column flanges with 3/4 inch nominal bolts of grade A325. The corresponding experimental M-ϕ curve and the idealised M-ϕ model as a series of trilinear curves are shown in Figure 4.17.

4.3.1.5 Response of the Sway Frame

Figure 4.18(a) shows the load deflection response at the second storey of the sway frame due to increasing lateral load. As can be seen from the figure, the predicted load-deflection response agrees reasonably well with the test result. The nonlinearity behaviour of the load-deflection response as observed in the experiment is also demonstrated by the analytical prediction. Clearly, the program can trace the real behaviour of the load-deflection of the real sway frame.

Similarly, Figure 4.18(b) shows the analytical load-deflection response at the first storey of the sway frame as compared against the test result. As demonstrated in this figure, the program closely traces the test load-deflection response which demonstrates the validity of the computer program to be used for analysing the response of sway frames under horizontal loading. No experimental results were available for testing the program for column failure.

4.3.2 Comparison of the SERIFA Prediction with the Other Analytical Results

In order to verify further the ability of the SERIFA program, the author decided to compare the results with the Deierlein's program [4-6]. Figure 4.19 shows the Deierlein's frame as used by Foley and Vinnakota to verify their program [4-6], [4-7].

The analytical model of the frame is shown in Figure 4.20. The frame was modelled with four elements for each beam and four elements for each column. It should be mentioned that Foley and Vinnakota quoted Deierlein as employing four elements for each beam and two elements for each column.

The frame consisted of two different semi-rigid connections identified as TSAW-ave1 and TSAW-ave2 and were employed at the first storey and the second storey of the frame respectively. Figure 4.21 shows the M-ϕ curve models of the connections with the corresponding parameters of the curve are given in Table 4.4.

The modulus elasticity was taken as E = 200 kN/mm^2 (29,000 ksi) and the yield strength was taken as σ_y = 248 N/mm^2 (36 ksi). The beams at the first and second storeys were W21 × 50 and W16 × 36 respectively. Whilst, the external and internal columns were W12 × 16 and W10 × 33 respectively.

The frame was designed by Deierlein with a factored design load of *1.2DL + 0.5LL + 1.3WL*, where *DL* is the dead load, *LL* is the live load and *WL* is the wind load. In order to check the performance of the frame, a numerical load test was performed by applying a series of load increment denoted as γ *(1.2DL + 0.5LL + 1.3WL*) to the frame. The value of γ was increased from the load level of γ = 0.0 up to γ_{ult}, where γ is the load factor at various load levels and γ_{ult} is the ultimate load factor in which the frame reaches its collapse load.

Figure 4.22 shows the comparison of the analytical result as obtained from the SERIFA program with the Deierlein's program. It is seen from the figure that the load-deflection response as predicted by the SERIFA program agrees well with the Deierlein's result. The observed difference of load-deflection paths may be attributed by the different number of finite elements used in the frame models and the method of modelling the spread of yield.

Table 4.5 presents the corresponding results of maximum connection rotations as obtained from the different programs. It can be seen from the table that the SERIFA program gives the maximum connection rotation of 38 milliradians as compared to the Deierlein's program which gives 42 milliradians. In the case of collapse load factor, the SERIFA programs gives γ_{ult} of 1.8 as compared to 1.84 as obtained by Deierlein. The results show that the SERIFA predictions are in good agreement with the responses predicted by the Deierlein's program.

The good comparisons with the analytical results of the other researchers show that the SERIFA program can predict favourably realistic analysis of semi-rigid sway frames.

4.4 Conclusions

The SERIFA program as formulated in Chapter 3 has been verified against the experimental tests.

In the case of non-sway frames, it was pointed out that it is difficult to accurately simulate an experimental result. This is due to the presence of complex imperfections such as the wide variation of residual stresses and yield strength, the load eccentricity and the possible effect of experimental errors. These factors may lead to some discrepancies in certain cases of the analytical results. However by incorporating the complex imperfections with a larger initial geometrical imperfection, it was then possible to achieve a closer representation.

In the case of sway frames, the analytical results compared favourably with the experimental results as well as with the analytical results of the other researchers.

Based on the results of the verification, it can be concluded that the program can accurately predict the actual response of real frames both in non-sway and sway modes. With regard to this, the program can therefore be employed for extensive use in the analytical studies. Any result obtained from the program can be regarded as valid for representing the true behaviour of real frames.

4.5 References

[4-1] Davison, J.B., 'Strength of beam-columns in flexibly connected steel frames', Ph.D. Thesis, Department of Civil and Structural Engineering, University of Sheffield, U.K., June, 1987.

[4-2] Moore, D.B., Nethercot, D.A. and Kirby, P.A., 'Steel frames: Testing steel frames at full scale', The Structural Engineer, Volume 71, Nos. 23 & 24/7, December 1993, pp. 418-427.

[4-3] Lau, S.M., 'The response of non-sway steel-framed structures with semi-rigid connections', Ph.D. Thesis, Department of Civil & Structural Engineering, University of Sheffield, U.K., December, 1993.

[4-4] Ahmed, I., 'Semi-rigid action in steel frames', Ph.D. Thesis, Department of Civil & Structural Engineering, University of Sheffield, U.K., August, 1992.

[4-5] Stelmack, T.W., Marley, M.J. and Gerstle, K.H., 'Analysis and tests of flexibly connected steel frames', Journal of Structural Engineering, ASCE, Vol. 112, No. 7, July, 1986, pp. 1573-1588.

[4-6] Deierlein, G.G., Hsieh, S.H. and Shen, Y.J., 'Computer-aided design of steel structures with flexible connections', Proceedings of the National Steel Construction Conference, AISC, Kansas City, MO, U.S.A, March 14-17, pp. (9-1) - (9-21), 1990.

[4-7] Foley, C.M. and Vinnakota, S., 'Inelastic behaviour of multi-storey partially restrained steel frames - Part 1', Journal of Structural Engineering, ASCE, still in press, 1998.

[4-8] AISC, 'Manual of steel construction', American Institute of Steel Construction, Inc., 7th. edition, New York, 1970.

[4-9] Gibbons, C., 'The strength of biaxially loaded columns in flexibly connected steel frames', Ph.D. Thesis, Department of Civil and Structural Engineering, University of Sheffield, U.K., December, 1990.

[4-10] Nadjai, A., 'The behaviour of steel frames with semi-rigid joints containing unreinforced infill panels', Ph.D. Thesis, Department of Civil and Structural Engineering, University of Sheffield, U.K., April, 1993.

Column designation	Experimental (kN)	Analytical (SERIFA) using actual initial out-of-straightness and σ_y=285 N/mm^2 (see Figure 4.8(a)) (kN)	Analytical (SERIFA) using actual initial out-of-straightness and σ_y=275 N/mm^2 (see Figure 4.8(b)) (kN)
C4	560	609	560

Table 4.1 Comparison of the experimental and analytical failure loads of column C4 in frame 1

Column designation	Experimental (kN)	Analytical (SERIFA) using actual initial out-of-straightness and σ_y=285 N/mm^2 (see Figure 4.10(a)) (kN)	Analytical (SERIFA) using larger initial out-of-straightness and σ_y=265 N/mm^2 (see Figure 4.10(b)) (kN)
C2	590	666	591

Table 4.2 Comparison of the experimental and analytical failure loads of column C2 in frame 2

Column designation	Experimental (kN)	Analytical (SERIFA) using actual initial out-of-straightness and σ_y=285 N/mm^2 (see Figure 4.11(a)) (kN)	Analytical (SERIFA) using larger initial out-of-straightness and σ_y=285 N/mm^2 (see Figure 4.11(b)) (kN)
C5	620	705	632

Table 4.3 Comparison of the experimental and analytical failure loads of column C5 in frame 2

Connection designation	*Connection stiffness (kNm/rad)			*Connection rotation x 10^{-3} radians		
	k_1	k_2	k_3	ϕ_1	ϕ_2	ϕ_3
TSAW-ave2	15071	3853	624	1.95	8.05	50
TSAW-ave1	22189	4267	987	2.8	11.44	50

Note:

* The values of connection stiffnesses k_1, k_2, k_3 and the connection rotations ϕ_1, ϕ_2, ϕ_3 correspond to Figure 3.13(b) of Chapter 3.

Table 4.4 Parameters for M-ϕ curve models shown in Figure 4.21 [4-6], [4-7]

Maximum connection rotation and ultimate load factor due to *(1.2DL+0.5LL+1.3WL)* γ	SERIFA	Deierlein [4-6], [4-7]
Max. connection rotation (milliradians)	38	42
γ_{ult}	1.8	1.84

Table 4.5 Maximum connection rotations at ultimate load condition and ultimate load factor

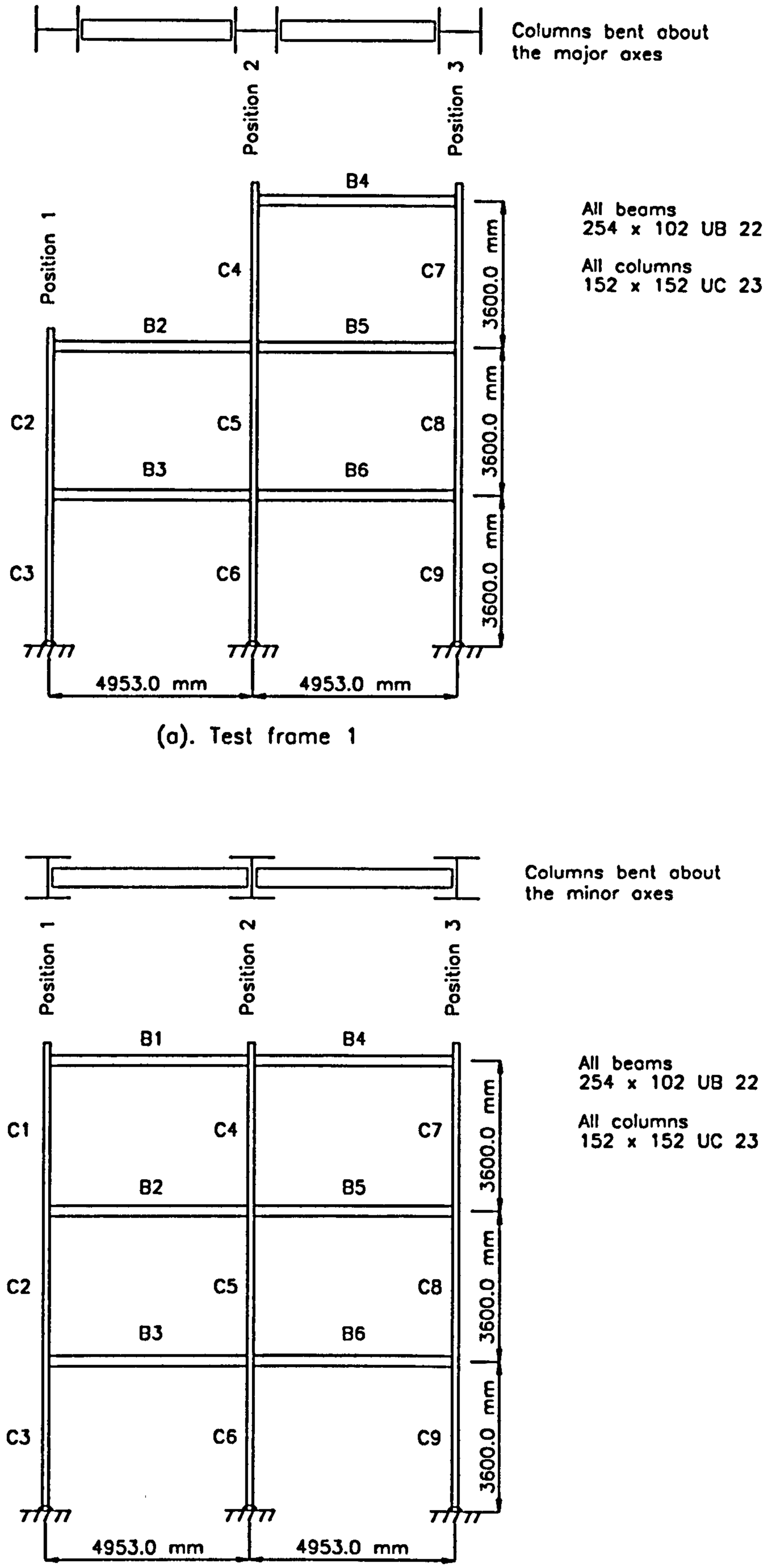

Figure 4.1 Non-sway Test Frames

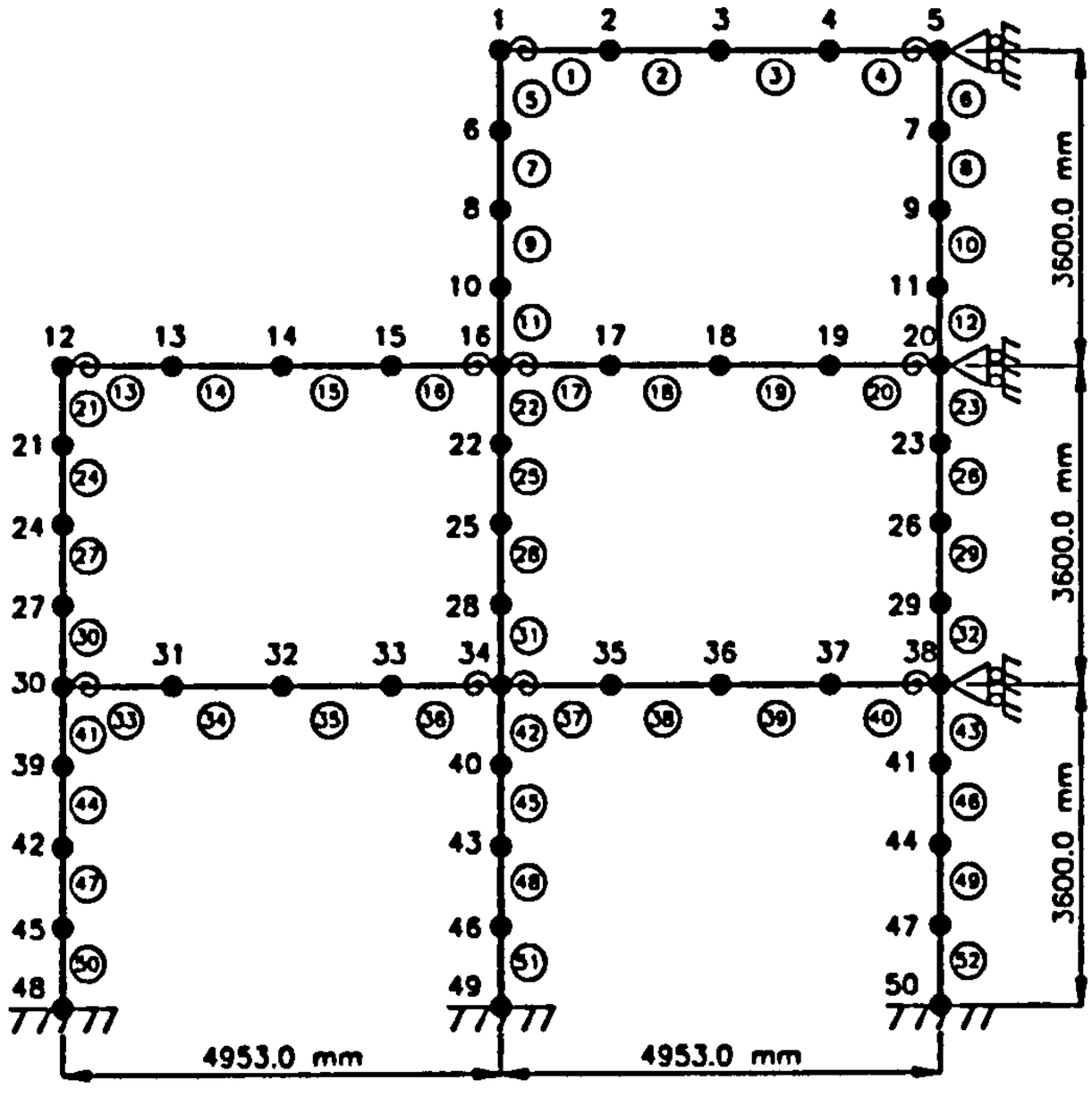

(a). Frame 1

Notation:

- Node
- 3 Node number
- ③ Element number
- Semi-rigid connection
- Lateral displacement prevented

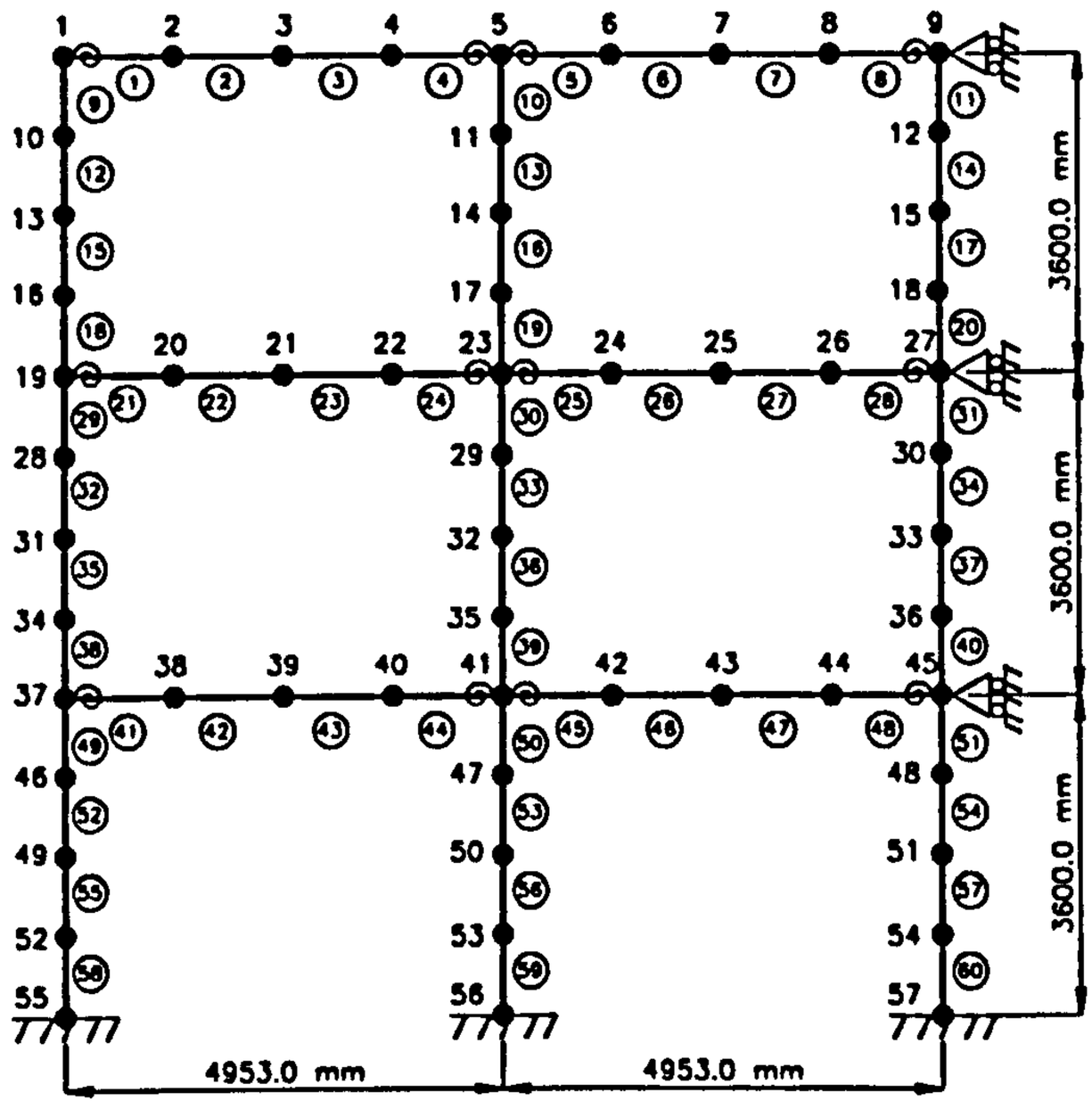

(b). Frame 2

Figure 4.2 Analytical model

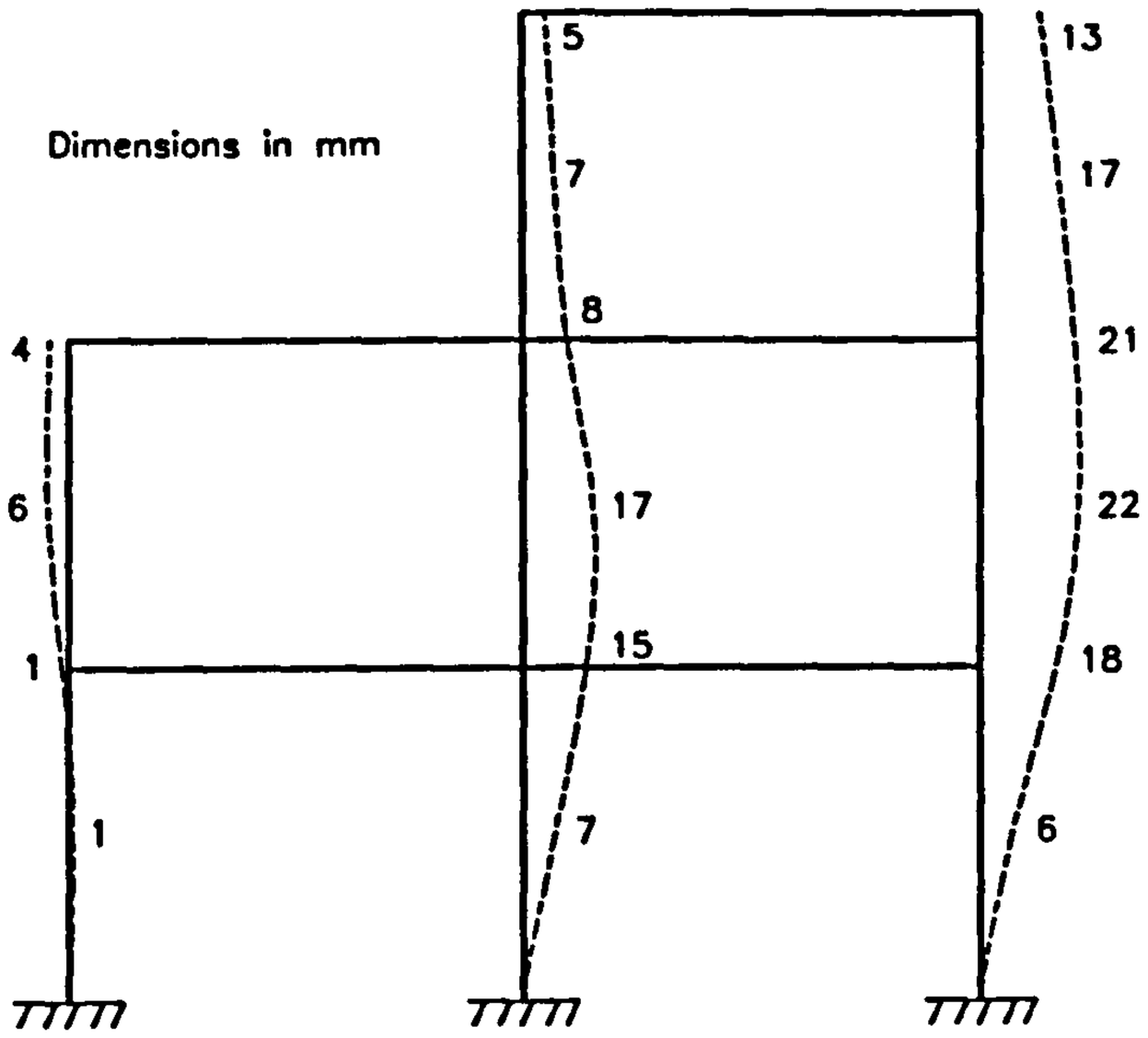

(a). Frame 1

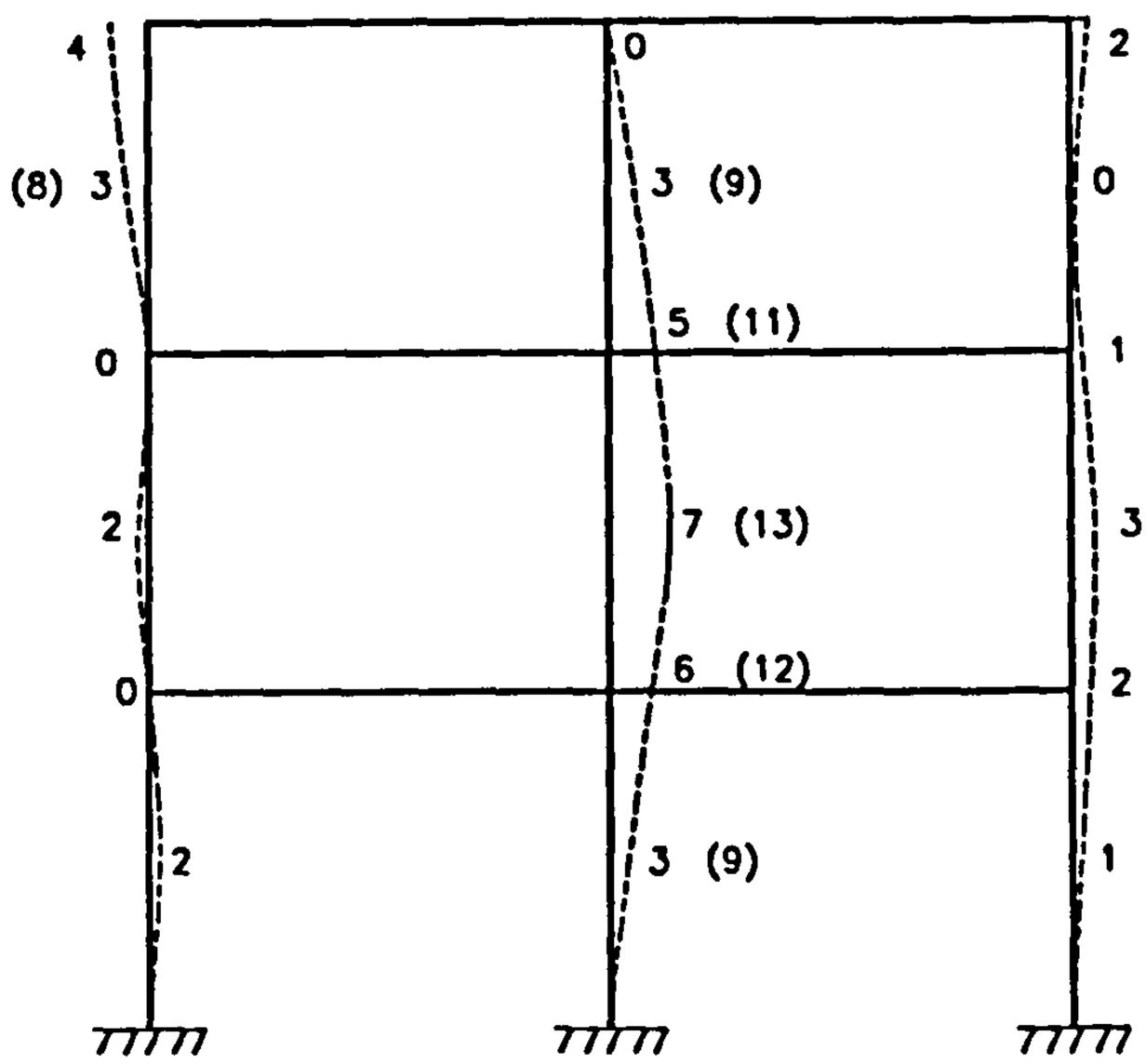

1. Dimensions in mm
2. Values not in bracket are based on the measured initial out-of-straightness
3. Values in bracket are for larger initial out-of-straightness model

(b). Frame 2

Figure 4.3 Initial out-of-straightness in columns

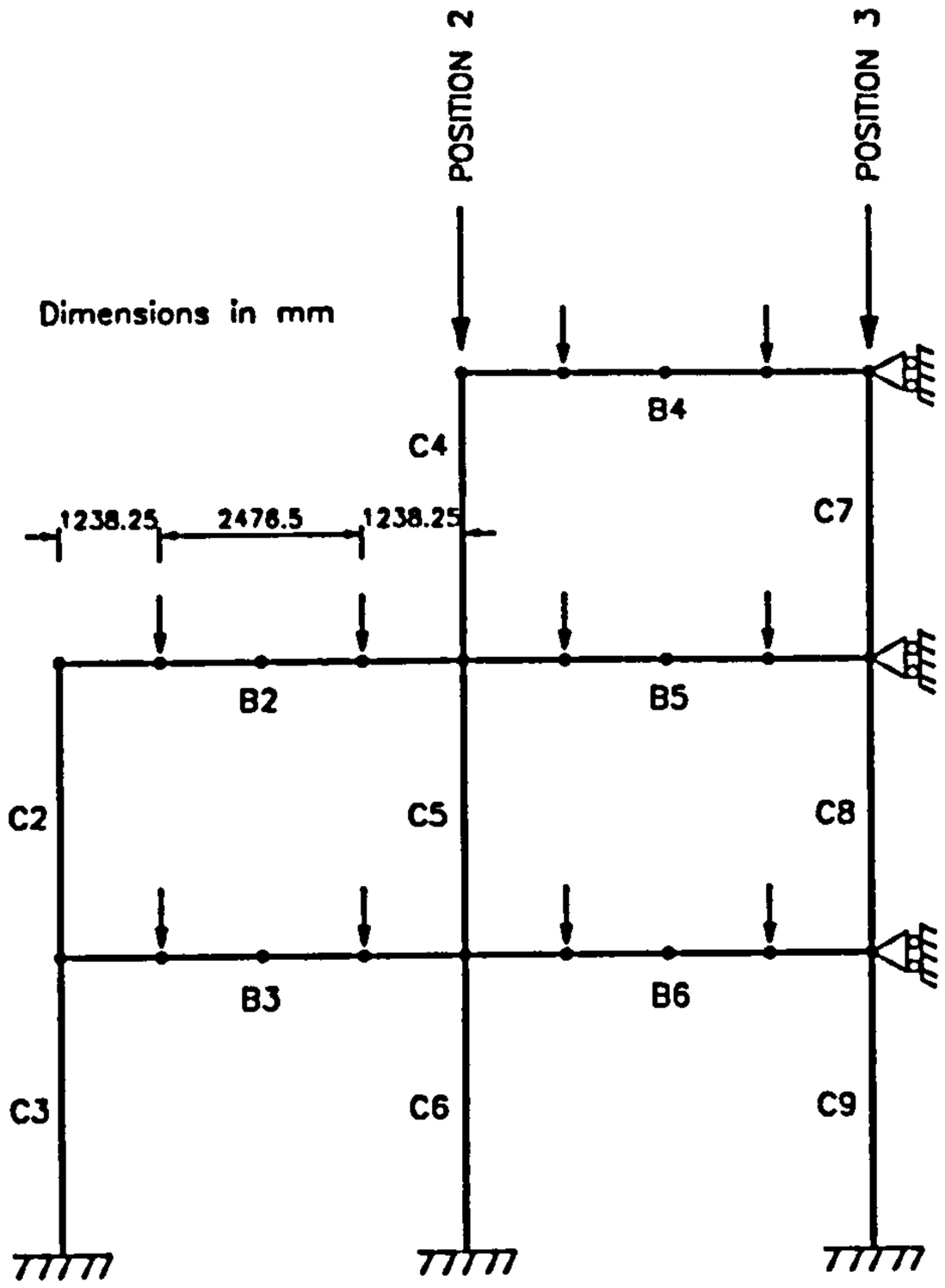

(a). Frame 1

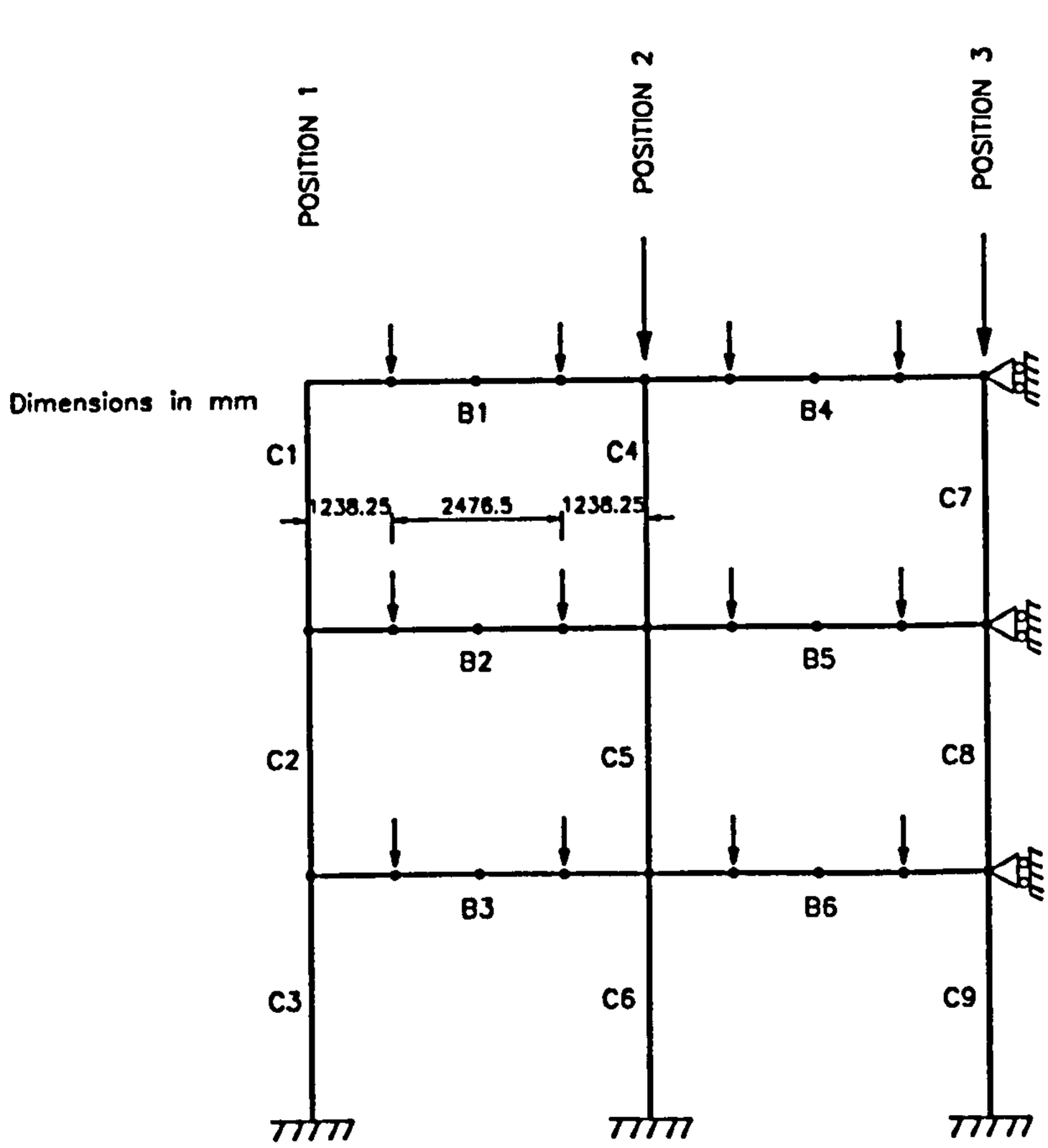

(b). Frame 2

Figure 4.4 Loading arrangement

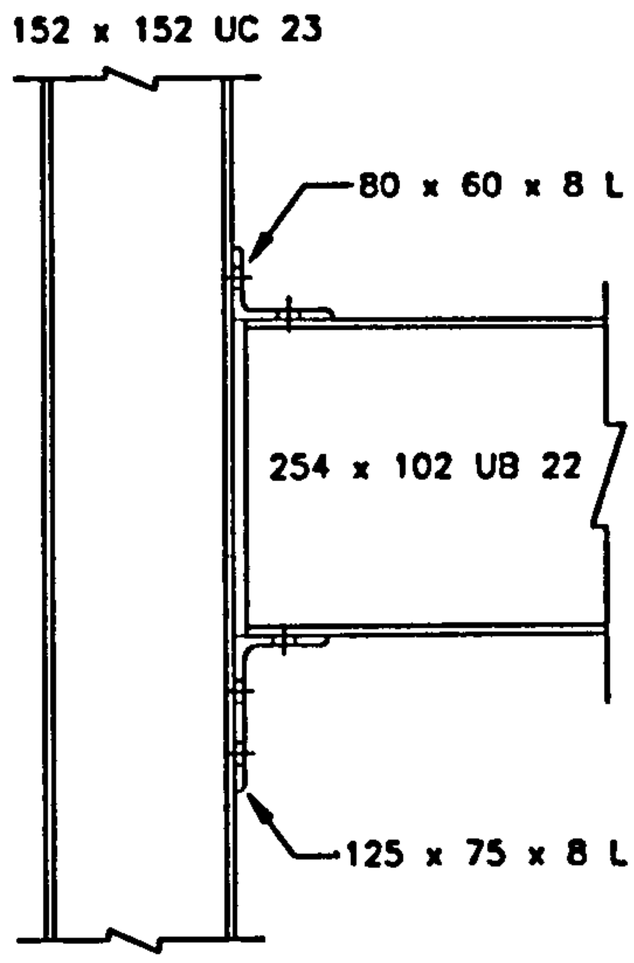

(a). Major axis connection employed in frame 1

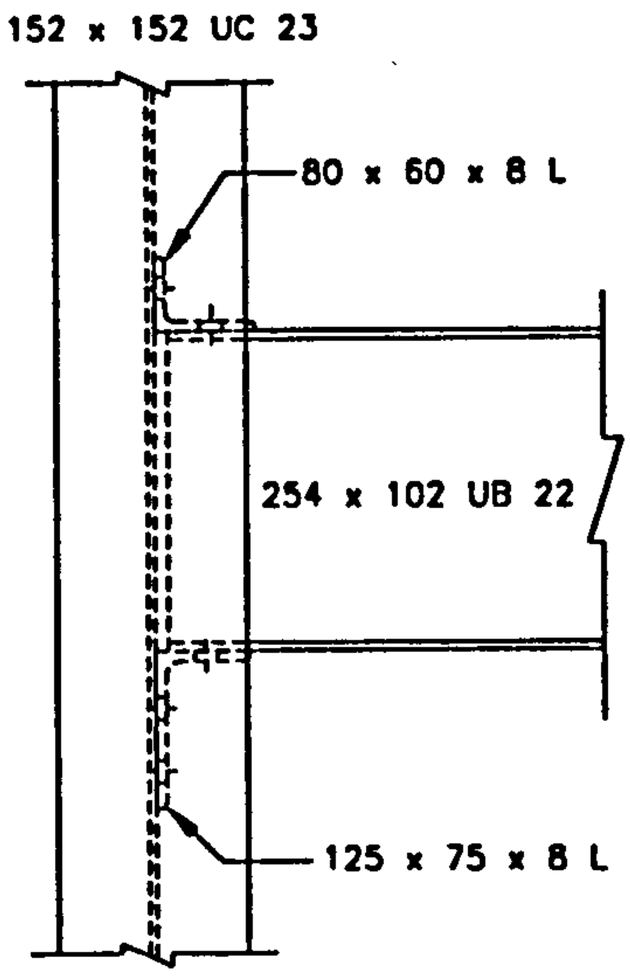

(b). Minor axis connection employed in frame 2

Figure 4.5 Semi-rigid connections employed in the test frames

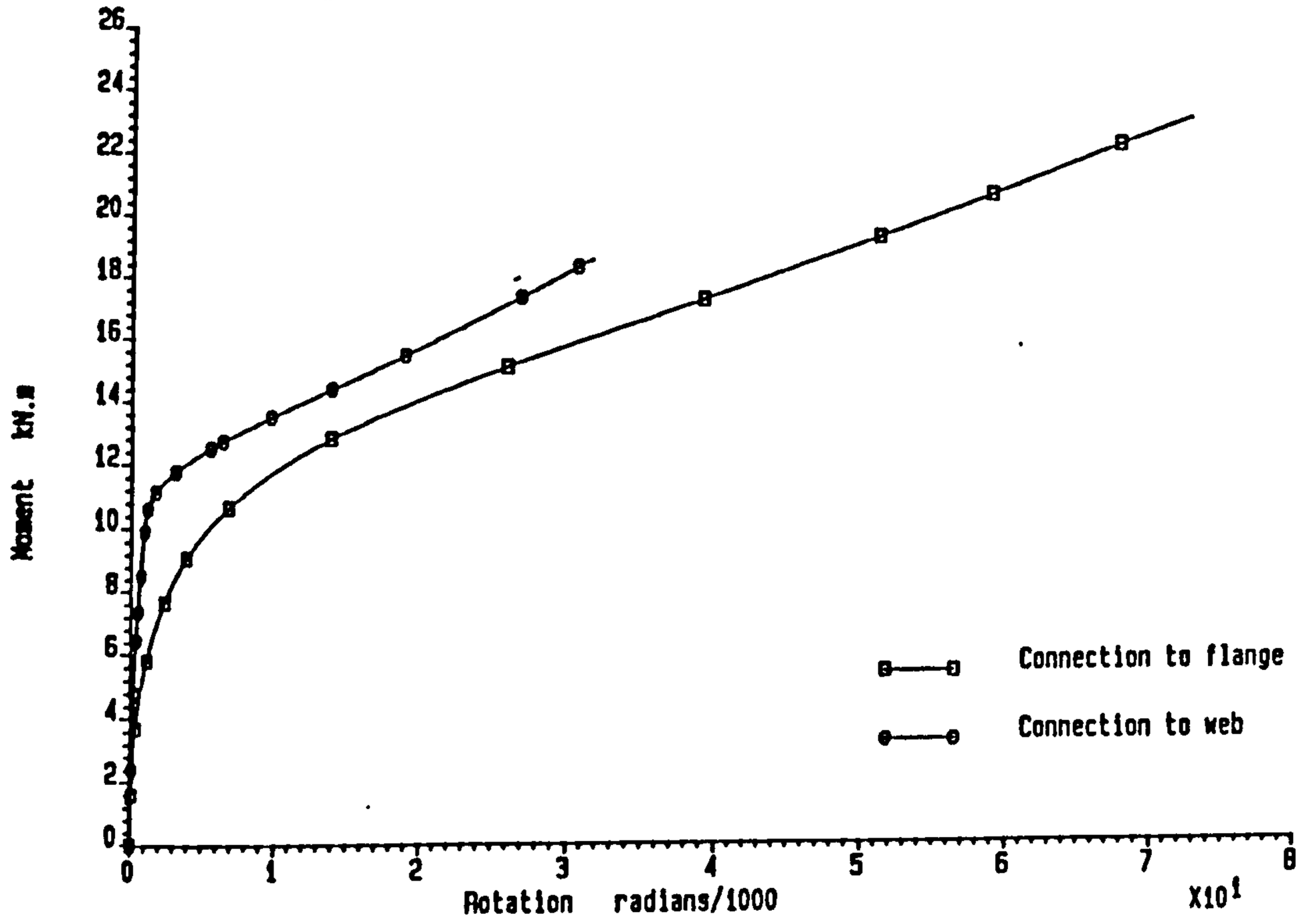

Figure 4.6(a) Experimental M-ϕ curves [4-1]

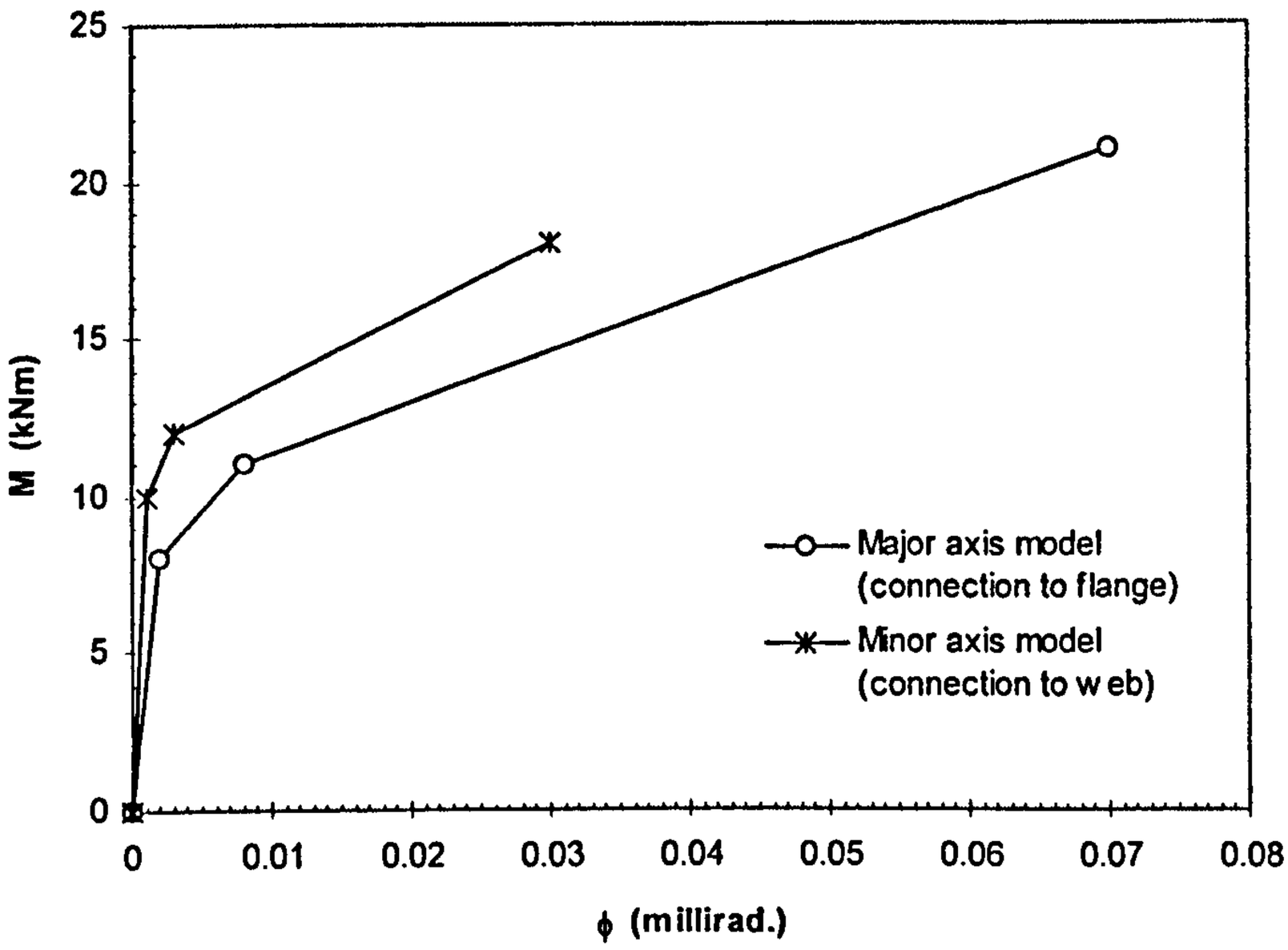

Figure 4.6(b) Trilinear M-ϕ curves of Figure 4.6(a) as used in the analysis

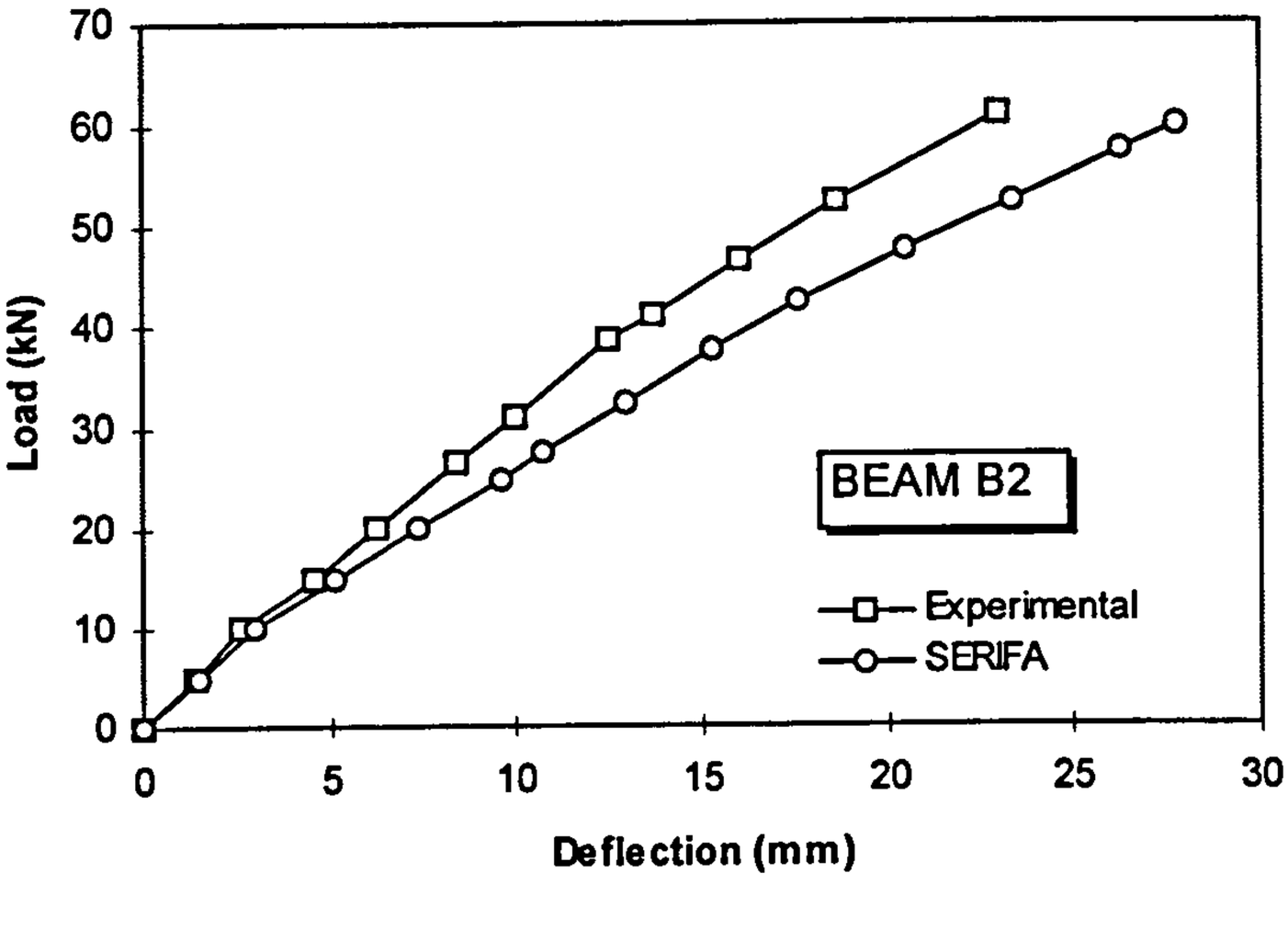

(a). Beam B2

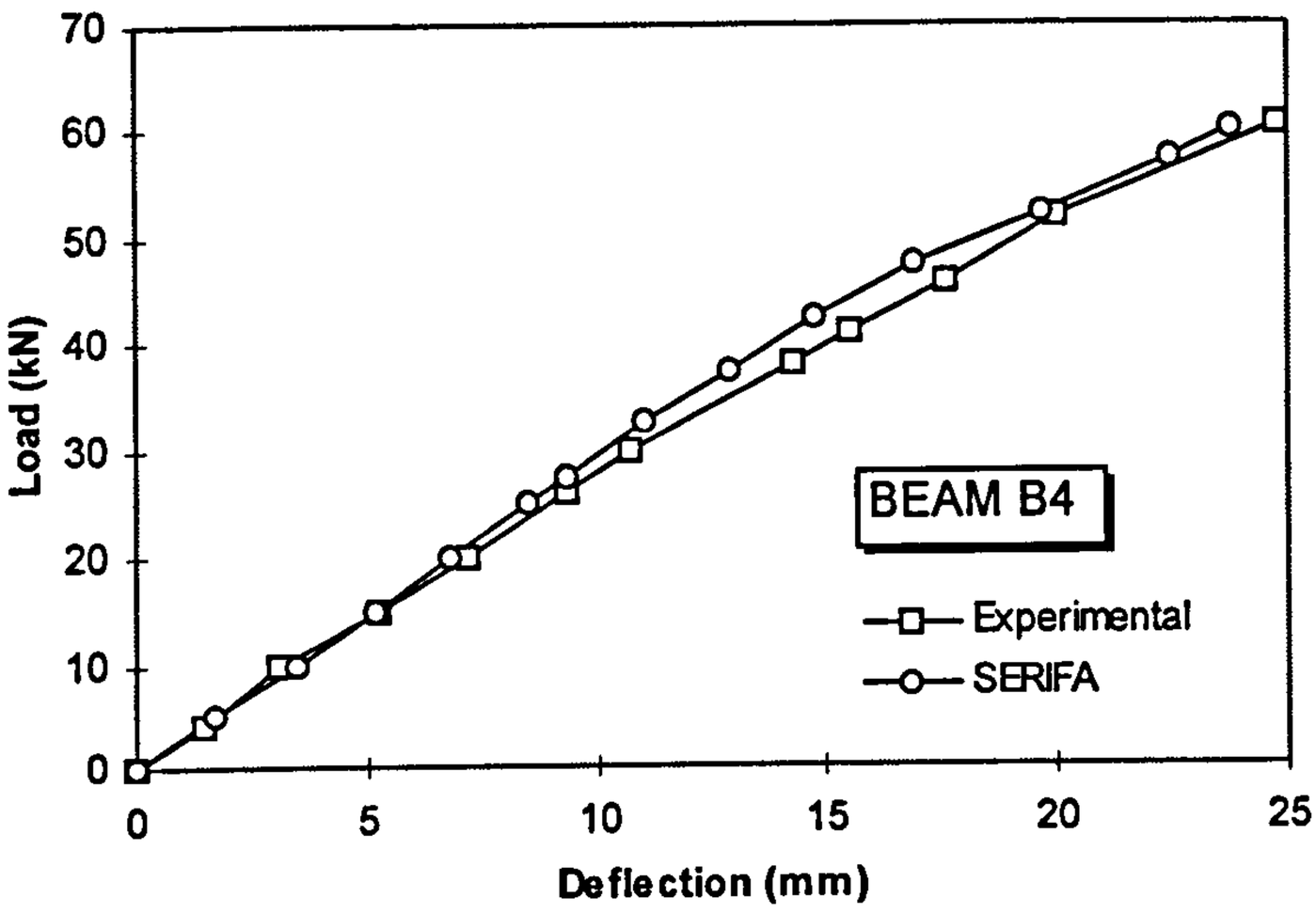

(b). Beam B4

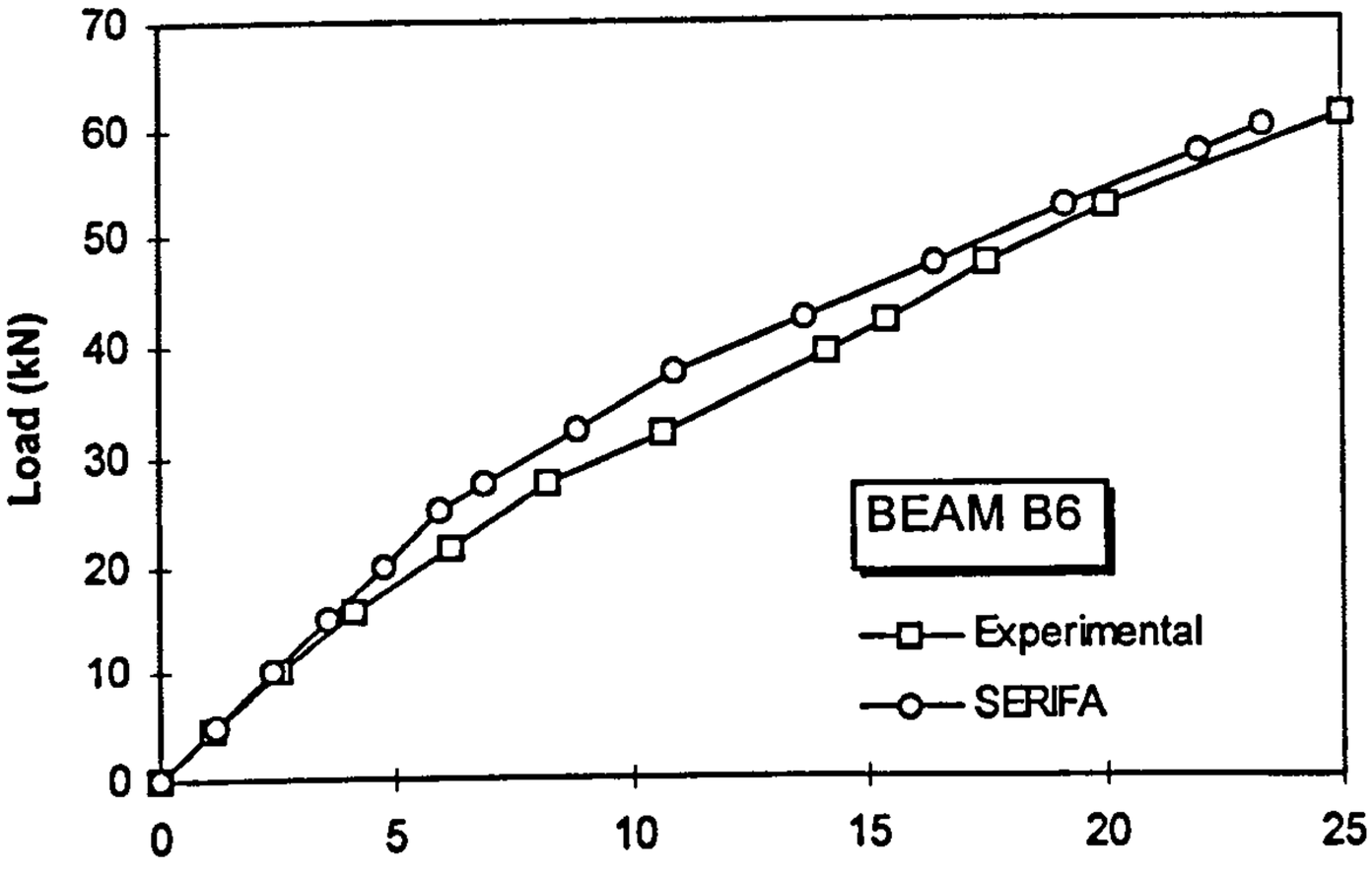

(c). Beam B6

Figure 4.7 Comparison of the experimental and analytical beam load-deflection responses for frame 1

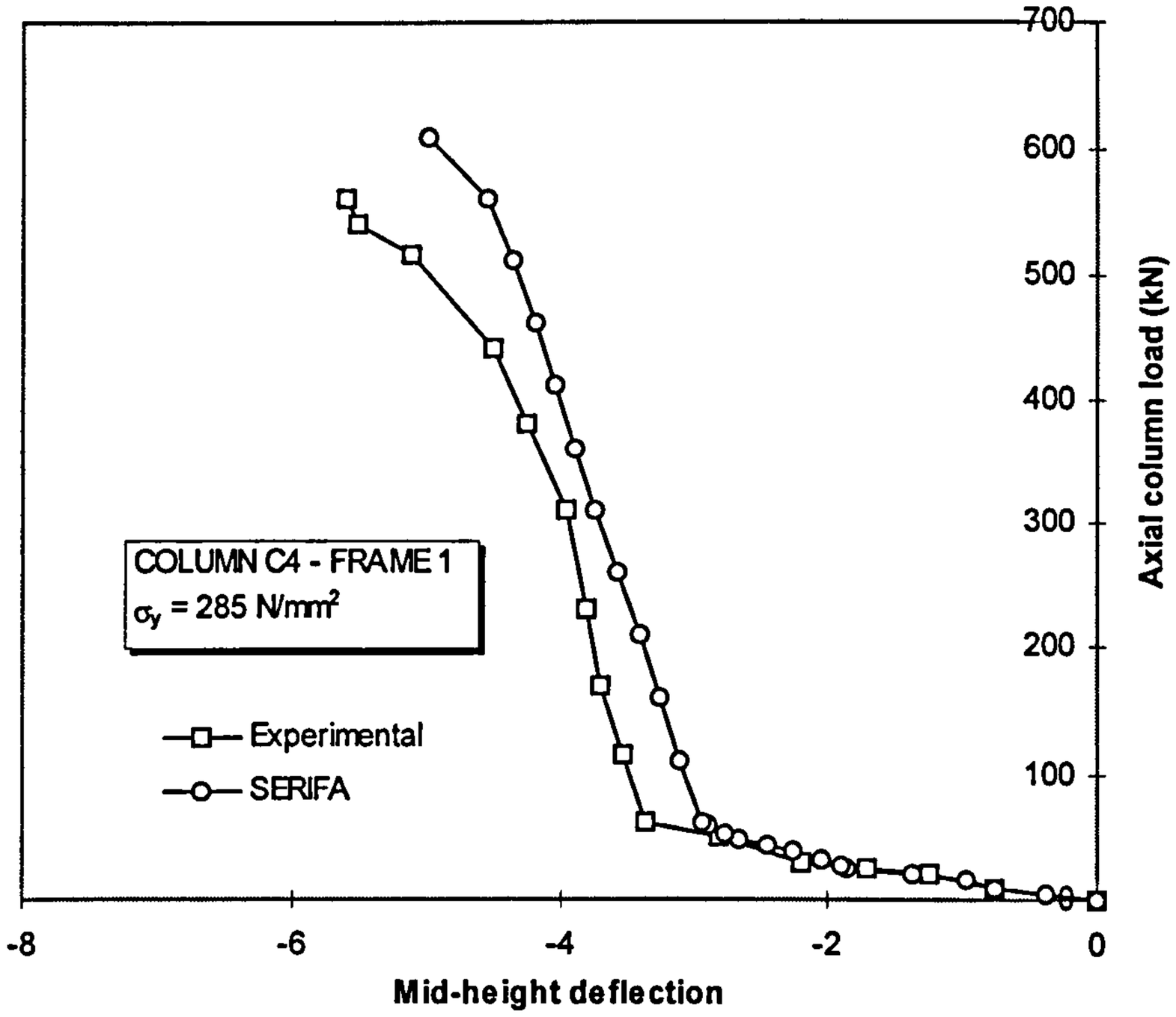

Figure 4.8(a) Comparison between experimental and analytical load-deflection response using $\sigma_y = 285$ N/mm^2 - Column C4/frame 1

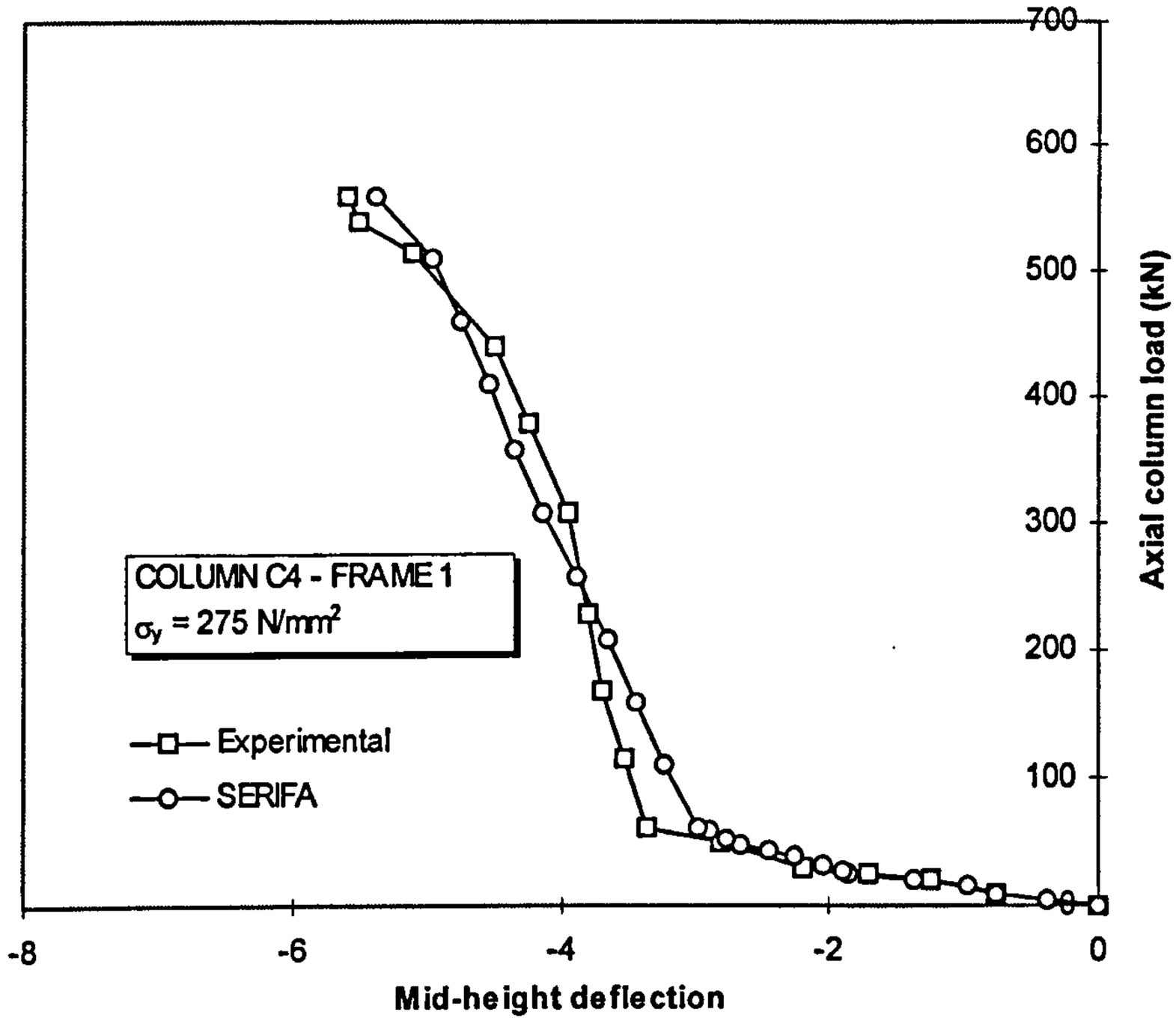

Figure 4.8(b) Comparison between experimental and analytical load-deflection response using $\sigma_y = 275$ N/mm^2 - Column C4/frame 1

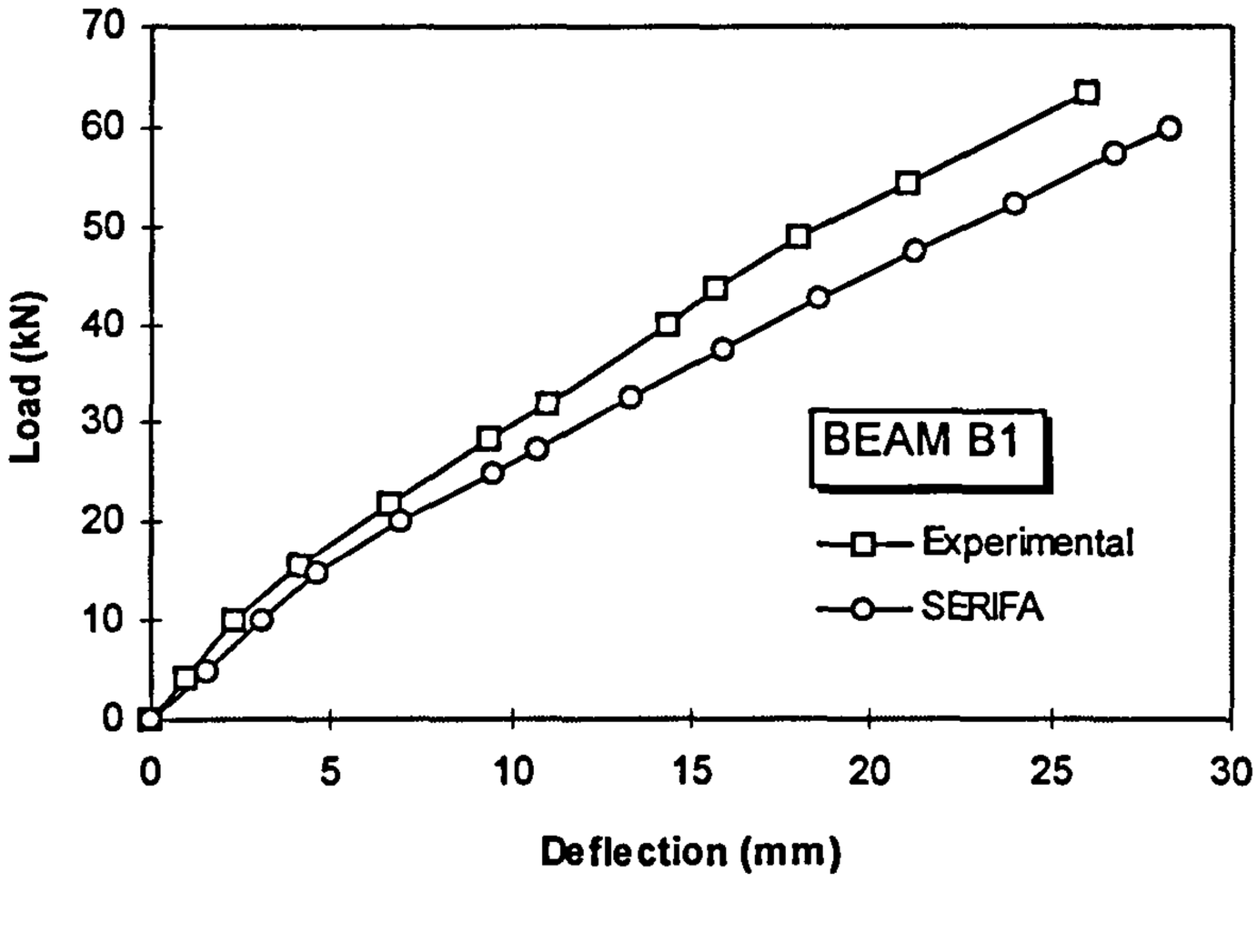

(a). Beam B1

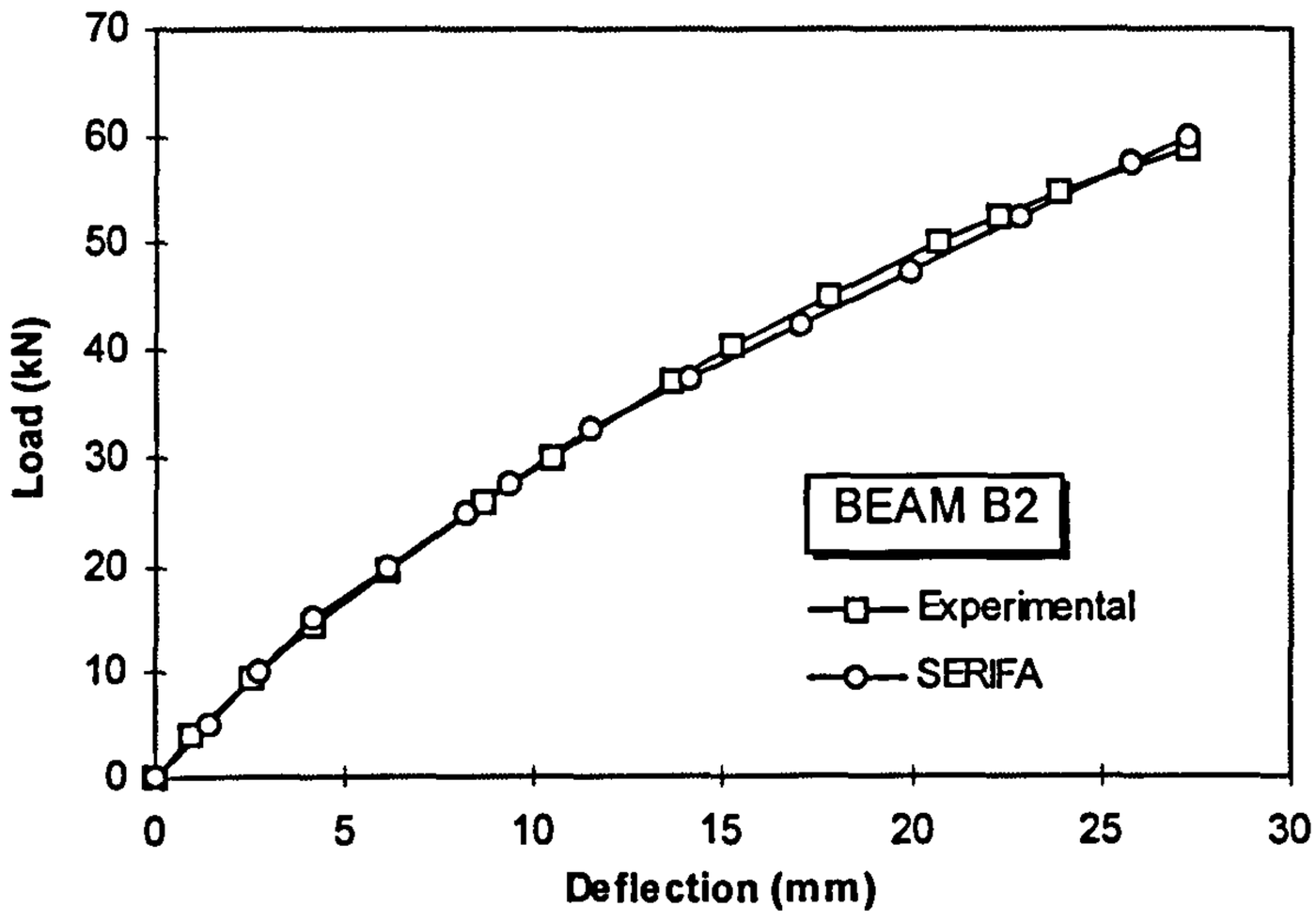

(b). Beam B2

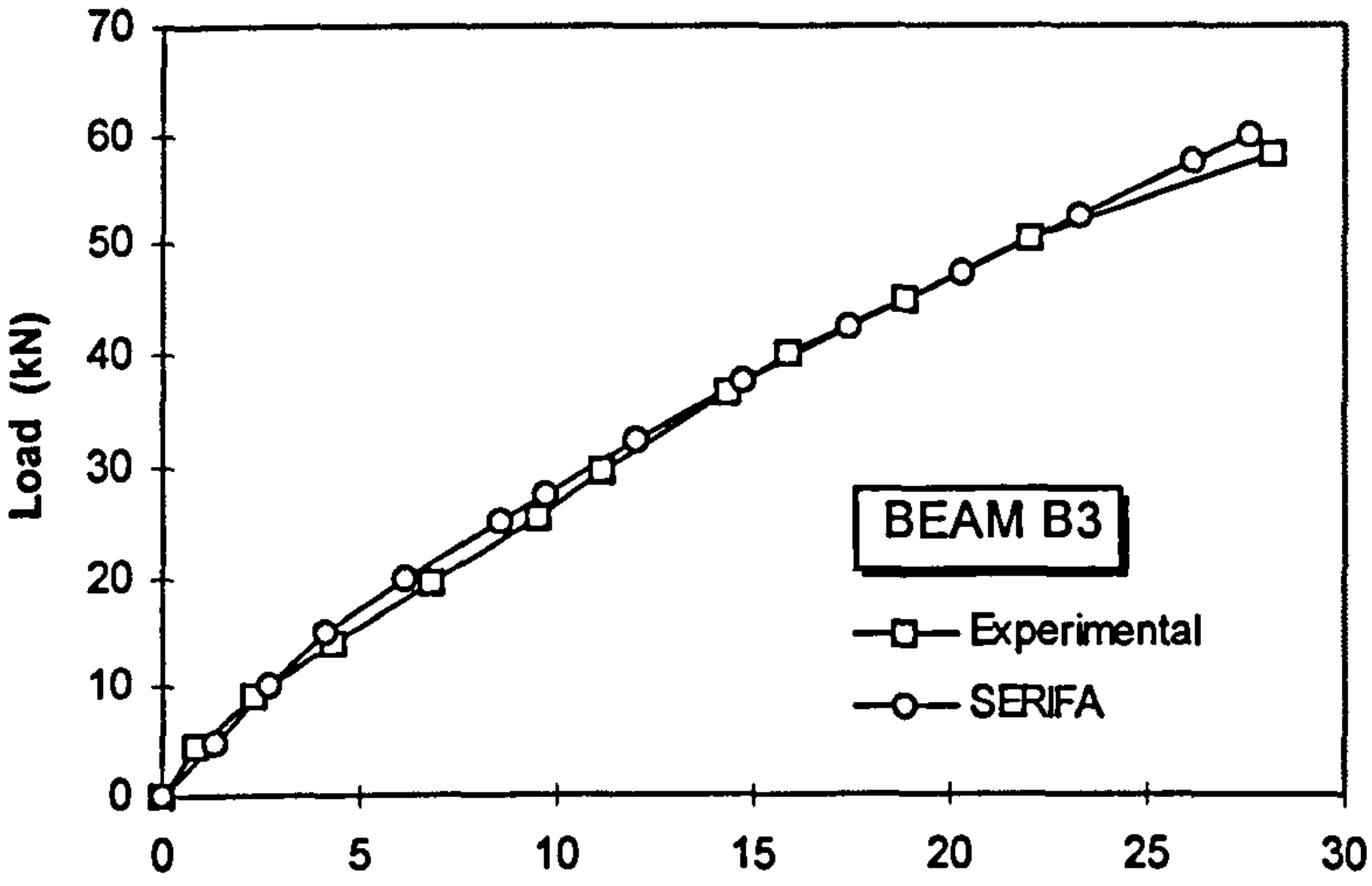

(c). Beam B3

Figure 4.9 Comparison of the experimental and analytical beam load-deflection responses for frame 2 (continue)

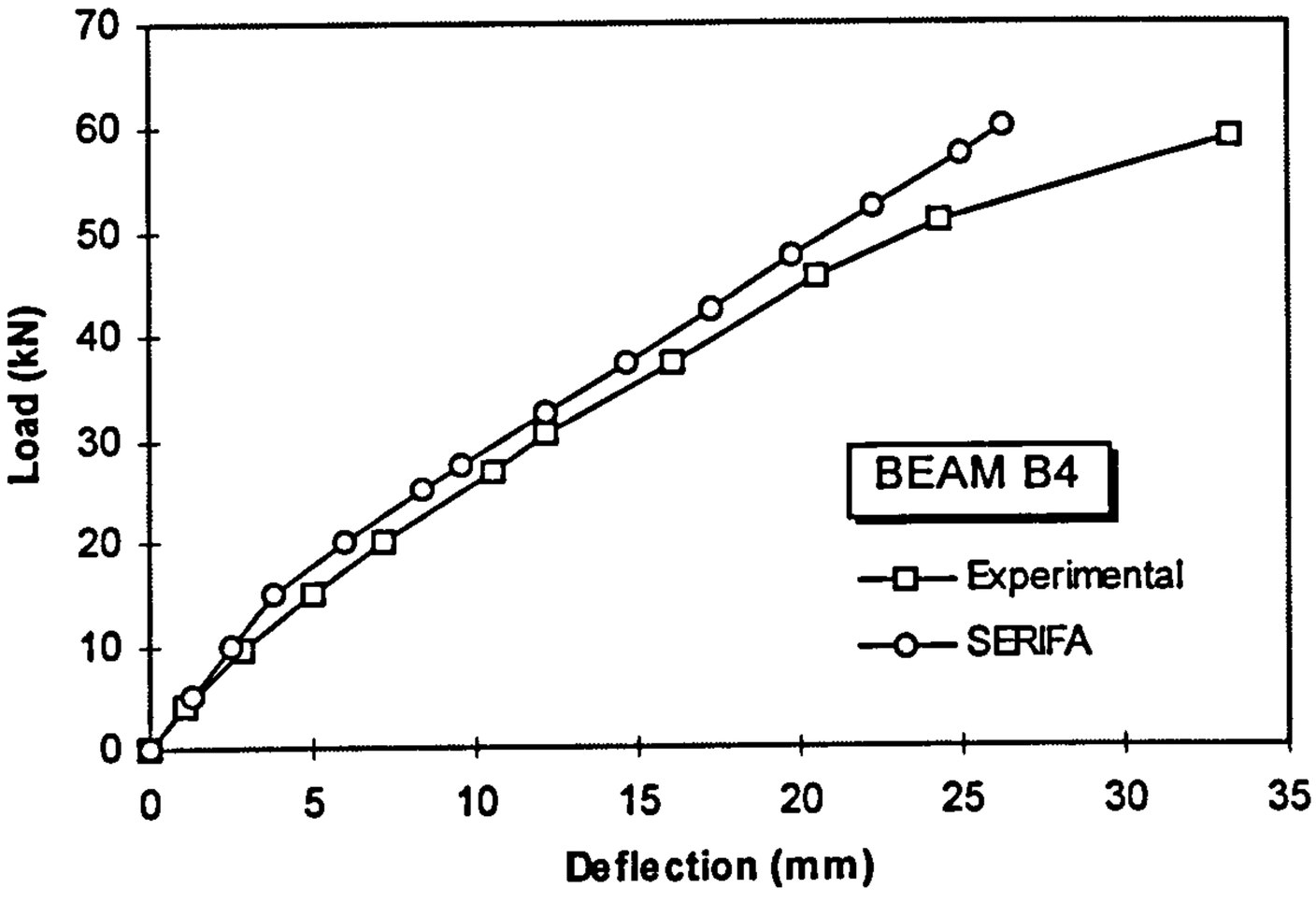

(d). Beam B4

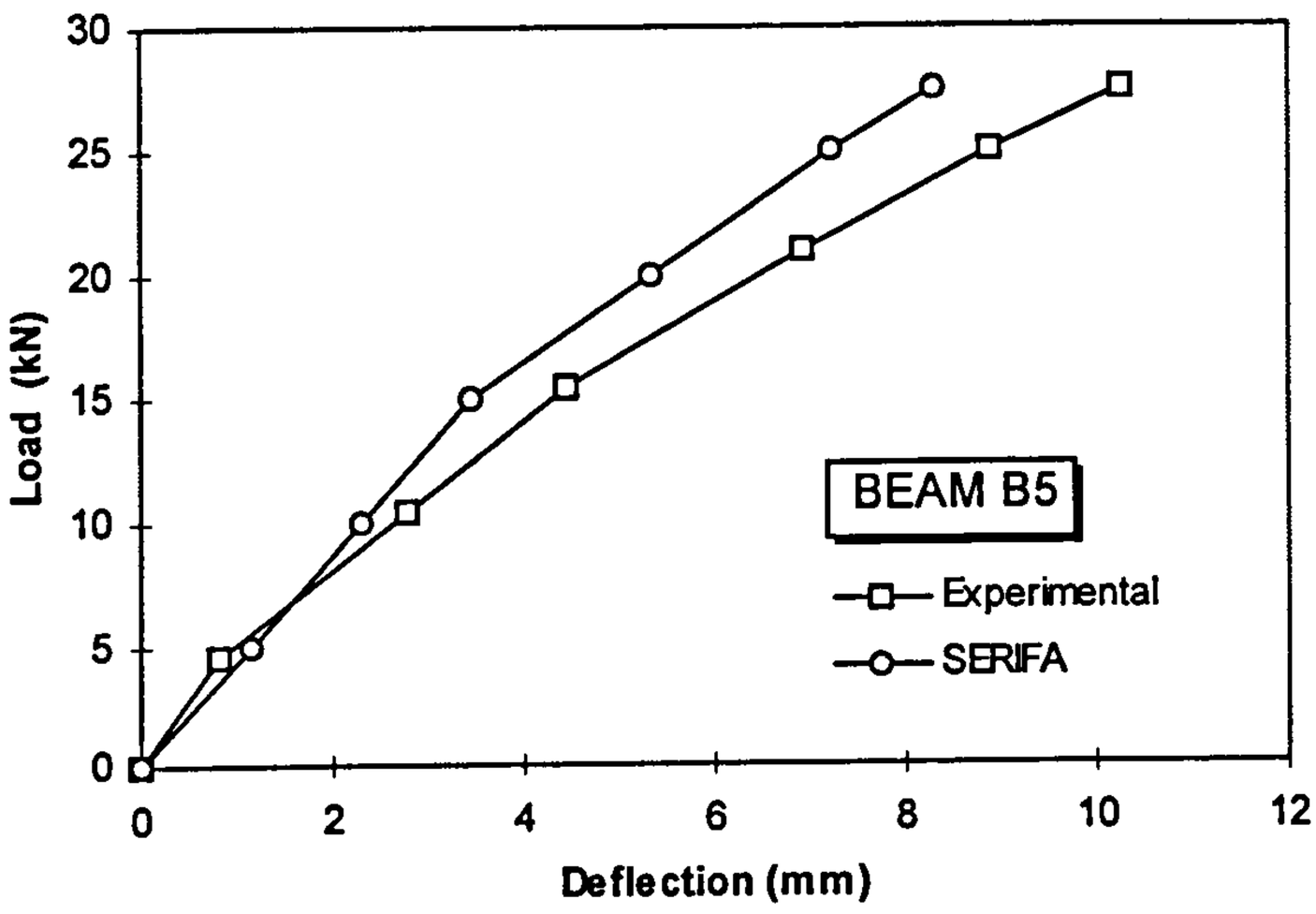

(e). Beam B5

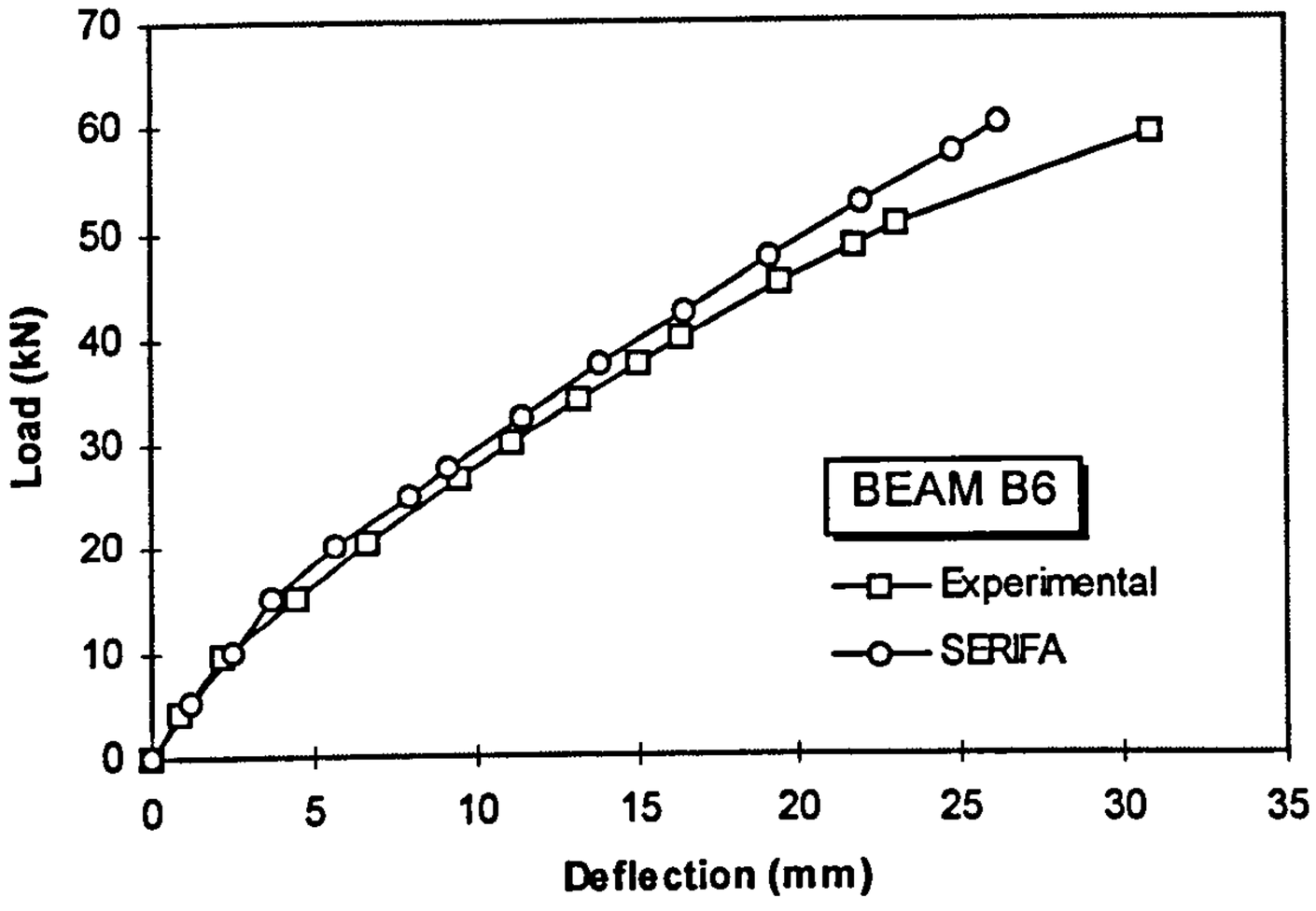

(f). Beam B6

Figure 4.9 Comparison of the experimental and analytical beam load-deflection responses for frame 2

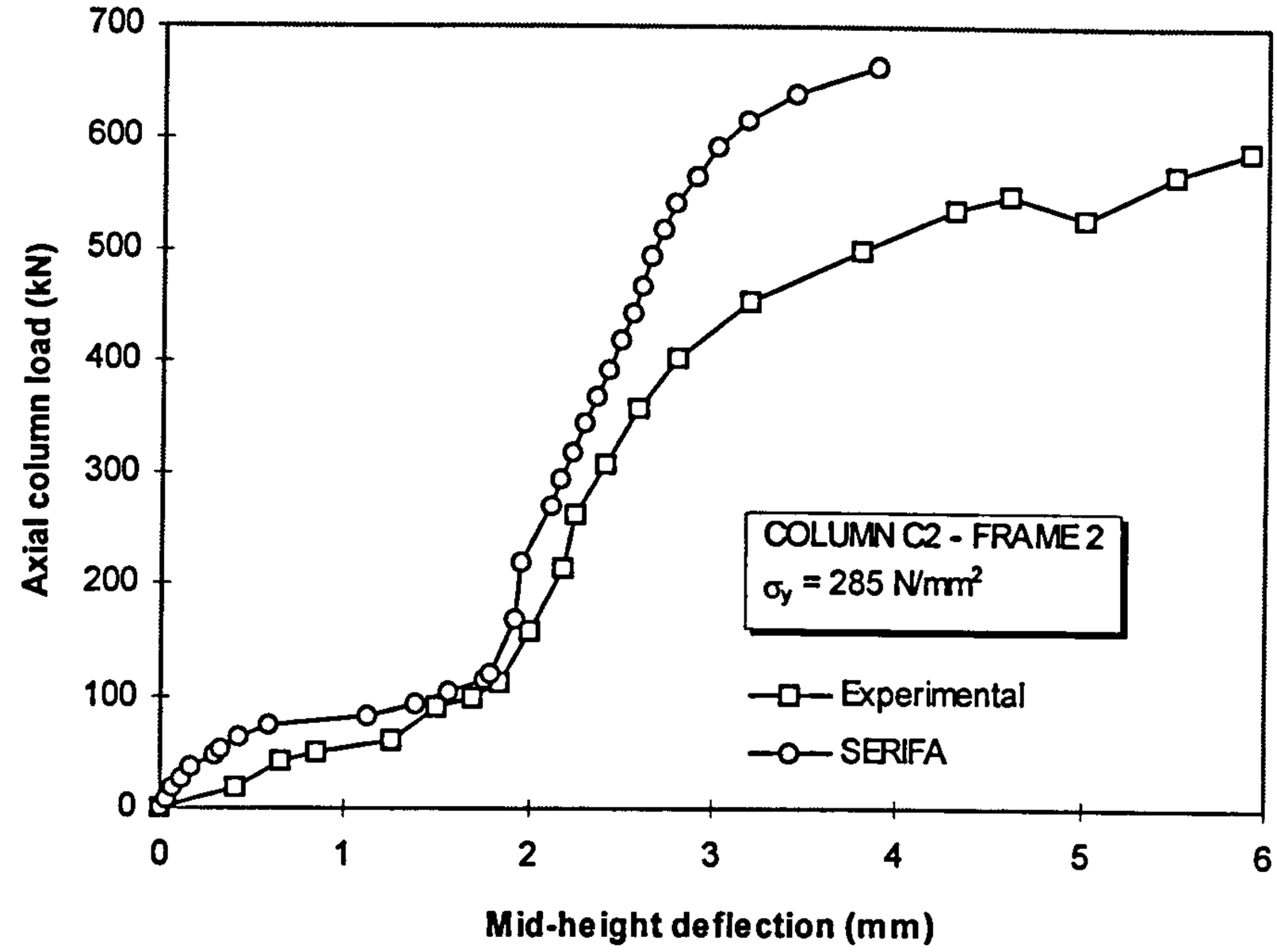

Figure 4.10(a) Comparison of the experimental and analytical load-deflection responses using $\sigma_y = 285$ N/mm^2 and the actual initial out-of-straightness : Column C2/frame 2

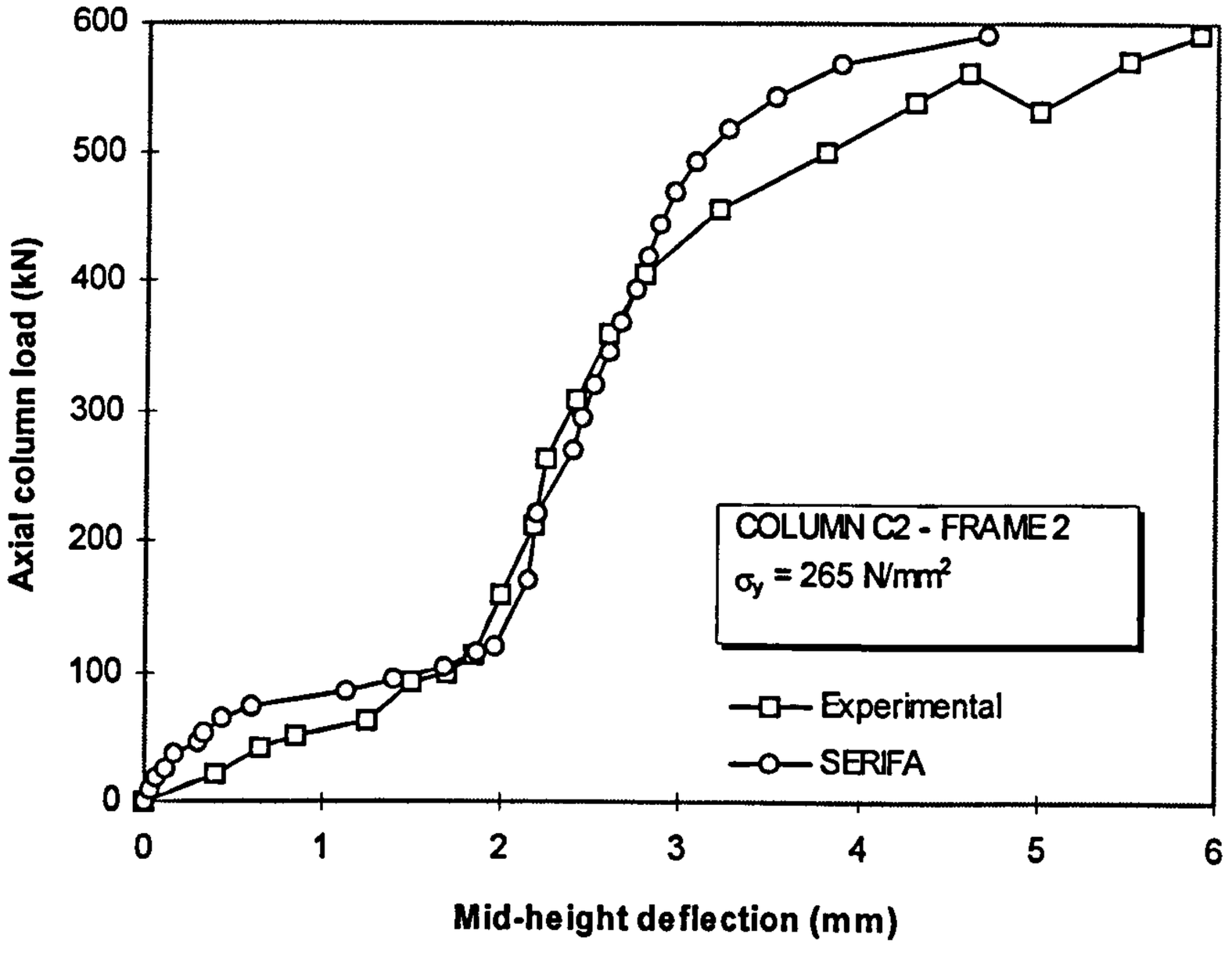

Figure 4.10(b) Comparison of the experimental and analytical load-deflection responses using $\sigma_y = 265$ N/mm^2 and the larger initial out-of-straightness : Column C2/frame 2

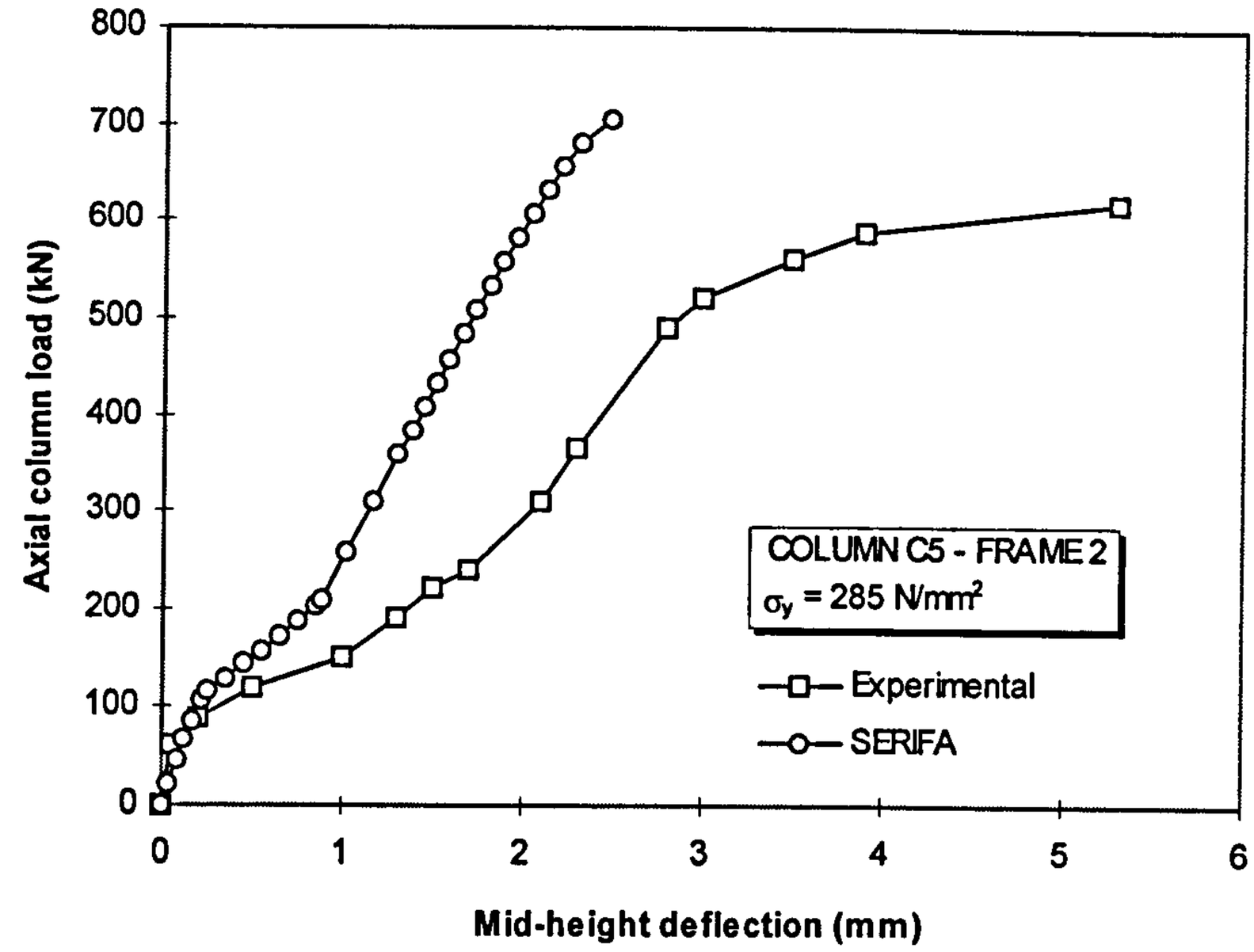

Figure 4.11(a) Comparison of the experimental and analytical load-deflection responses using the actual initial out-of-straightness : Column C5/frame 2

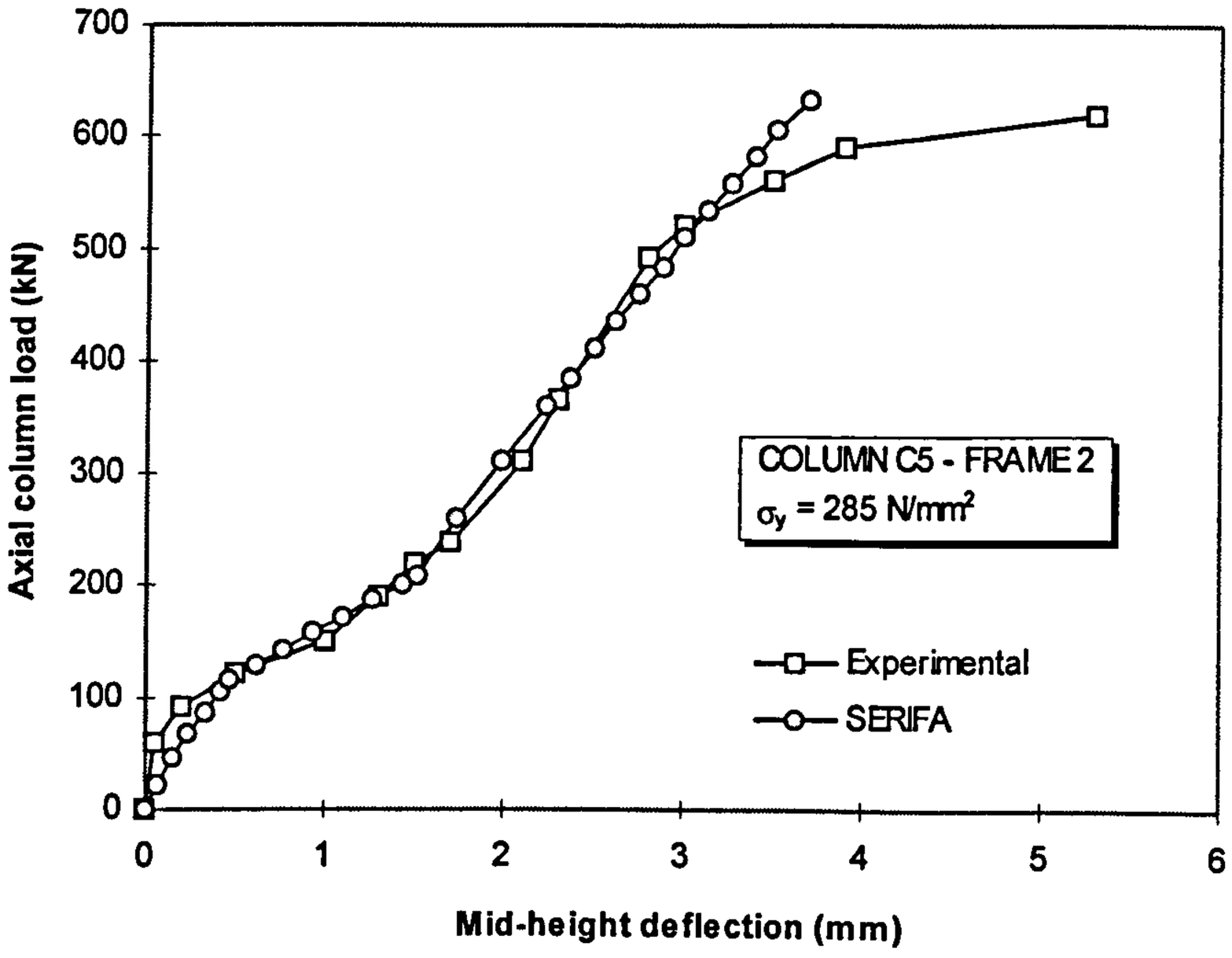

Figure 4.11(b) Comparison of the experimental and analytical load-deflection responses using the larger initial out-of-straightness : Column C5/frame 2

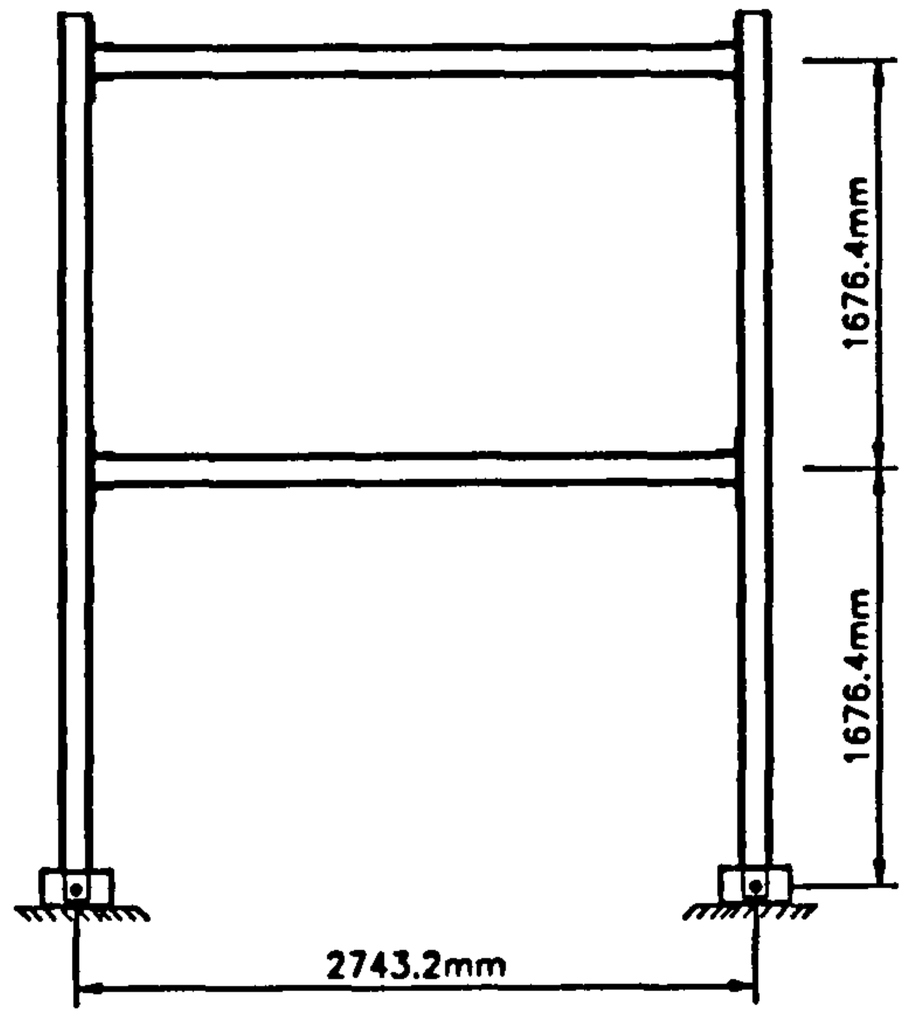

Figure 4.12 Stelmack's sway frame

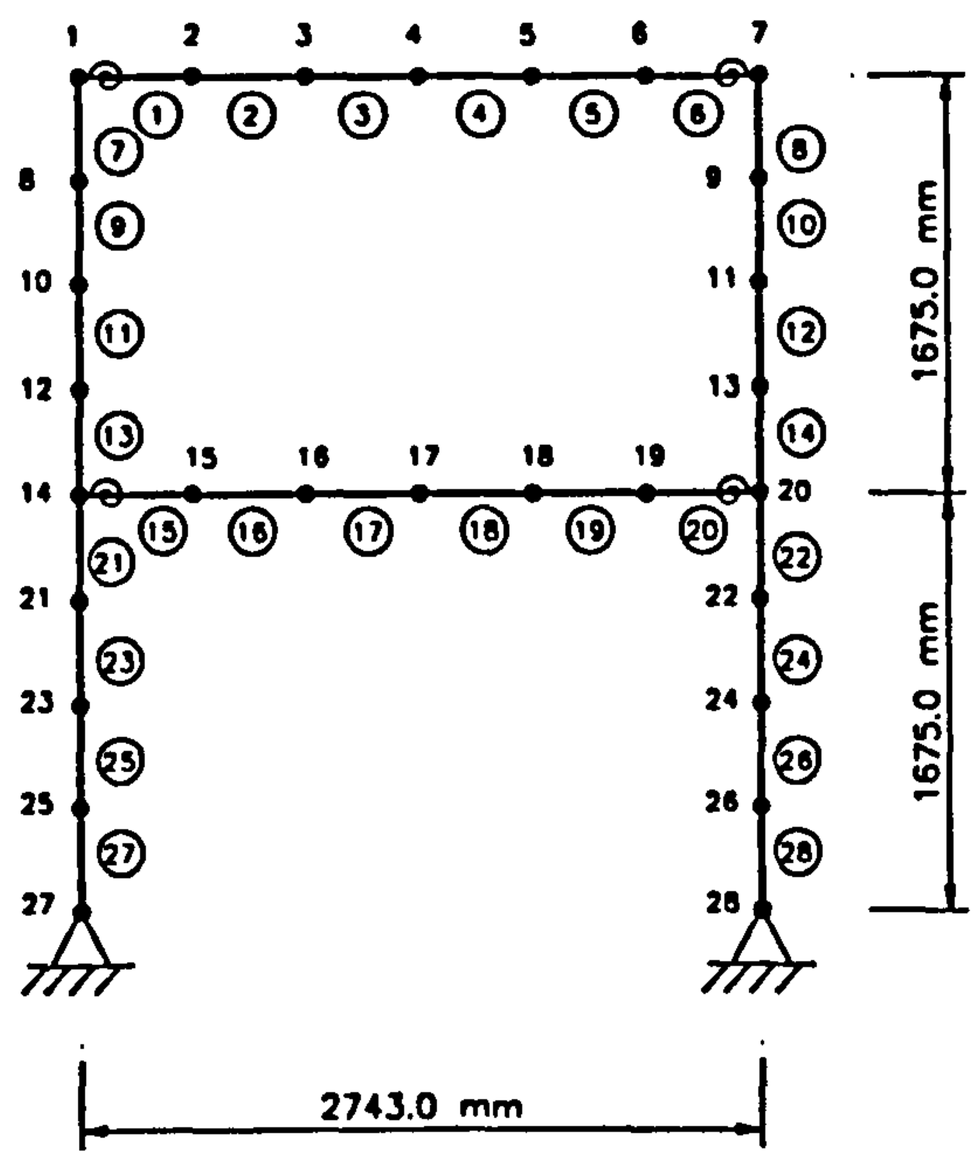

Figure 4.13 Analytical model of the Stelmack's sway frame

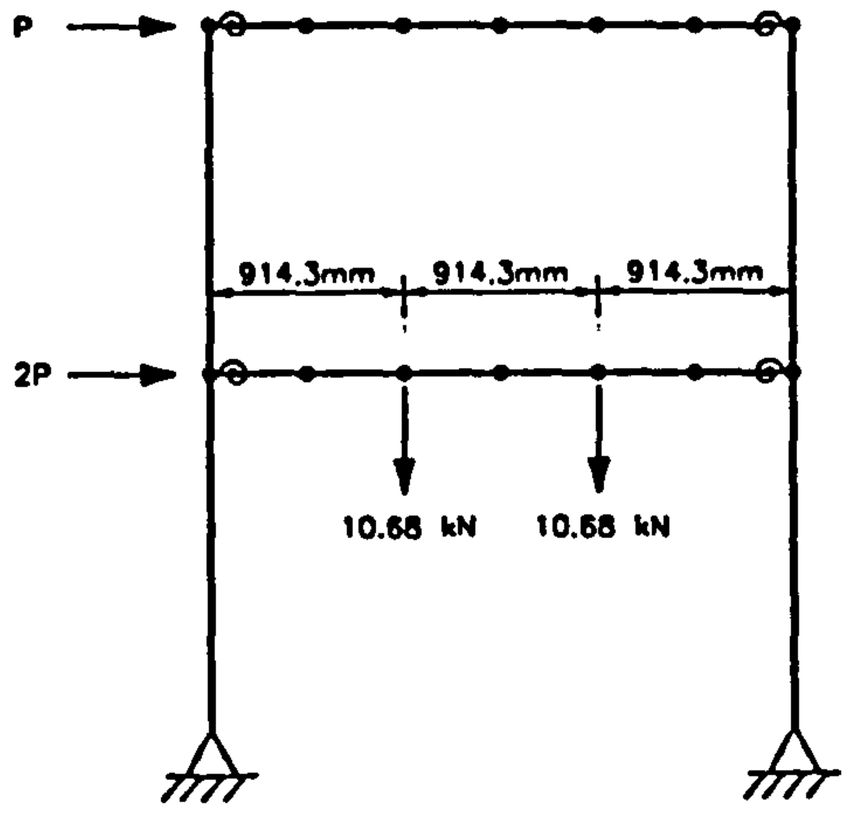

Figure 4.14 Loading arrangements

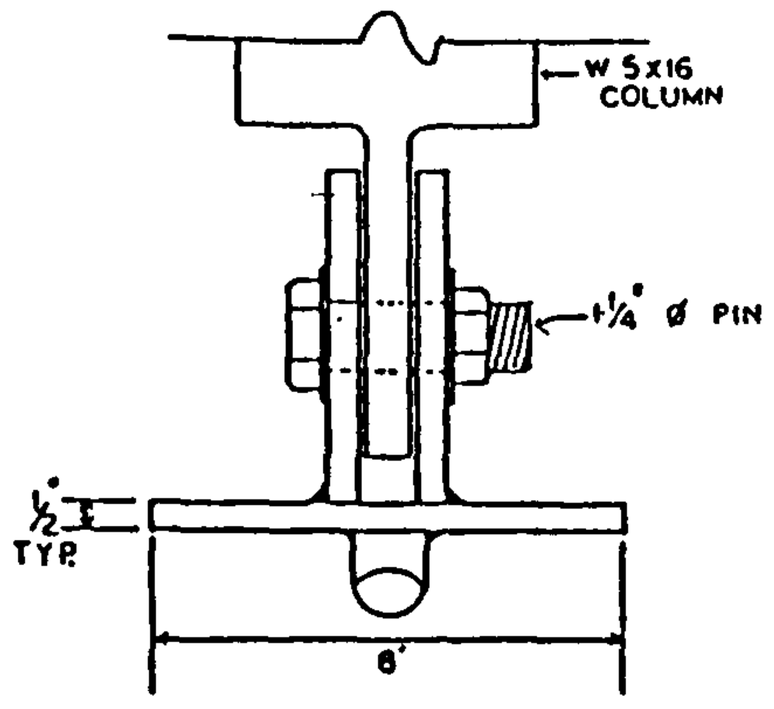

Figure 4.15 Pinned support at column base [4–5]

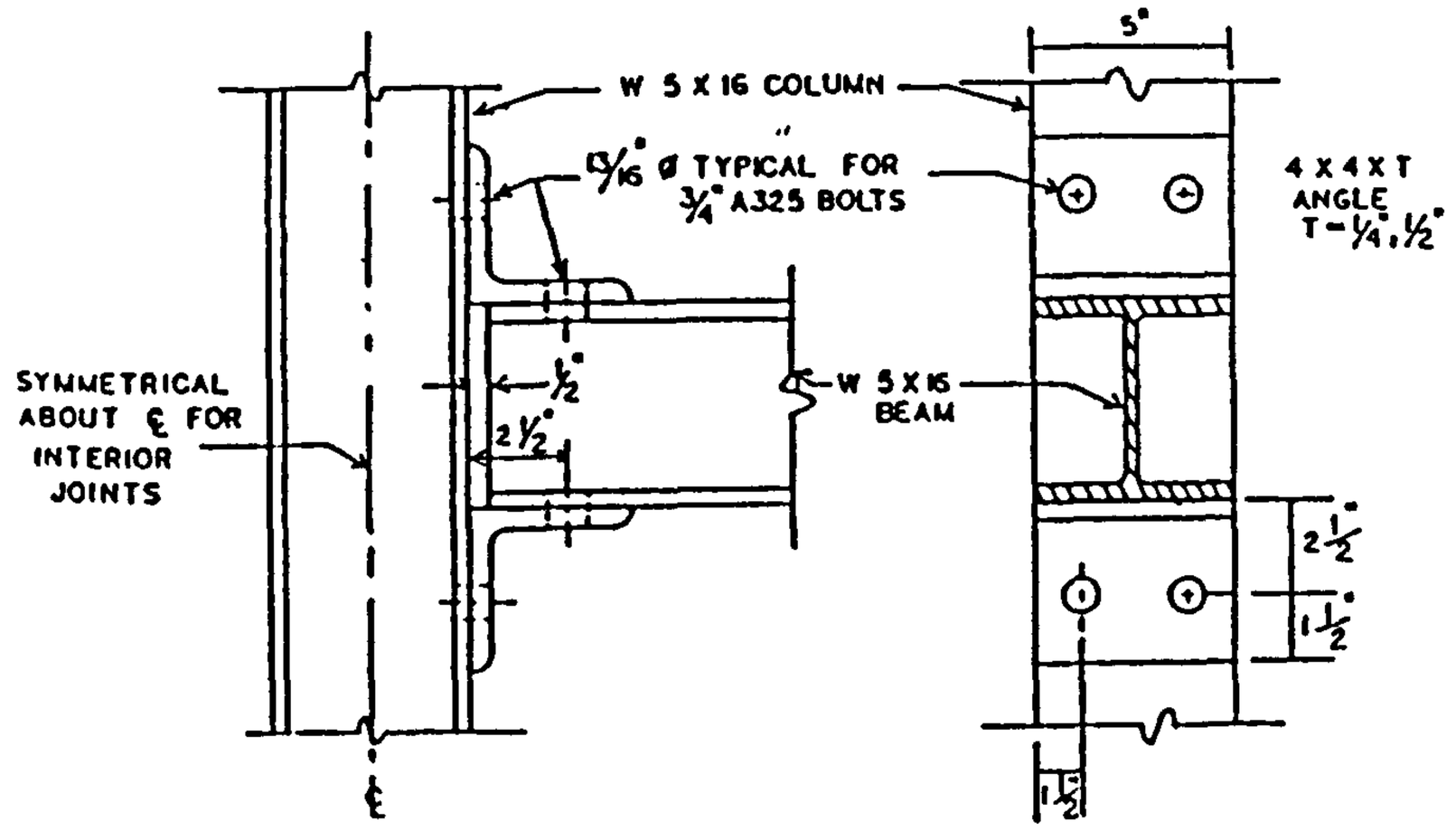

Figure 4.16 Details of beam-to-column connections [4-5]

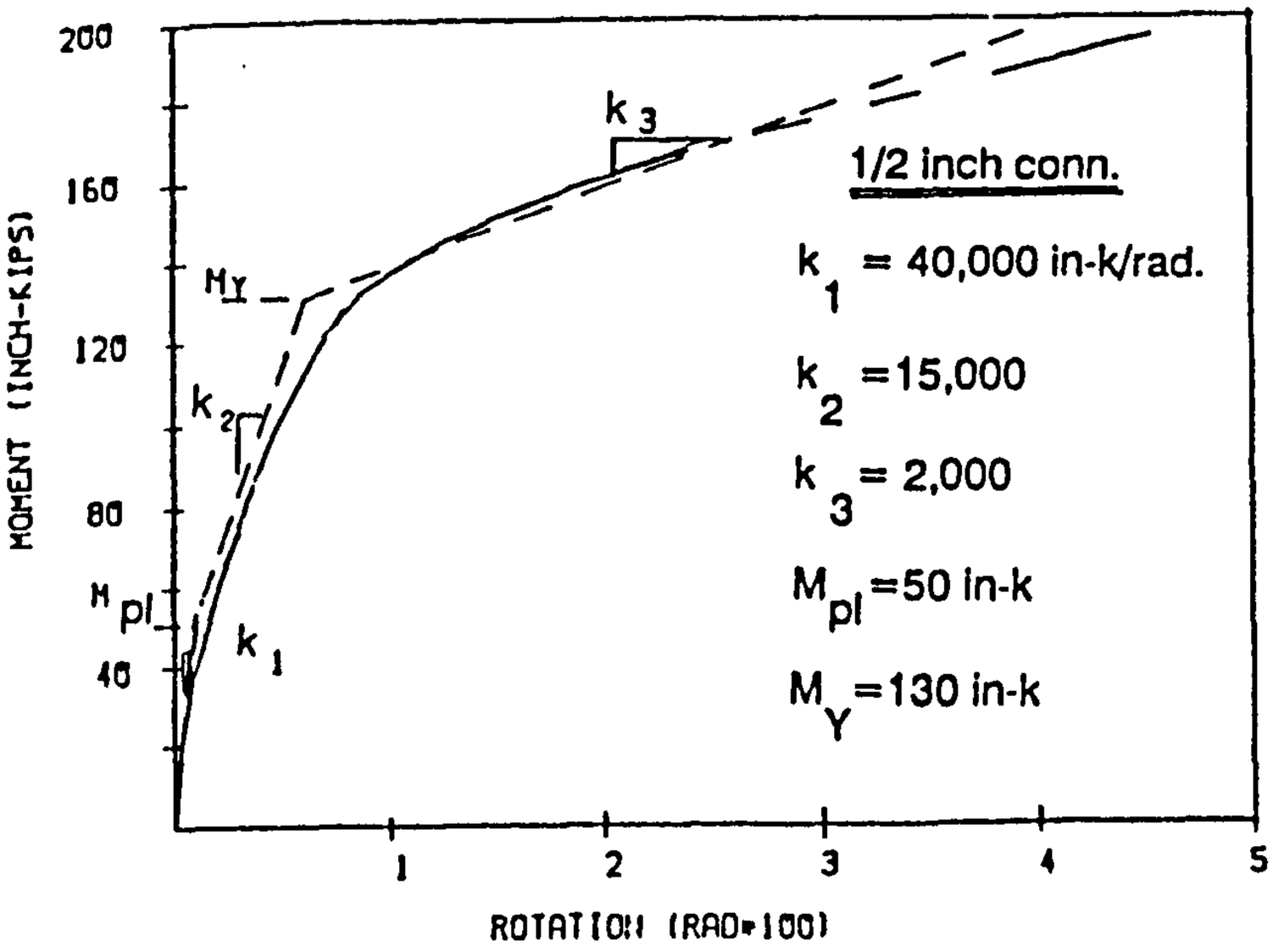

Figure 4.17 Trilinear M-ϕ curve with the use of 1/2 inch thick angle connections [4-4], [4-5]

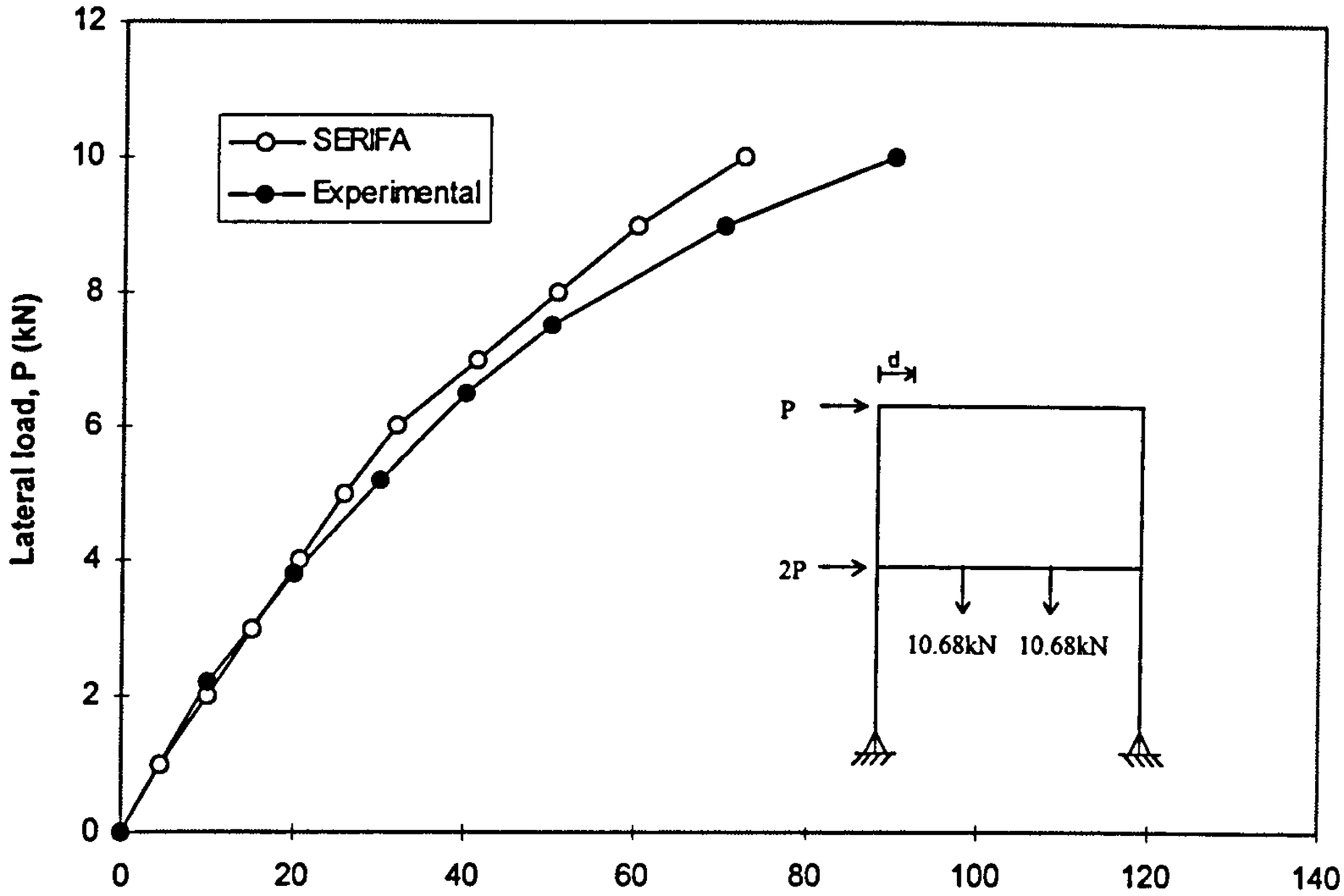

Figure 4.18(a) Comparison of the experimental and analytical load-deflection responses at the first storey of the Stelmack's sway frame

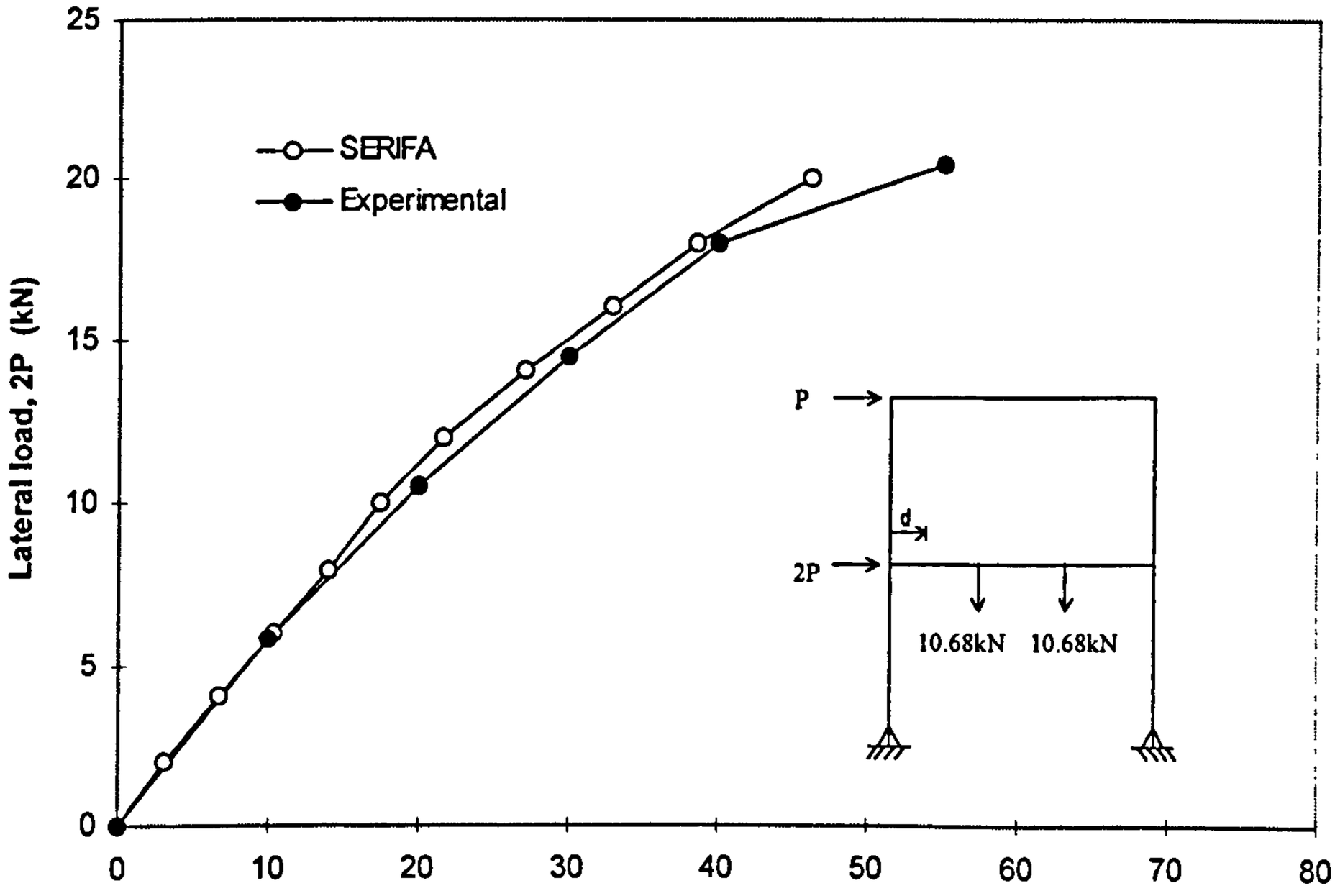

Figure 4.18(b) Comparison of the experimental and analytical load-deflection responses at the second storey of the Stelmack's sway frame

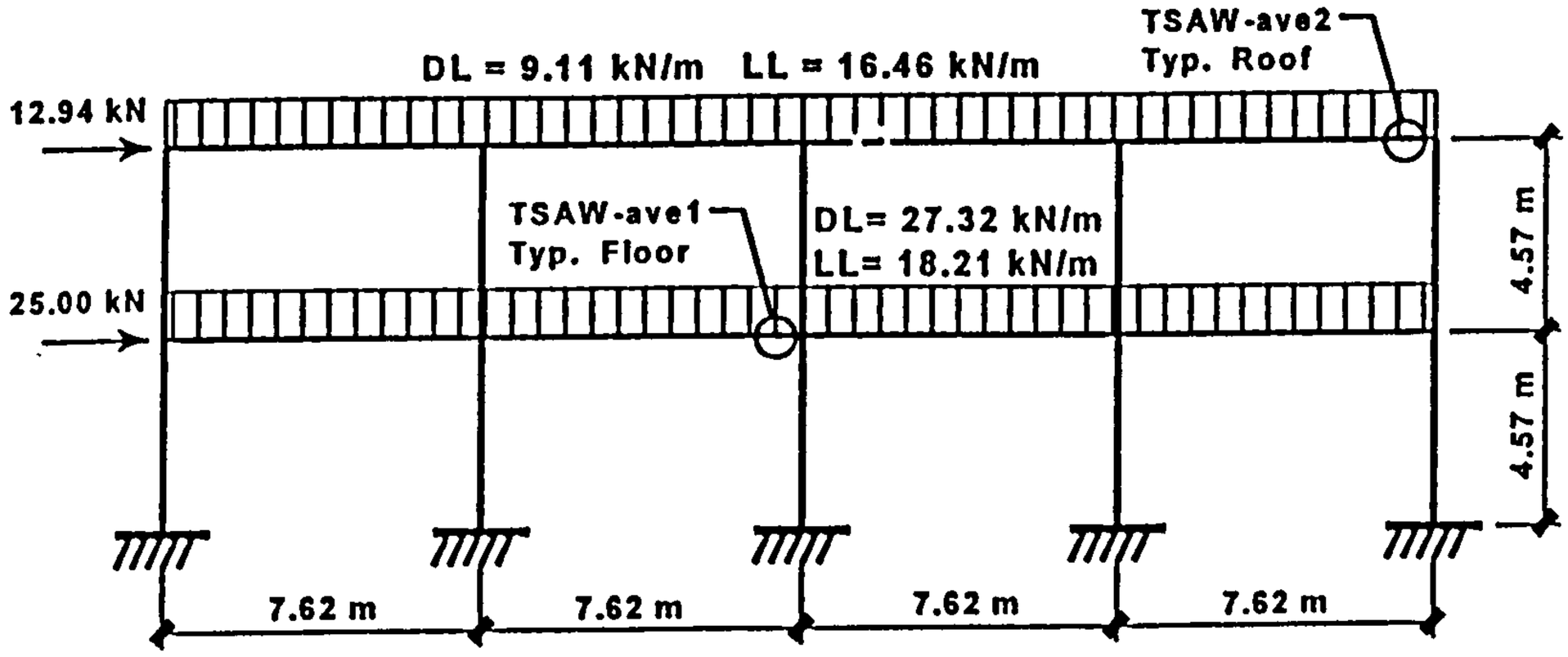

Figure 4.19 Deierlein's frame as analysed by Foley & Vinnakota [4-7]

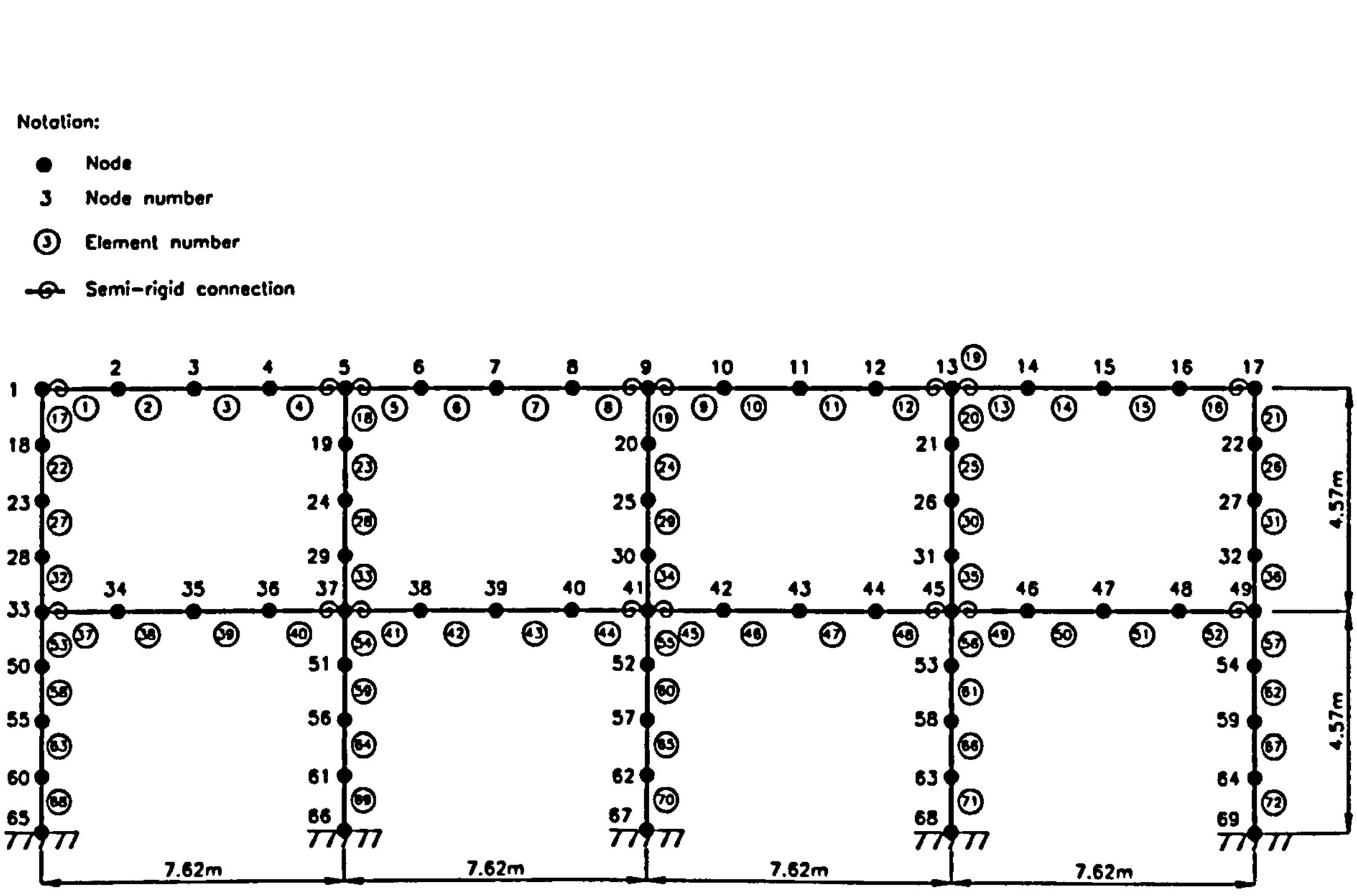

Figure 4.20 Finite element model of the frame shown in Figure 4.21 for the SERIFA program

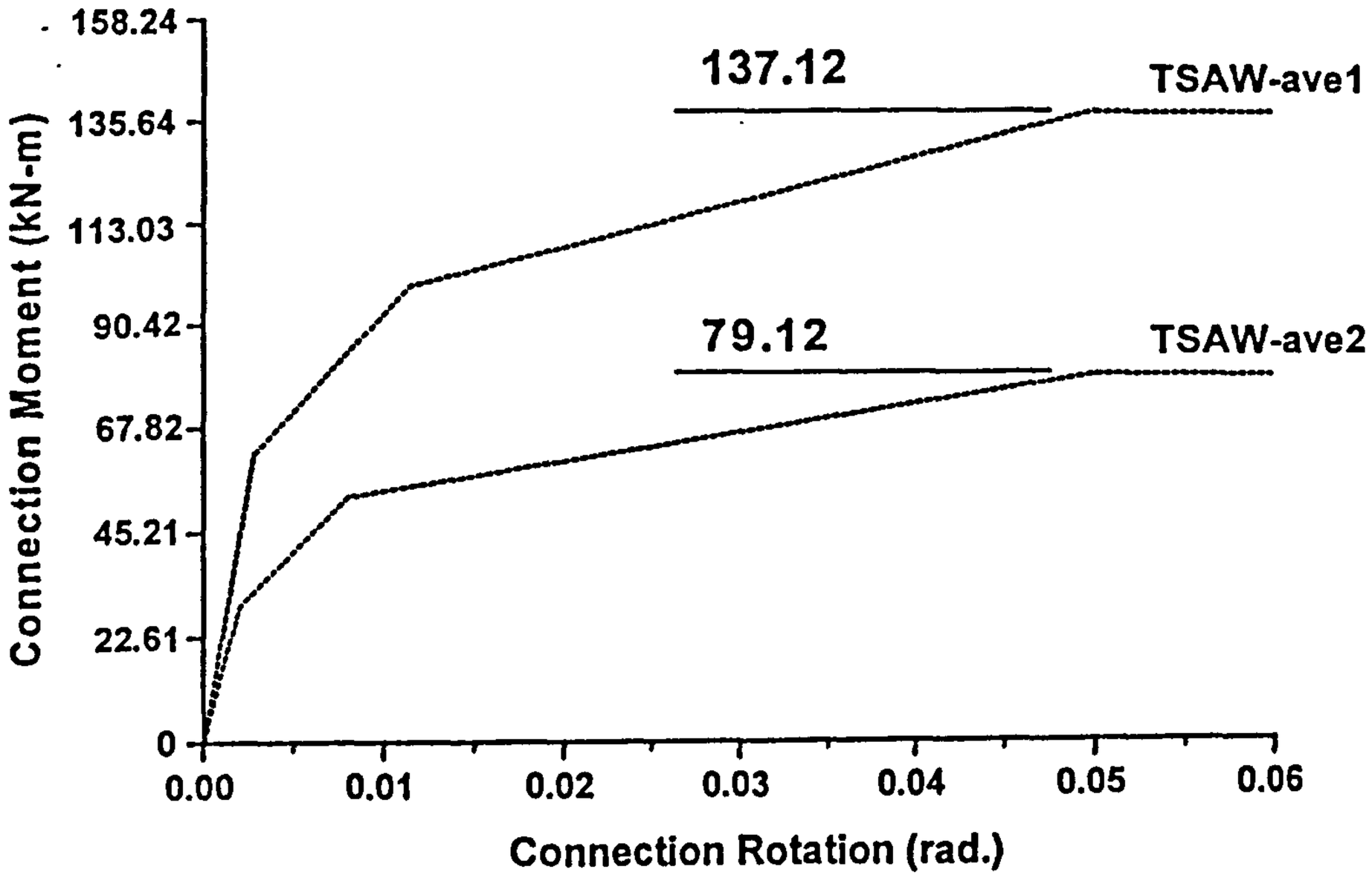

Figure 4.21 M-ϕ curve model used in the analysis [4-6], [4-7]

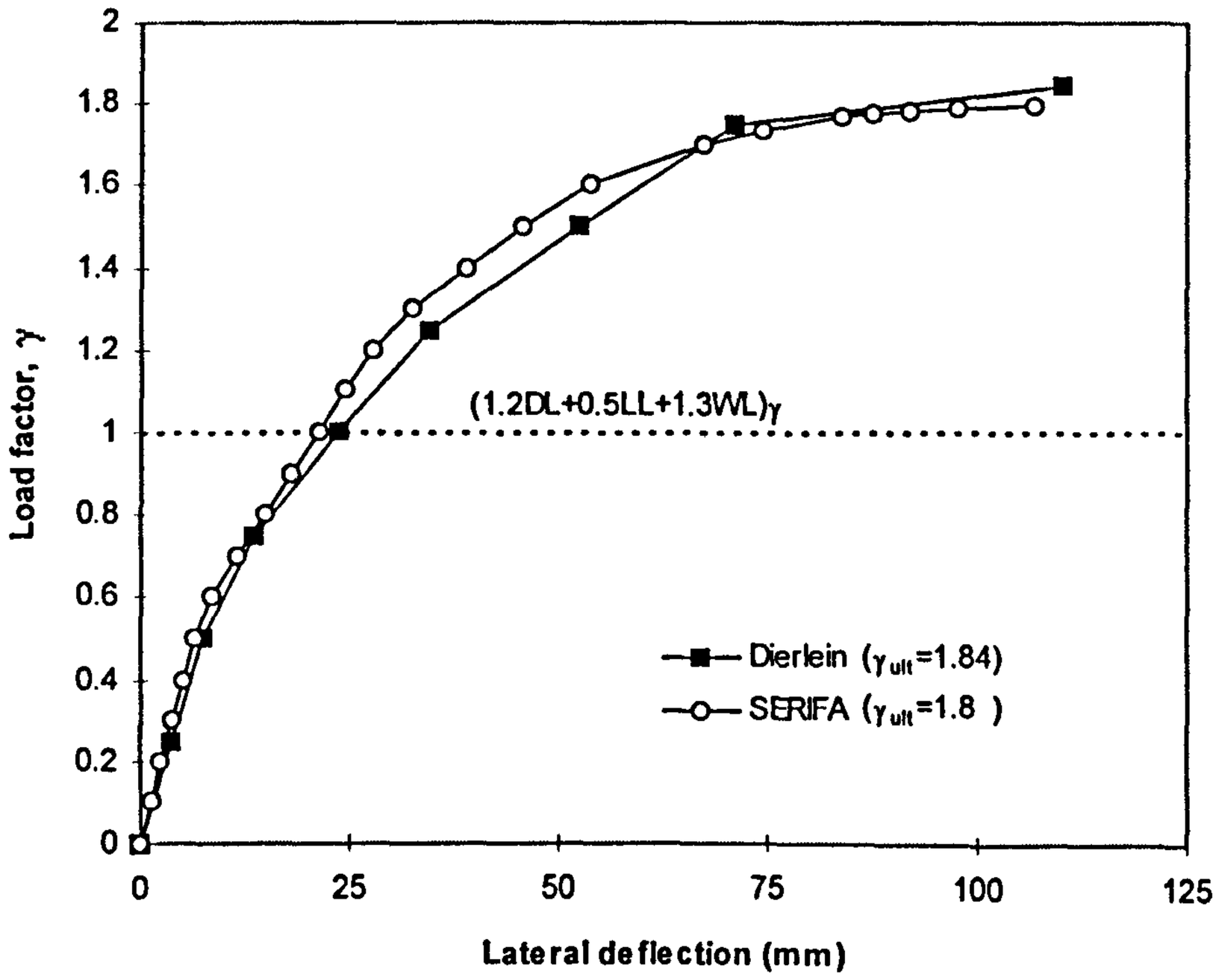

Figure 4.22 Comparison of frame response between the SERIFA and Deierlein programs [4-6], [4-7]

Chapter 5

Behaviour of SHS Beam-columns with Semi-rigid Connections in Non-sway Frames

5.1 Introduction

The verification presented in Chapter 4 showed that the program can give a reasonably good prediction of real frame response. The program was used subsequently to analyse a series of one-bay two-storey plane frames employing various types of semi-rigid connections.

The aim of the study presented in this chapter is to investigate the behaviour of SHS columns with various types of connections in both elastic and inelastic ranges. This includes the investigation on the following aspects:

- the phenomenon of moment shedding and its effect to the column performance
- the influence of semi-rigid connections to the behaviour of the columns.

The study in this chapter, however, is limited to the response of a one-bay two-storey frame employing different types of connections.

5. 2 Scope of the Parametric Study

The study was conducted on a one-bay two-storey non-sway frame as shown in Figure 5.1. The storey heights and the bay width were taken as 4m and 6m respectively. The frame consisted of 200 x 200 x 8 SHS columns and 356 x 171 x 45 UB beams. In the case of EEP connections, the 356 x 171 x 45 UB beams were also utilised assuming that the use of thicker end plates will give a similar M-ϕ curve as shown in Figure 5.9(c) (the actual M-ϕ curve was based on 356 x 171 x 67 UB beams). The base was assumed to be perfectly pinned. The reason for using the pinned base was to observe the effect of moment shedding at the top end of the column without the influence of any restraint at the base. The corresponding lower left column C3 and joint J3 which were chosen as the references for the investigation are shown in Figure 5.1. The finite element model of the analytical frame is shown in Figure 5.2. The material was assumed to behave as elastic-perfectly plastic as shown in Figure 5.3. Finally, Figure 5.4 shows the deformed angle α, that is the angle between the beam centre-line to the column centre-line located at the underside of the beam. Also included in the figure are the various types of rotations that occur at the joint.

5.2.1 Connection Types

Five different connection types with different degrees of rotational stiffness were chosen, ranging from the most flexible "PINNED" connections to the extreme RIGID connections. Other connections between these extremes; partial-depth end plate (PDEP), flush end plate (FEP) and extended end plate (EEP) were also utilised (see Figures 5.5(a), 5.5(b) and 5.5(c)).

The corresponding M-ϕ characteristics of the semi-rigid connections are shown in Figure 5.6. All the M-ϕ curves were obtained from the full scale joint test results conducted by France [5-1]. The classifications of the connections by both strength and stiffness which are in accordance to EC3 [5-2] are shown in Figures 5.7 and 5.8 respectively.

The M-ϕ curves were modelled as a series of trilinear curves as given in Figures 5.9(a), 5.9(b) and 5.9(c). The "PINNED" connection is assumed to have a very small linear stiffness of 13, 333 kNcm/rad to simulate the real pin connection.

5.2.2 Imperfections

Research carried out in three different countries by Bjorhovde & Birkemoe [5-3] in USA, Davison & Birkemoe [5-4] in Canada and Selveranas as reported by Kato [5-5] in Mexico shows that rectangular tubular columns have smaller geometrical imperfections ranging from L/3000 to L/6500. Bjorhovde also indicated that the maximum geometrical imperfection of columns with a practical length of about 4m to 5m is L/3000. Therefore based on this justification, the imperfection of L/3000 was adopted in this study. The imperfection e_o = L/3000 was taken at the column mid-height to represent the sinusoidal shape of the column. The imperfection shape was calculated as $y = e_o.sin(\pi x/L)$, where y is the lateral initial deflection due to the imperfection, x is the node latitude and L is the column height. The imperfection was applied to the lower columns only as shown in Figure 5.1.

5.2.3 Loading

A uniform distributed load of 30 kN/m was selected as an appropriate maximum load that will not cause any yielding to beams in all the five connection types considered in this study . In the first stage of the loadings, the uniform distributed load was applied to beam B2 to induce moment at the top end of column C3. The uniform load of 30 kN/m was modelled as a series of point loads shown in Figure 5.2. The beam loads were kept constant and then followed by the application of incremental axial column loads located at both column heads of the upper storey columns up to collapse. Based on the beam and column loadings and the pin bases, the failure will occur at the lower storey columns and hence the performance of beam-column C3 can be explored.

5.3 Behaviour at Column Mid-height

This section discusses the response observed at the mid-height of the column with specific reference to Figures 5.10 to 5.20 unless otherwise stated. The actual deformed shapes at both service and collapse loads of the frame are shown in Figure 5.10.

The two important issues to be investigated are:

(i). the response of load versus deflection

(ii). the spread of yield, loss of stiffness and reserve of strength.

5.3.1 Response of Load versus Deflection

The fundamental behaviour of a beam-column as part of a frame can be interpreted by first analysing the load-deflection response. Figure 5.11 illustrates the load-deflection response of the lower left column (column C3) with PDEP connections. The load-deflection behaviour is analysed based on the response observed at the column mid-height.

As can be seen from Figure 5.11, there are two distinct regions in which the column behaves quite differently, first is the elastic range (**OAB**) and secondly, is the inelastic range (**BC**) which is shown in grey colour. The column will demonstrate its elastic behaviour from **O** to **B** and the inelastic behaviour from **B** to **C**.

Line **OA** shows the response of the initial column deflection under the application of a uniform distributed load of 30 kN/m beam load. The level of the initial deflection depends on the magnitude of the beam load, the connection stiffness and the stiffness of columns C1 and C3.

The increase in axial column load P as the beam load is kept constant gives curve **AB**. The response is nonlinear since at the early stage of the column loading due to the existence of column axial load and the column deflection which induced an extra moment of P-δ. Hence, in the load-deflection response the only non linear effects are geometric. Laszlo [5-6] also reported the similar geometrical nonlinear response. In

range **OAB**, the deflection may be categorised as elastic-stable deflection because the column requires a significant load to induce a small deflection.

When the curve reaches point **B**, the column starts to develop yield which indicates a first sign of material deterioration and hence the column starts to buckle inelasticly. Beyond point **B**, the load-deflection response is influenced by the elastic-plastic material behaviour which brings about the material nonlinearity effects. In the inelastic range **BC**, the material yielding has become an important factor which greatly influences the behaviour and the performance of the column. Due to material yielding, the column stiffness starts to deteriorate to a new lower level which can be observed from the reduction in the slope of the curve, particularly in the sudden shift from curves **AB** to **BC**. The nonlinearity of the curve is more obvious due to a combination of both geometric and material nonlinearities.

In the inelastic range it is observed that a small axial load increment will cause the column mid-height deflection to increase rapidly. The column, however, is still stable. Due to this behaviour, the deflection in this range may be categorised as an inelastic-stable deflection. The column is still able to sustain additional loads up to point **C** which is the maximum load the column can carry. The load at this level is also known as the collapse load or the ultimate load. At point **C** the column is still stable with the internal and external forces are in equilibrium which is in accordance with Moy [5-7]. Any small load increment beyond this point will cause the column to become unstable with the internal and external forces not in equilibrium which indicates the collapse of the structure. According to Salmon & Johnson [5-8] the ultimate load is defined as the load which becomes the boundary between stable and unstable deflections of a compression member. Therefore any deflection up to point **C** is categorised as stable and any point beyond point **C** as unstable.

In range **BC**, the process of progressive yielding or plastification along the member length and across the cross section at mid-height of the column has occurred. During the development of yield spreading there is nevertheless an increase in column strength that can be seen from the rise of inelastic curve from **B** to **C** , that is the difference between the collapse load and the load at first yield.

Near the peak of the curve, it can be seen that a small load increment will induce a significantly large deflection. This gives a signal indicating that the column is approaching failure as a result of loss of stiffness.

5.3.2 Spread of Yield, Loss of Stiffness and Reserve of Strength

One of the important observation from Figure 5.11 is the sudden shift of the load-deflection response from the elastic curve **AB** to the inelastic curve **BC**. This sudden shift is associated with the loss of stiffness in the column. The other term for loss of stiffness as used by Wood [5-9] is the vanishing stiffness. This phenomenon develops as a result of yield spreading in the elastic-plastic columns. Figure 5.12 relates the development of loss of stiffness at the critical section in the column to the load-deflection response shown in Figure 5.11. The loss of stiffness at a section can be monitored by knowing the percentage of reduction values of *EI* due to yielding at that particular section [5-10] .

Figure 5.12 shows the loss of stiffness at the column mid-height cross section. As loss of stiffness is related to spread of yield, then the discussions of the phenomenon of loss of stiffness is predominantly due to the behaviour of yield spreading at this particular section.

As can be observed from Figure 5.12, in the elastic range from **O** to **B**, no yielding has occurred and hence there is no loss of stiffness due to material degradation. The column stiffness starts to vanish after the formation of first yield at point **B** and continue to lose its stiffness up to point **C**. Once the first yield has formed, a further small load increment has caused a significant spread out of yield across the section and followed by the spreading along the element. This behaviour eventually has caused a sudden drop in the column stiffness. The slope of curve **BC** represents the rate of yield spreading with increasing axial load *P*. The greatly reduced slope of curve **BC** indicates that the rate of stiffness loss is very dramatic in which a small load *P* has caused a significant amount of stiffness loss.

Hence, it can be seen that yielding is the parameter that has caused significant deterioration in the column stiffness. On the other hand, however, in terms of column strength, the yielded zone has reached its maximum yield stress, σ_y in which the product of yield stress and the yielded area gives the maximum strength offered by that area ($P = \sigma_y \times A_{yield}$). This contributes to the increase in column capacity. Therefore, any further load increment will be resisted by the development of plastic zone absorbing the remaining elastic core as well as the strength contributed from the elastic section itself. However the increase in column strength due to inelastic action is normally limited by the lower bound failure due to vanishing stiffness and increase in column flexibility.

Other important results of the study show that, in the case of columns which are subjected to axial load, bending and imperfections, it is observed that at collapse load, the cross section which corresponds to the maximum deflection normally has about 50% of its section yielded in the compression face. This is in agreement with Baker [5-11] and Gent & Milner [5-12] who noted that for a single curvature column, the instability always occurs below the full plastic moment.

Another observation from Figure 5.12 shows that about 60% stiffness loss has occurred at the mid-height critical section. This also means that at the point just before column collapse (point **C**), the column stiffness at the critical section is about 60% lower than that of the original elastic stiffness.

The loss of stiffness is a useful parameter and has been used in many design methods such as those due to Gent and Milner [5-12] and Wood [5-9]. Studies by Gent & Milner [5-12] on open section columns had shown that the column stability is controlled by one flange , that is at failure load, one of the flanges will tend to remain elastic while the other becomes plastic and hence they estimated that about a 50% loss of stiffness would occur. As a result of this, they adopted a reduction factor of 0.5 in their design method. Wood [5-9] agreed with the concept of 50% vanishing stiffness. However, he used a factor of 40% reduction in column stiffness instead of 50% in his variable stiffness method to give a more conservative approach.

In tangent modulus theory, the loss of stiffness which reduces the column strength is modelled by assuming that, at time of failure, the column material has the tangent modulus E_t which is less than the elastic modulus E [5-13]. This leads to the prediction of the failure loading for axially loaded columns by incorporating the reduced modulus E_t into Euler equation, i.e. the Engesser equation:

$$\sigma_{cr} = \frac{(\pi^2 E_t)}{(KL/r^2)} \tag{5.1}$$

where σ_{cr} = critical stress just before the column buckles,

K = effective length factor, L = column length, r = radius of gyration

The reason for highlighting the various design methods is to show the importance of loss of stiffness and how it is incorporated into design. As in the simplified design method (see sections 6.6.2 and 7.3), the results of the collapse loads which are employed as the fundamental criteria for the design method have already considered the effect of vanishing stiffness, i.e. through the incorporation of a bilinear stress-strain σ–ε model in the analyses.

The Perry-Robertson design method assumes the maximum strength of the column is achieved after the first yield [5-9]. This assumption neglects the benefits of any extra reserve of strength in the inelastic range as shown in this study. Baker [5-11] suggested that columns can sustain further loading after the first yield. This is in agreement with Wood who suggested that the maximum strength in a column is achieved when the column stiffness has vanished. This vanishing stiffness only occurs at a certain point beyond the first yield. As the column stiffness completely vanishes, it will experience an infinite displacement. This is in agreement with the definition by Salmon & Johnson [5-8] who argued that beyond the ultimate load the column has unstable deflections.

In this section, the instability of the column has been described by the deterioration of the column stiffness, which in line with Wood [5-14], who suggested that instability in elastic-plastic range is best demonstrated by the deterioration of stiffness.

5.4 Behaviour at Column Top End

This section discusses the corresponding response occurring at the column top end of joint J3 (see Figure 5.1). Unless otherwise stated the discussion will refer to Figures 5.10 to 5.20. The two main important responses to be investigated are:

(i). the column rotation at the joint

(ii). the moment shedding at the column top end.

It is also of interest to note the relationship between the response of column rotation and the amount of moment shedding particularly in the inelastic range.

5.4.1 Behaviour of Rotations at the Joint

There is an interaction between the lateral deflection at column mid-height and rotation at the column top end (joint J3). At the initial stage of beam loading, the rotation at column top end influences the level of column deflection. As the column load P is applied incrementally, the effect of extra moment of P-δ influences the rate of column end rotation. When the column loses its stiffness, the sudden increase in lateral deflections causes the end column to rotate very rapidly. Clearly, it can be seen that the interaction between column end rotation, beam rotation and connection rotation can influence the frame behaviour. This section will explain further the development of beam end rotation, connection rotation and column end rotation which directly influence the performance of the column under investigation.

Figure 5.13 shows the response of the moment-rotation of the connection at joint J3. When the beam load is applied, the connection rotates up to point **A**. However, as can be observed from the curve, the moment at the connection reduces with increasing column load P and this has caused the connection to unload to point **C**. The reason of connection unloading is explained in Section 5.4.2.2. Due to the connection unloading, the connection contributes its initial stiffness k_1 to the stiffness of the column up to collapse. Hence it can be said that the deterioration of the column

stiffness discussed in section 5.3.2 is not due to any deterioration in the stiffness of the connection.

Figure 5.14 shows the response of the rotations at joint J3 with increasing axial load *P*. Lines **OA** represent the initial rotations of the column end, beam end and the connection at joint J3 due to the applied beam loads. When the column load is increased from **A** to **B**, it is observed that the column end rotation increases at a faster rate than the beam end rotation. This is expected because the axial load *P* is directly applied to the already deflected column which then increases the column deflection and eventually the column end rotation. As for the connection rotation, it decreases immediately after the commencement of the application of the column axial loads. A decrease in connection rotation represents an unloading which is in accordance with the M-ϕ curve response shown in Figure 5.13.

Referring back to Figure 5.14, when the curve has reached point **B** in which the first yield has formed, the column will be subjected to an abrupt stiffness loss. This effect has caused the column to become more flexible and eventually has triggered a sudden increase in lateral deflection and a large end rotation, i.e. a large ϕ_{column}.

To explain this further, it is of interest to use a term called the stiffness factor. According to Rygol [5-15], the stiffness factor is a true measure of the capacity to resist rotation. In this case, the stiffness factor at the column end is defined as the column end moment divided by the column end rotation, i.e. M_c / ϕ_{column}. In this regard, the yielded column with a large ϕ_{column} has a low value of stiffness factor. This means that the column can no longer provide resistance against the rotation at its end. As a result, the column end rotation increases very rapidly with the increase in column loads. Consequently, the deteriorated column allows the large column end rotations to propagate. This is followed by the rapid unloading of the connection and the rapid increase in the beam rotation. The rapid change of all the rotations can be observed clearly after the formation of first yield from **B** to **C**. This behaviour can be seen even more clearly in the cases of columns with stiffer connections such as FEP, EEP and RIGID which are shown in Figures 5.25, 5.36 and 5.47 respectively. It can be

seen from the steep slope **BC** of the curves indicating a small increase in column axial load has caused very abrupt changes in all the beam, column and connection rotations.

Another observation from Figure 5.14 is that, the rate of end beam rotation is not as rapid as the column end rotation. The rapid column end rotations relative to moderate beam rotations have caused the connection rotations to decrease and unload very rapidly. Referring back to Figure 5.4(b), as the $\phi_{connection}$ unloads, the angle α increases with increasing axial load. Physically, this action indicates that the beam, with the help of the connection has restrained and pulled the column top end back towards its initial position as the mid-height column deflection continues to increase (see Figure 5.4(a)). The use of stiffer connections will have larger restraint effects and permit the column to undergo larger deflections with consequently larger end rotations.

5.4.2 Moment Shedding & Redistribution of Moment at Ultimate State

5.4.2.1 Behaviour of Moment Shedding

The responses of load-deflection, loss of stiffness and column end rotation have been discussed in the previous sections. Consequently, the most important phenomenon associated with these responses is the progressive shedding of moment at the top end of column C3.

Figure 5.15 shows the response of moment at the top column end using PDEP connections with increasing axial column loads. The moment at **A** is the moment due to the beam load. Further inspection of this figure shows that this moment is actually shed and can be relaxed to almost zero at the ultimate load level. This response of moment shedding as the structure approaches its ultimate load has been studied experimentally by many researchers [5-11], [5-12], [5-16].

Moment shedding is a phenomenon in which the existing end moment supported by the column end is shed to the adjoining members. This moment shedding occurs in two different stages:

(i). Moment shedding in the elastic range.

(ii). Moment shedding in the inelastic range.

Referring back to Figure 5.15, it can be seen that the moment shedding in the elastic range starts to develop from **A** to **B** immediately after the application of column loads. It is seen that the rate of moment shedding shows a constant rate in the elastic range (**AB**) and subsequently followed by an increasing rate in the inelastic range (**BC**).

As the column attains its collapse load (point **C**), a significant amount of moment at the column top end is released and hence the remaining moment is very small - if it is relaxed to zero, it is analogous to a pin ended column. In some cases the moment at collapse load actually changes sign and induces a reversal of moment. Hence, it is observed from this behaviour that the detrimental effect of vanishing stiffness due to yielding has contributed to another effect which is the beneficial effect of relaxing the column end moment.

Another observation is that the moment at column mid-height keeps increasing as the column failure load is approached (see Figure 5.16). This behaviour occurs due to the increasing lateral deflections at the column mid-height with the increase in column loads. This in turn produces increasing strains and stresses at the column mid-height cross section. As a result, this effect contributes to the increasing bending moments as can be seen from the figure.

The release of the column end moment from column C3 causes the redistribution of bending moments of the adjoining members beam B2 and column C1. Of most interest is the redistribution of moment at beam B2 as shown in Figure 5.17. The redistribution of moments from beam end M_a to midspan M_b occurred quite rapidly in the inelastic range which is associated with the dramatic moment shedding at the column top end. As the beam end moment reduced rapidly, the beam midspan moment increased accordingly. This behaviour is more obvious for columns which

utilised stiffer connections such as EEP and RIGID which are shown in Figures 5.39 and 5.50 respectively.

The reduction of beam end moment indicates a reduction in end restraint moment. Figure 5.18 shows the percentage of beam end restraint moment in terms of M_p up to collapse load, where M_p is the beam plastic moment. It shows that the end restraints start to decrease at point **A** and the reduction becomes more significant after the first yield (point **B**). The corresponding M-ϕ response of the connection as a result of the variation of moments at the beam ends is shown in Figure 5.13. The presence of the connection initial stiffness k_I as a result of unloading from **B** to **C** implies that the reduction of end restraint is not due to the deterioration of the connection rotational stiffness but is rather due to deterioration of the column stiffness. The column, which normally assists the connection to restraint the beam, has yielded and becomes more flexible and hence reduces the effective end restraint at the beam end. This is in agreement with the current state of knowledge in which the degree of restraint provided by the connection is dependent on the relative stiffness of the beam-to-column connection, the beam and the column [5-17].

The plot of the end restraint moment in this aspect is to quantify the maximum moment distributed to the midspan and the minimum effective restraint the joint can offer. With this knowledge, the beam can be designed safely to provide the required moment resistance due to the moment redistribution at ultimate loads.

5.4.2.2 Redistribution of Moment at the Joint

This section discusses the response of column rotation at joint J3 which leads to the moment redistribution. Gent & Milner [5-12] suggested that one of the main parameters which mainly influence the moment redistribution in rigid frames is the joint rotation. That is true because the rigid joint will undergo a single global rigid body rotation. Hence, the joint rotation can be either the beam rotation or the column rotation. In the case of semi-rigid frames, however, the author suggests that the column end rotation is one of the important parameters influencing the response of

moment shedding. This is due to the fact that the increase in column rotations has caused the column to lose its resistance which causes the moment redistribution.

The behaviour of the interaction between the column end rotation and the moment distribution at the joint is shown in Figure 5.19. At point **A**, the initial beam load has contributed end moment M_a to the joint. Moment M_a has caused the lower and upper column to rotate and, in order to maintain equilibrium, moment M_a is resisted by the moment at the upper column, M_u and the moment at the lower column, M_c .

As the column load is applied incrementally, the column end rotation increases very gradually in the elastic range (**AB**). At this stage the lower column (column C3) has to resist moment from the beam load, which is negative in direction, as well as moment from the axial load which is positive in direction (see section 5.6). As a result of these moments which act in opposite directions, moment reversal has taken place and hence the column starts to relax its end moment which causes M_c to decrease. In order to maintain compatibility, the released moment from the column end is distributed to the upper column (column C1) and the beam (beam B2). As the distributed moment is negative in direction, it increases the negative upper column moment and reduces the positive beam end moment. Therefore, as can be seen from Figure 5.19, the curve M_u increases and curve M_b decreases with increasing column end rotations. It should be mentioned that, after point **A**, the increasing column end rotation shown in the figure is associated with the increasing in column axial loads.

In the inelastic range (**BC**), the column stiffness has deteriorated due to yielding which causes the column end to rotate very rapidly. The column has lost its resistance against the end moments and hence releases the moment to the upper column and the beam at a very dramatic rate which then causes sudden moment redistribution. Similarly, as has occurred in the elastic range, the negative moment released from the column end has increased the upper column moment and reduced the beam end moment. As a result, curve M_u continues to increase and curve M_a continues to decrease at a very dramatic rate. The reduction of moment M_a has caused the unloading of the connection.

5.4.2.3 Configuration of Bending Moments at Ultimate Load

The development of moment redistribution as described in section 5.4.2.2 shows that there is a significant change in the bending moment configuration as the collapse load (ultimate load) is approached. Therefore, another important aspect which needs to be considered is the configuration of bending moments of the frame at collapse load. The focus is now given to the configuration of moment on the failed column (column C3), on the upper column C1 and on the beam B2.

Results of the study show that the bending moments at the ultimate load are totally different to those at the service load and this has important implications on the development of the design method. The comparisons and the behaviour of the bending moment are as follows:

1. Upper column (see Figure 5.20(a)) - At collapse load, the moment diagram of the upper column shows the sign of plastic moment. This indicates the development of plastic zone absorbing the elastic core at the lower part of the upper column in order to provide enough resistance to the moment released by the lower column. This response, however, has not caused collapse of the upper column.

2. Beam B2 (see Figure 5.20(b)) - the configuration of the bending moment at ultimate load shows that the beam can be treated as simply supported, and with a certain percentage of restraining moment.

3. Lower column (see Figure 5.20(c)) - At service load the column has to carry both moment and axial load. In the current design method these actions have to be considered in the interaction equation. However at collapse load, the bending moment of the column is similar to the bending moment of a pin ended column. This occurs due to the relaxation of the column top end moment. This behaviour is in accordance with the finding of Gent & Milner [5-12], who concluded that the condition of the column when it has largely relaxed at its end moments is similar to an axially loaded column with an initial curvature. This behaviour shows that the column at ultimate load can be treated as carrying axial load only.

On the basis that at the collapse load (ultimate load), the frame is in a state of stable equilibrium then the response of such bending moments can be adopted as a fundamental feature for a simplified design approach.

5.5 The Influence of Connection Restraint on the Column Behaviour

Sections 5.3 to 5.4 have discussed the overall beam-column behaviour with semi-rigid connections. The behaviour of beam-columns with respect to a more specific connection type will be discussed in this section.

5.5.1 Column Behaviour with Various Connection Types

5.5.1.1 PDEP Connections

The discussion on the behaviour of the lower column will refer back to Figures 5.10 to 5.20.

One important observation from the load-deflection response (see Figure 5.11) is that the steeper ascending slope of curve **AB** indicates that in the elastic range, the flexible PDEP connections demonstrate the ability to provide substantial restraint so that the column can sustain high axial loads. However, as the column yielded, it is seen that in the inelastic range, this relatively flexible connection can no longer provide sufficient restraint and additional stiffness to the column as shown by the dramatic change in the slope **BC**.

Due to the fact that the PDEP connection itself has limited rotational stiffness, then the effective restraint offered by the column and the connection at the beam ends is minimal. The corresponding end restraint moment due to 30 kN/m beam load is 7.1 kNm (see Figure 5.17). In order to maintain compatibility at the joint, the lower column is able to provide resistance of -3.2 kNm and the remaining moment is

transferred to the upper column (see Figure 5.15). The small amount of moment transferred to the column has caused the column to undergo a small end rotation of about 0.6 milliradian and hence a small mid-height deflection of -0.4 mm (see Figures 5.14 and 5.11 respectively).

In the column loading stage, it is seen that the formation of first yield is delayed until 1615 kN as a result of small strains associated with the small initial deflections (see Figure 5.11). As the first yield is delayed, the corresponding percentage of moment shedding in the elastic range is quite large, i.e. about 36% has been relaxed (see Figure 5.15).

After the first yield, the column is capable of carrying additional loads due to inelastic action up to 1638 kN, that is 1.4% of reserve of strength above the first yield load (see Figure 5.11). It is observed that at collapse load, a corresponding of 60% loss of stiffness has occurred at the critical section located at mid-height of the column (see Figure 5.12). The corresponding moment shedding in the inelastic stage is 58% (see Figure 5.15). Hence, it is observed that a total of 94% of the detrimental moment has been shed from the column end and consequently has been relaxed to almost zero.

The plot of rotations with increasing loads shows that in the inelastic range, the PDEP connection is unable to provide sufficient restraint which can increase the column stiffness and then permit the column to undergo larger end rotation (see Figure 5.14). The evidence can be seen from the extent of the column end rotation in the inelastic range from **B** to **C** which is only about 0.3 milliradian. Hence, it can be concluded that columns with PDEP connections have a very low rotation in the inelastic range. The maximum column rotation is 1.3 milliradians and the maximum connection rotation is 9.5 milliradians.

The effective beam end restraint moment at service load is observed at about 3.4% of M_p of the beam (see Figure 5.18). However at collapse load, this has been decreased to 3.2% of M_p as a result of moment shedding. The corresponding reduction of beam end restraint moment is followed by the increase of 0.3% in the midspan moment.

The distribution of moment at joint J3 shows that most of the shed (released) moment as indicated by the descending slope of curve M_c from the lower column is largely

attracted by the upper column as shown by the steep ascending slope of curve M_u (see Figure 5.19). On the other hand, the moderate slope of curve M_a shows that the beam only attracted a small amount of the shed moment. This is due to the fact that the PDEP connections only permit a small amount of shed moment to be redistributed back to the beam.

The plot of bending moments at collapse load, as shown in Figure 5.20, indicates that by utilising PDEP connections which are classified as pin by EC3 (see Figure 5.8), the frame members can be treated individually. The effect of moment eccentricity as required in the current U.K. design method can be neglected. The beam can be treated as simply supported with zero end restraint and the column can be designed as axially loaded without any load eccentricity. This is a straightforward design method which is based on actual frame response.

5.5.1.2 FEP Connections

The discussion in this section refers to Figures 5.21 to 5.31.

With the use of FEP connections, the effective restraint offered by the column and the connection at the beam ends has increased. As a result of beam loading, the corresponding end restraint moment at beam ends is 20.5 kNm (see Figure 5.28). The lower column is able to provide resistance of about -9.7 kNm and the balance is transferred to the upper column (see Figure 5.26). The moment transferred to the lower column has induced 1.7 milliradians column end rotation and -1.24 mm mid-height deflection (see Figures 5.25 and 5.22 respectively).

Due to larger initial column deflections, an earlier formation of first yield is observed at 1535 kN (see Figure 5.22). In the elastic range, about 19% of moment shedding has occurred (see Figure 5.26). This is followed by 79% of moment shedding in the inelastic range. The column end moment at collapse load has been relaxed to -1.6 kNm which corresponds to a total of 98% of the moment shedding. The collapse load is observed at 1592 kN (see Figure 5.22). The reserve of strength is 3.7% above the first yield load.

The use of FEP connections has increased the value of the column rotation in the inelastic range (from **B** to **C**) to about 1.2 milliradians as compared to 0.3 milliradian with PDEP connections (see Figure 5.25). Associated with the larger inelastic column rotation is the larger amount of moment shedding in the inelastic range, that is 79% of the moment has been shed as compared to 58% with PDEP connections. It is also observed that the maximum column rotation is 3.5 milliradians. Whilst, the maximum connection rotation is 6.7 milliradians.

The effective beam end restraint moment at service load has increased to 9.8% of M_p (see Figure 5.29) as compared to 3.4% of M_p with the PDEP connections. At collapse load, the end restraint moment has decreased to 7.8% of M_p due to the moment shedding.

Figure 5.30 shows the development of moment distribution at the joint. The shed moment is partly distributed to the upper column and the beam. The descending slope of curve M_a indicates that the beam with FEP connections has attracted a quite large amount of the shed moment as compared with the PDEP connections. This implies that the stiffer FEP connections permit a larger amount of shed moment to be redistributed back to the beam.

Due to the relaxation of moment at column top end, the plot of bending moments at collapse load of column C3 shows similarity to that of an axially loaded case (see Figure 5.31). Hence, a beam-column with FEP connections can be designed as an axially loaded compression member. Subsequently, the beam with FEP connections can be designed as simply supported with an end restraint moment of 5% of M_p of the beam.

5.5.1.3 EEP Connections

The discussion for columns with EEP connections will refer to Figures 5.32 to 5.42.

The initial end restraint moment due to beam loading is 44.1 kNm (see Figure 5.39). The lower column provides resistance of about -21.1 kNm and the balance is resisted

by the upper column (see Figure 5.37). The transferred moment has induced -3.7 milliradians column end rotation and -2.8 mm mid-height deflection (see Figures 5.36 and 5.33 respectively). Early formation of first yield is observed at 1390 kN. At first yield load, the column end moment has decreased to -17.9 kNm which indicates that about 15% of moment shedding has occurred in the elastic stage (see Figure 5.37).

As can be observed from Figure 5.36, the column end rotation in the inelastic range develops very rapidly with increasing axial loads. The extent of the rotation in the inelastic range from **B** to **C** is 2.8 milliradians indicating larger inelastic rotation at the column end. This implies that the column will experience a larger amount of moment shedding and is able to sustain more axial load in the inelastic range. Another important observation is that the maximum column rotation with EEP connections is 7 milliradians, whereas the maximum connection rotation is 1.7 milliradians.

The collapse load is 1540 kN with the reserve of strength 11% above the first yield load (see Figure 5.33). The detrimental negative moment of -21.1 kNm has been shed by 100% before changing to a positive moment of +1.27 kNm (see Figure 5.37). It can be seen that the detrimental column moment has been relaxed to almost zero and has changed sign to become a restraining moment.

The effective beam end restraint moment at service load is 21.2% of M_p (see Figure 5.40). At collapse load, the beam end restraint moment has decreased to 11.1% of M_p but is greater than 10% of M_p . The descending slope of curve M_a indicates that the beam with EEP connections has attracted a large amount of shed moment as compared to the FEP connections (see Figure 5.41). This is due to the fact that the EEP connections permit a large amount of shed moment to be redistributed back to the beam.

The bending moment of the lower beam-column at collapse load shown in Figure 5.42 is similar to that the bending moment of an axially loaded column. Again, the beam-column can be designed as axially loaded compression member. Whereas, the beam can be designed as simply supported with end restraint moment equal to 10% of M_p of the beam.

5.5.1.4 RIGID Connections

The discussion for columns with RIGID connections will refer to Figures 5.43 to 5.53.

The results show that with RIGID connections, the end restraint moment is 51.3 kNm (see Figure 5.50). The lower column provides resistance of about -23.4 kNm and the balance is resisted by the upper column (see Figure 5.48). The transferred moment has induced -4.1 milliradians column end rotation and -3.1 mm mid-height deflection (see Figures 5.47 and 5.44 respectively). Due to large initial deflections, first yield is achieved early at 1375 kN. At first yield, the column end moment has decreased to -19.7 kNm which indicates that about 16% of moment shedding has occurred in the elastic stage (see Figure 5.48).

As can be observed from Figure 5.47, the column end rotation in the inelastic range develops very rapidly with increasing axial loads. The extent of column end rotation in the inelastic range (from **B** to **C**) is 3.3 miliradians as opposed to 0.3 milliradian with PDEP connections. The large extent of the column end rotation also indicates that columns with RIGID connections possess larger rotation to permit larger moment redistribution, thus enabling the column to sustain more axial load. The maximum column rotation is 7.9 milliradians. It is seen that the columns with RIGID connections show good behaviour in the inelastic range in terms of reserves of strength and ability to undergo large deflections. Another observation is that, the column rotation is in close agreement with the beam rotation. This demonstrates a close agreement with the theory in which when rigid connections are employed, the column rotation is equal to the beam rotation (see Figure 5.4(b)).

The collapse load is observed at 1538 kN with the reserve of strength increased to 11.9% above the first yield load (see Figure 5.44). The final column end moment is +1.8 kNm in which the negative moment has been shed by 100% before changing to the positive moment (see Figure 5.48).

The effective beam end restraint moment at service load is 24.6% of M_p (see Figure 5.51). At collapse load, the end restraint moment has decreased to 10.8% of M_p but is greater than 10% of M_p. The descending slope of curve M_a indicates that the beam

with RIGID connections has attracted a large amount of shed moment as compared to the other PDEP and FEP connections (see Figure 5.52).

The bending moment of the lower column at collapse load is similar to the bending moment of an axially loaded compression member (see Figure 5.53). Hence, the column can be designed as axially loaded only. Whereas, the beam can be designed as simply supported with end restraint moment equal to 10% of M_p of the beam.

Comparisons of results between EEP and RIGID connections show considerably similarity and indicate that EEP connections behave very closely to rigid connections.

5.5.1.5 PDEP Connections with Eccentricity Moment

The discussion will refer to Figures 5.54 to 5.64.

The most significant observation from this study is that the column end moment due to eccentricity is also shed and relaxed to almost zero as the column undergone yielding. The configuration of bending moment diagrams at collapse load, again, shows that the column can be designed as axially loaded and the beam as simply supported. These results give more evidence that columns with flexible connections can be designed without incorporating the eccentricity moment as normally used in practise.

5.5.1.6 "PINNED" Connections

The discussion will refer to Figures 5.65 to 5.75.

The significant observation from the response of columns using "PINNED" connections is that even with a significantly small stiffness connection (see Figure 5.68), the column still demonstrates a high column stiffness in the elastic range. It is evident from the steep slope of the load-deflection response from **A** to **B** as shown in Figure 5.66. The first yield is seen at 1645 kN and the collapse load is 1655 kN. It is

observed that a significant proportion of the axial column load capacity occurs in the elastic range.

The maximum connection rotation is observed at 10.7 milliradians (see Figure 5.68) which in very good agreement with the connection rotation calculated by theory, i.e.

$\phi_{pin} = wL^3 / 24EI$

$= [(30\ \text{N/mm}) \times (6000\text{mm})^3] \ / \ [24 \times (205 \times 10^3\ \text{N/mm}^2) \times (12100 \times 10^4\ \text{mm}^4)]$

$= 0.01088$ radian

$= 10.9$ milliradians

Furthermore, it can be observed from Figure 5.69 that the connection rotation is in close agreement with the beam rotation. Again, this demonstrates a close agreement with the theory in which when pinned connections are employed, the connection rotation is equal to the beam rotation (see Figure 5.4(b)).

On the other hand, the maximum column rotation is only 0.6 milliradian (see Figure 5.69). After the attainment of first yield the column only managed to rotate for about 0.1 milliradian (from **B** to **C**). This reflects the inability of this almost "PINNED" connection to contribute additional stiffness to the columns in the inelastic range.

Assuming that the "PINNED" connection has perfectly zero stiffness, it is the elastic column stiffness that play a dominant role in sustaining the axial loads. Hence, it suggests that the connection stiffness is not an important parameter for the column to sustain high axial loads in the elastic range.

Considering the behaviour of all connection types dealt with this frame, it can be seen that it is the presence of the connection that is the most important. This is in agreement with Kirby et al. [5-18] who suggested that for column design it is the presence of semi-rigid connection that is the most important feature, the stiffness of that connection being of secondary consideration.

It is believed that the importance of connection stiffness is most dominant in the inelastic stage, i.e. when the column has yielded and lost its stiffness. This is evident from the comparison of load-deflection responses between "PINNED" and RIGID (see Figures 5.66 and 5.44 respectively) which show that the "PINNED" connected

column can only sustain an additional axial of 10 kN whereas the RIGID connection can sustain 163 kN above that which causes first yield.

5.5.2 Comparison of Column Behaviour with Various Connection Types

The comparison of columns with PDEP, FEP and RIGID connections are made on the basis that all member sizes, loading and frame dimensions are the same - the only variable is the connection type. Therefore, any differences in the behaviour of the columns are attributed to the connection effects. Figure 5.76 shows clear evidence of different responses of exaggerated deformed shapes as a result of using various types of connections.

In the following comparisons PDEP connections will be identified as flexible connections whereas EEP and RIGID as stiffer connections. FEP connections normally show a response intermediate between the two.

5.5.2.1 Comparison of Load-deflection Responses

A direct comparison of load deflection response for columns with PDEP , FEP and RIGID connection is shown in Figure 5.77. The load-deflection plot shows clearly the response of columns with various connection types.

It can been seen that the use of flexible connections has the following effects on the column response:

1. Limit the transfer of detrimental beam end moment to the column resulting in a small initial column deflection during the beam loading phase.
2. The small initial load deflection delays the formation of first yield. However, when the first yield is approached, the transition of the load-deflection response from the elastic to the inelastic range is very sudden due to the dramatic reduction in the column stiffness.

3. A small load increment in the inelastic range caused a significant spread of yield and hence a more sudden loss of stiffness in the column. Subsequently when 50% of the critical section has yielded, this is immediately followed a small load increment causing the ultimate load condition.
4. Large axial column load capacity in the elastic range.
5. Low inelastic column stiffness as can be seen for a very moderate and sudden load-deflection response in the inelastic range.
6. Small reserve of strength above first yield.

In contrast, the use of stiffer connections has the following effects to the columns:

1. Induced larger initial column deflections in the beam loading phase. This is expected because the stiffer connection transmits a larger detrimental beam end moment into the column which result in a larger column end rotation and consequently a larger initial column deflection.
2. The presence of large initial column deflections is accompanied by large initial strains which eventually led to the early formation of first yield.
3. The gradual transition of the load-deflection response from elastic to the inelastic range resulting in a gradual loss of column stiffness.
4. The effect of stiffer connections increased the end restraints and hence the connections have the ability to restrain the column as it undergoes large deflection particularly after the attainment of the first yield (in the inelastic range).
5. Higher inelastic column stiffness as can be observed from the gradual slope of the load-deflection curve in the inelastic range.
6. Large reserve of strength above first yield.

5.5.2.2 Comparison of Loss of Stiffness

Figure 5.78 shows the comparison of stiffness loss for columns with various connection types which influence the load-deflection response.

It can been seen that the use of flexible connections has the following effects on the loss of stiffness:

1. The plot of stiffness loss with increasing column loads is very moderate indicating that a small load increment has caused a significant amount of stiffness loss in the column.
2. The sudden loss of column stiffness is the factor for the abrupt change in the load-deflection curve.

The use of stiffer connections has the following effects to the loss of stiffness:

1. The inelastic slope of the load versus stiffness loss curves are steeper which indicate that the rate of stiffness loss is more gradual with increasing axial loads.
2. Associated with gradual stiffness loss is the gradual spread of yield. Consequently the formation of 50% yielded at the critical section is delayed and hence, the remaining elastic stiffness of the column and the stiffness of the connection can be of benefit to sustain additional loads.

5.5.2.3 Comparison of Beam End Restraints

The interaction behaviour between the deteriorated column and the connection unloading has contributed to a variation in the end restraint. Figure 5.79 shows the percentage of the effective end restraint moment for various connection types.

As can been seen, the use of flexible connections has the following effect to the beam end restraints:

1. Small reduction of beam end restraint moment at ultimate load levels.

The use of stiffer connections has the following effect to the beam end restraints:

1. Large reduction of beam end restraint moment, however, it is seen in this study that for all the cases considered, the restraints at ultimate load levels are greater than 5% of M_p.

5.5.2.4 Comparison of M-ϕ Responses

Figure 5.80 shows the response of M-ϕ characteristics with various connection types. The reduction in column stiffness has caused the connection to unload and hence all connections have contributed their largest stiffness, k_1 throughout the loading stage.

As can been seen, the use of flexible connections has the following effect to the M-ϕ characteristics:

1. The unload effect is very small indicating a small amount of moment reduction.

The use of stiffer connections has the following effect to the M-ϕ characteristics:

1. A significant amount of unloading which indicates a large amount of end moment previously carried by the connections has been released to the beam midspan.

5.5.2.5 Comparison of Column End Rotation

Figures 5.81 to 5.83 show the comparisons of beam rotations, column rotations and connection rotations.

Referring to Figure 5.82, it can be seen that the use of flexible connections has the following effect to the column end rotations:

1. Small column end rotation in the inelastic range.

The use of stiffer connections has the following effects to the column end rotations:

1. Large column end rotation in the inelastic range which can cause more moment being redistributed to the adjoining members.

5.5.2.6 Comparison of Moment Shedding

Figure 5.84 shows the response of moment shedding at the column top end. It can be observed that the column end moments are relaxed to almost zero for all types of connections.

The use of flexible connections has the following effect to the moment shedding:

1. A very small amount of moment shedding in the inelastic range.

The use of stiffer connections has the following effects to the moment shedding:

1. Early sudden moment shedding in the inelastic range due to early formation of first yield.
2. The rate of moment shedding in the elastic range is more rapid as indicated by the steeper curves. This is due to the fact that stiffer connections has induced larger initial column deflections which enhance the P-δ effect as the axial loads are applied. Consequently, the load increment P induced a larger amount of reverse moment in the negative direction which reduces significantly the positive beam end moments and hence increases the rate of moment shedding.
3. Larger amount of moment shedding in the inelastic range.

The shed moments have affected the neighbouring member particularly the beams. Figure 5.85 shows the bending moments of the beams at service loads and at ultimate loads for various connection types.

The use of flexible connections has the following effect on the beam:

1. Permits a small percentage of shed moment to be redistributed back to the beam.

The use of stiffer connections has the following effect on the beam:

1. Permits a larger percentage of shed moment to be redistributed back to the beam.

5.5.2.7 Comparison of Moment Redistribution

The development of moment redistribution at joint J3 up to collapse load for various types of connections is shown in Figure 5.86.

The use of flexible connections has the following effects on the beam:

1. A very moderate slope of M_a indicating that only a small amount of released moment from the lower column is attracted by the connection and consequently a smaller amount of moment is redistributed back to the beam.
2. The connection can only attract a small amount of the shed moment due to the limitation in the connection rotational stiffness. Consequently at collapse load, the bending moment in the beam has not changed significantly.
3. As can be seen from the shaded areas of Figures 5.86(a) and 5.86(b), the column rotations in the inelastic stage for both cases are small, that is less than 0.5 milliradian. This implies that the moment redistribution to the adjoining members in the inelastic stage is very abrupt.

The use of stiffer connections has the following effects to the beam:

1. The slope M_a has undergone a quite steep reduction indicating that a larger amount of shed moment is redistributed back to the beam.
2. It can be seen that stiffer connections have the ability to attract more released moment from the lower column and then redistribute the moment back to the beam. Thus, at collapse load, the beam has undergone a significant change of moment due to the redistribution.
3. As can be seen from the shaded areas of Figures 5.86(c), 5.86(d) and 5.86(e), the column rotations in the inelastic stage for the three cases are larger but still small, that is within the range of 1 to 4 milliradians. This implies that the moment redistribution to the adjoining members in the inelastic stage is fairly gradual.

5.5.3 The Effect of Connections on Column Reserve Strength, Beam End Restraints, Column Rotation and Connection Rotation

Table 5.1 shows direct comparisons of the column reserve of strength $(P_{sr} - P_y) / P_y$ with respect to various types of connections, where P_{sr} is the collapse load and P_y is the load at first yield. It is seen that flexible connections such as "PINNED" and PDEP have very small axial load reserve of strength which are less than 1.5%. As the connection stiffness is increased, the reserve of strength in the column increases. This

can be seen in the reserve of strength shown by FEP, EEP and RIGID connections with values of 3.7%, 11% and 11.9% respectively. It can be concluded that the use of stiffer connections will provide larger reserves of strength in the columns.

Table 5.2 shows comparisons of beam end restraint moments with different connection types. It can be observed from this table that the stiffer the connection the larger is the reduction in the beam end restraint moment. The reduction in the end restraint moment is mainly attributed to the deterioration in the column stiffness as a result of yielding.

Table 5.3 shows comparisons of column rotations at various conditions with different connection types. At collapse loads, it is seen that columns with "PINNED" and PDEP connections are unable to sustain additional axial loads when the column rotations are higher than 1.3 milliradians. Further observations show that frames with FEP connections fail when the column rotation is a maximum of 3.5 milliradian. Whilst, in the case of EEP and RIGID connections, the maximum column rotations are about 7 and 8 milliradians respectively. It can be concluded that the stiffer the connection the larger is the column end rotation at failure.

Finally, Table 5.4 shows comparisons of connection rotations with various types of connections. It can be seen from the table that the maximum connection rotation for practical connections such as PDEP, FEP and EEP are not more than 10 milliradians. This is in agreement with the finding made by Ahmed and Kirby [5-19] who suggested that the anticipated maximum value of connection rotation in the case of semi-rigid non-sway frames of normal geometries up to collapse is in the vicinity of 10 milliradians.

5.6 Further Aspects of Moment Shedding

It was mentioned in section 5.4.2.1 that the moment shedding at the column end starts to occur in the elastic stage. This section will explain further aspects of moment shedding in the elastic range. Two cases of analytical studies were considered.

In case 1, a simple parametric study on a frame with outwards initial out-of-straightness at the lower columns was carried out. In the first loading phase, the frame was loaded with a constant beam load of 30 kN/m. The response of column end moment with increasing load is as shown in Figure 5.87(a). It is assumed that the bending moment transmitted to the column end does not change with increasing column loads. As can be seen from the figure, the beam load has induced negative moment M_{beam} at the column end, acting in a clockwise direction.

In the second loading phase, the frame was loaded with incremental axial loads without the presence of beam load. The response of the column is shown in Figure 5.87(b). The application of axial loads to the column with an imperfection of L/3000 has induced positive bending moment M_{axial} at the column end.

In the main parametric study (see section 5.2.3), the beam is loaded first prior to the incremental axial column loads. Hence to simulate this loading, the response in the first loading phase is superimposed on the response in the second loading phase. The result is shown in Figure 5.87(c). The superimposed of M_{axial} and M_{beam} gives M_c. It can be seen that the column end moment M_c decreases with increase in column load. The reduction of column end moment before yielding occurs in the column is identified as the moment shedding in the elastic range. As can be seen from Figures 5.87(a), 5.87(b) and 5.87(c), the phenomenon of moment shedding is a consequence of the reversal moments acting at the joint. In this case, it can be seen that the reduction of moment in the elastic range is not dominant in which the column end moment is still significant (see Figure 5.87(c)). This implies that moment shedding in the inelastic range plays a significant role in relaxing the column end moment.

In case 2, i.e. in the case of columns with inwards initial out-of-straightness, it is seen that both the gravity and axial loads have produced negative moments (see Figures 5.88(a) and 5.88(b)). The addition of M_{axial} and M_{beam} has caused the column end moment, M_c to increase with increase in column load (see Figure 5.88(c)).

The above response is based on the superimposed loads. The true phenomenon of moment shedding for both cases 1 and 2 with the beam load applied first and followed by the incremental axial loads to failure is shown in Figures 5.89 and 5.90

respectively. It is seen that the column with inwards initial out-of-straightness gives smaller amount of moment shedding in both the elastic and inelastic ranges. The percentage values of moment shedding for each case are shown in Figures 5.89 and 5.90 respectively. The column in case 2 failed at 1568 kN as compared to 1581 kN in case 1 (see Figure 5.91). However, the difference of the ultimate loads is small, i.e. about 0.8%. The study conducted in this thesis is focused on the outwards initial out-of-straightness columns only.

5.7 Relation to Design

Results of the study show that beyond yielding the configuration of moment in the frame has changed dramatically due to the phenomenon of moment shedding. The configuration of moments at ultimate load shows that a beam-column with end restraints can be treated as an axially loaded compression member. As for the beams, the bending moment configuration diagram can be simplified as simply supported with a certain amount of end restraint. Preliminary studies on a series of two-storey and one-bay frames conducted in this chapter show that the suggested amount of end restraint moment of the external ends of external beams may be taken as; 0% for flexible connections such PDEP connections, 5% of M_p of the connected beams for semi-rigid FEP connections and also 5% of M_p of the connected beams for EEP and RIGID connections. It should be mentioned that the end restraint moment of 5% of M_p instead of 10% of M_p (see sections 5.5.1.3 and 5.5.1.4) is adopted for EEP and RIGID connections for a more conservative approach. The connections can be determined as either flexible, semi-rigid or rigid connections based on the current connection stiffness classification method.

Table 5.5 shows some of the beneficial and detrimental items that may be useful for design considerations.

5.8 Conclusions

The parametric study on the behaviour of beam-columns with semi-rigid connections in the elastic and inelastic ranges for non-sway frames has been discussed. The study, however, is limited to a one-bay and two-storey frame only.

The results show that the behaviour beyond yielding is significantly different from the behaviour in the elastic range. This is due to the effect of moment shedding which significantly influenced the form of moment transfer from the initial beam loads up to the collapse condition. At the collapse load, the structure is seen to become analogous to a statically determinate system in which the columns and the beams can be treated individually.

On the basis that at collapse load the structure is still in a state of stable equilibrium, the configuration of the bending moments can be adopted as a fundamental feature for a true simplified design method. The results have shown that at collapse load, the column end moment reduced and usually can be relaxed to zero ($\pm$ 0). Therefore, the bending moment diagram of a beam-column at ultimate load is similar to that the bending moment diagram of an axially loaded compression member. On this basis, the columns with semi-rigid connections can be designed as carrying axial load loads only.

As a result of moment redistribution due to moment shedding, beams with semi-rigid connections can be treated as simply supported with a certain degree of fixed end restraint. Beams with simple semi-rigid connections such as PDEP connections can be designed as simply supported with zero end restraints. Similarly, the external ends of external beams with semi-rigid connections such as FEP and EEP connections can be designed assuming a restraining moment equal to 5% of M_p of the connected beam to take into account the semi-rigid effect.

The most significant advantage of this simplified design method is that both beams and columns design are independent of the connection M-ϕ characteristics.

Another important conclusion from this study is that it is seen that the occurrence of moment shedding is more obvious when columns buckle about minor axes. It is believed that one of the factors that may contribute to this effects is the smaller second moment of area in the minor axes such as I_{yy} for H columns and I_{xx} or I_{yy} for SHS columns. This can be explained by the fact that, once the column has yielded, more sudden vanishing stiffness occurs due to the smaller values of EI that are associated with the minor axis flexure. This in turn causes a larger effect of moment shedding.

In addition, columns with imperfections carrying axial loads and moments which failed in single curvature are seen to have about 50% of the area at the mid-height in a yield condition prior to collapse. This is observed in columns of intermediate slenderness, approximately those with $20 < \lambda < 100$. It is also seen that the presence of bending moments at column ends due to beam loads can be concluded to be analogous to a pin ended column with imperfections as both will reduce the ultimate capacity.

Further important conclusions regarding the connection characteristics which can influence the column performance are as follows:

1. The degree of restraint offered by the connections influences the attainment of first yield, rate of yield spreading and the rate of vanishing stiffness in the columns.

2. In this loading regime with beam loads applied first followed by increasing axial loads to failure, columns with the more flexible connections have small initial deflections which delays the formation of first yield.

3. The use of flexible connections leads to some effects such as small initial column deflections, small column rotations and high first yield loads. As a result, a significant proportion of the axial column load capacity is achieved in the elastic range. It can be concluded that the use of flexible connections is analogous to a pin ended column with a small imperfection that can provide high ultimate load capacity.

4. It is seen that the stiffness of the connections is more important and becomes more dominantly utilised in the inelastic stage, that is when the column starts to lose its stiffness after the attainment of first yield.

5. In the inelastic range, columns with more flexible connections experience more rapid rate of yielding and hence dramatic loss of stiffness. This effect has resulted in the column being able to carry only small additional axial loads and hence only small reserve of strength.

6. Increasing the column end restraints will enable the connection to further restrain the column after the attainment of first yield and permit larger column end rotations and larger column deflections. This effect delays the spread of yield and consequently delays the loss of stiffness. This in turn will enable the column to carry larger additional axial loads as the detrimental moment is being shed and relaxed. Consequently, the columns with stiffer connections offer larger reserves of strength above first yield.

7. The extent of column rotation in the inelastic range is influenced by the connection restraint. The stiffer the connection the larger is the value of the column end rotation at failure and consequently permits larger moment shedding in the inelastic range.

8. The amount of moment shedding redistributed from the column ends to the beams depends on the degree of connection restraint. Less stiff connections will attract a small amount of shed moment and hence permit a small amount of the moment to be redistributed back to the beam. As a consequence, the beam with flexible connections will not undergo significant change of bending moment as a result of moment redistribution.

5.9 References

[5-1] France, J.E., 'Bolted connections between open section beams and box columns', Ph.D. Thesis, Department of Civil & Structural Engineering, University of Sheffield, U.K., January, 1997.

[5-2] Eurocode 3, 'Design of steel structures - Part 1.1: General rules and rules for buildings', ENV 1993-1-1.

[5-3] Bjorhovde, R. and Birkemoe, P.C., 'Limit states design of HSS columns', Canadian Journal of Civil Engineering, 6, 1979, pp. 276-291.

[5-4] Davison, T.A and Birkemoe, P.C., 'Column behaviour of cold-formed hollow structural steel shapes', Canadian Journal of Civil Engineering, 10, 1983, pp. 125-141.

[5-5] Kato, B. 'Cold-formed welded steel tubular members', in Axial compressed structures : Stability and strength, editor R. Narayanan, Applied Science Publisher, London, 1982, pp. 149-180.

[5-6] Laszlo, H., 'Computer simulation of semi-rigid frame behaviour', Stability of Steel Structures, International Colloquium - European Session, Technical University of Budapest, Hungary, Vol. 2, September, 1995, pp. 11/17-11/28.

[5-7] Moy, S.S.J., 'Plastic methods for steel and concrete structures', Macmillan, 2nd. edition, 1996.

[5-8] Salmon, C. G. and Johnson, J. E, 'Steel structures, design and behaviour', 2nd. edition, Harper & Row, Publisher, New York, 1980.

[5-9] Wood, R.H., 'A new approach to column design', Department of the Environment Building Research Establishment, Her Majesty's Stationery Office, 1974.

[5-10] Rifai, A. M., 'Behaviour of columns in sub-frames with semi-rigid joints', Ph.D. Thesis, Department of Civil and Structural Engineering, University of Sheffield, U.K., June, 1987.

[5-11] Baker, J.F., Horne, M.R. and Heyman J., 'The steel skeleton', Cambridge University Press, Vol. 2, 1956.

[5-12] Gent, A.R. and Milner, H.R., 'The ultimate load capacity of elastically restrained H-columns under biaxial bending', Proceedings, Institution of Civil Engineers, Vol. 41, December, 1968, pp. 685-704.

[5-13] Hibbeler, R.C., 'Mechanics of materials', Macmillan Publishing Company, New York, 1991.

[5-14] Wood, R. H., 'The stability of tall buildings', Proceedings, Institution of Civil Engineers, Vol. 11, September, 1958, pp. 685-704.

[5-15] Rygol, J., 'Structural analysis by direct moment distribution', Crosby Lockwood & Sons Ltd., 1968.

[5-16] Gibbons, C., Kirby, P.A. and Nethercot, D.A., 'Experimental behaviour of partially restrained steel columns', Proceeding of Institution of Civil Engineers, Structures and Buildings, 99, February, 1993, pp. 29-42.

[5-17] Davison, J.B., Kirby, P.A. and Nethercot, D.A., 'Column behaviour in PR construction: Experimental behaviour', Journal of Structural Engineering, ASCE, Vol. 113, No. 9, September, 1987, pp. 2032-2050.

[5-18] Kirby, P.A., Bitar, S. and Gibbons, C., 'The design of columns in non-sway semi-rigidly connected frames', First World Conference on Constructional Steel Design', Acapulco, Mexico, December, 1992, pp. 54-63.

[5-19] Ahmed, I and Kirby P.A., 'Maximum connection rotations in non-sway semi-rigid frames', Journal of Constructional Research, Vol. 40, No. 1, 1996, pp. 1-15.

[5-20] BS 5950: Part 1: 1990, 'Structural use of steelwork in building', Part 1. Code of practice for design in simple and continuous construction : hot rolled sections, British Standard Institution.

[5-21] Gent, A.R., 'Elastic-plastic column stability and the design of no-sway frames', Proceedings, Institution of Civil Engineers, Vol. 34, June, 1966, pp. 129-152.

[5-22] Gibbons, C., Nethercot, D.A., Kirby, P.A. and Wang, Y.C., 'An appraisal of partially restrained column behaviour in non-sway steel frames', Proceeding of Institution of Civil Engineers, Structures and Buildings, 99, February, 1993, pp. 15-28.

[5-23] Foley, C.M. and Vinnakota, S., 'Inelastic analysis of partially restrained unbraced steel frames', Engineering Structures, Vol. 19, No. 11, 1997, pp. 891-902.

[5-24] Technical Committee 8 - Structural stability, Technical working group 8.1/8.2: Skeletal structures, 'Analysis and design of steel frames with semi-rigid joints', 1st. edition, 1991.

LOAD		Connection Types				
		"PINNED"	PDEP	FEP	EEP	RIGID
Collapse load, P_{sr}	(kN)	1655	1638	1592	1540	1538
First yield load, P_y	(kN)	1645	1615	1535	1390	1375
Reserve of strength(1)	(kN)	10	23	57	150	163
Percentage of reserve of strength(2)	(%)	0.6%	1.4%	3.7%	11%	11.9%

Note:
(1). Reserve of strength = P_{sr} - P_y

(2). Percentage of reserve of strength = $\dfrac{\left(P_{sr} - P_y\right)}{P_y} \times 100\%$

Table 5.1 Comparisons of collapse loads, first yield load and reserve of strength with different connection types

PERCENTAGE OF EFFECTIVE END RESTRAINT MOMENT		Connection Types				
		"PINNED"	PDEP	FEP	EEP	RIGID
At beam load	(% of M_p)	0.68%	3.4%	9.8%	21.2%	24.6%
At collapse load	(% of M_p)	0.66%	3.2%	7.8%	11.1%	10.8%
Percentage of reduction(1)	(%)	2.9%	6.8%	20.4%	47.6%	56.1%

Note:
(1). Percentage of reduction = [% at beam load - % at collapse load) / % at beam load] × 100%

Table 5.2 Percentage of effective end restraint moment at beam ends

COLUMN ROTATION		Connection Types				
		"PINNED"	PDEP	FEP	EEP	RIGID
(1). At beam load	(millirad.)	-0.1	-0.6	-1.7	-3.7	-4.1
(2). At first yield load	(millirad.)	-0.5	-1.0	-2.3	-4.2	-4.6
(3). At collapse load	(millirad.)	-0.6	-1.3	-3.5	-7	-7.9
(4). Elastic rotation(a)	(millirad.)	-0.4	-0.4	-0.6	-0.5	-0.5
(5). Inelastic rotation(b)	(millirad.)	-0.1	-0.3	-1.2	-2.8	-3.3

Note :
(a). Elastic rotation = rotation at first yield load - rotation at beam load
(b). Inelastic rotation = rotation at collapse load - rotation at first yield load

Table 5.3 Comparisons of column rotations with different connection types

CONNECTION ROTATION		Connection Types				
		"PINNED"	PDEP	FEP	EEP	RIGID
(1). At beam load	(millirad.)	-10.7	-9.5	-6.7	-1.7	0
(2). At first yield load	(millirad.)	-10.3	-9.1	-6.3	-1.6	0
(3). At collapse load	(millirad.)	-10.2	-8.9	-5.4	-0.9	0
(4). Maximum rotation	(millirad.)	10.7	9.5	6.7	1.7	0

Table 5.4 Comparisons of connection rotations with different connection types

Items	Beneficial effects to columns	Detrimental effects to columns
Yielding in columns	• Moment shedding	• Loss of stiffness
Flexible connections	• Smaller values of column rotations and column deflections • High first yield load • High axial load capacity in the elastic range	• Small axial load capacity (small reserve of strength) in the inelastic range
Stiffer connections	• High axial load capacity (high reserve of strength) in the inelastic range	• Large values of column rotations and column deflections • Early formation of first yield

Table 5.5 List of beneficial and detrimental items to columns

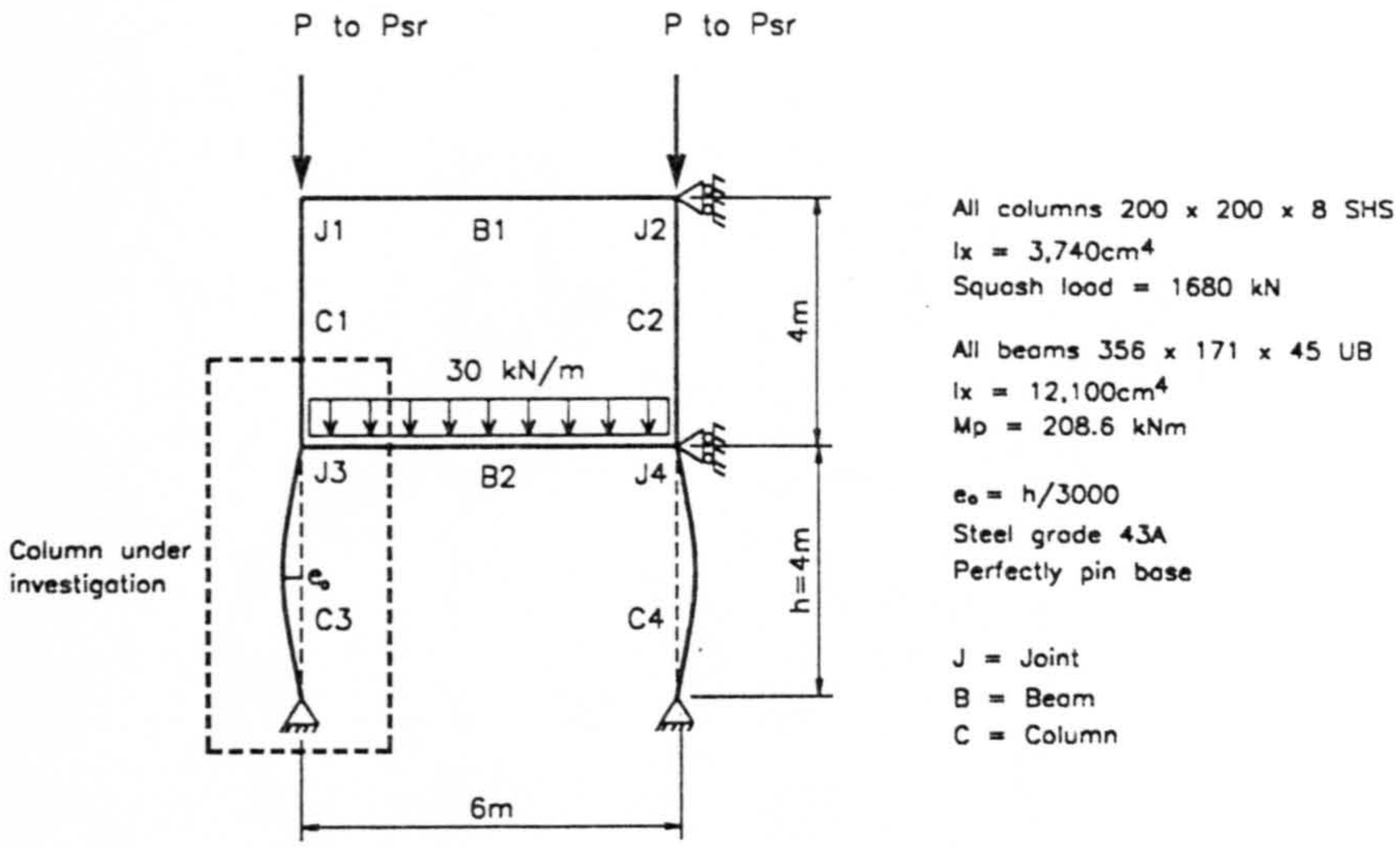

Figure 5.1 Frame dimensions and loadings

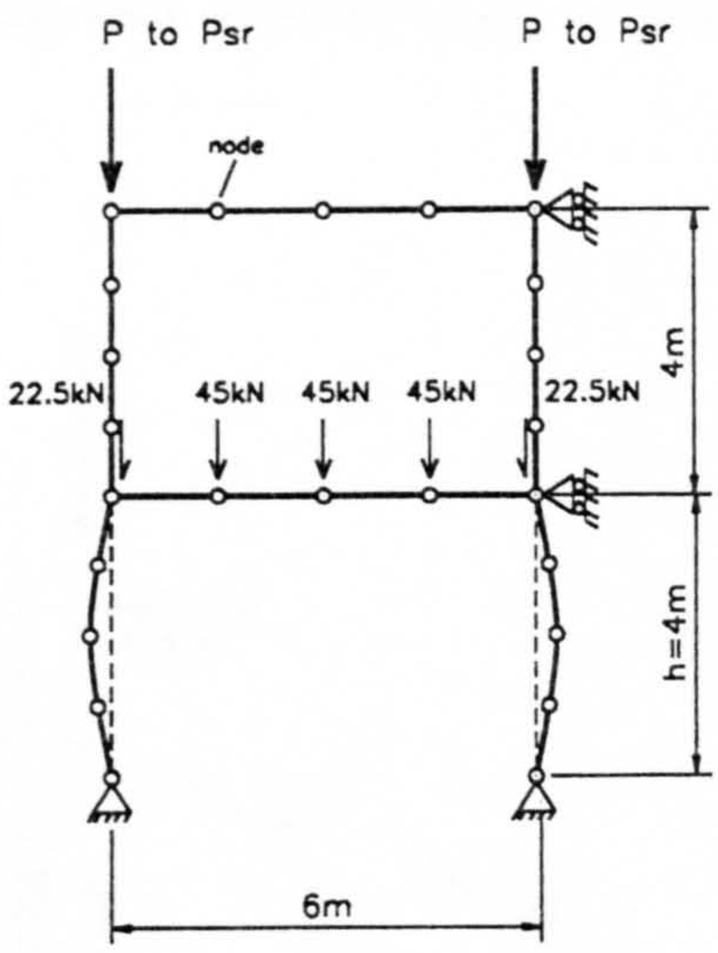

Figure 5.2 Finite element model and equivalent 30kN/m uniform distributed loads

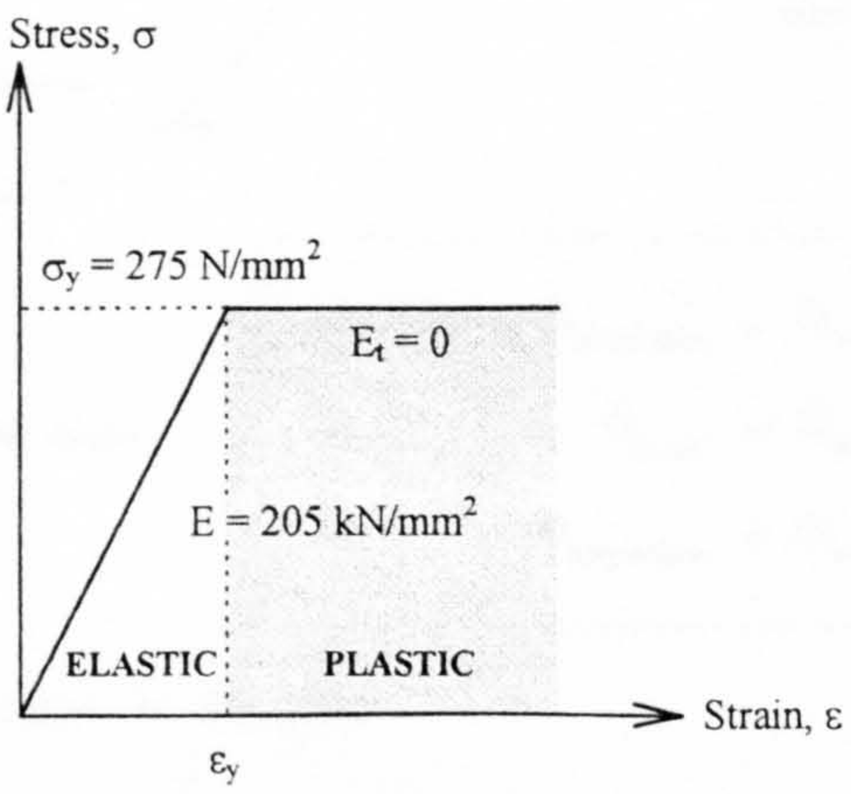

Figure 5.3 Bilinear elastic–perfectly plastic material model used in the study

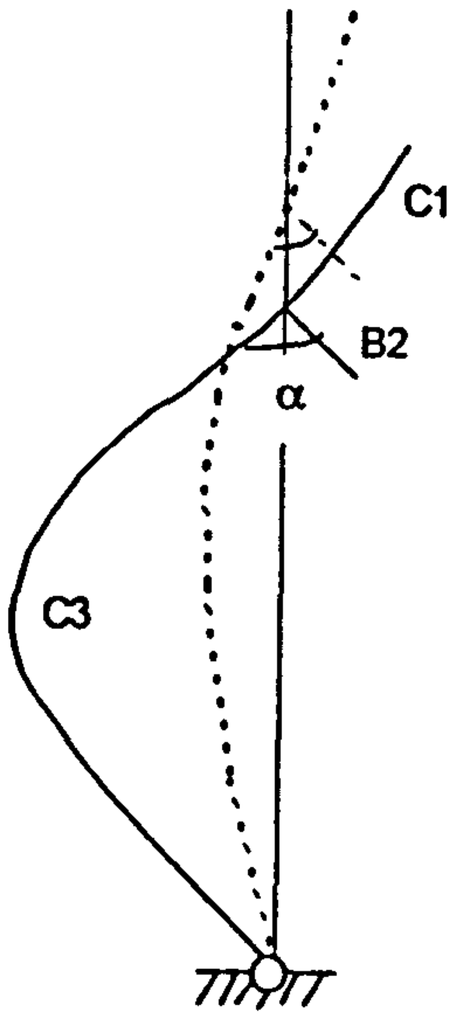

(a). Deformed angle α between beam and lower column

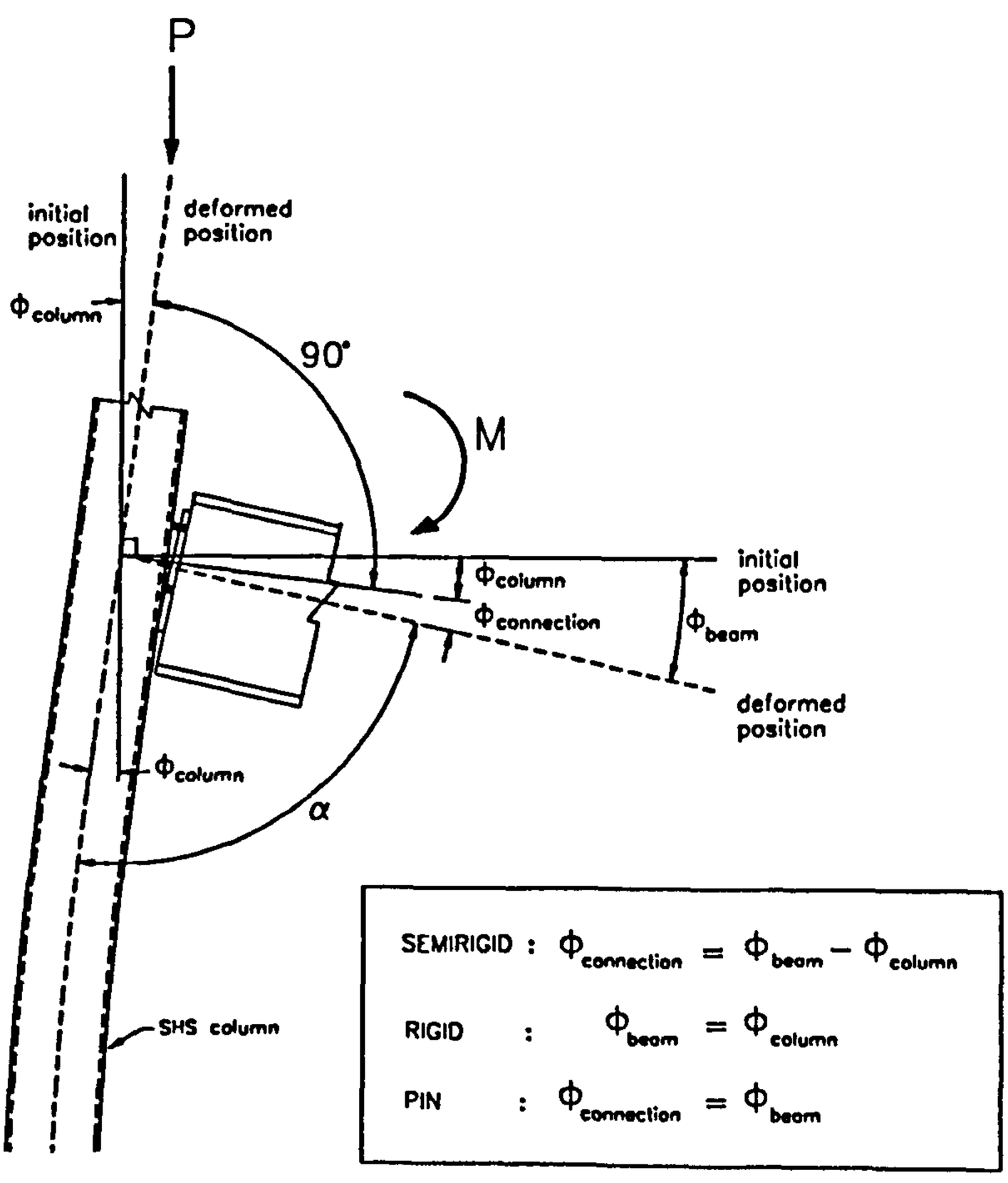

(b). Types of rotation at the joint

Figure 5.4

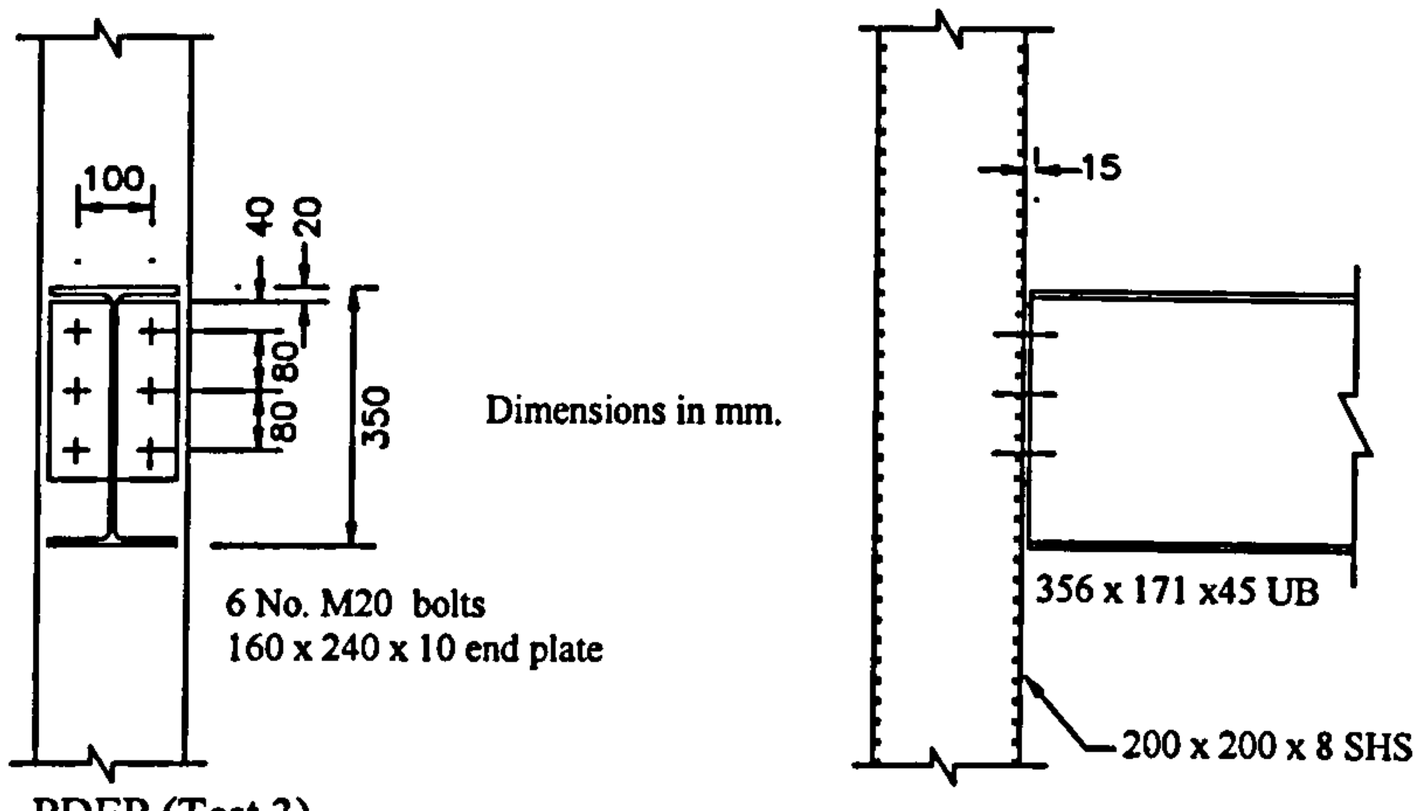

PDEP (Test 3)

(a). Partial depth end plate, PDEP (Test 3)

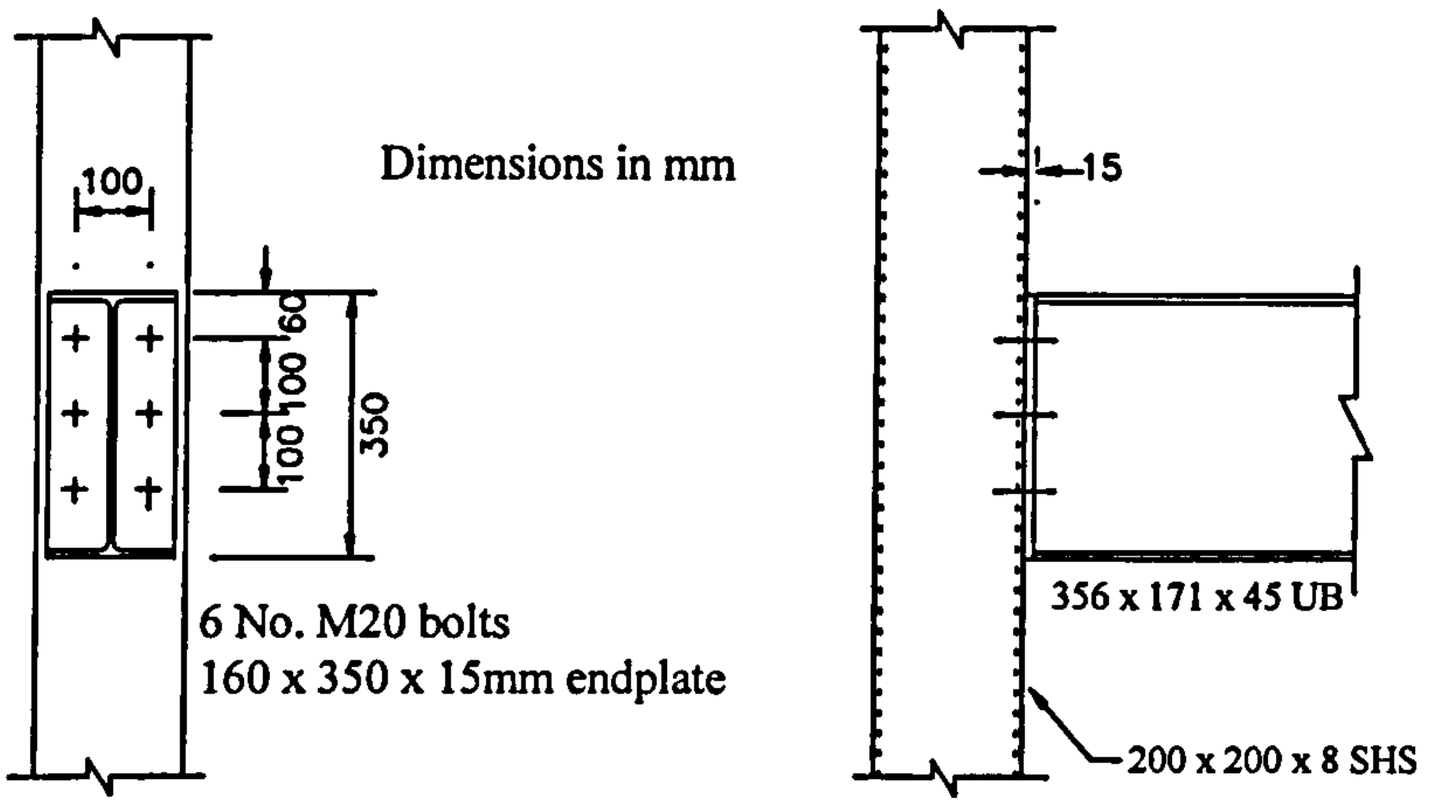

FEP (Test 18)

(b). Flush end plate, FEP (Test 18)

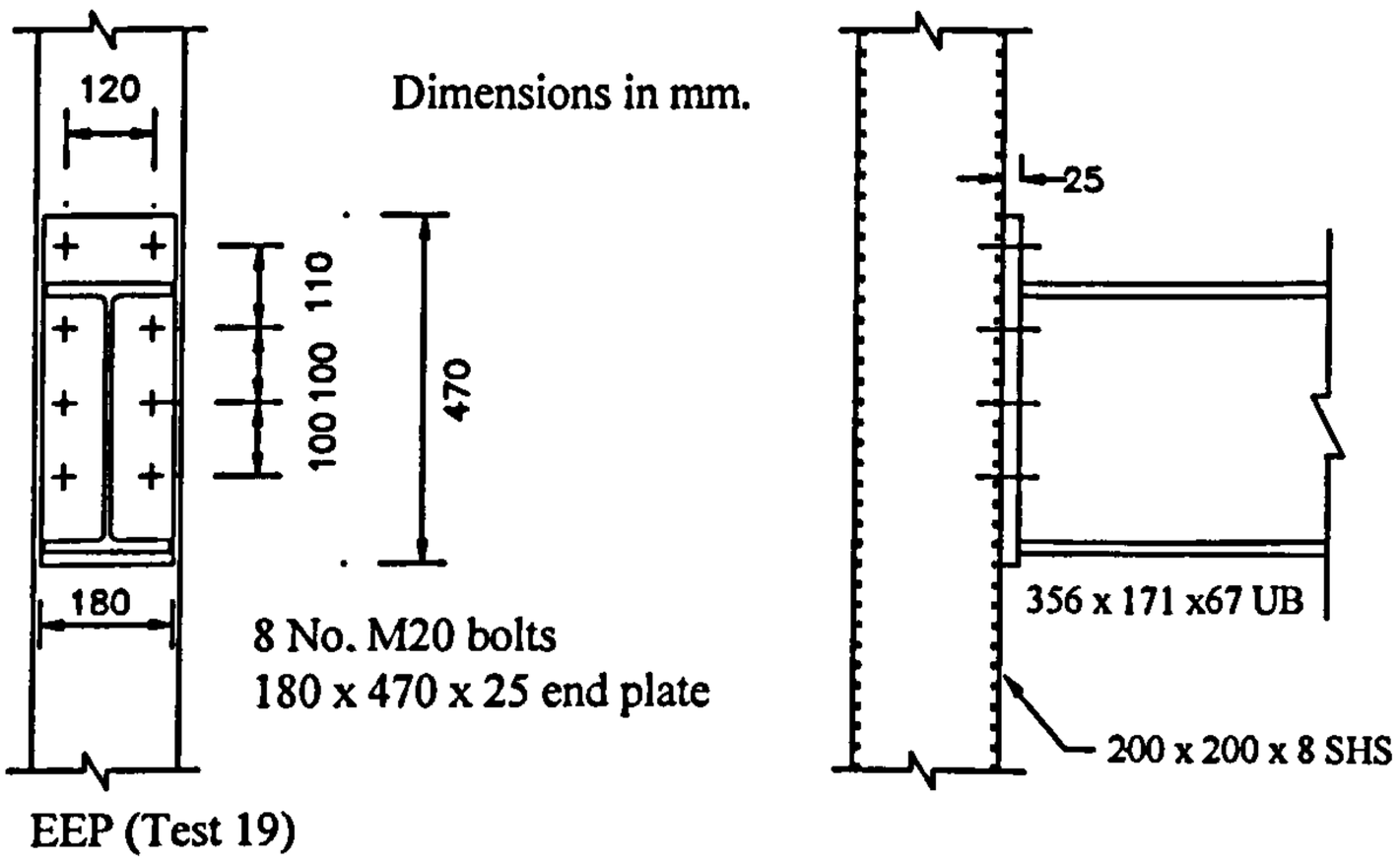

EEP (Test 19)

(c). Extended end plate, EEP (Test 19)

Figure 5.5 Types of flowdrill connections used in the study [5-1]

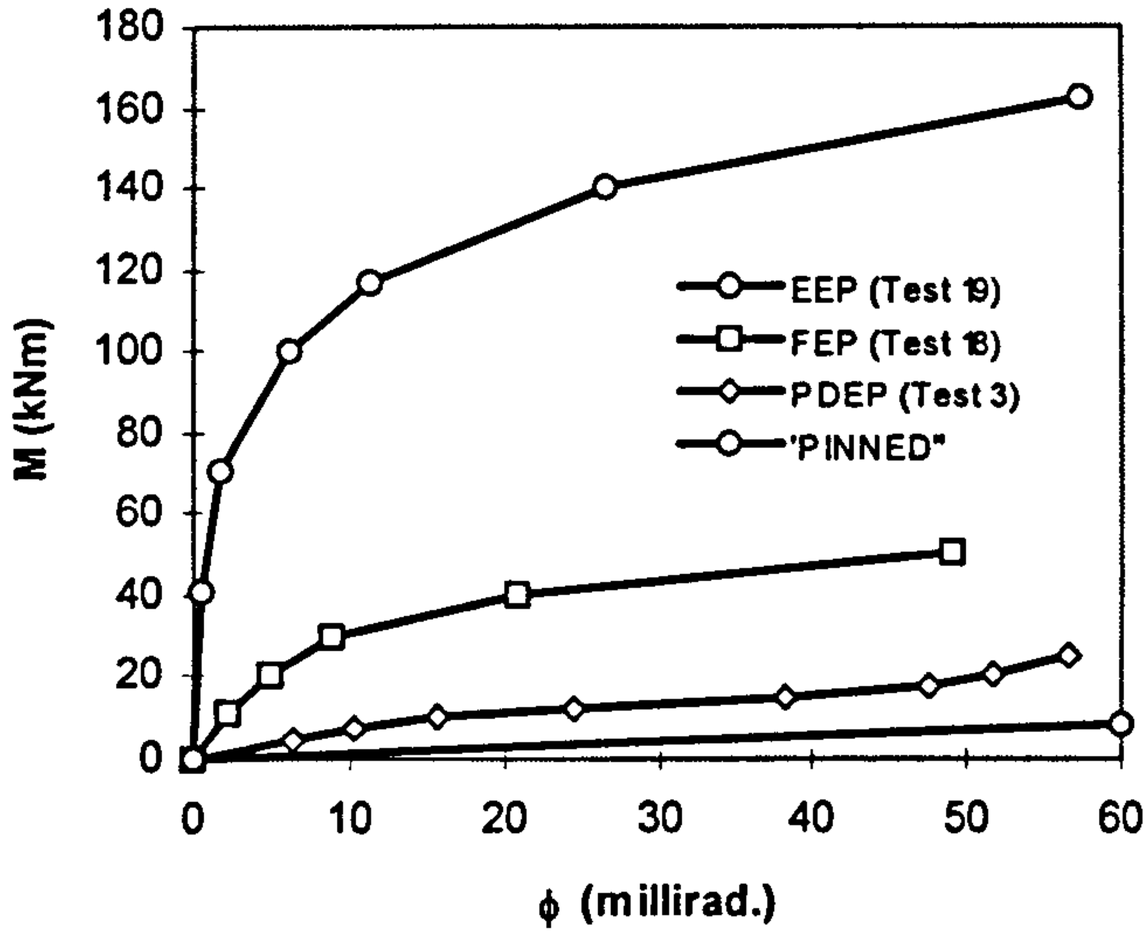

Figure 5.6

Experimental M-ϕ curves for PDEP, FEP and EEP connections shown in Figure 5.5 [5-1] and M-ϕ for "PINNED" connections

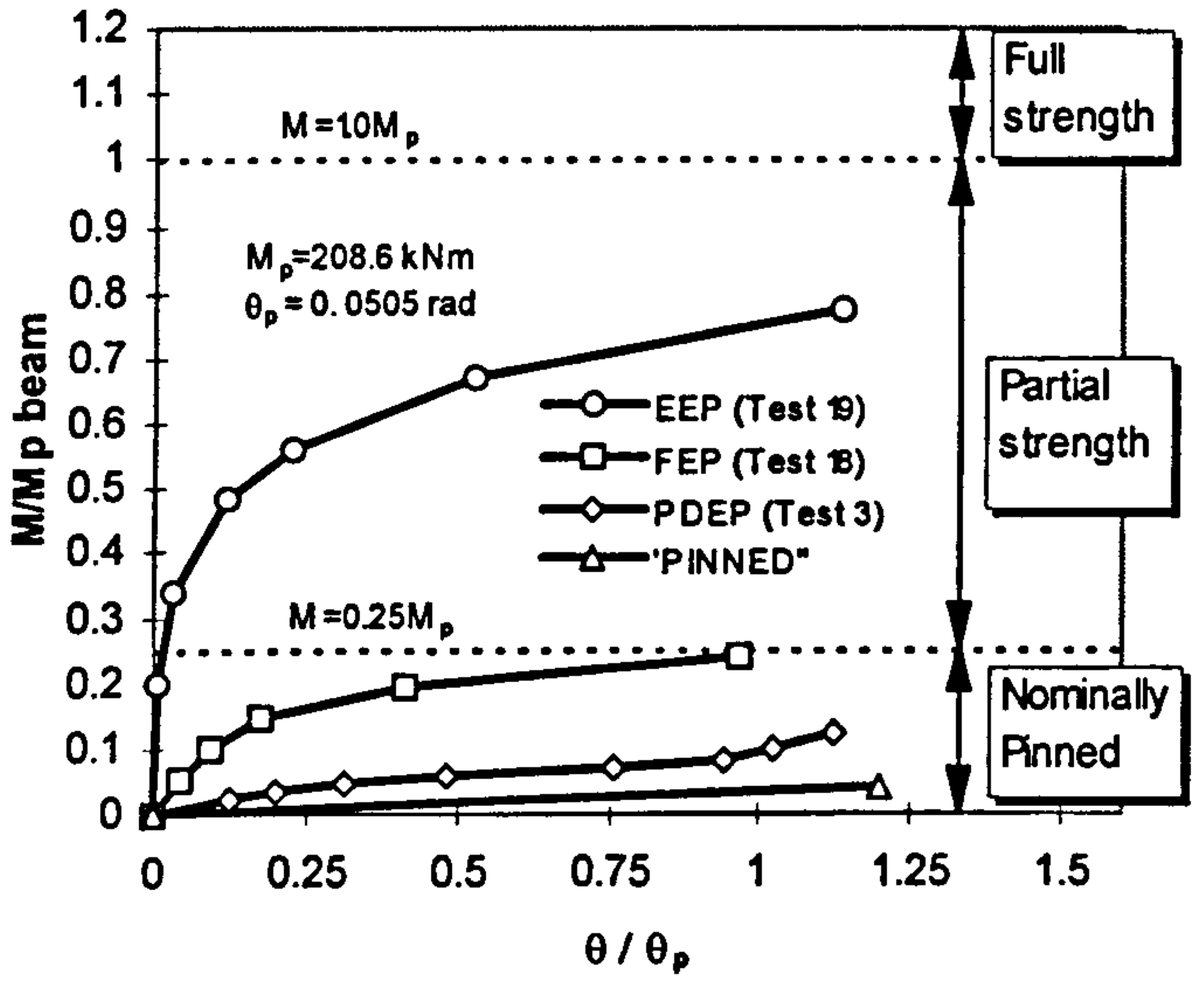

Figure 5.7

EC3 connection classification by strength [5-2]

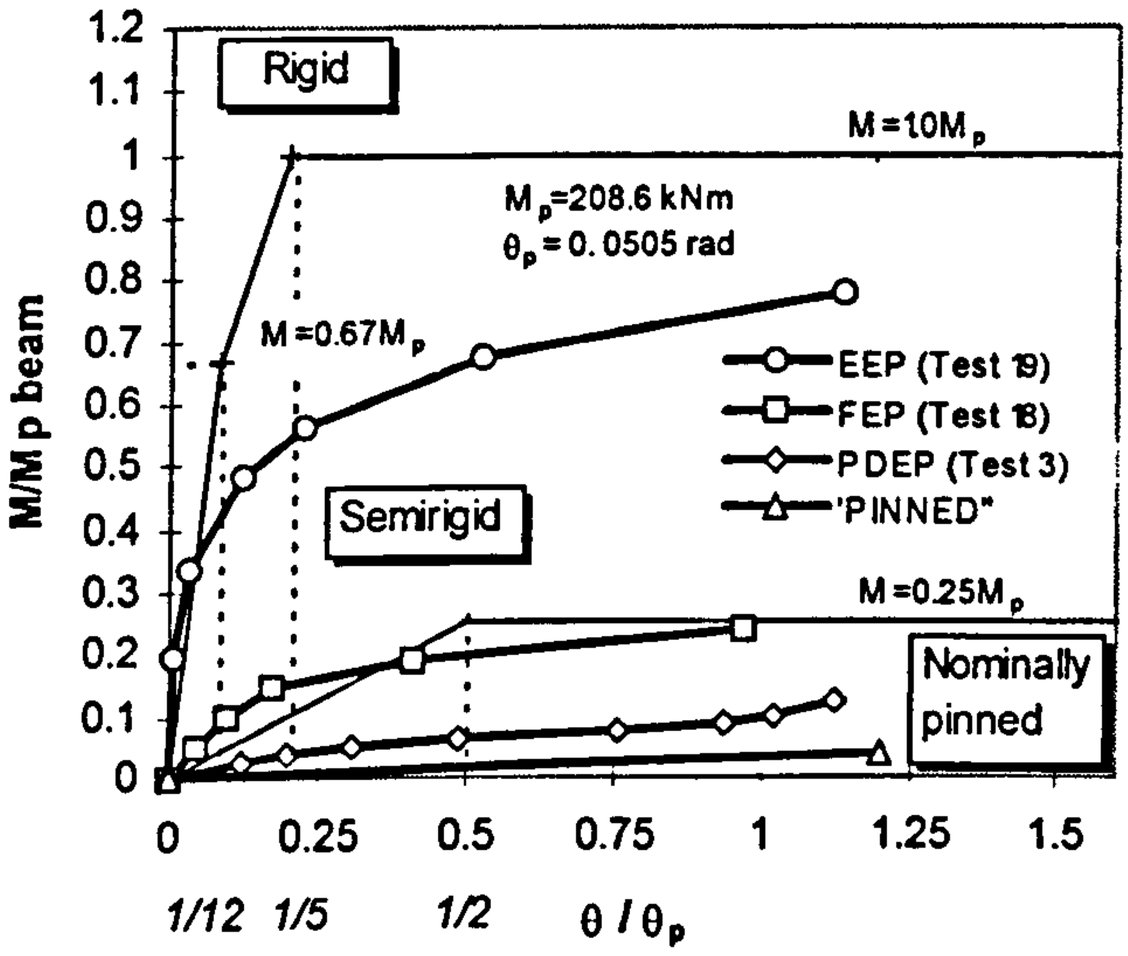

Figure 5.8

EC3 connection classification by rotational stiffness [5-2]

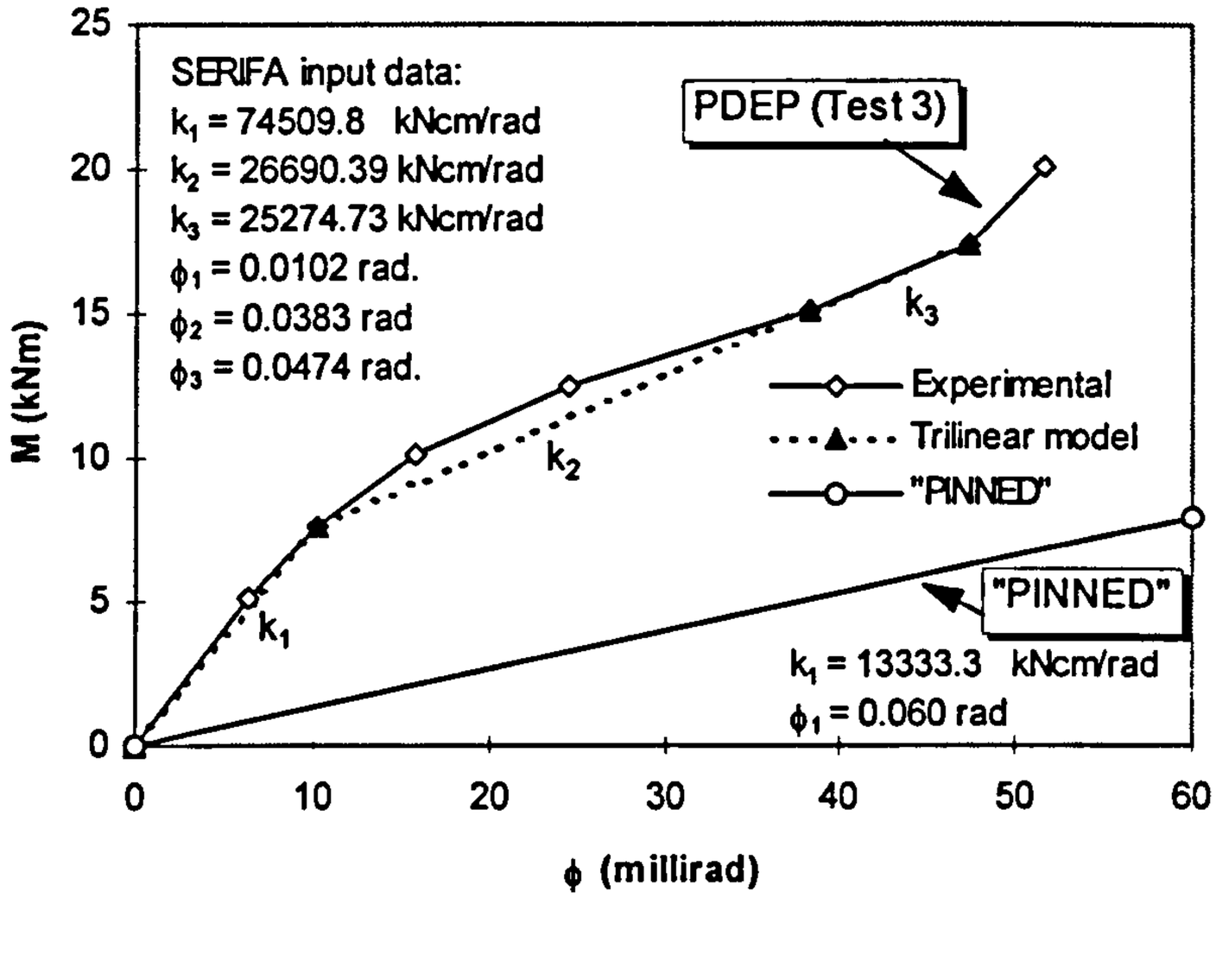

(a).

Partial depth end plate, PDEP (Test 3) and "PINNED"

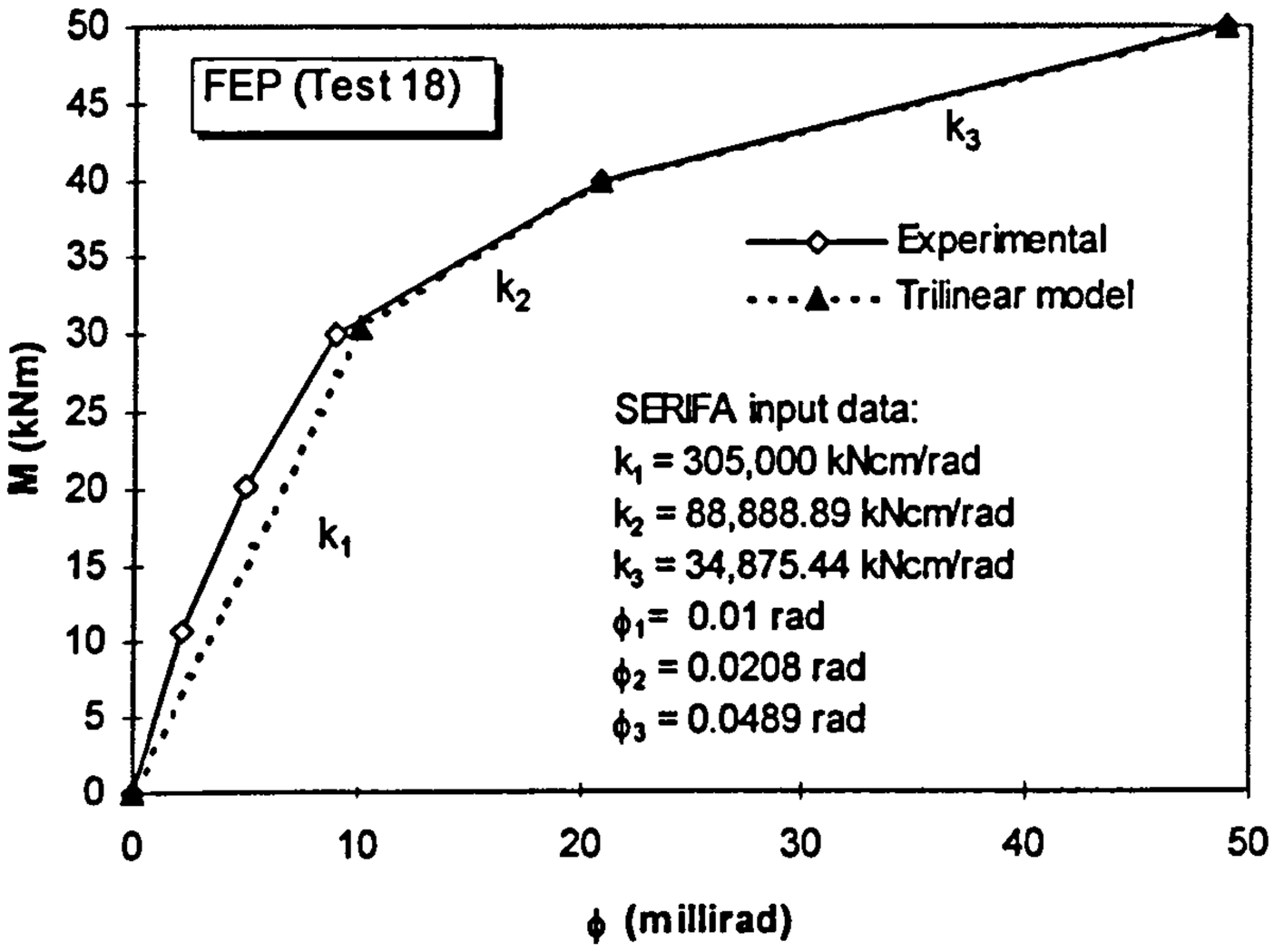

(b).

Flush end plate, FEP (Test 18)

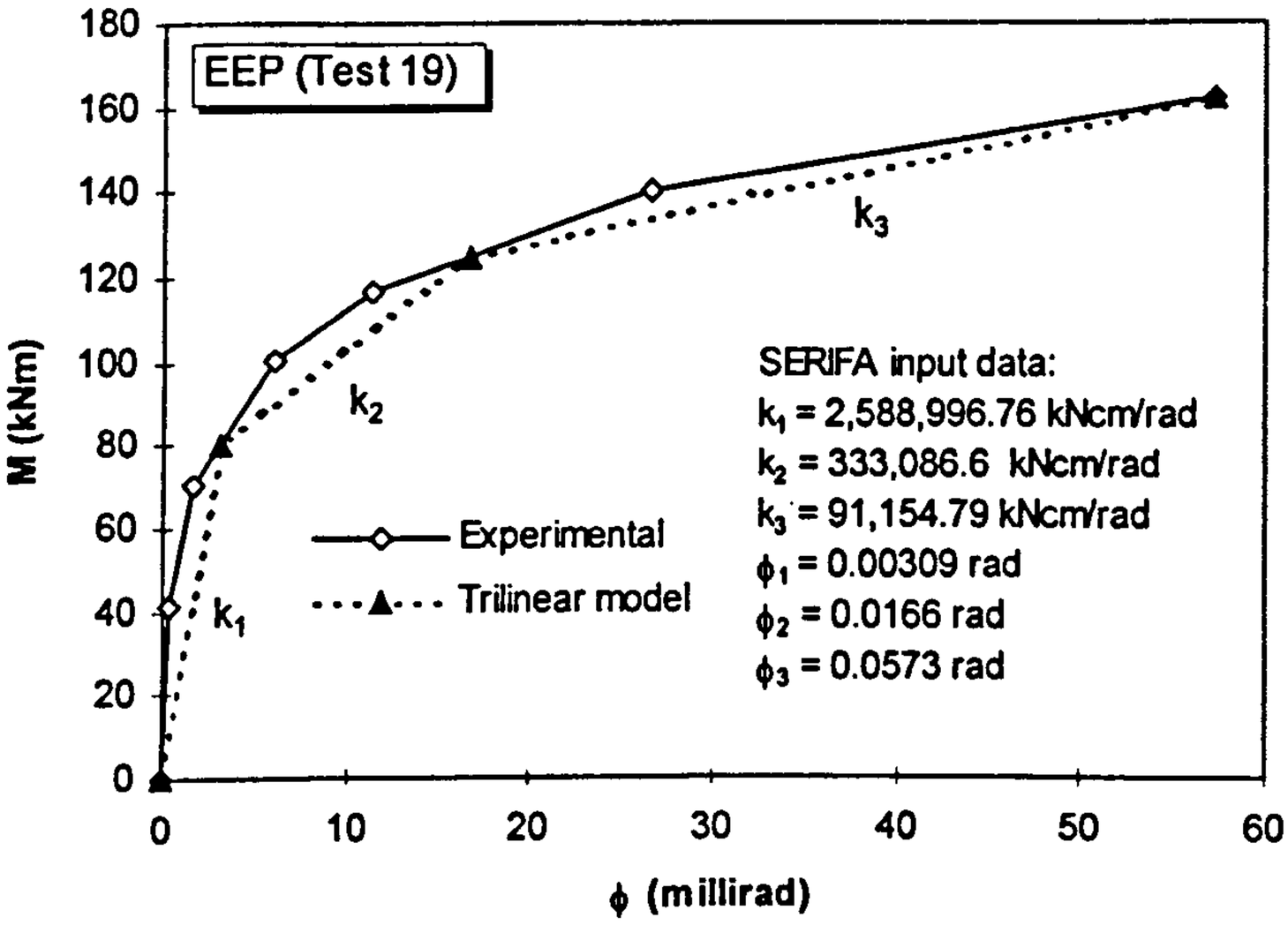

(c).

Extended end plate, EEP (Test 19)

Figure 5.9 *M-ϕ* curve models for connection types PDEP, "PINNED" , FEP and EEP respectively

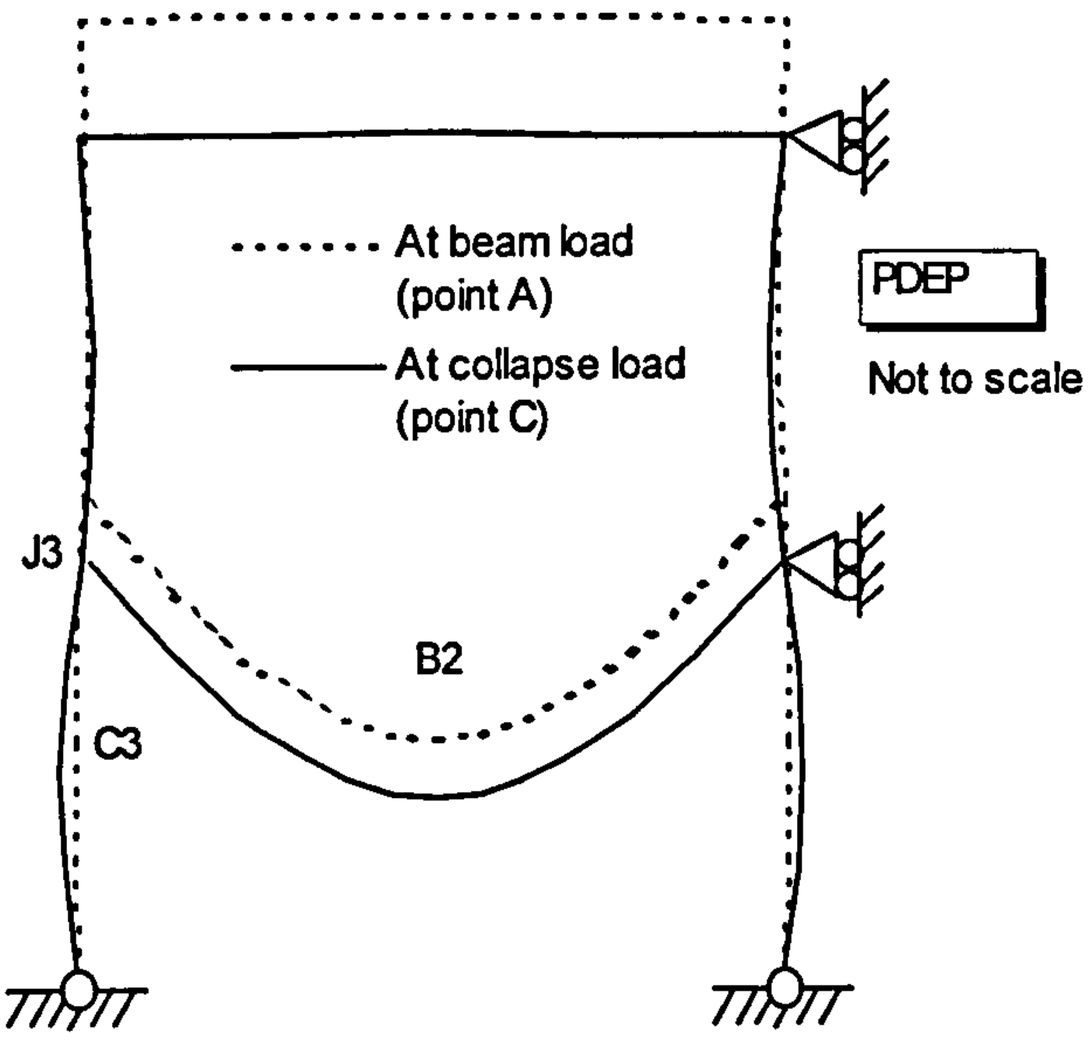

Figure 5.10 Exaggerated deformed shape of frame with PDEP connections

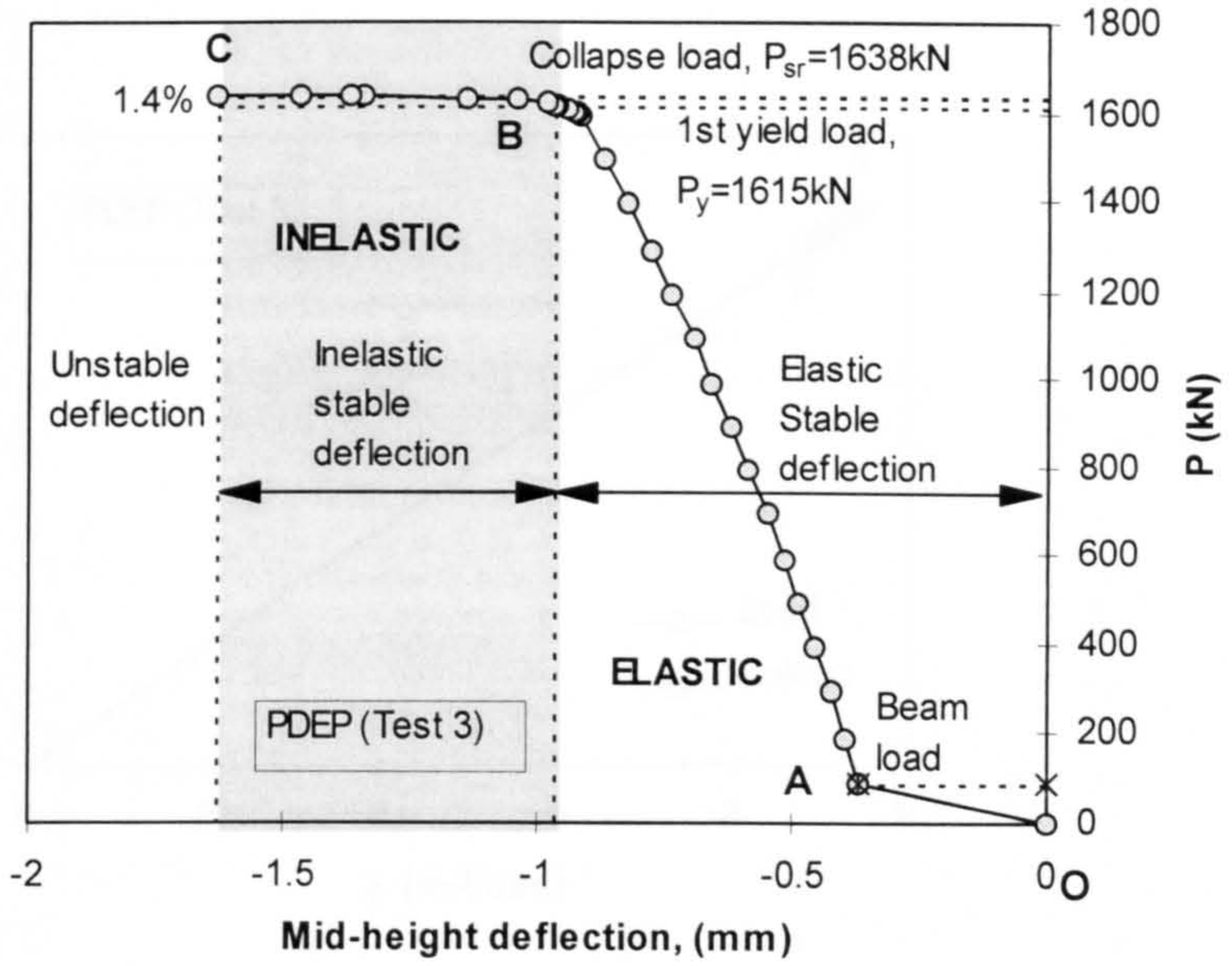

Figure 5.11 Load deflection response at column mid-height with PDEP connections

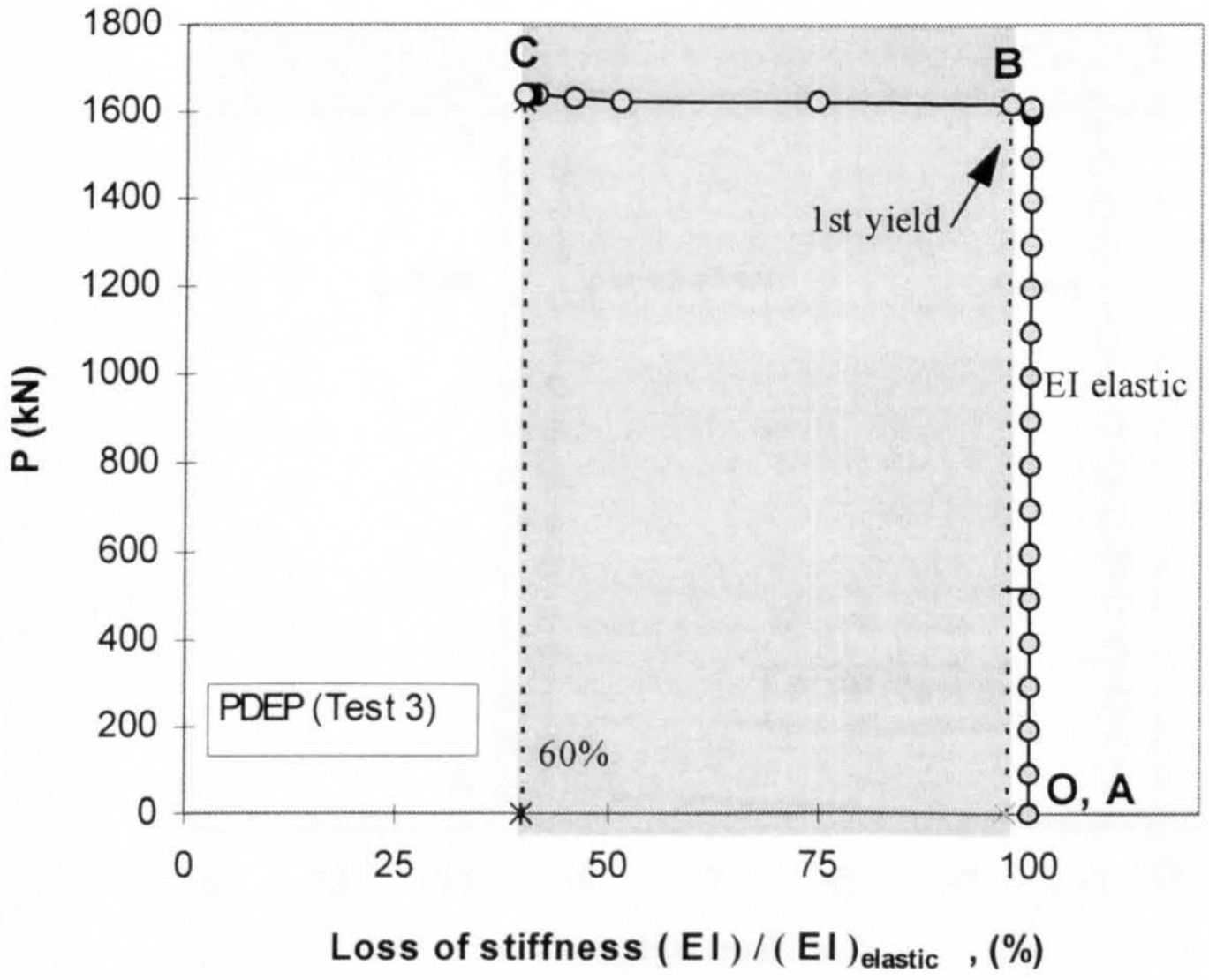

Figure 5.12 Loss of stiffness at column mid-height with PDEP connections

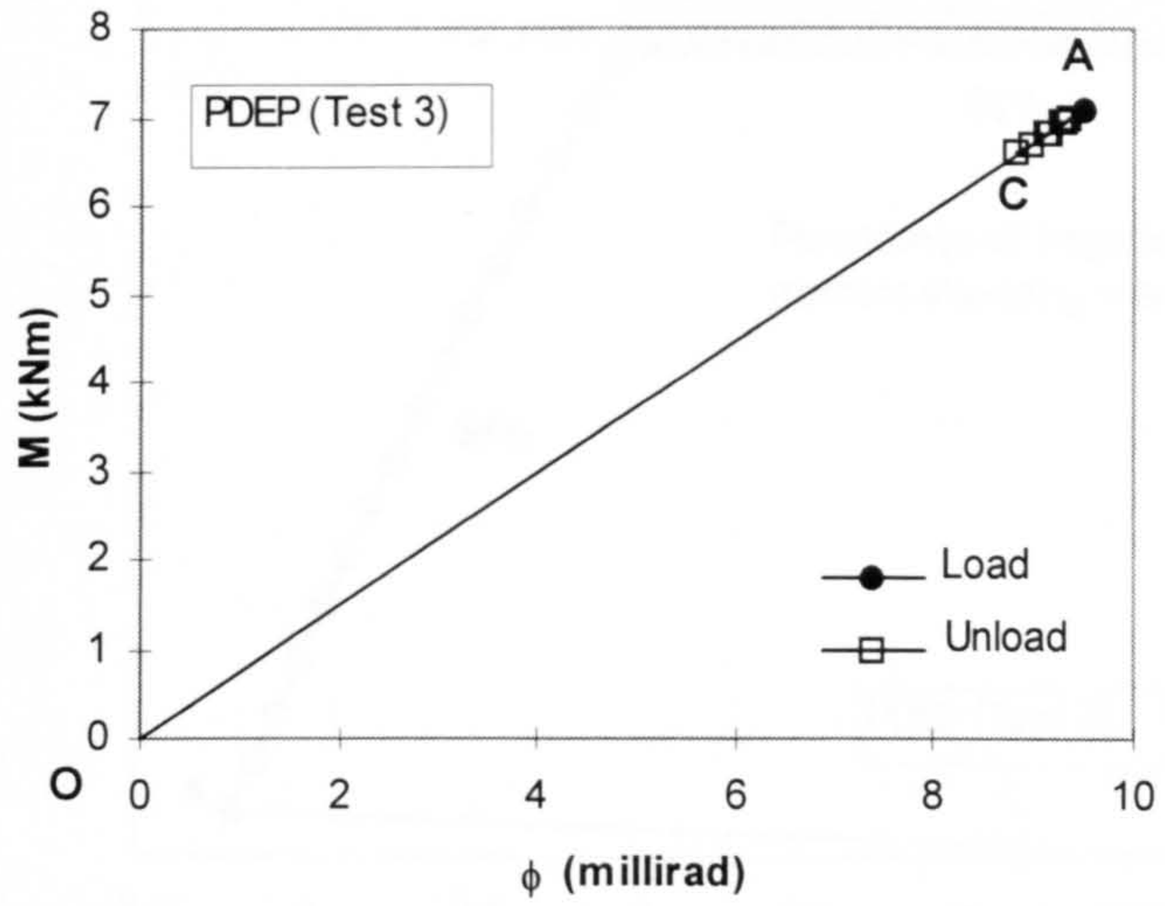

Figure 5.13 M-ϕ response at column top end with PDEP connections

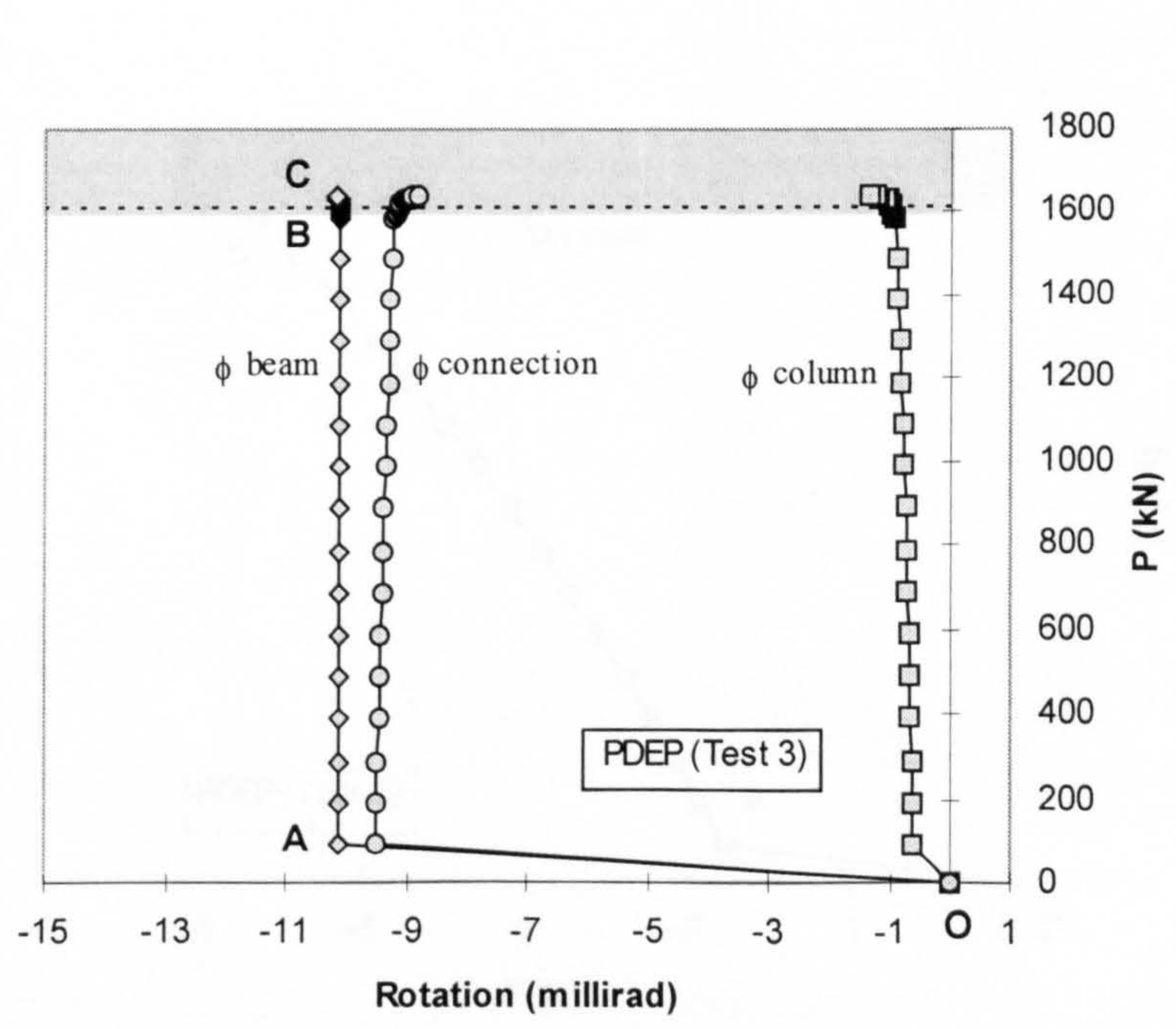

Figure 5.14 Development of beam, column and connection rotations with PDEP connections

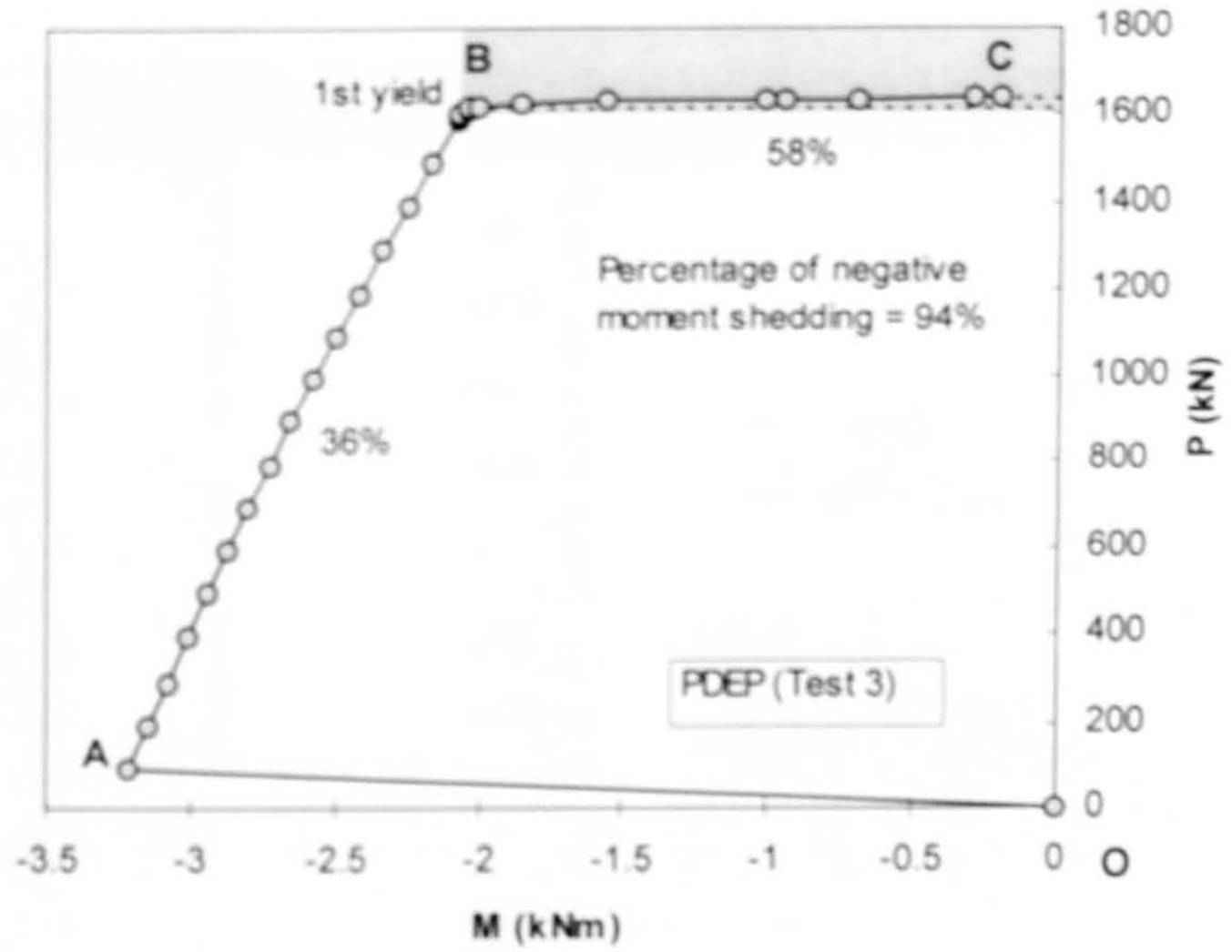

Figure 5.15 Response of moment shedding at column top end with PDEP connections

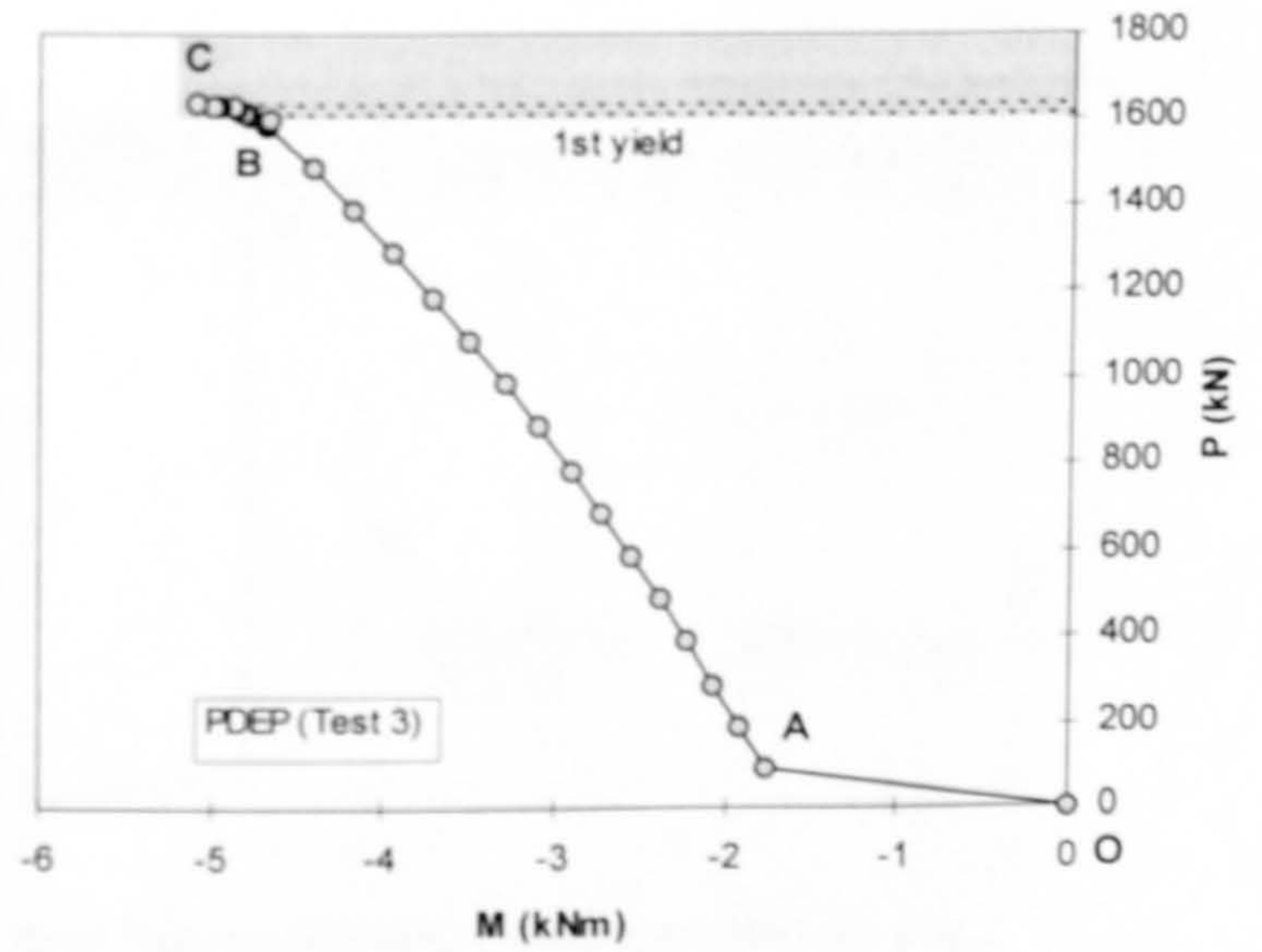

Figure 5.16 Response of moment at column mid-height with PDEP connections

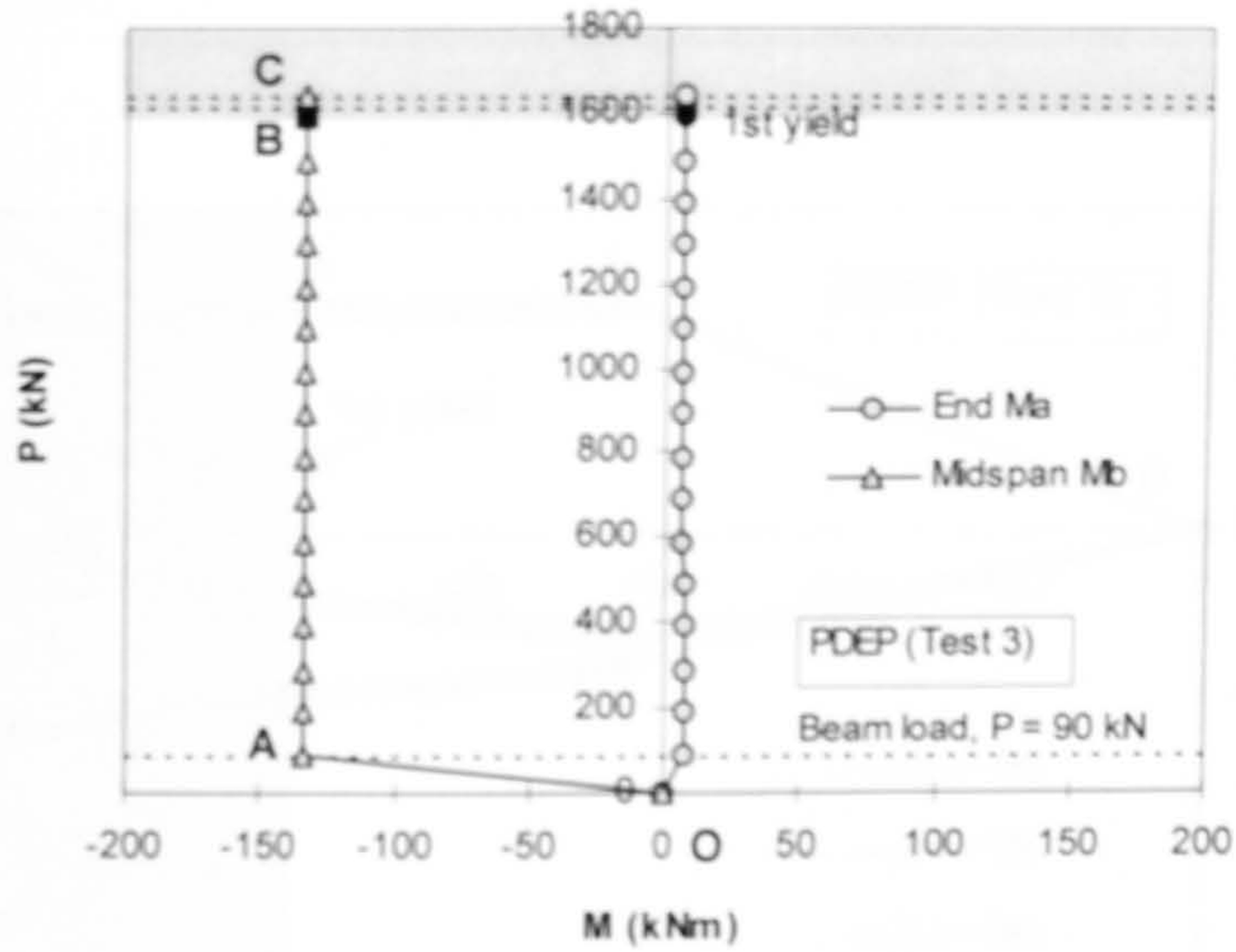

Figure 5.17 Response of moments at both beam end and beam midspan with PDEP connections

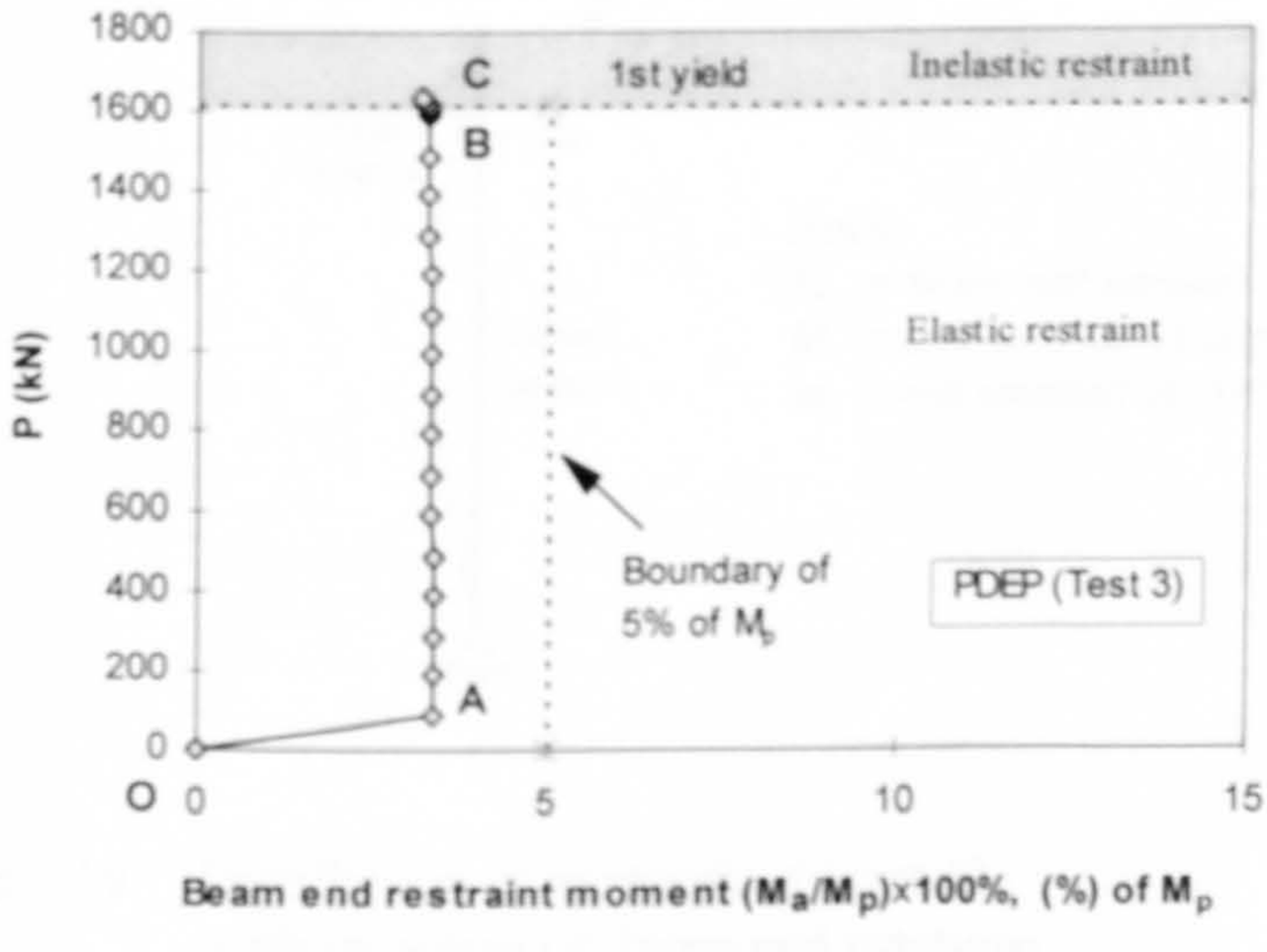

Figure 5.18 Development of beam end restraint moment with PDEP connections

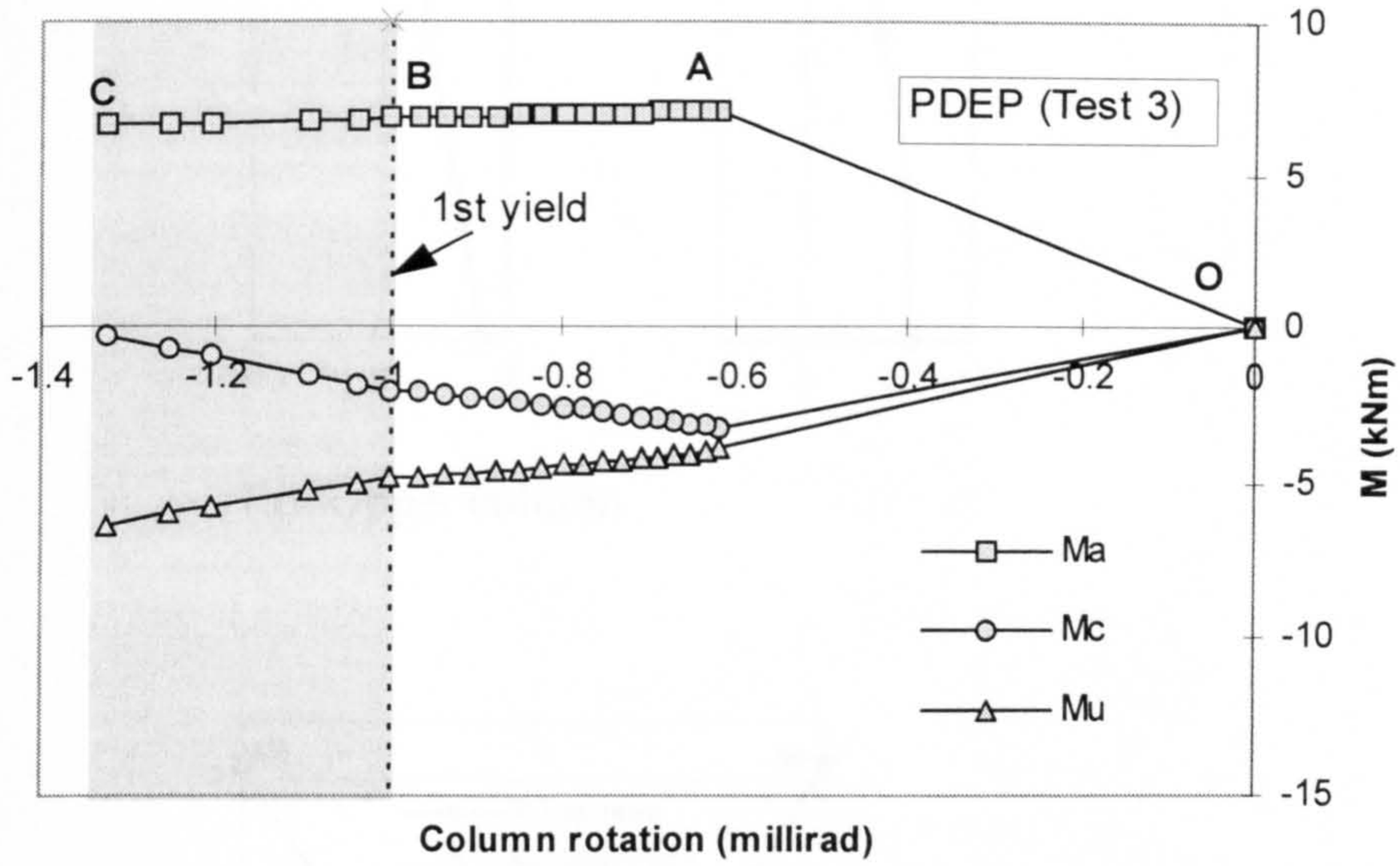

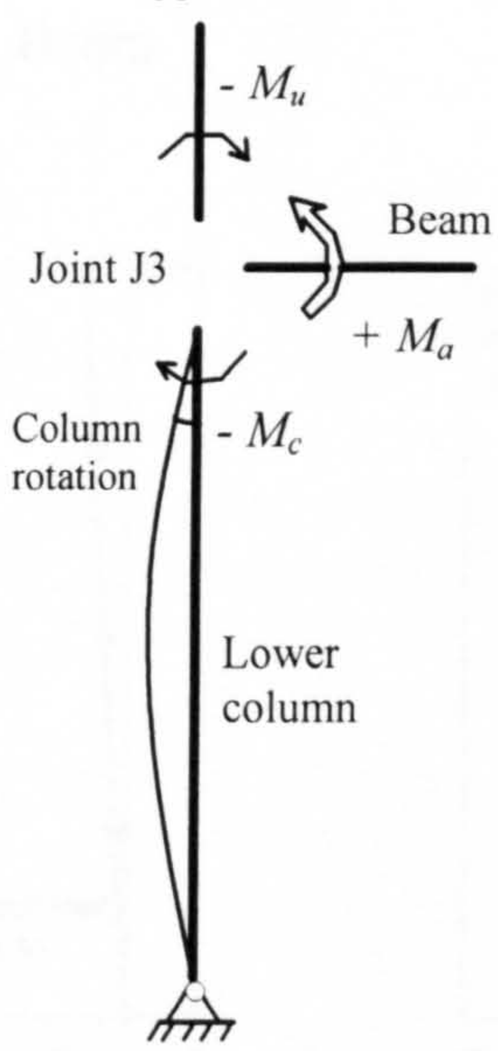

Notes:
M_a = beam end moment
M_u = end moment of upper column
M_c = end moment of lower column

Figure 5.19 Distribution of moments at joint J3 with increasing column end rotations

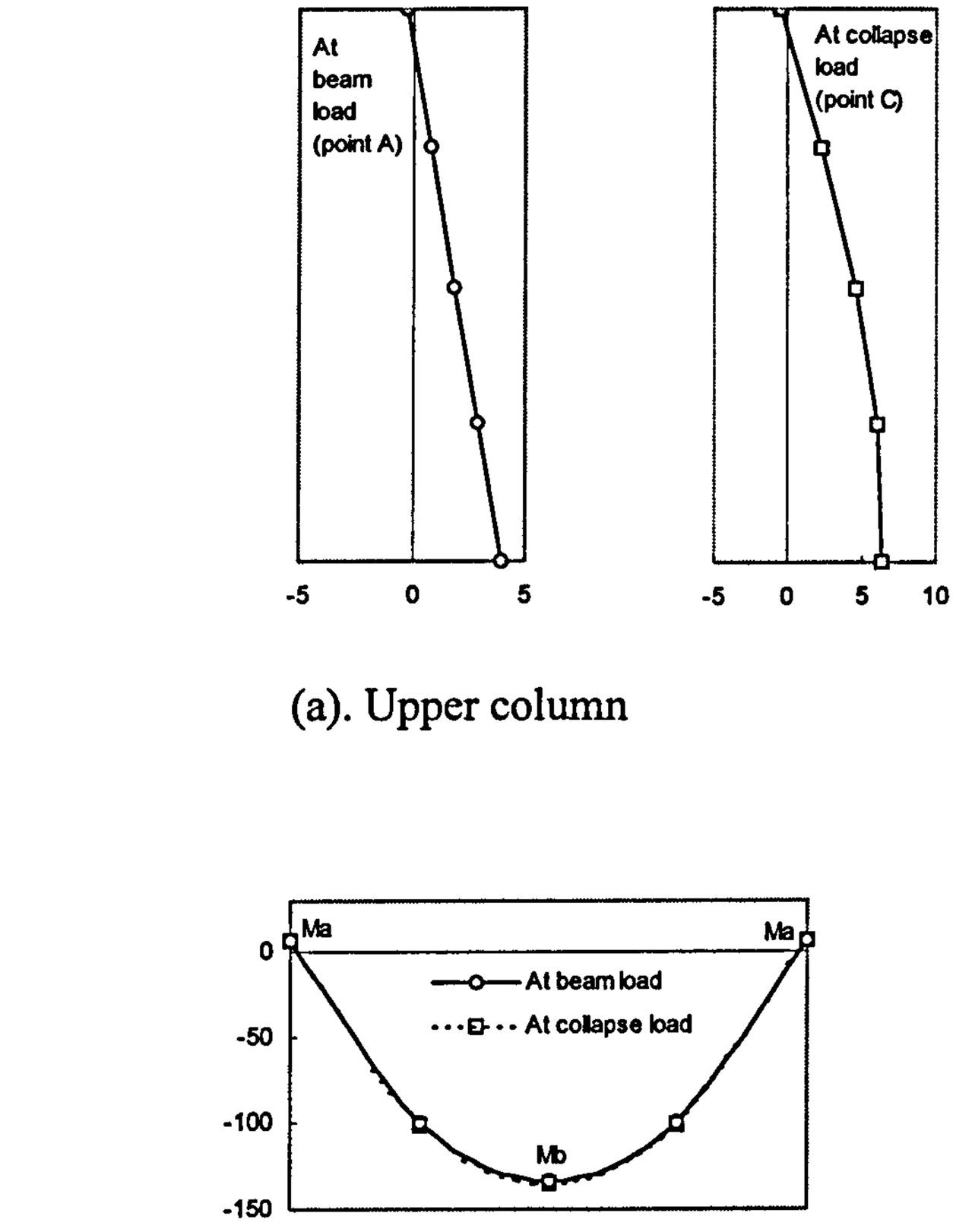

(a). Upper column

(b). Beam

(c). Lower column.

Figure 5.20 Smoothed bending moment diagrams at beam loads and at collapse loads in kNm with PDEP connections

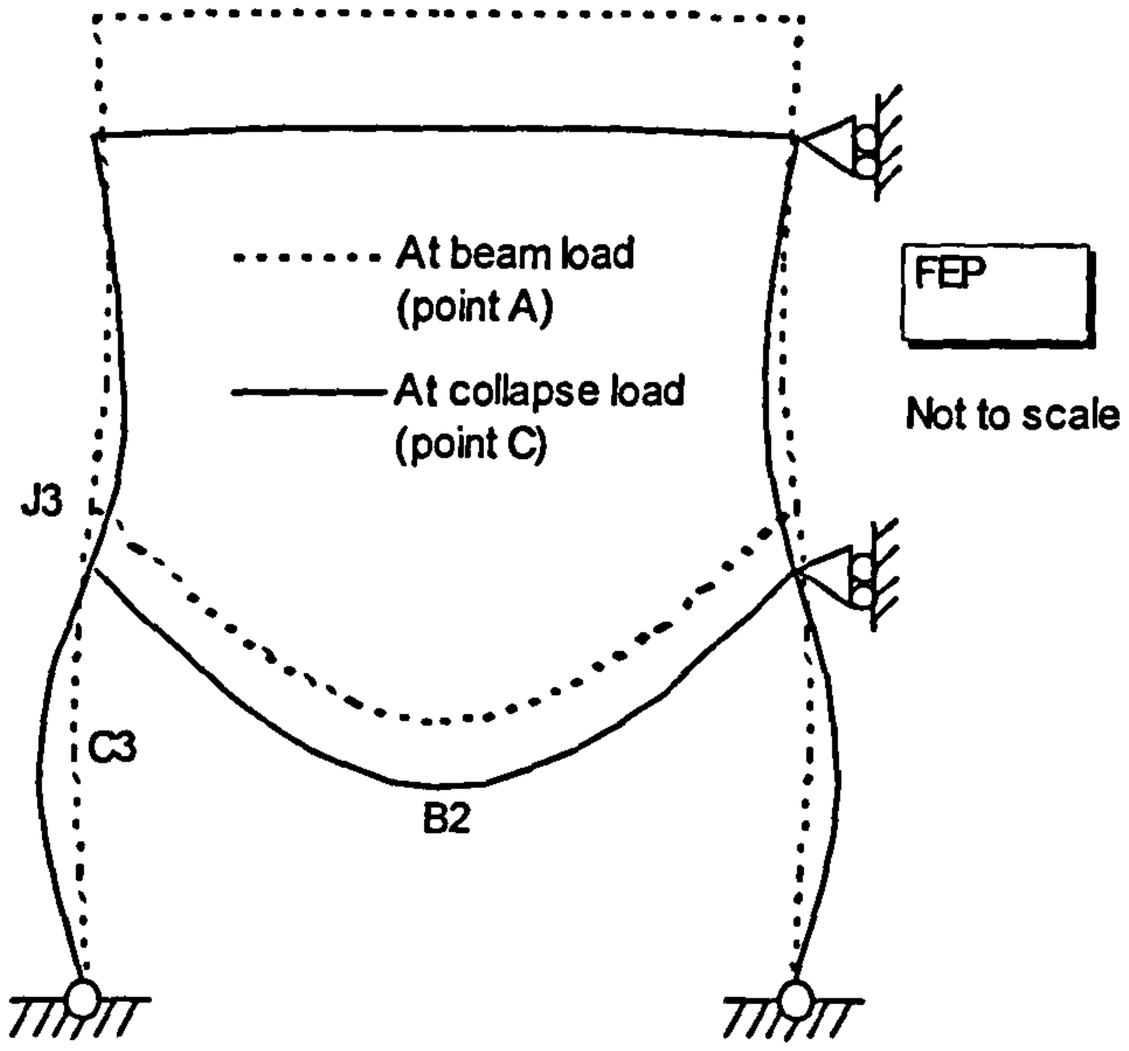

Figure 5.21 Exaggerated deformed shape of frame with FEP connections

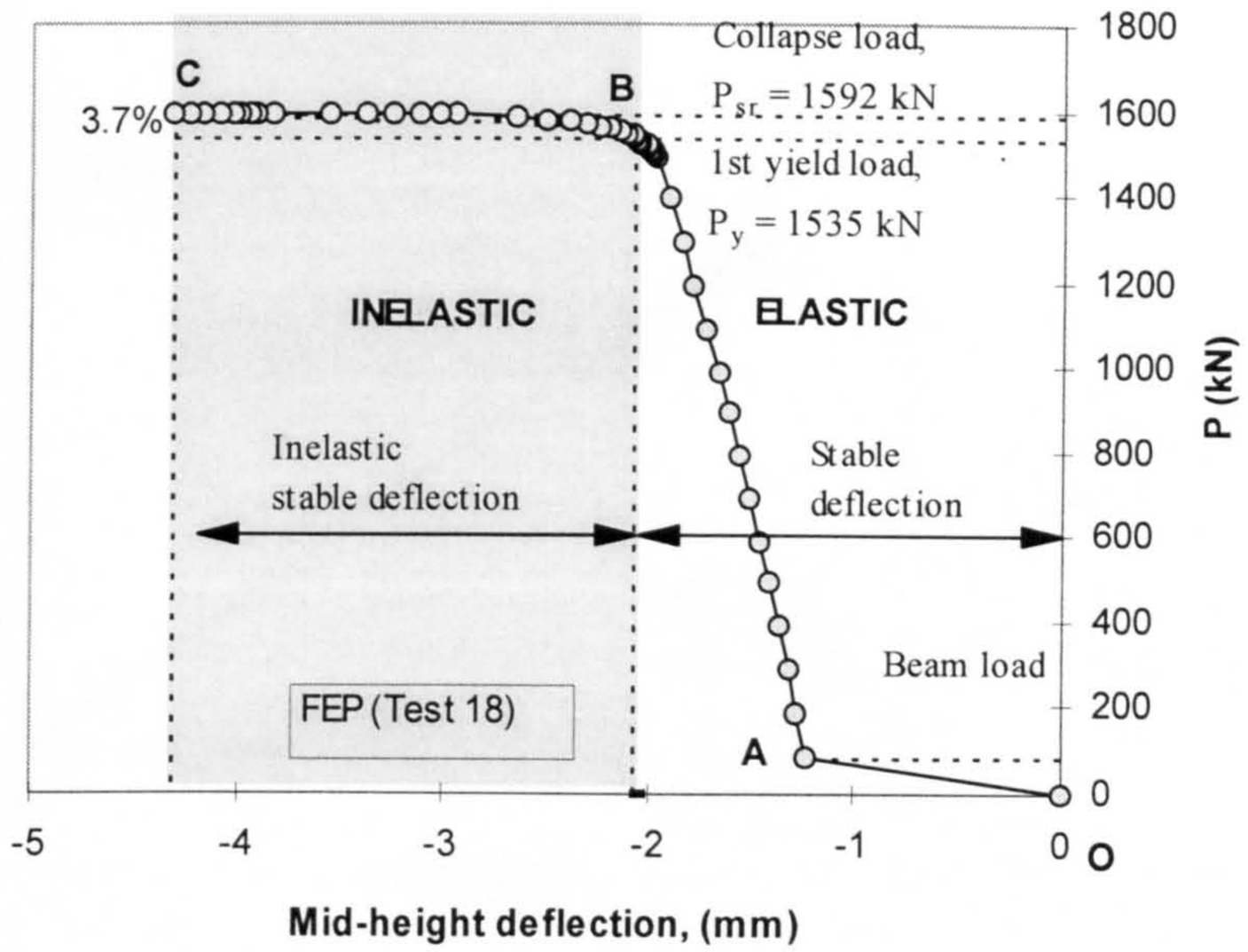

Figure 5.22 Load deflection response at column mid-height with FEP connections

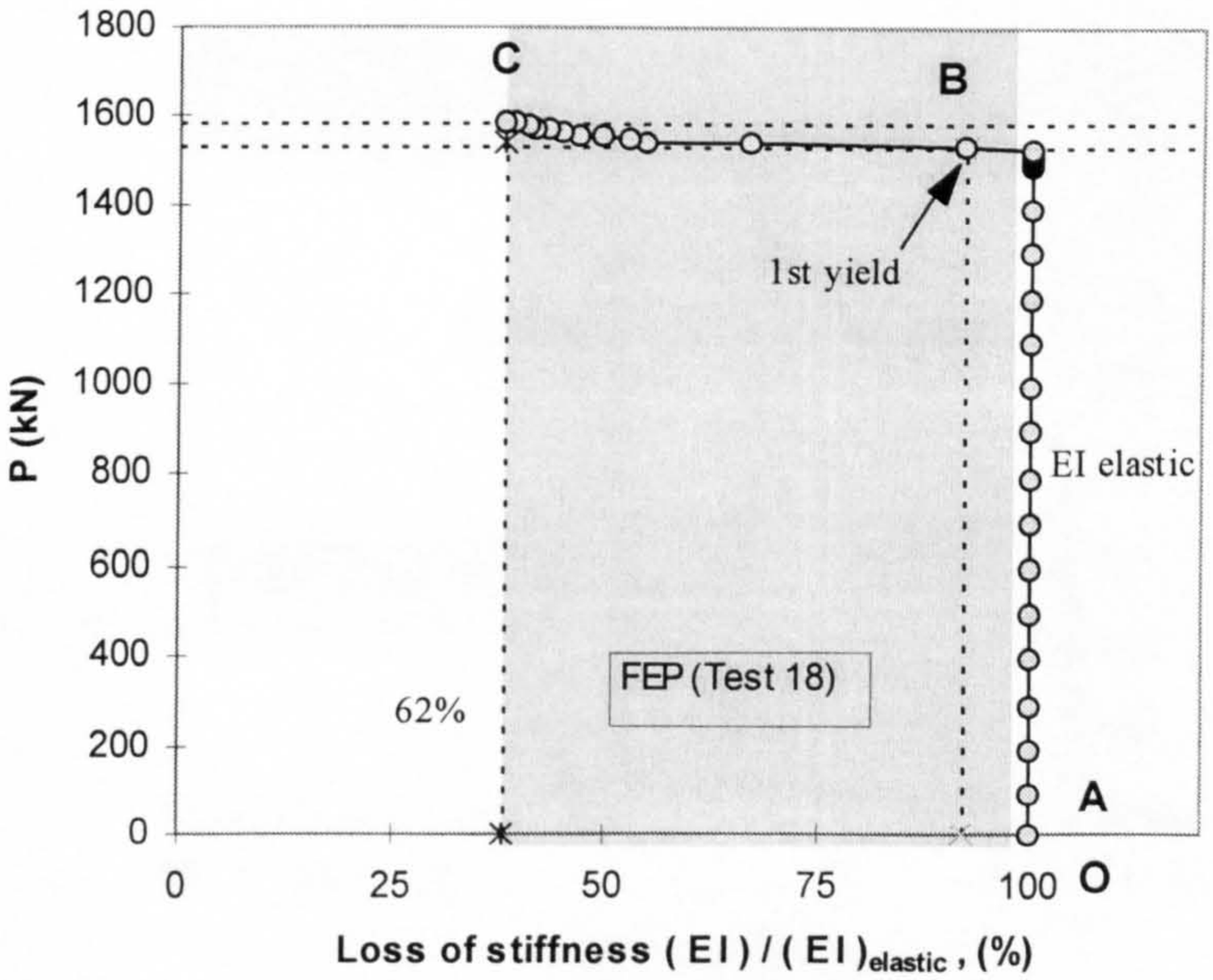

Figure 5.23 Loss of stiffness at column mid-height with FEP connections

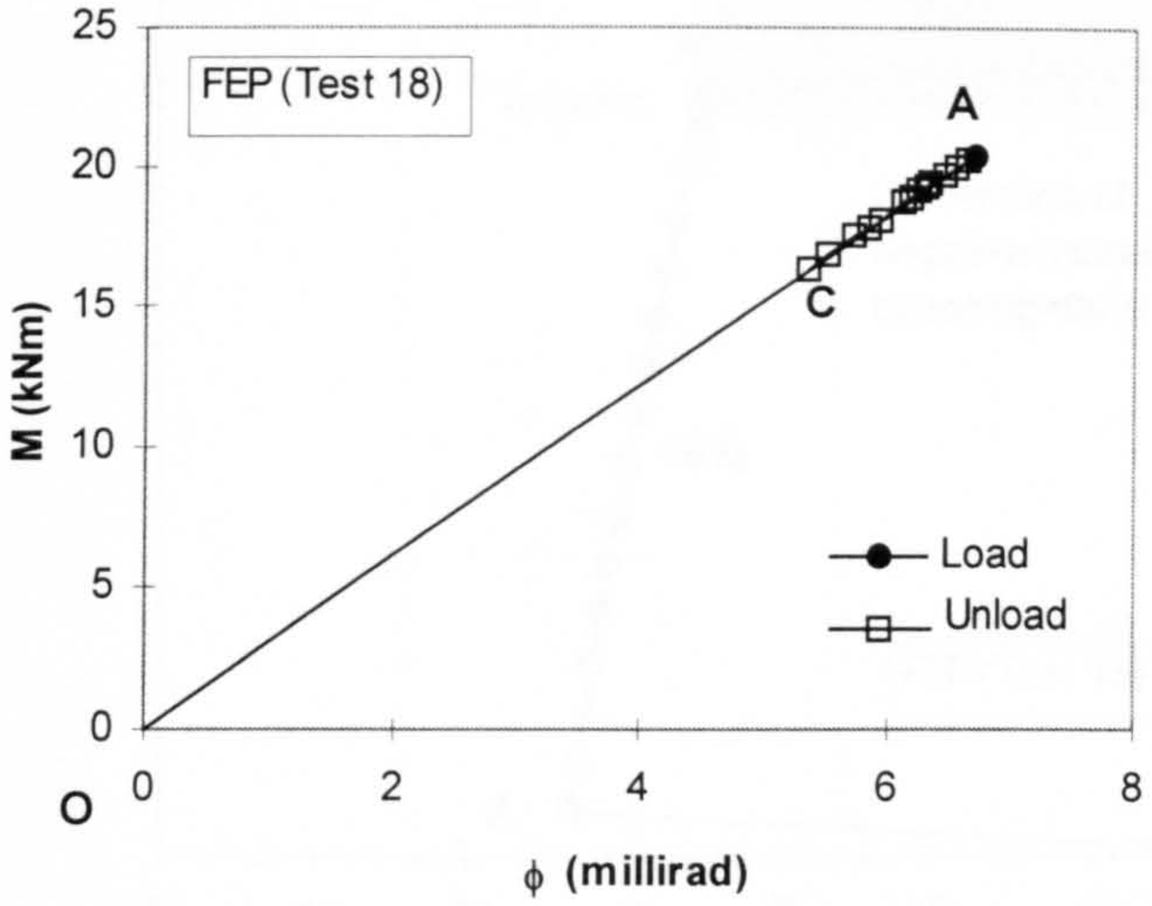

Figure 5.24 M-ϕ response at column top end with FEP connections

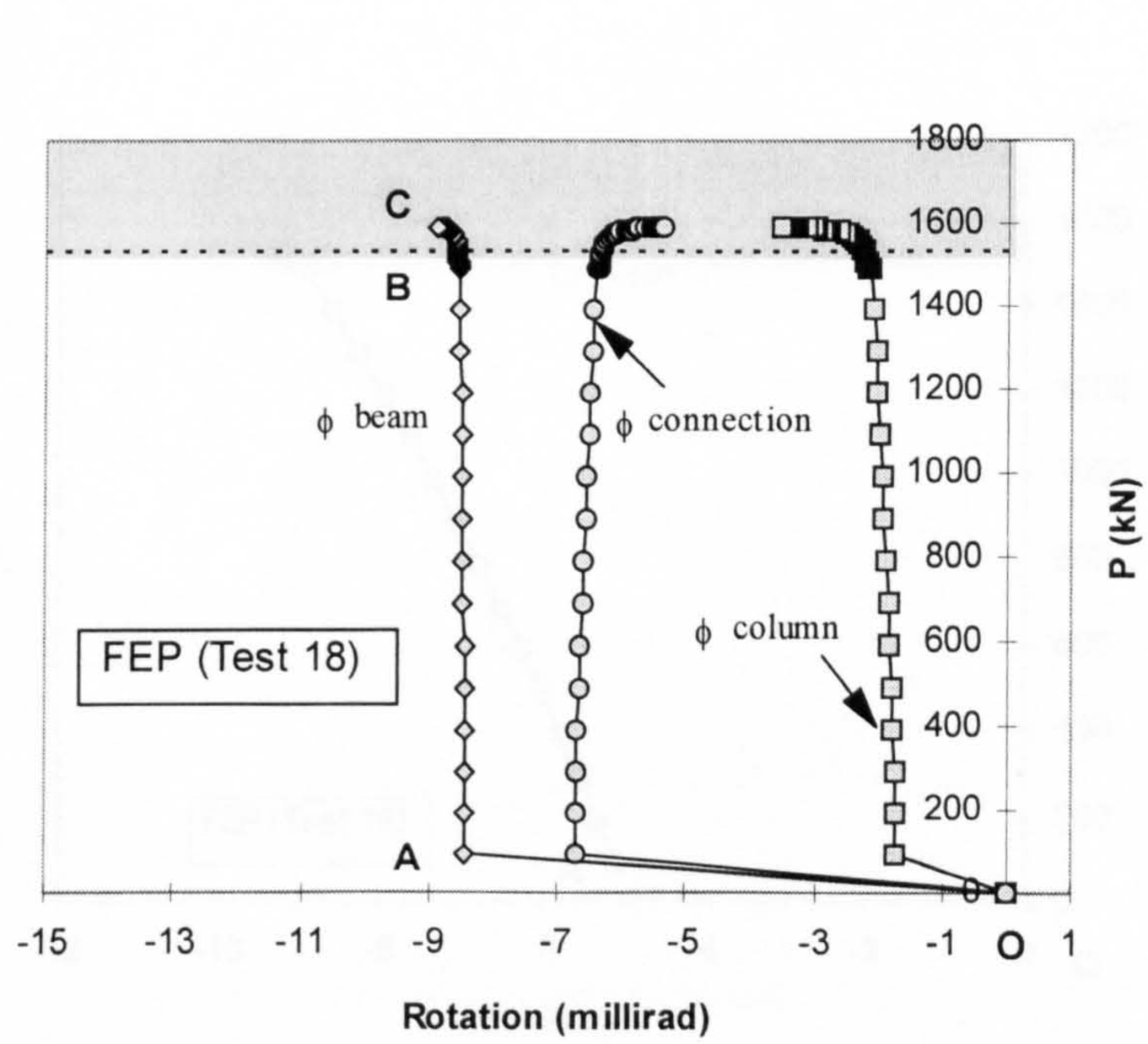

Figure 5.25 Development of beam, column and connection rotations with FEP connections

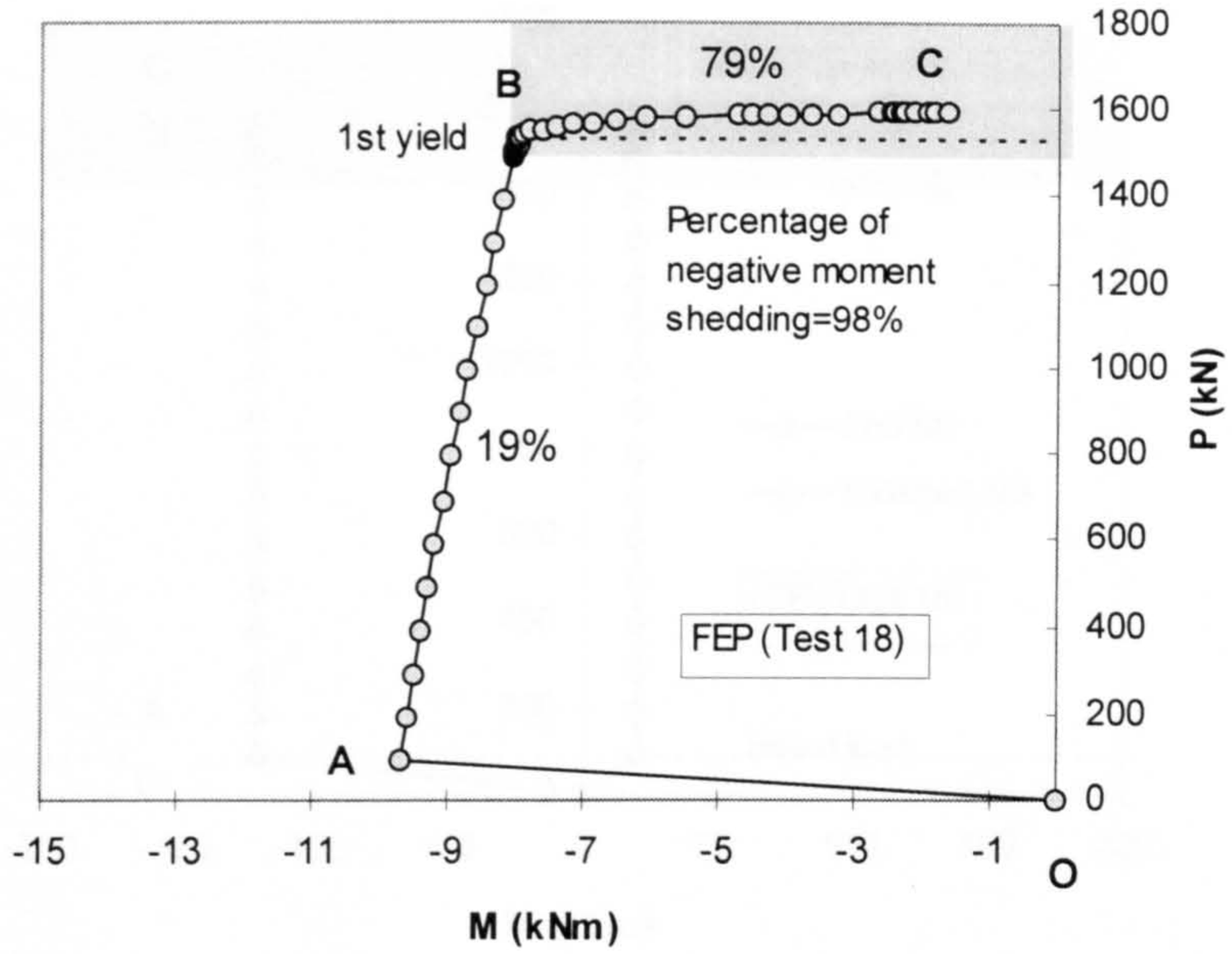

Figure 5.26 Response of moment shedding at column top end with FEP connections

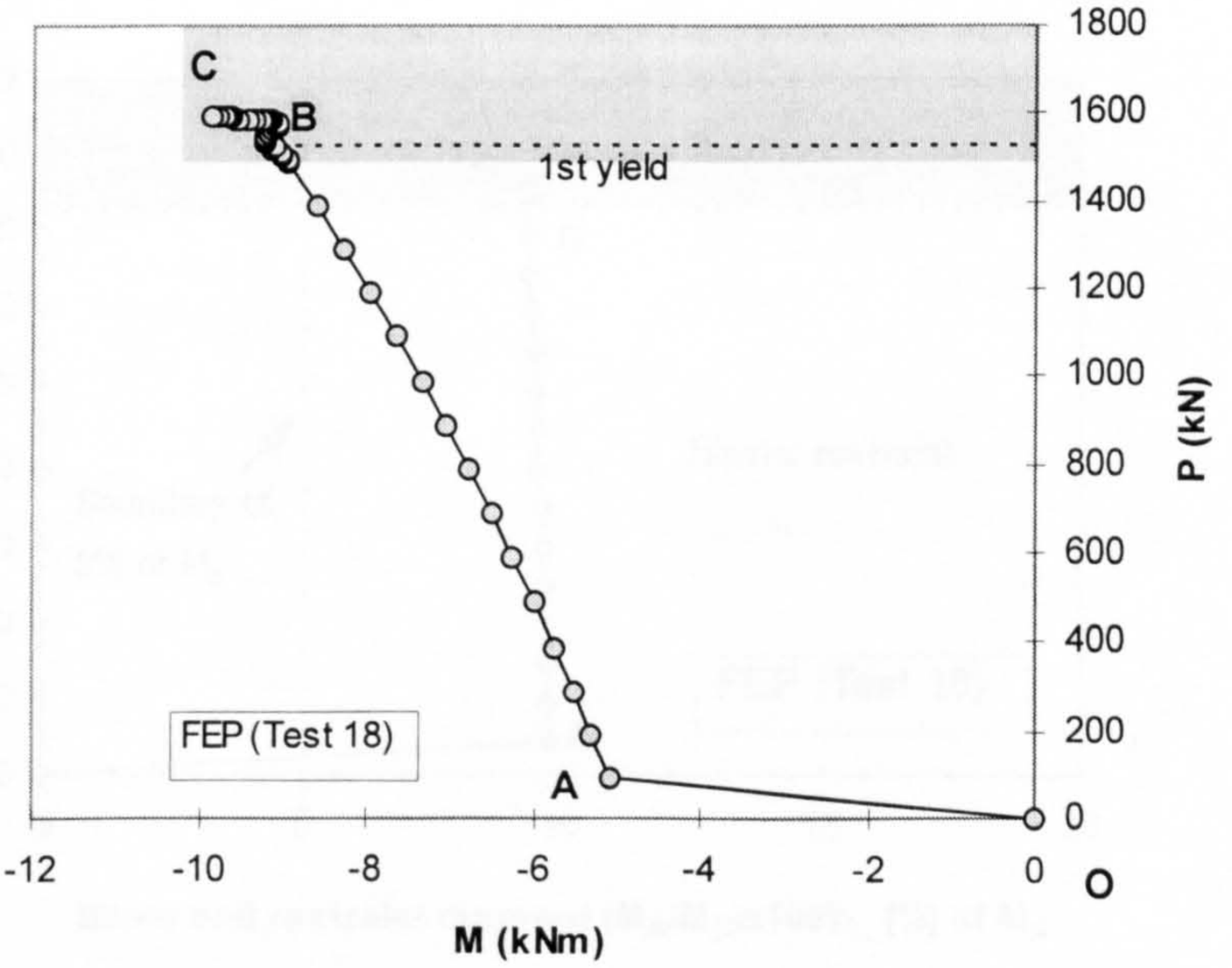

Figure 5.27 Response of moment at column mid-height with FEP connections

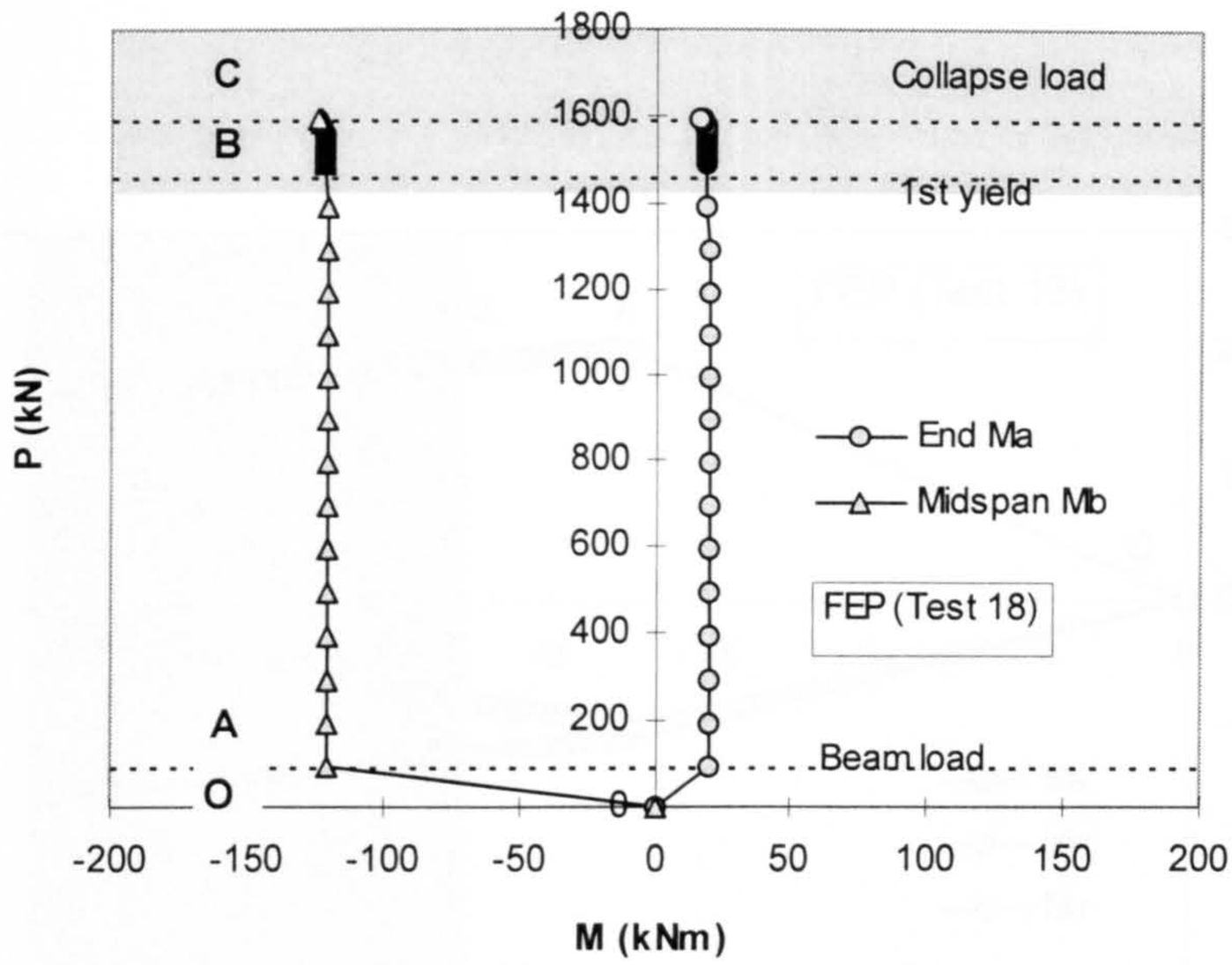

Figure 5.28 Response of moments at both beam end and beam midspan with FEP connections

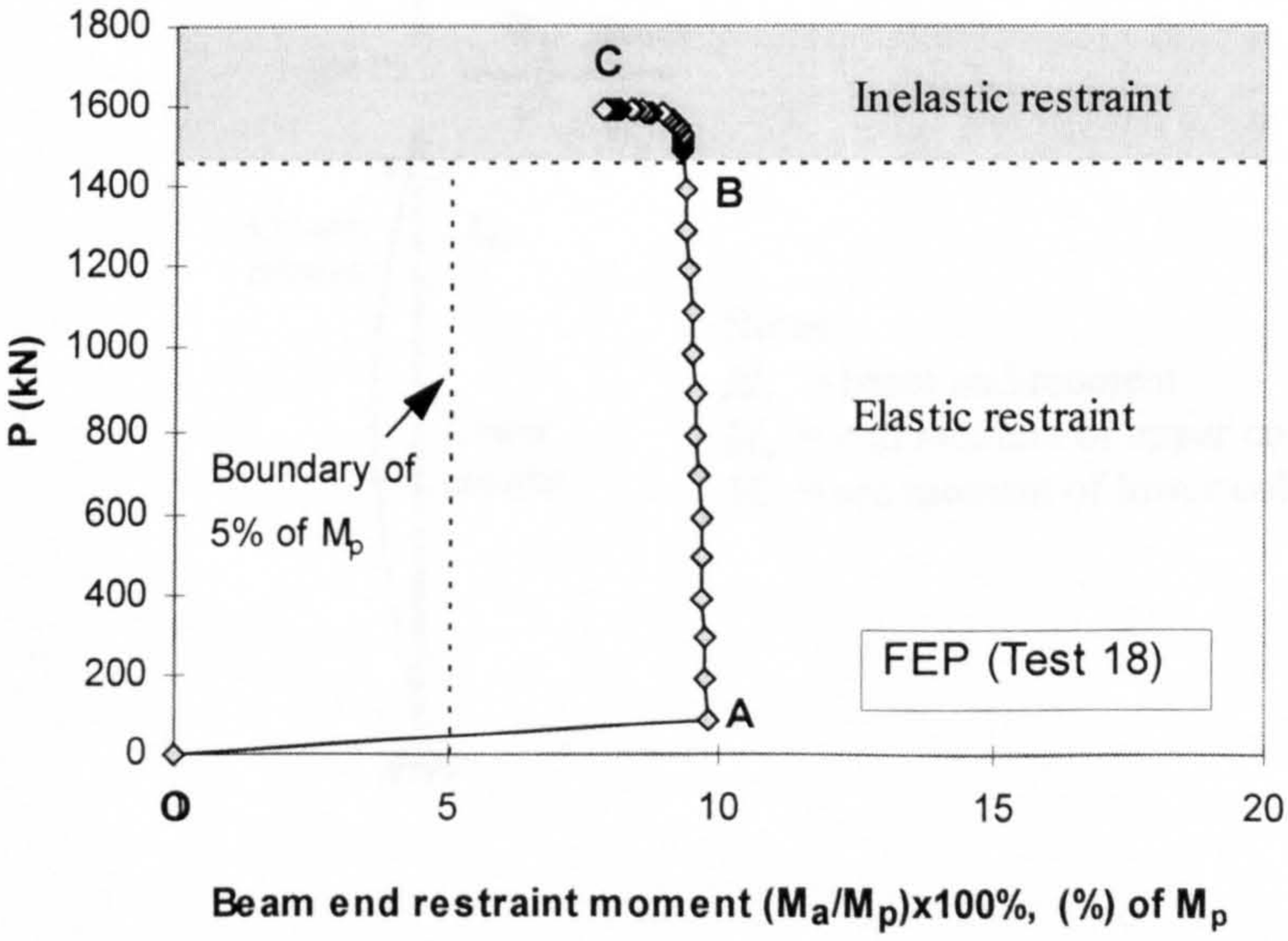

Figure 5.29 Development of beam end restraint moment with FEP connections

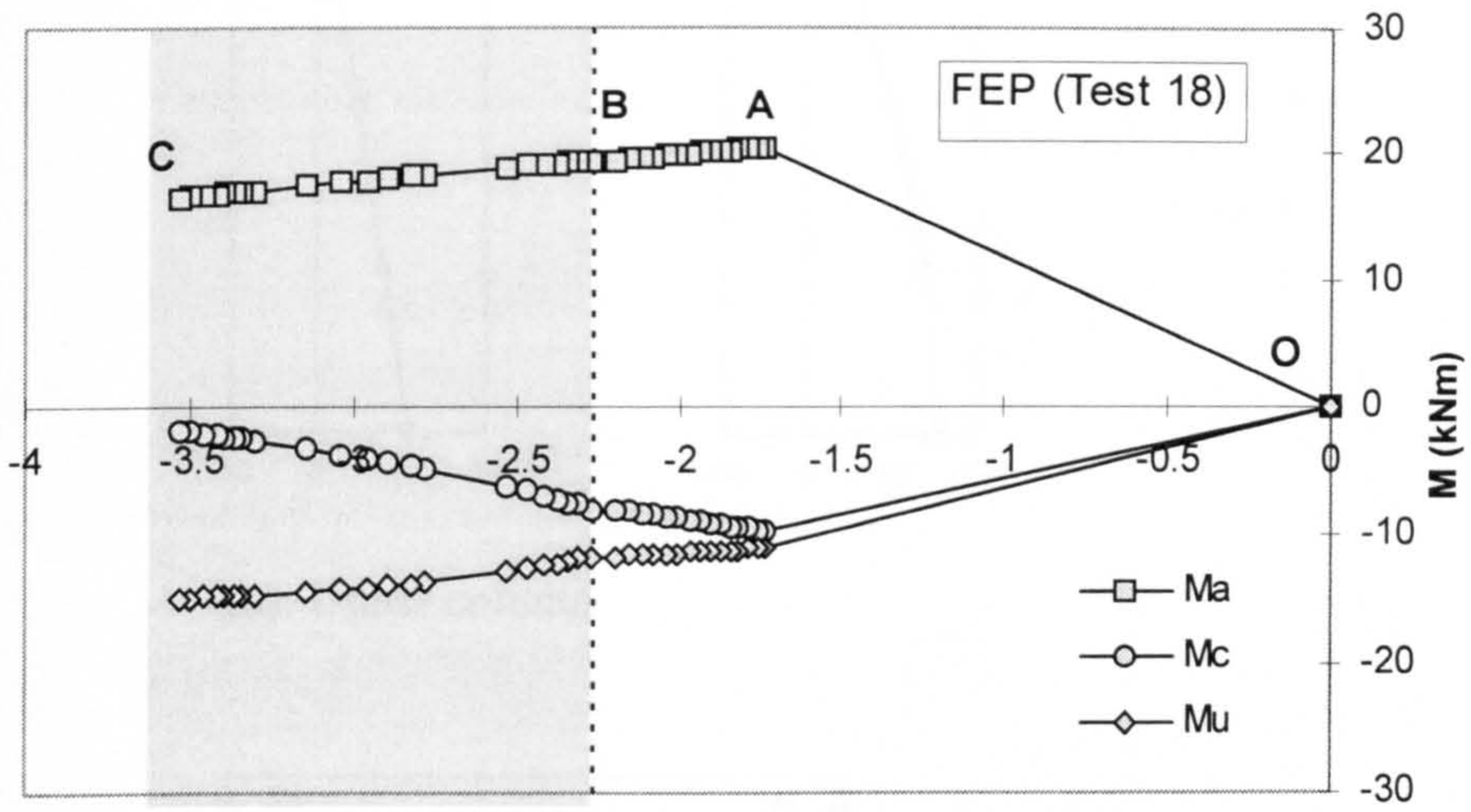

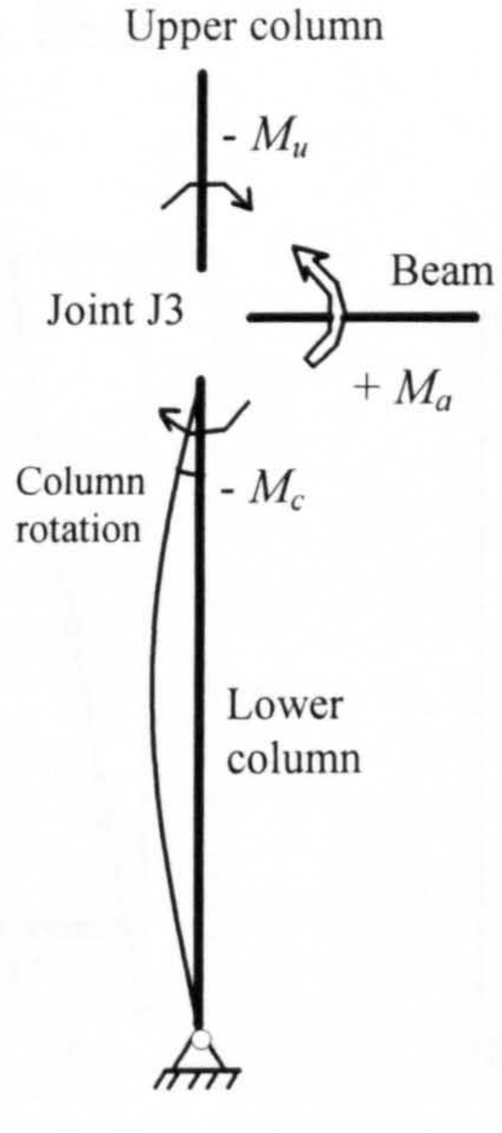

Notes:
M_a = beam end moment
M_u = end moment of upper column
M_c = end moment of lower column

Figure 5.30 Distribution of moments at the joint J3 with increasing column end rotation using FEP connections

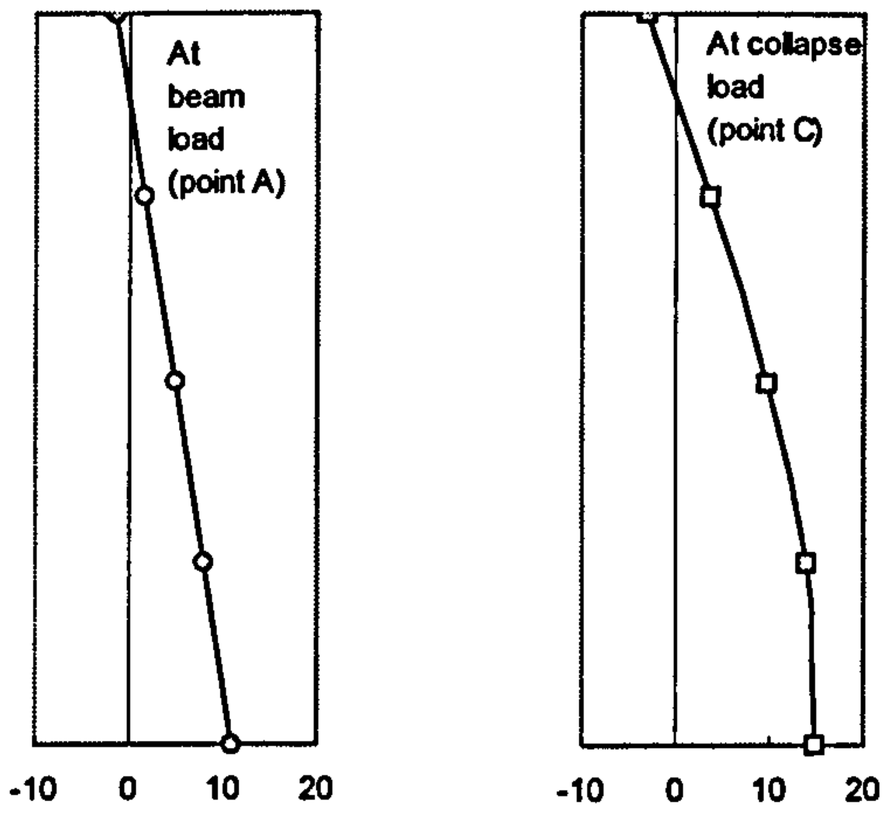

(a). Upper column

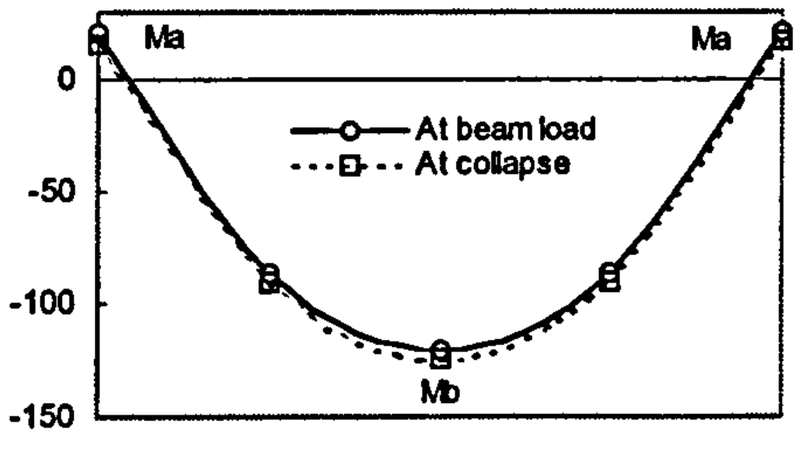

(b). Beam

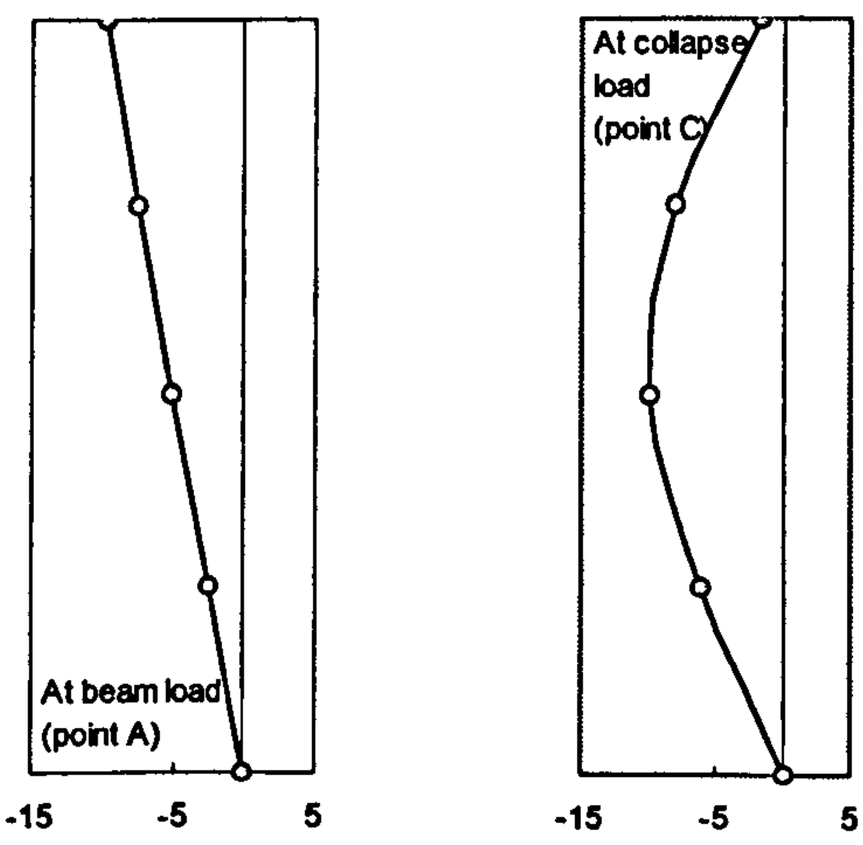

(c). Lower column

Figure 5.31 Smoothed bending moment diagrams at service loads and at collapse loads in kNm with FEP connections

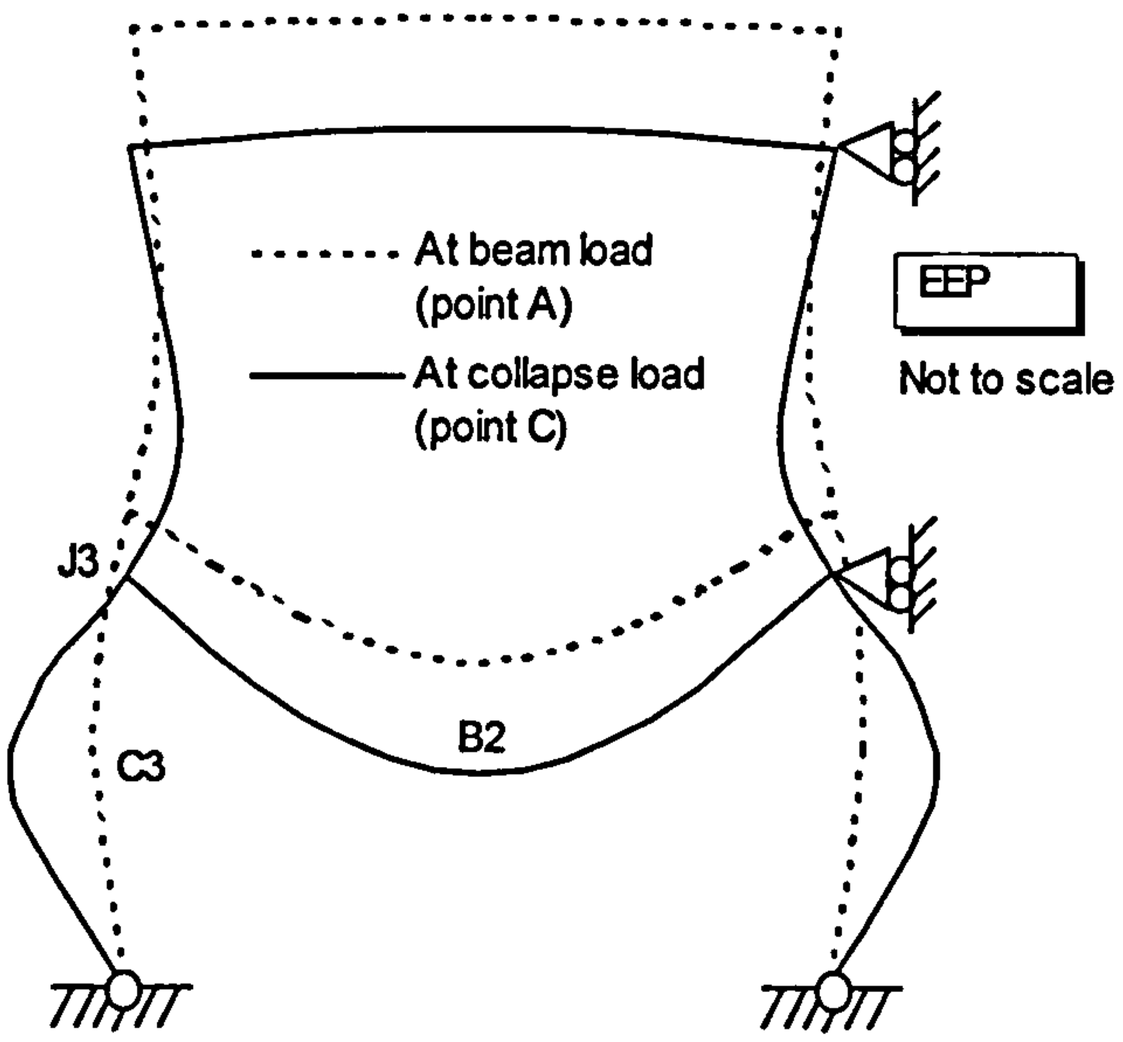

Figure 5.32 Exaggerated deformed shape of frame with EEP connections

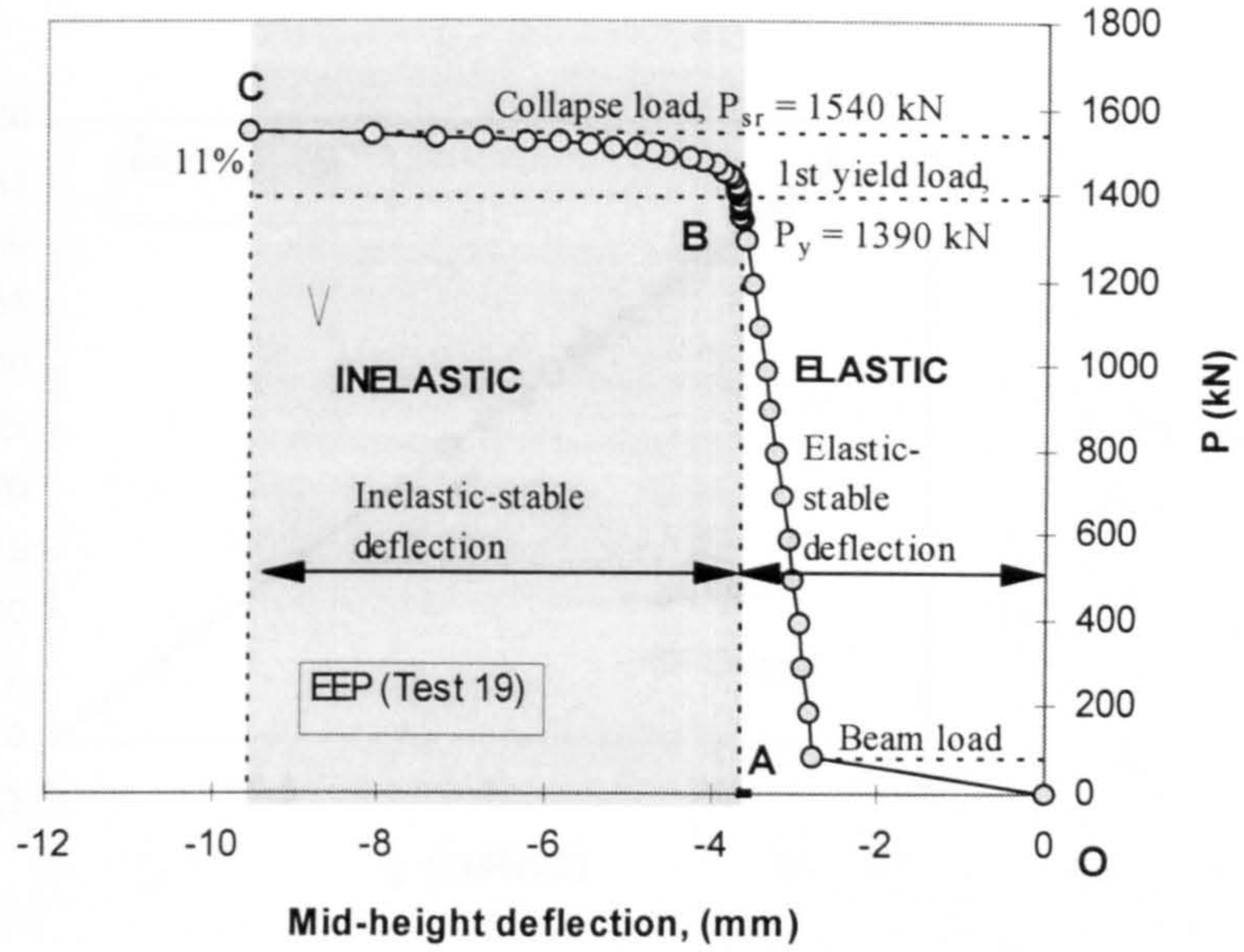

Figure 5.33 Load deflection response at column mid-height with EEP connections

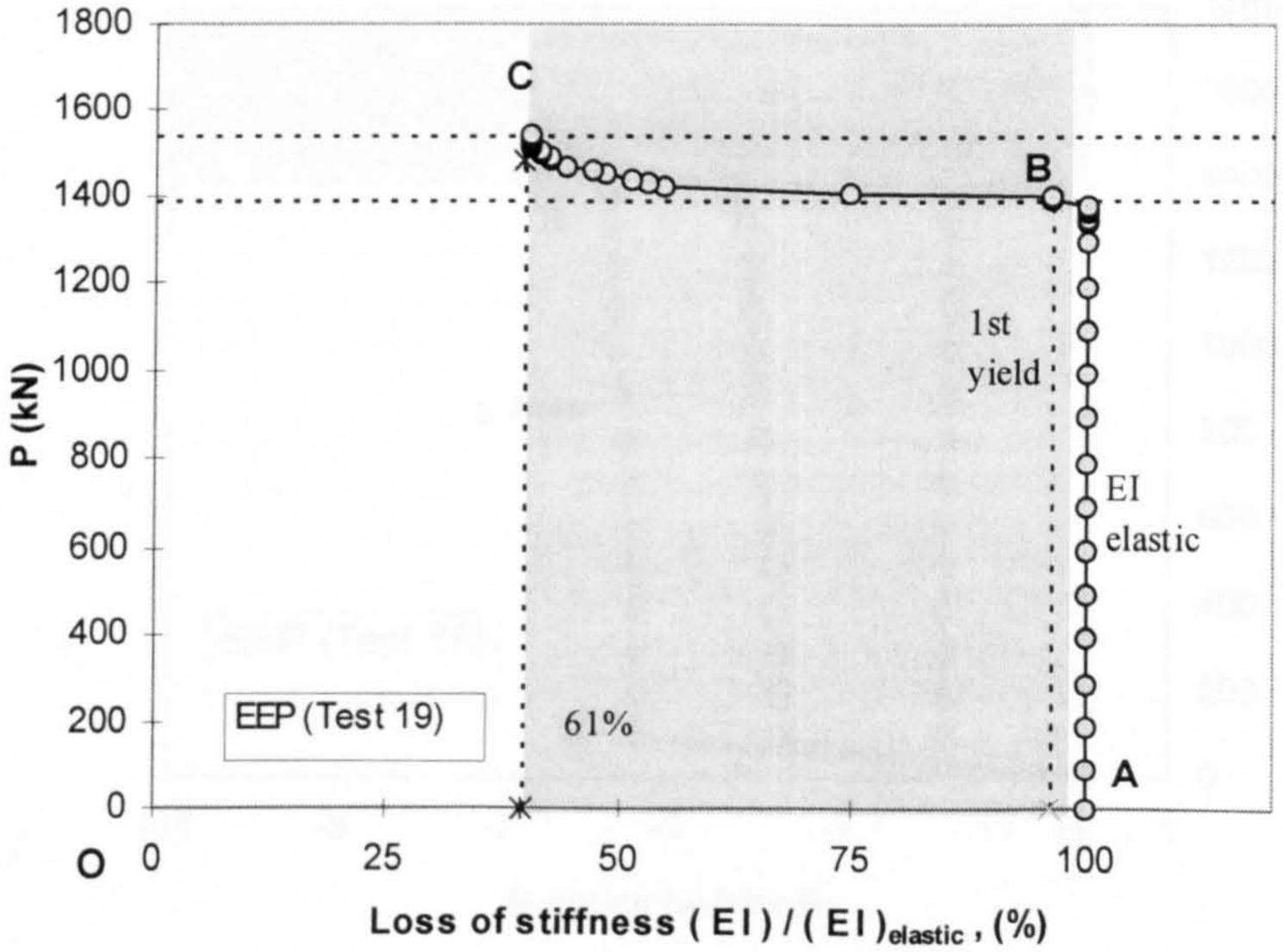

Figure 5.34 Loss of stiffness at column mid-height with EEP connections

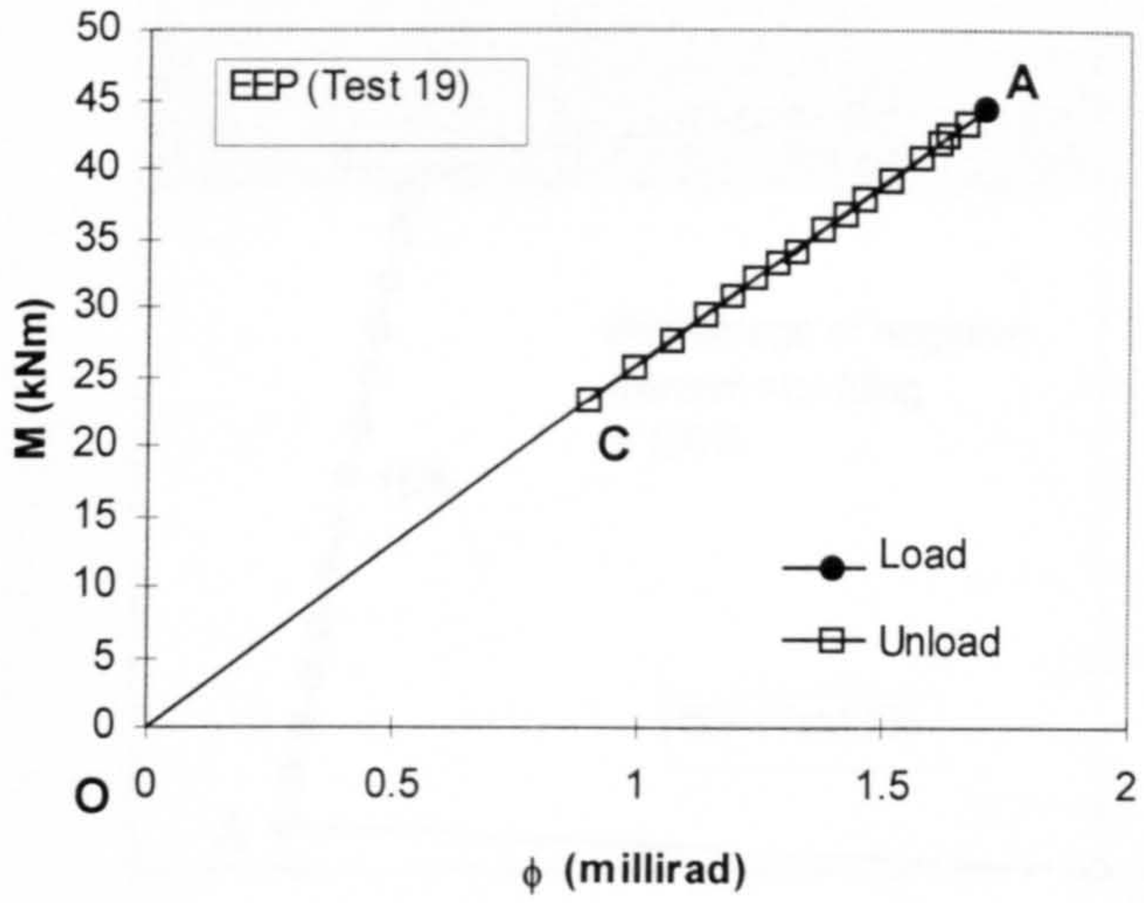

Figure 5.35 M-ϕ response at column top end with EEP connections

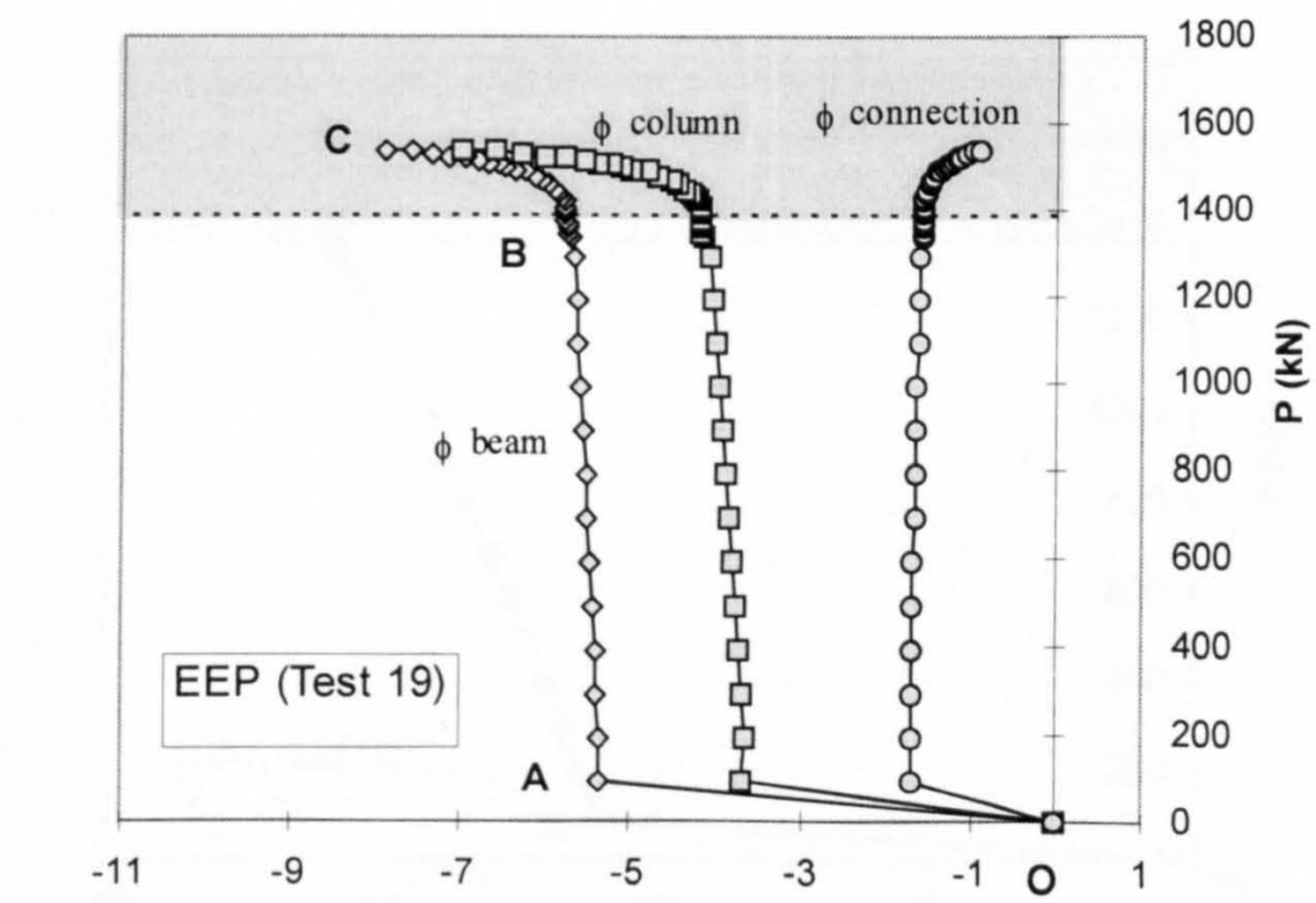

Figure 5.36 Development of beam, column and connection rotations with EEP connections

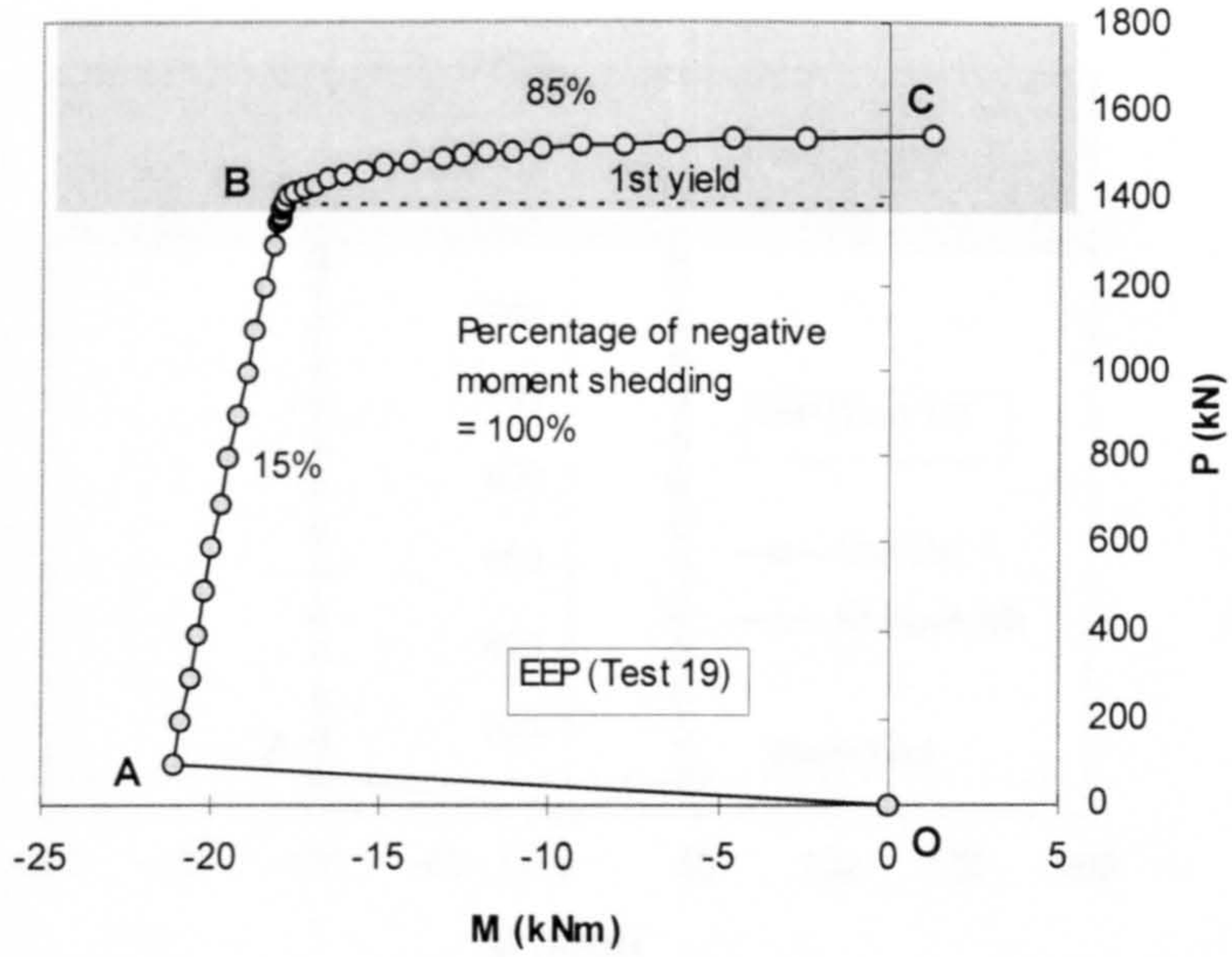

Figure 5.37 Response of moment shedding at column top end with EEP connections

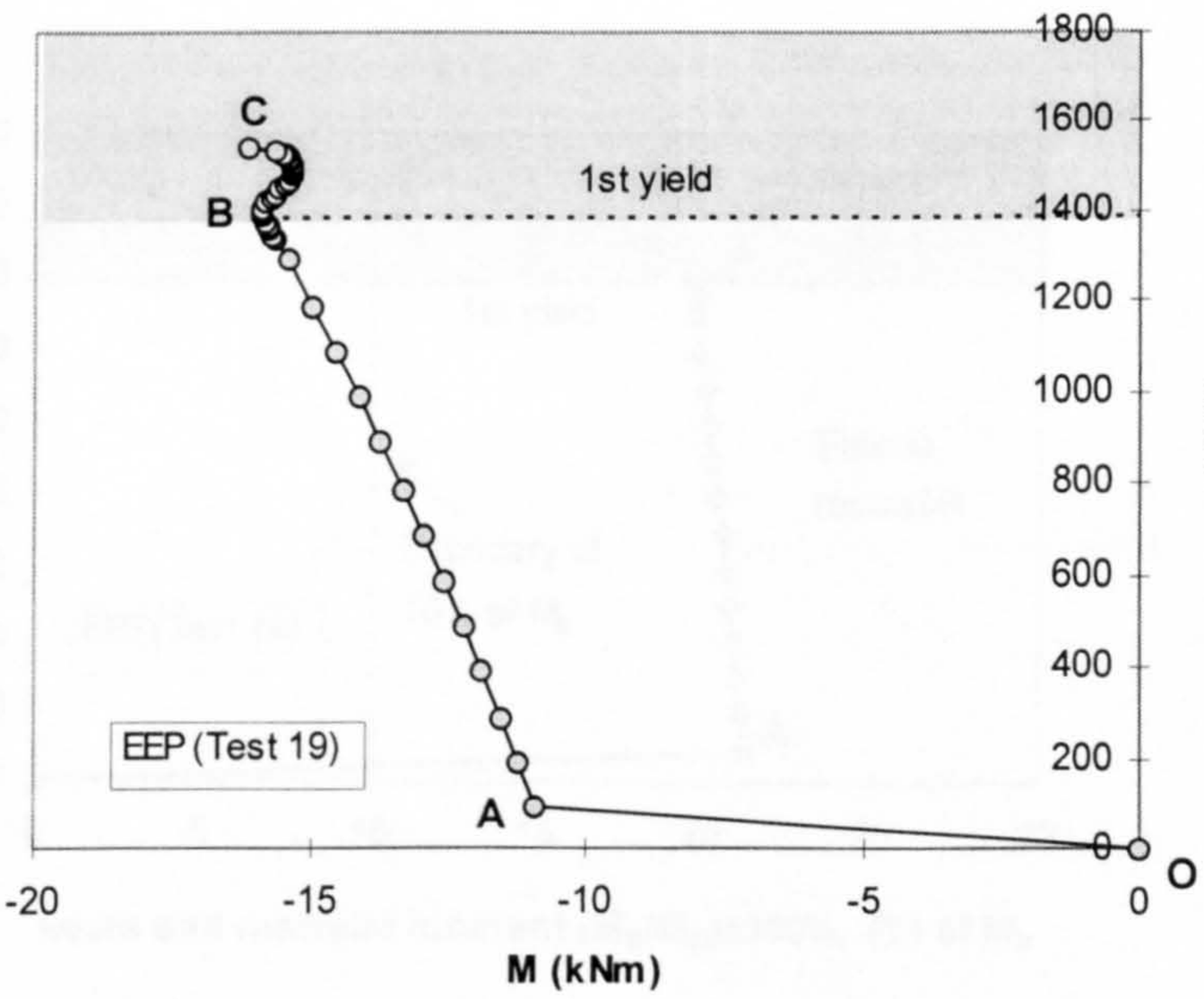

Figure 5.38 Response of moment at column mid-height with EEP connections

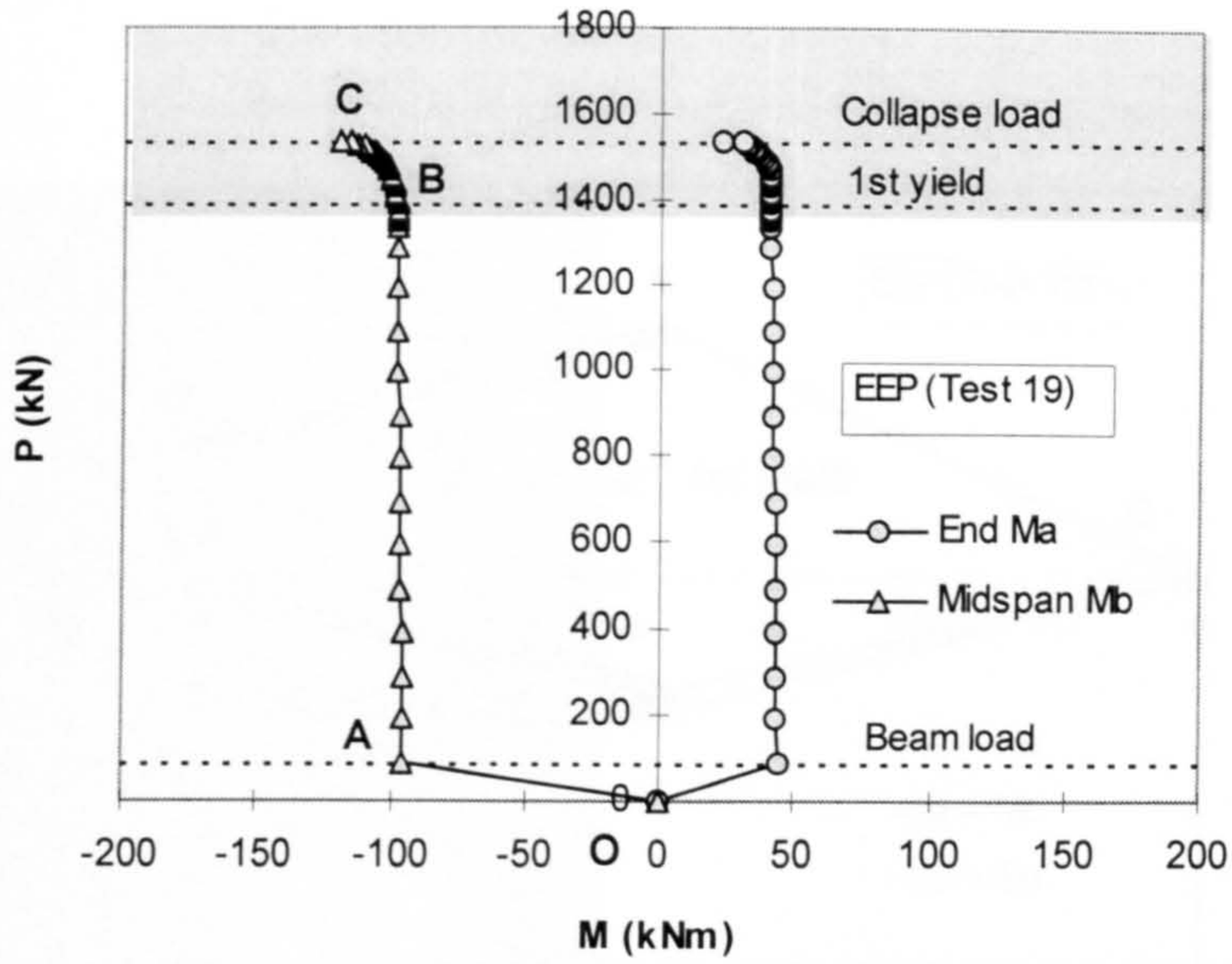

Figure 5.39 Response of moments at both beam end and beam midspan with EEP connections

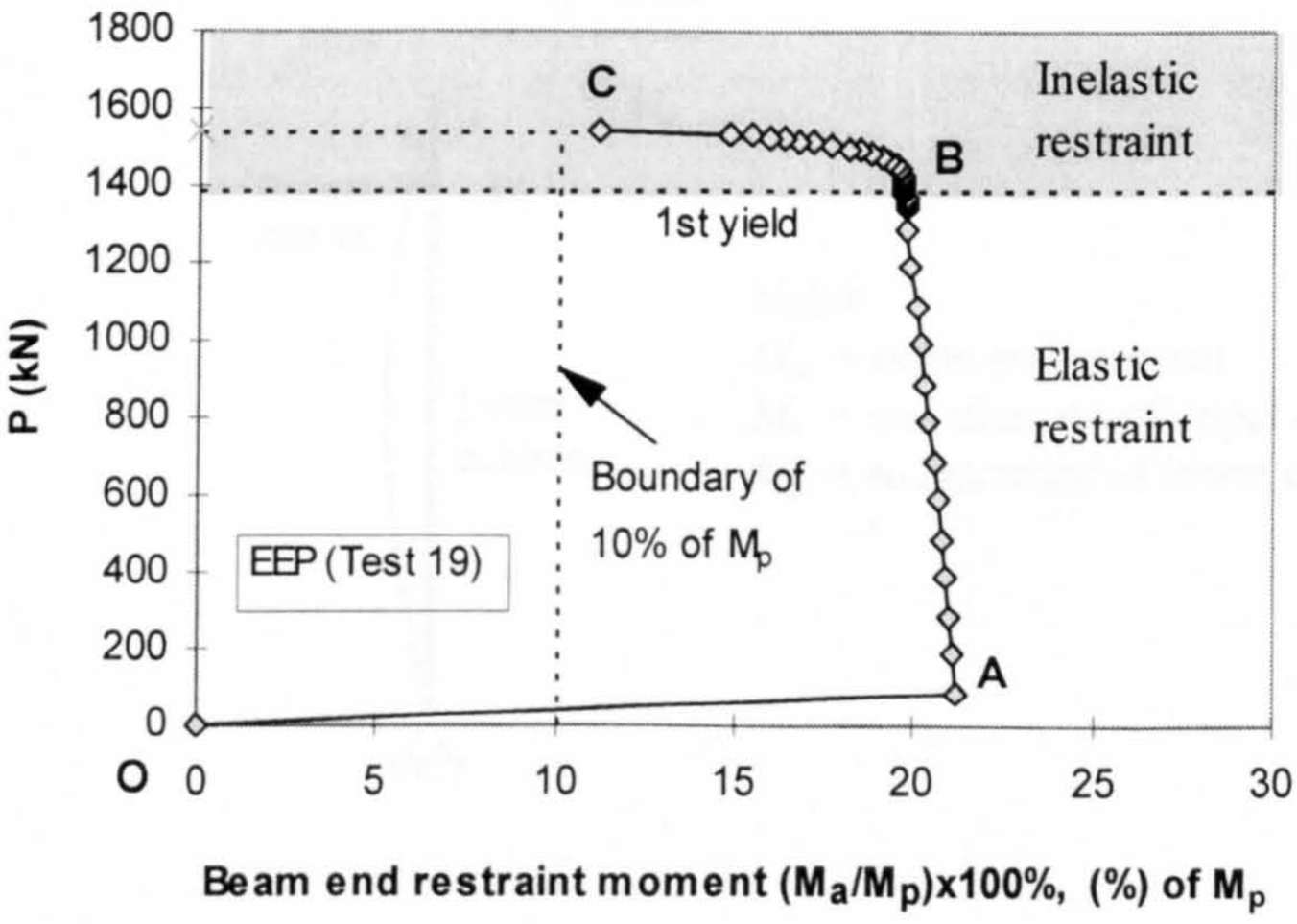

Figure 5.40 Development of beam end restraint moment with EEP connections

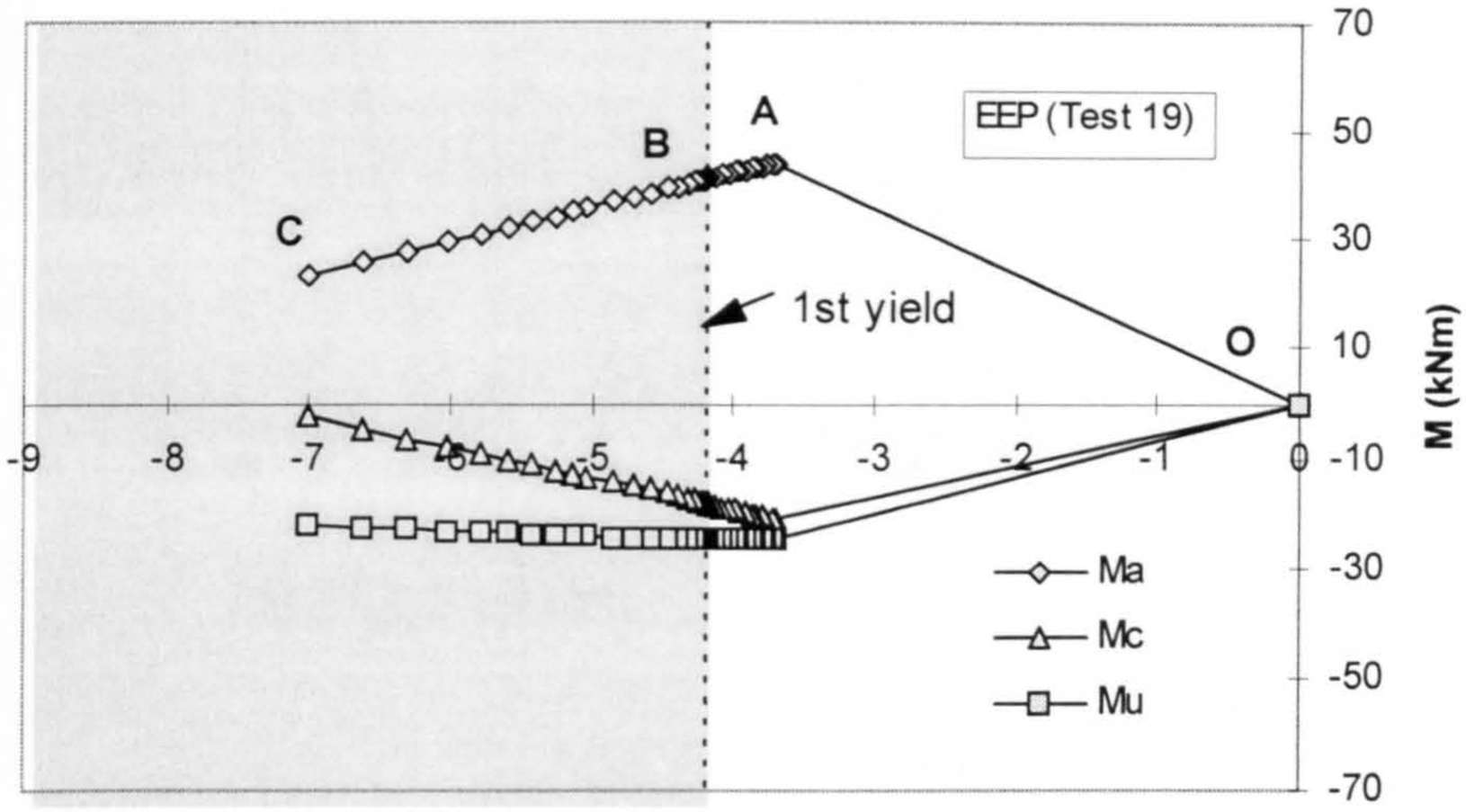

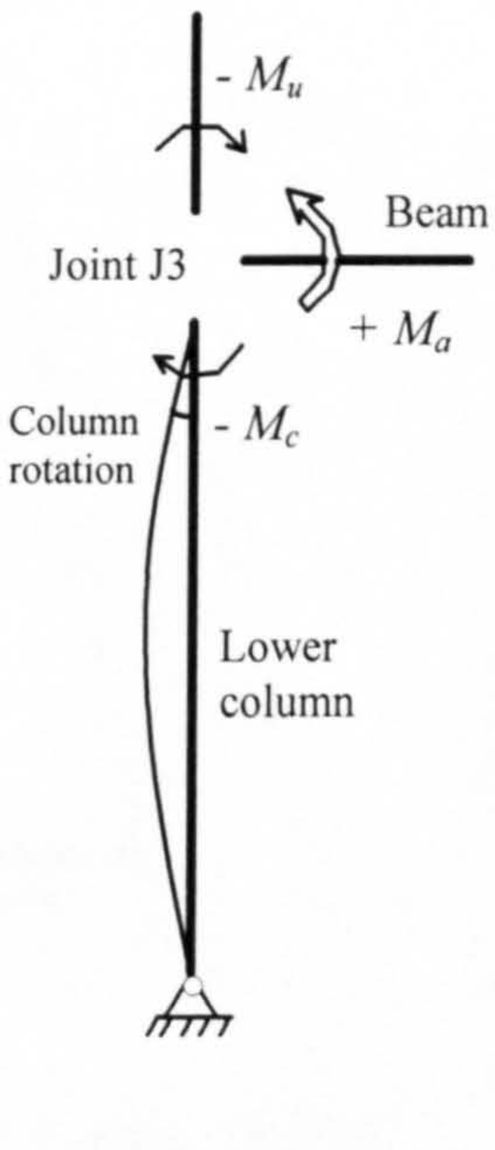

Notes:
M_a = beam end moment
M_u = end moment of upper column
M_c = end moment of lower column

Figure 5.41 Distribution of moments at joint J3 with increasing column end rotations using EEP connections

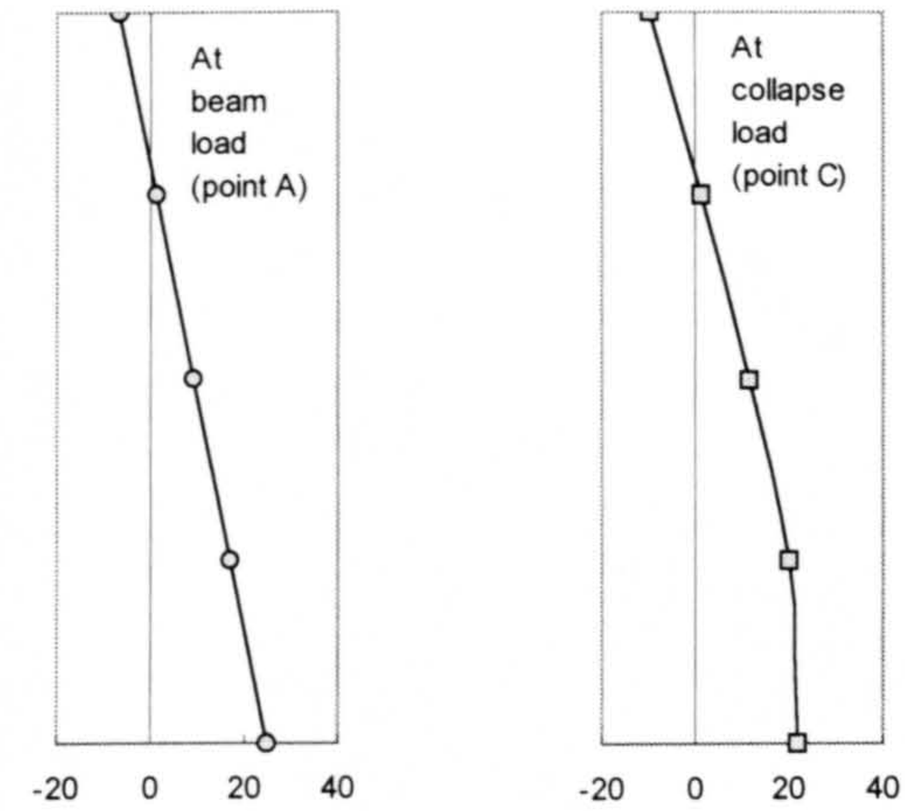

(a). Upper column

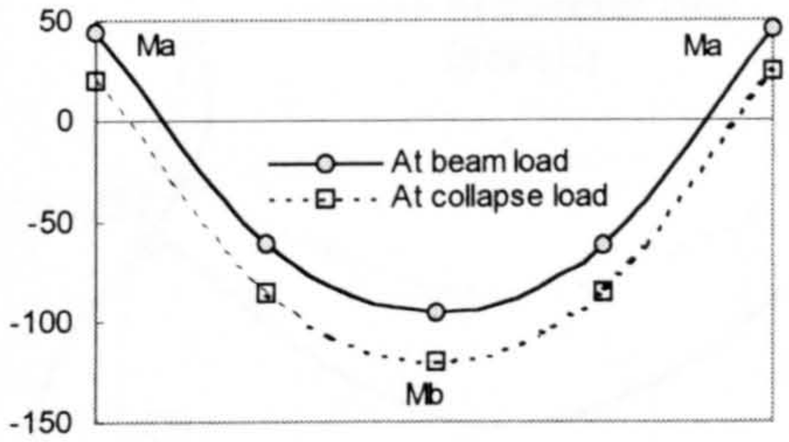

(b). Beam

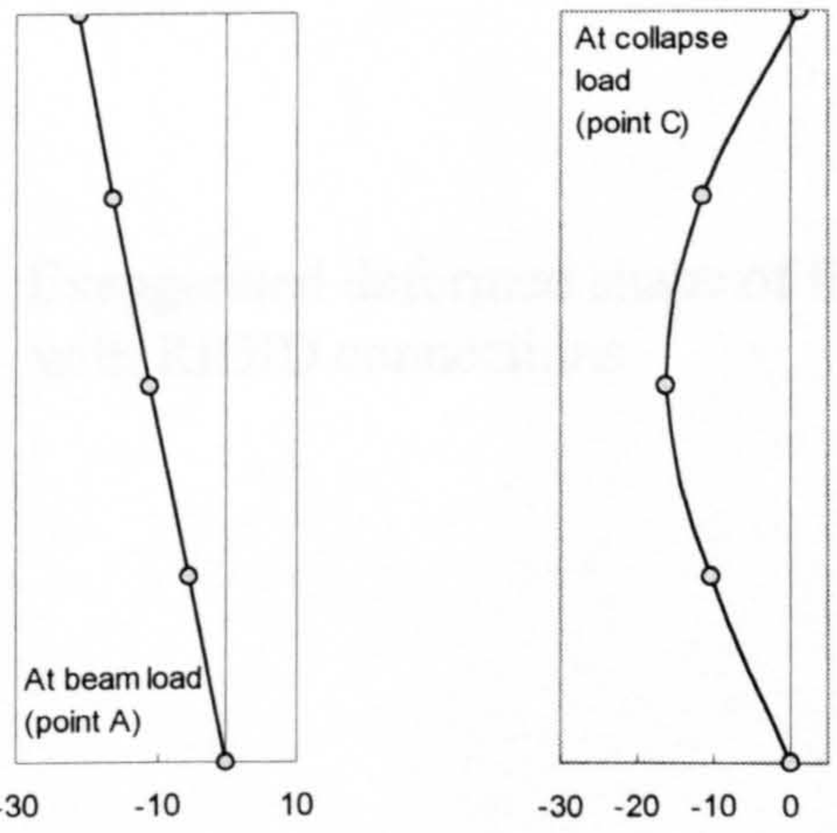

(c). Lower column

Figure 5.42 Smoothed bending moment diagrams at service loads and at collapse loads in kNm with EEP connections

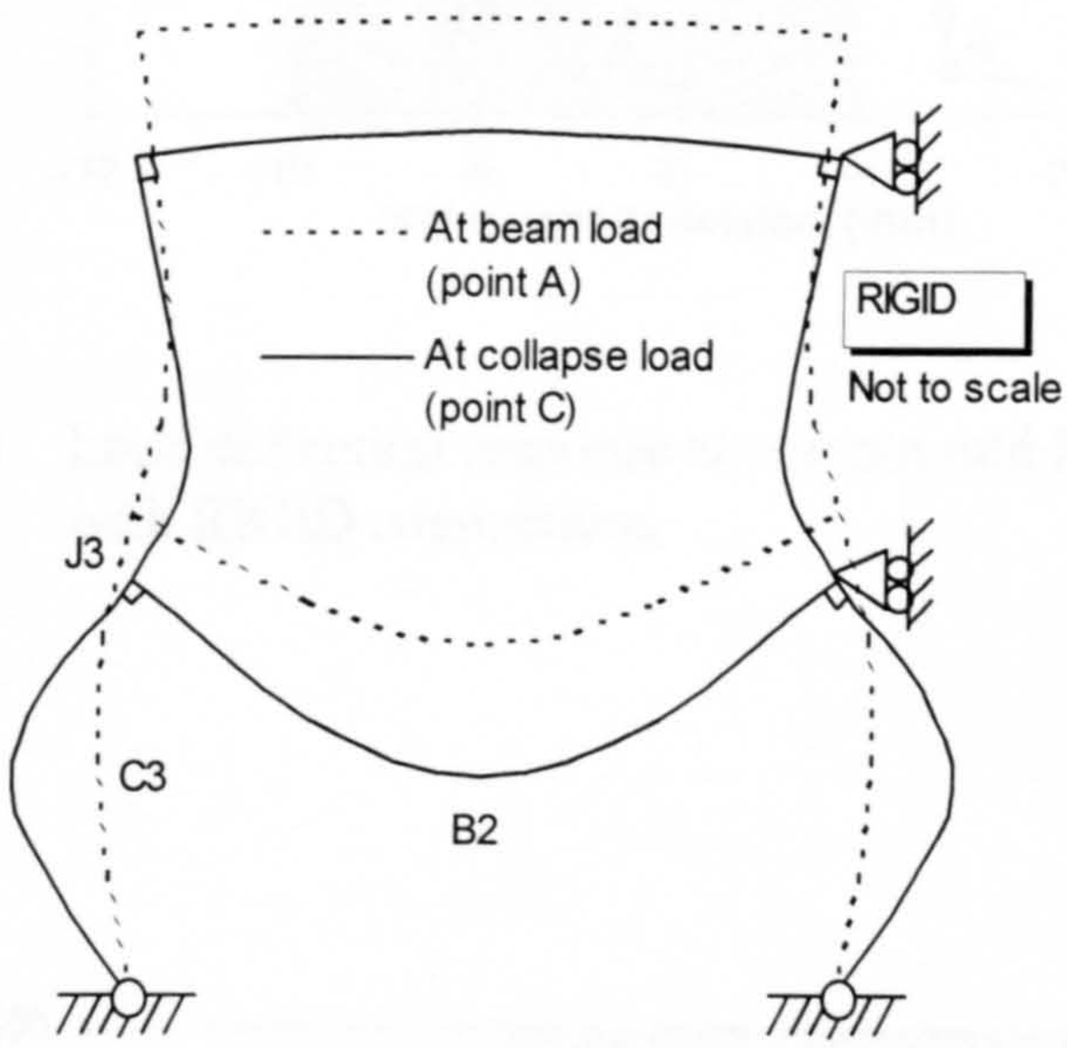

Figure 5.43 Exaggerated deformed shape of frame with RIGID connections

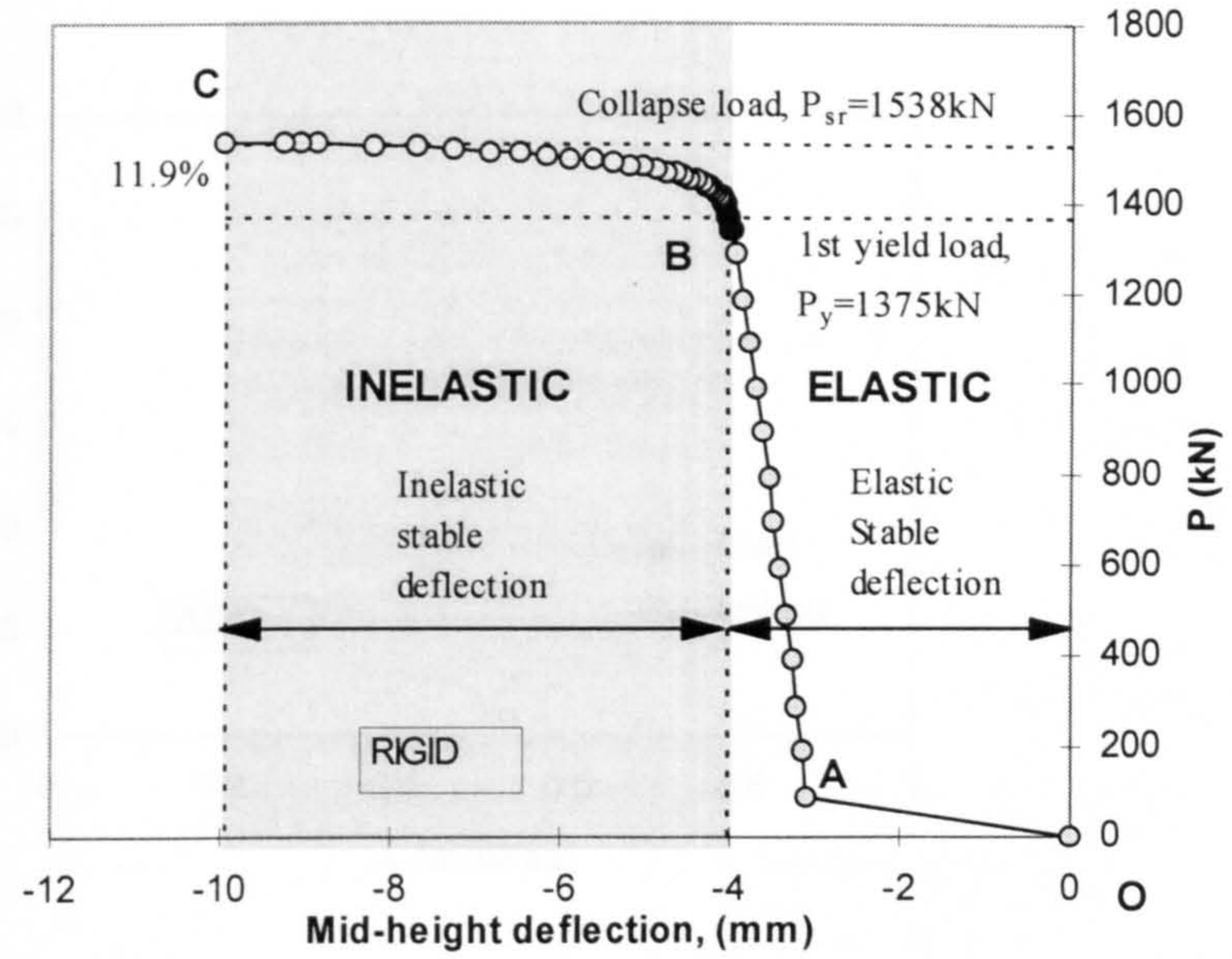

Figure 5.44 Load deflection response at column mid height with RIGID connections

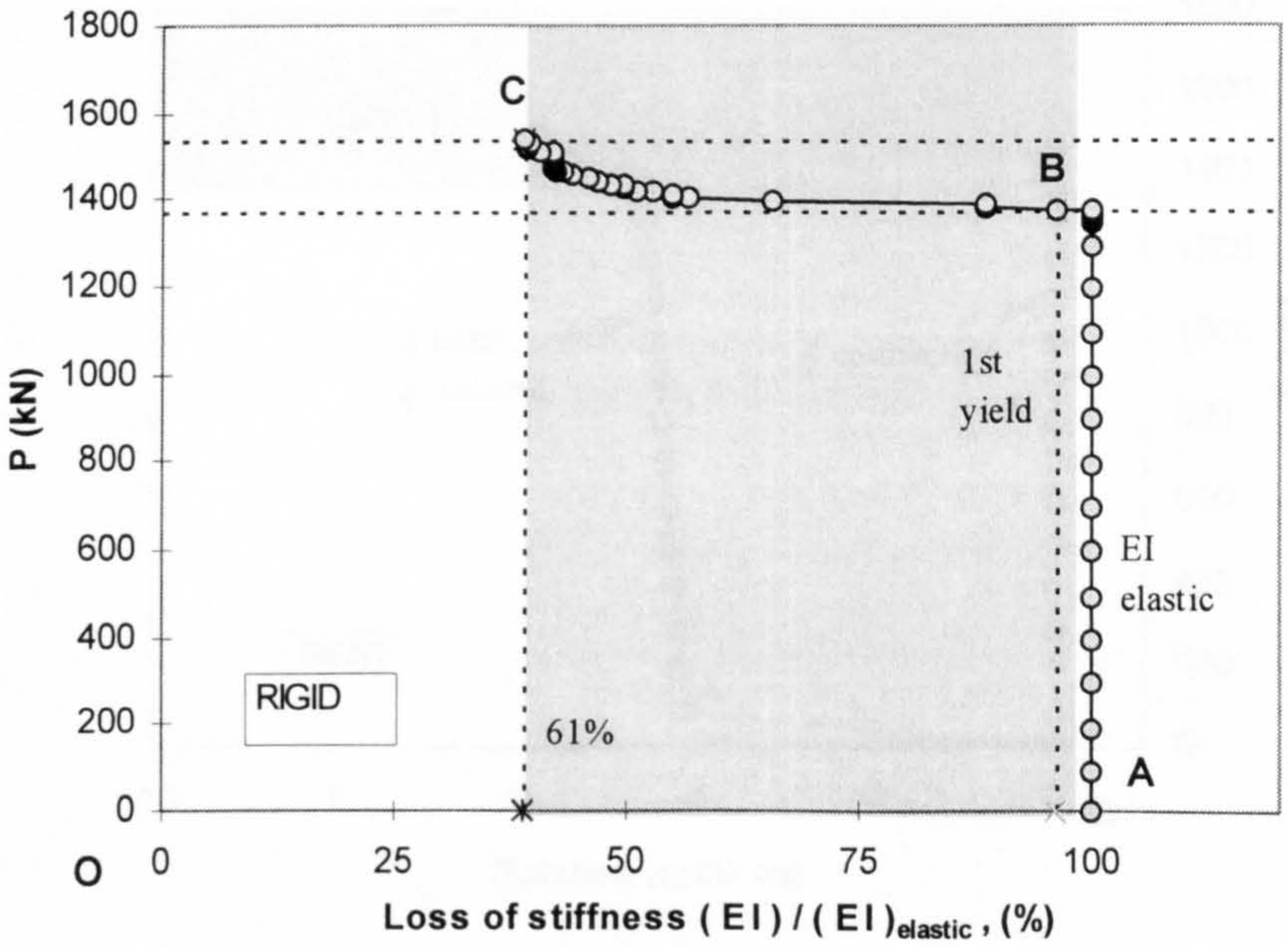

Figure 5.45 Loss of stiffness at column mid-height with RIGID connections

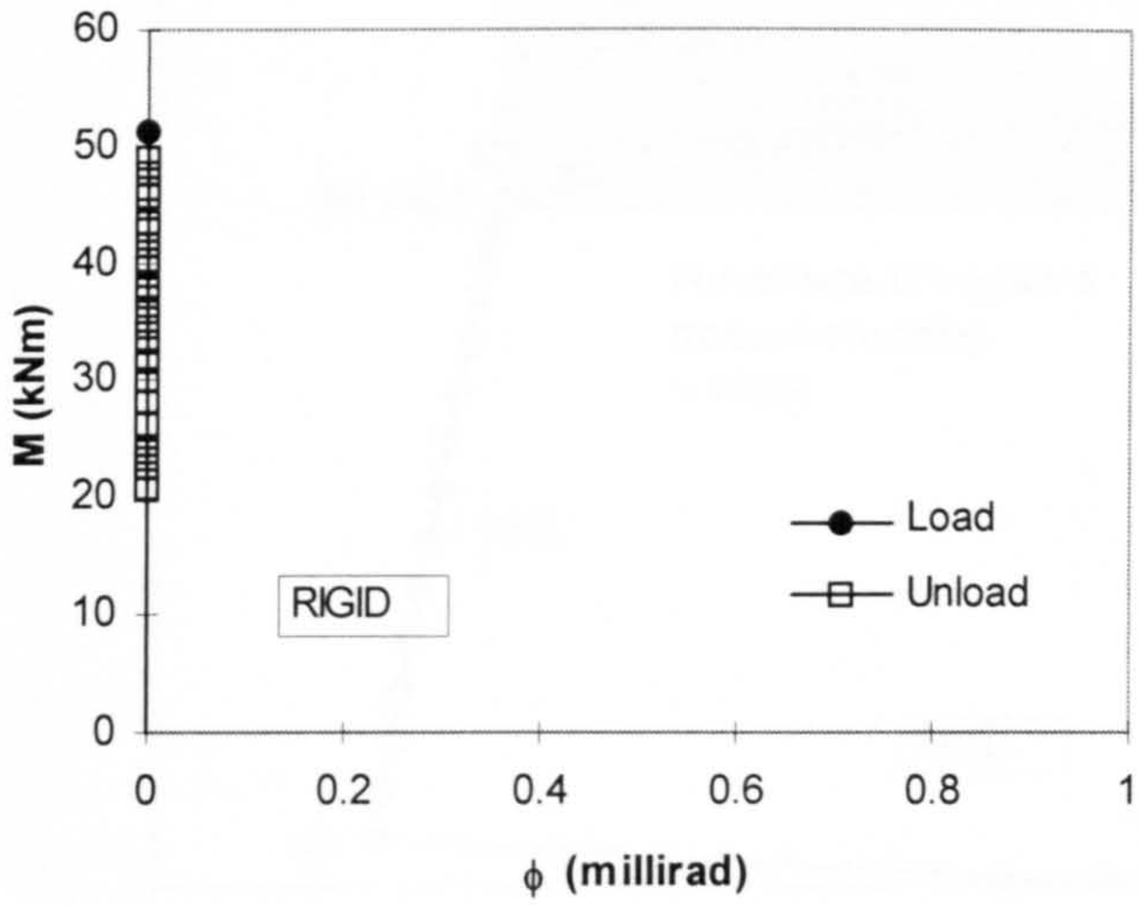

Figure 5.46 *M-ϕ* response at column top end with RIGID connections

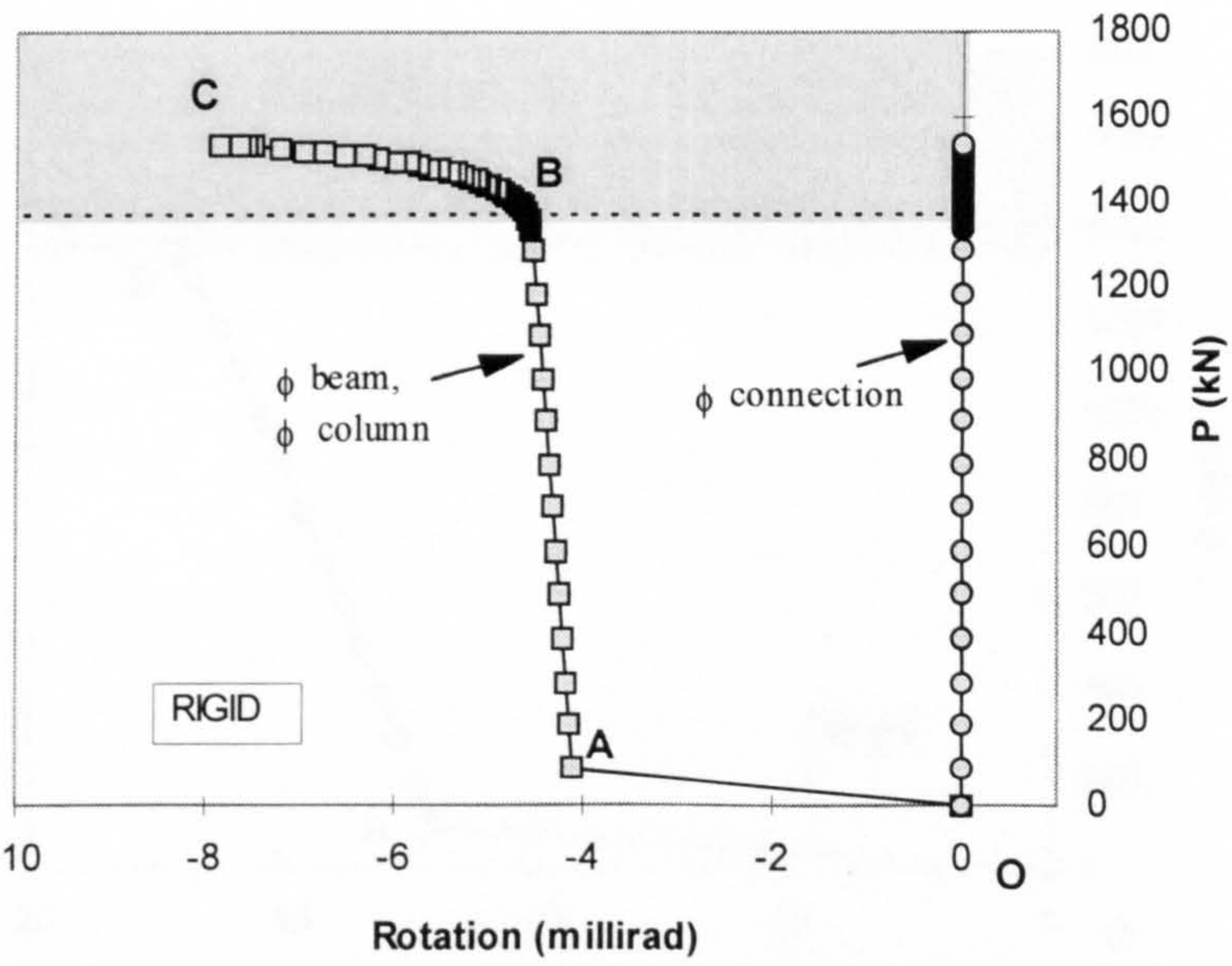

Figure 5.47 Development of beam, column and connection rotations with RIGID connections

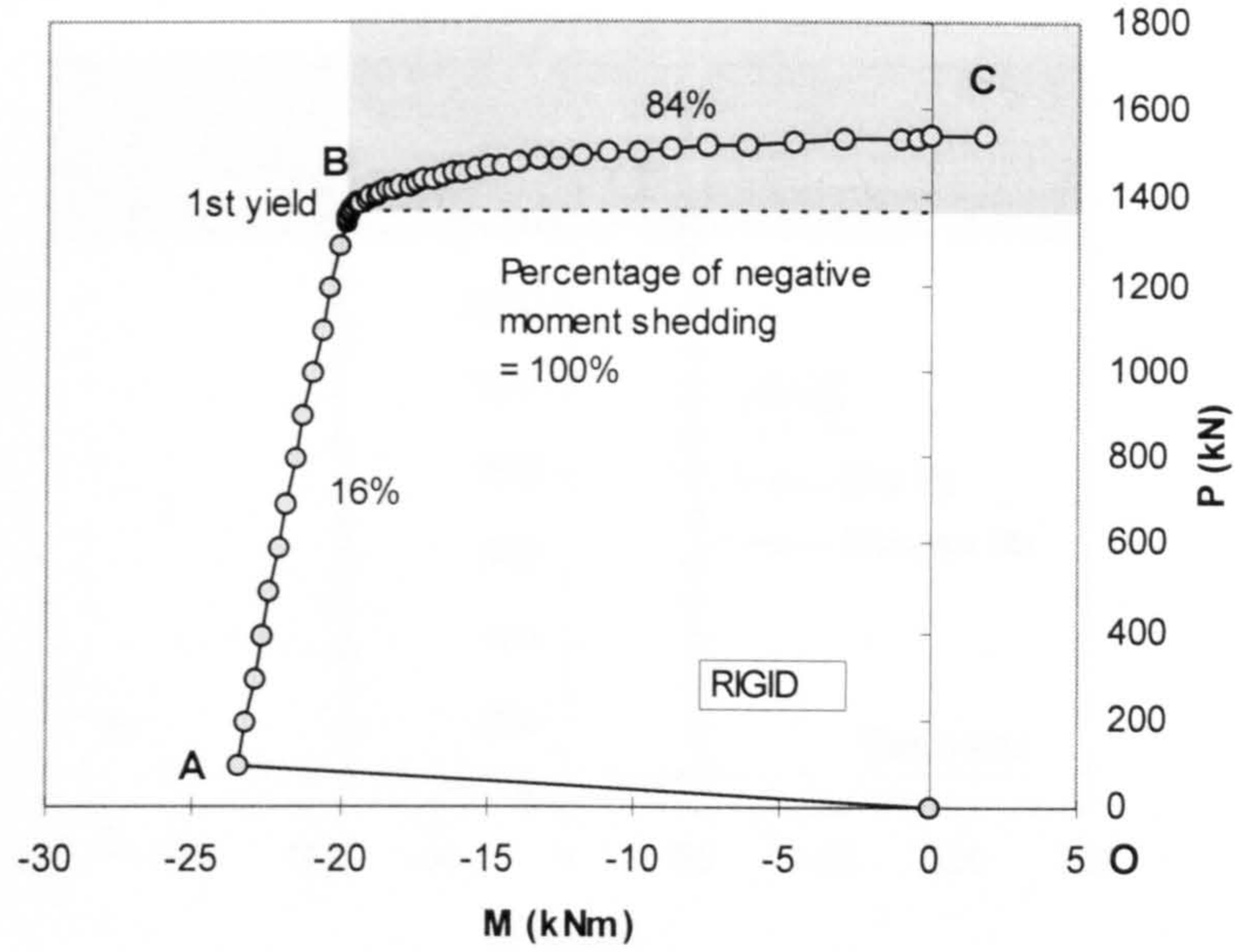

Figure 5.48 Response of moment shedding at column top end with RIGID connections

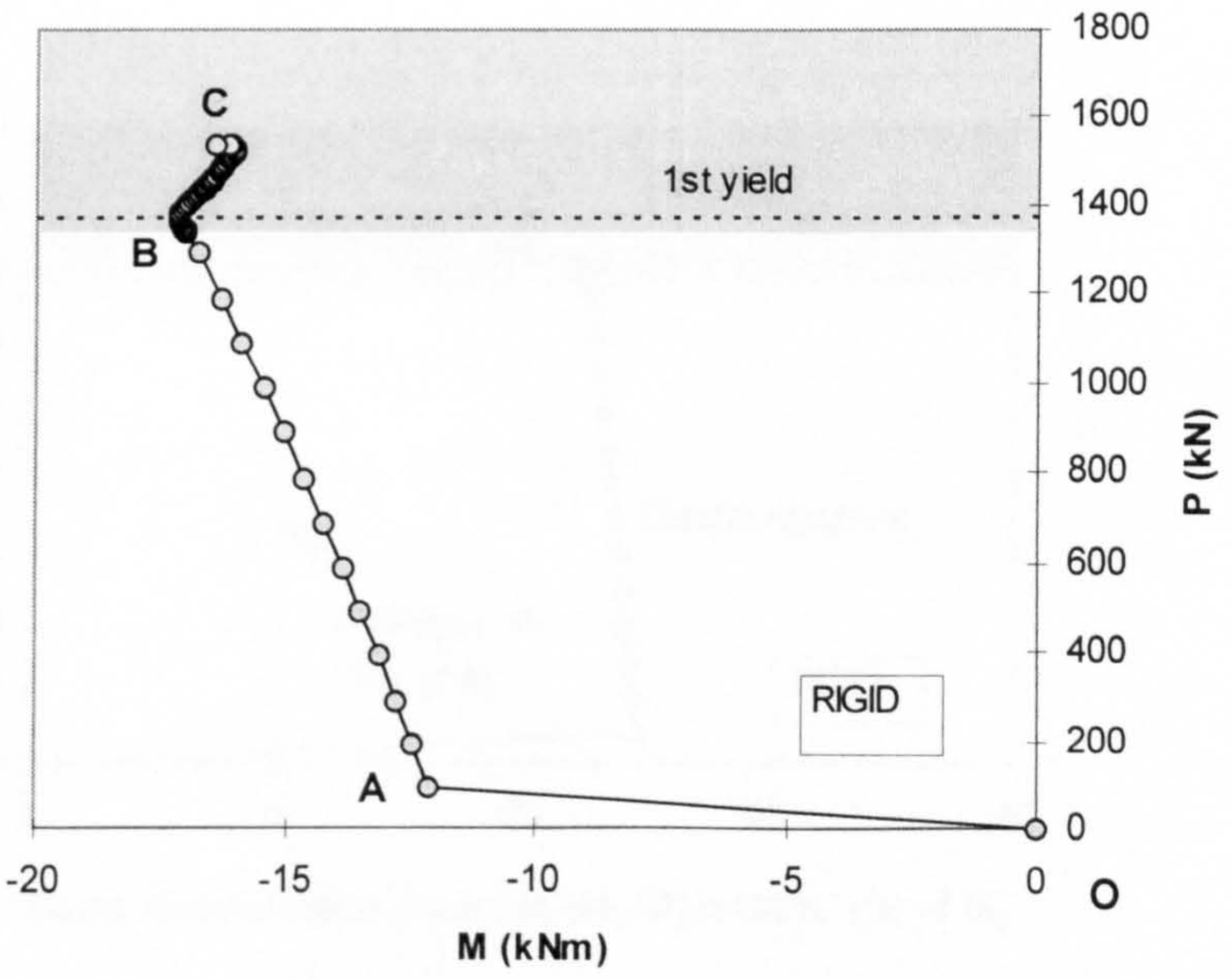

Figure 5.49 Response of moment at column mid-height with RIGID connections

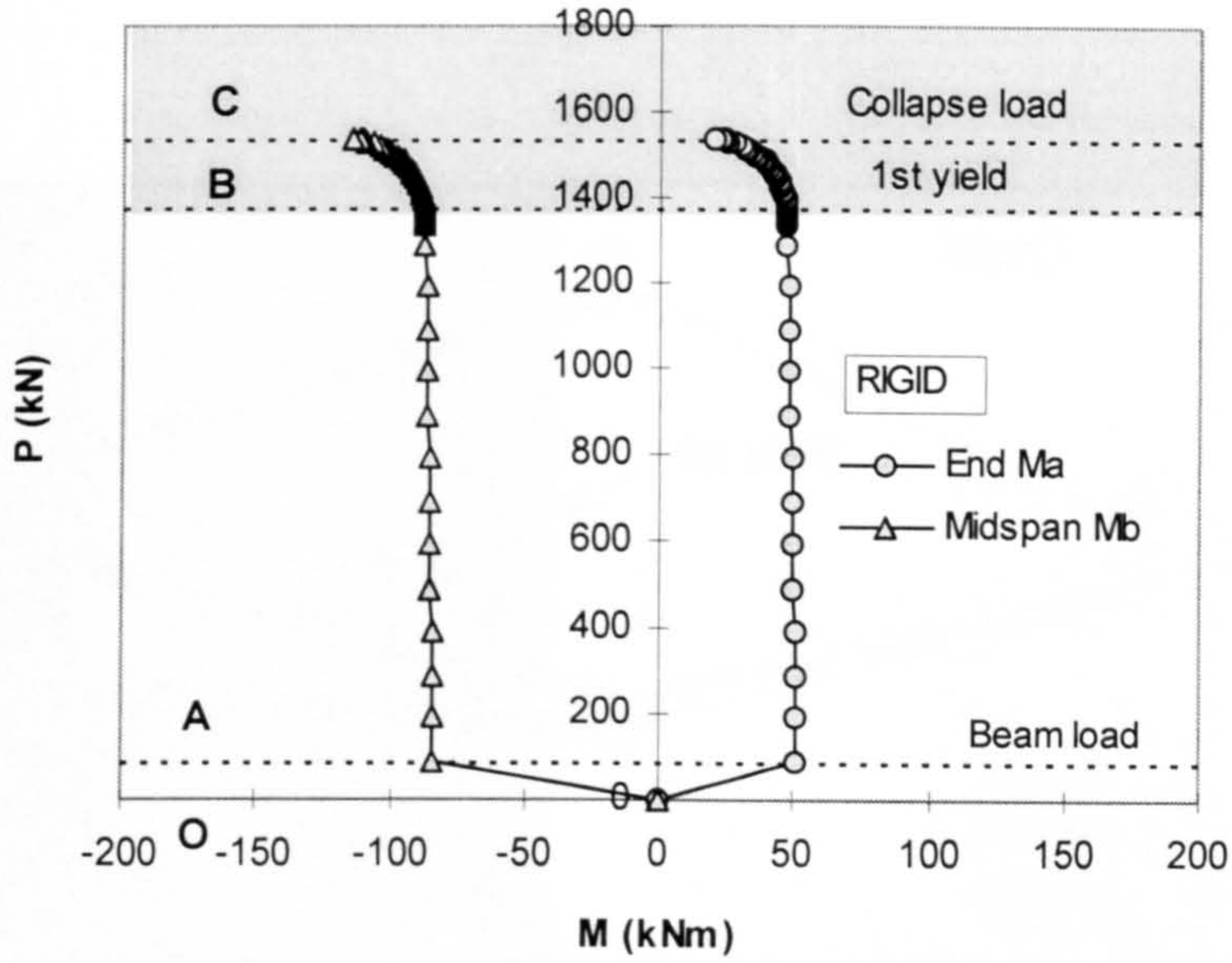

Figure 5.50 Response of moments at both beam end and beam midspan with RIGID connections

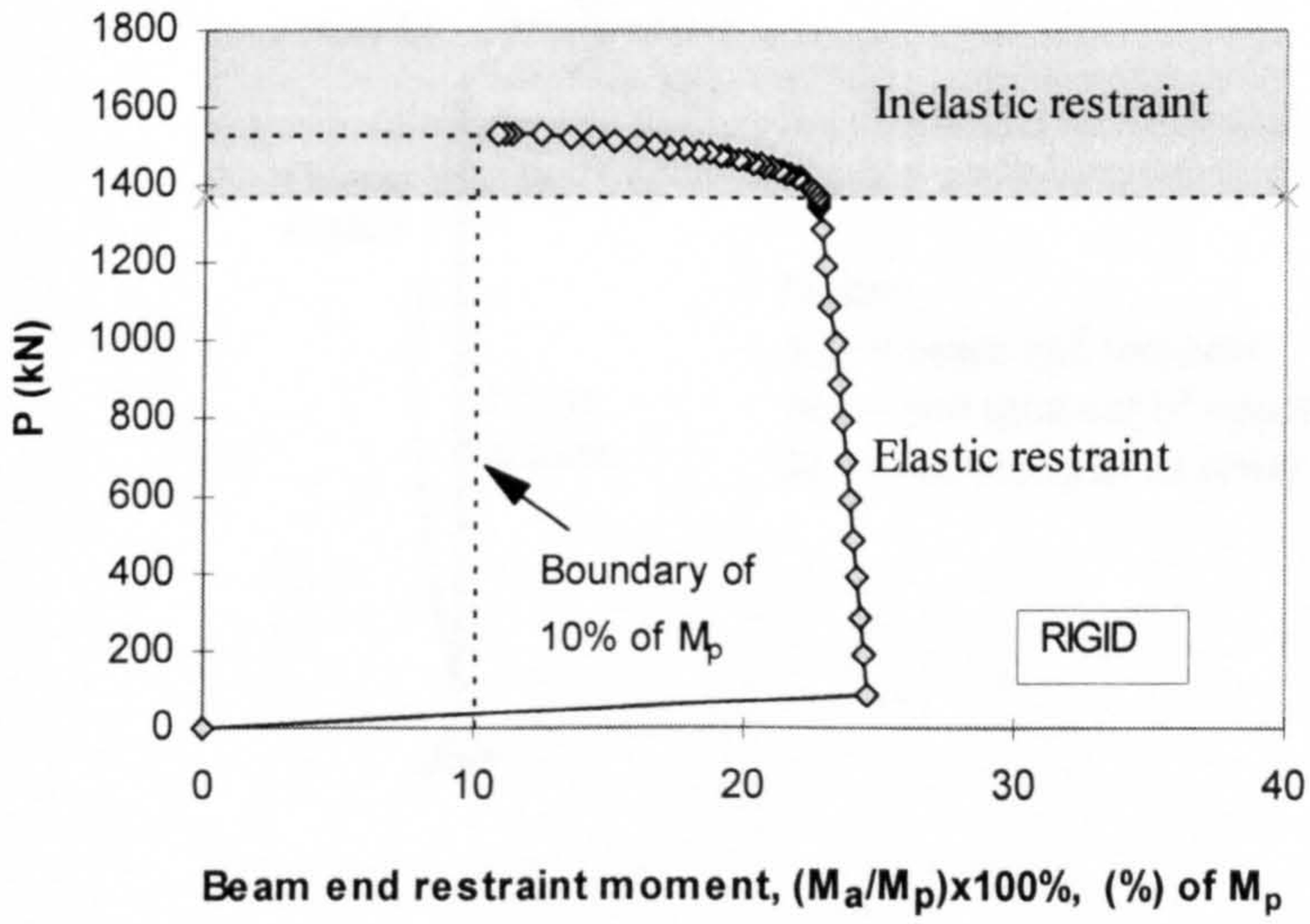

Figure 5.51 Development of beam end restraint moment with RIGID connections

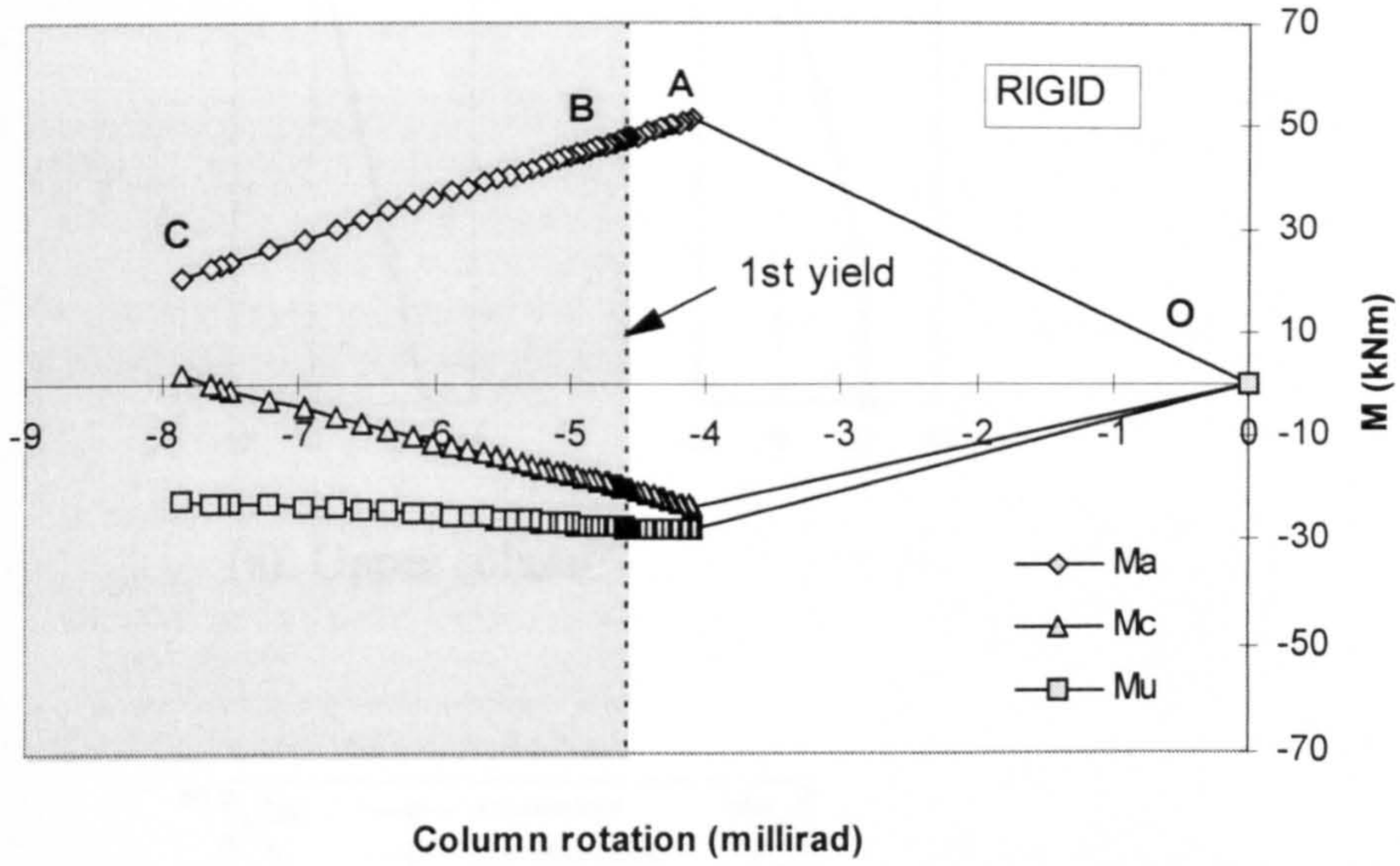

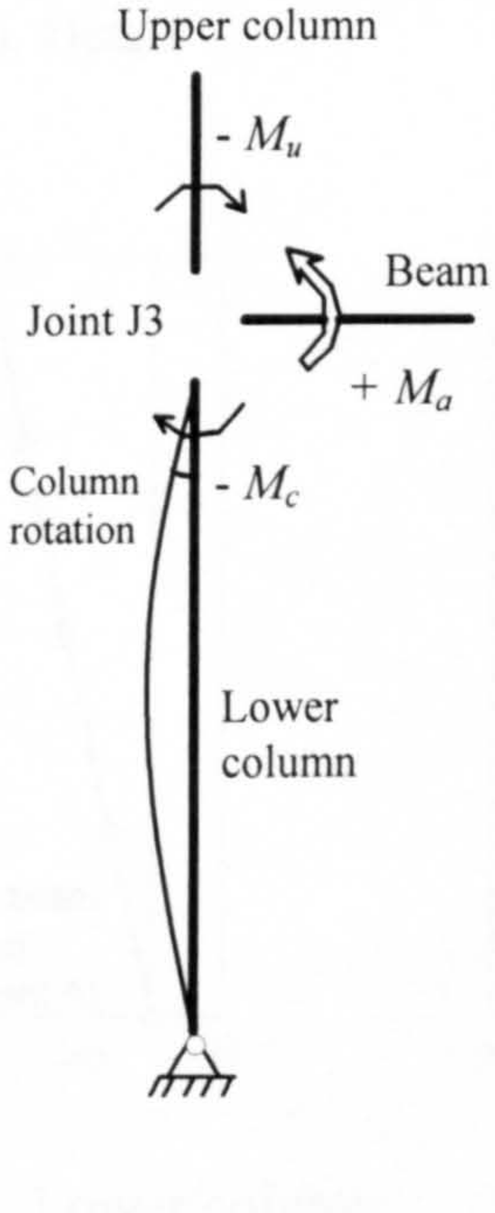

Notes:
M_a = beam end moment
M_u = end moment of upper column
M_c = end moment of lower column

Figure 5.52 Distribution of moments at joint J3 with increasing column end rotations using RIGID connections

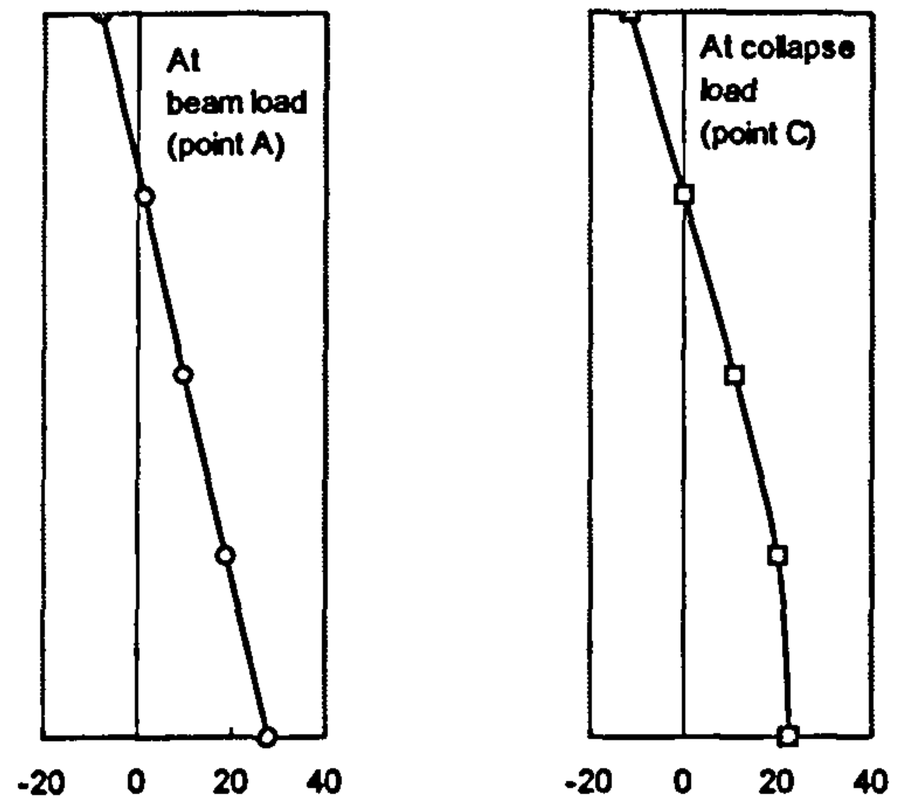

(a). Upper column

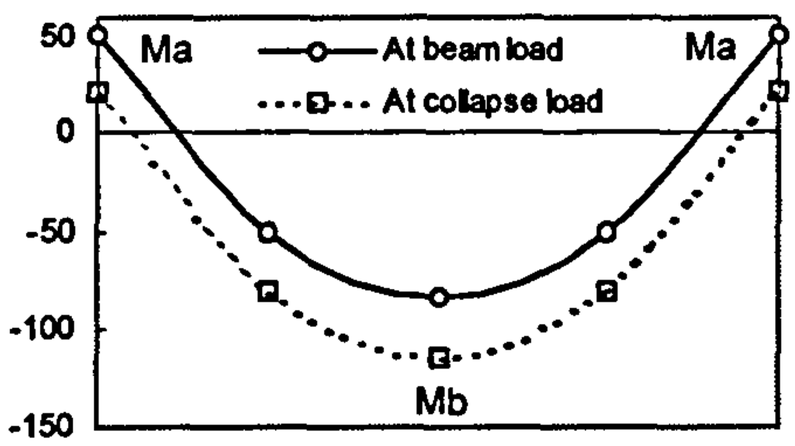

(b). Beam

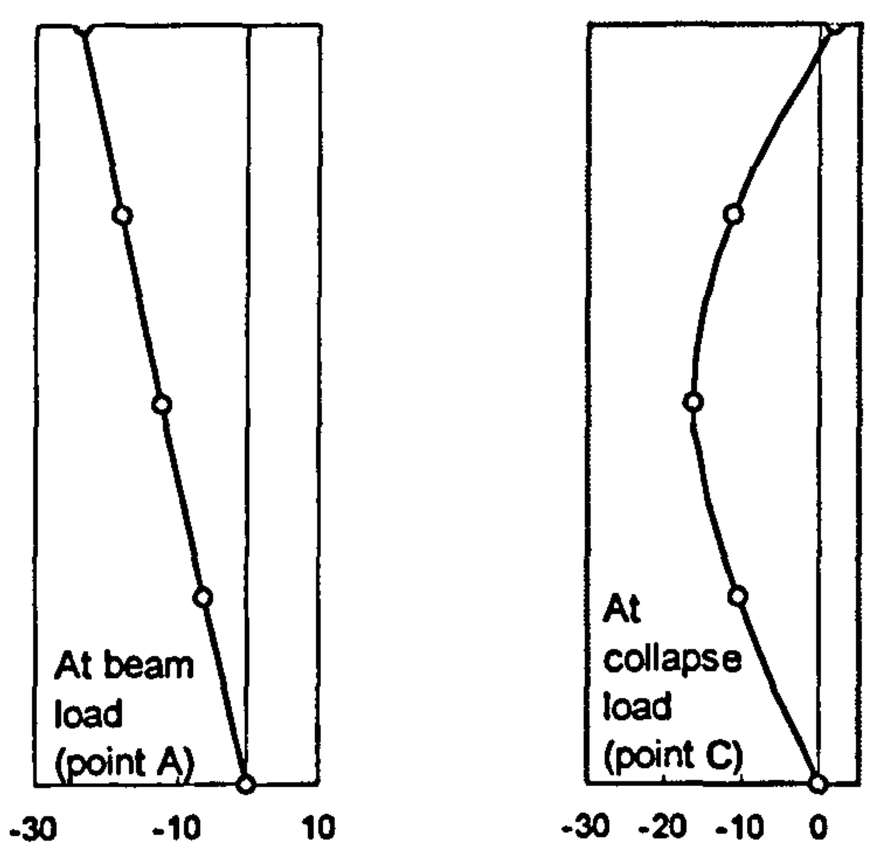

(c). Lower column

Figure 5.53 Smoothed bending moment diagrams at service loads and at collapse loads in kNm with RIGID connections

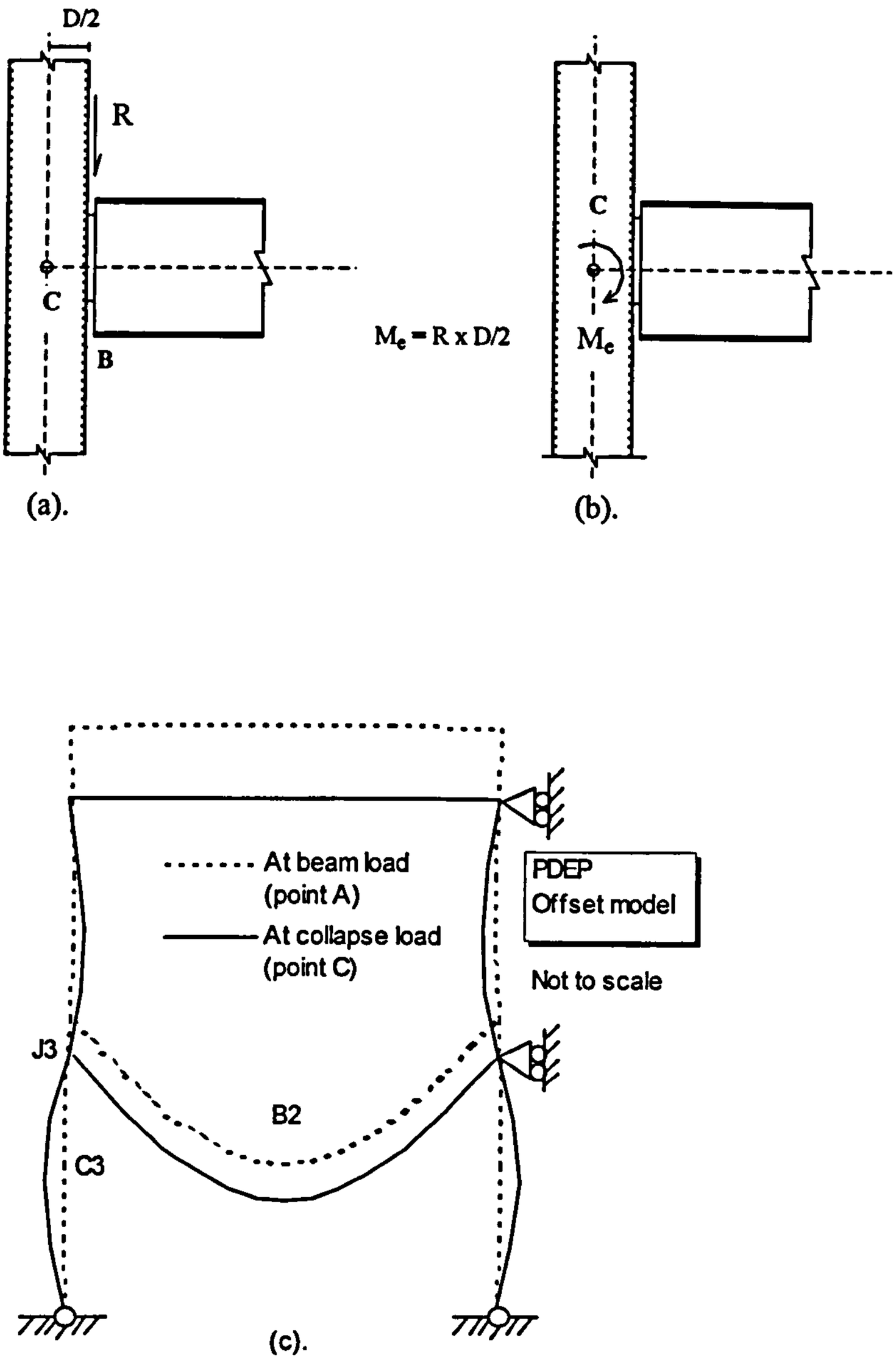

Figure 5.54 (a). Actual location of connection with load eccentricity at column face
(b). Applied moment, M_e at intersection between beam centre-line and column centre-line to model the eccentricity load
(c). Exaggerated deformed shape of frame with PDEP connections modelled at column face

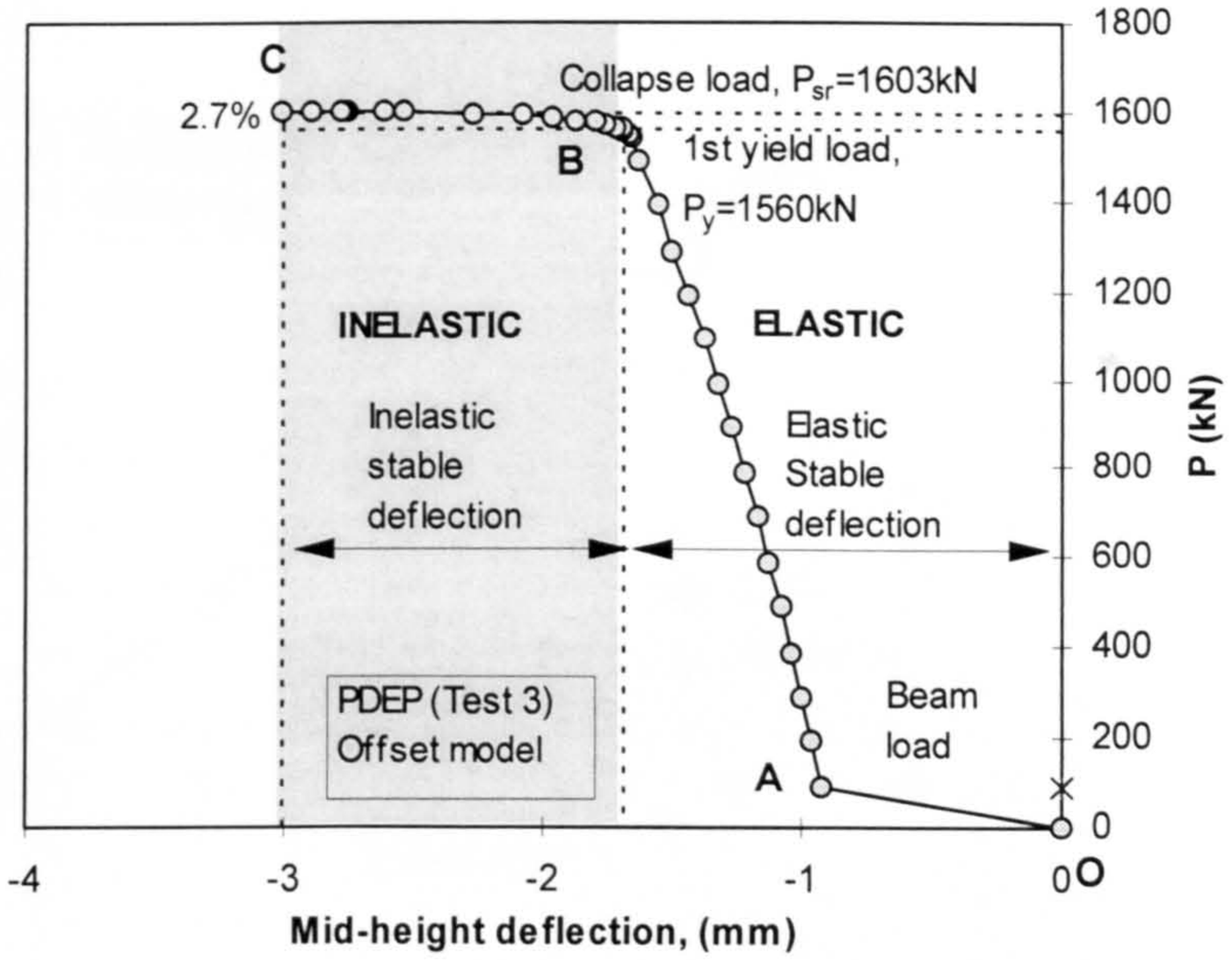

Figure 5.55 Load deflection response at column mid-height with PDEP connections modelled at column face

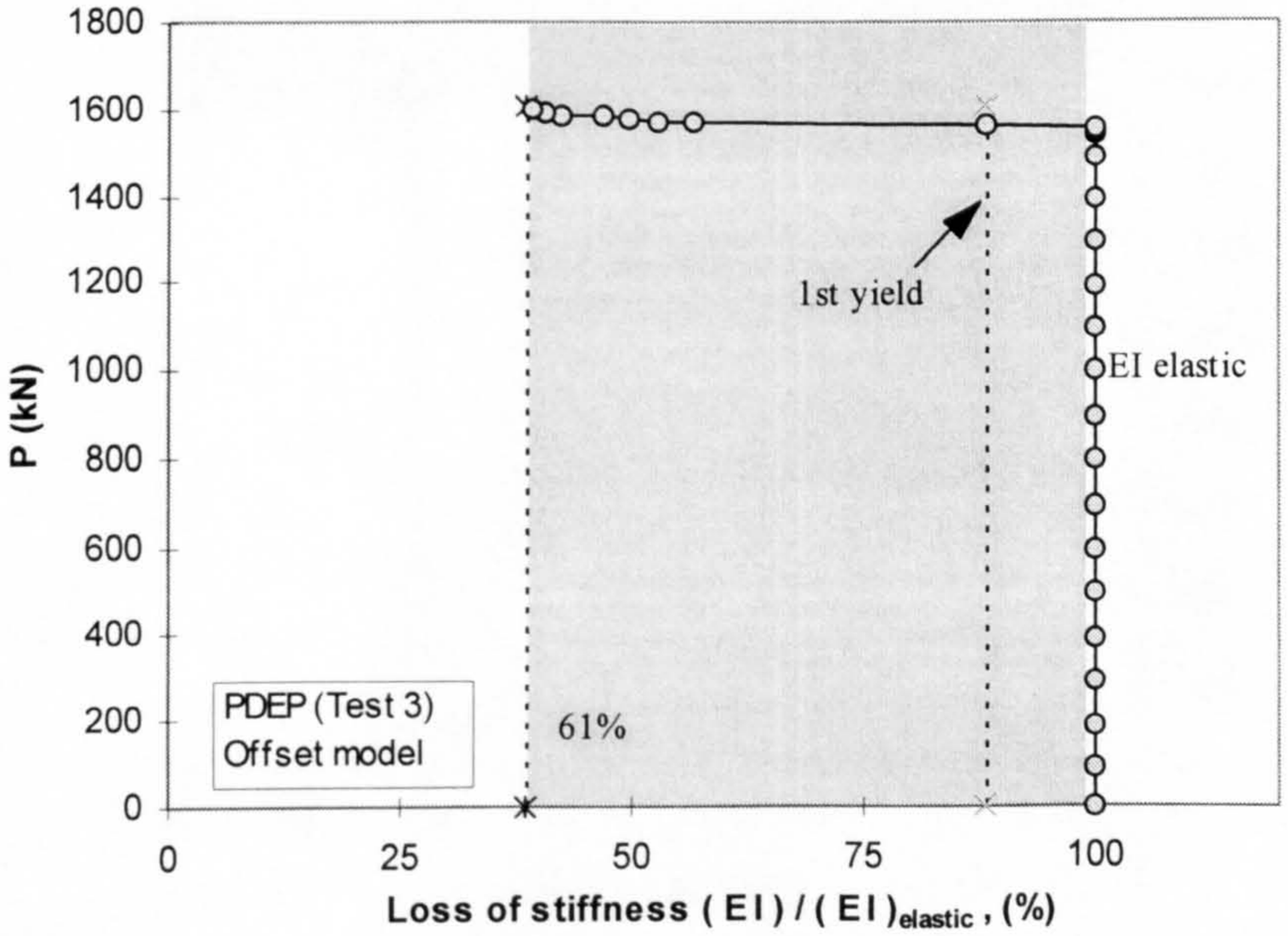

Figure 5.56 Loss of stiffness at column mid-height with PDEP connections modelled at column face

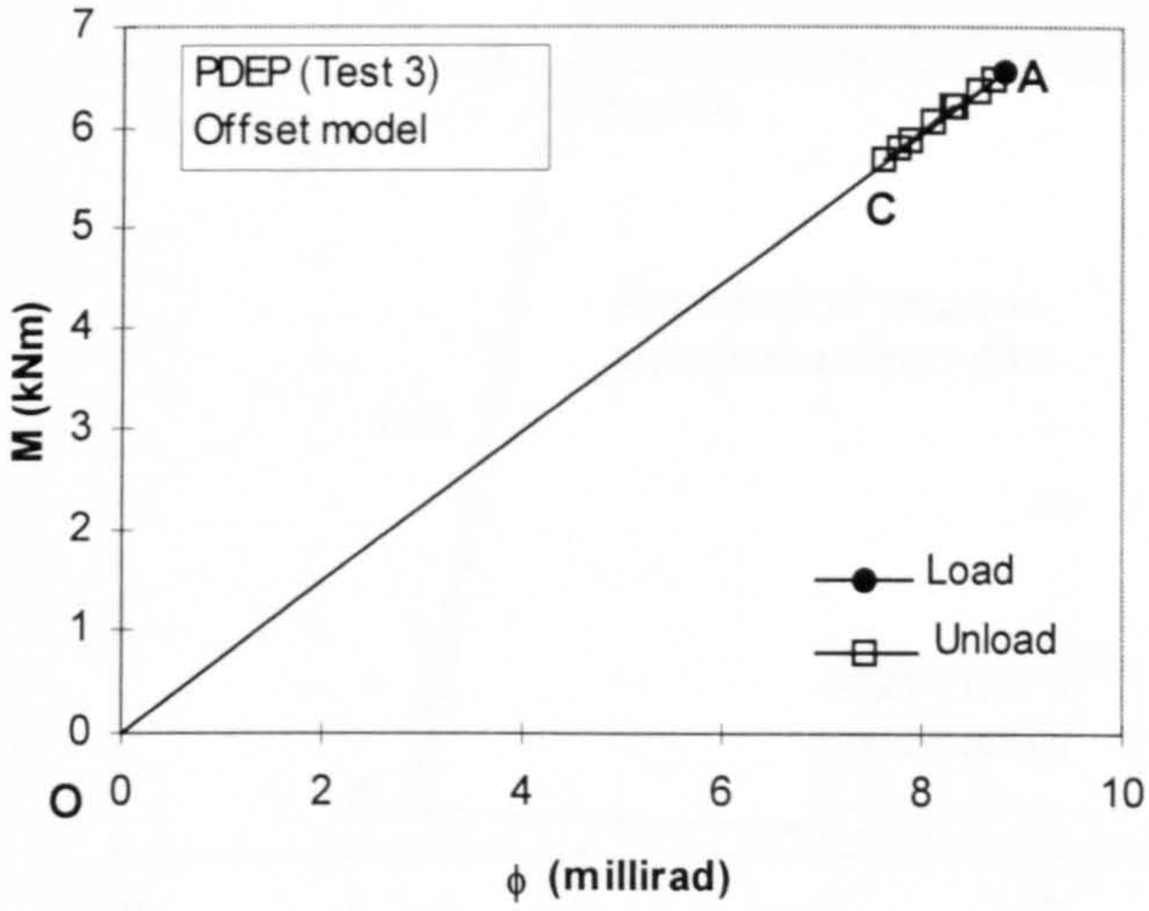

Figure 5.57 *M-φ* response at column top end with PDEP connections modelled at column face

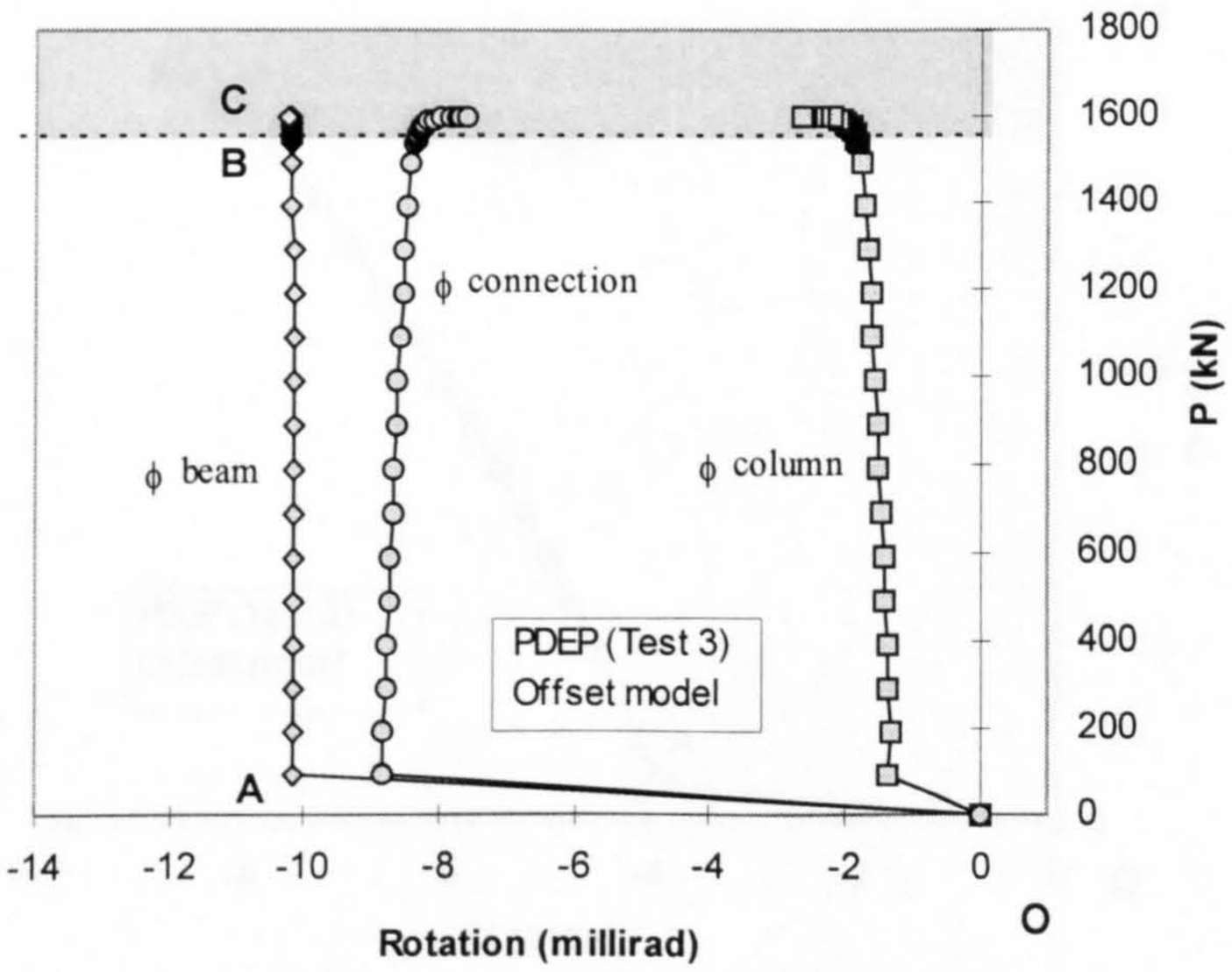

Figure 5.58 Development of beam, column and connection rotations with PDEP connections modelled at column face

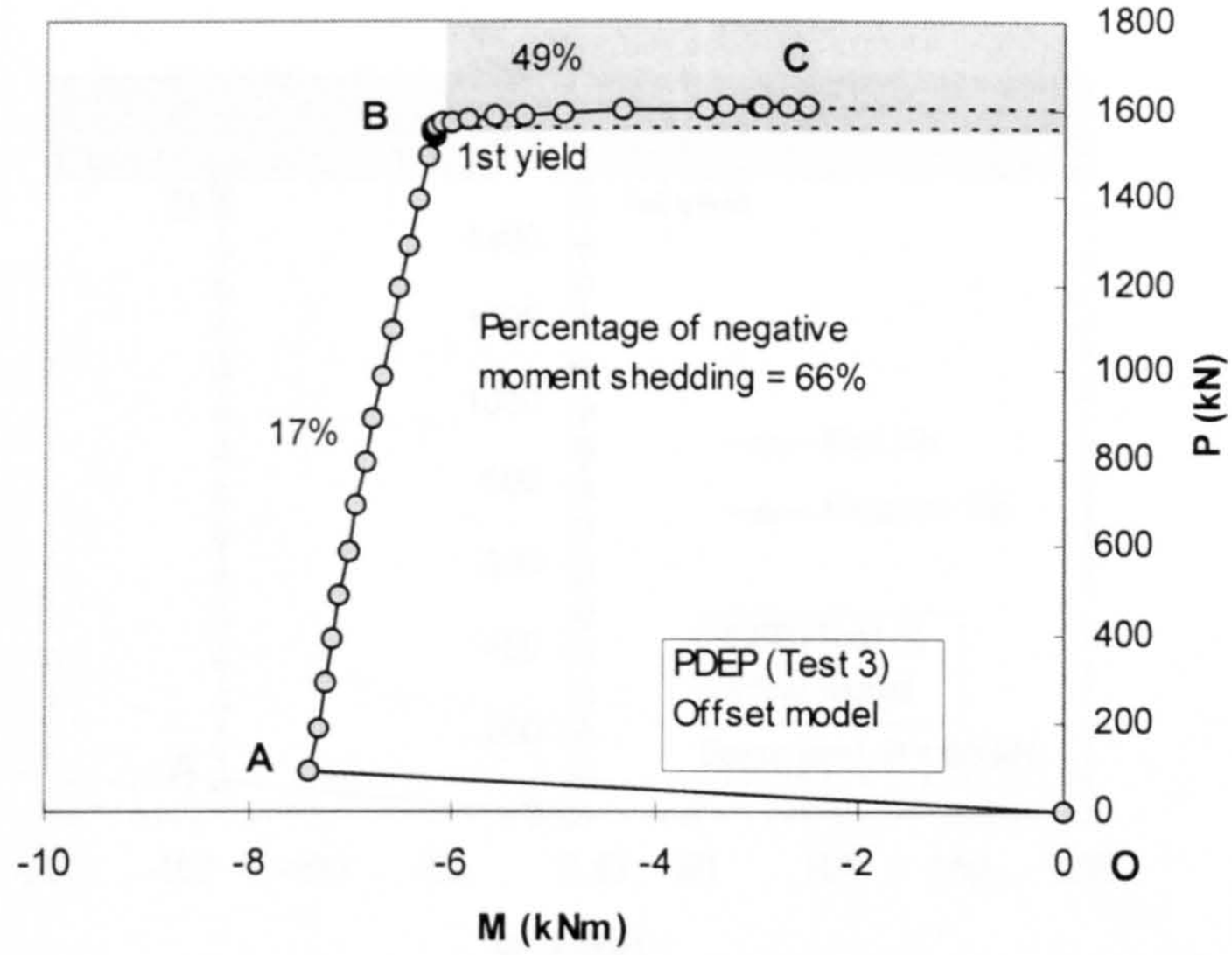

Figure 5.59 Response of moment shedding at column top end with PDEP connections modelled at column face

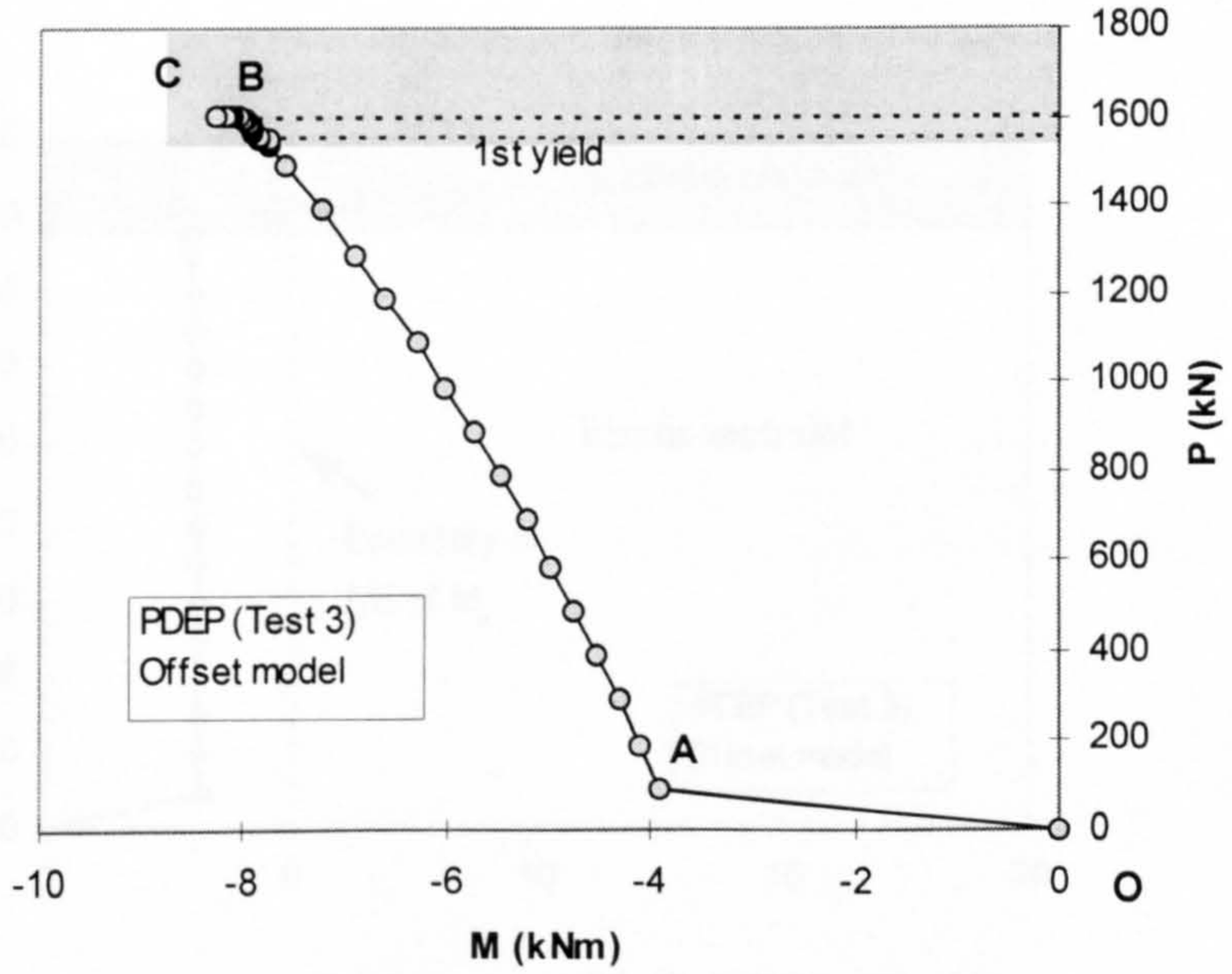

Figure 5.60 Response of moment at column mid height with PDEP connections modelled at column face

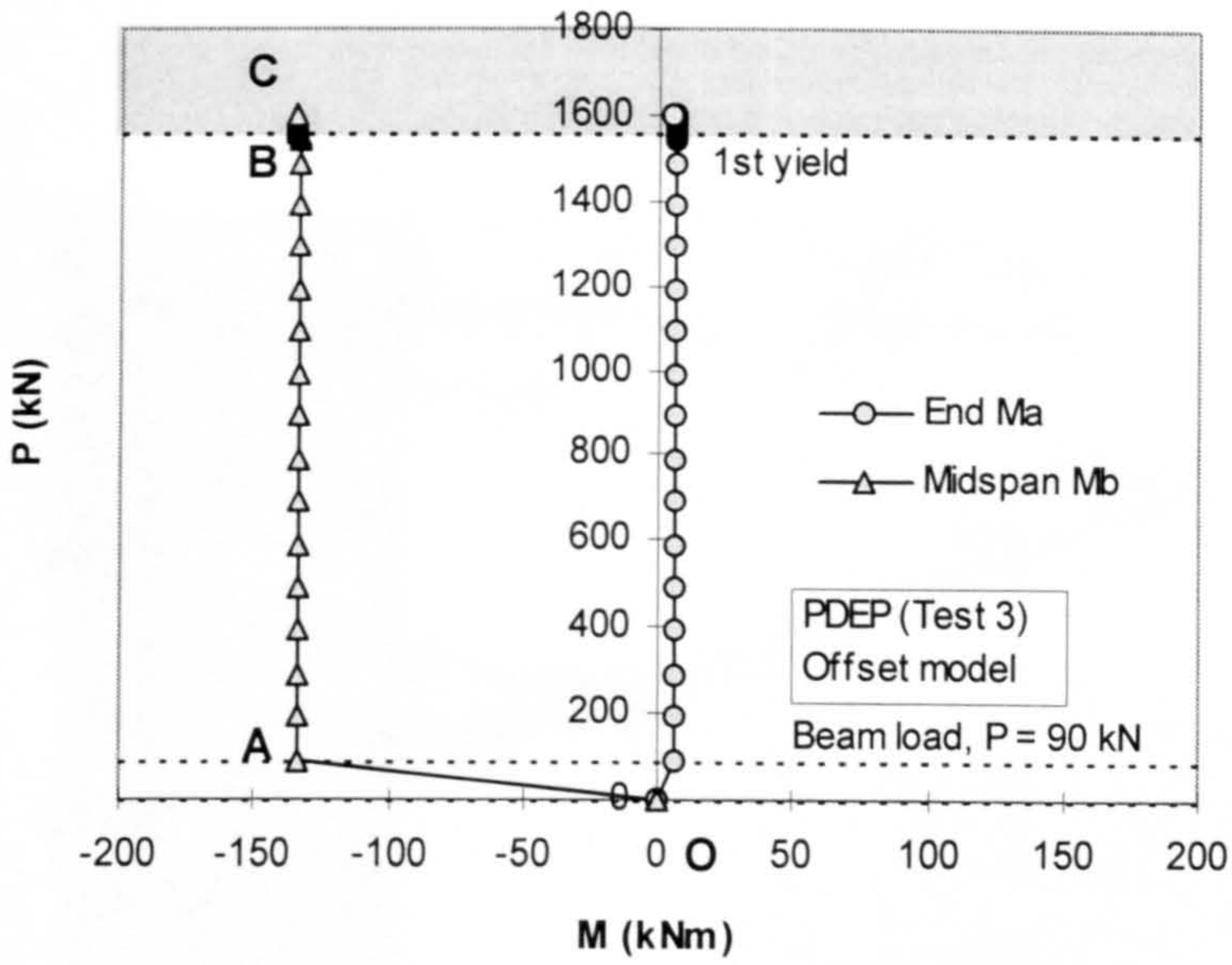

Figure 5.61 Response of moments at both beam end beam midspan with PDEP connections modelled at column face

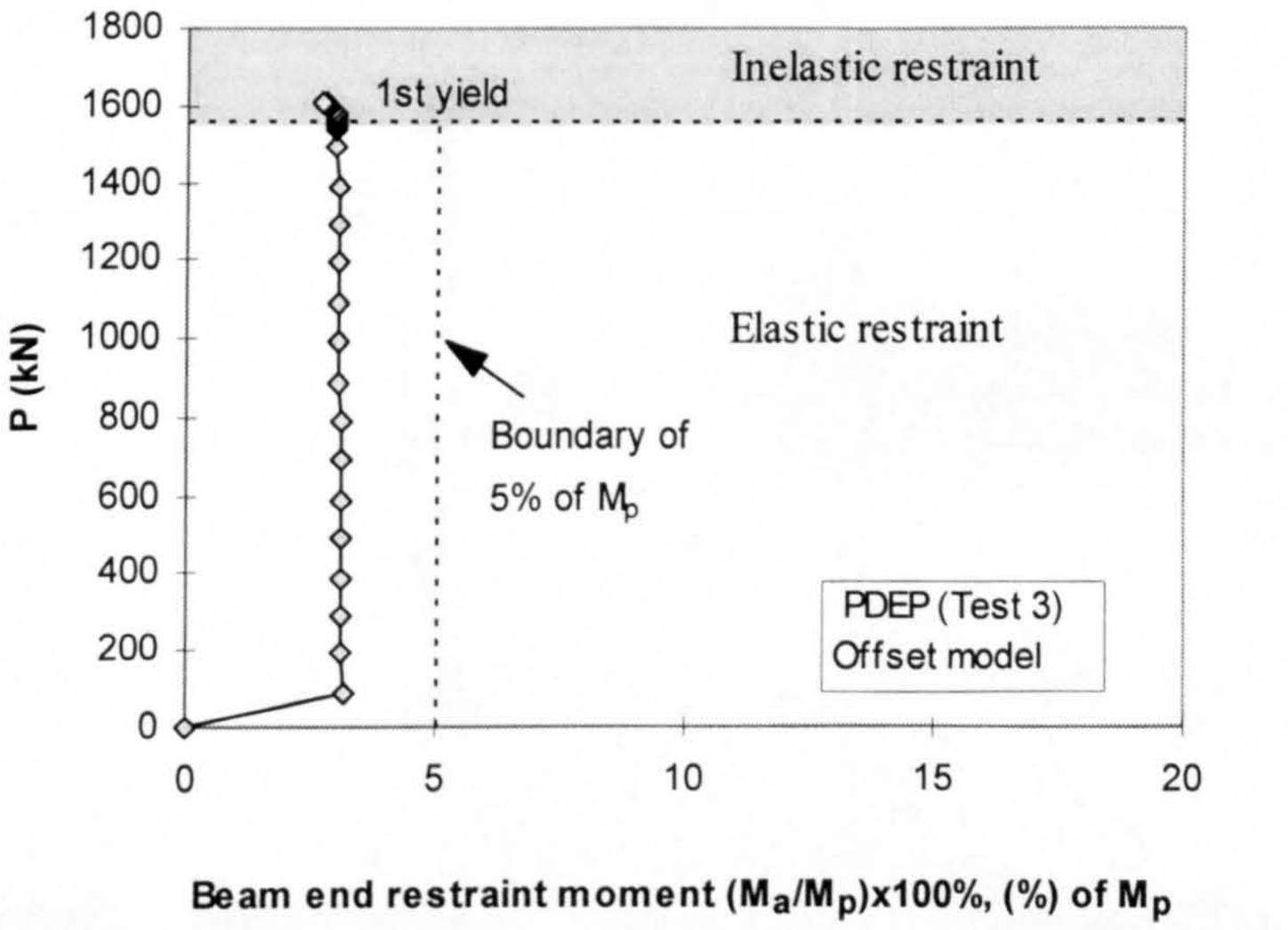

Figure 5.62 Development of beam end restraint moment with PDEP connections modelled at column face

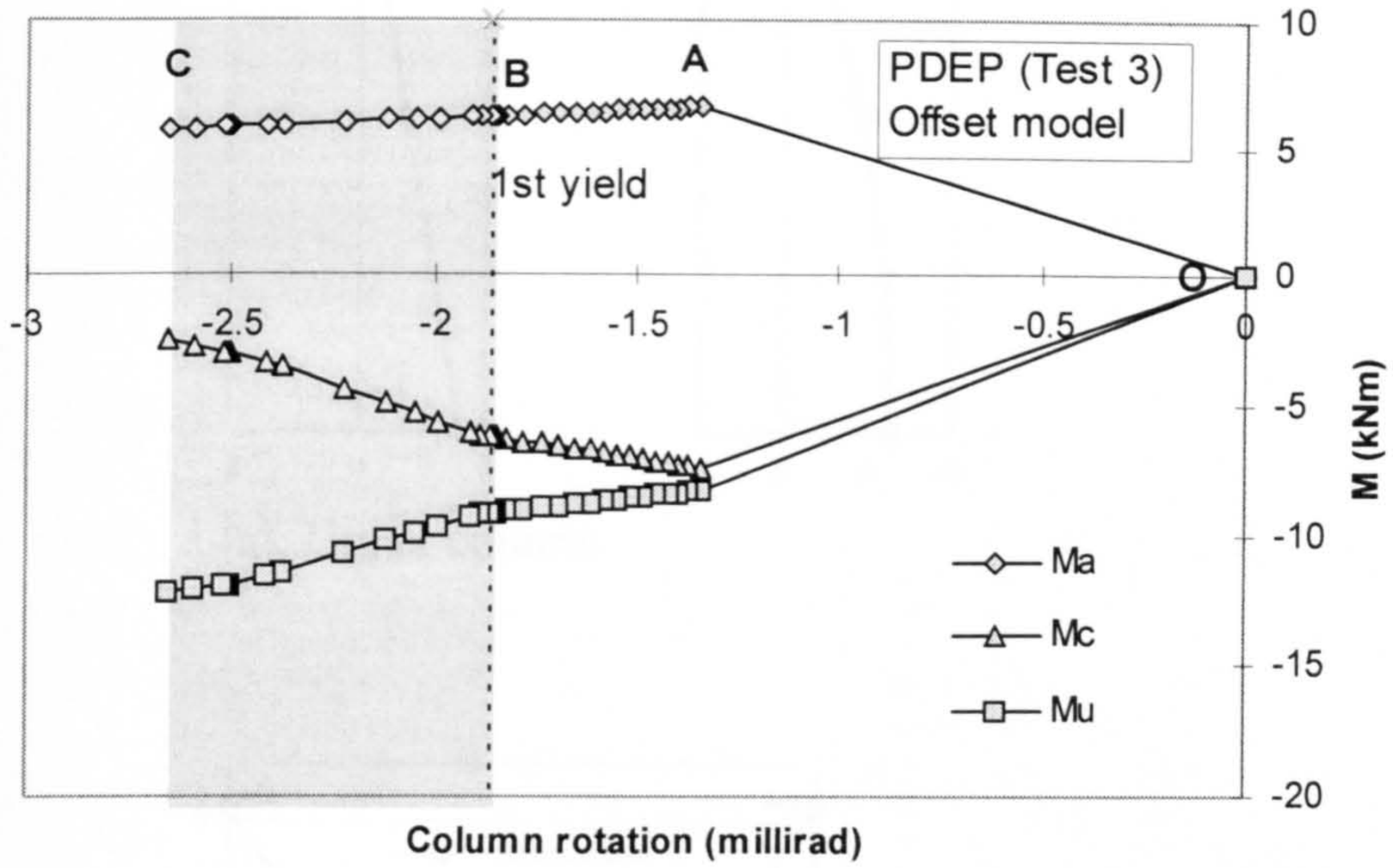

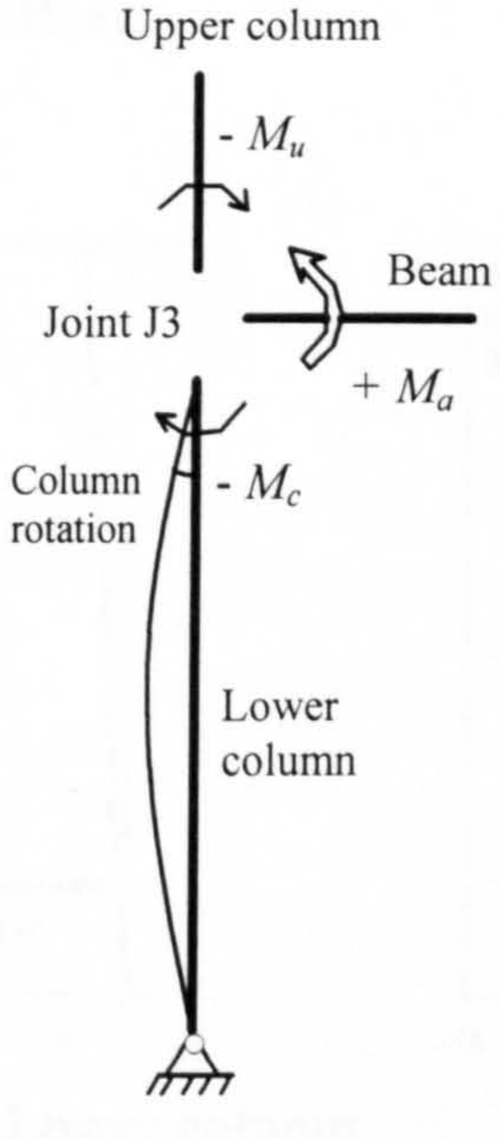

Notes:
M_a = beam end moment
M_u = end moment of upper column
M_c = end moment of lower column

Figure 5.63 Distribution of moments at joint J3 with increasing column end rotation

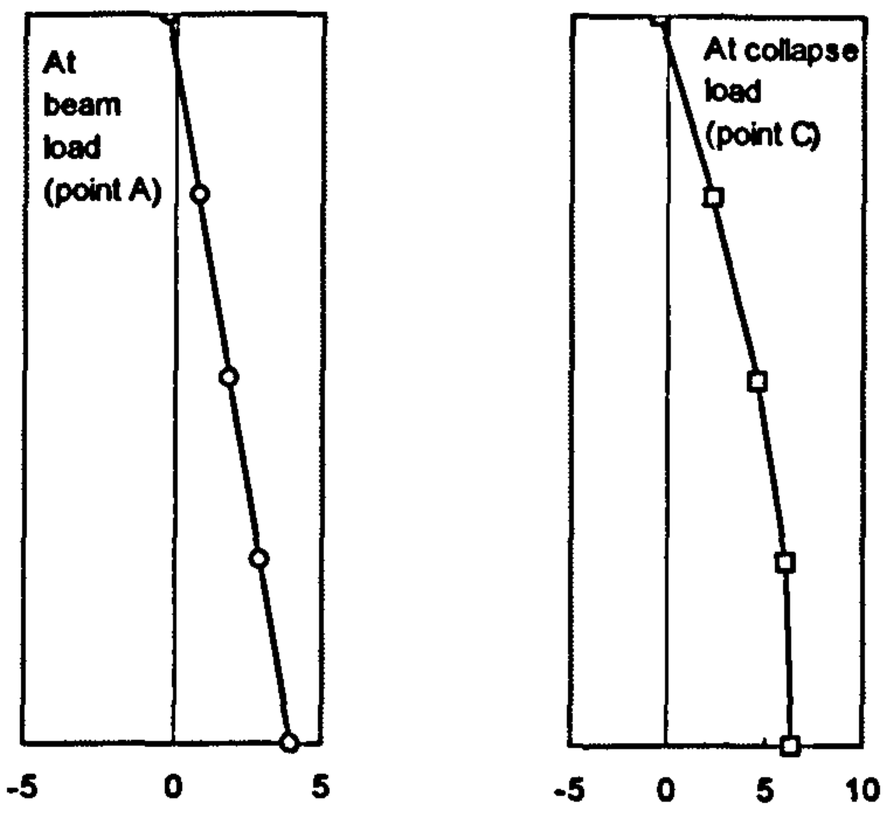

(a). Upper column

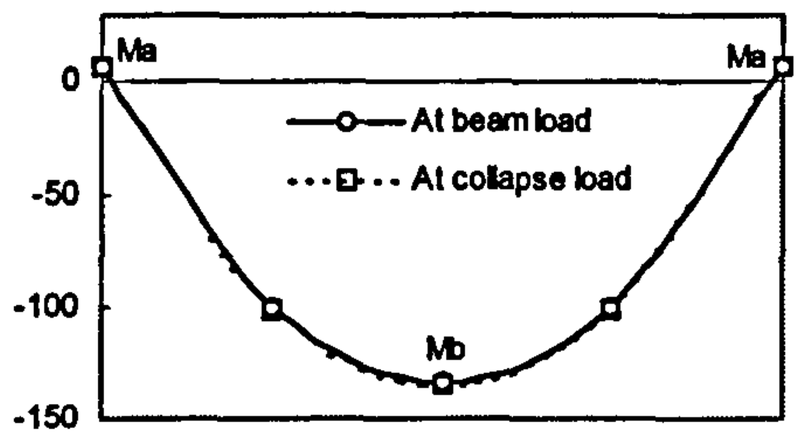

(b). Beam

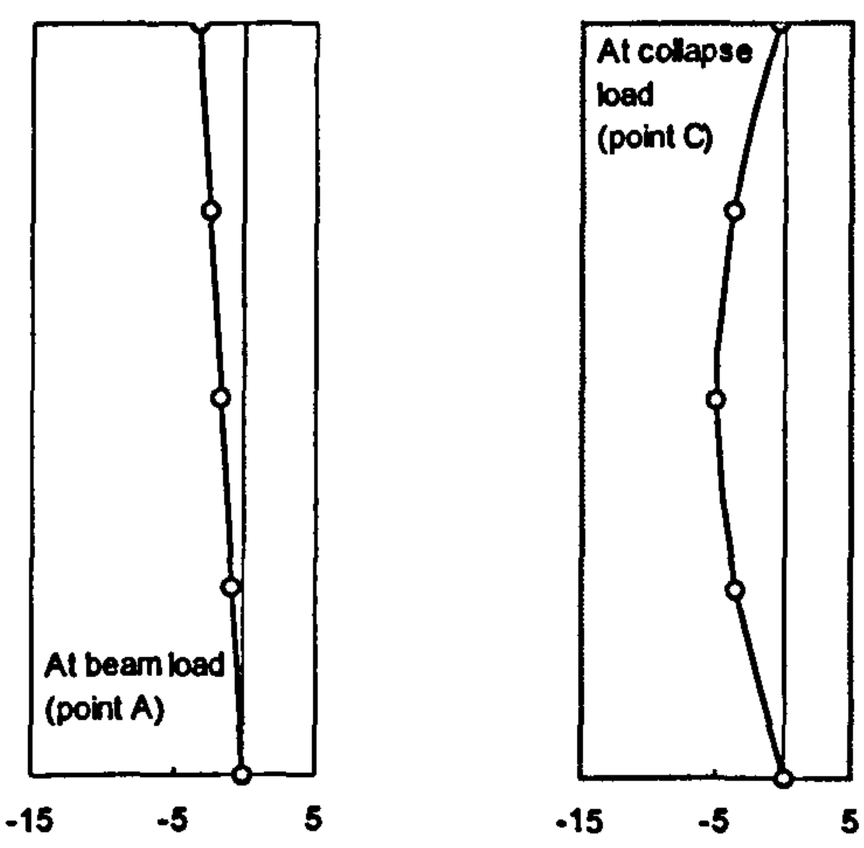

(c). Lower column

Figure 5.64 Smoothed bending moment diagrams at beam loads and at collapse loads in kNm with PDEP connections modelled at face of column

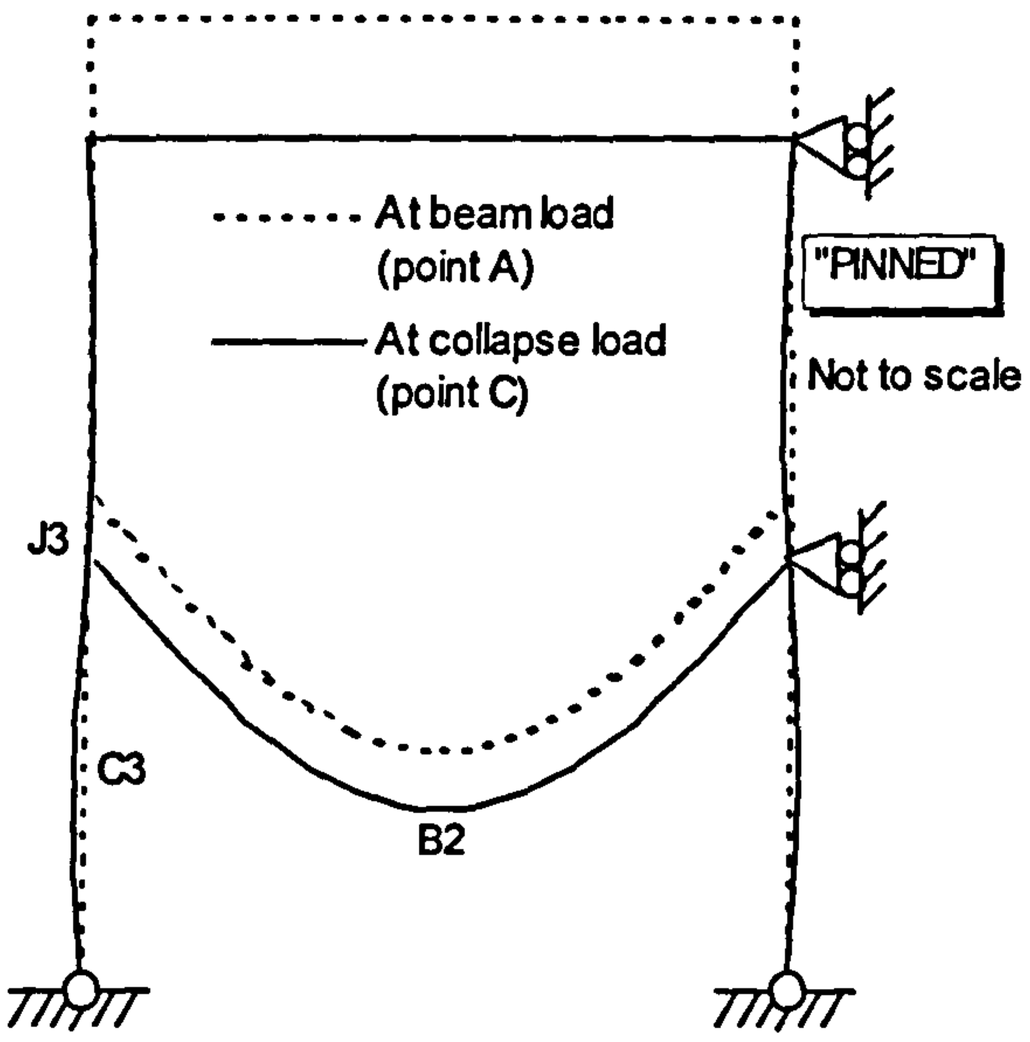

Figure 5.65 Exaggerated deformed shape of frame with "PINNED" connections

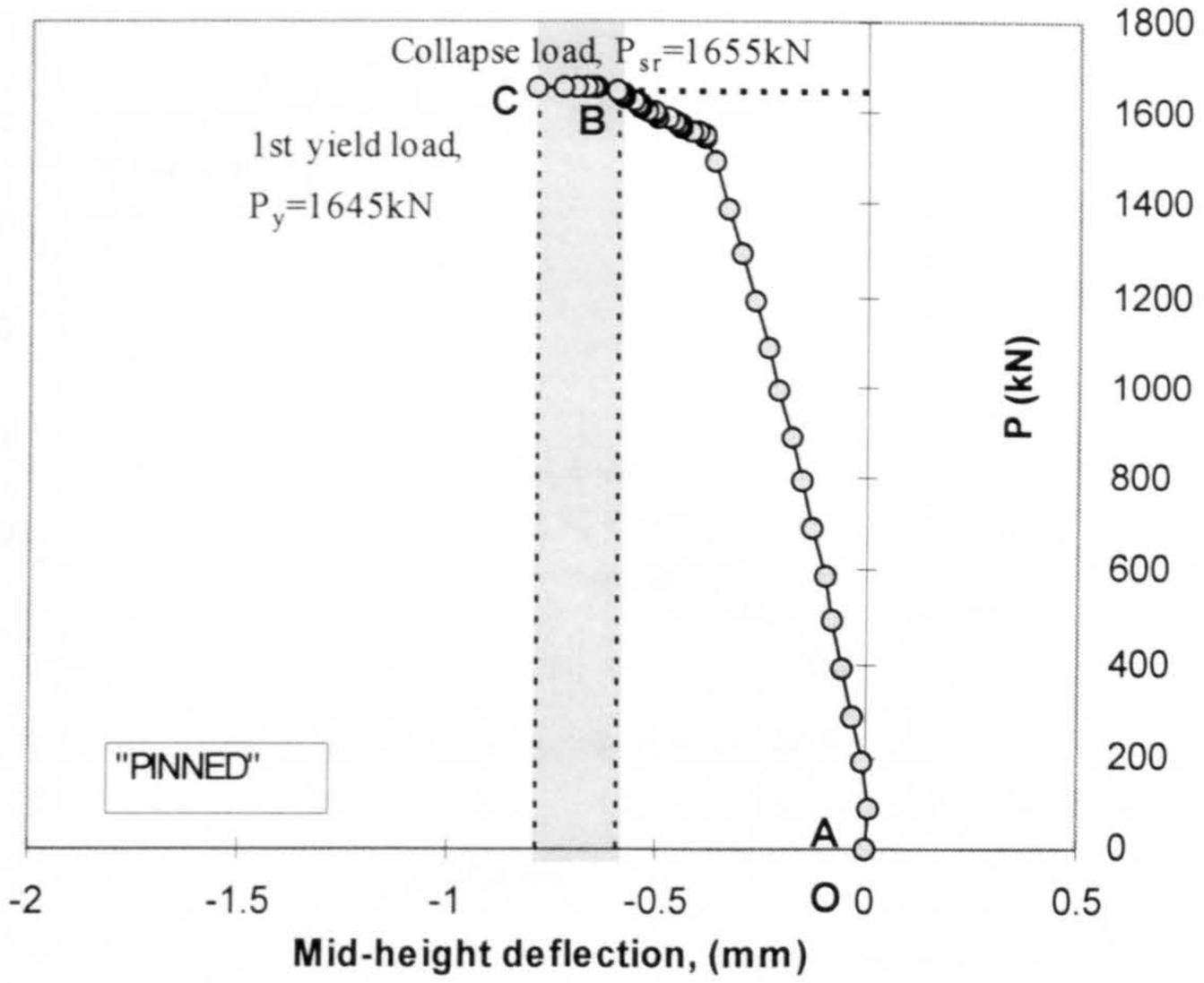

Figure 5.66 Load deflection response at column mid-height with "PINNED" connections

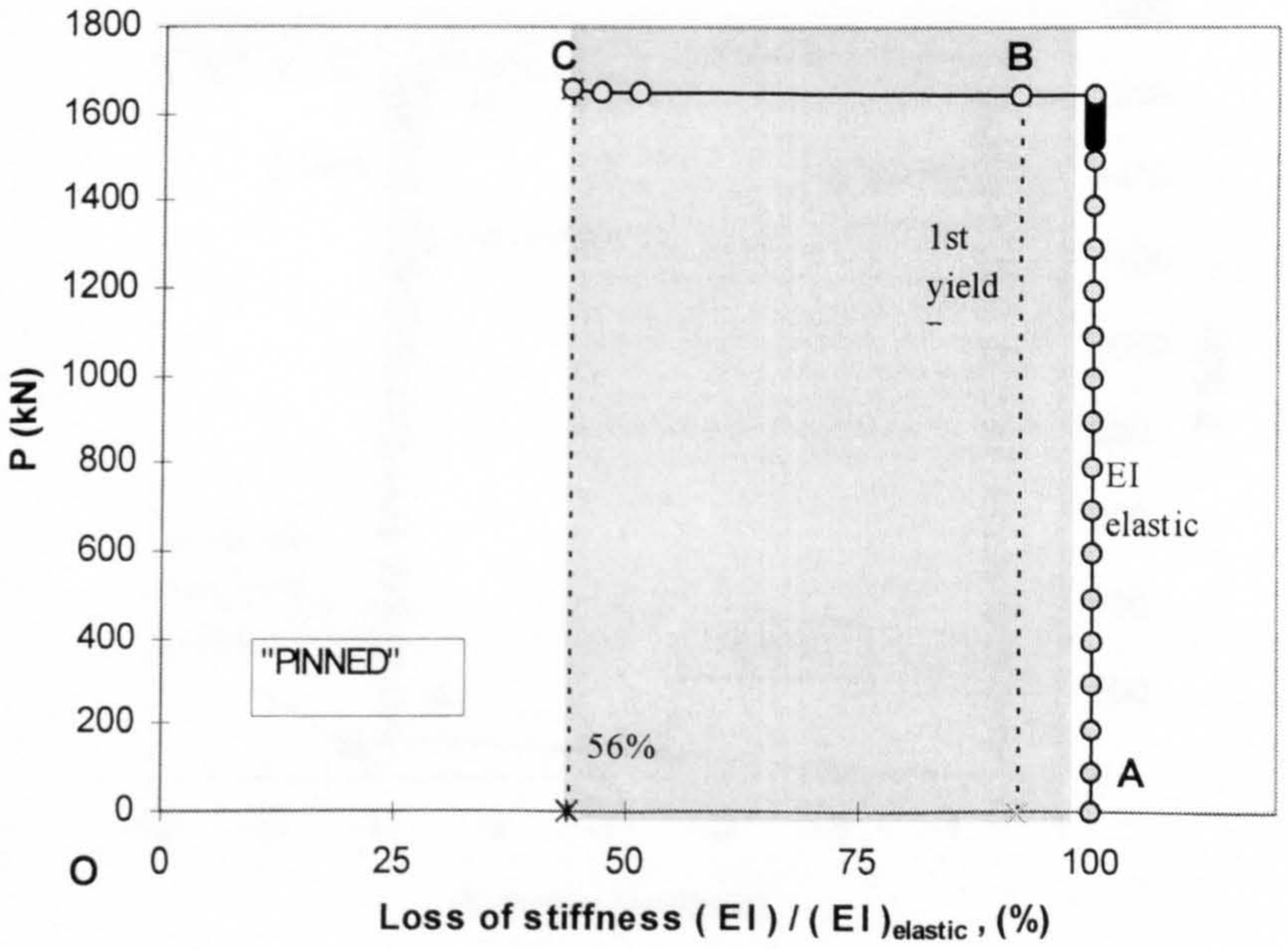

Figure 5.67 Loss of stiffness at column mid-height with "PINNED" connections

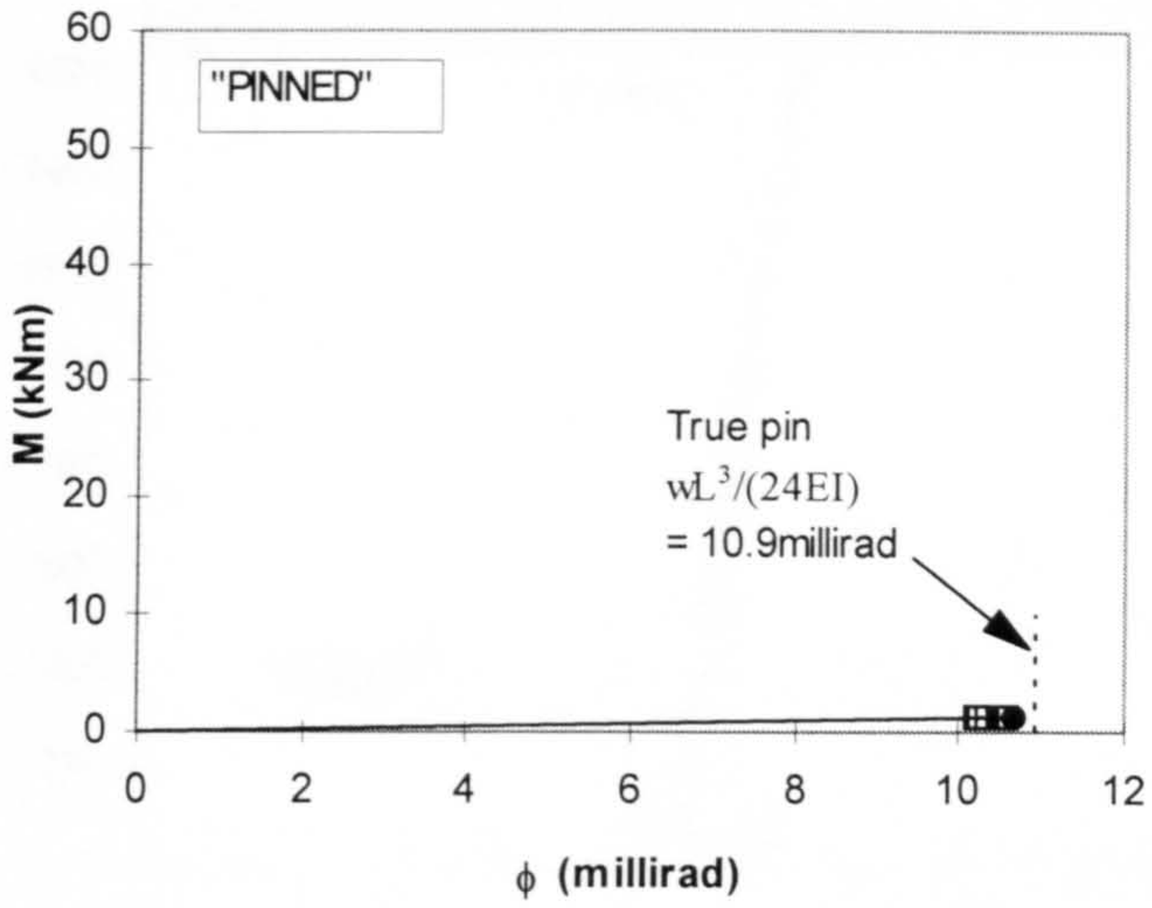

Figure 5.68 *M-ϕ* response at column top end with "PINNED" connections

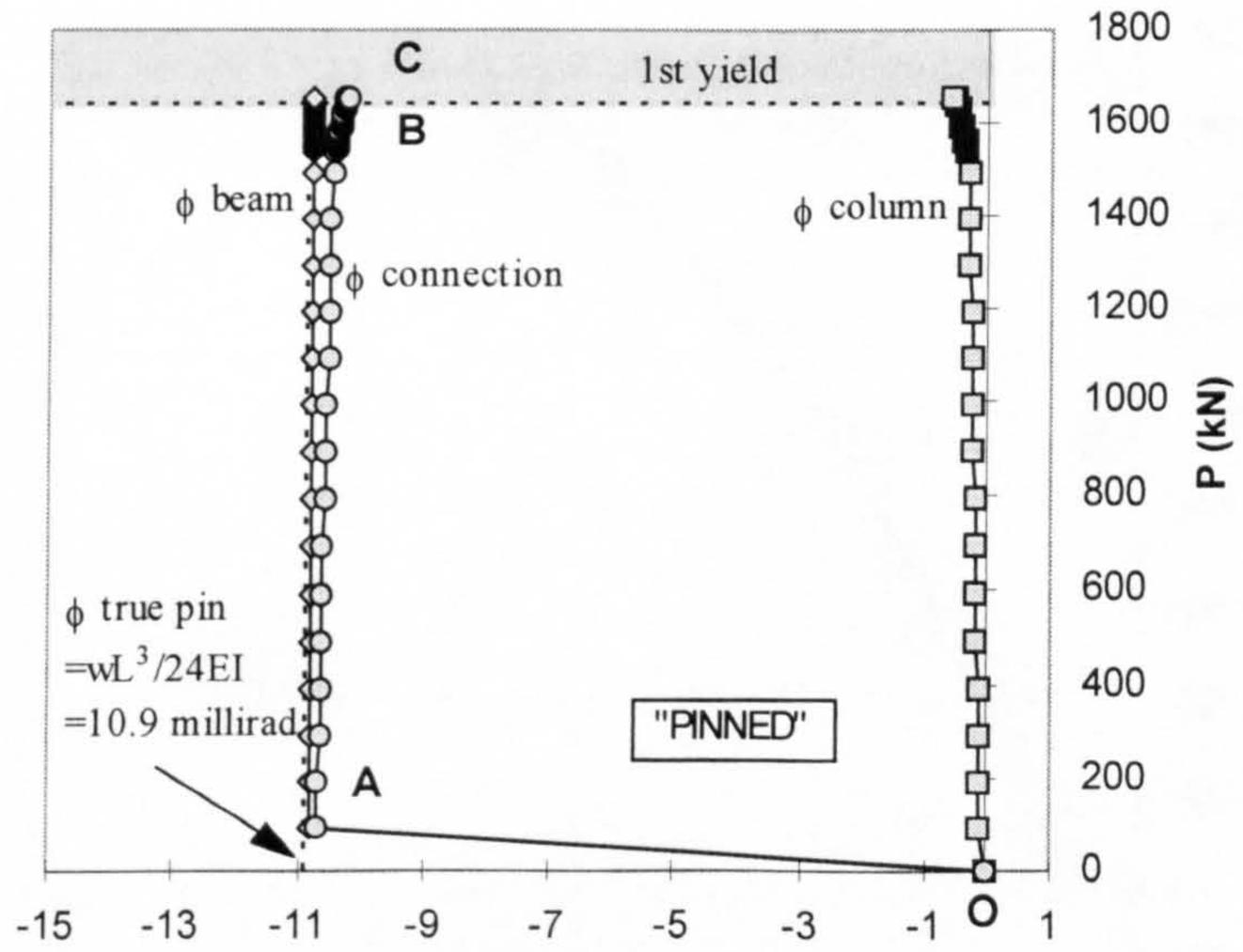

Figure 5.69 Development of beam, column and connection rotations with "PINNED" connections

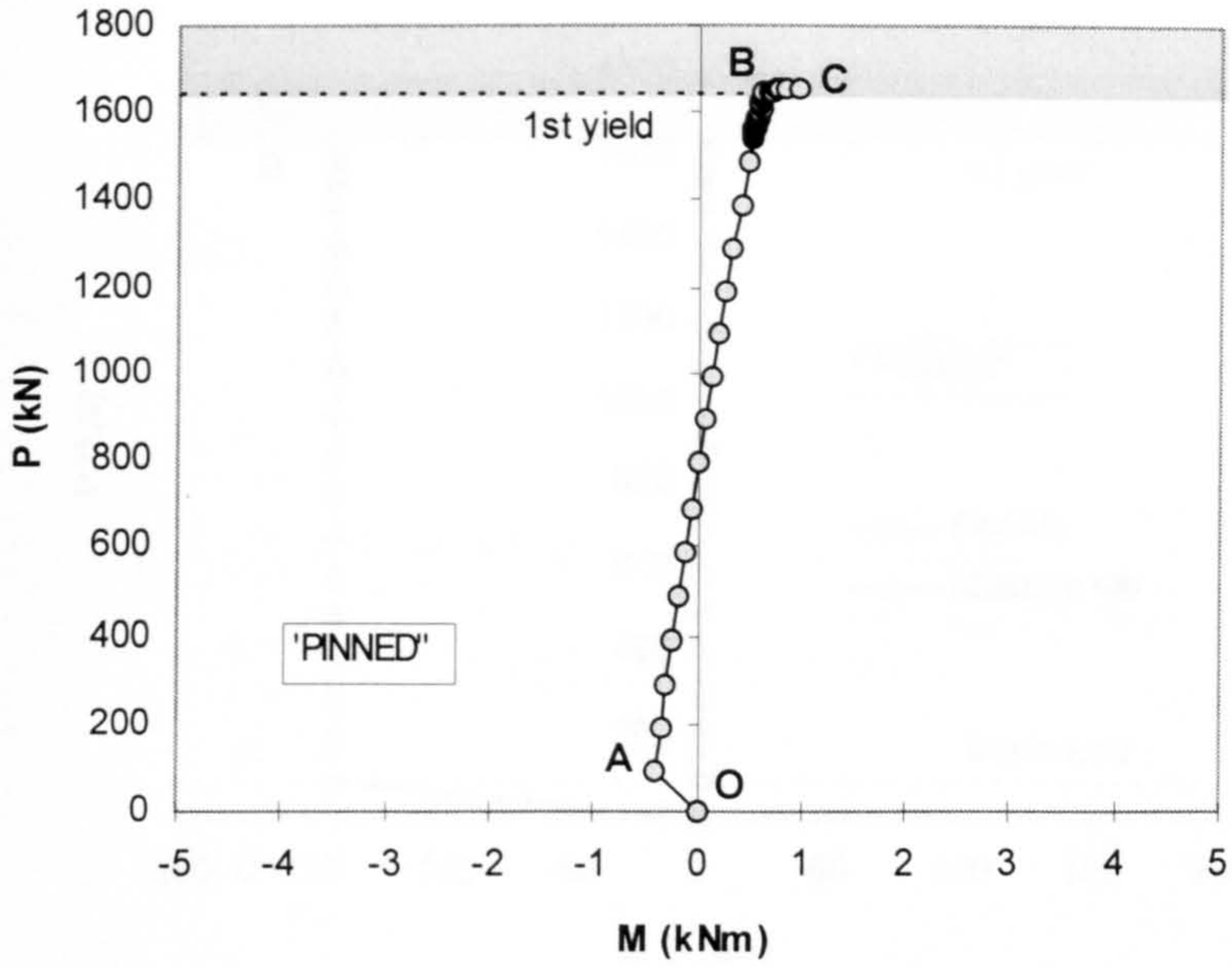

Figure 5.70 Response of moment shedding at column top end with "PINNED" connections

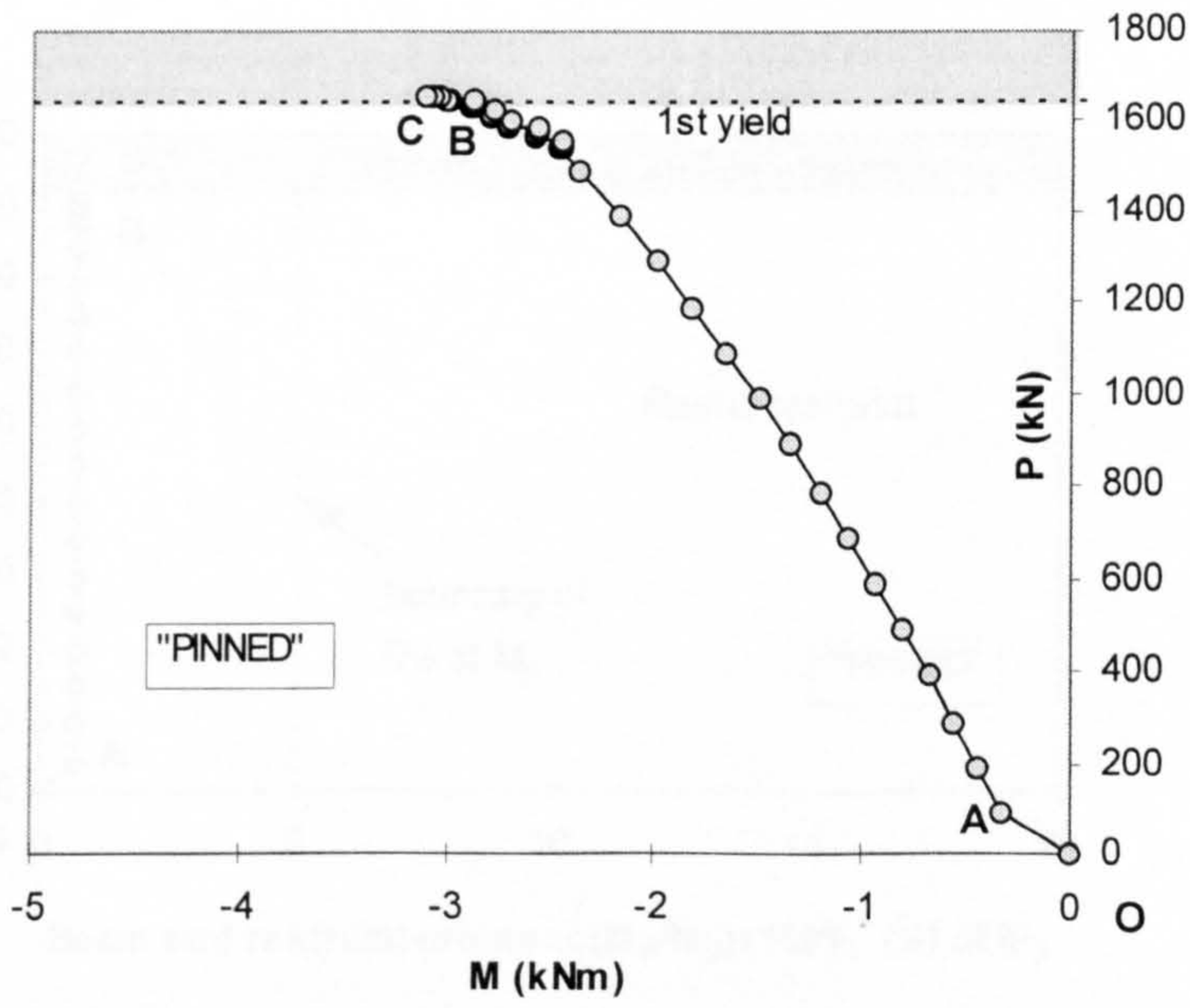

Figure 5.71 Response of moment at column mid-height with "PINNED" connections

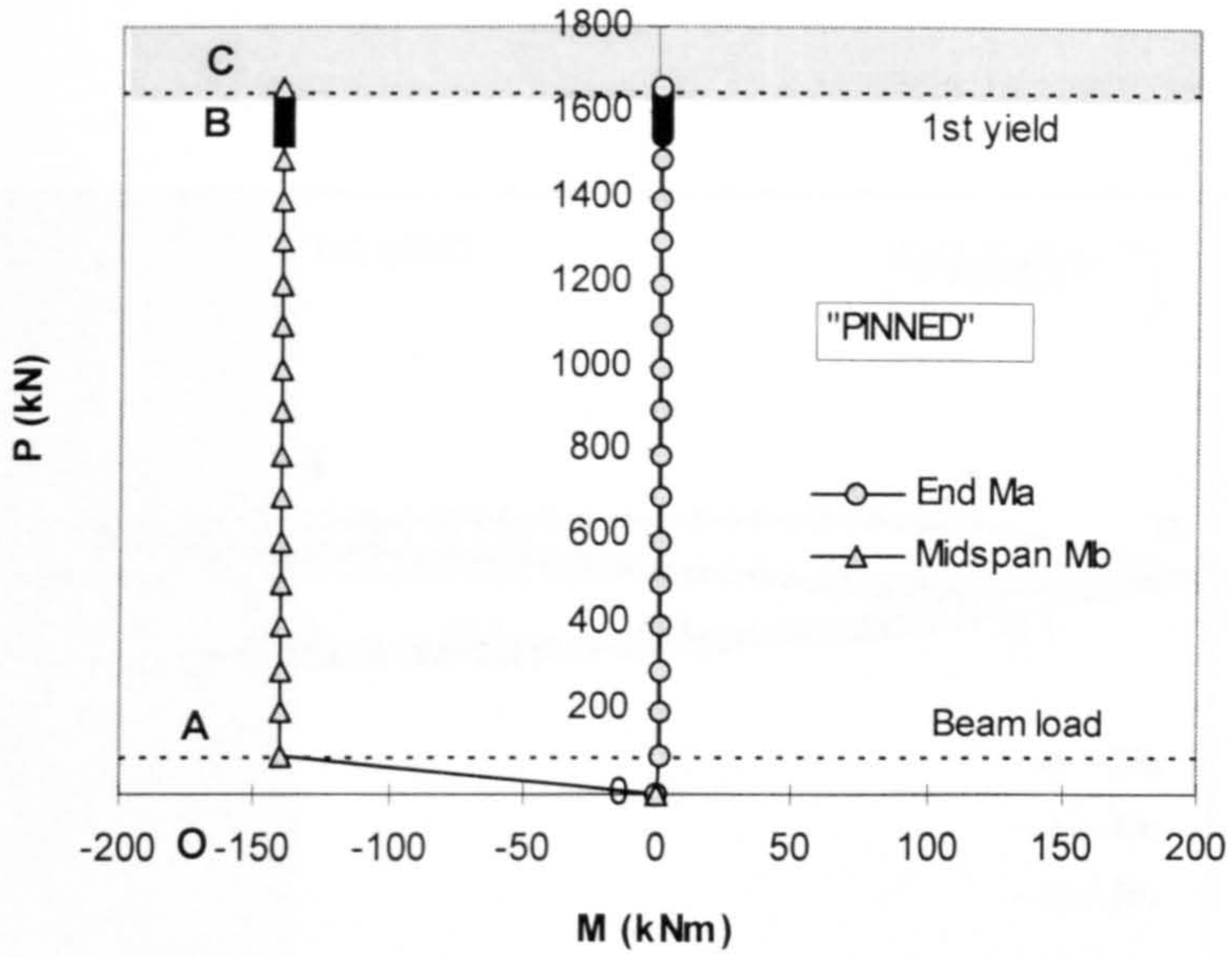

Figure 5.72 Response of moments at both beam end and beam midspan with "PINNED" connections

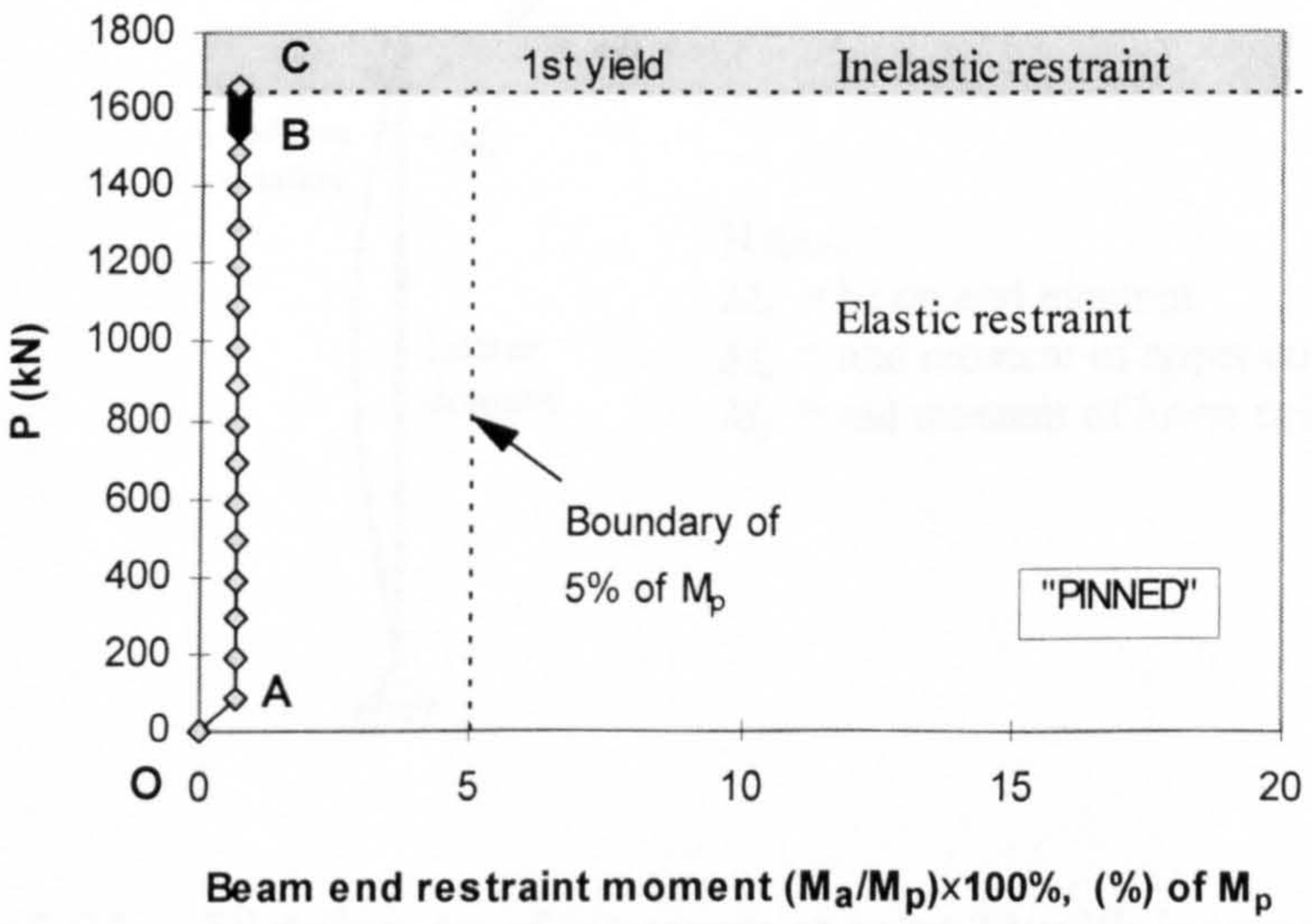

Figure 5.73 Development of beam end restraint moment with "PINNED" connections

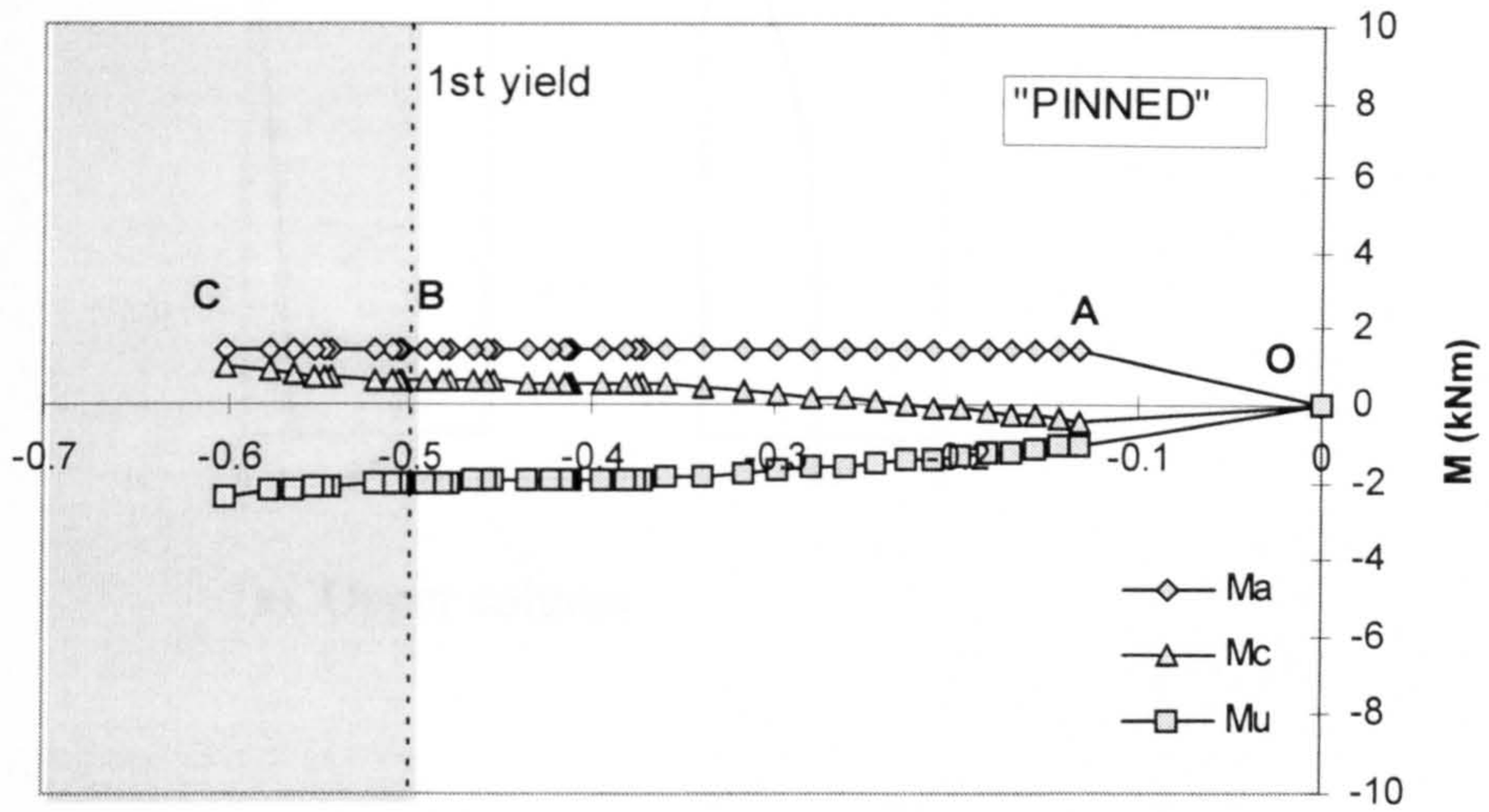

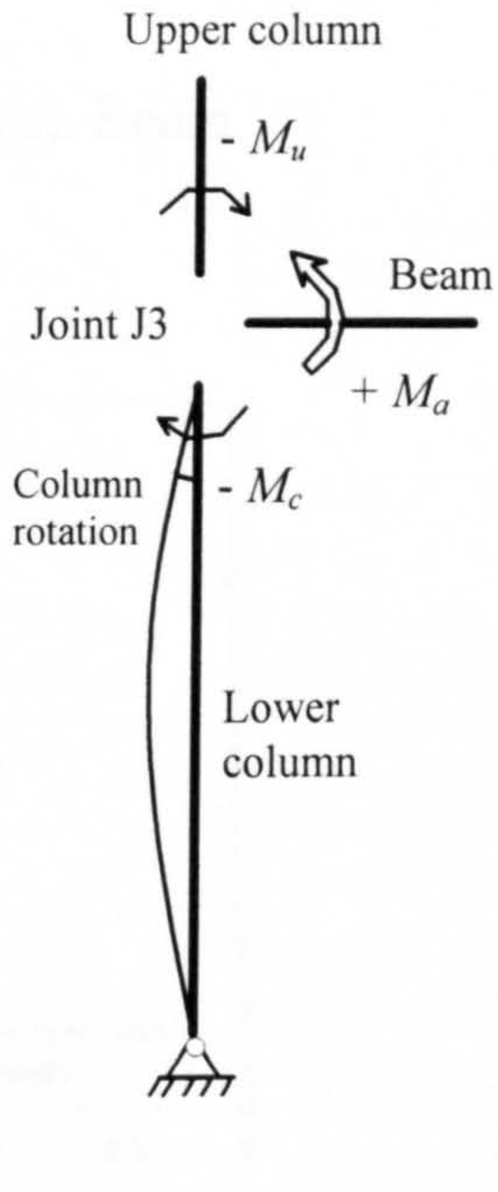

Notes:
M_a = beam end moment
M_u = end moment of upper column
M_c = end moment of lower column

Figure 5.74 Distribution of moments at joint J3 with increasing column end rotations using "PINNED" connections

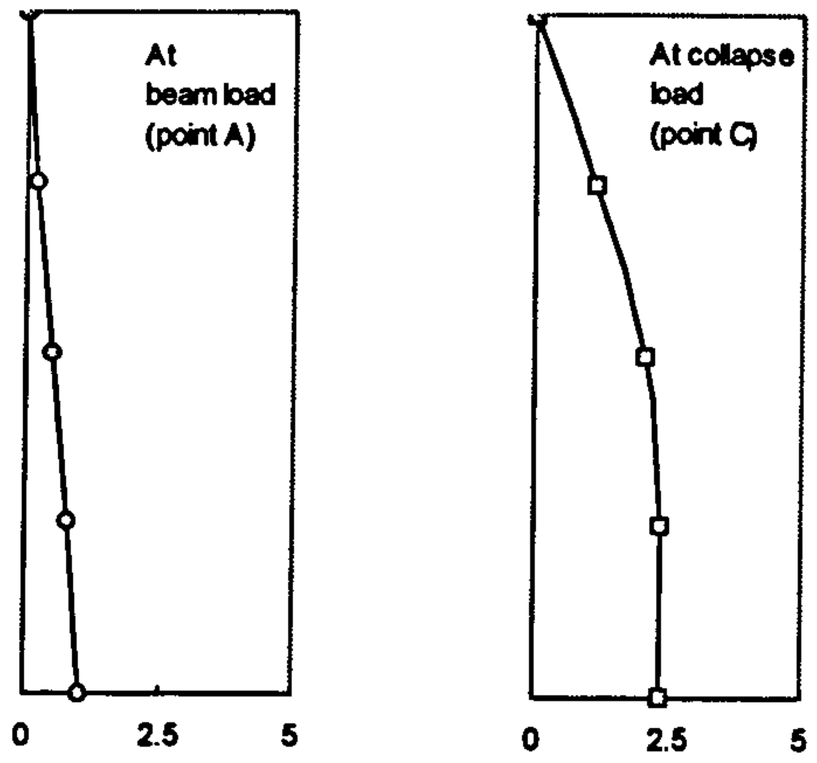

(a). Upper column

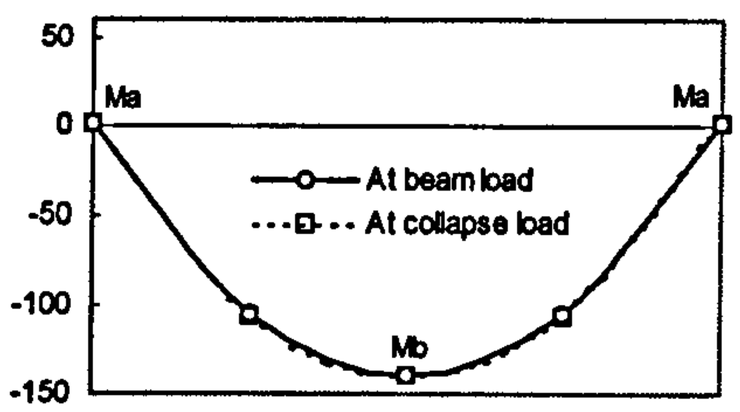

(b). Beam

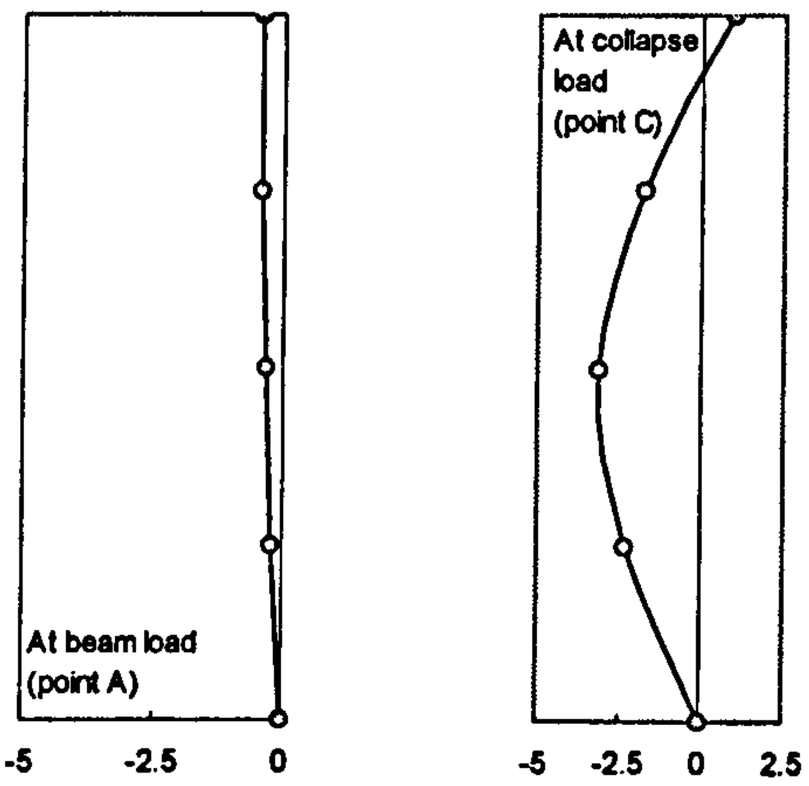

(c). Lower column

Figure 5.75 Smoothed bending moment diagrams at service loads and at collapse loads in kNm with "PINNED" connections

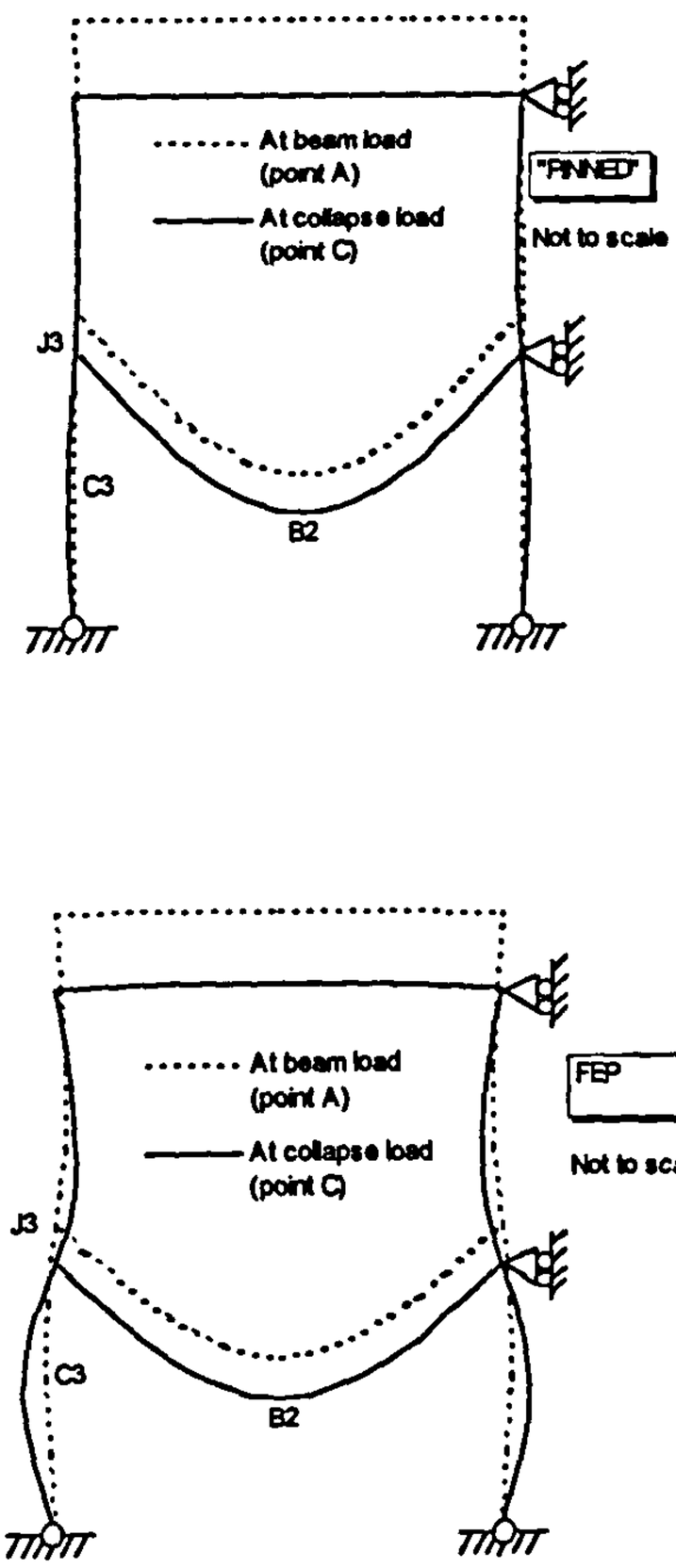

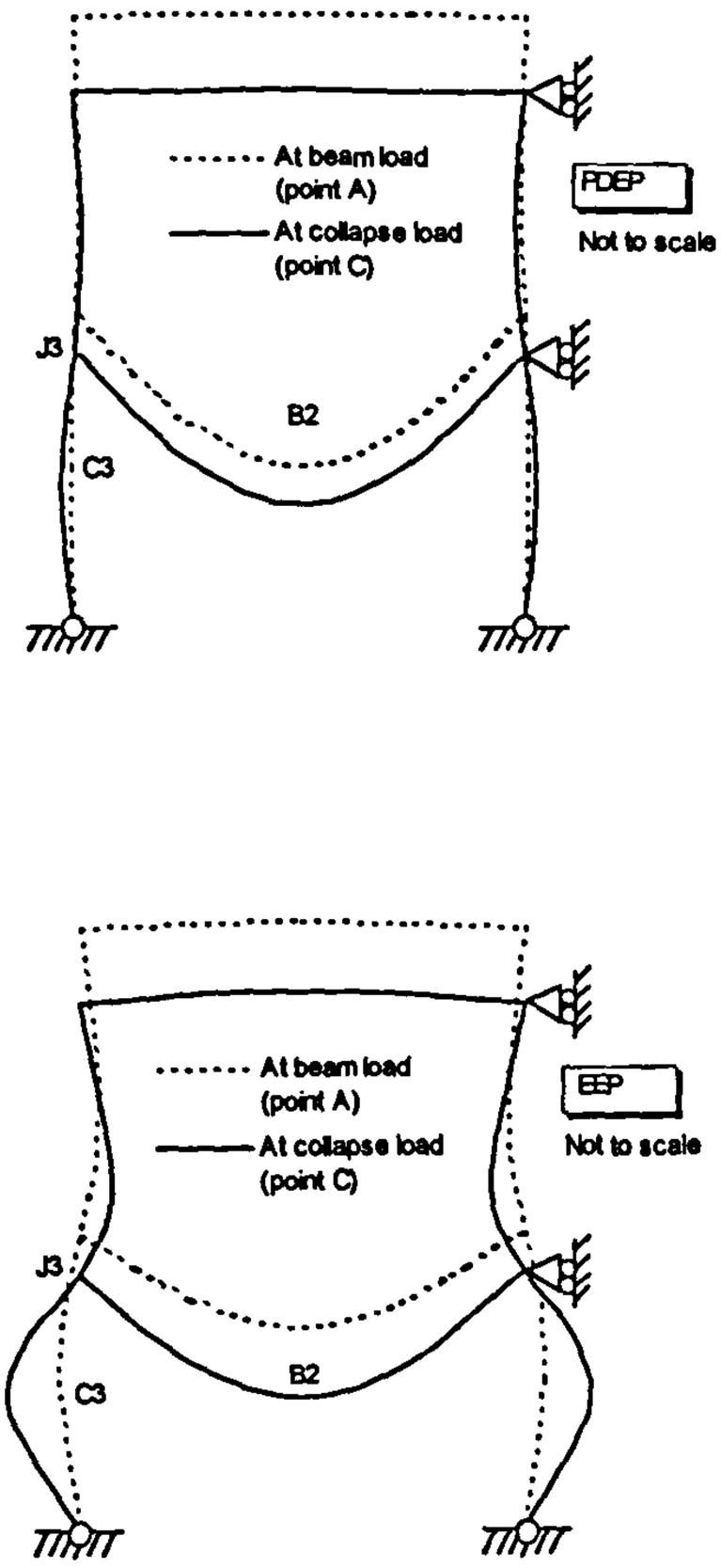

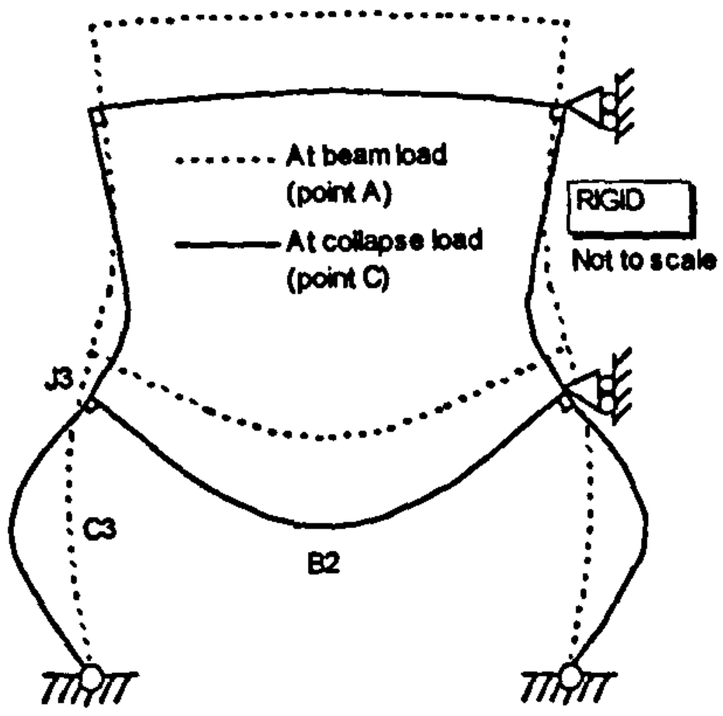

Figure 5.76 Exaggerated deformed shapes of frames with various types of connections

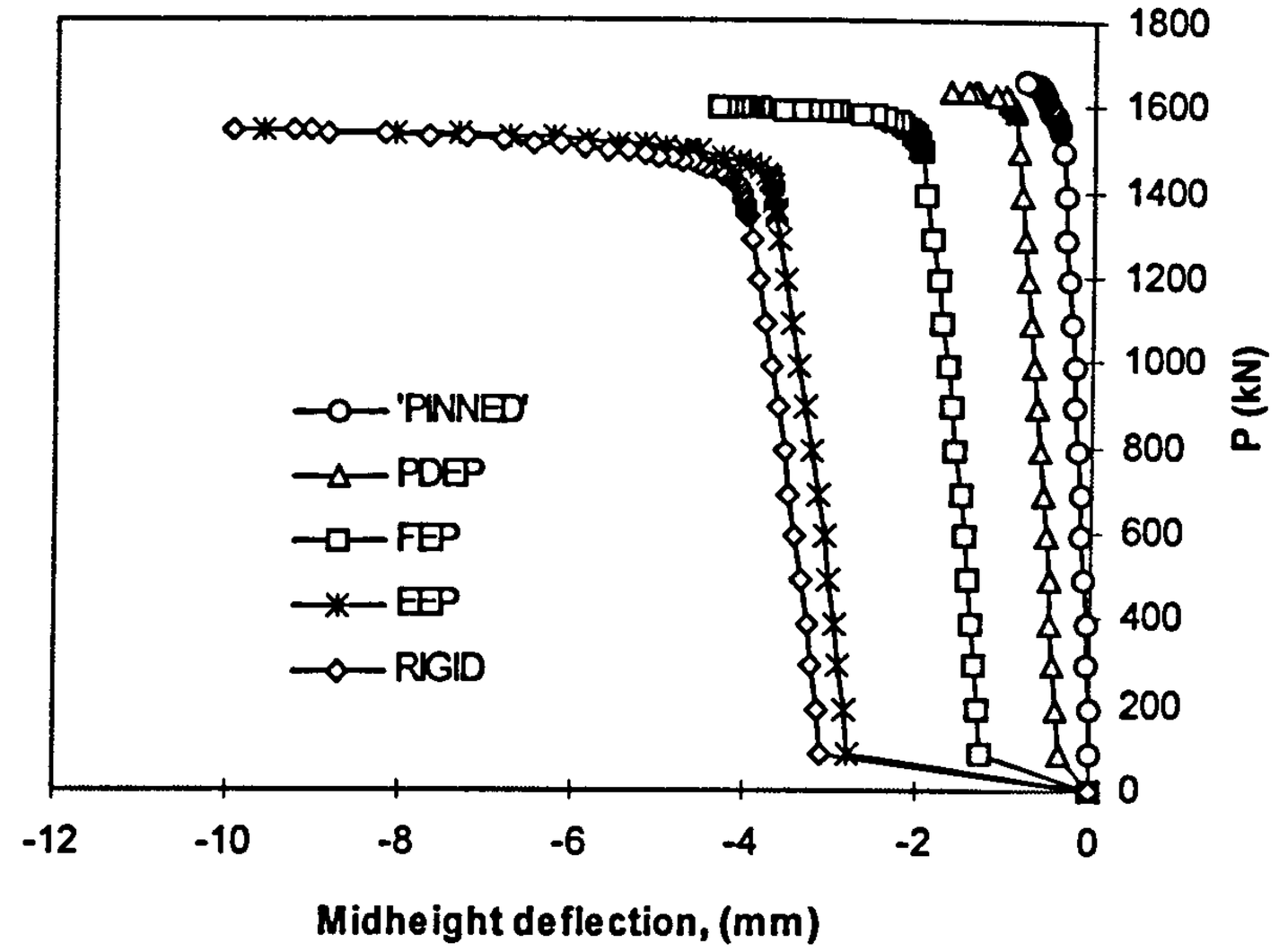

Figure 5.77 The effect of connection types on the load-deflection response at column mid height

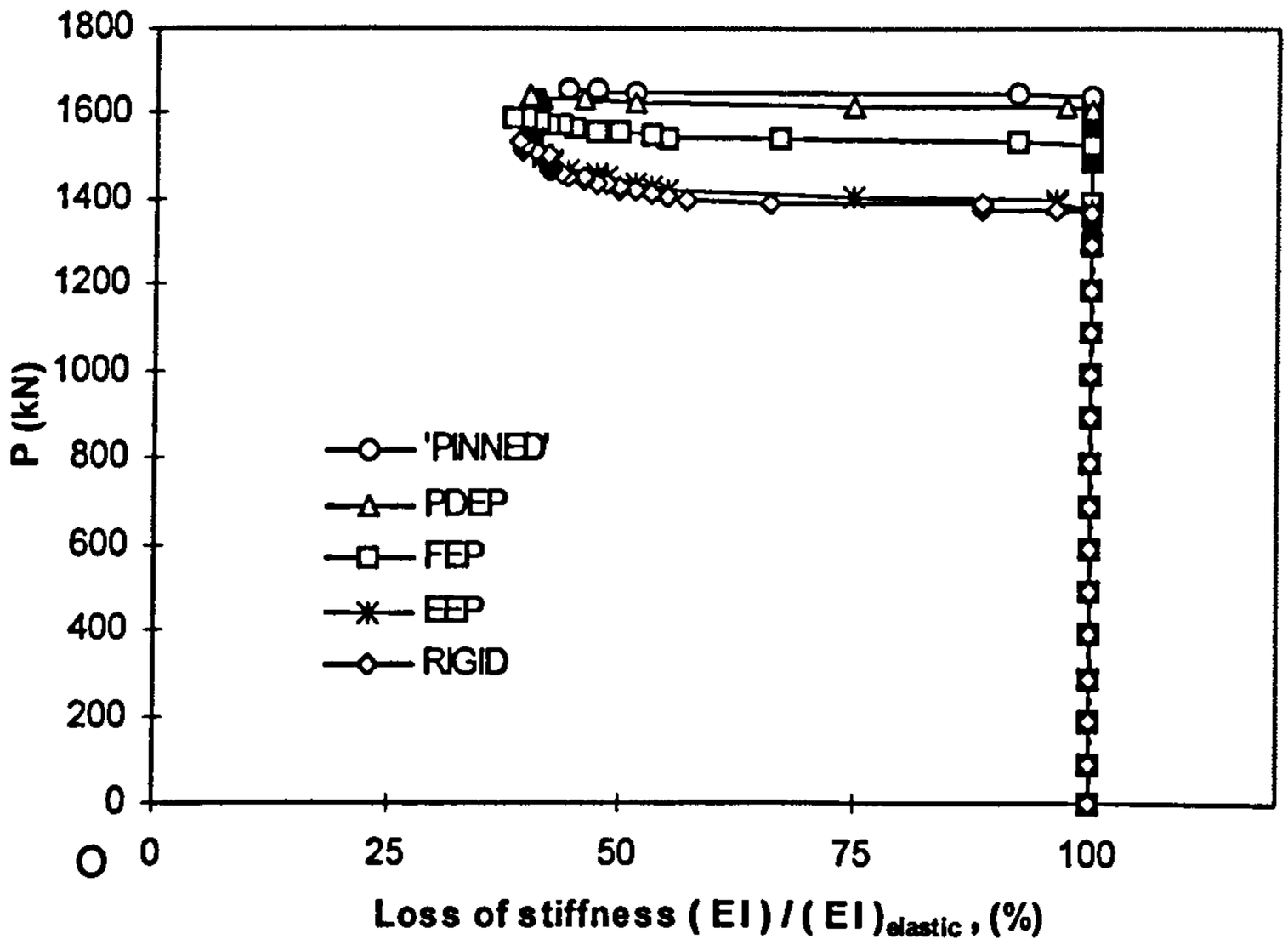

Figure 5.78 The effect of connection types on the loss of stiffness at column mid height

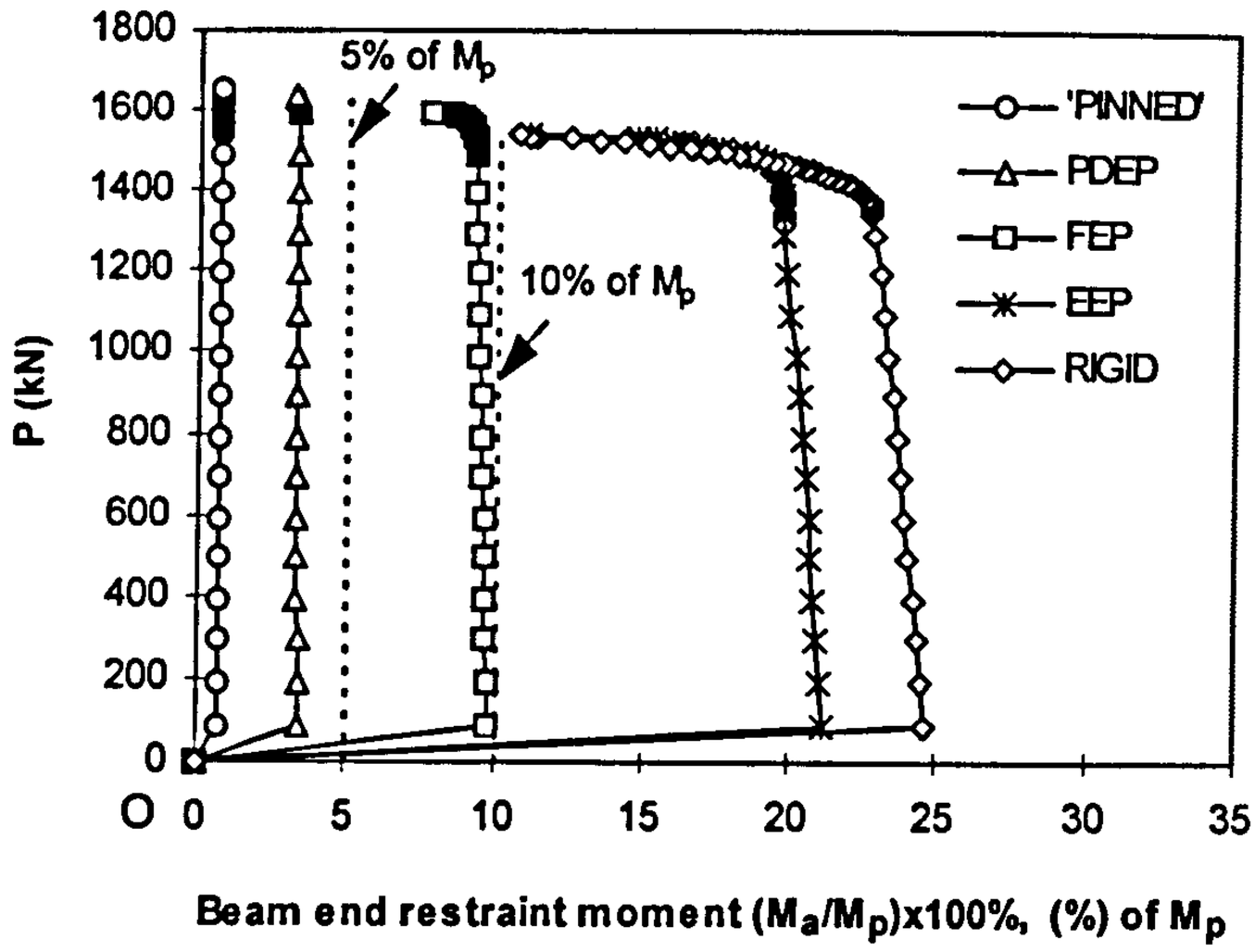

Figure 5.79 The effect of connection types on beam end restraints

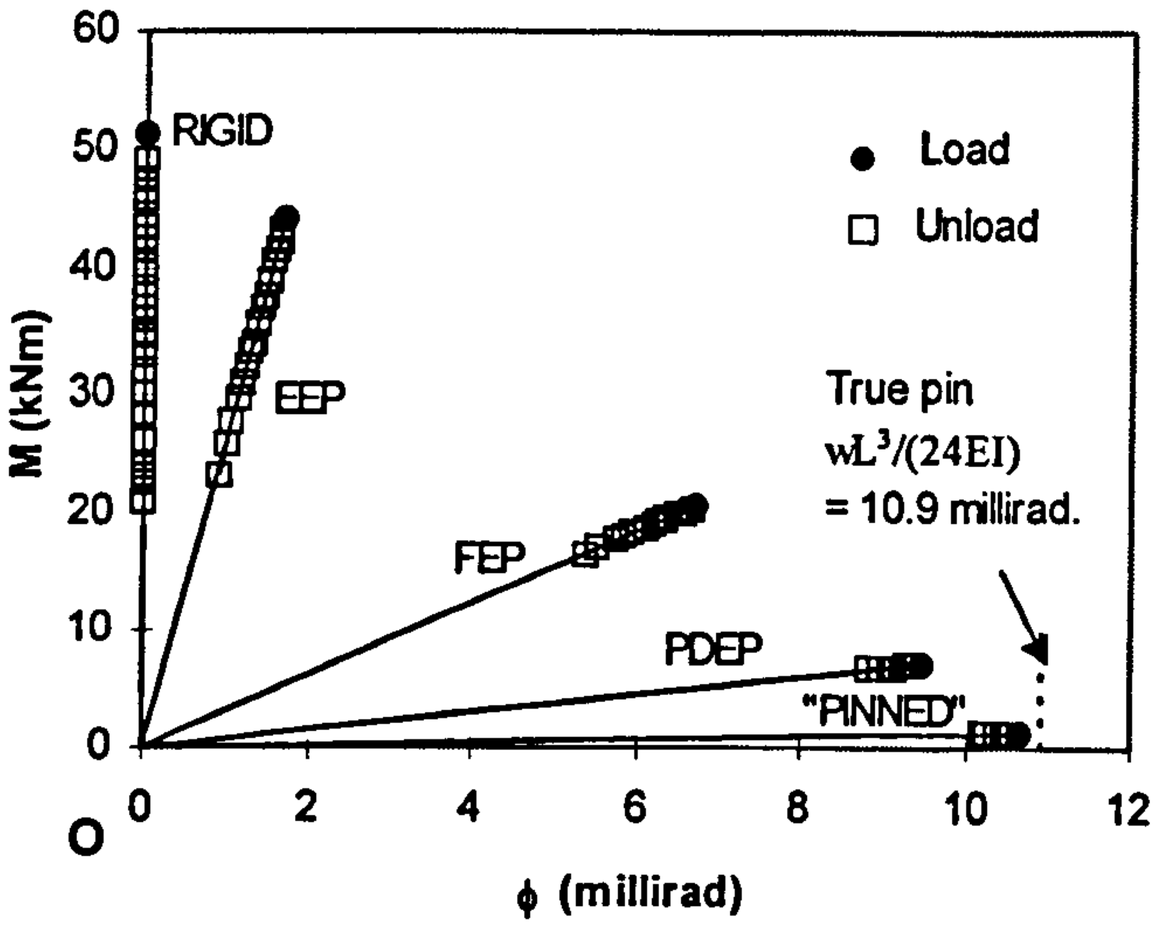

Figure 5.80 M-ϕ response with different types of connections

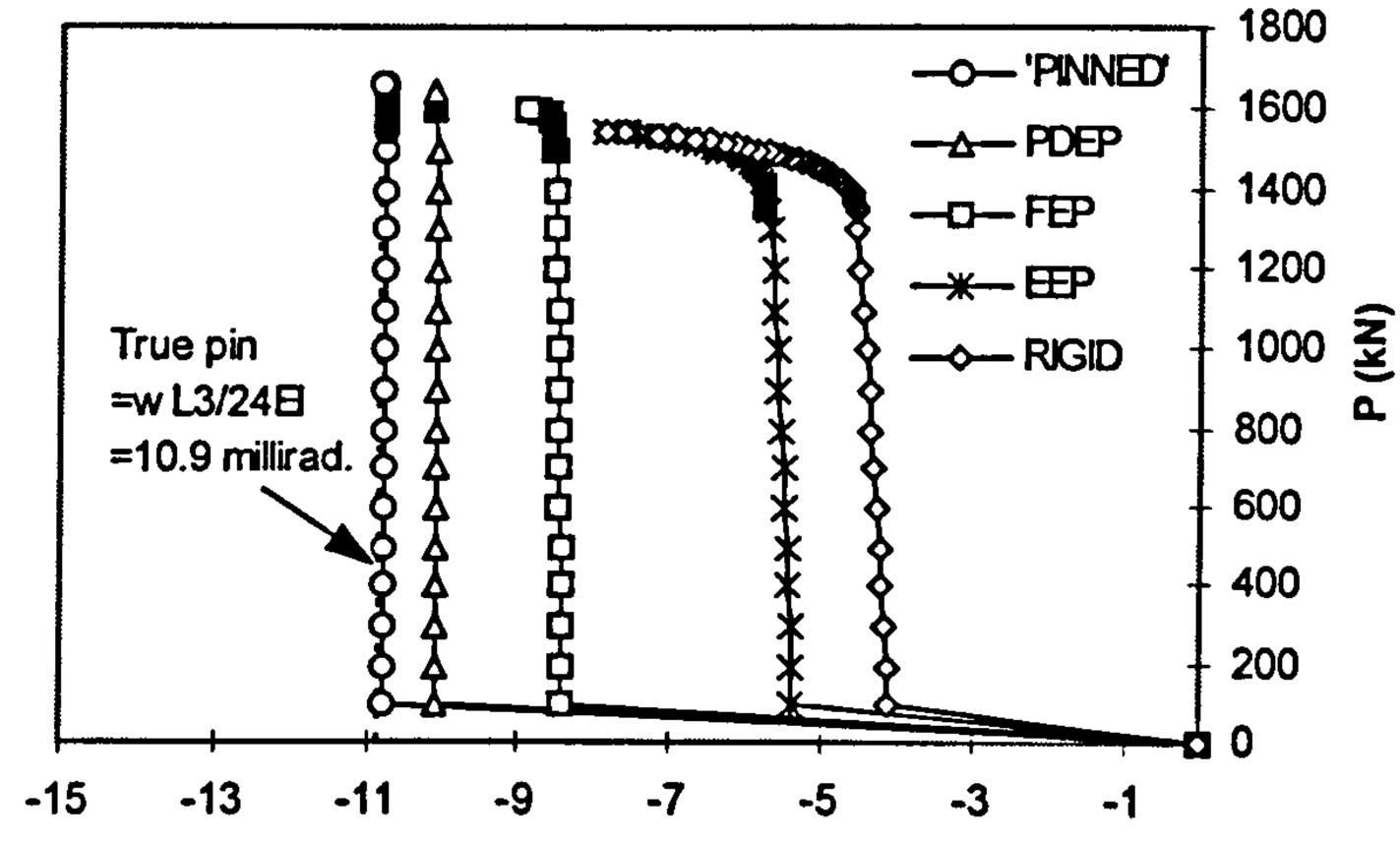

Figure 5.81
The effect of connection types on beam rotations

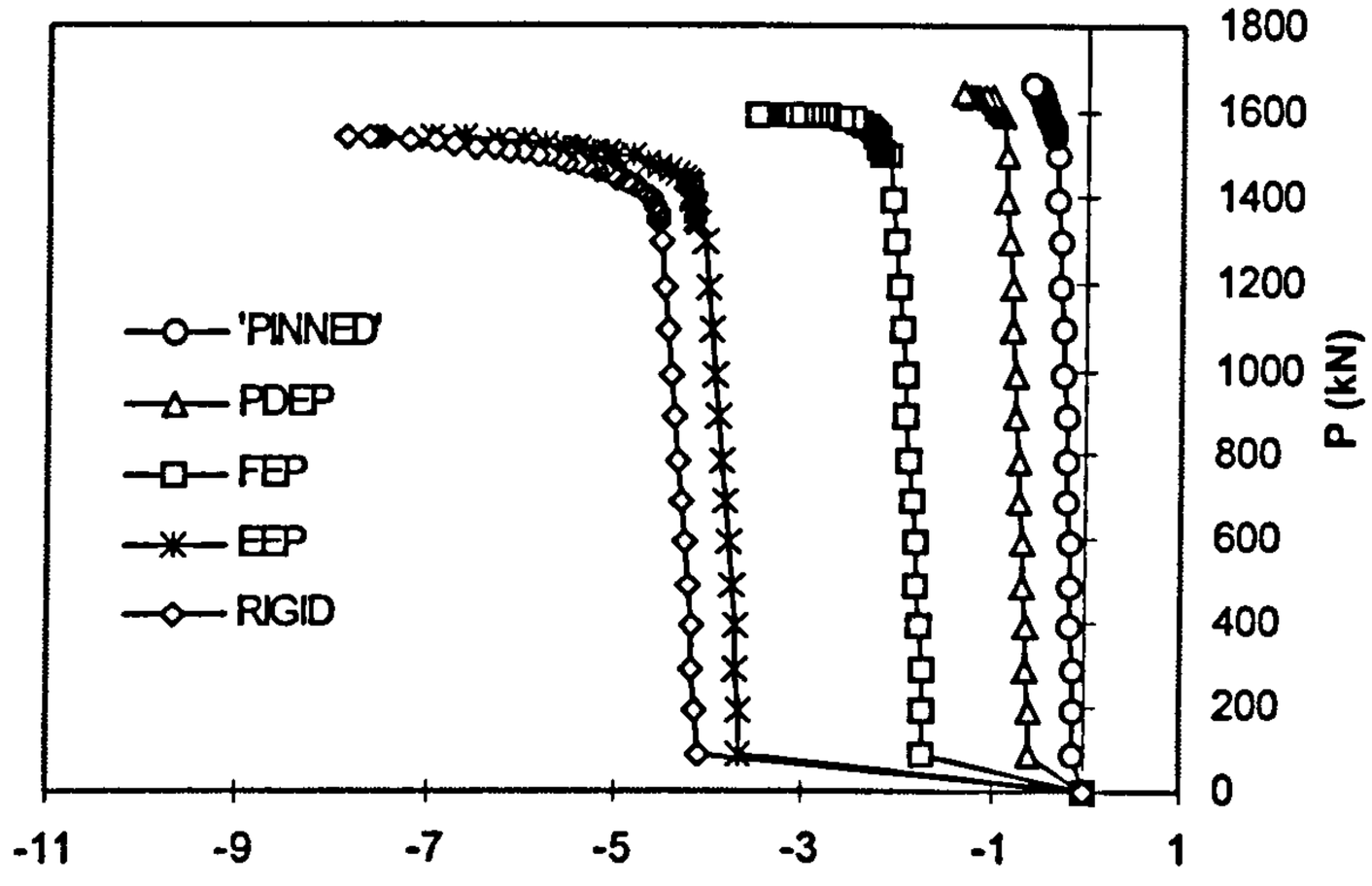

Figure 5.82
The effect of connection types on column rotations

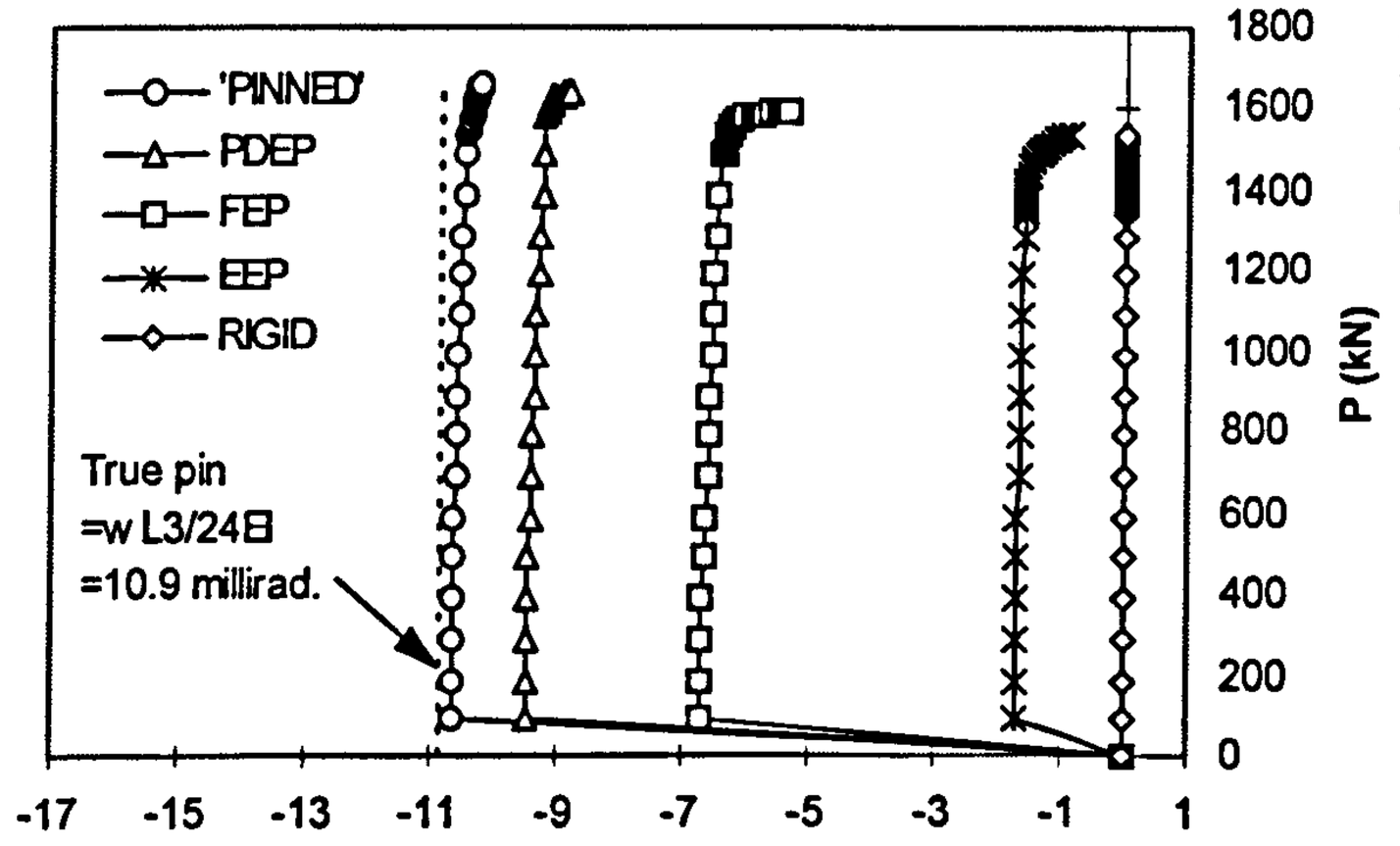

Figure 5.83
Response of different connection rotations

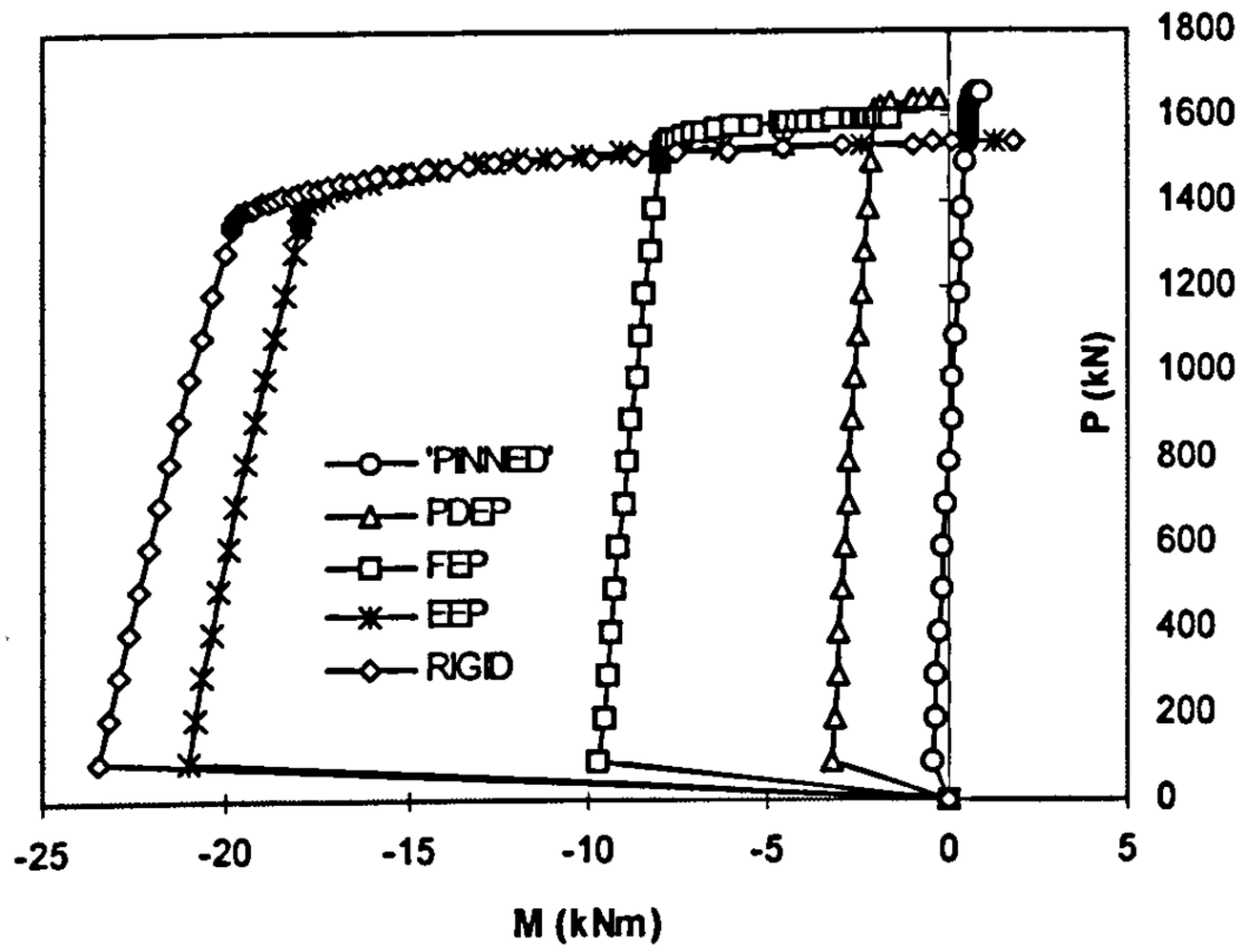

Figure 5.84 The effect of connection types on the response of moment shedding at column top end

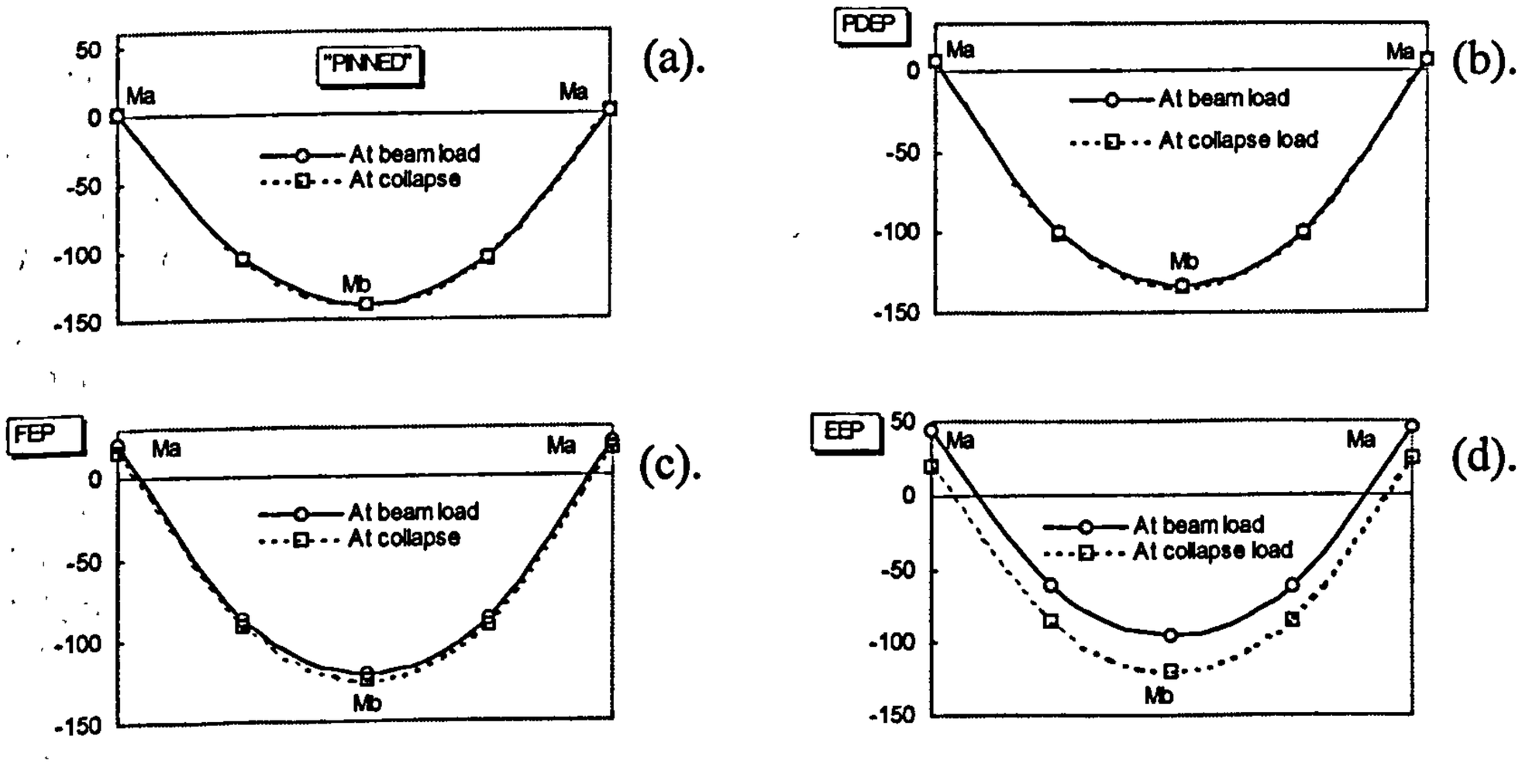

Figure 5.85 The effect of connection types on the redistribution of beam moments at collapse loads

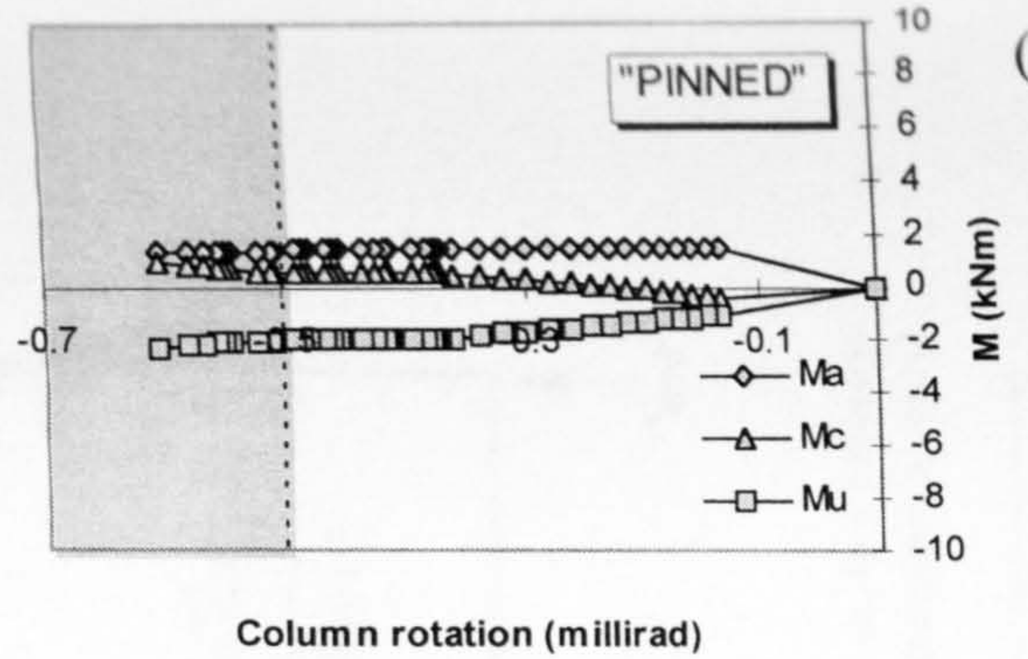

(a).

Figure 5.86
The effect of connection types on the redistribution of moments at joint J3

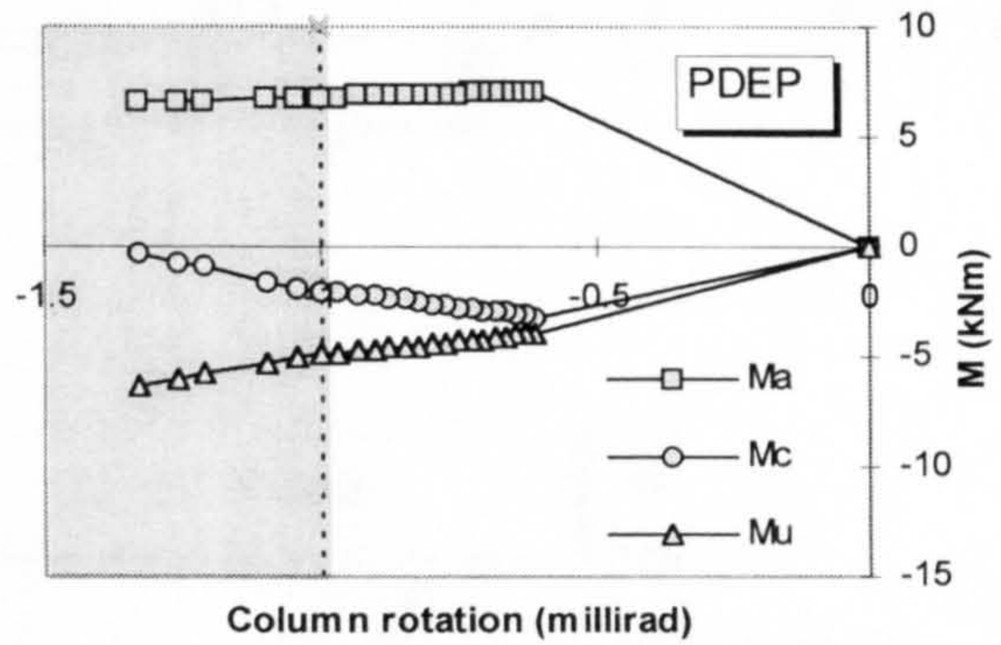

(b).

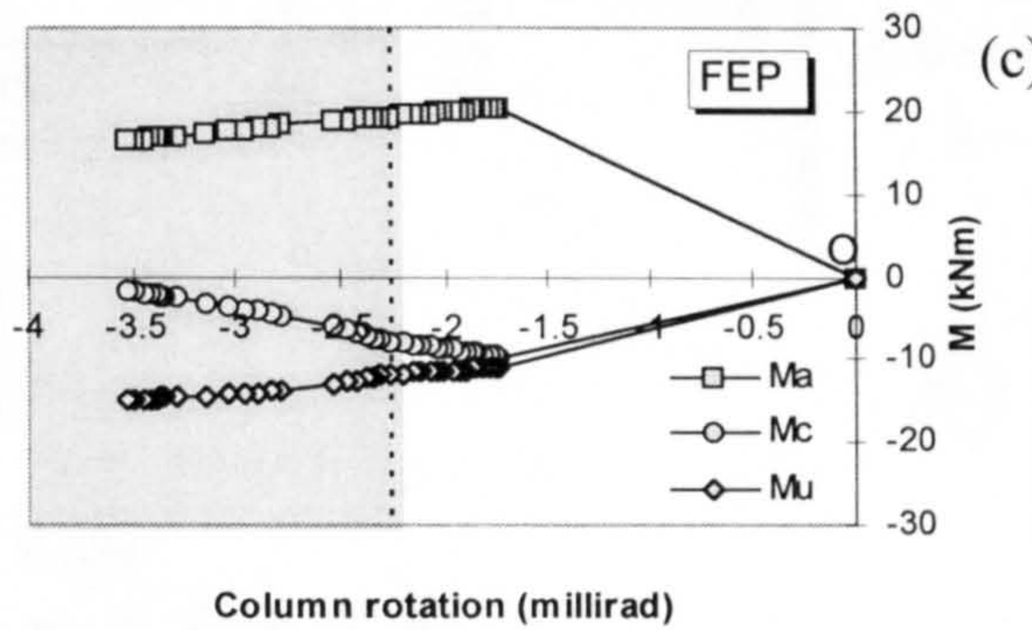

(c).

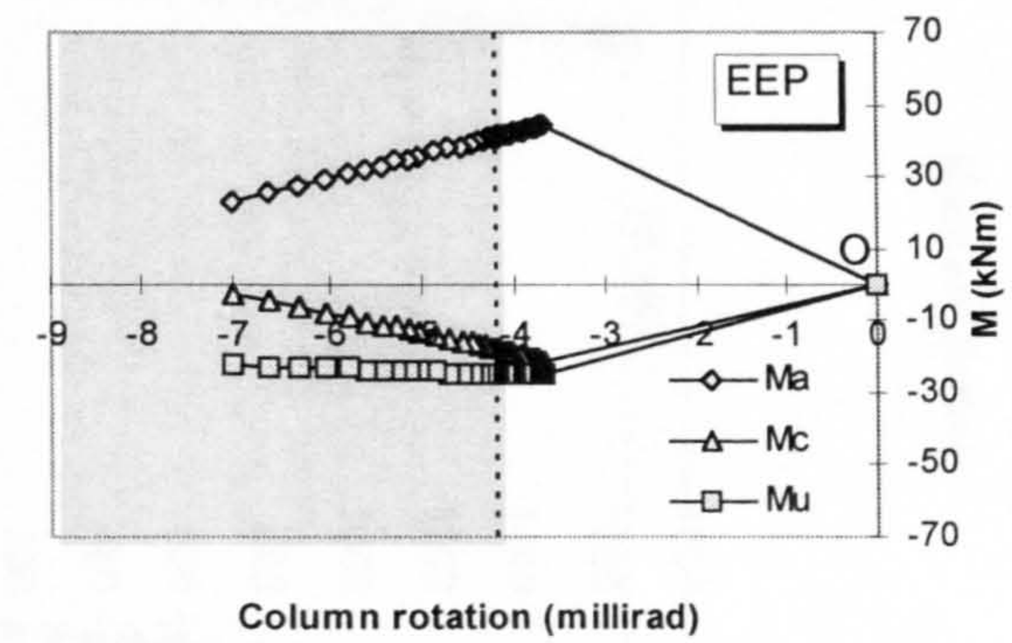

(d).

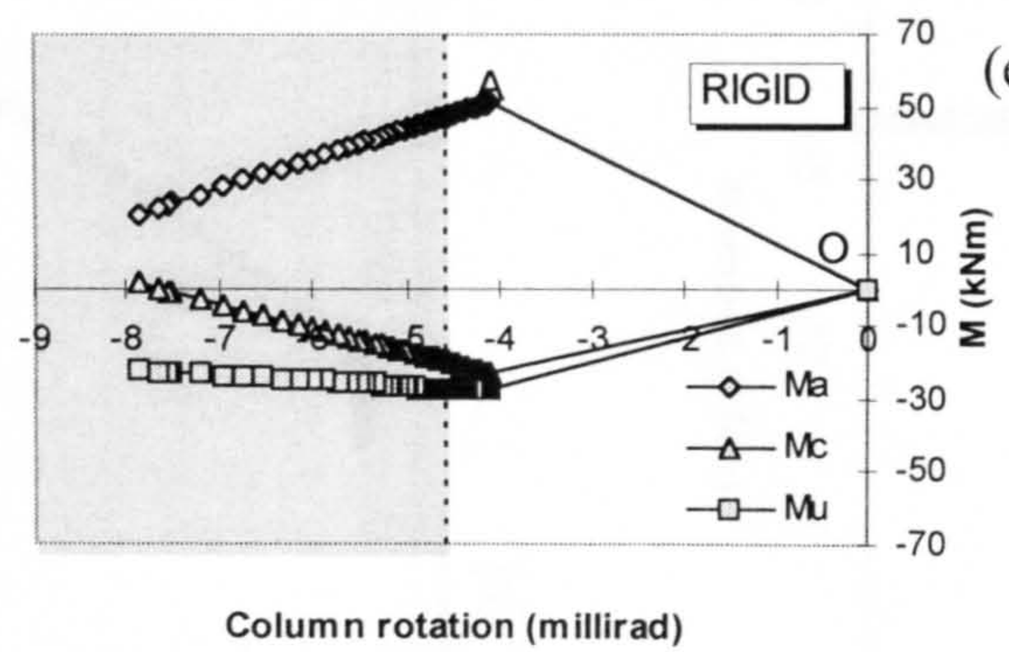

(e).

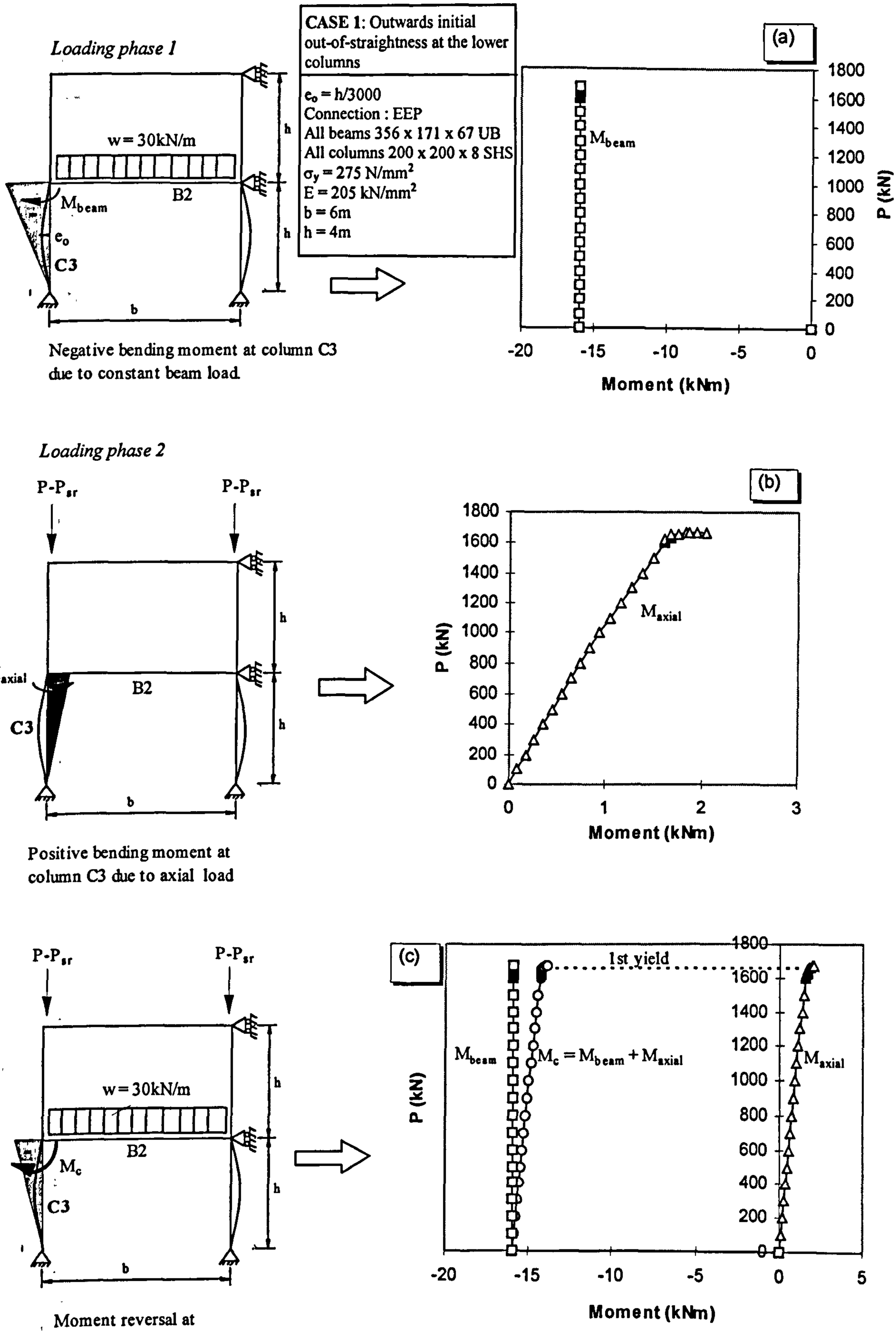

Figure 5.87 Response of end moment at top end of column C3-Case 1 due to :
(a). beam load only
(b). column axial load only
(c). superimpose of beam load and column axial load

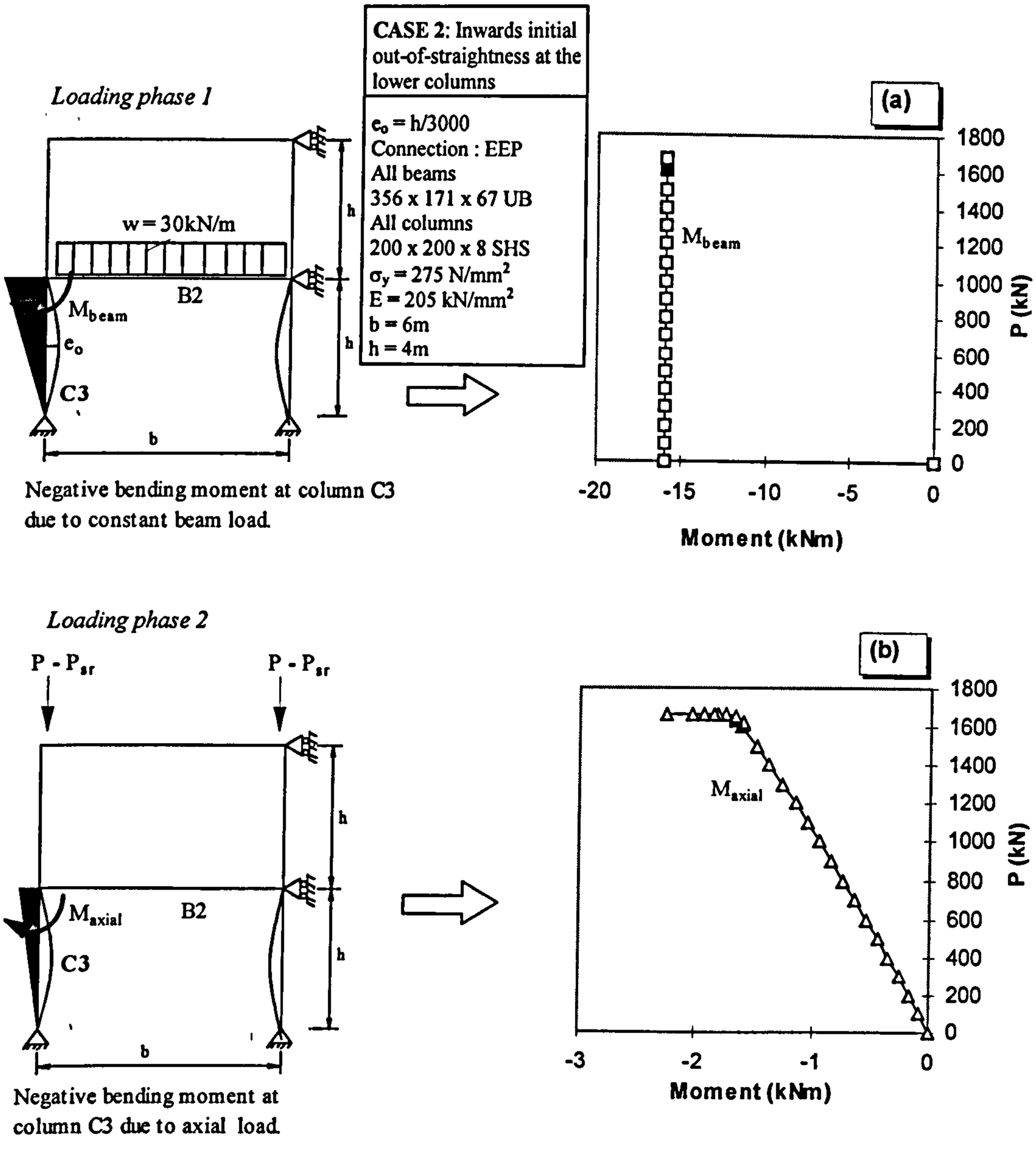

Negative bending moment at column C3 due to constant beam load.

Negative bending moment at column C3 due to axial load.

Bending moment at column C3 due to beam and axial loads

Figure 5.88 Response of end moment at top end of column C3-Case 2 due to :
(a). beam load only
(b). column axial load only
(c). superimpose of beam load and column axial load

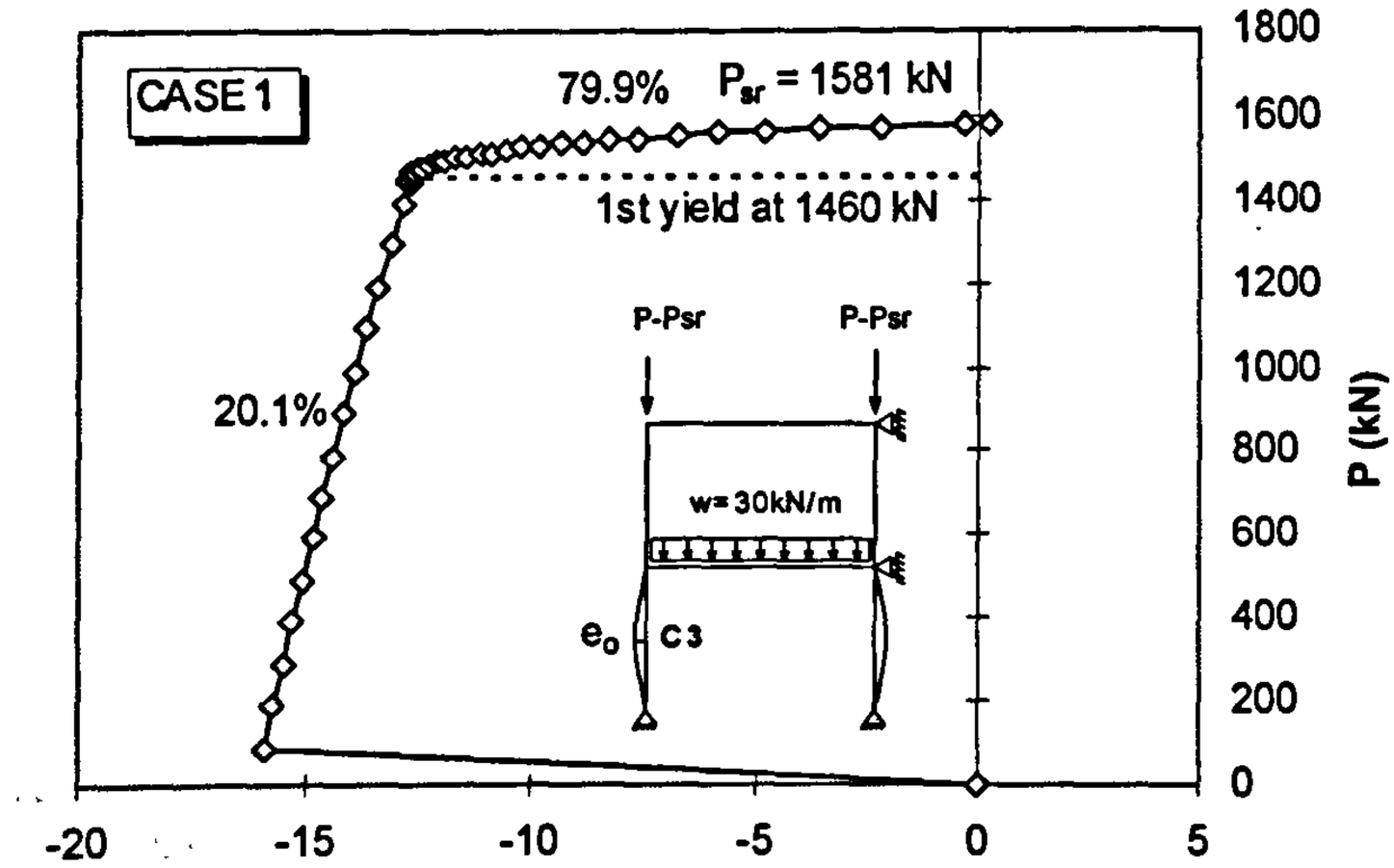

Figure 5.89
Actual response of moment shedding at top end of column C3-case 1 in both elastic and inelastic ranges

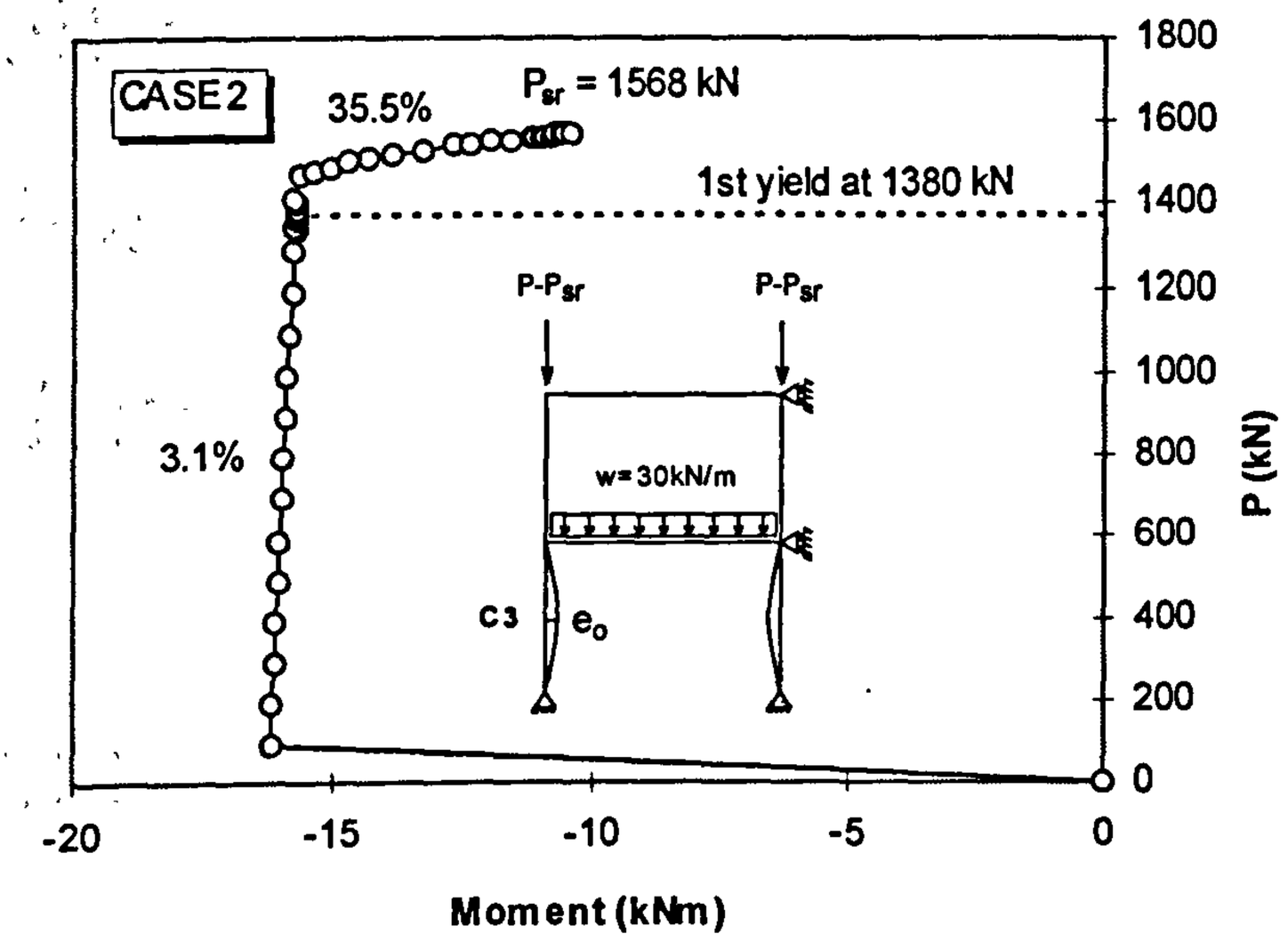

Figure 5.90
Actual response of moment shedding at top end of column C3-case 2 in both elastic and inelastic ranges

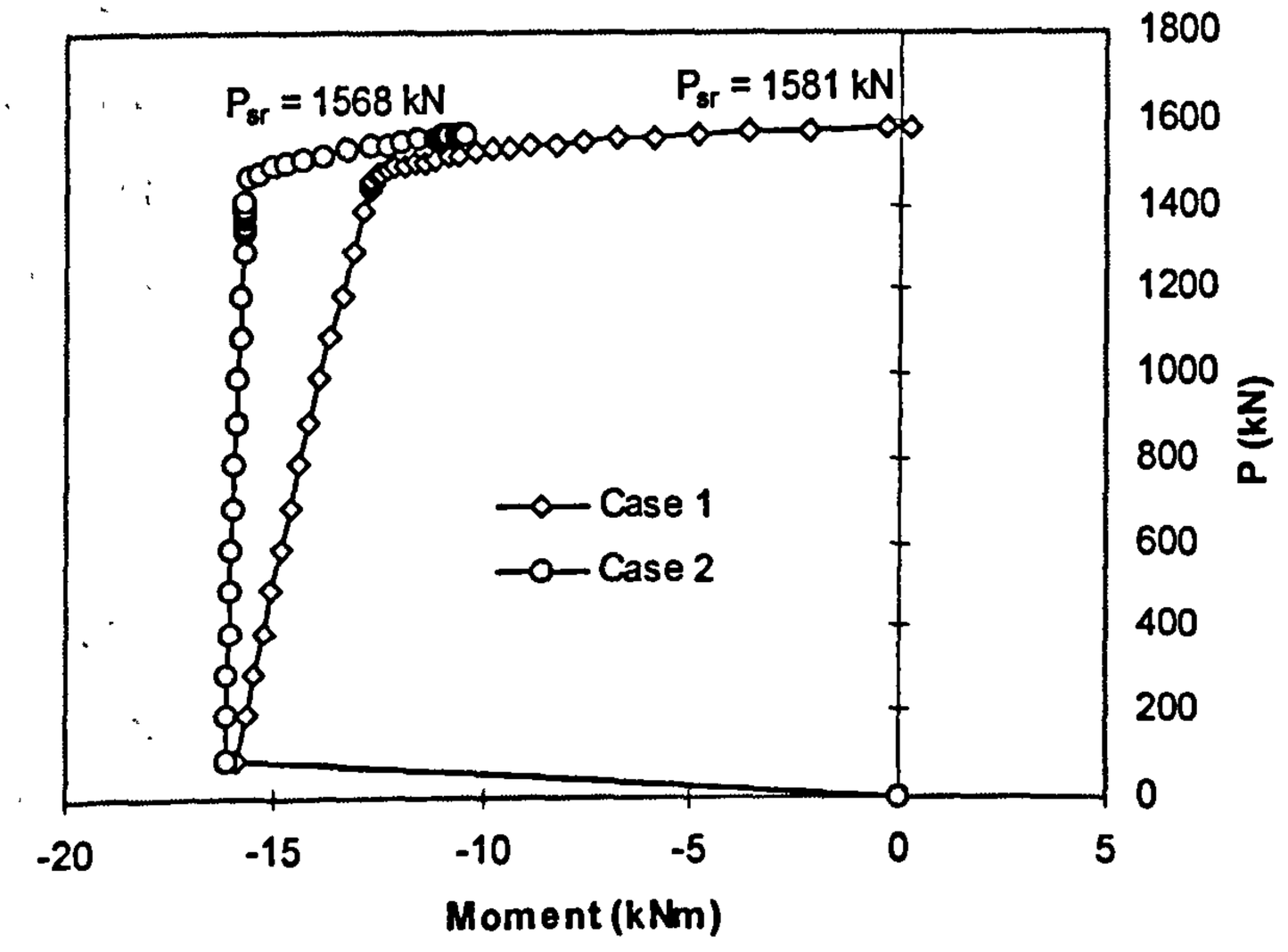

Figure 5.91
Comparison of moment shedding between case 1 and case 2

Chapter 6

Ultimate Strength of SHS Beam-columns with Semi-rigid Connections in Non-sway Frames

6.1 Introduction

The significant behaviour observed in the study conducted in Chapter 5 was the development of moment shedding at the column top end as the collapse load is approached. Related issues concerning the behaviour at ultimate load levels such as the loss of stiffness and moment redistribution were discussed. These responses eventually lead to a simple configuration of bending moment in the beams and columns. As a consequence, the column can be treated as an axially loaded compression member and the beam as a simply supported member with a certain value of end restraint moment.

The analysis of the beam-column behaviour described in Chapter 5 focused on the problems of external columns with pinned bases and various types of restraint at the top end only. In view of this matter and to extend the investigation further, this

chapter studies the other beam-column cases, i.e. the upper edge, the upper intermediate and the internal columns.

The studies are conducted to:

- investigate the behaviour of internal columns
- investigate the redistribution of moment at ultimate load levels
- investigate the values of end restraint moment to be used for designing beams with semi-rigid connections
- investigate the applicability of the upper external, the upper intermediate and the internal beam-columns to be designed as axially loaded compression members
- investigate the ultimate axial load strength of beam-columns with semi-rigid connections
- study the factors that influence the ultimate strength of beam-columns
- investigate the relation between the behaviour at the ultimate load levels and the proposed simplified design method.

The parametric study was limited to a series of low rise two and three storey frames with SHS columns. The analyses were carried out without the incorporation of residual stress as this effect is considered negligible in tubular columns [6-1].

Finally, before commencing to the main parametric study, it is also of interest to understand the basic behaviour of columns with pinned connections. This is due to the fact that the behaviour of pin ended column is normally employed as a basis for understanding the behaviour of semi-rigidly restrained columns.

6.2 Behaviour and Strength of Axially Loaded Columns with Pinned End Connections

The behaviour of a pin ended column is well understood so that it has become the reference of strength for other column types. Thus, pin ended columns are normally taken as the anchor point for determining the strength of columns with semi-rigid connections.

In order to demonstrate the behaviour of a pin ended column, a simple parametric study using the SERIFA program was conducted on the portal frame shown in Figure 6.1. The connections used were perfectly pinned. The column heights were varied from 1m up to 10m with the initial geometric imperfection of L/800. Incremental axial loads were applied at the column heads up to failure.

The plots of the ultimate strength curves of pin ended columns are shown in Figure 6.2. The upper bound to buckling load consists of the plastic squash load **AB** and the theoretical Euler elastic buckling load curve **BC**. The slenderness λ_t is the transition slenderness from curve **AB** to curve **BC**. In the case of perfect pin ended columns, when λ is less than λ_t, the ultimate strength of the column is denoted by the squash load curve **AB**. Whereas, in the case of perfect pin ended columns with $\lambda > \lambda_t$ the ultimate strength is denoted by the elastic Euler buckling curve **BC**. However in reality, the columns are not really perfect, the presence of initial imperfections such as initial-out-of straightness and residual stresses reduces the column ultimate strength. Examples of pin ended column strength curves with the inclusion of imperfections are the BS 5950 [6-2] and the SERIFA curves as shown in the figure. The SERIFA strength curve which demonstrates the good agreement with the BS 5950 curve is obtained by using an initial geometrical imperfection of L/800. Referring to the SERIFA curve, the columns are then classified into three different categories namely "short", "intermediate" and "slender" columns. As can be seen from the figure, the difference between the upper bound buckling load and the SERIFA buckling load is more obvious in the intermediate range of the column slenderness. This is due to the fact that in this range, both material and geometrical imperfections are present both of which reduce the column ultimate strength significantly.

Figure 6.3(a) shows the load-deflection response which explains the three types of failure modes for columns in each of the three categories. In the first failure mode, it can be observed that the "short" column fails by squashing. In this case, the stiffness loss in the column is attributed to the yielding of the material only. As can be seen from Figure 6.3(b) the actual deflection is significantly small which suggests that the effect of geometrical deformation does not influence the column stiffness. In the second failure mode, an "intermediate" column fails by elastic-plastic buckling. The

failure is influenced by the stiffness loss due to both geometrical deformation and material degradation (yielding). Finally in the third failure mode, a "slender" column fails due to excessive deflections and shows the response of pure elastic buckling without any form of yielding throughout the section. This implies that the loss of stiffness in "slender" columns is mainly attributed from the effect of geometrical deformation. The associated diagrammatic failure modes of the three column categories are shown in Figure 6.4. Most practical columns in multi-storey buildings fall in the category of the "intermediate" columns and hence show the elastic-plastic behaviour.

Knowing the behaviour of pin ended columns, the study is extended to the behaviour and strength of semi-rigidly restrained columns as described in the following sections.

6.3 Parametric Study on Beam-columns with Semi-rigid Connections

6.3.1 Description of the Frames

In order to investigate the behaviour and ultimate strength of external and internal columns at collapse load level, the following types of frames were examined (see Figure 6.5) :

(i). Frame 1, a two-storey one-bay frame.
(ii). Frame 2, a two-storey two-bay frame.
(iii). Frame 3, a three-storey two-bay frame.

Frames 1, 2 and 3, respectively, were employed to investigate the strength of the upper edge column C1, the upper intermediate column C2 and the internal column C5. These columns were then referred as the studied columns. The storey height h was taken as 2m, 3m, 4m, 5m, 6m and 7m. This in turn gives a practical column slenderness ratio ranging from 25 to 90. In practice, typical columns normally will have slenderness ratios well below 75 and in many cases as low as 30 [6-3]. The frame bay width b was taken as 6m for all cases. The beams were all 356 x 171 x 45 UB. All

the studied columns were taken as 200 x 200 x 8 SHS. In order to ensure failure of the studied columns, the first storey of each frame was designed to have larger column sizes of 200 x 200 x 10 SHS coupled with fully fixed bases (except in frame 1, where the first storey columns also consisted of 200 x 200 x 8 SHS columns).

All members were designated to have grade 43A steel with the yield stress value of 275 N/mm^2. The steel was assumed to possess an elastic-perfectly plastic stress-strain relationship as shown in Figure 6.6. The modulus of elasticity was taken as 205 kN/mm^2.

6.3.2 Imperfection and Connection Characteristics

The initial geometrical imperfection of L/3000 (see Figure 6.7) was included in all the three frames used in this parametric study due to the reasons discussed in section 5.2.2 of Chapter 5. The geometrical imperfection was applied to the studied column only.

In the case of connections, four types of flowdrill connections namely PDEP, FEP, EEP and RIGID connections were employed in the parametric study (see Chapter 5, Figure 5.5). The connection characteristics were those obtained by France [6-4] who conducted investigations on the behaviour of flowdrill connections in isolated subassemblage tests. The corresponding M-ϕ characteristics, the connection classifications by strength and by stiffness are shown in Figures 5.6, 5.7 and 5.8 of Chapter 5. The trilinear model of the connection M-ϕ relationships used in the analyses are shown in Figure 5.9 of Chapter 5.

6.3.3 Loading

The columns were all tested under the loading system described below.

- In phase one of the loading, a uniform distributed load was loaded to the right beam which was connected to the top end of the column under investigation (see Table 6.1). The purpose was to transfer the detrimental beam end moment to the

top end of the column. The beam load was then kept constant throughout the second loading loading phase. Except in frame 3, another beam loading was applied at the left beam connected to the lower end of the studied column. The reason was to induce a single curvature type of column buckling. According to Wood [6-5], this type of buckling is the most critical for columns with high axial loads.

- In the second phase of the loading, incremental column axial loads were applied at the column head of the studied column up to failure. Hence in all the cases considered, the frames failure were triggered by the failure of the studied columns.

The beam loads used were 30 kN/m and 45 kN/m. The justification of employing the 30 kN/m load was based on the following aspects:

- The distribution of floor loading was assumed as in Figure 6.8. The spacing between plane frames was taken as 5 m. The secondary beam spacing was taken as 2.5m. The unfactored dead load DL was considered as 4.0 kN/m^2. The typical live load LL was taken as 4.0 kN/m^2 as being typical for buildings in UK [6-6]. The corresponding factored dead load was assessed as 1.4DL + 1.6LL = 12 kN/m^2. Assuming precast concrete floor planks spanning in one way resulted in the factored distributed load of 30 kN/m on the beam.

- The beam remains elastic with different connection types and column heights.

In the case of 45 kN/m beam load, it was the maximum load as obtained by designing the beam as a simply supported member in accordance with BS 5950 [6-2]. With this model, the maximum free moment of the beam was obtained as $wL^2/8 = 202.5$ kNm, where w is the uniformly distributed load and L is the beam length. The free moment was just below the plastic moment capacity of the beam, i.e. $M_p = 212.9$ kNm. As a result of the large distributed load of 45 kN/m, it was observed that the beam with PDEP connections had its section partially yielded. However the yielded beam did not cause any failure to the frame.

6.4 Behaviour of Internal Beam-columns with Semi-rigid Connections

In presenting the parametric study results, this section discusses the two fundamental responses of load-moment and load-deflection of the internal columns based on the parametric study on frame 3. These responses coupled with the knowledge of behaviour presented in Chapter 5 can provide further understanding of the column behaviour and its significance in design.

6.4.1 Response of Load-Deflection

Figure 6.9(a) shows the load-deflection characteristics of an internal column with 4m height and the corresponding slenderness ratio of 51.1. It can be seen that the slopes of load-deflection curves in the elastic range are almost similar for PDEP, FEP, EEP and RIGID connections. This implies that in the elastic range, the stiffness of the column is not much influenced by the connection stiffness. However, a closer observation to the final slope of the load-deflection curves in the inelastic range shows that there is a role played by the various types of connections. It can be noticed that after the formation of first yields, the slopes are much steeper with EEP and RIGID connections as compared to the FEP and PDEP connections. It is evident from this response that the important of connection stiffness is more significant in the inelastic range of the column. The significant contribution of the stiffer connection is to delay the rate of stiffness loss in the column. This response coupled with the shedding of the detrimental moment permits the column with the stiffer connections to sustain larger axial loads in the inelastic range. Hence, the columns with stiffer connections are able to provide larger reserves of strength as compared to the columns with less stiffer connections. On the other hand, it is also seen that the use of less stiffer connections such as PDEP and FEP connections can enhance the column axial failure load to almost close to that of EEP and RIGID connections. This is due to the fact that the use of less stiff connections have some beneficial aspects such as less detrimental

moment and the ability to delay the first yield. This in turn permits the column with PDEP connections to sustain high axial failure load.

Figure 6.10(a) shows the load-deflection response of the more slender column with 7m height and the corresponding slenderness ratio of 89.4. It can be seen that in the elastic range, the slopes with EEP and RIGID connections are slightly steeper than the slopes with FEP connections. However as can be seen from the figure, the stiffening effect is very small and has little significance to the column. Hence, it indicates that increasing connection restraint has little influence on the performance of the slender column in the elastic range.

Figure 6.11(a) shows the comparison of load-deflection responses between the columns with slenderness ratio of 51.1 and 89.4. It can be seen in the elastic range **AB** that the load-deflection curves of columns with higher slenderness ratios are more gradual than the curves of the columns with lower slenderness ratios irrespective of connection types. The gradual slopes indicate that in the elastic range, the slender columns are more vulnerable to the rapid stiffness loss due to the geometrical deformation as compared to the columns with lower slenderness. This initiated an early first yield and hence an early inelastic moment shedding.

6.4.2 Response of Load-moment and Moment Shedding

Figure 6.9(b) shows the load-moment response of the column with slenderness ratio of 51.1 with the corresponding load-deflection response shown in Figure 6.9(a). Similarly, Figure 6.10(b) shows the load-moment response of the column with slenderness ratio of 89.4 with the corresponding load-deflection response shown in Figure 6.10(a). As can be seen from the two load-moment figures, the plots of axial loads against end moments show that the initial detrimental moment is progressively shed with increasing axial load. Eventually, dramatic moment shedding is observed when the column start to undergo yielding.

After the detrimental negative moment is relaxed to zero, the moment will then act as a reverse moment (positive moment). This reversal of moment acts in the opposite direction to the column rotation. This in turn results in the column being restrained further at its ends.

It is also of interest to compare the response of moment shedding of the columns with respect to different slenderness ratios. In view of this, Figure 6.11(b) shows the comparison of moment shedding between the column with slenderness ratio of 51.1 and the columns with higher slenderness ratio of 89.4. For each slenderness ratio, four different connection types are utilised. It is seen that in the elastic range, irrespective of connection types used, the slopes of load-moment responses **A** to **B** are more gradual with the higher slenderness columns than the lower slenderness columns. This reflects the fact that in the elastic range, more rapid moment shedding occurs in the slender columns. This is because the slender columns tend to have more appreciable loss of elastic stiffness with increasing axial load as shown in the gradual load-deflection response **A** to **B** of Figure 6.11(a).

The results of the comparison suggest that:

- The rate of moment shedding is dependent on the rate of stiffness loss. The more rapid is the loss of stiffness, the quicker is the rate of moment shedding.
- Columns with higher slenderness tend to have higher stiffness loss in the elastic range due to geometric deformation. Hence, it can be concluded that the higher the slenderness of the columns the more rapid is the rate of moment shedding.

As a result of a smaller detrimental moment and rapid rate of moment shedding, a slender column will undergo a large restraining moment effect at the collapse load level. This suggests that the more slender columns tend to have larger restraining effect from the reversal of moment. This behaviour is also noted by Gent and Milner [6-7].

6.4.3 Response of Beam-columns with the Inclusion of Eccentric Loads

In this study, the analyses were performed by modelling the connection to be located at the concentrated point of the intersection between beam and column centre-lines. Figures 6.12(a) and 6.12(b), respectively, show the actual beam-to-column connection and the connection model which neglects the offset.

The study of connection offset in open section was investigated by Rifai [6-8]. According to Rifai, in the case of open section columns, the model neglecting connection offset is acceptable only if the column buckles in minor axis. This is due to the fact that in this case, the beam is connected to the column web in which the offset between the connection and the column centre-line is minimal [6-9]. Thus, the moment due to eccentricity load is negligible. However in the case of the beam is connected to the column flange, the offset may be significant and needs to be considered . This effect is modelled by Rifai by employing an extra rigid element with a length of *D/2* between the intersection of the beam-column centreline and the actual location of the connection at the column face, where D is the column depth (see Figure 6.12(c)).

In this study, however, a different approach is used to model the connection offset. An additional eccentricity moment which is equivalent to that of $M = R \times e$ is applied at the intersection of beam and column centre-lines, where R is the beam reaction and e is the offset (see Figure 6.12(d)). The connection location remains at the intersection of the beam and column centre-lines. Eventually, the total applied moments at the intersection consist of the eccentricity moment, $M = R \times e$ and the moment transmitted by the actual connection restraint. The study on the offset model was limited to the internal column in frame 3 only. It is expected that other column problems may also show similar fashion of response. The results of the study using the offset model are presented in Figures 6.13 to 6.16.

Figure 6.13(a) shows the load-deflection response of the internal column with 4m height and PDEP connections. It can be observed that the inclusion of additional

moment due to connection offset has caused larger column deflection. As a result, the ultimate axial load reduced slightly by 2.4%, that is from 1660 kN to 1620 kN. This is due to the fact that the larger column deflection has triggered an earlier formation of first yield which caused the column to lose its stiffness earlier. In the case of FEP, EEP and RIGID connections, the load-deflection responses are shown in Figures 6.14(a), 6.15(a) and 6.16(a) respectively. It is observed that as the connection stiffness is increased, the difference in the load-deflection path as well as the difference in the ultimate load decreases. This can be seen clearly in the case of EEP and RIGID connections where the difference of load-deflection response is minimal. This in turn resulted in a very small difference in the column axial failure loads. For example, with EEP connections the column axial failure load with the offset model is only reduced by 0.3% from 1650 kN to 1645 kN. The results show that the modelling of connection at column face are seen to have little effects on the collapse load and the load-deflection response of the columns with the use of EEP and RIGID connections. The explanation to this is that the EEP and RIGID connections can provide almost full continuity in the transmission of forces within the beams and columns. Hence the effect of eccentricity is minimal.

The corresponding behaviour of moment shedding in the case of columns with PDEP, FEP, EEP and RIGID connections is shown in Figures 6.13(b), 6.14(b), 6.15(b) and 6.16(b) respectively. As can be seen from these figures, the inclusion of connection offset has caused a variation in the distribution of moments. However the other important observation is that even with the offset model, the column head is still subjected to the shedding phenomenon in which the moment is eventually relaxed to zero and then act as restraining moment. This phenomenon shows more evidence that the column with eccentricity moment also behaves as axially loaded compression member at the ultimate load level.

6.5 Configuration of Bending Moments

As a result of the moment shedding and the corresponding redistribution of moments, it is important to identify the bending moments which are meaningful for design purposes. In view of this, it is noted that the bending moment diagrams at the initial beam load levels (lower load levels) and at the collapse load levels are recognised as the important bending moments for design criteria. The bending moments at the lower load levels are used for designing the connections, whereas, the bending moments at the higher load levels are used for designing the beams and the columns.

The load levels mentioned above refer to the levels of column loads. Figure 6.17(a) shows the levels of column loads namely the lower load level P_1 and the higher load levels P_2 , P_3 and P_{sr} . The corresponding responses of beneficial and detrimental items that are present at the column ends with respect to different load levels are shown in Figure 6.17(b). The higher load levels P_2 , P_3 and P_{sr} are defined as the various equilibrium points near the ultimate loads at which the column can still be considered as an axially loaded compression member.

The load levels P_1 , P_2 , P_3 and P_{sr} are associated with the column loads P_1 , P_2 , P_3 and P_{sr} respectively. The definition of the various column loads are as follows:

- P_1 is the column load due to beam loads with the presence of maximum acting moment.
- P_2 is the column load with the presence of small acting moment. At this load level, the presence of connection restraint permits the column to sustain high axial load which is greater than the strength of pin ended column. Hence, the column can be treated as axially loaded.
- P_3 is the column load with the presence of zero moments or moments that are close to zero. At this load level the column is behaving as an axially loaded member.
- P_{sr} is the collapse load of the column, sometimes with the presence of restraining moments. At this load level the column is behaving as an axially loaded member.

The following sections discuss the configuration of bending moments at the lower and higher load levels and their effects on the design of connections, beams and columns.

6.5.1 Beam Moments at Lower Load Levels and the Connection Capacity

In the proposed simplified design method (see Chapter 7, section 7.6.3), it is suggested that the end restraint moments at beam ends to be used for beam design are adopted based on the inelastic end restraint moments (due to inelastic column) at the ultimate load level. The suggested inelastic end restraint moments for the simplified beam design method are as follows:

- 0% of end restraint moment for both external and internal beams with the use of pinned connections.
- 5% of M_p for external ends of external beams and 10% of M_p for internal ends with the use of semi-rigid and rigid connections.

The above inelastic end restraint moments are associated with the values of elastic end restraint moments at the lower load levels. This in turn corresponds to the connection capacities at the lower load levels.

In view of the above, sections 6.5.1.1, 6.5.1.2 and 6.5.1.3 discuss the requirements of the connections at the lower load levels in order to obtain the required inelastic end restraint moments at the higher load levels.

6.5.1.1 Pinned Connections

Tables 6.2(a), 6.3(a) and 6.4(a) show the values of elastic end restraint moments at the lower load level P_1 as obtained from frames 1,2 and 3 respectively.

Referring to PDEP connections, it is seen that the values of elastic end restraint moment in all the three frames are less than 5%. Such values of elastic end restraint moments can provide inelastic end restraint moments at the higher load levels of less than 5% (see Tables 6.2(b), 6.2(c), 6.3(b), 6.3(c), 6.4(b), 6.4(c) and 6.4(d)). This satisfies the 0% of end restraint moment as suggested in the proposed simplified design.

Examination of the M-ϕ classification shows that the connection has its moment capacity less than 5% of M_p and is classified as pinned (see Chapter 5, Figures 5.7 and 5.8). Based on this justification, it is suggested that the pinned connections to be used in the proposed simplified design should satisfy the following conditions:

- The connection must have a minimum moment capacity of 5% of M_p as classified by strength.
- The connection must be within the pinned boundary as classified by stiffness.

The connections should be classified based on the EC3 specifications [6-10].

6.5.1.2 Semi-rigid Connections

In the case of semi-rigid connections, it is seen that the values of elastic end restraint moments with FEP, EEP and RIGID connections at the lower load level P_1 are within the range of 13% - 15%, 24% - 36%, 27% - 47% respectively (see Tables 6.2(a), 6.3(a) and 6.4(a)). Such values of elastic end restraint moments can provide inelastic end restraint moments at the higher load levels of more than $0.05M_p$ for the external beams and $0.10M_p$ for the internal beams (see Tables 6.2(b), 6.3(b) and 6.4(b)).

To justify the requirement of the connections, it is appropriate to refer the FEP connection which have the lowest inelastic end restraint moments as compared to EEP and RIGID connections. Examination of the M-ϕ classifications shows that the maximum moment capacity of the FEP connection is close to $0.25M_p$ and it is just qualified to be classified as semi-rigid connections (see Chapter 5, Figures 5.7, 5.8). Hence, based on this justification, it is suggested that the semi-rigid connections to be used in the proposed simplified design should satisfy the following conditions:

- The connection must have a minimum moment capacity of 25% of M_p as classified by strength.
- The connection must be within the semi-rigid boundary as classified by stiffness.

Similarly, the connections should be classified based on the EC3 specifications.

6.5.1.3 Rigid Connections

In this study, the rigid connections follow the same requirement of the semi-rigid connections. With this respect, the connections should satisfy the following:

- The connection must be within the rigid boundary as classified by stiffness.

The connections should be classified based on the EC3 specifications.

6.5.2 Beam Moments at Higher Load Levels and the Restraining End Moments at Beam Ends

In the case of beam design based on conditions at the ultimate load level, the inelastic end restraint moment is selected when the column reaches its ultimate load. So far in this study, the investigation on the end restraint moment at the beam ends is concentrated on the exact state of the column collapse load. The disadvantage is that small values of inelastic end restraint moment occur at the beam ends as the column failure load is approached. This is due to the fact that the values of end restraint moment decreases with the increased in axial load.

In view of the above, various equilibrium points at higher load levels P_2 , P_3 and P_{sr} are investigated to obtain larger values of inelastic end restraint moment at the beam ends.

6.5.2.1 Values of inelastic end restraint moments of external beams

Tables 6.2(b) and 6.2(c) show the values of inelastic end restraint moment of the external beams of frame 1 at load levels P_2 and P_{sr} respectively.

It can be observed from the tables that in the case of PDEP connections, the end restraint moment satisfies the requirements of 0% end restraint moment at both load levels P_2 and P_{sr} .

In the case of FEP, EEP and RIGID connections, the values of end restraint moment are satisfied at load level P_2 . Thus, based on this justification, it is possible to obtain the inelastic end restraint moment at the external ends of the external beams up to $0.05M_p$ with the use of FEP, EEP and RIGID connections. Hence, the suggested values of end restraint moment to be used at the external ends of the external beam are as follows:

- 0% for PDEP connections.
- 5% of M_p for FEP, EEP and RIGID connections.

6.5.2.2 Values of inelastic end restraint moments of internal beams

Tables 6.3(b), 6.3(c) and 6.3(d) show the values of end restraint moment of the upper internal beams of frame 2 at load levels P_2 , P_3 and P_{sr} respectively.

It is seen that the PDEP connection satisfies the 0% requirement at all load levels P_2 , P_3 and P_{sr} . In the case of FEP connections, the suggested end restraint moment of 10% of M_p is satisfied at load level P_2 . Whilst, with the EEP and RIGID connections, the suggested inelastic restraint moment is satisfied at all the three load levels P_2, P_3, and P_{sr} .

Similarly, Tables 6.4(b), 6.4(c) and 6.4(d) show the values of inelastic end restraint moment for the internal beams of frame 3 at load levels P_2 , P_3 and P_{sr} respectively. It is observed that with PDEP, EEP and RIGID connections, the requirement of the end restraint moment is satisfied at load level P_{sr} . However in the case of FEP connections, the end restraint moment is only satisfied at load level P_3 but not at load level P_{sr} .

Based on the above results, it is suggested that the values of inelastic end restraint moment at the internal beam ends to be used in beam design are as follows:

- 0% for PDEP connections.
- 10% of M_p with FEP, EEP and RIGID connections.

As can be seen from the tables, the value of end restraint moment is defined in terms of M_p of the beam. This corresponds to the capacities of the connections which are also classified in terms of M_p of the beams.

6.5.3 Column Moments at Ultimate Load Levels

Figures 6.18(a), 6.19(a) and 6.20(a) show the response of column top end moment with increasing column load for the upper edge of frame 1, the upper intermediate column of frame 2 and the internal column of frame 3 respectively. The important phenomenon to be observed from this figure is the decreasing rate of column top end moment due to moment shedding. This phenomenon has resulted in the change of column bending moment configuration at the ultimate load level. The corresponding bending moments of the studied column before and after the moment shedding phenomenon are shown in Figures 6.18(b), 6.19(b) and 6.20(b) respectively. These figures show the comparison of bending moment diagrams at the initial beam load level and at the collapse (ultimate) load level with respect to various connection types. Clearly, in all the limited cases considered and irrespective of connection types, the bending moments at collapse loads are in the general forms of the bending moments of axially loaded restrained columns. It is evident from these results that at ultimate load levels, the restrained beam-column behaves in a similar manner as an axially loaded compression member with a certain degree of end restraint.

Based on the analysis results presented above, it is now recognised that beam-columns behave differently at both service and ultimate load levels. At the lower load level, the moment transferred by the beam causes a detrimental effect to the column (see Figure 6.21(a)). The corresponding bending moment is shown in Figure 6.21(b). On the other hand, at the ultimate load level, the column top end moment instead of being detrimental has become beneficial by inducing a reversal of moment which restrained the column (see Figure 6.21(c)). The typical corresponding column bending moment diagram at this stage is shown in Figure 6.21(d). Based on this figure, it is believed that as a result of the moment reversal, a point of inflection can develop at the point of transition between negative and positive moments. Experimental observations by

Davison [6-11] showed evidence of such existence of inflection points within the column length employing "simple" semi-rigid connections of web cleat types.

6.6 Ultimate Strength of Beam-columns

The problem of interaction between the axial load and moment which occurs at the lower load level diminishes as the ultimate load level is approached as a result of moment shedding phenomenon. As a consequence, the bending moment diagrams of beam-columns at collapse load are analogous to the bending moment diagrams of axially loaded columns with end restraints. This response demonstrates that beam-columns can be treated as axially loaded members.

In view of the above, the values of the ultimate strength of the beam-columns obtained from the analysis can be utilised to relate the ultimate strength of semi-rigid end restrained beam-columns to the ultimate strength of the pin ended columns. In other words, the failure load of the beam-columns which are treated as axially loaded at ultimate load can be compared directly to the ultimate axial failure load of the pin ended columns.

Consequently, the ultimate strength of beam-column can be presented as follows:

1. The strength curves (see Figure 6.22(a)).
2. The α_{pin} values (see Figure 6.22(b)).

6.6.1 Ultimate Strength of Beam-columns Using the Strength Curves

The maximum axial load strength of semi-rigidly restrained beam-columns over a wide spectrum of slenderness can be presented in the form of these curves. Consequently, the comparison between the strength of semi-rigid end restrained beam-columns and the strength of pin ended columns can be described by the plots of such column curves. Referring to Figure 6.22(a), if P_{sr} is greater than $P_{pin\ BS\ 5950}$, it indicates that the ultimate axial load of the semi-rigid beam-column is greater than the

ultimate axial load of the pin ended column as specified by BS 5950. This implies that the use of BS 5950 pin ended strength curve to design the beam-column as an axially loaded column will result in a safe design method.

The other important criterion of beam-column strength curve is that it can be employed to determine the effective length factor of a beam-column with semi-rigid end restraints.

6.6.1.1 The Effective Length and the Solution of Beam-Columns at the Ultimate Load Level

The ultimate axial load of an axially loaded column with end restraints can be evaluated using the effective length method. The concept of effective length is widely used in design as a simplified method to take into account the effect of connection restraints at the column ends. The term effective length *KL* is defined as the length of the buckled deflected shape between points of zero curvature. This is the length of an equivalent pin ended column which has the same load capacity as the end restraint column [6-12].

Figure 6.23(a) shows the condition of a beam-column at ultimate load level which behaves as an axially loaded restrained member. In some cases, at the ultimate load level, the column end moments reverse in sign and act in the opposite direction to the column rotation. This results in the column ends being restrained further by the reversal of moment. Hence, the equivalent solution of the restrained beam-column at ultimate load level is shown in Figure 6.23(b). As can be seen from the figure, the beam-column can be modelled as a pin ended column but with a reduced effective length. Hence, knowing the effective length factor K, will enable the ultimate axial load P_{sr} of the end restrained beam-column with the length L to be calculated as if it were a pin ended column with the length KL.

Consequently, the ultimate strength of beam-column P_{sr} can be compared with the ultimate strength of an equivalent pin ended column P_{pin} as shown in Figure 6.23(c). Knowing this relation will enable the restrained beam-column to be designed as a pin

ended column with a reduced effective length. In this study the ultimate strength of restrained beam-column is compared directly against the strength of pin ended column as that specified by the BS 5950 and EC3 specifications. The reason is that the restrained beam-column can then be designed as axially loaded based on these two specifications.

According to Jones et al. [6-13], the effective length can also be defined as the length (slenderness) which gives the same strength on the basic column curve for pinned ends as the failure load for the actual column with its actual end restraint. Based on this definition, the effective length factor K is obtained by dividing the pinned column slenderness to the restrained column slenderness, i.e. $\lambda_{pin} / \lambda_{sr}$ as shown in Figure 6.22(a). In this study, the corresponding effective length factors of the studied columns as obtained by this method are presented in Table 6.5. Inspection of the results show that with the use of PDEP and FEP connections, the effective length factors vary from 0.8 to 0.85 for the external column, 0.62 to 0.63 for the upper intermediate column and 0.55 to 0.57 for the internal column. Whereas, in the case of EEP and RIGID connections, the effective length factors vary from 0.7 to 0.77 for the external column and 0.5 to 0.52 for the upper intermediate and the internal columns.

Hence, to avoid complexity in determining the effective length factors, it is suggested that the simplified forms of effective length factors are adopted. In the case of both ends are restrained with semi-rigid connections such as PDEP and FEP connections, the effective length factors of 1.0 and 0.85 are employed for the external and internal columns respectively. Whereas, when both ends are restrained with EEP or RIGID connections, the effective length factors of 1.0 and 0.7 are used for external and internal columns respectively.

6.6.2 Ultimate Strength of Beam-columns Using the α_{pin} Values

Another method of investigating the results of the beam-column strength is by using the α_{pin} values. The diagrammatic relation between the beam-column strength curves

and the α_{pin} values can be seen by referring back to Figures 6.22(a) and 6.22(b). The α_{pin} is defined as

$$\alpha_{pin} = P_{sr} / P_{pin} \qquad (6.1)$$

in which P_{sr} is the ultimate axial load (collapse load) of semi-rigidly connected column, P_{pin} is the ultimate axial load of equivalent perfectly pin ended column. The concept of α_{pin} was first introduced by Kirby et al. [6-15] as an index to identify the beneficial effect of connection restraints as opposed to the detrimental effects of the connections.

The beneficial and detrimental effects are present due to the fact that the connection has dual functions in the column response [6-16]. The response at the column ends as a result of these dual functions of the connection is illustrated in Figure 6.17(b). First, the connection contributes to the detrimental effect by transferring a disturbing moment to the column which reduces the column axial load strength. Secondly, the connection contributes to the beneficial effect by providing restraint to the column which enhances the column axial load strength.

Knowing the detrimental and the beneficial effects, the α_{pin} values provide a simple approach to identify which one of the two effects is more dominant.

The use of α_{pin} values enable the following assessment to be made:

1. When $\alpha_{pin} > 1.0$

- The beneficial effect of connection restraint outweighs the detrimental effect of the column moment.
- The strength of beam-columns with semi-rigid connections is greater than the strength of the equivalent pin ended axially loaded column.
- The beam-column can be designed as axially loaded member without the consideration of moment.

2. When $\alpha_{pin} = 1.0$

- The beneficial effect of connection restraint is equal to the detrimental effect of the column moment.
- The strength of beam-columns with semi-rigid connections is equal to the strength of the equivalent pin ended axially loaded column.
- The beam-column can be designed as axially loaded member without the consideration of moment.

3. When $\alpha_{pin} < 1.0$

- The detrimental effect of the column moment outweighs the beneficial effect of the connection restraint.
- The strength of beam-columns with semi-rigid connections is less than the strength of the equivalent pin ended axially loaded column.
- The beam-column should be designed using interaction equations considering both the axial load and the detrimental moment.

The justification of designing beam-columns as axially loaded compression members is based on the behaviour of beam-columns discussed in Chapter 5. Consequently, based on the α_{pin} values, in-depth studies on the ultimate strength of beam-columns with respect to various types of parameters can be carried out.

In this study, the results of ultimate strength of the beam-columns in terms of α_{pin} values are presented in Tables 6.6 - 6.17.

As can be seen from the tables, the ultimate strength of semi-rigidly restrained beam-column P_{sr} is compared against the ultimate strength of pin ended column $P_{pin\ BS\ 5950}$ as specified by clause 4.7.4 of BS 5950 [6-2], giving the value of α_{pin}. This is due to the fact that the strength of the beam-column with semi-rigid connections will later be designed using the ultimate strength of the pin ended column specified by the BS 5950 code. In addition, the ultimate strength of semi-rigidly restrained beam-columns P_{sr} is also compared with the strength of pin ended column $P_{pin\ EC3}$ as specified by clause 5.5.1 of EC3 [6-10] to obtain the α_{pin} value. The results show that in all 288 cases considered, all the α_{pin} values are in excess of unity except

in three cases where the α_{pin} values are slightly less than unity, i.e. 0.99. This shortfall is related to the edge columns and only represents 1% of all the cases considered. These results suggest that semi-rigidly restrained beam-columns can be designed safely as axially loaded members using the BS 5950 or EC3 pin ended column curves.

6.7 Parameters Influencing the Axial Load Strength of Beam-columns

Knowing that beam-columns can be treated as axially loaded members, it is of interest to study the important parameters that can influence the ultimate axial load of the semi-rigidly restrained beam-columns.

6.7.1 Influence of Column Slenderness

Figures 6.24 to 6.28 show the ultimate strength curves of the selected beam-column problems considered in this study. The overall range of the column slenderness is from 25.5 to 89.4. It can be seen from these figures, that the strength of the beam-columns with the slenderness ranging from 25 to 50, irrespective of connection types, is not less than 90% of the squash load. Whereas for the slenderness ranges between 50 to 90, it is seen that the ultimate carrying capacity of the column is greater than 80% of the squash load. This implies that within the practical range of column slenderness, the connection stiffness is seen not to be the main parameter in controlling the ultimate column load. For comparison, full scale test results on rigid frames also show that the failure loads of the intermediate columns are close to 97% of the squash load [6-5].

On the other hand, Tables 6.6(a), 6.7(a), 6.8(a) and 6.9(a) presented the values of α_{pin} for columns with PDEP, FEP, EEP and RIGID connections respectively. The values of α_{pin} are presented for various column slendernesses. In general, it can be seen that increasing the column slenderness increases the values of α_{pin}. For example, the value

of α_{pin} increases from 1.06 with 4m column to 1.35 with 7m column (see Table 6.6(a)). Other results presented in Tables 6.10 to 6.17 also show similar patterns of increasing α_{pin} values with the increase of column slenderness. This implies that the effect of increasing column strength with the use of stiffer connections is more significant for slender columns. The higher values of α_{pin} with the higher slenderness columns indicate the more significant effect of the connection restraint as opposed to the detrimental effect of the acting moment. This is to be expected as the higher slenderness column induces a smaller detrimental moment and sufficiently have larger effect of restraining moment. This is in agreement with Jones et al. [6-17] who suggested that the greater improvements in column strength can only be achieved significantly in column with slenderness beyond practical range.

6.7.2 Influence of Beam Loads

Figures 6.24 and 6.26, respectively, show the ultimate strength curves of the upper edge and the upper intermediate beam-columns with 30 kN/m beam load. Similarly, Figures 6.25 and 6.27 respectively, show the ultimate strength curves of the upper edge and upper intermediate columns with 45 kN/m beam load. In general, it is observed that irrespective of connection types, increasing the beam load from 30 kN/m to 45 kN/m reduces the column ultimate axial load. This is to be expected because the column end moment increases as the beam load is increased. This in turn resulting in larger deflection, earlier first yield and earlier stiffness loss in the column. Consequently, these effects reduce the ultimate strength of the columns. Hence, the effect of increasing beam load is analogous to increasing the column imperfection. This is in agreement with Gent and Milner [6-7] who first suggested that the effect of beam load is analogous to the column imperfection.

However, it is seen that even with the presence of high bending due to the large beam load, the ultimate axial loads of the external and internal columns are reduced to not less than 80% of the squash load (see Figures 6.25 and 6.27 respectively). Baker et al. [6-18] also noted that for open section columns, the most severe case of column end moment does not reduce the ultimate column capacity by more than 21.5%. Hence, it

is seen that the effect of bending moment transferred to the column is small in reducing the ultimate collapse load of the column.

Tables 6.6 to 6.13 show the comparison of the α_{pin} values between the beam loads of 30 kN/m and 45 kN/m. As can be observed from the tables, for each column height the values of α_{pin} decrease as the beam load is increased from 30 kN/m to 45 kN/m. For example, the value of α_{pin} for column with 4m height decreases from 1.06 to 1.04 with PDEP connections, from 1.04 to 1.02 with FEP connections, from 1.06 to 1.02 with EEP connections and from 1.07 to 1.04 with RIGID connections (see Tables 6.6(a) & 6.6(b), 6.7(a) & 6.7(b), 6.8(a) & 6.8(b) and 6.9(a) & 6.9(b) respectively). This implies that a larger detrimental moment transmitted by the beam load reduces the column axial load capacity. However even with the presence of the very large beam load of 45 kN/m, the values of α_{pin} are all above unity except in three cases which are very close to unity (see Tables 6.6(b), 6.7(b), 6.8(b)). This implies that even with the presence of large detrimental moment, the column can still sustain high axial failure load. This result is in agreement with Baker et al. [6-18] and Gent [6-19] who suggested that the ultimate axial load capacity of the column is not seriously affected by the column end moment.

6.7.3 Influence of Load Eccentricity

This section discusses the effect of load eccentricity to the internal column only. Hence, the results presented are limited to the internal columns. It is expected that other cases of columns will demonstrate a similar behaviour.

The higher ultimate strength of columns associated with PDEP connections as compared to the FEP, EEP and RIGID connections is due to the fact that the effect of load eccentricity at the column face is not taken into account (see Figure 6.28). However when the model of connection offset is adopted then the ultimate load of column with PDEP connections is lower than the columns with FEP, EEP and RIGID connections (see Figure 6.29). The similar response is also observed with the use of

FEP connections in which the ultimate strength is larger than the ultimate strength with the EEP connections (see Figure 6.25).

Figure 6.30 shows the comparison of the ultimate strength curves as modelled including the connection offset and not including the connection offset. On the other hand, Table 6.18 shows the percentage difference in the ultimate load as modelled using the two methods. The results show that in terms of ultimate load capacity, the inclusion of offset connection reduced the column capacity by not more than 6% with the most flexible PDEP connections and less than 3% with FEP connections. In other words, modelling the connection at the beam-column centre-line intersections can give a higher prediction of the column ultimate strength by not more than 6% with PDEP connections and not more than 3% with FEP connections. There is no significant difference in the ultimate loads between the two models when the stiffer connections such as EEP and RIGID connections are utilised. The effect of connection offset can be seen even more clearly in Figure 6.31. It can be seen that the stiffer the connection the lesser is the effect of modelling the connection at the true location.

Tables 6.14 to 6.17 show the α_{pin} values with different connection types and were obtained based on the two models described above. As can be observed from the tables, the α_{pin} values reduce slightly with the incorporation of eccentricity moment. For example, the value of α_{pin} for column with 4m height decreases from 1.08 to 1.06 with PDEP connections, from 1.07 to 1.06 with FEP connections, from 1.08 to 1.07 with EEP connections and from 1.09 to 1.08 with RIGID connections (see Tables 6.14(a) & 6.14(b), 6.15(a) & 6.15(b), 6.16(a) & 6.16(b) and 6.17(a) & 6.17(b) respectively). The values of α_{pin} are well above unity. This indicates that even if eccentricity moment is included, the benefit of connection restraint is still dominant.

6.7.4 Influence of Connection Stiffness

Figures 6.24 to 6.30 show the ultimate strength curves of beam-columns with semi-rigid end restraints. It can be seen that the failure loads of the beam-columns with quite flexible connections such as PDEP and FEP are close to the failure loads

with EEP and RIGID connections. It is also seen that in this range of slenderness, the use of less stiff connections such as PDEP and FEP connections can enhance the column strength to more than 80% of the squash load.

Figure 6.32 shows the ultimate loads of the internal columns with semi-rigid connections as compared to the strength of columns with rigid connections. It is seen that PDEP and EEP connections can sustain the column axial loads up to 95% of the strength of columns with RIGID connections. In the case including connection offset, the use of PDEP and FEP connections can attain 90% and 95% of the columns with RIGID connections respectively (see Figure 6.33).

Tables 6.6 to 6.9 show the effect of different connection types such as PDEP, FEP, EEP and RIGID connection types on the ultimate strength of beam-columns as a part of frame 1. It can be seen that by changing flexible connections to stiffer connections has not increased the α_{pin} values significantly. For example, in the case of column with 4m height, the value of α_{pin} only increases from 1.06 with PDEP connections to 1.07 with RIGID connections (see Tables 6.6(a) and 6.9(a) respectively). In other words, even with the use of less stiff connections such as PDEP and FEP connections, the α_{pin} values are seen to be close to the α_{pin} with EEP and RIGID connections. Similarly, examination of the α_{pin} values in frame 2 as presented in Tables 6.10 to 6.13 also show that the increase of α_{pin} values with respect to increasing connection stiffness is not significant.

The results of the ultimate strength curves and the α_{pin} values suggest that the use of flexible and less stiff semi-rigid connections are able to enhance the column strength to almost the strength of columns with rigid connections. Hence in this range of slenderness, it is seen that increasing the end restraints has less effect in increasing the column ultimate strength.

These results are in agreement with the observation made in the testing of full scale semi-rigid frames carried out at BRE [6-20],[6-21]. In fact, the behaviour observed in this full-scale frame test has been incorporated in the latest amendment in IStructE steelwork building structures design manual [6-22]. The basis of the amendment is

such that it is now believed that ordinary connections of beams to columns can develop the full stiffness of the beam members [6-23]. Clearly, the flexible and semi-rigid connections possess some degree of restraint which reduces the column effective length and hence increases the column capacity.

Wood [6-5] noted in his research that the column collapse load is not sensitive to the connection stiffness. Furthermore, according to Kirby et al. [6-15] , it is the presence of the connection that is the most important while the connection stiffness is of secondary importance. Studies conducted by Chen also show that increasing the stiffness of the joint does not necessarily increase the load carrying capacity of the frame [6-24]. Other results of Chen [6-25] show that the ultimate load-carrying capacity of a portal frame is not dependent on the connection types used. He suggested that as long as the connection has enough strength to carry the moment, the failure of the frame can be obtained by assuming the connection to be rigid. Overall, it can be concluded that the variation in connection rotational stiffness has very little influence on the value of the ultimate column loads.

Gent [6-19] also noted that the rigidity of the connections had no influence on the column design. He then suggested that the principal effect of semi-rigid connections is just to reduce the initial column end moment as compared to rigid connections.

Having recognised that the use of less stiff connections can also enhance the column axial failure load, it is therefore possible to design the column by employing less stiff connections without reducing the column strength. This in turn will minimise the connection cost. In practice, however, many designers continue to specify unnecessary full-strength or fully welded connection which eventually increases the connection cost [6-26]. In view of this matter, designers should be aware of the limited benefit of employing full-strength connections in increasing the column strength. Indeed, the IStrucE Committee has recognised that even connections designed to develop the full resistance moment of the beams full strength connections may not develop the full stiffness [6-23].

6.8 Relation to Design

As a result of moment shedding phenomenon and the limited study on the α_{pin} values, it is reasonably justified that a simplified design method can be carried out as follows:

- The beam can be treated as a simply supported member with a certain value of end restraint moment to include the effect of semi-rigid end restraint.
- The beam-column can be treated as an axially loaded compression member perhaps with a reduced effective length to include the effect of semi-rigid end restraint.

6.8.1 Design of Beams

The results of the study show that at higher load levels, beams with PDEP connections are seen to have very small values of inelastic end restraint moment, i.e. less than 5% of M_p . Based on these results, it is suggested that for designing beams in simple construction, the end restraint moment at beam ends is taken as zero.

On the other hand, it is seen that at higher load levels, the beams with FEP, EEP and RIGID connections can still possess a certain amount of inelastic end restraint moment which may be beneficial for reducing the beam mid-span moment. This in turn can result in more economical beams. Based on the results of the parametric study, it is suggested that the following values of end restraint moment may be used for designing beams in semi-rigid and rigid constructions:

(i). $0.05M_p$ at external ends of external beams.

(ii). $0.10M_p$ at all internal beam ends.

It is also worth noting that the use of FEP connections as opposed to the PDEP connections can change the structural system from simple construction to semi-rigid construction in which further savings in beam design can be achieved. In addition, further benefits may be attained at serviceability conditions as the semi-rigid joints will significantly reduce deflections.

6.8.2 Design of Columns

The results of the study show that the design of restrained beam-columns at the ultimate load level in non-sway frames can be performed in a simple manner as only axial loadings are considered. The design approach is based on the elastic-plastic behaviour of the column as it approaches the ultimate limit state.

It was discussed in section 6.6.2 that the connection has dual role functions. First, by inducing the detrimental moment and secondly by providing the beneficial restraint effects. These two aspects are incorporated in design as discussed herein.

In the current column BS 5950 [6-2] design method, in order to incorporate the detrimental effect of the actual moment transferred to the column, it is required to have an accurate knowledge of M-ϕ curve characteristics. However in the case of a design method based on the ultimate load level as in the proposed simplified elastic-plastic α_{pin} design method, the detrimental moment acting on the column diminishes and no longer present. This indicates that it is not necessary to determine the actual moment transferred to the column. Hence, the design of a beam-column with semi-rigid end restraints at the ultimate load level is no longer dependent on the M-ϕ characteristics.

On the other hand, in order to include the beneficial effect of the end restraint at the column ends, the reduced column effective length is employed. Consequently, realising that there is no significant difference in the ultimate column load due to the variation in connection stiffness, it is suggested that a simplified form of effective length is used for determining the axial resistance of the column. The suggested effective lengths are as follows:

(i). In the case where both ends are restrained by semi-rigid connections such as PDEP, FEP connections, the effective lengths are $L_e = 0.85L$ and $L_e = 1.0L$ for the internal and external columns respectively.

(ii). In the case of both ends are restrained by EEP or rigid connections, the effective lengths are $L_e = 0.7L$ and $L_e = 1.0L$ for the internal and external columns respectively.

The above effective lengths are based on the results discussed in section 6.6.1.1.

6.8.3 Design of Connections

It is possible to design the connection without having to match the strength of the connected beam in order to achieve high ultimate column capacity. This is based on the justification that the use of flexible PDEP connection can achieve almost 90% of the column load with RIGID connections. However the use of flexible connections may result in an uneconomical beam design. Therefore, in order to achieve economy in beam design, the FEP connection is suggested to be employed to get the benefit of the end restraint moment at the beam ends. Furthermore, the use of the FEP connections may not increase the connection cost significantly above PDEP connections unlike the use of EEP or RIGID connections.

The other important design criteria of the connection is that in order to achieve the suggested inelastic restraint moment of $0.05M_p$ at external ends of external beams and $0.10M_p$ at internal beam ends at the ultimate load level, the connection should have a minimum moment capacity of *0.25Mp* as classified by strength using the EC3 classification.

6.9 Conclusions

The parametric study on the behaviour and strength of SHS beam-columns at ultimate load level has been presented. It is seen that the study on the behaviour of elastic-plastic columns at higher load level leads to a more realistic design method. Moreover, the problem of the detrimental moment acting at the column end which normally occurs at a lower level diminishes as the column loses its stiffness at higher load levels. As a result, the design procedure based on the response at the ultimate load level is nothing more involved than the simple analysis and design of individual members of beams and columns.

The parametric study described in this chapter was limited to a series of low rise multi-storey plane frames in the range of two to three storeys. The frames consisted of SHS columns with flowdrill connections. The study on the connection offset is limited

to the internal columns only. It is expected that other column problems may follow a similar response. Furthermore, it should be pointed out that the effect of residual stress has not been taken into account in the analysis as it is considered negligible in tubular columns [6-1].

The study on the ultimate strength of beam-column was conducted on a column slenderness ratio in the range between 25 to 90. Such a range of column slenderness has already covered a wide range of practical SHS columns. As a result of the limited study, several important conclusions are presented as follows:

1. The rate of decrease (shedding) in moment is dependent on the rate of stiffness loss in the columns. The more rapid the loss of stiffness in the column, the more sudden is the moment shedding.

2. It is seen that a significant decrease of moments in the elastic range occurs in columns with high slenderness ratios. This is associated with the high stiffness loss in the elastic column as a result of large geometrical deformation.

3. As a result of the moment shedding phenomenon, it is seen that at ultimate load level, the external and internal beam-columns can be designed as axially loaded compression members.

4. The development of restraining moments which further enhance the column axial failure load is seen to be more significant with slender columns.

5. In all cases considered, the results of α_{pin} values are all above unity except in three cases which are just below unity. This shortfall only represents 1% of all the cases considered. This implies that SHS beam-columns can be designed safely as axially loaded compression members based on the BS 5950 or the EC3 pin ended column curves.

6. The interior columns tend to have higher values of α_{pin} as opposed to the external columns. This indicates that the effect of detrimental moment is minimal for the interior columns.

7. The earlier first yield load P_y in the column with stiffer connections is counteracted by the larger reserve of axial load strength in the inelastic range. This in turn results in columns with stiffer connections being able to sustain larger axial failure loads than equivalent columns with more flexible connections.

8. The additional eccentricity moment at the column end is also subject to the moment shedding phenomenon at the ultimate load level. The moment is relaxed to almost zero resulting in the column to behave as axially loaded only. The important implication is that, columns in simple construction can be designed as axially loaded without the inclusion of nominal (eccentricity) moment as employed in the current design method.

9. The effect of increasing connection stiffness is seen to be less important for columns with practical slendernesses. It is seen that the use of flexible PDEP connections can enhance the ultimate column strength to about 90% of the column strength with RIGID connections. Therefore, in the practical range of column slenderness, there are no significant benefits of increasing connection restraints in order to enhance the column ultimate load.

10. The only benefit of increasing connection stiffness is the increase of the restraint moments at the beam ends. This in turn reduces the maximum mid-span moment of the beams and hence resulting in shallower or lighter beam sections. In view of this, it is suggested that the use of FEP connections can minimise the unnecessary restraint in columns and can slightly enhance the end restraint at beam ends as opposed to the PDEP connections.

11. In terms of stability and strength, SHS columns coupled with flowdrill connections are suitable for low-rise multi-storey non-sway frames.

6.10 References

[6-1] Needham, F.H., 'Local buckling and section classification', in Introduction to Steelwork Design to BS 5950: Part 1, The Steel Construction Institute, 1988, pp. (5-1) - (5-9).

[6-2] BS 5950: Part 1: 1990, 'Structural use of steelwork in building', Part 1. Code of practice for design in simple and continuous construction : hot rolled sections, British Standard Institution.

[6-3] Ackroyd, M.H. and Bjorhovde R., "Discussion of 'Effects of semi-rigid connections on steel column strength' by Jones, S.W., Kirby, P.A. and Nethercot D.A., Journal of Constructional Steel Research, Vol. 1, No, 1, September, 1980, pp. 38-46 ", Journal of Constructional Steel Research, Vol. 1, No.3, May, 1981, pp. 48-51.

[6-4] France, J.E., 'Bolted connections between open section beams and box columns', Ph.D. Thesis, Department of Civil and Structural Engineering, University of Sheffield, U.K., January, 1997.

[6-5] Wood, R.H., 'A new approach to column design', Her Majesty's Stationery Office, 1974.

[6-6] BS 6399: Part 1: 1984, 'Code of practice for dead and imposed loads', British Standard Institution.

[6-7] Gent, A.R. and Milner H.R., 'The ultimate load capacity of elastically restrained H-columns under biaxial bending', Proceedings, Institution of Civil Engineers, Vol. 41, December, 1968, pp. 685-704.

[6-8] Rifai, A.M., 'Behaviour of columns in sub-frames with semi-rigid joints', Ph.D. Thesis, Department of Civil and Structural Engineering, University of Sheffield, U.K., June, 1987.

[6-9] Nethercot, D.A., Kirby, P.A. and Rifai, A.M., 'Columns in partially restrained construction: analytical studies', Canadian Journal of Civil Engineering, 14, 1987, pp. 485-497.

[6-10] Eurocode 3, 'Design of steel structures - Part 1.1: General rules and rules for buildings', ENV 1993-1-1.

[6-11] Davison, J.B., Kirby, P.A. and Nethercot, D.A., 'Column behaviour in PR construction: Experimental behaviour', Journal of Structural Engineering, ASCE, Vol. 113, No. 9, September, 1987, pp. 2032-2050.

[6-12] Kirby, P.A., 'Continuous multi-storey frames', in Introduction to Steelwork Design to BS 5950: Part 1, The Steel Construction Institute, Berkshire, 1988, pp. (15-1) - (15-10).

[6-13] Jones, W. S., Kirby, P.A. and Nethercot D.A., 'Columns with semi-rigid joints', Journal of the Structural Division, ASCE, Vol. 108, No. ST2, February, 1982.

[6-14] Jones, W.S., 'Semi-rigid connections and their influence on steel column behaviour', Ph.D. Thesis, Department of Civil and Structural Engineering, University of Sheffield, U.K., 1980.

[6-15] Kirby, P.A., Bitar, S.S. and Gibbons, C., 'Design of columns in non-sway semi-rigidly connected frames', First World Conference on Constructional Steel Design', Acapulco, Mexico, December, 1992, pp. 54-63.

[6-16] Kirby, P.A. and Davison, J.B., 'Full scale testing of semi-rigid response in non-sway steel frames', in Structural Assessment: The Role of Large and Full Scale Testing, Joint IStructE/City University International Seminar, City University, London, 1-3 July, 1996, pp. 77.1-77.8.

[6-17] Jones, S.W., Kirby, P.A. and Nethercot, D.A., 'Effect of semi-rigid connection on steel column strength', Journal of Constructional Steel Research, Vol. 1, No.1, September, 1980, pp. 38-46.

[6-18] Baker, J.F., Horne, M.R. and Heyman J., 'The steel skeleton', Cambridge University Press, Vol. 2, 1956.

[6-19] Gent, A.R., 'Elastic-plastic column stability and the design of non-sway frames', Proceedings, Institution of Civil Engineers, Vol. 41, December, 1968, pp. 685-704.

[6-20] Moore, D.B., Nethercot, D.A. and Kirby, P.A., 'Steel frames: Testing steel frames at full scale', The Structural Engineer, Volume 71, Nos. 23 & 24, December, 1993, pp. 418-427.

[6-21] Moore, D.B. and Nethercot, D.A., 'Testing steel frames at full scale: Appraisal of results and implications for design', The Structural Engineer, Volume 71, Nos 23 & 24, December, 1993 , pp. 428-435.

[6-22] Institution of Structural Engineers, 'Manual for the design of steelwork building structures', Institution of Structural Engineers, November, 1989.

[6-23] The Structural Engineer, 'Amendment to IStructE steelwork design manual', in Structural News, The Structural Engineer, Vol. 76, No.2, January, 1998, p. A3.

[6-24] Chen, W.F. and Zhou, S.P., 'Inelastic analysis of steel braced frames with flexible joints', International Journal of Solid and Structures, Vol. 23, No. 5, 1987, pp. 631-649.

[6-25] Chen, W.F., 'Analysis of steel frames with flexible joints', in Structural Connections : Stability and Strength, ed. Narayanan, R., Elsevier Applied Science, 1989, pp. 335-444.

[6-26] Gibbons, C., 'Economic steelwork design', The Structural Engineer, Vol. 73, No. 15/1, 1995, pp. 250-253.

[6-27] Rifai, A.M., Nethercot D.A. and Kirby P.A., 'Stability of column subassemblages with semi-rigid connections', in Stability of Steel Structures, Technical University of Budapest, Hungary, 1988, pp. 443-449.

[6-28] Gibbons, C., Kirby, P.A. and Nethercot, D.A., 'Calculation of serviceability deflections for non-sway frames with semi-rigid connections', Proceeding of Institution of Civil Engineers Structures and Buildings, May, 1996, 111, pp. 186-193.

[6-29] Lau, S.M., 'The response of non-sway steel framed structures with semi-rigid connections', Ph.D. Thesis, Department of Civil & Structural Engineering, University of Sheffield, U.K., December, 1993.

[6-30] Anderson, D. and Tahir, M.M., 'Economic comparisons between simple and partial-strength design of braced frames', in Connections in Steel Structures III, Behaviour, Strength and Design, Proceedings of the Third International Workshop, Trento, Italy, May 1995, Pergamon, pp. 527-533.

[6-31] Bjorhovde, R., 'Effect of end restraint on column strength - Practical applications', Engineering Journal, American Institute of Steel Construction, First quarter, Vol. 21, No.1, 1984, pp. 1-13.

Frame type	Base type	Loaded beam no.	Studied column no.
Frame 1 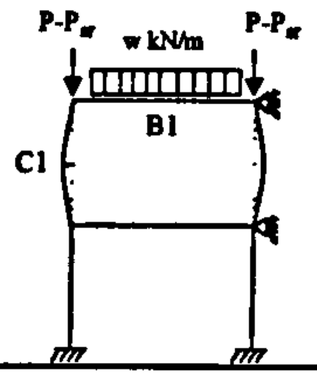	Rigid	B1	C1
Frame 2 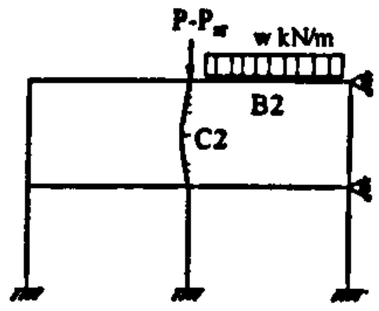	Rigid	B2	C2
Frame 3 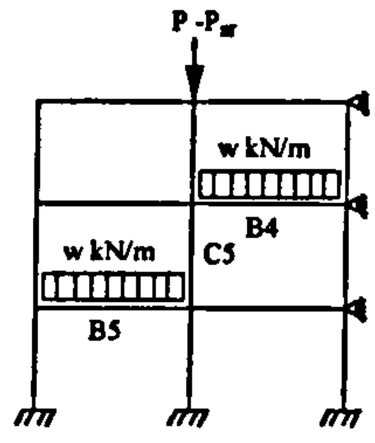	Rigid	B4 & B5	C5

Table 6.1 Loading combinations

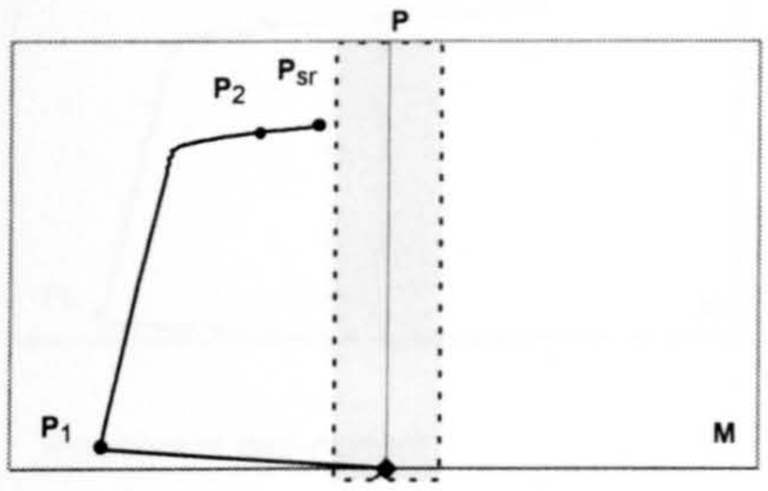

Response of load-moment

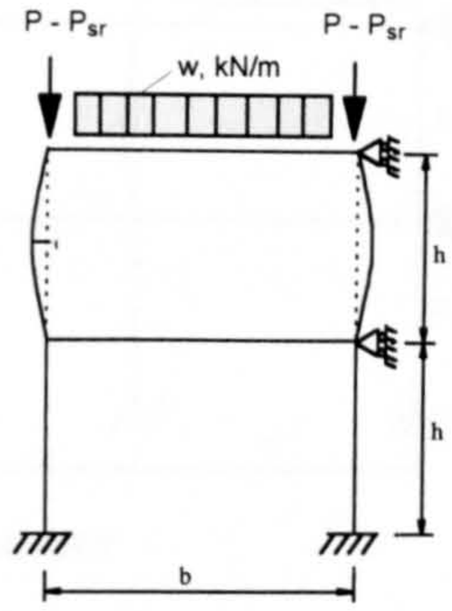

FRAME 1

For all frames :
w = 45 kN/m
h = 4m
b = 6m

Free moment = $wb^2/8$ =	202.5	kNm
Nominal beam plastic moment, M_p =	213	kNm
P_{pin} BS 5950 =	1530	kN

(a). Values of end restraint moment at P_1

Connection	Beam end Moment (kNm)	Elastic end restraint moment % of M_p
PDEP	10.2	4.8%
FEP	27.2	12.8%
EEP	51.7	24.3%
RIGID	58.4	27.4%

(b). Values of end restraint moment at P_2

Connection	P_2 (kN)	α_{pin} BS 5950	Beam end Moment (kNm)	Inelastic end restraint moment % of M_p	Suggested restraint moment % of M_p	Satisfy the suggested restraint moment
PDEP	1535	1.00	9.9	4.6%	**0%**	✓
FEP	1545	1.01	11.2	5.3%	**5%**	✓
EEP	1530	1.00	10.8	5.1%		✓
RIGID	1530	1.00	12.9	6.1%		✓

(c). Values of end restraint moment at P_{sr}

Connection	P_{sr} (kN)	α_{pin} BS 5950	Beam end Moment (kNm)	Inelastic end restraint moment % of M_p	Suggested restraint moment % of M_p	Satisfy the suggested restraint moment
PDEP	1590	1.04	8	3.8%	**0%**	✓
FEP	1560	1.02	9	4.2%	**5%**	X
EEP	1565	1.02	0.3	0.1%		X
RIGID	1585	1.04	0.64	0.3%		X

Table 6.2 Values of end restraint moment for external beams of frame 1

(a). Upper edge column (see Figure 6.25)

Connection	P_{sr} / P_y	λ_{pin}	λ_{sr}	$K = \lambda_{pin}/\lambda_{sr}$
PDEP, FEP	0.92	47	55	0.855
	0.83	68	85	0.800
RIGID	0.88	59	76.6	0.770
	0.84	66	89.4	0.738

(b). Upper intermediate column (see Figure 6.27)

Connection	P_{sr} / P_y	λ_{pin}	λ_{sr}	$K = \lambda_{pin}/\lambda_{sr}$
PDEP, FEP	0.95	40	64	0.625
	0.89	55	89	0.618
EEP, RIGID	0.95	40	76.6	0.522
	0.94	45	89.4	0.503

(c). Internal column (see Figure 6.28)

Connection	P_{sr} / P_y	λ_{pin}	λ_{sr}	$K = \lambda_{pin}/\lambda_{sr}$
PDEP, FEP	0.98	30	55	0.545
	0.91	51	89	0.573
EEP, RIGID	0.99	32	63.9	0.501
	0.97	40	76.6	0.522

Table 6.5 Calculation of effective length factor, K using beam-column strength curves

SUMMARY OF α_{pin} VALUES
UPPER EDGE COLUMN (C2)
Connection type : PDEP (Test 3)

Frame 1

b = 6 m

All beams
356 x 171 x 45 UB
Grade 43A

Upper columns
200 x 200 x 8 SHS
Grade 43A

Lower columns
200 x 200 x 10 SHS
Grade 43A

Beam elements = 4 nos.
Column elements = 4 nos.

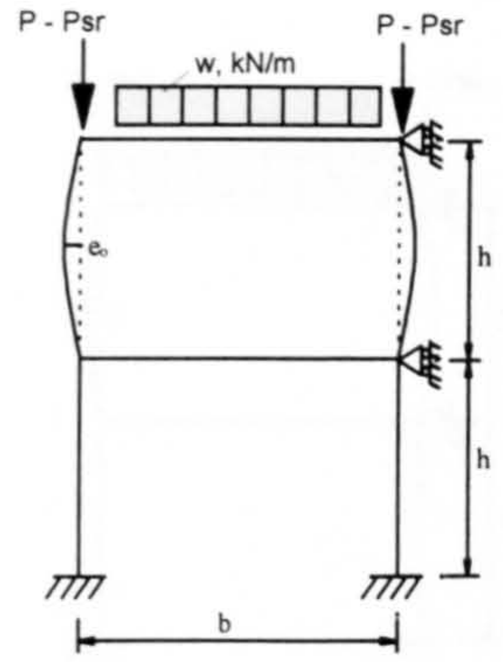

(a). P_{pin} BS5950 and P_{sr} with w = 30 kN/m

w = 30 kN/m			
	[1]	[2]	[1] / [2]
Storey height h (m)	P_{sr} SERIFA (kN)	**P_{pin} BS 5950 (kN)**	α_{pin}
2	1655	**1650**	1.00
3	1635	**1600**	1.02
4	1615	**1530**	1.06
5	1585	**1430**	1.11
6	1550	**1290**	1.20
7	1500	**1110**	1.35

(b). P_{pin} BS5950 and P_{sr} with w = 45 kN/m

w = 45 kN/m			
	[1]	[2]	[1] / [2]
Storey height h (m)	P_{sr} SERIFA (kN)	**P_{pin} BS 5950 (kN)**	α_{pin}
2	1640	**1650**	0.99
3	1620	**1600**	1.01
4	1590	**1530**	1.04
5	1560	**1430**	1.09
6	1515	**1290**	1.17
7	1455	**1110**	1.31

(c). P_{pin} EC3 and P_{sr} with w = 30 kN/m

w = 30 kN/m			
	[1]	[2]	[1] / [2]
Storey height h (m)	P_{sr} SERIFA (kN)	**P_{pin} EC3 (kN)**	α_{pin}
2	1655	**1565**	1.06
3	1635	**1504**	1.09
4	1615	**1427**	1.13
5	1585	**1323**	1.20
6	1550	**1186**	1.31
7	1500	**1024**	1.46

(d). P_{pin} EC3 and P_{sr} with w = 45 kN/m

w = 45 kN/m			
	[1]	[2]	[1] / [2]
Storey height h (m)	P_{sr} SERIFA (kN)	**P_{pin} EC3 (kN)**	α_{pin}
2	1640	**1565**	1.05
3	1620	**1504**	1.08
4	1590	**1427**	1.11
5	1560	**1323**	1.18
6	1515	**1186**	1.28
7	1455	**1024**	1.42

Table 6.6 Values of α_{pin} of upper edge columns with PDEP connections

SUMMARY OF α_{pin} VALUES
UPPER EDGE COLUMN (C1)
Connection type : FEP (Test 18)

Frame 1

b = 6 m

All beams
356 x 171 x 45 UB
Grade 43A

Upper columns
200 x 200 x 8 SHS
Grade 43A

Lower columns
200 x 200 x 10 SHS
Grade 43A

Beam elements = 4 nos.
Column elements = 4 nos.

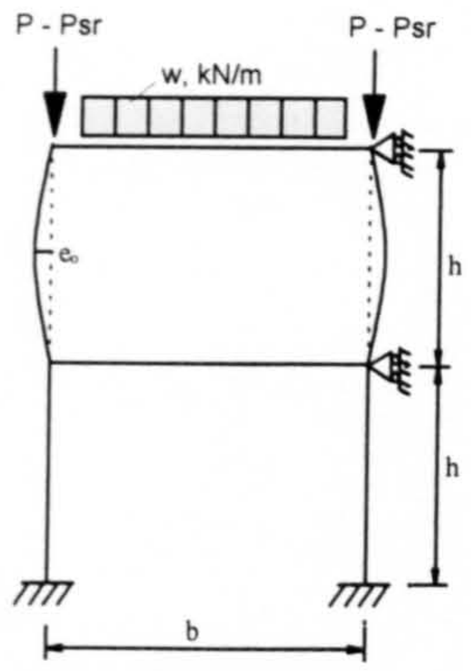

(a). P_{pin} BS5950 and P_{sr} with w = 30 kN/m

w = 30 kN/m			
	[1]	[2]	[1] / [2]
Storey height h (m)	P_{sr} SERIFA (kN)	**P_{pin} BS 5950 (kN)**	α_{pin}
2	1660	**1650**	1.01
3	1630	**1600**	1.02
4	1595	**1530**	1.04
5	1550	**1430**	1.08
6	1505	**1290**	1.17
7	1455	**1110**	1.31

(b). P_{pin} BS5950 and P_{sr} with w = 45 kN/m

w = 45 kN/m			
	[1]	[2]	[1] / [2]
Storey height h (m)	P_{sr} SERIFA (kN)	**P_{pin} BS 5950 (kN)**	α_{pin}
2	1640	**1650**	0.99
3	1605	**1600**	1.00
4	1560	**1530**	1.02
5	1500	**1430**	1.05
6	1440	**1290**	1.12
7	1380	**1110**	1.24

(c). P_{pin} EC3 and P_{sr} with w = 30 kN/m

w = 30 kN/m			
	[1]	[2]	[1] / [2]
Storey height h (m)	P_{sr} SERIFA (kN)	**P_{pin} EC3 (kN)**	α_{pin}
2	1660	**1565**	1.06
3	1630	**1504**	1.08
4	1595	**1427**	1.12
5	1550	**1323**	1.17
6	1505	**1186**	1.27
7	1455	**1024**	1.42

(d). P_{pin} EC3 and P_{sr} with w = 45 kN/m

w = 45 kN/m			
	[1]	[2]	[1] / [2]
Storey height h (m)	P_{sr} SERIFA (kN)	**P_{pin} EC3 (kN)**	α_{pin}
2	1635	**1565**	1.04
3	1605	**1504**	1.07
4	1560	**1427**	1.09
5	1500	**1323**	1.13
6	1440	**1186**	1.21
7	1380	**1024**	1.35

Table 6.7 Values of α_{pin} of upper edge columns with FEP connections

SUMMARY OF α_{pin} VALUES
UPPER EDGE COLUMN (C1)
Connection type : EEP (Test 19)

Frame 1

b = 6 m

All beams
356 x 171 x 45 UB
Grade 43A

Upper columns
200 x 200 x 8 SHS
Grade 43A

Lower columns
200 x 200 x 10 SHS
Grade 43A

Beam elements = 4 nos.
Column elements = 4 nos.

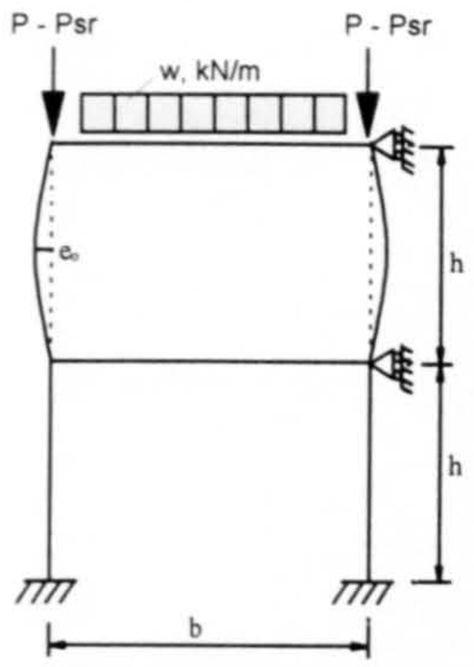

(a). P_{pin} BS5950 and P_{sr} with w = 30 kN/m

(w = 30 kN/m			
	[1]	[2]	[1] / [2]
Storey height h (m)	P_{sr} SERIFA (kN)	**P_{pin} BS 5950 (kN)**	α_{pin}
2	1670	**1650**	1.01
3	1650	**1600**	1.03
4	1620	**1530**	1.06
5	1575	**1430**	1.10
6	1520	**1290**	1.18
7	1465	**1110**	1.32

(b). P_{pin} BS5950 and P_{sr} with w = 45 kN/m

w = 45 kN/m			
	[1]	[2]	[1] / [2]
Storey height h (m)	P_{sr} SERIFA (kN)	**P_{pin} BS 5950 (kN)**	α_{pin}
2	1640	**1650**	0.99
3	1605	**1600**	1.00
4	1565	**1530**	1.02
5	1505	**1430**	1.05
6	1435	**1290**	1.11
7	1370	**1110**	1.23

(c). P_{pin} EC3 and P_{sr} with w = 30 kN/m

w = 30 kN/m			
	[1]	[2]	[1] / [2]
Storey height h (m)	P_{sr} SERIFA (kN)	**P_{pin} EC3 (kN)**	α_{pin}
2	1670	**1565**	1.07
3	1650	**1504**	1.10
4	1620	**1427**	1.14
5	1575	**1323**	1.19
6	1520	**1186**	1.28
7	1465	**1024**	1.43

(d). P_{pin} EC3 and P_{sr} with w = 45 kN/m

w = 45 kN/m			
	[1]	[2]	[1] / [2]
Storey height h (m)	P_{sr} SERIFA (kN)	**P_{pin} EC3 (kN)**	α_{pin}
2	1640	**1565**	1.05
3	1605	**1504**	1.07
4	1565	**1427**	1.10
5	1505	**1323**	1.14
6	1435	**1186**	1.21
7	1370	**1024**	1.34

Table 6.8 Values of α_{pin} of upper edge columns with EEP connections

After the detrimental negative moment is relaxed to zero, the moment will then act as a reverse moment (positive moment). This reversal of moment acts in the opposite direction to the column rotation. This in turn results in the column being restrained further at its ends.

It is also of interest to compare the response of moment shedding of the columns with respect to different slenderness ratios. In view of this, Figure 6.11(b) shows the comparison of moment shedding between the column with slenderness ratio of 51.1 and the columns with higher slenderness ratio of 89.4. For each slenderness ratio, four different connection types are utilised. It is seen that in the elastic range, irrespective of connection types used, the slopes of load-moment responses **A** to **B** are more gradual with the higher slenderness columns than the lower slenderness columns. This reflects the fact that in the elastic range, more rapid moment shedding occurs in the slender columns. This is because the slender columns tend to have more appreciable loss of elastic stiffness with increasing axial load as shown in the gradual load-deflection response **A** to **B** of Figure 6.11(a).

The results of the comparison suggest that:

- The rate of moment shedding is dependent on the rate of stiffness loss. The more rapid is the loss of stiffness, the quicker is the rate of moment shedding.

- Columns with higher slenderness tend to have higher stiffness loss in the elastic range due to geometric deformation. Hence, it can be concluded that the higher the slenderness of the columns the more rapid is the rate of moment shedding.

As a result of a smaller detrimental moment and rapid rate of moment shedding, a slender column will undergo a large restraining moment effect at the collapse load level. This suggests that the more slender columns tend to have larger restraining effect from the reversal of moment. This behaviour is also noted by Gent and Milner [6-7].

SUMMARY OF α_{pin} VALUES
UPPER INTERMEDIATE COLUMN (C2)
Connection type : PDEP (Test 3)

Frame 2

b = 6m

All beams
356 x 171 x 45 UB
Grade 43A

Upper columns
200 x 200 x 8 SHS
Grade 43A

Lower columns
200 x 200 x 10 SHS
Grade 43A

Beam elements = 4 nos.
Column elements = 4 nos.

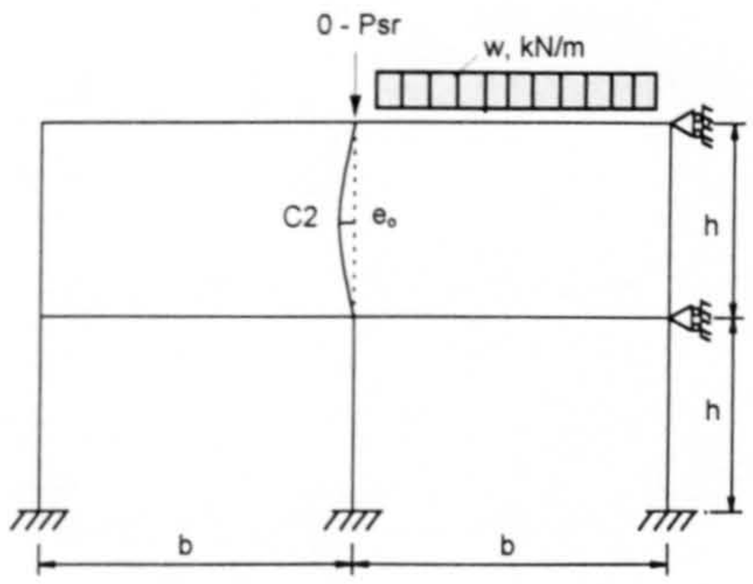

(a). P_{pin} BS5950 and P_{sr} with w = 30 kN/m

w = 30 kN/m			
	[1]	[2]	[1] / [2]
Storey height h (m)	P_{sr} SERIFA (kN)	**P_{pin} BS 5950 (kN)**	α_{pin}
2	1659	**1650**	1.01
3	1645	**1600**	1.03
4	1625	**1530**	1.06
5	1610	**1430**	1.13
6	1590	**1290**	1.23
7	1560	**1110**	1.41

(b). P_{pin} BS5950 and P_{sr} with w = 45 kN/m

w = 45 kN/m			
	[1]	[2]	[1] / [2]
Storey height h (m)	P_{sr} SERIFA (kN)	**P_{pin} BS 5950 (kN)**	α_{pin}
2	1650	**1650**	1.00
3	1635	**1600**	1.02
4	1605	**1530**	1.05
5	1585	**1430**	1.11
6	1560	**1290**	1.21
7	1525	**1110**	1.37

(c). P_{pin} EC3 and P_{sr} with w = 30 kN/m

w = 30 kN/m			
	[1]	[2]	[1] / [2]
Storey height h (m)	P_{sr} SERIFA (kN)	**P_{pin} EC3 (kN)**	α_{pin}
2	1659	**1565**	1.06
3	1645	**1504**	1.09
4	1625	**1427**	1.14
5	1610	**1323**	1.22
6	1590	**1186**	1.34
7	1560	**1024**	1.52

(d). P_{pin} EC3 and P_{sr} with w = 45 kN/m

w = 45 kN/m			
	[1]	[2]	[1] / [2]
Storey height h (m)	P_{sr} SERIFA (kN)	**P_{pin} EC3 (kN)**	α_{pin}
2	1650	**1565**	1.05
3	1635	**1504**	1.09
4	1605	**1427**	1.12
5	1585	**1323**	1.20
6	1560	**1186**	1.32
7	1525	**1024**	1.49

Table 6.10 Values of α_{pin} of upper intermediate columns with PDEP connections

SUMMARY OF α_{pin} VALUES
UPPER INTERMEDIATE COLUMN (C2)
Connection type : FEP (Test 18)

Frame 2

b = 6m

All beams
356 x 171 x 45 UB
Grade 43A

Upper columns
200 x 200 x 8 SHS
Grade 43A

Lower columns
200 x 200 x 10 SHS
Grade 43A

Beam elements = 4 nos.
Column elements = 4 nos.

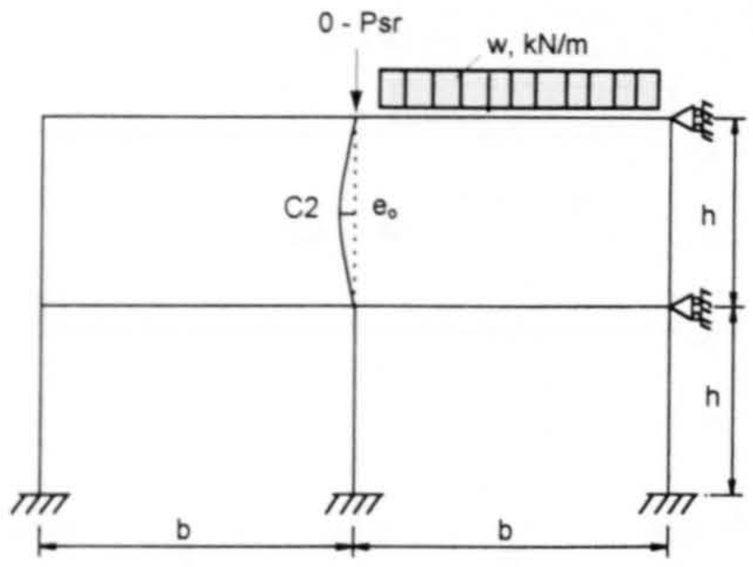

(a). P_{pin} BS5950 and P_{sr} with w = 30 kN/m

w = 30 kN/m			
	[1]	[2]	[1] / [2]
Storey height h (m)	P_{sr} SERIFA (kN)	**P_{pin} BS 5950 (kN)**	α_{pin}
2	1670	**1650**	1.01
3	1660	**1600**	1.04
4	1642	**1530**	1.07
5	1615	**1430**	1.13
6	1590	**1290**	1.23
7	1560	**1110**	1.41

(b). P_{pin} BS5950 and P_{sr} with w = 45 kN/m

w = 45 kN/m			
	[1]	[2]	[1] / [2]
Storey height h (m)	P_{sr} SERIFA (kN)	**P_{pin} BS 5950 (kN)**	α_{pin}
2	1670	**1650**	1.01
3	1656	**1600**	1.04
4	1630	**1530**	1.07
5	1590	**1430**	1.11
6	1548	**1290**	1.20
7	1504	**1110**	1.35

(c). P_{pin} EC3 and P_{sr} with w = 30 kN/m

w = 30 kN/m			
	[1]	[2]	[1] / [2]
Storey height h (m)	P_{sr} SERIFA (kN)	**P_{pin} EC3 (kN)**	α_{pin}
2	1670	**1565**	1.07
3	1660	**1504**	1.10
4	1642	**1427**	1.15
5	1615	**1323**	1.22
6	1590	**1186**	1.34
7	1560	**1024**	1.52

(d). P_{pin} EC3 and P_{sr} with w = 45 kN/m

w = 45 kN/m			
	[1]	[2]	[1] / [2]
Storey height h (m)	P_{sr} SERIFA (kN)	**P_{pin} EC3 (kN)**	α_{pin}
2	1670	**1565**	1.07
3	1656	**1504**	1.10
4	1630	**1427**	1.14
5	1590	**1323**	1.20
6	1548	**1186**	1.31
7	1504	**1024**	1.47

Table 6.11 Values of α_{pin} of upper intermediate columns with FEP connections

SUMMARY OF α_{pin} VALUES
UPPER INTERMEDIATE COLUMN (C2)
Connection type : EEP (Test 19)

Frame 2

b = 6m

All beams
356 x 171 x 45 UB
Grade 43A

Upper columns
200 x 200 x 8 SHS
Grade 43A

Lower columns
200 x 200 x 10 SHS
Grade 43A

Beam elements = 4 nos.
Column elements = 4 nos.

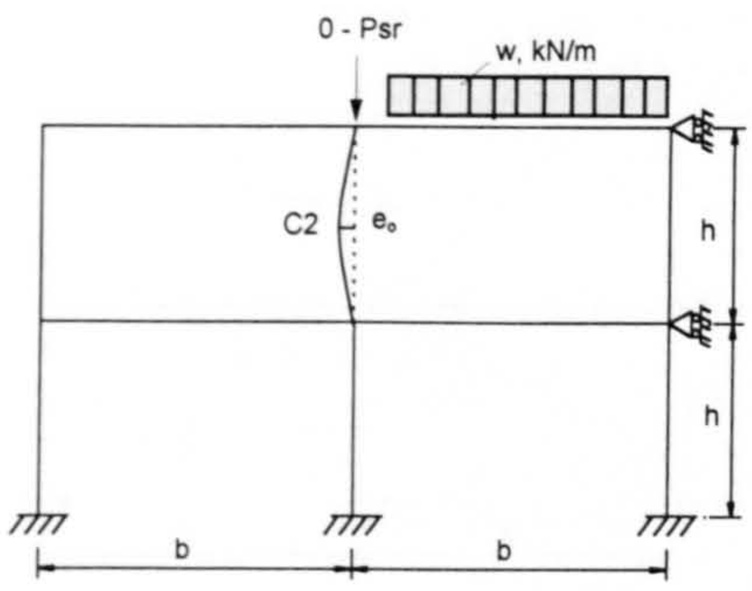

(a). P_{pin} BS5950 and P_{sr} with w = 30 kN/m

(w = 30 kN/m			
	[1]	[2]	[1] / [2]
Storey height h (m)	P_{sr} SERIFA (kN)	**P_{pin} BS 5950 (kN)**	α_{pin}
2	1675	**1650**	1.02
3	1670	**1600**	1.04
4	1655	**1530**	1.08
5	1640	**1430**	1.15
6	1620	**1290**	1.26
7	1590	**1110**	1.43

(b). P_{pin} BS5950 and P_{sr} with w = 45 kN/m

w = 45 kN/m			
	[1]	[2]	[1] / [2]
Storey height h (m)	P_{sr} SERIFA (kN)	**P_{pin} BS 5950 (kN)**	α_{pin}
2	1675	**1650**	1.02
3	1660	**1600**	1.04
4	1645	**1530**	1.08
5	1620	**1430**	1.13
6	1590	**1290**	1.23
7	1550	**1110**	1.40

(c). P_{pin} EC3 and P_{sr} with w = 30 kN/m

w = 30 kN/m			
	[1]	[2]	[1] / [2]
Storey height h (m)	P_{sr} SERIFA (kN)	**P_{pin} EC3 (kN)**	α_{pin}
2	1675	**1565**	1.07
3	1670	**1504**	1.11
4	1655	**1427**	1.16
5	1640	**1323**	1.24
6	1620	**1186**	1.37
7	1590	**1024**	1.55

(d). P_{pin} EC3 and P_{sr} with w = 45 kN/m

w = 45 kN/m			
	[1]	[2]	[1] / [2]
Storey height h (m)	P_{sr} SERIFA (kN)	**P_{pin} EC3 (kN)**	α_{pin}
2	1675	**1565**	1.07
3	1660	**1504**	1.10
4	1645	**1427**	1.15
5	1620	**1323**	1.22
6	1590	**1186**	1.34
7	1550	**1024**	1.51

Table 6.12 Values of α_{pin} of upper intermediate columns with EEP connections

SUMMARY OF α_{pin} VALUES
UPPER INTERMEDIATE COLUMN (C2)
Connection type : RIGID

Frame 2

b = 6m

All beams
356 x 171 x 45 UB
Grade 43A

Upper columns
200 x 200 x 8 SHS
Grade 43A

Lower columns
200 x 200 x 10 SHS
Grade 43A

Beam elements = 4 nos.
Column elements = 4 nos.

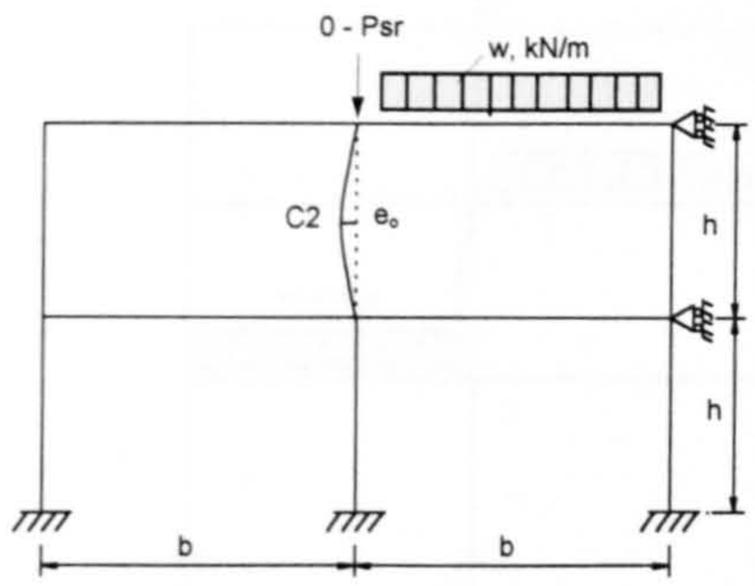

(a). P_{pin} BS5950 and P_{sr} with w = 30 kN/m

w = 30 kN/m			
	[1]	[2]	[1] / [2]
Storey height h (m)	P_{sr} SERIFA (kN)	**P_{pin} BS 5950 (kN)**	α_{pin}
2	1675	**1650**	1.02
3	1670	**1600**	1.04
4	1660	**1530**	1.08
5	1645	**1430**	1.15
6	1625	**1290**	1.26
7	1600	**1110**	1.44

(b). P_{pin} BS5950 and P_{sr} with w = 45 kN/m

w = 45 kN/m			
	[1]	[2]	[1] / [2]
Storey height h (m)	P_{sr} SERIFA (kN)	**P_{pin} BS 5950 (kN)**	α_{pin}
2	1665	**1650**	1.01
3	1660	**1600**	1.04
4	1645	**1530**	1.08
5	1625	**1430**	1.14
6	1595	**1290**	1.24
7	1560	**1110**	1.41

(c). P_{pin} EC3 and P_{sr} with w = 30 kN/m

w = 30 kN/m			
	[1]	[2]	[1] / [2]
Storey height h (m)	P_{sr} SERIFA (kN)	**P_{pin} EC3 (kN)**	α_{pin}
2	1675	**1565**	1.07
3	1670	**1504**	1.11
4	1660	**1427**	1.16
5	1645	**1323**	1.24
6	1625	**1186**	1.37
7	1600	**1024**	1.56

(d). P_{pin} EC3 and P_{sr} with w = 45 kN/m

w = 45 kN/m			
	[1]	[2]	[1] / [2]
Storey height h (m)	P_{sr} SERIFA (kN)	**P_{pin} EC3 (kN)**	α_{pin}
2	1665	**1565**	1.06
3	1660	**1504**	1.10
4	1645	**1427**	1.15
5	1625	**1323**	1.23
6	1595	**1186**	1.34
7	1560	**1024**	1.52

Table 6.13 Values of α_{pin} of upper intermediate columns with RIGID connections

SUMMARY OF α_{pin} VALUES
INTERMEDIATE COLUMN (C5)
Connection type : PDEP (Test 3)

b = 6m

All beams
356 x 171 x 45 UB
Grade 43A

2nd & 3rd storey columns
200 x 200 x 8 SHS
Grade 43A

1st storey columns
200 x 200 x 10 SHS
Grade 43A

Beam elements = 4 nos.
Column elements = 4 nos.

Frame 3

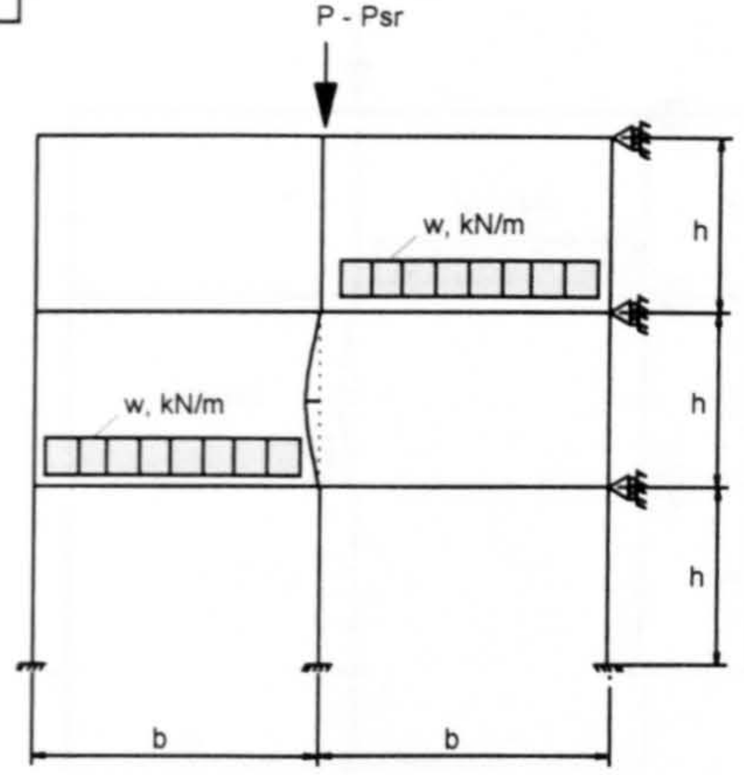

(a). P_{pin} BS5950 and P_{sr} without offset model

w = 45 kN/m			
	[1]	[2]	[1] / [2]
Storey height h (m)	P_{sr} SERIFA (kN)	**P_{pin} BS 5950 (kN)**	α_{pin}
2	1680	**1650**	1.02
3	1675	**1600**	1.05
4	1660	**1530**	1.08
5	1635	**1430**	1.14
6	1595	**1290**	1.24
7	1535	**1110**	1.38

(b). P_{pin} BS5950 and P_{sr} with offset model

w=45 kN/m			
	[1]	[2]	[1] / [2]
Storey height h (m)	P_{sr} SERIFA (kN)	**P_{pin} BS 5950 (kN)**	α_{pin}
2	1660	**1650**	1.01
3	1645	**1600**	1.03
4	1620	**1530**	1.06
5	1585	**1430**	1.11
6	1525	**1290**	1.18
7	1455	**1110**	1.31

(c). P_{pin} EC3 and P_{sr} without offset model

w = 45 kN/m			
	[1]	[2]	[1] / [2]
Storey height h (m)	P_{sr} SERIFA (kN)	**P_{pin} EC3 (kN)**	α_{pin}
2	1680	**1565**	1.07
3	1675	**1504**	1.11
4	1660	**1427**	1.16
5	1635	**1323**	1.24
6	1595	**1186**	1.34
7	1535	**1024**	1.50

(d). P_{pin} EC3 and P_{sr} with offset model

w=45 kN/m			
	[1]	[2]	[1] / [2]
Storey height h (m)	P_{sr} SERIFA (kN)	**P_{pin} EC3 (kN)**	α_{pin}
2	1660	**1565**	1.06
3	1645	**1504**	1.09
4	1620	**1427**	1.14
5	1585	**1323**	1.20
6	1525	**1186**	1.29
7	1455	**1024**	1.42

Table 6.14 Values of α_{pin} of internal columns with PDEP connections

SUMMARY OF α_{pin} VALUES
INTERMEDIATE COLUMN (C5)
Connection type : FEP (Test 18)

b = 6m

All beams
356 x 171 x 45 UB
Grade 43A

2nd & 3rd storey columns
200 x 200 x 8 SHS
Grade 43A

1st storey columns
200 x 200 x 10 SHS
Grade 43A

Beam elements = 4 nos.
Column elements = 4 nos.

Frame 3

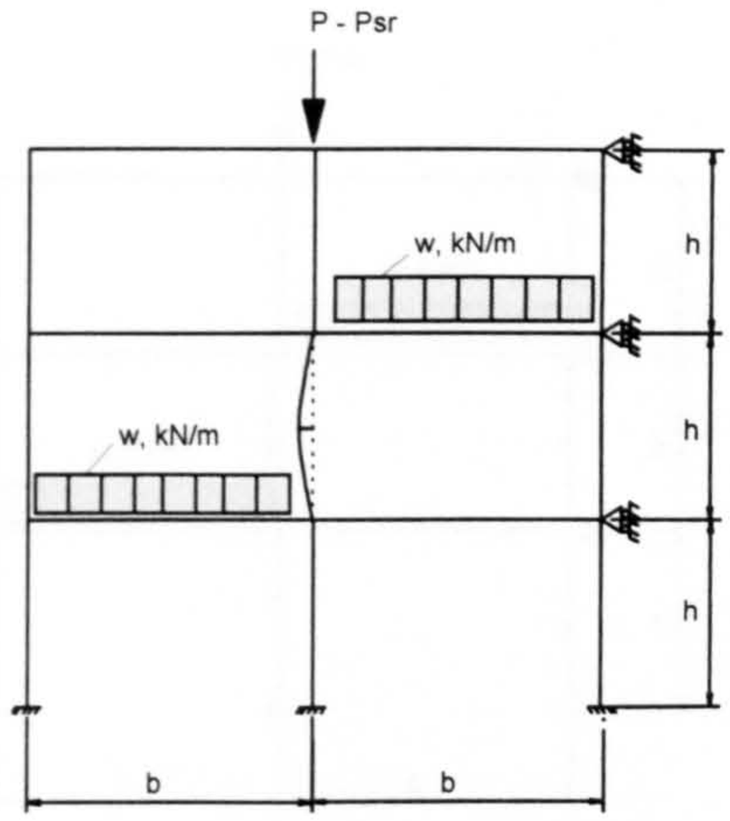

(a). P_{pin} BS5950 and P_{sr} without offset model

w = 45 kN/m			
	[1]	[2]	[1] / [2]
Storey height h (m)	P_{sr} SERIFA (kN)	**P_{pin} BS 5950 (kN)**	α_{pin}
2	1675	**1650**	1.02
3	1660	**1600**	1.04
4	1640	**1530**	1.07
5	1610	**1430**	1.13
6	1575	**1290**	1.22
7	1530	**1110**	1.38

(b). P_{pin} BS5950 and P_{sr} with offset model

w = 45 kN/m			
	[1]	[2]	[1] / [2]
Storey height h (m)	P_{sr} SERIFA (kN)	**P_{pin} BS 5950 (kN)**	α_{pin}
2	1665	**1650**	1.01
3	1650	**1600**	1.03
4	1621	**1530**	1.06
5	1590	**1430**	1.11
6	1550	**1290**	1.20
7	1495	**1110**	1.35

(c). P_{pin} EC3 and P_{sr} without offset model

w = 45 kN/m			
	[1]	[2]	[1] / [2]
Storey height h (m)	P_{sr} SERIFA (kN)	**P_{pin} EC3 (kN)**	α_{pin}
2	1675	**1565**	1.07
3	1660	**1504**	1.10
4	1640	**1427**	1.15
5	1610	**1323**	1.22
6	1575	**1186**	1.33
7	1530	**1024**	1.49

(d). P_{pin} EC3 and P_{sr} with offset model

w = 45 kN/m			
	[1]	[2]	[1] / [2]
Storey height h (m)	P_{sr} SERIFA (kN)	**P_{pin} EC3 (kN)**	α_{pin}
2	1665	**1565**	1.06
3	1650	**1504**	1.10
4	1621	**1427**	1.14
5	1590	**1323**	1.20
6	1550	**1186**	1.31
7	1495	**1024**	1.46

Table 6.15 Values of α_{pin} of internal columns with FEP connections

SUMMARY OF α_{pin} VALUES
INTERMEDIATE COLUMN (C5)
Connection type : EEP (Test 19)

Frame 3

b = 6m

All beams
356 x 171 x 45 UB
Grade 43A

2nd & 3rd storey columns
200 x 200 x 8 SHS
Grade 43A

1st storey columns
200 x 200 x 10 SHS
Grade 43A

Beam elements = 4 nos.
Column elements = 4 nos.

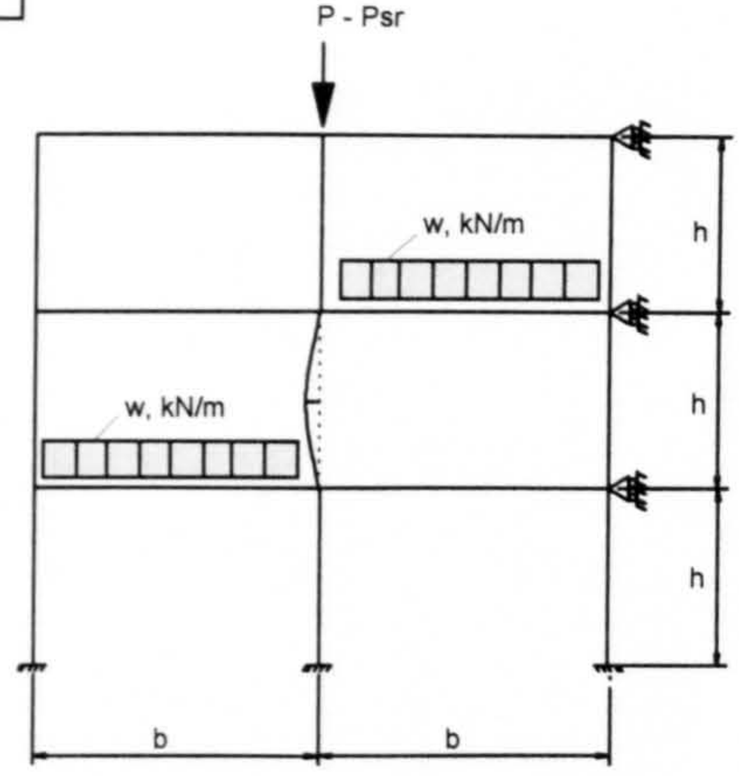

(a). P_{pin} BS 5950 and P_{sr} without offset model

w = 45 kN/m			
	[1]	[2]	[1] / [2]
Storey height h (m)	P_{sr} SERIFA (kN)	**P_{pin} BS 5950 (kN)**	α_{pin}
2	1675	**1650**	1.02
3	1665	**1600**	1.04
4	1650	**1530**	1.08
5	1625	**1430**	1.14
6	1600	**1290**	1.24
7	1565	**1110**	1.41

(b). P_{pin} BS 5950 and P_{sr} with offset model

w = 45 kN/m			
	[1]	[2]	[1] / [2]
Storey height h (m)	P_{sr} SERIFA (kN)	**P_{pin} BS 5950 (kN)**	α_{pin}
2	1675	**1650**	1.02
3	1660	**1600**	1.04
4	1645	**1530**	1.07
5	1620	**1430**	1.13
6	1590	**1290**	1.23
7	1555	**1110**	1.40

(c). P_{pin} EC3 and P_{sr} without offset model

w = 45 kN/m			
	[1]	[2]	[1] / [2]
Storey height h (m)	P_{sr} SERIFA (kN)	**P_{pin} EC3 (kN)**	α_{pin}
2	1675	**1565**	1.07
3	1665	**1504**	1.11
4	1650	**1427**	1.16
5	1625	**1323**	1.23
6	1600	**1186**	1.35
7	1565	**1024**	1.53

(d). P_{pin} EC3 and P_{sr} with offset model

w = 45 kN/m			
	[1]	[2]	[1] / [2]
Storey height h (m)	P_{sr} SERIFA (kN)	**P_{pin} EC3 (kN)**	α_{pin}
2	1675	**1565**	1.07
3	1660	**1504**	1.10
4	1645	**1427**	1.15
5	1620	**1323**	1.22
6	1590	**1186**	1.34
7	1555	**1024**	1.52

Table 6.16 Values of α_{pin} of internal columns with EEP connections

SUMMARY OF α_{pin} VALUES
INTERMEDIATE COLUMN (C5)
Connection type : RIGID

Frame 3

b = 6m

All beams
356 x 171 x 45 UB
Grade 43A

2nd & 3rd storey columns
200 x 200 x 8 SHS
Grade 43A

1st storey columns
200 x 200 x 10 SHS
Grade 43A

Beam elements = 4 nos.
Column elements = 4 nos.

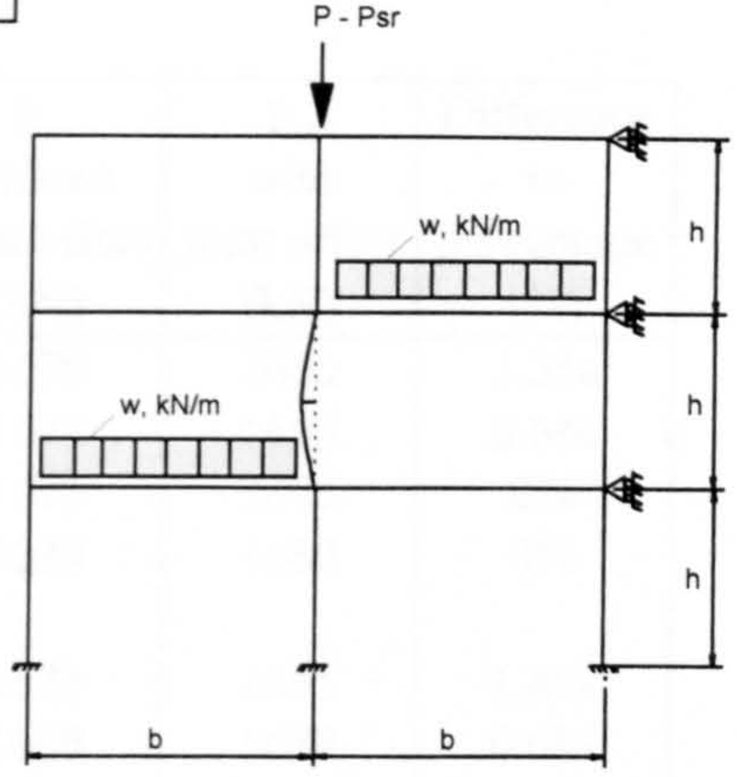

(a). P_{pin} BS 5950 and P_{sr} without offset model

w = 45 kN/m

Storey height h (m)	[1] P_{sr} SERIFA (kN)	[2] **P_{pin} BS 5950 (kN)**	[1] / [2] α_{pin}
2	1680	**1650**	1.02
3	1680	**1600**	1.05
4	1665	**1530**	1.09
5	1645	**1430**	1.15
6	1620	**1290**	1.26
7	1585	**1110**	1.43

(b). P_{pin} BS 5950 and P_{sr} with offset model

w = 45 kN/m

Storey height h (m)	[1] P_{sr} SERIFA (kN)	[2] **P_{pin} BS 5950 (kN)**	[1] / [2] α_{pin}
2	1680	**1650**	1.02
3	1675	**1600**	1.05
4	1660	**1530**	1.08
5	1640	**1430**	1.15
6	1615	**1290**	1.25
7	1580	**1110**	1.42

(c). P_{pin} EC3 and P_{sr} without offset model

w = 45 kN/m

Storey height h (m)	[1] P_{sr} SERIFA (kN)	[2] **P_{pin} EC3 (kN)**	[1] / [2] α_{pin}
2	1680	**1565**	1.07
3	1680	**1504**	1.12
4	1665	**1427**	1.17
5	1645	**1323**	1.24
6	1620	**1186**	1.37
7	1585	**1024**	1.55

(d). P_{pin} EC3 and P_{sr} with offset model

w = 45 kN/m

Storey height h (m)	[1] P_{sr} SERIFA (kN)	[2] **P_{pin} EC3 (kN)**	[1] / [2] α_{pin}
2	1680	**1565**	1.07
3	1675	**1504**	1.11
4	1660	**1427**	1.16
5	1640	**1323**	1.24
6	1615	**1186**	1.36
7	1580	**1024**	1.54

Table 6.17 Values of α_{pin} of internal columns with RIGID connections

Column height (m)	Connection type	P_{sr} without joint offset (kN)	P_{sr} with joint offset (kN)	Difference in percentage (%)
2	PDEP	1680	1660	1.2%
	FEP	1675	1665	0.6%
	EEP	1675	1675	0%
	RIGID	1680	1680	0%
3	PDEP	1675	1645	1.8%
	FEP	1660	1650	0.6%
	EEP	1665	1660	0.3%
	RIGID	1680	1675	0.3%
4	PDEP	1660	1620	2.4%
	FEP	1640	1621	1.2%
	EEP	1650	1645	0.3%
	RIGID	1665	1660	0.3%
5	PDEP	1635	1585	3.1%
	FEP	1610	1590	1.2%
	EEP	1625	1620	0.3%
	RIGID	1645	1640	0.3%
6	PDEP	1595	1525	4.4%
	FEP	1575	1550	1.6%
	EEP	1600	1590	0.6%
	RIGID	1620	1615	0.3%
7	PDEP	1535	1455	**5.2%**
	FEP	1530	1495	**2.3%**
	EEP	1565	1555	0.6%
	RIGID	1585	1580	0.3%

Table 6.18 The effect of joint offset to the ultimate strength of the columns with beam load of 45 kN/m

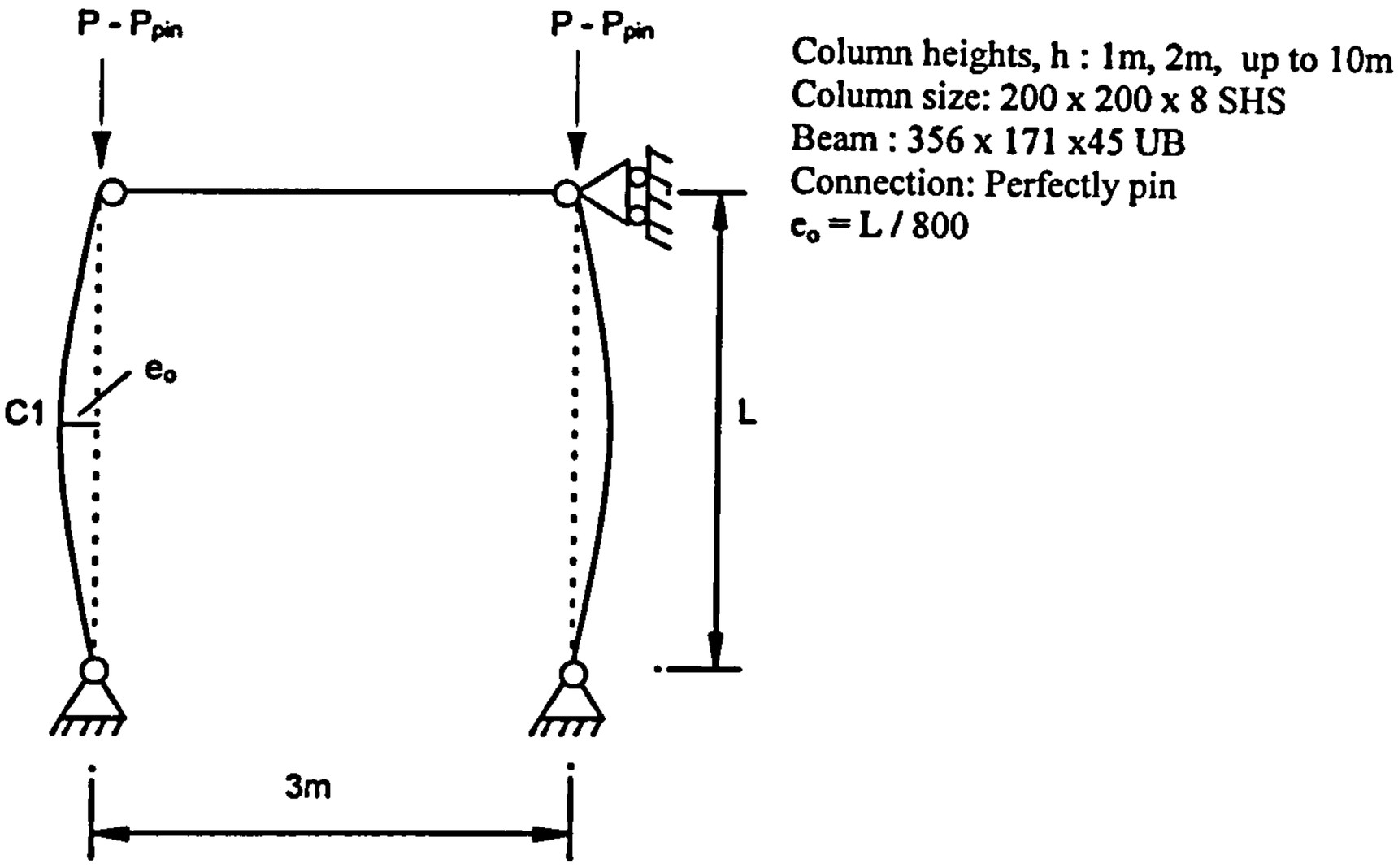

Column heights, h : 1m, 2m, up to 10m
Column size: 200 x 200 x 8 SHS
Beam : 356 x 171 x45 UB
Connection: Perfectly pin
$e_o = L / 800$

Figure 6.1 Portal frame model for determining P_{pin}

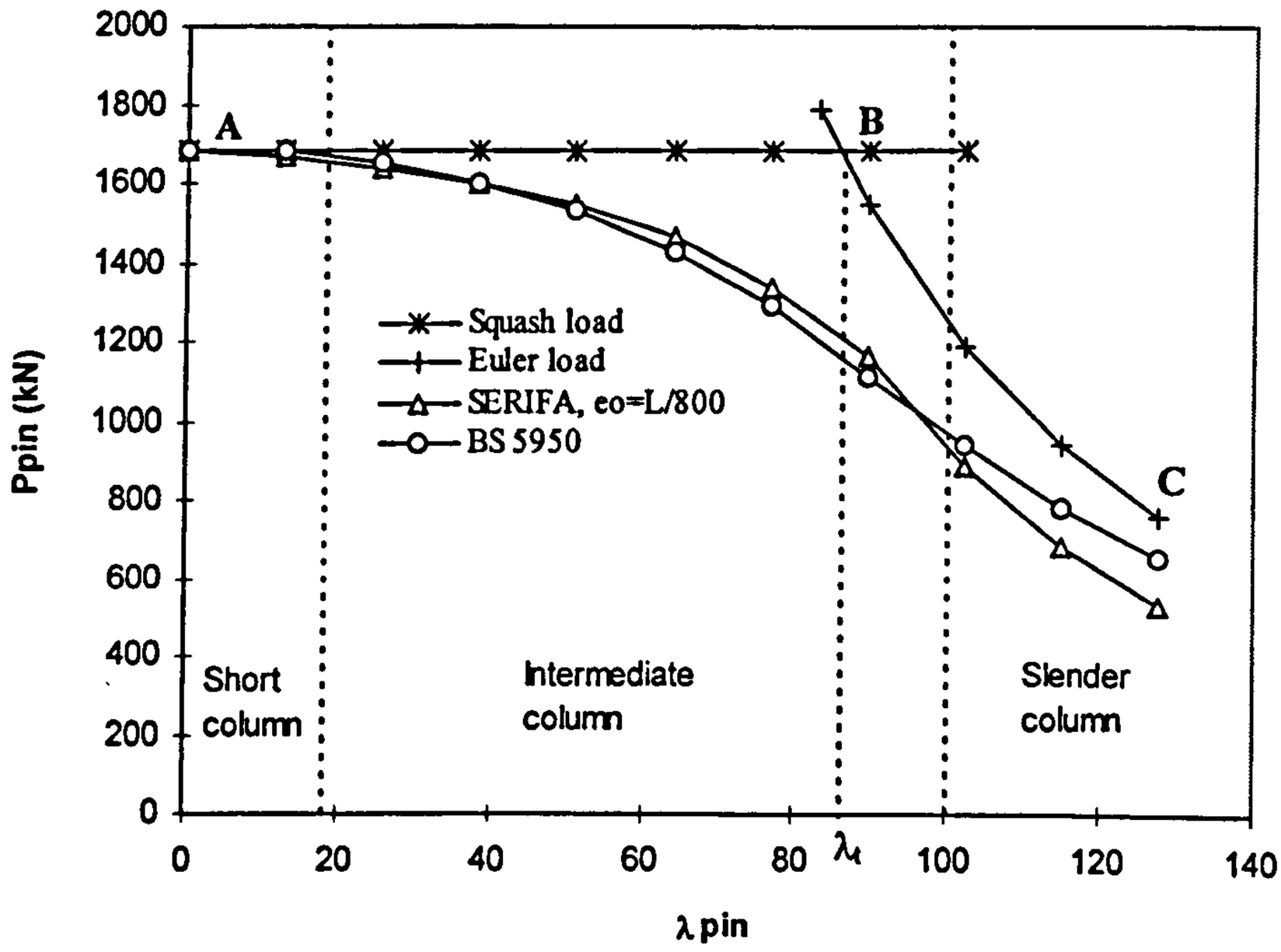

Figure 6.2 Strength curves of pin ended 200 x 200 x 8 SHS column

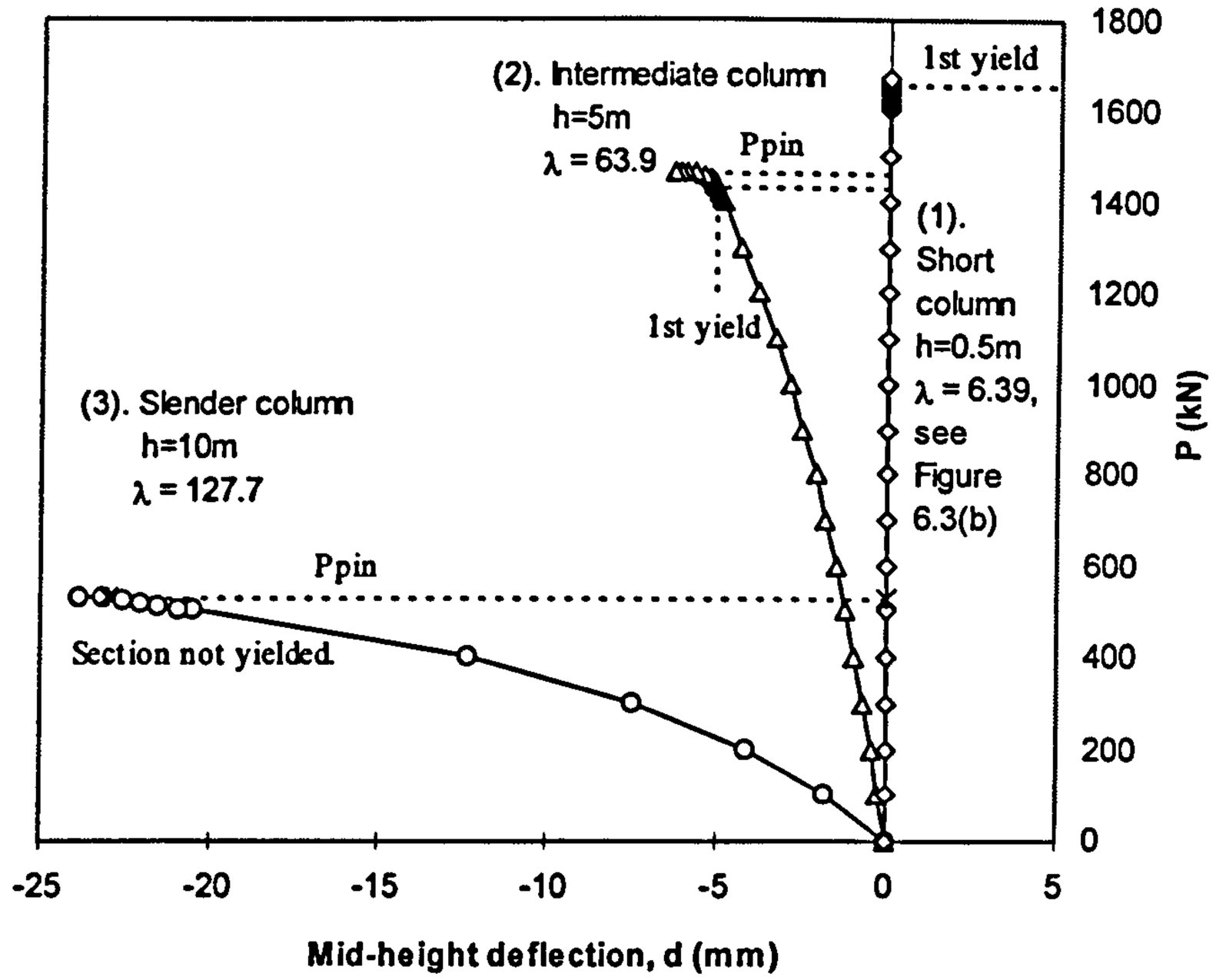

(a). Load-deflection responses of short, intermediate and slender columns

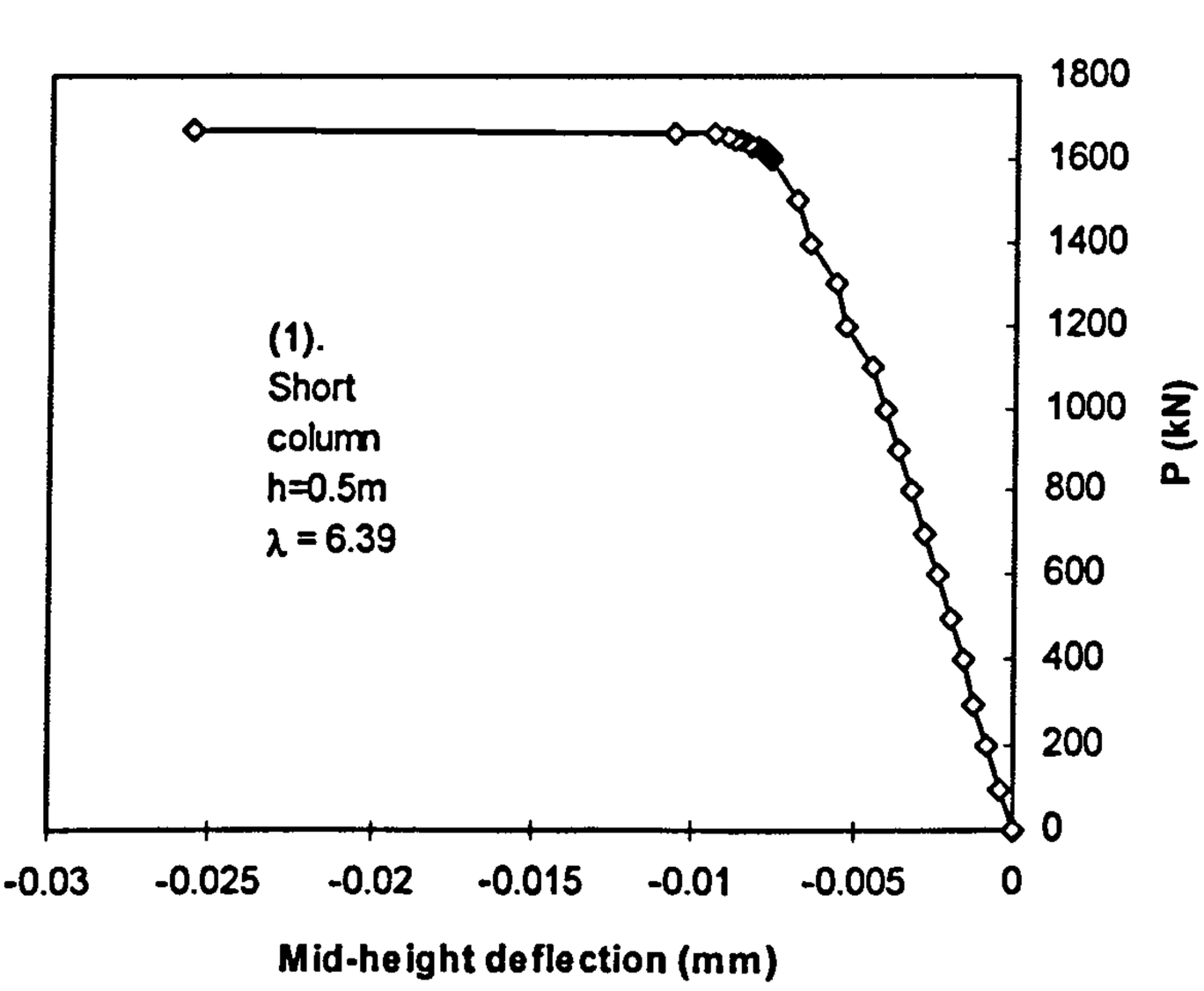

(b). Actual load-deflection response of the short column shown in Figure 6.3(a)

Figure 6.3 Load-deflection responses of pin ended columns

where:

d = mid-height deflection

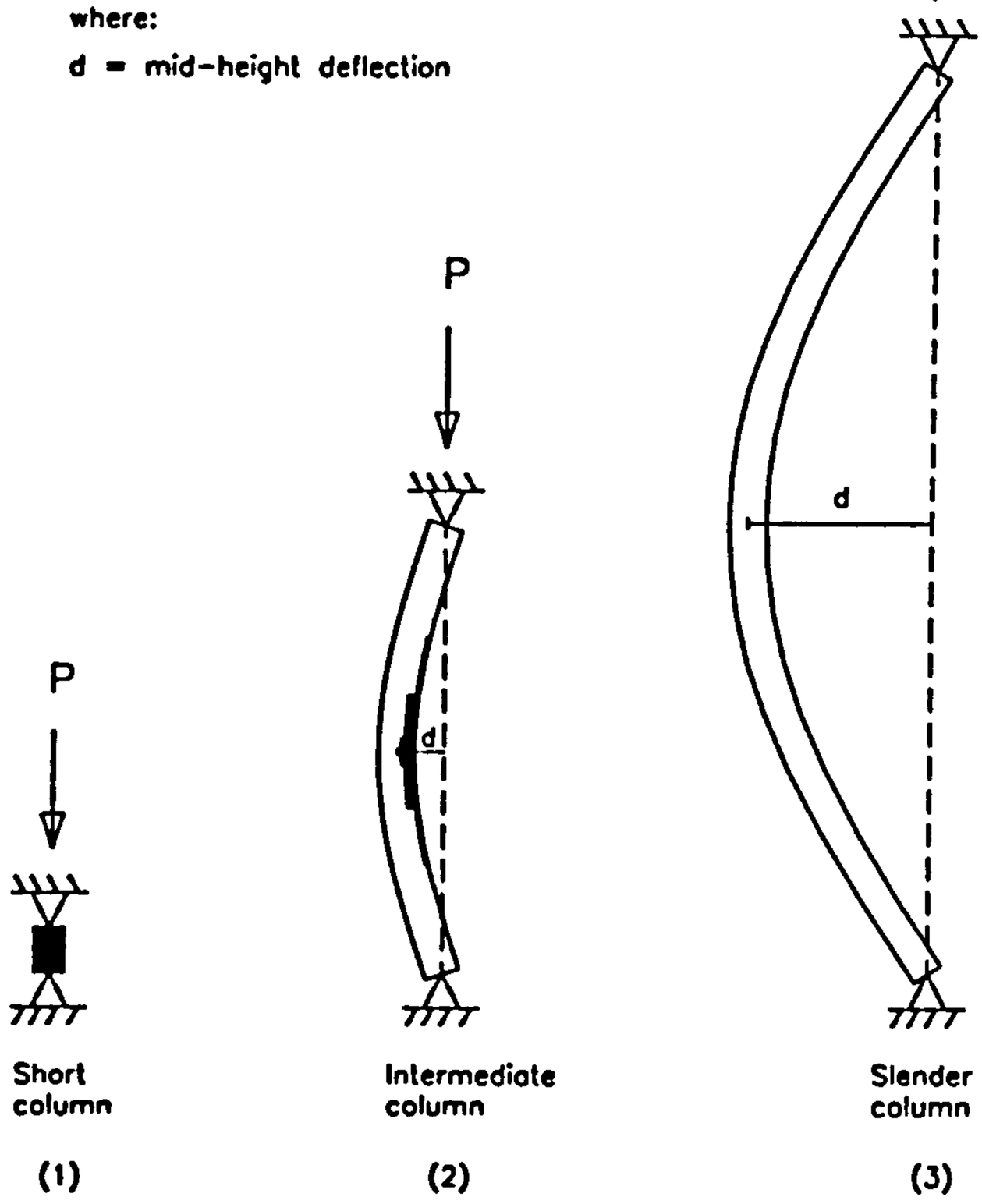

Figure 6.4 Failure modes of pin ended columns

(1). Squashing failure mode for 'short' column

(2). Elastic–plastic buckling mode for 'intermediate' column

(3). Elastic buckling mode for 'slender' column

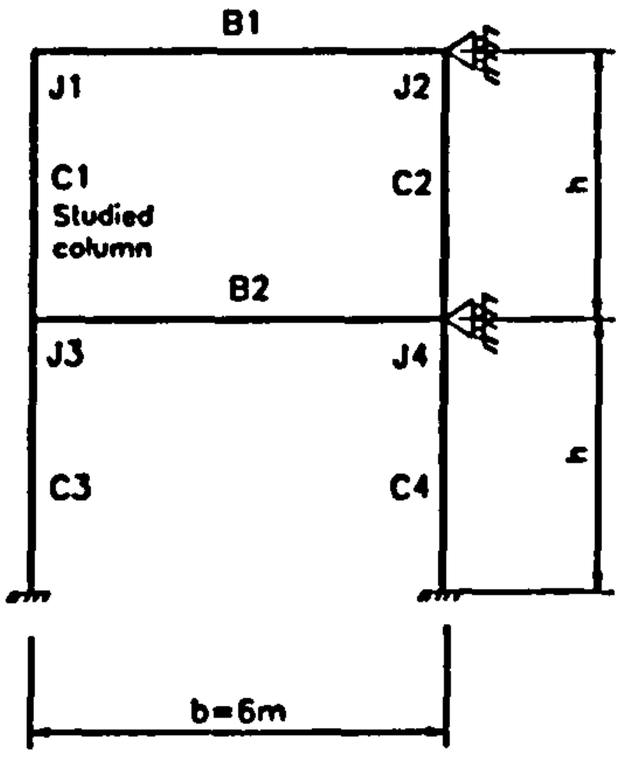

(a). Frame 1

All columns 200 x 200 x 8 SHS
All beams 356 x 171 x 45 UB
Steel grade 43A

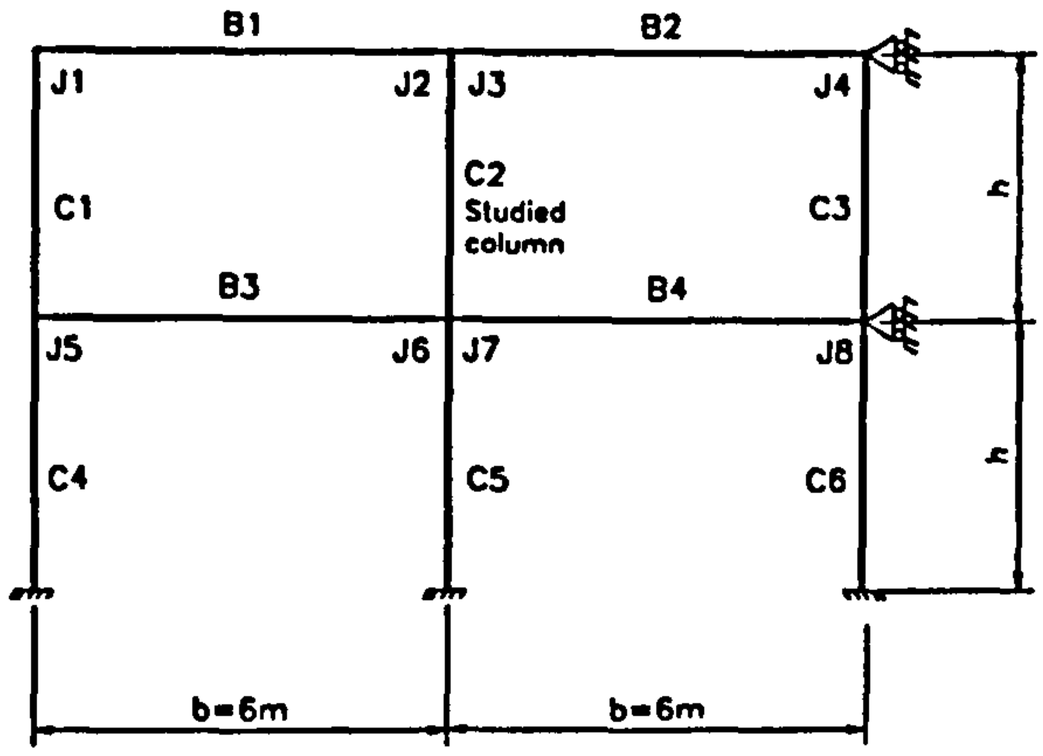

(b). Frome 2

First storey columns : 200 x 200 x 10 SHS
Other columns : 200 x 200 x 8 SHS
All beams 356 x 171 x 45 UB
Steel grade 43A

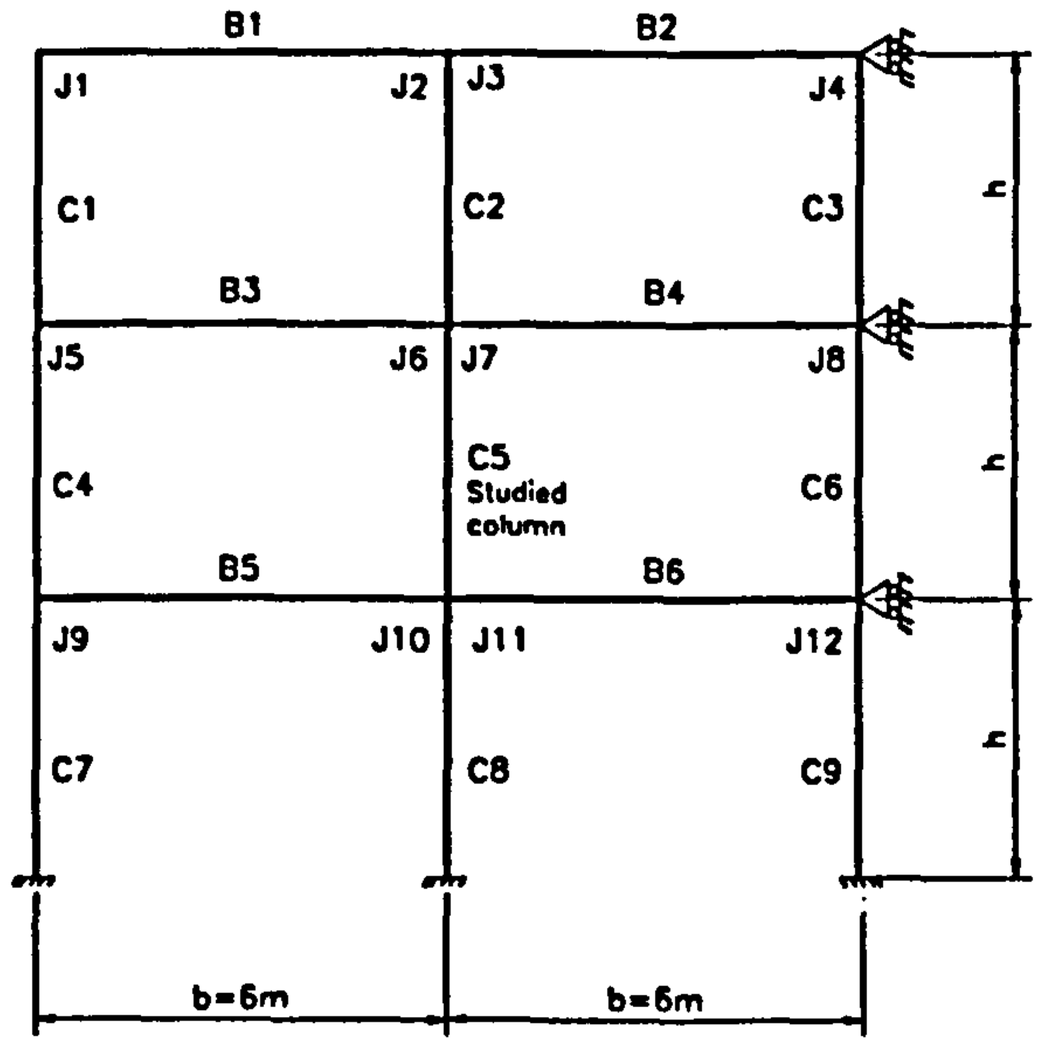

Notation:
B : Beam
C : Column
J : Connection
b : bay width
h : storey height

(c). Frame 3

First storey columns : 200 x 200 x 10 SHS
Other columns : 200 x 200 x 8 SHS
All beams 356 x 171 x 45 UB
Steel grade 43A

Figure 6.5 Frame geometry and member designation

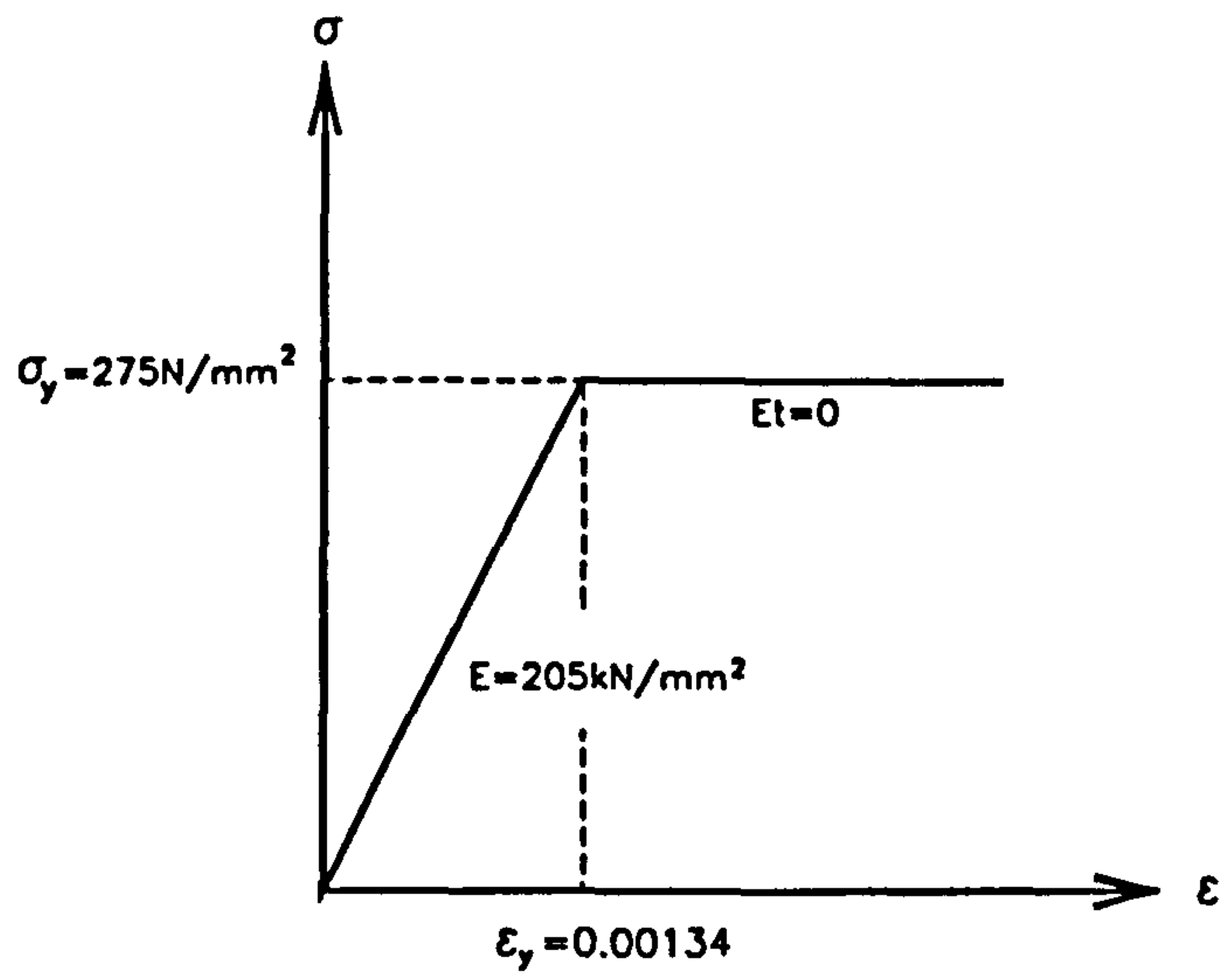

Figure 6.6 Bilinear material model

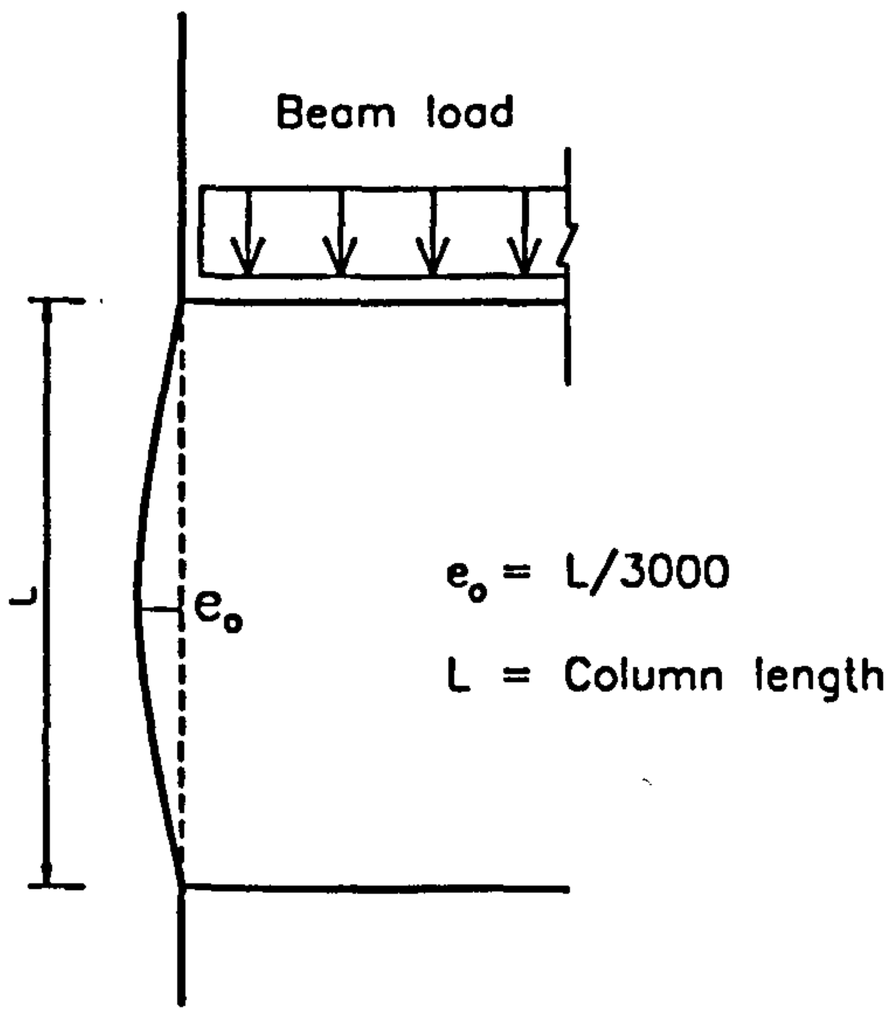

Figure 6.7 Geometrical imperfection

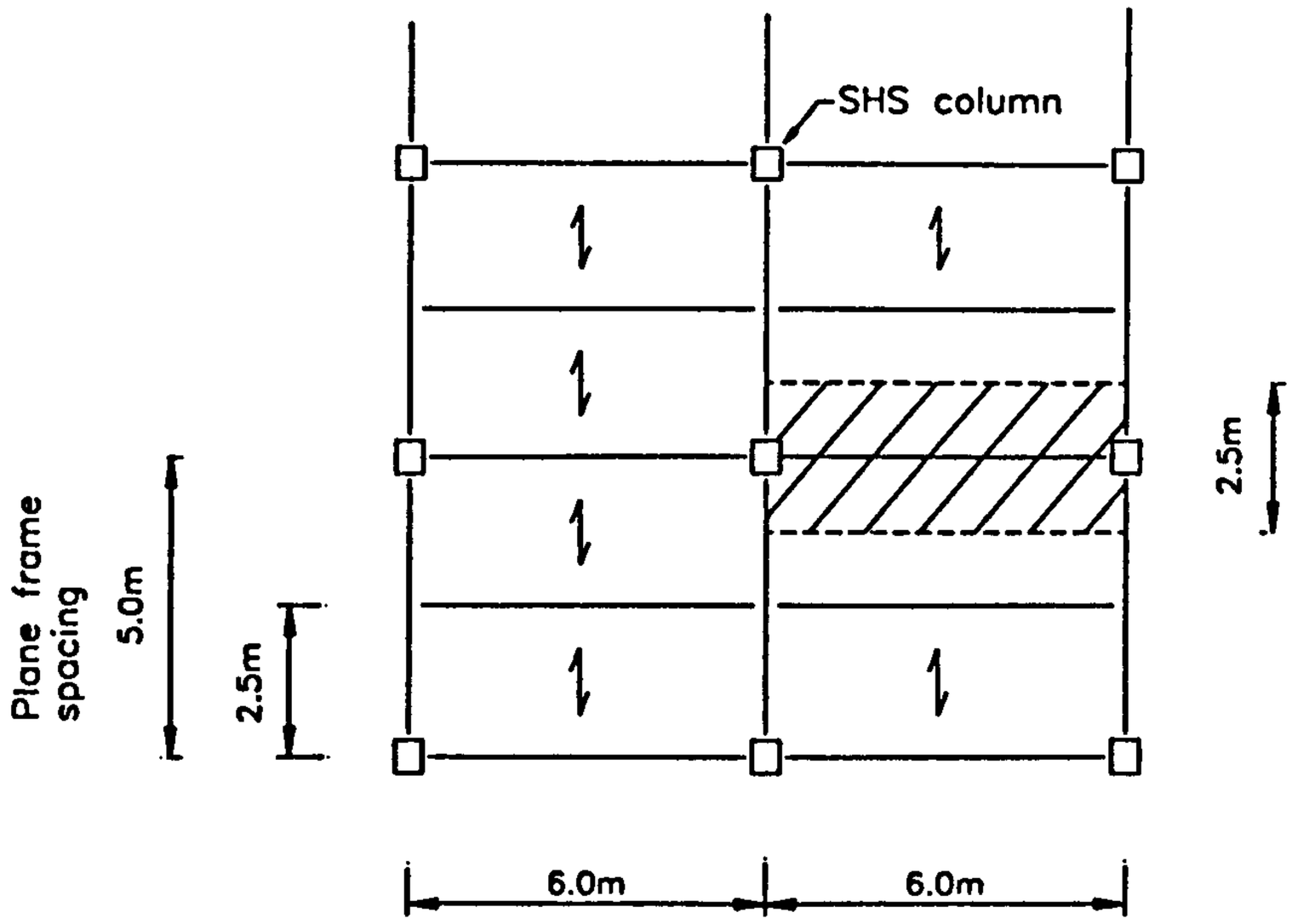

(a). One way spanning beam loading

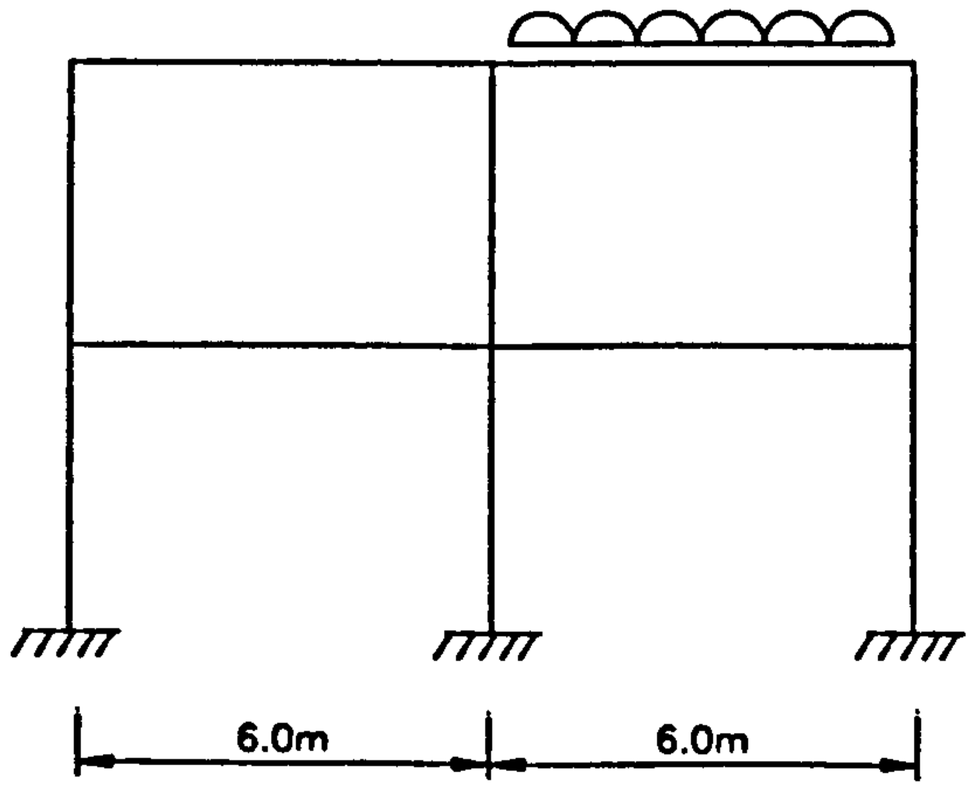

(b). Plane frame

Figure 6.8 Assumed distribution of beam loading

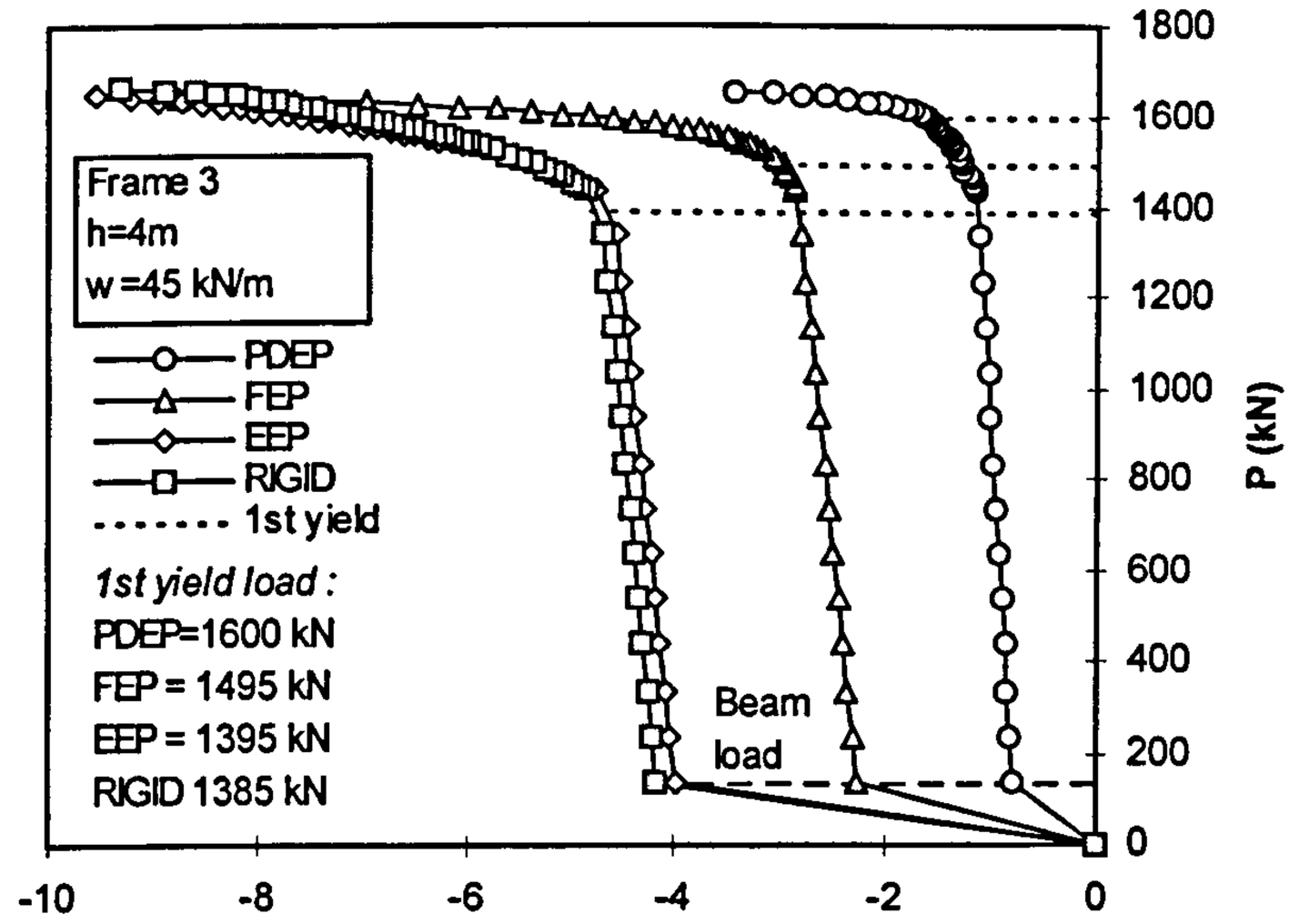

(a). Load-deflection response of columns with height of 4m using different connection types

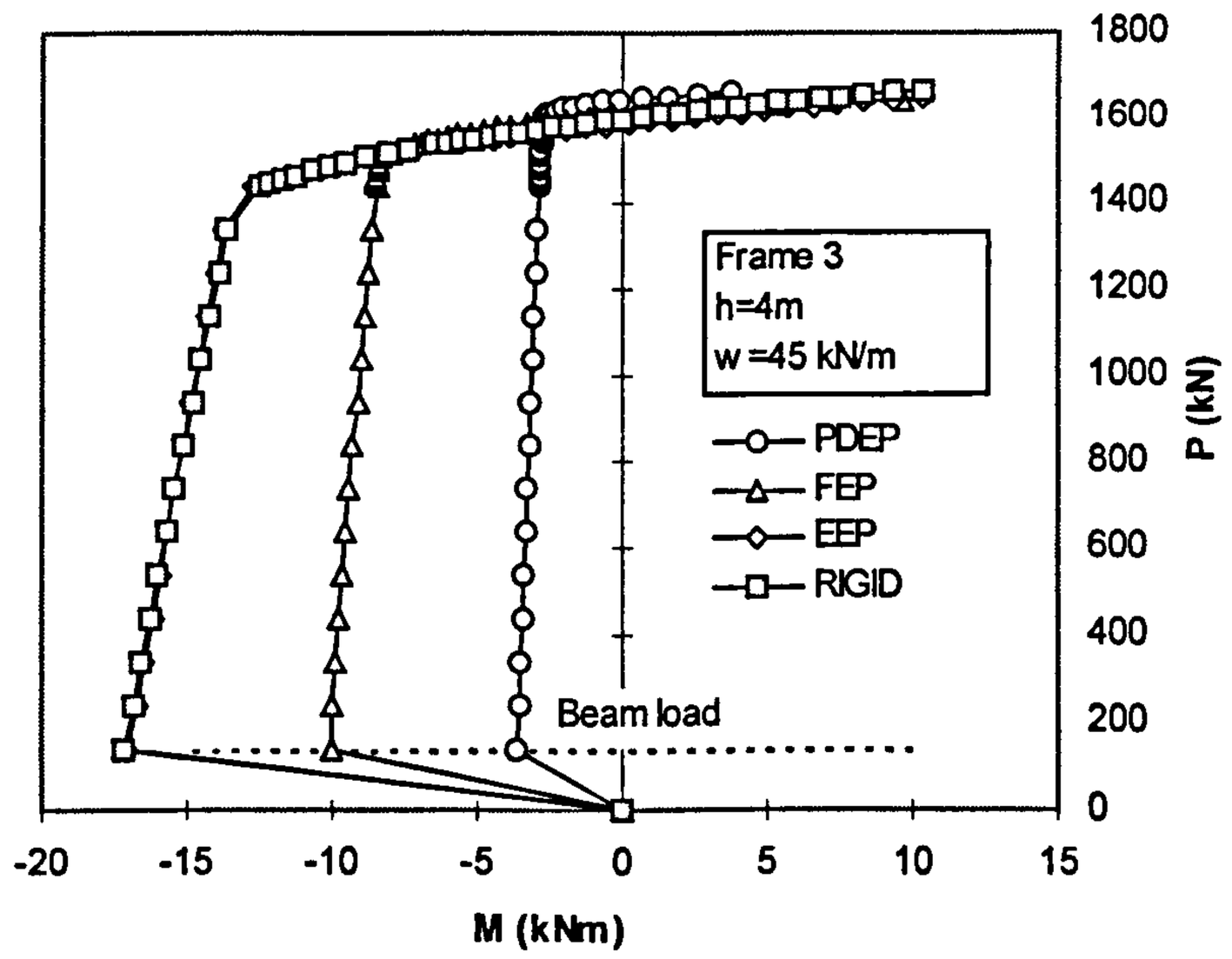

(b). Moment shedding response of columns with height of 4m using different connection types

Figure 6.9

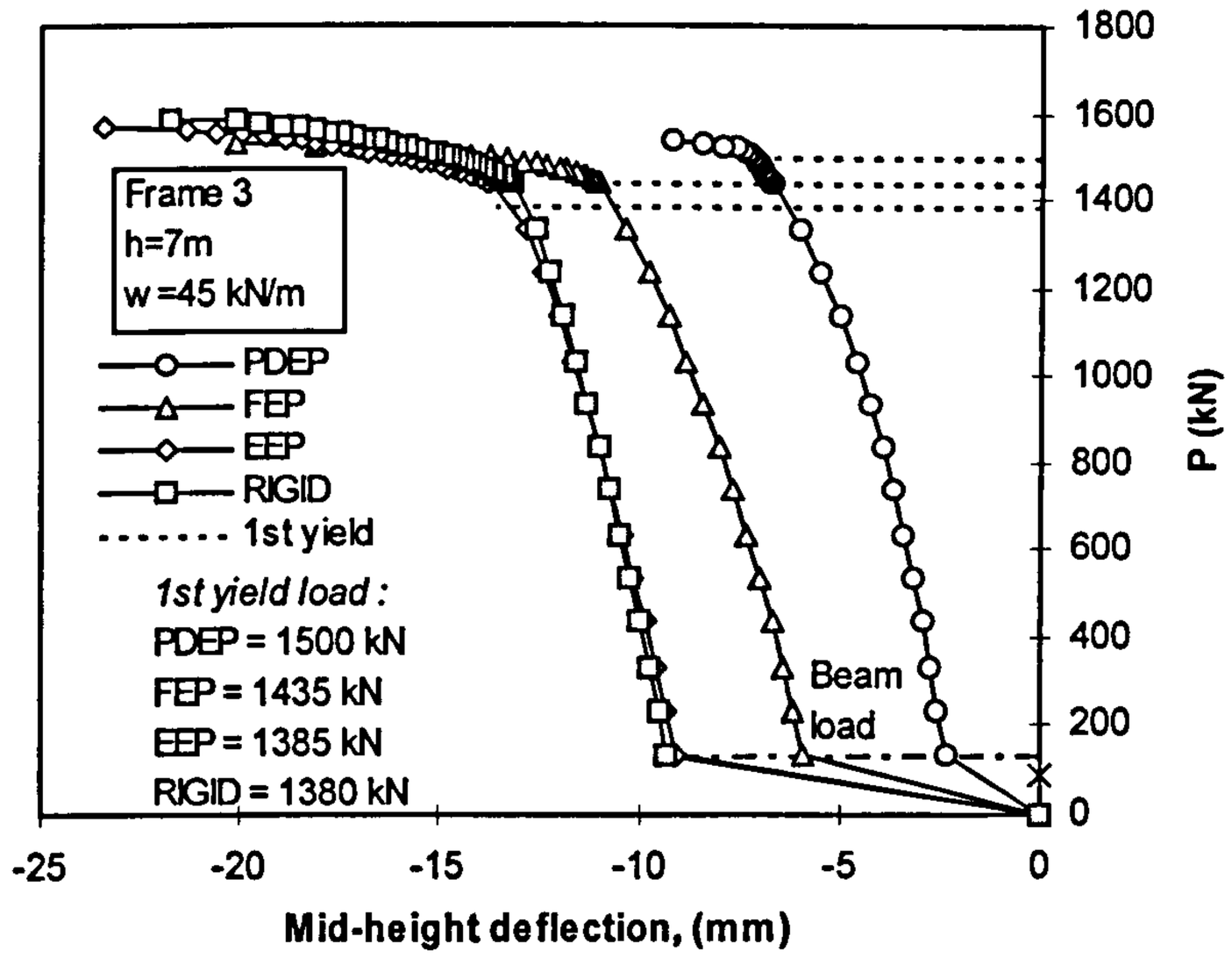

(a). Load-deflection response of columns with height of 7m using different connection types

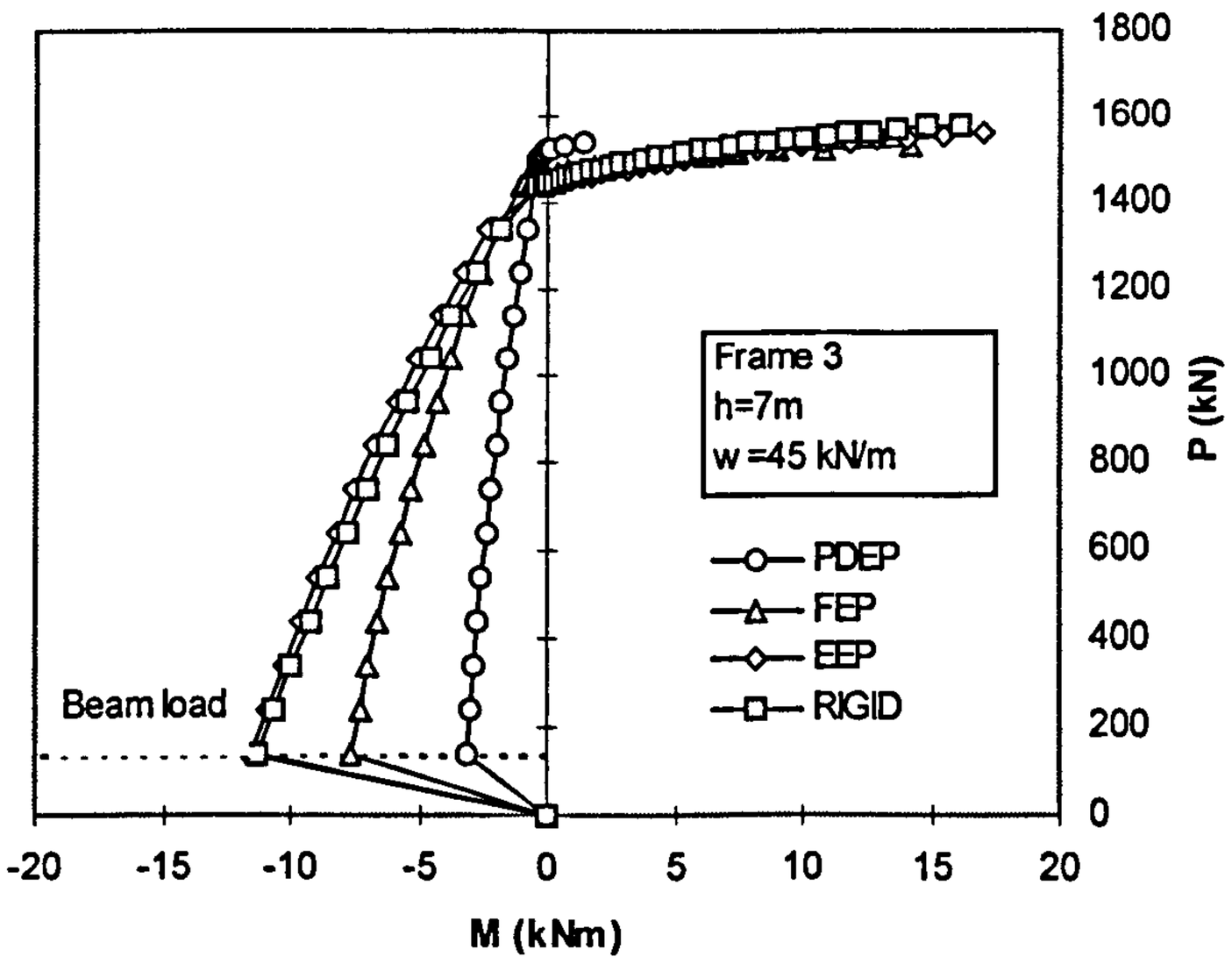

(b). Moment shedding response of columns with height of 7m using different connection types

Figure 6.10

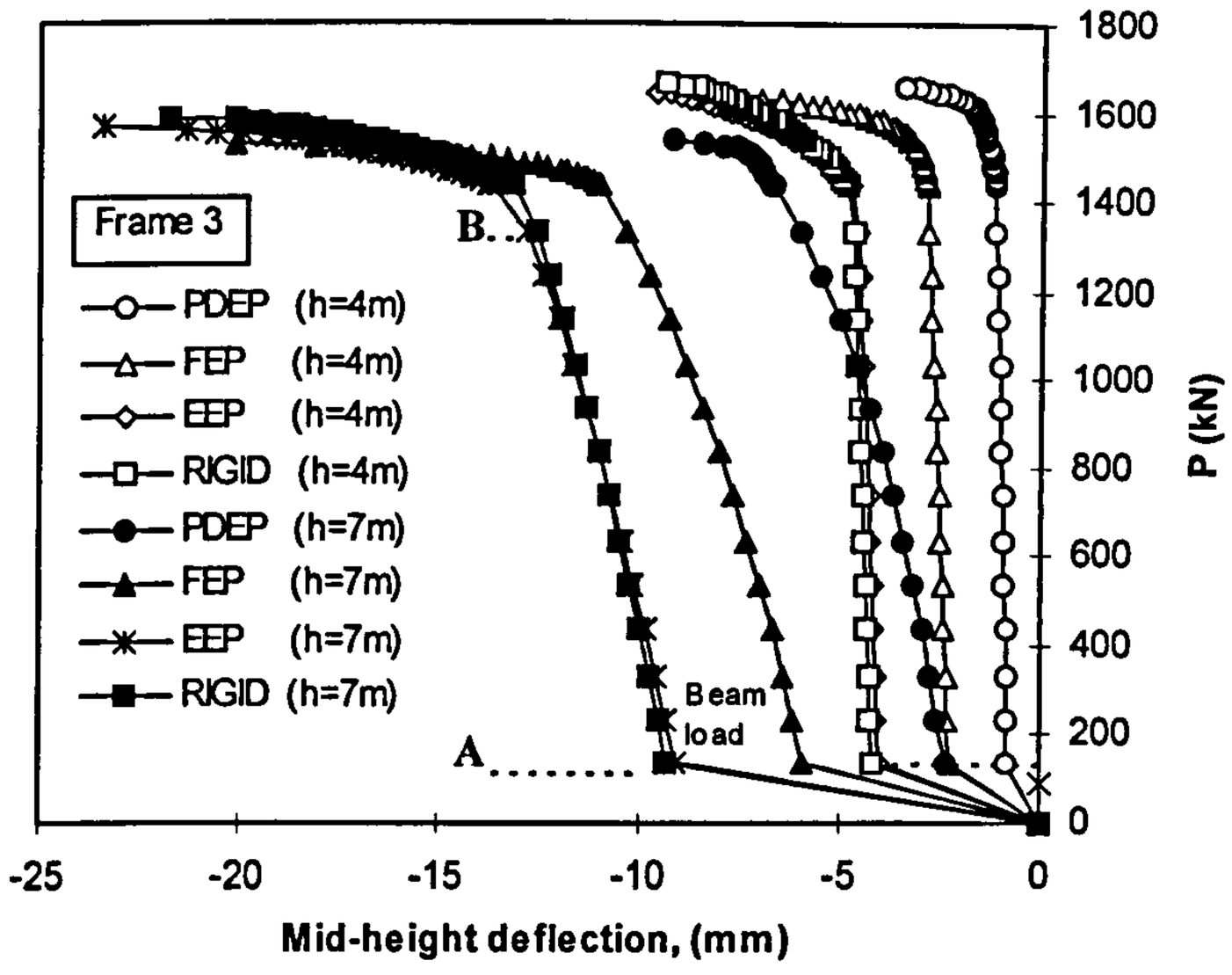

(a). Comparison of load-deflection responses

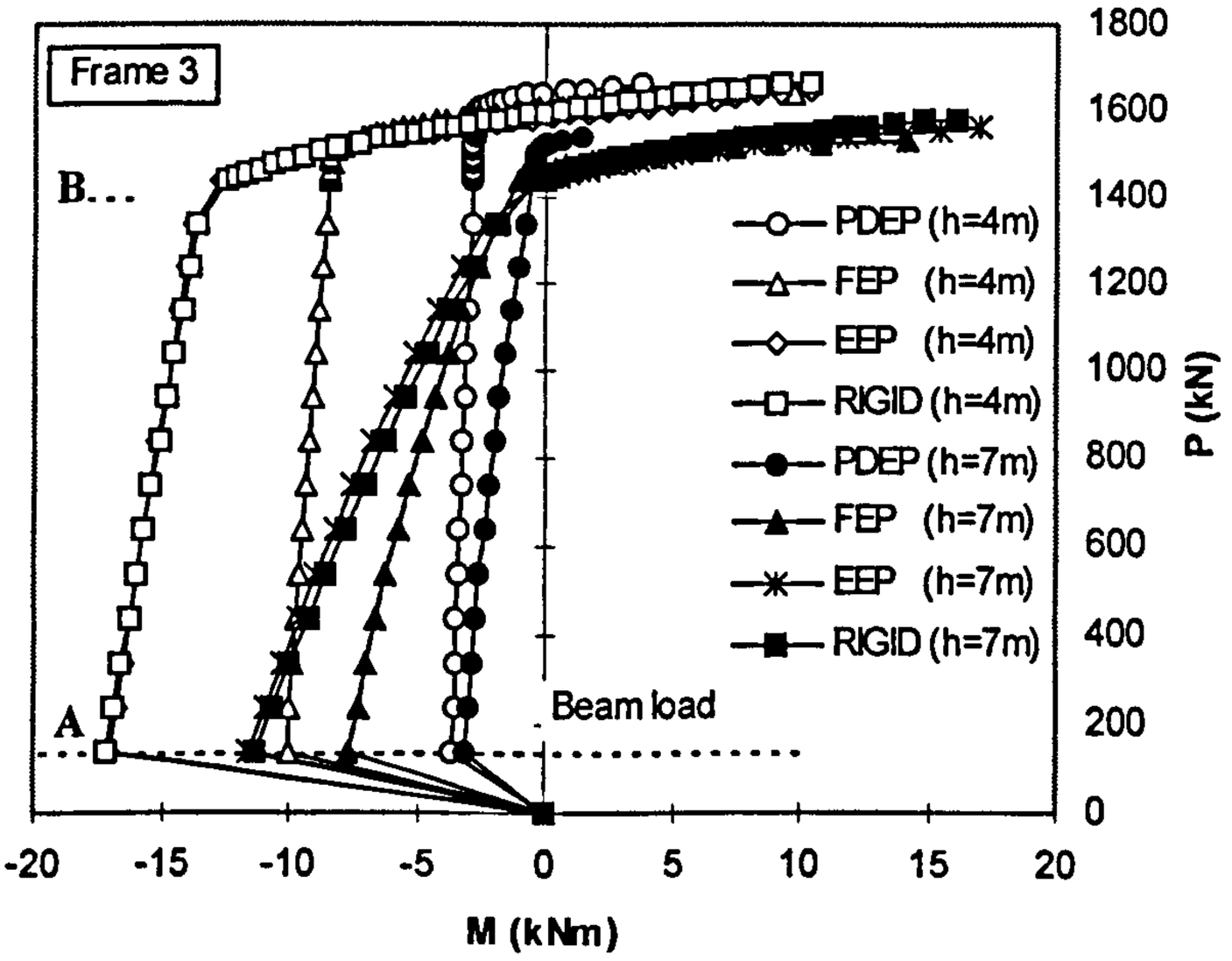

(b). Comparison of moment shedding responses

Figure 6.11

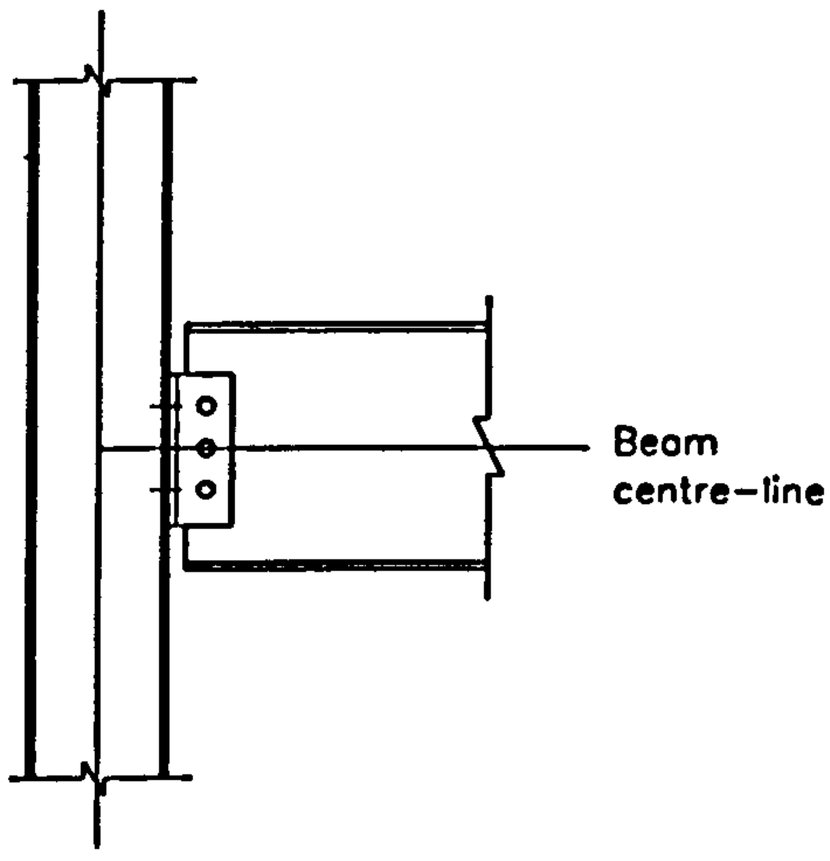

(a). Actual joint

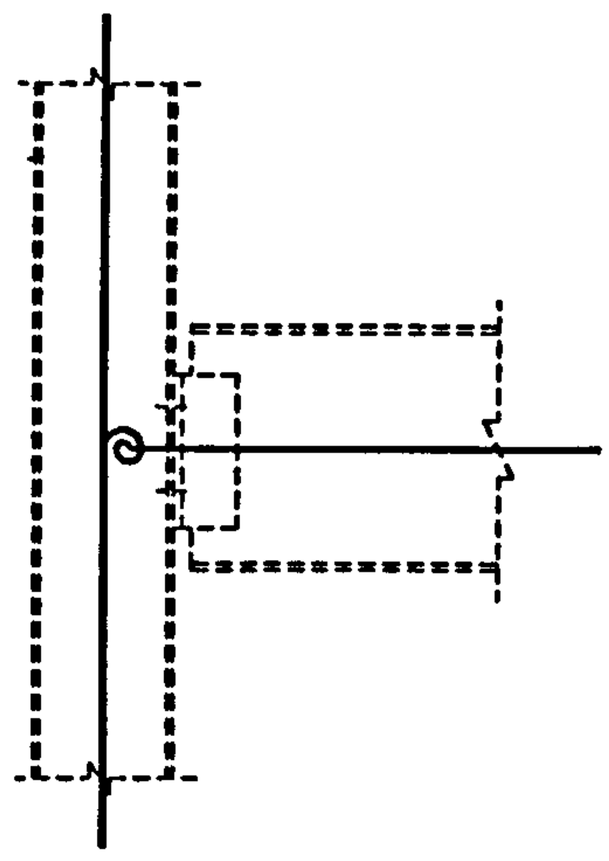

(b). Model neglecting joint offset

Notation:

rigid segment

semi-rigid connection

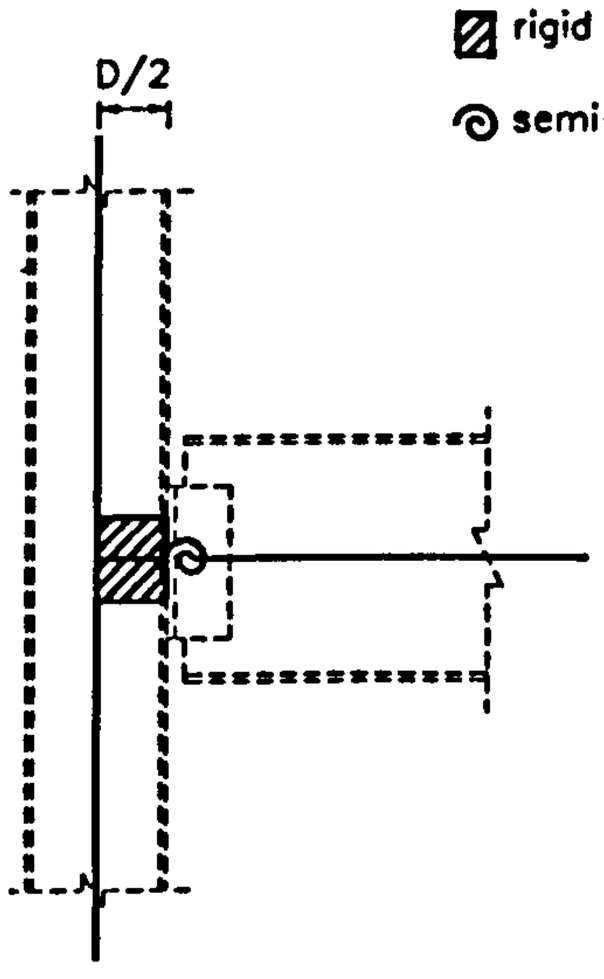

(c). Rigid segment
to model the joint offset

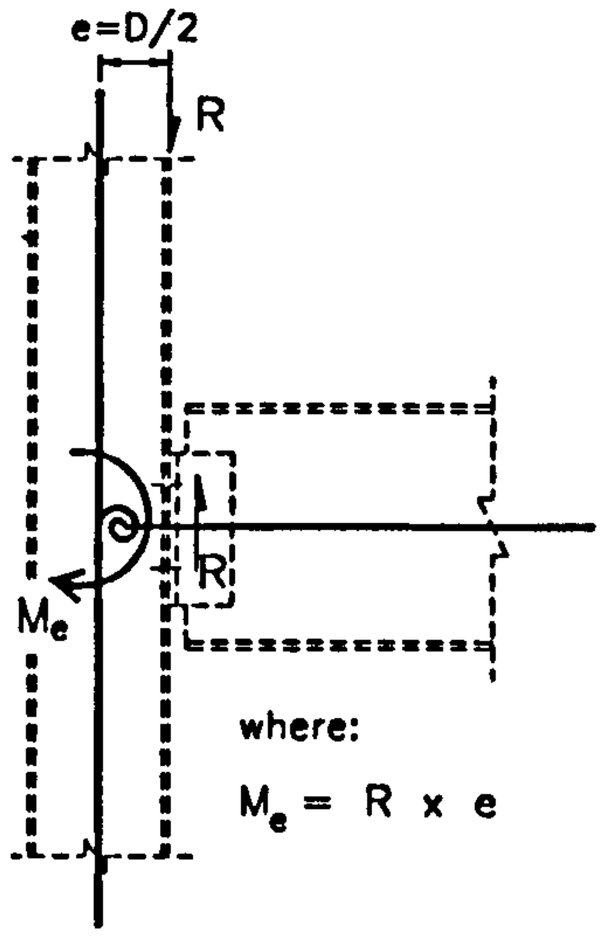

(d). Concentrated moment, M_e
to model the joint offset

Figure 6.12 Idealisation of connection

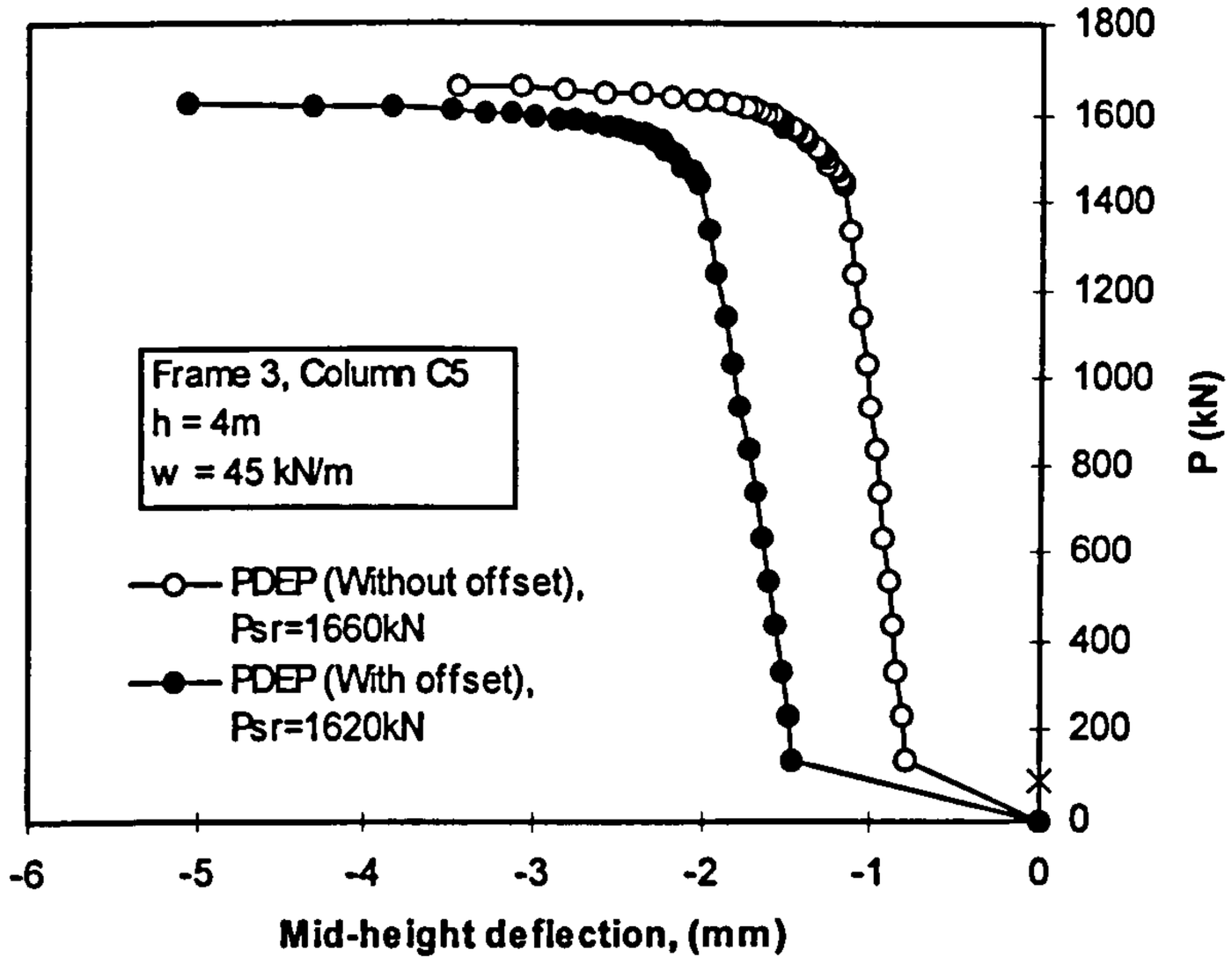

(a). The effect of load eccentricity on colum face to the load-deflection response using PDEP connections

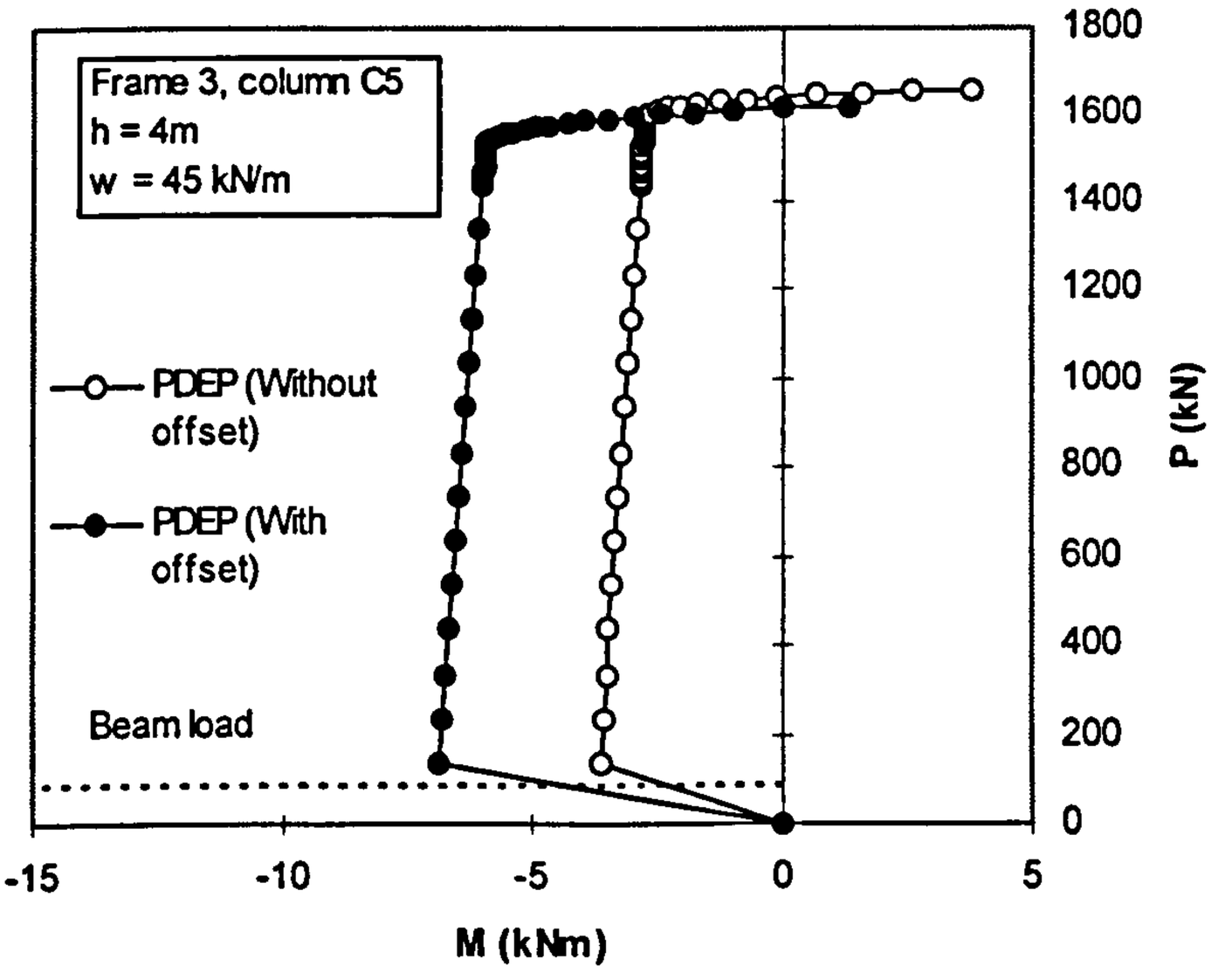

(b). The effect of load eccentricity on column face to the column end moment response using PDEP connections

Figure 6.13

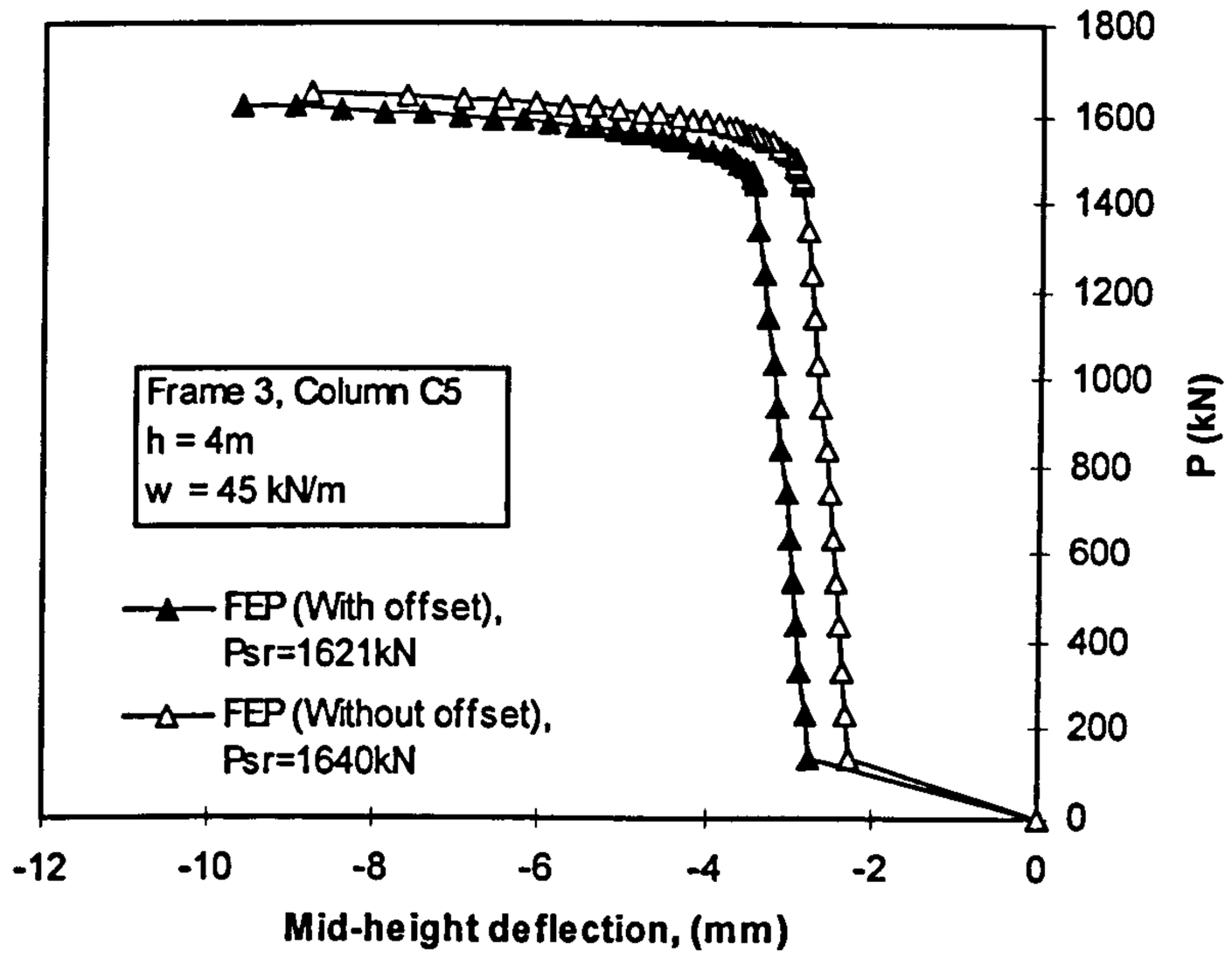

(a). The effect of load eccentricity on column face to the load-deflection response using FEP connections

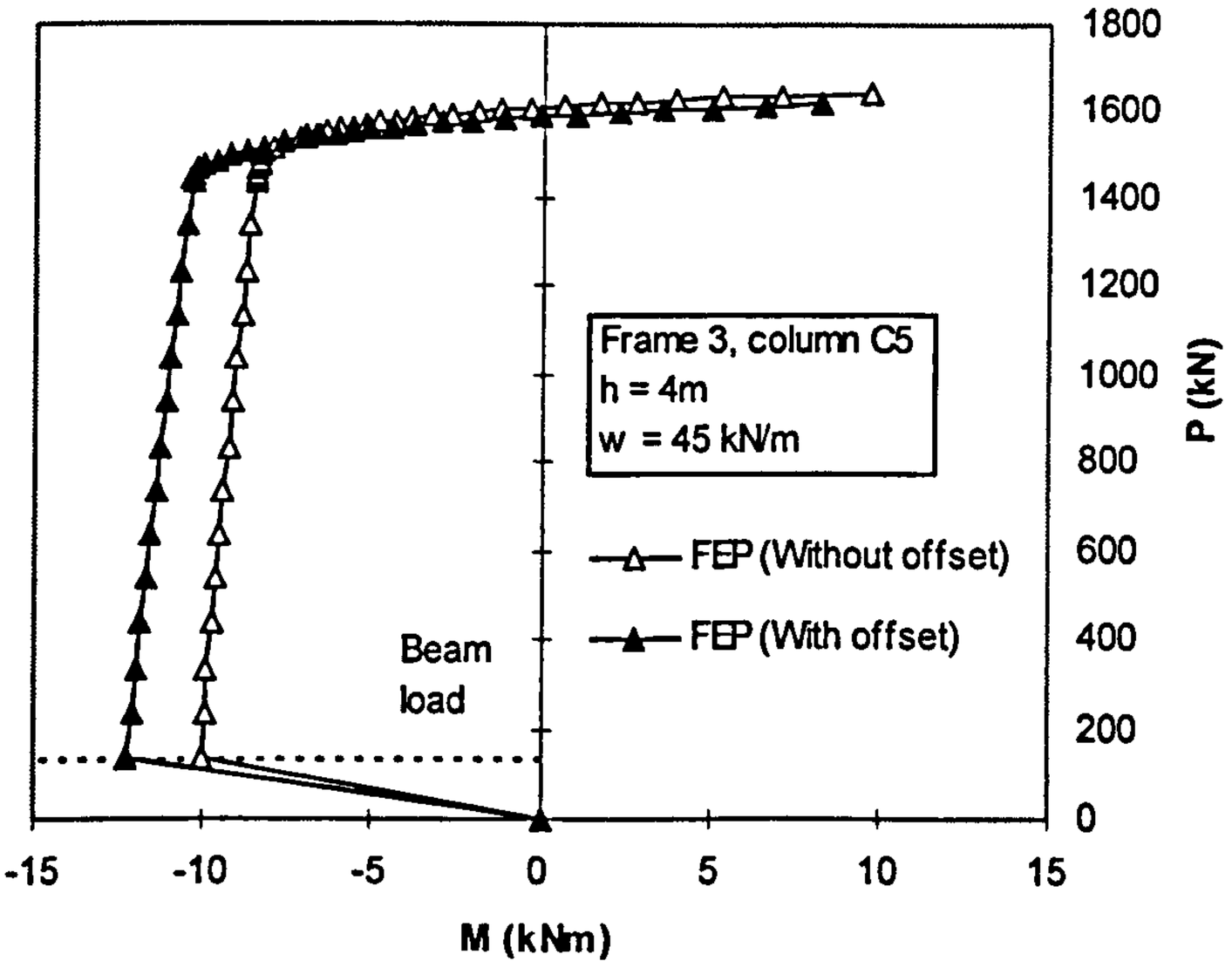

(b). The effect of load eccentricity on column face to the column end moment response using FEP connections

Figure 6.14

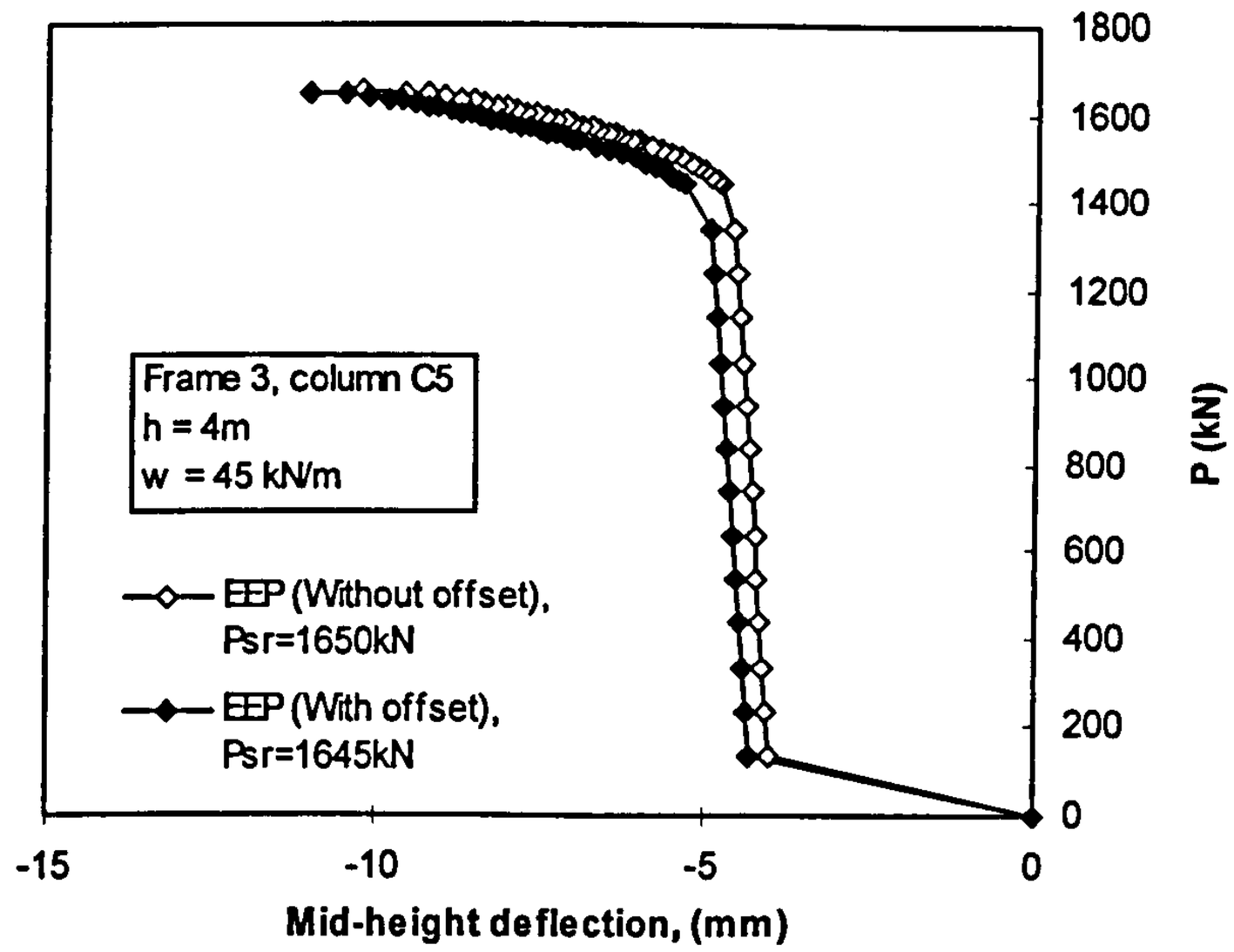

(a). The effect of load eccentricity on column face to the load-deflection response using EEP connections

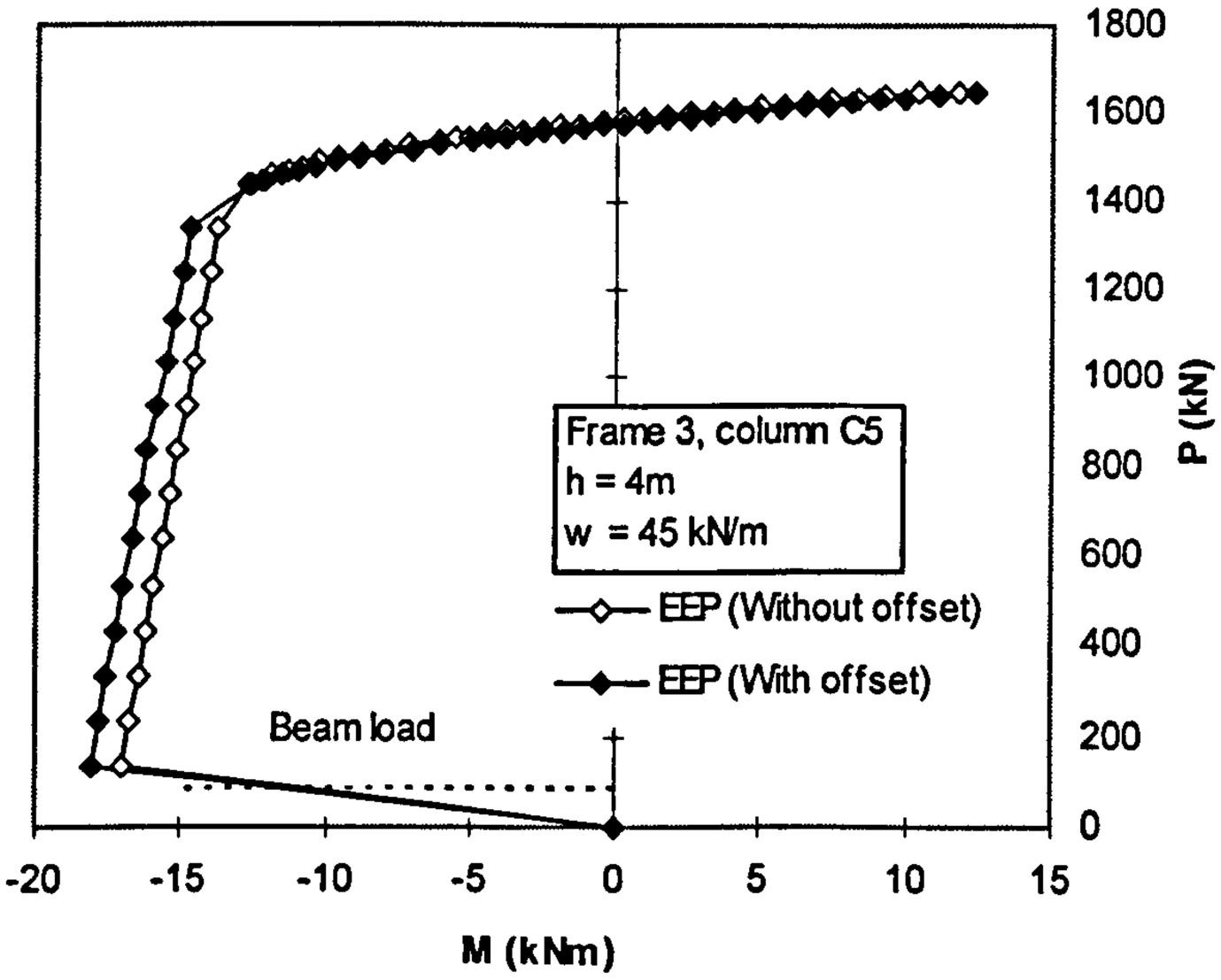

(b). The effect of load eccentricity on column face to the column end moment response using EEP connections

Figure 6.15

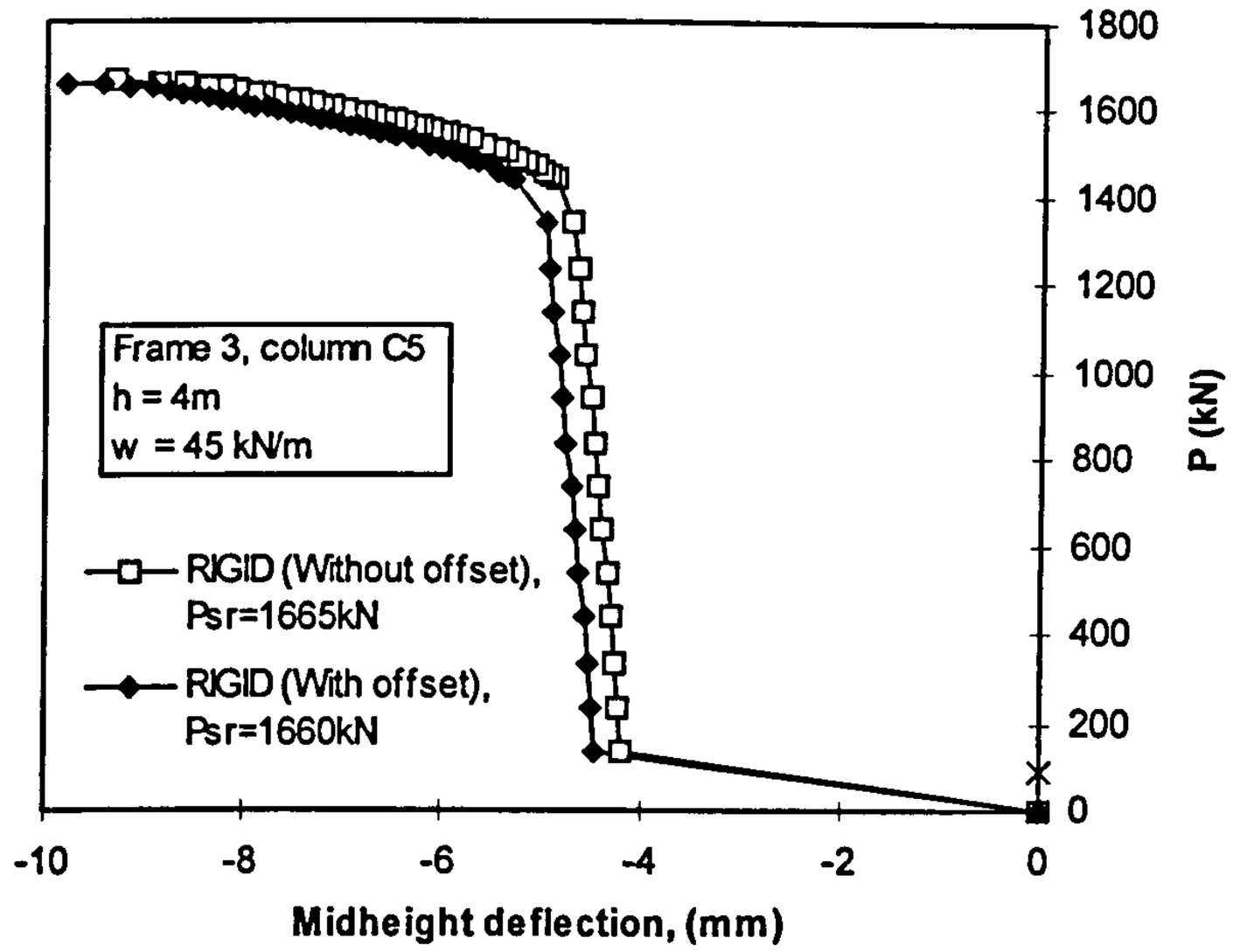

(a). The effect of load eccentricity on column face to the load-deflection response using RIGID connections

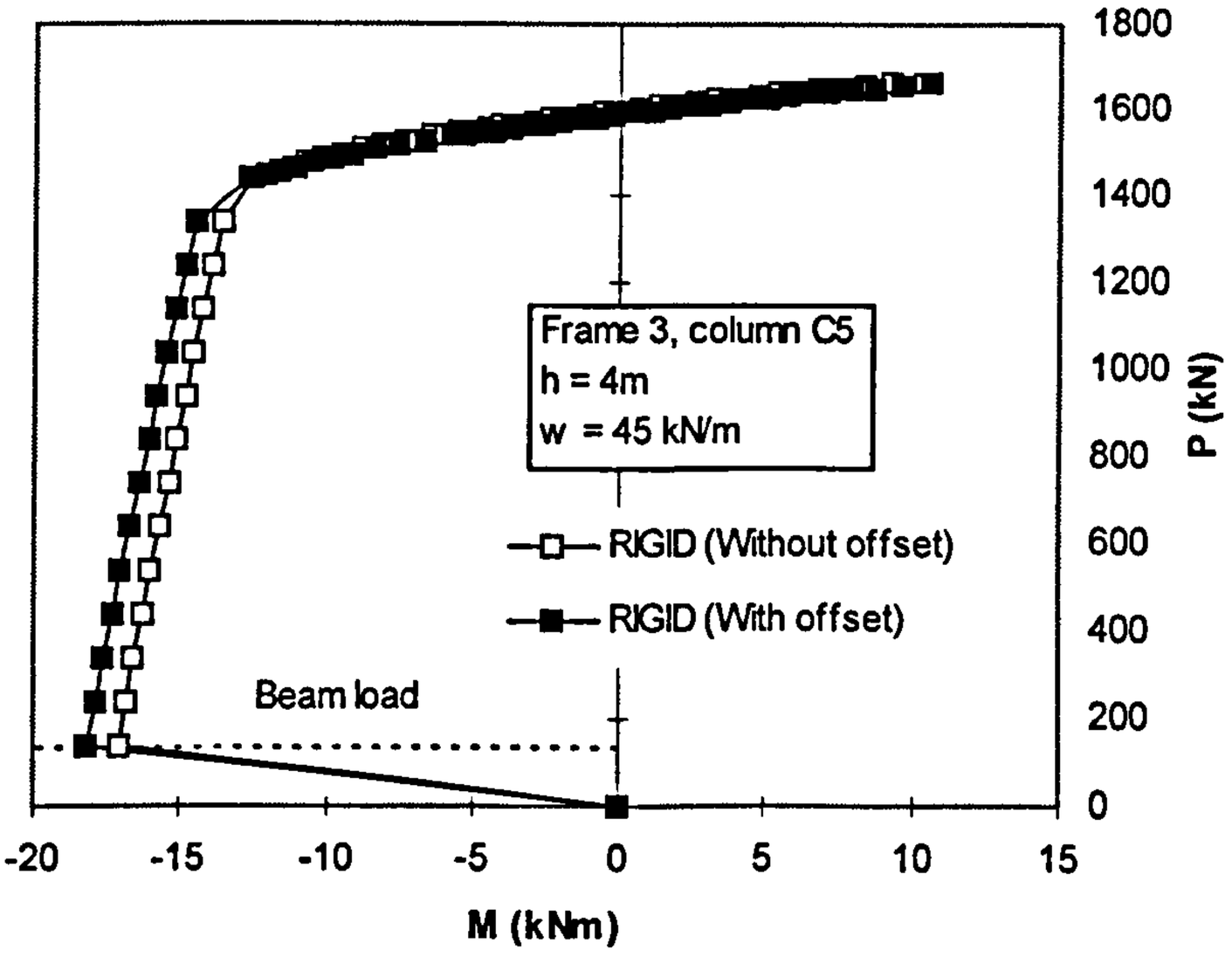

(b). The effect of load eccentricity on column face to the column end moment response using RIGID connections

Figure 6.16

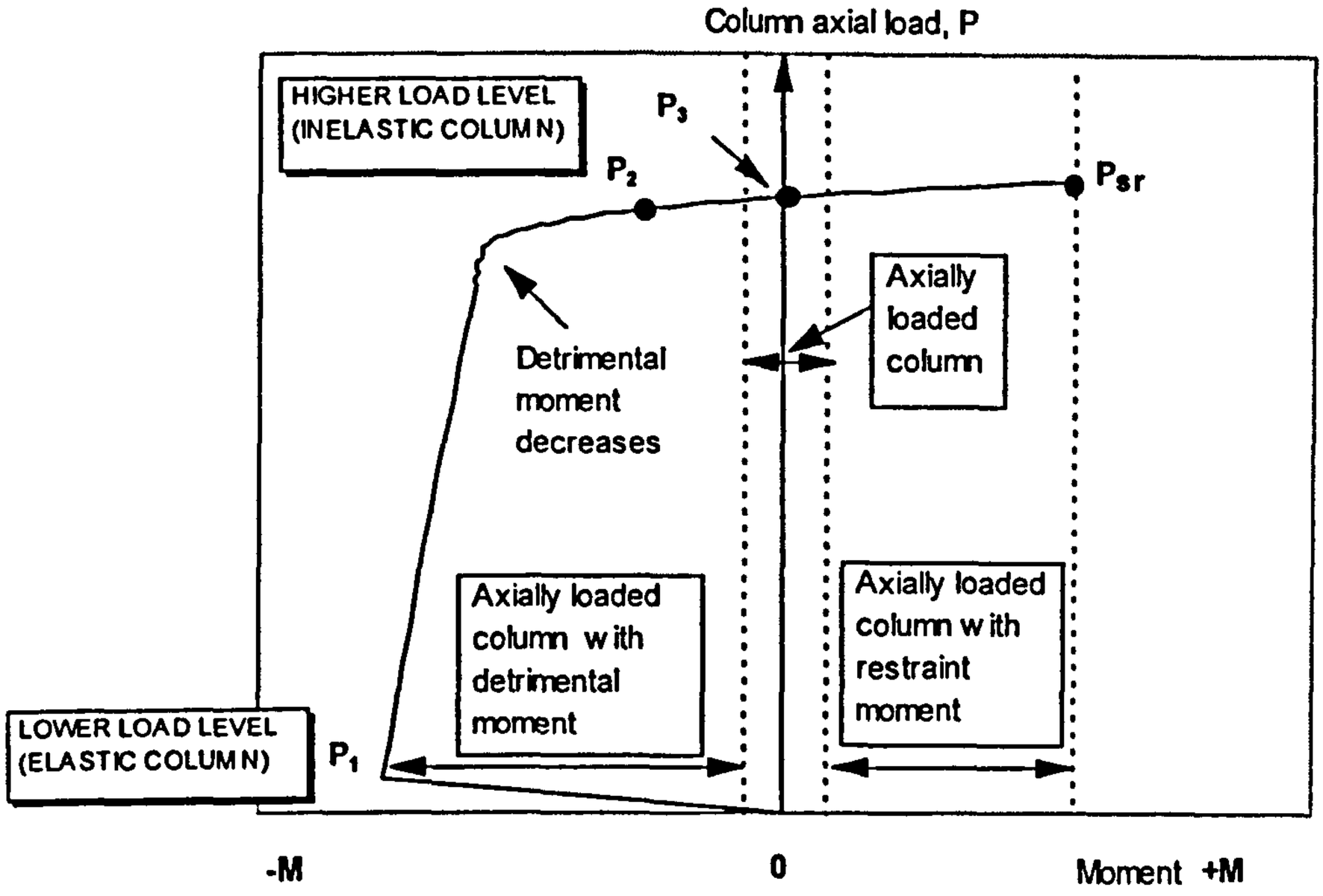

(a). Various responses of beam-columns

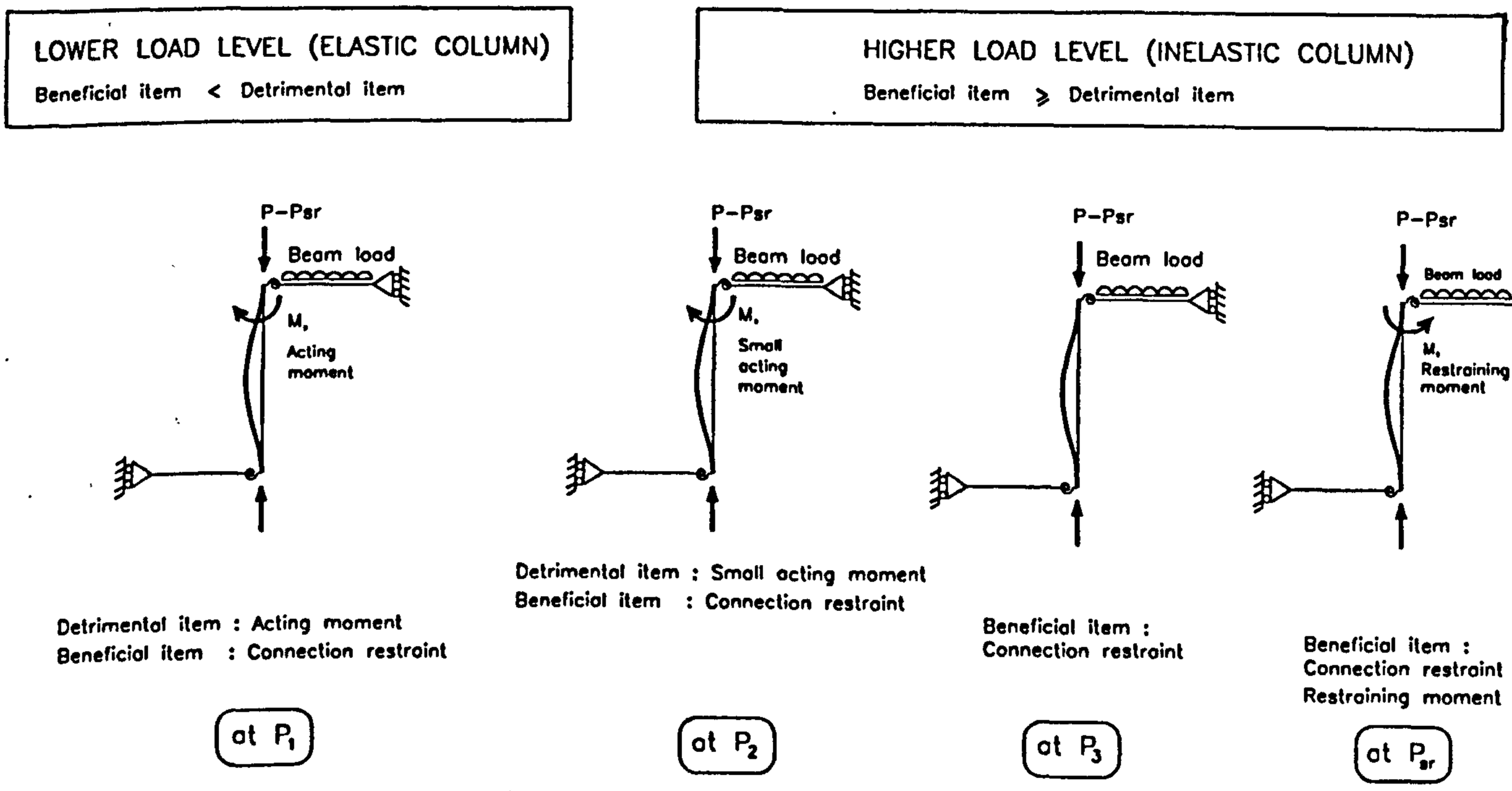

(b). Detrimental and beneficial items at column ends with respect to different axial load levels

Figure 6.17

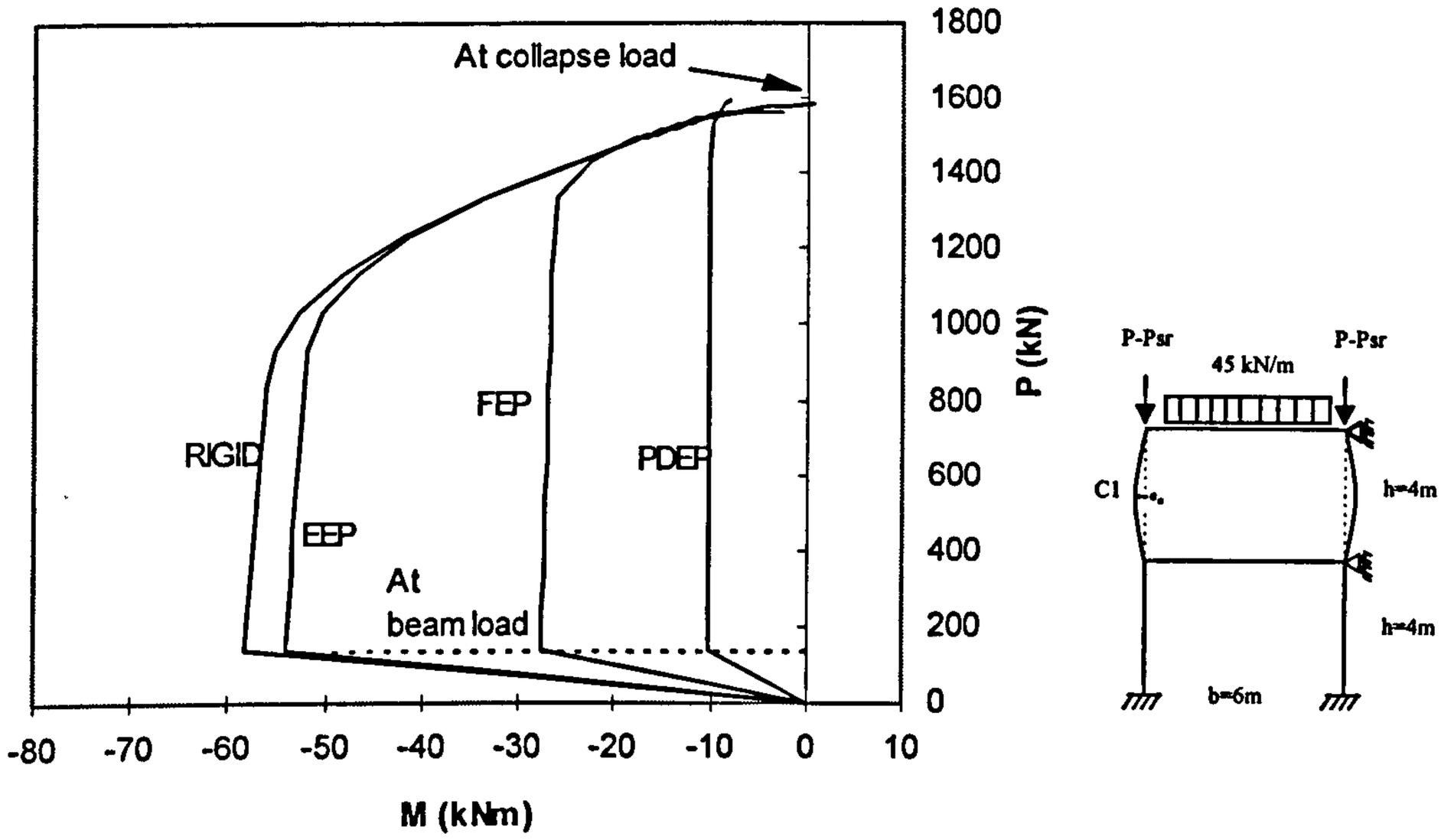

(a). Response of column top end moments with different connection types

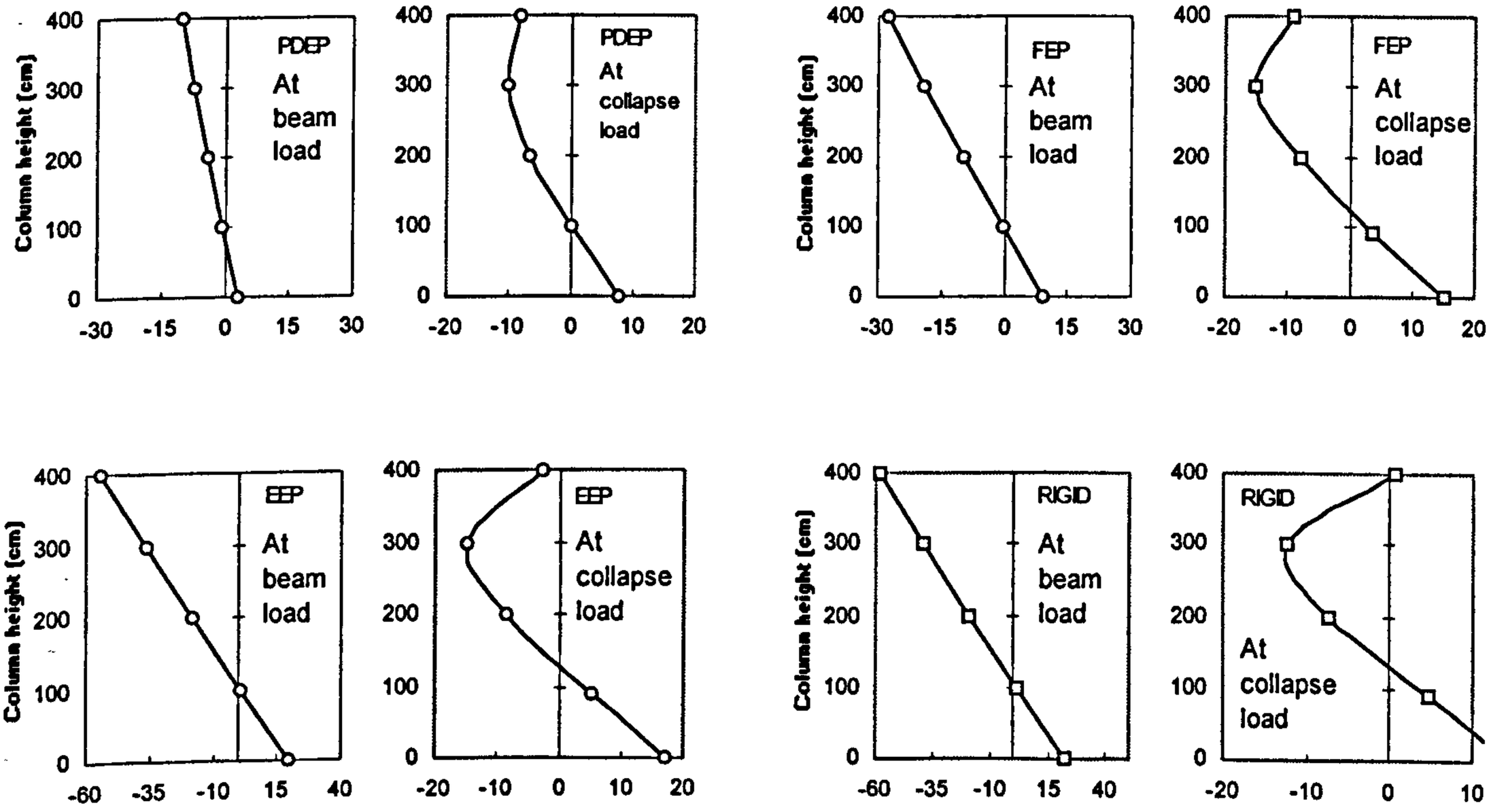

(b). Comparison of bending moments in column in kNm

Figure 6.18 Response of moment due to 45 kN/m beam load at column C1 of frame 1

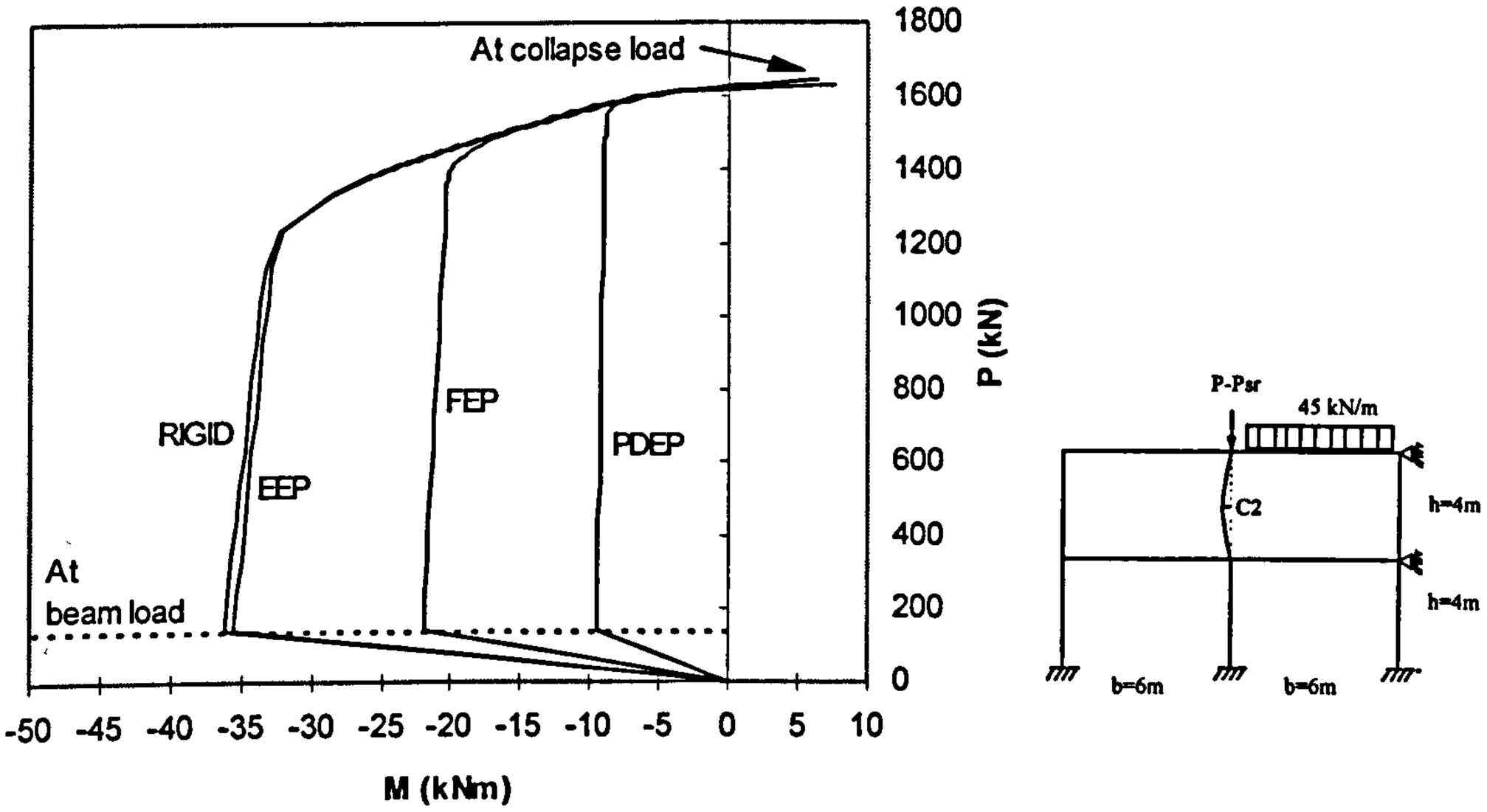

(a). Response of column top end moments with different connection types

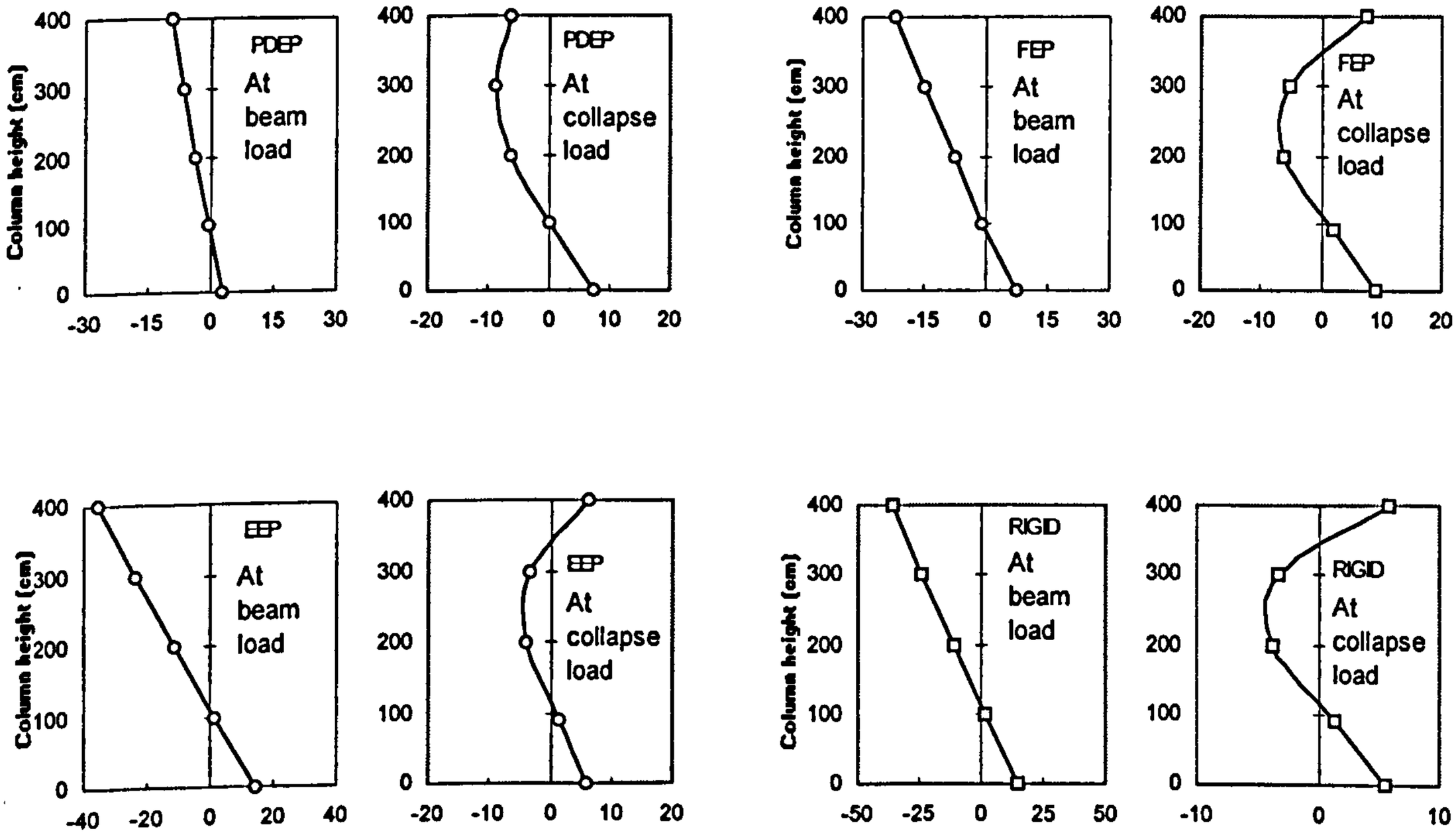

(b). Comparison of bending moments in column in kNm

Figure 6.19 Response of moments due to 45 kN/m beam load at column C2 of frame 2

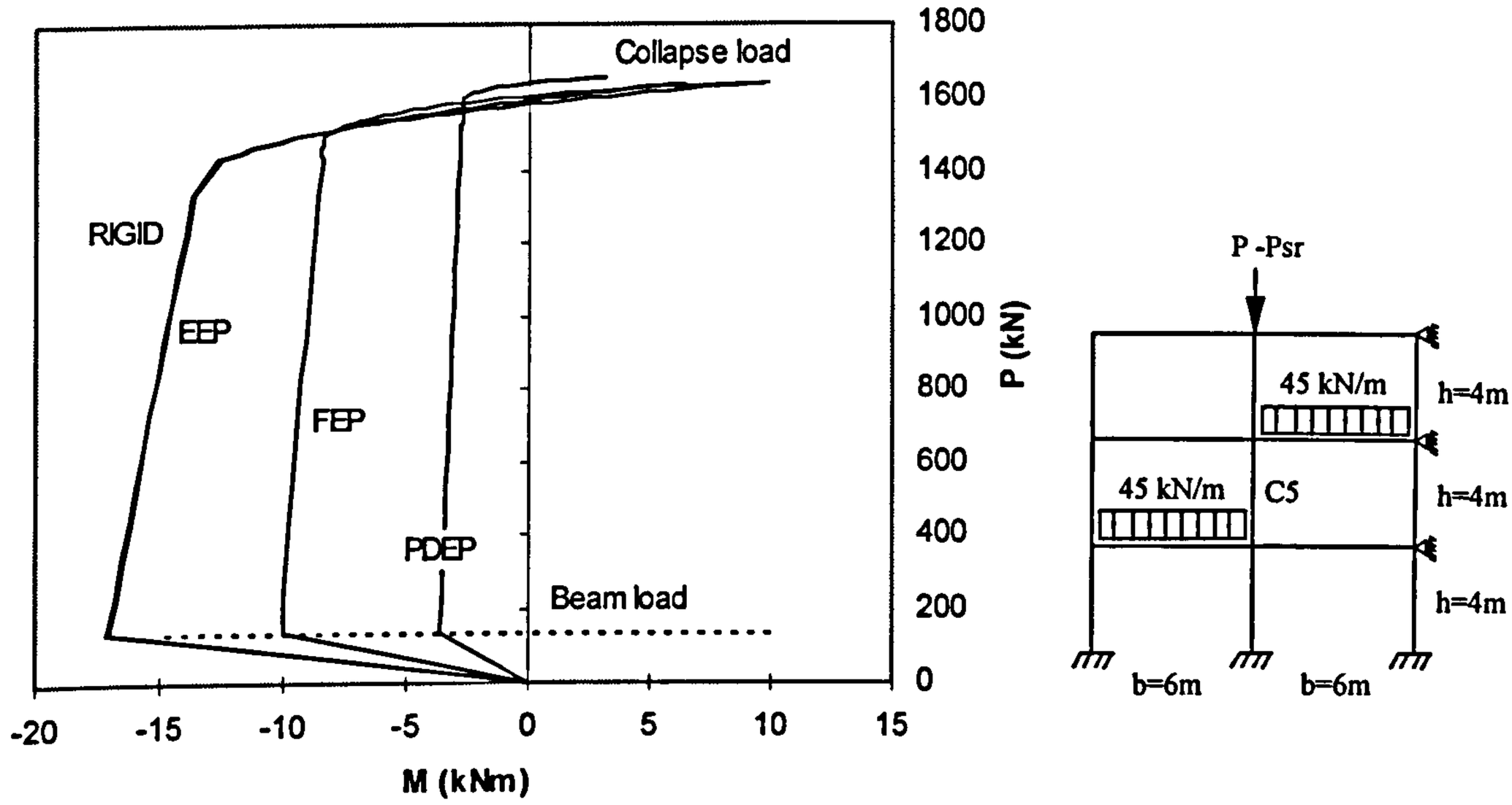

(a). Response of column top end moment with different connection types

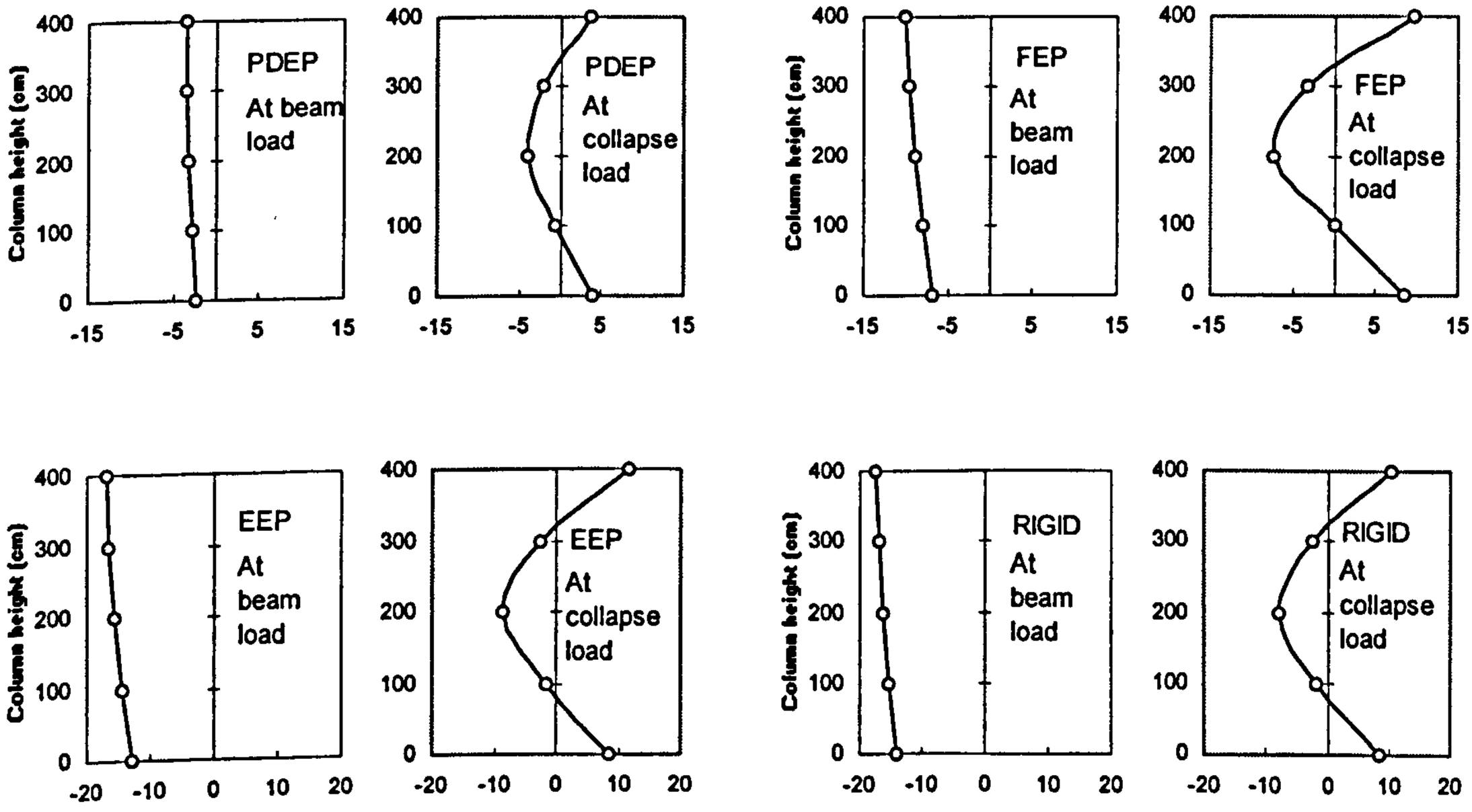

(b). Comparison of bending moments in column in kNm

Figure 6.20 Response of moments due to 45 kN/m beam load at column C5 of frame

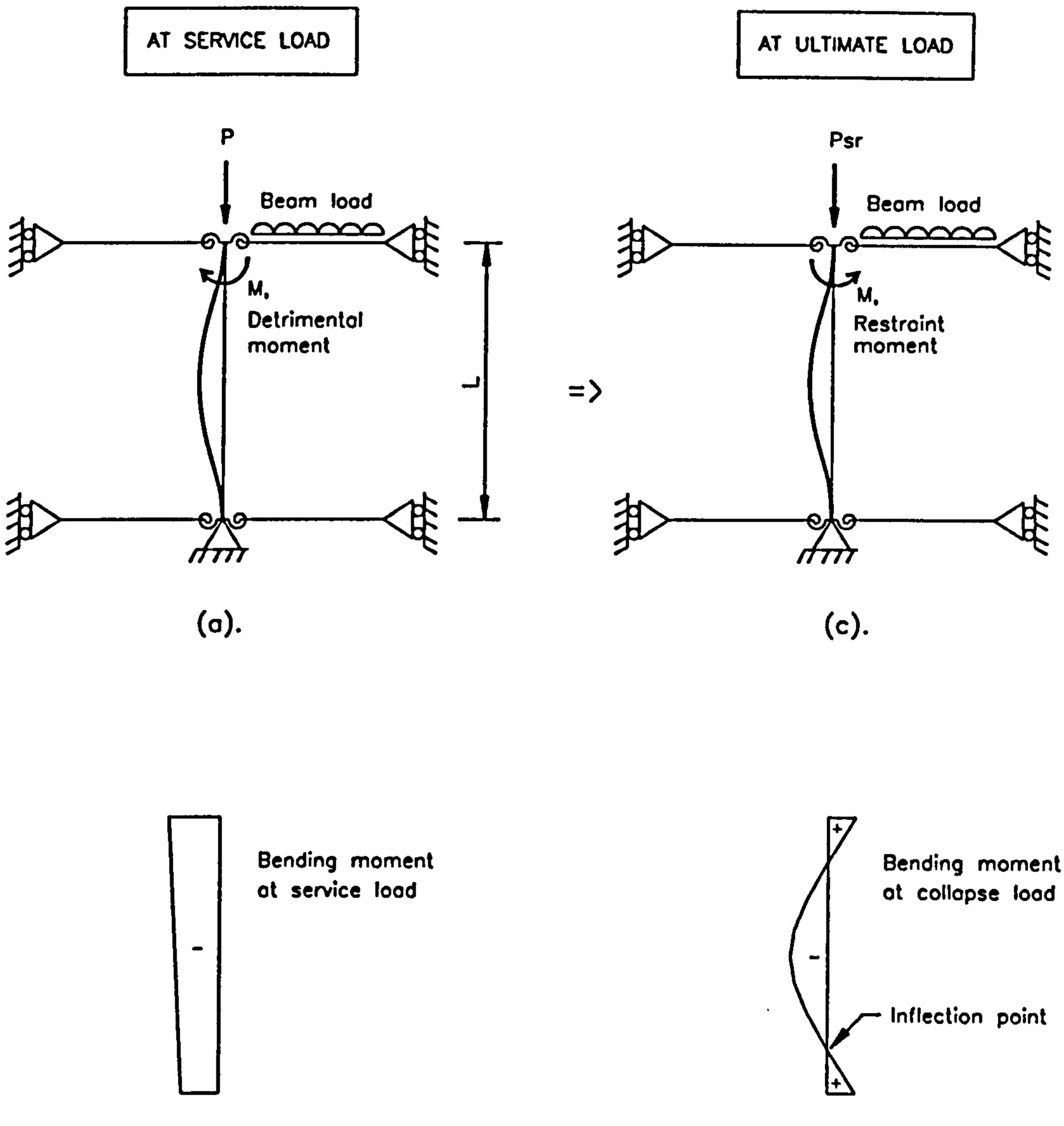

Figure 6.21 Response of moment at service and at ultimate load levels

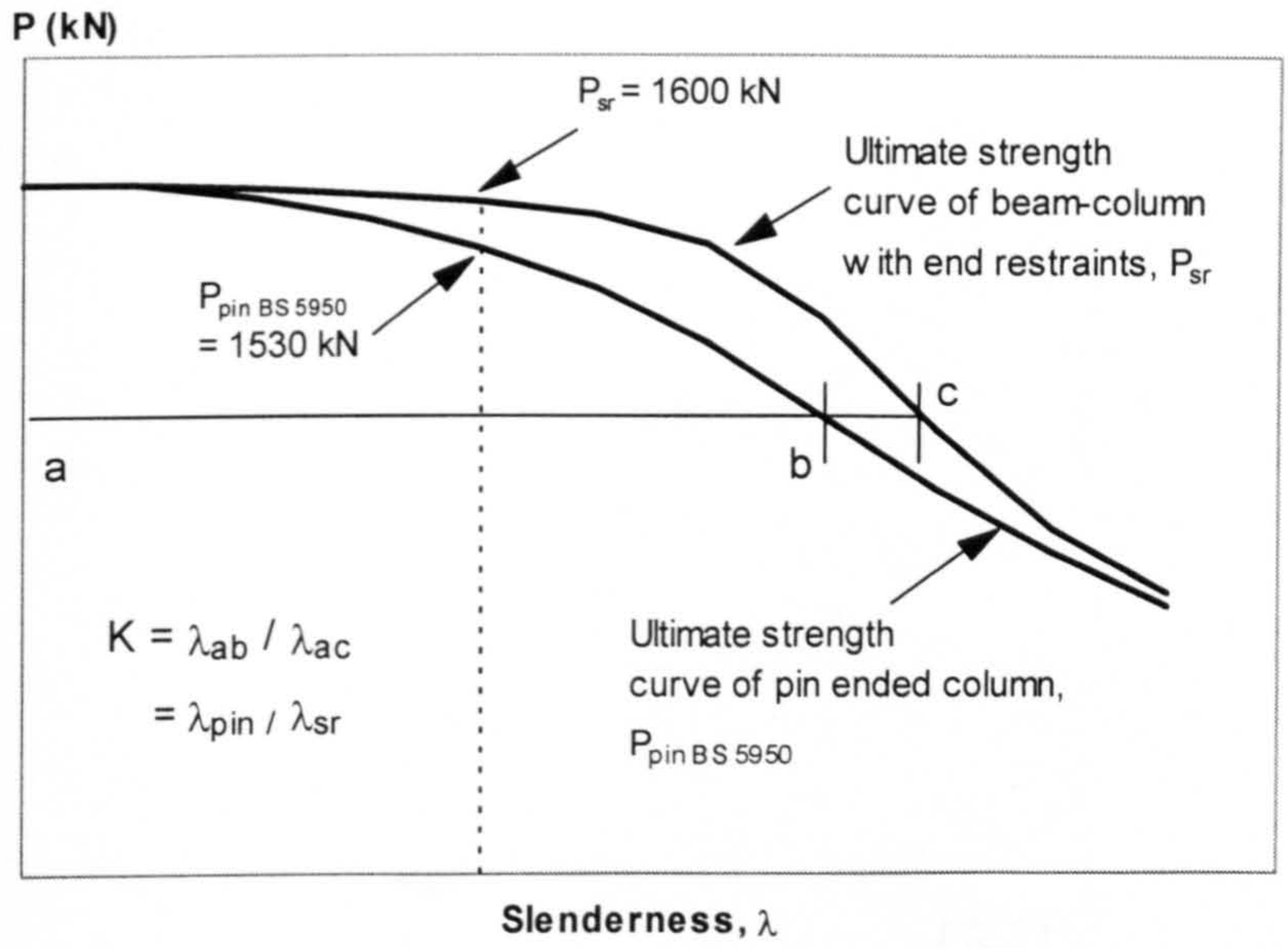

(a). Beam-column strength curve

P_{sr} (kN)	P_{pin} BS 5950 (kN)	α_{pin}
1600	1530	1.06

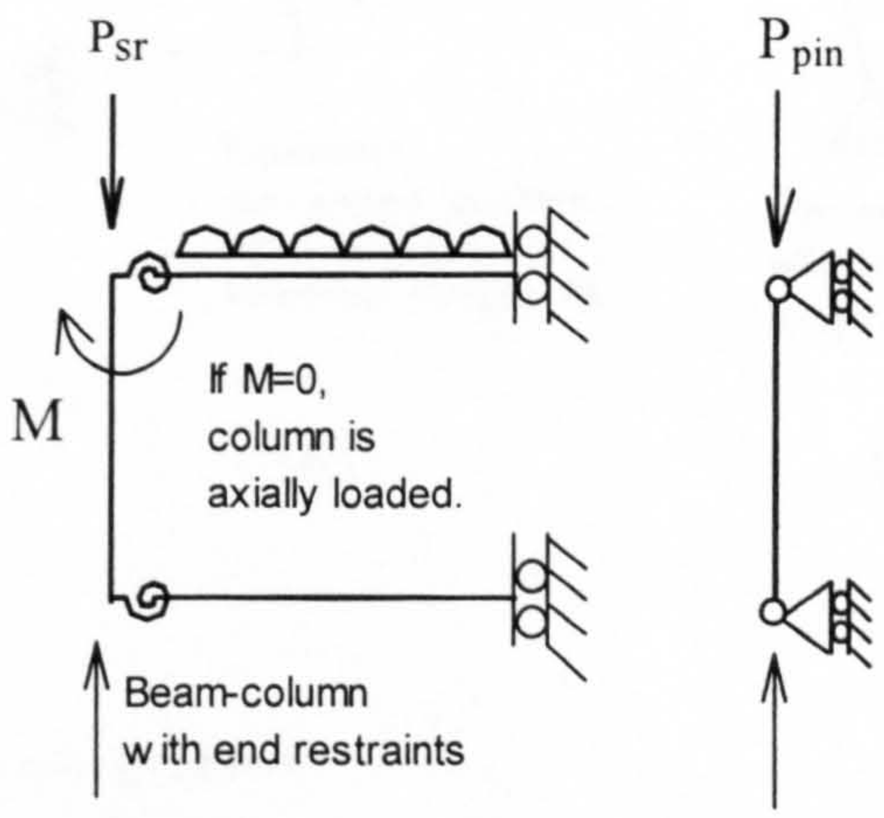

(b). α_{pin} values

Figure 6.22 Ultimate column strength curves and ultimate column strength ratio (α_{pin})

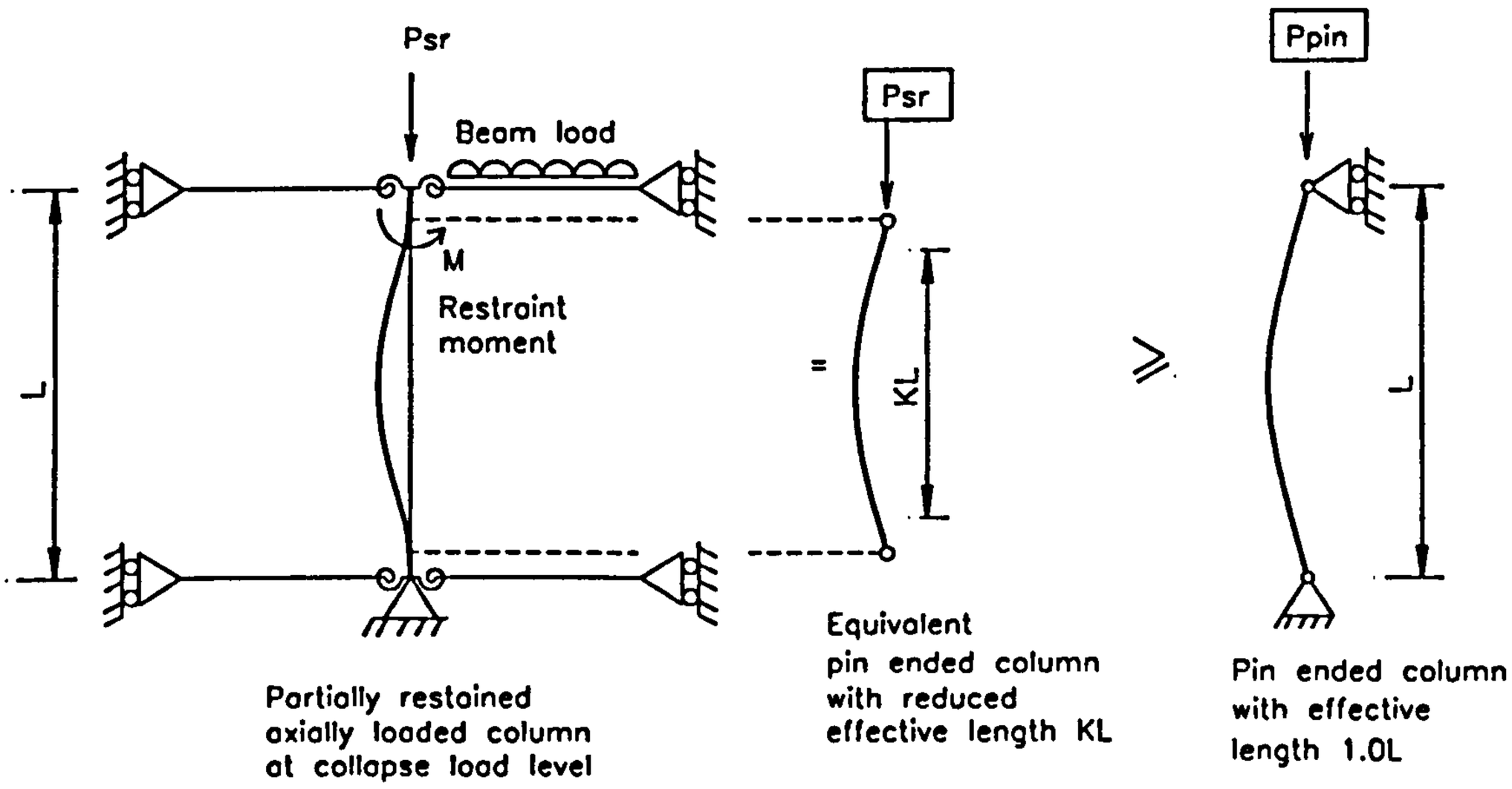

Figure 6.23 Solution of beam–column problem
at ultimate (collapse) load level using effective length method

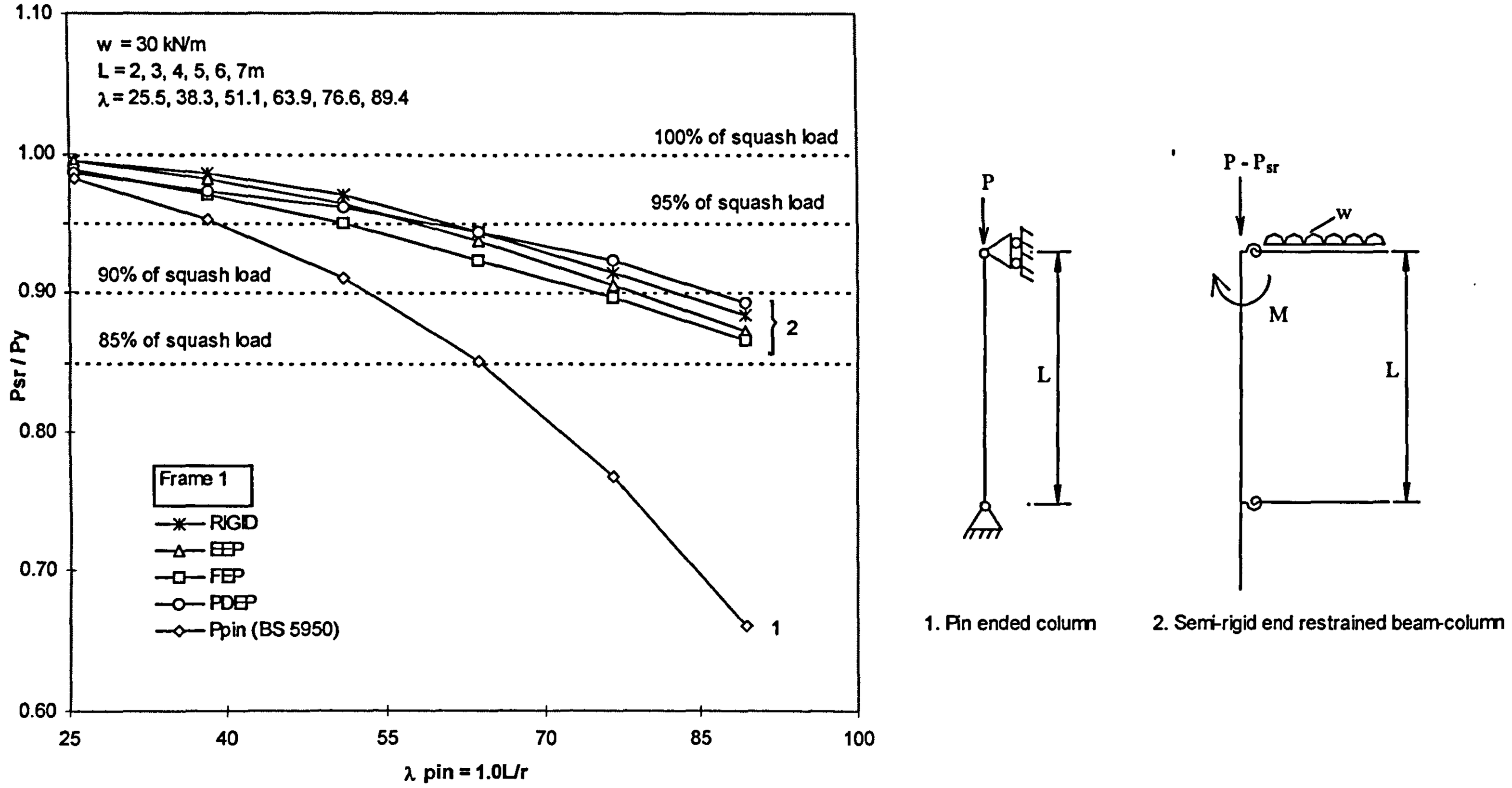

Figure 6.24 Beam-column ultimate strength curves of upper edge columns with various connection end types, w = 30 kN/m

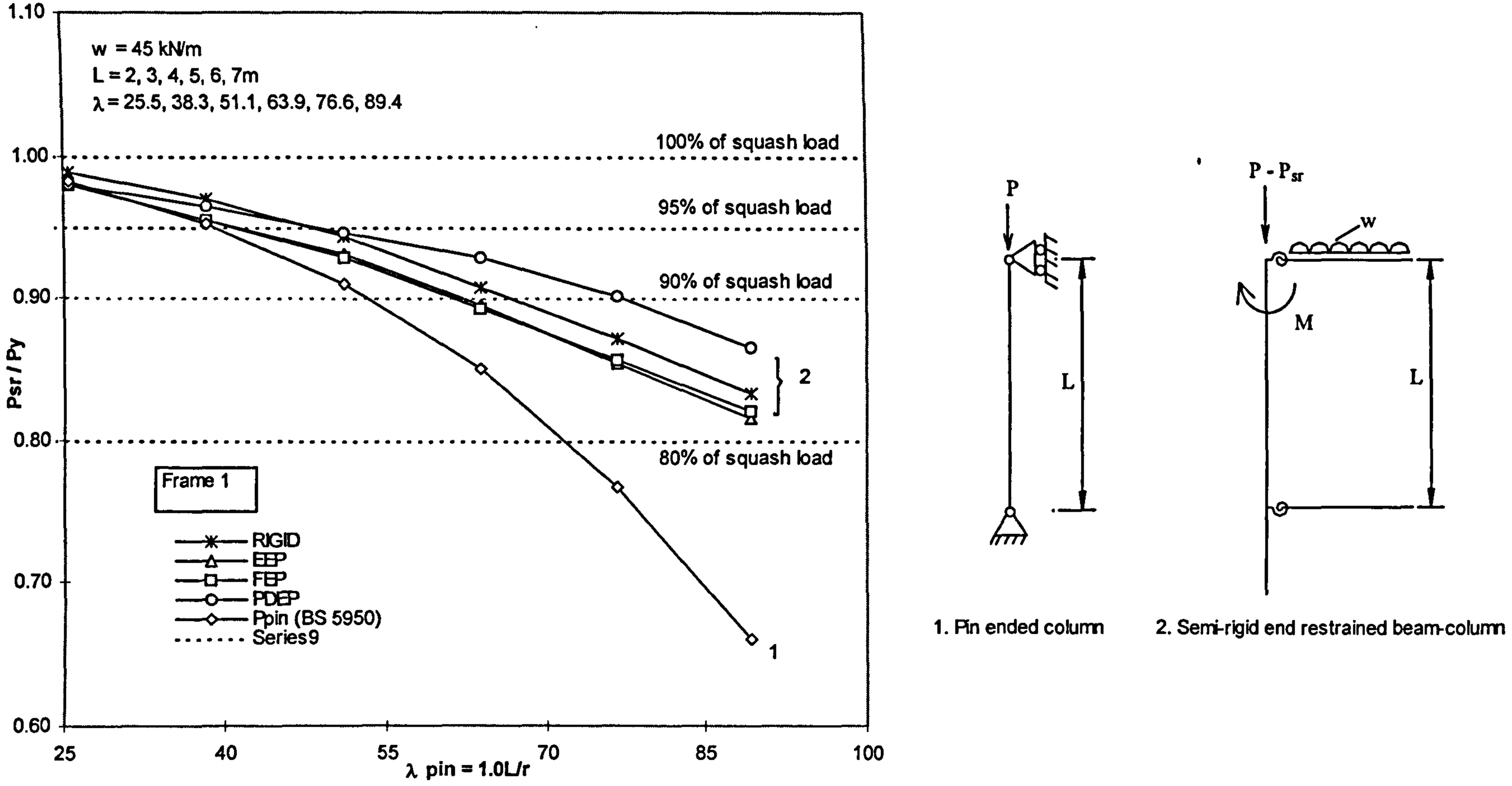

Figure 6.25 Beam-column ultimate strength curves of upper edge columns with various connection end types, w = 45 kN/m

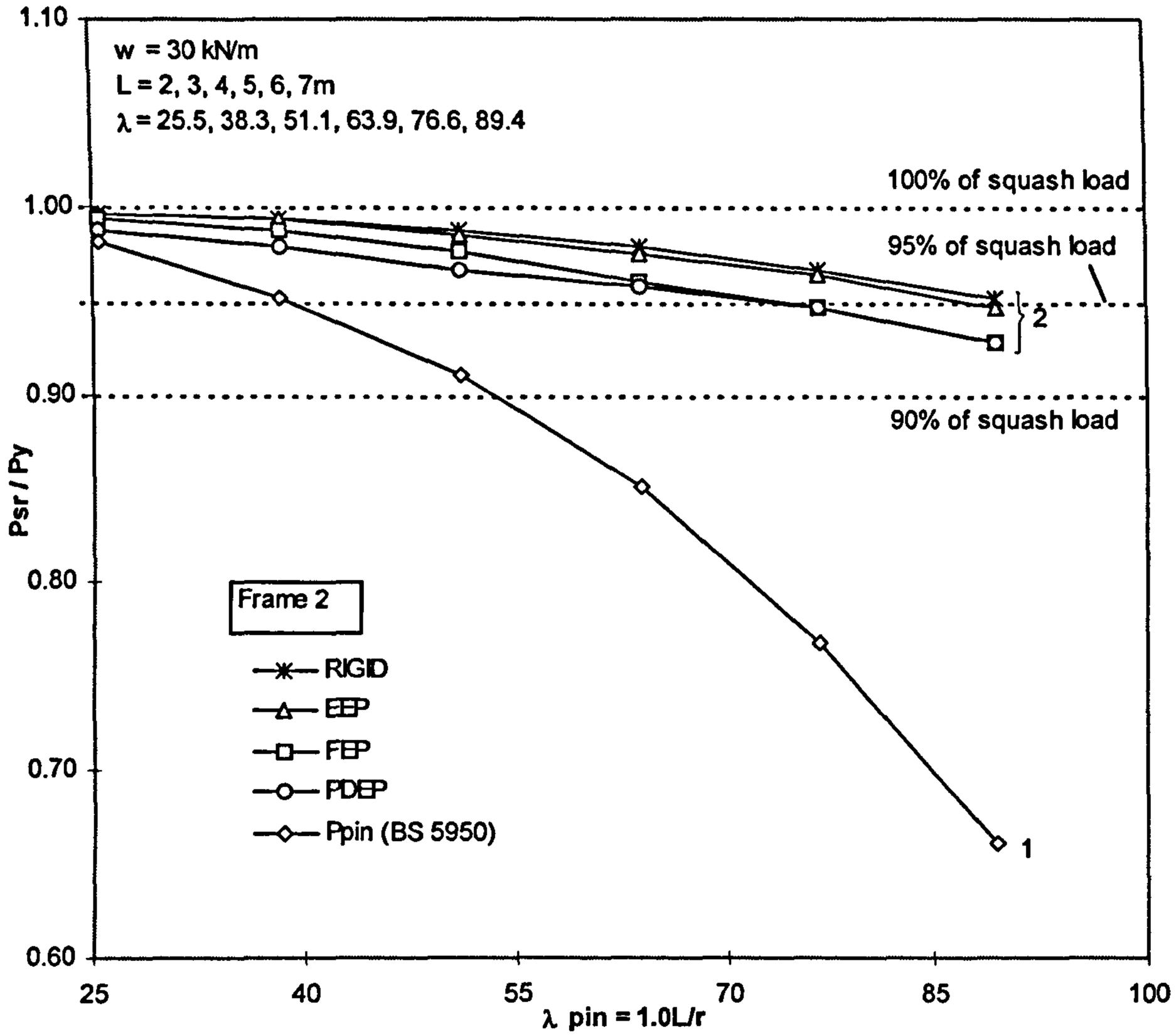

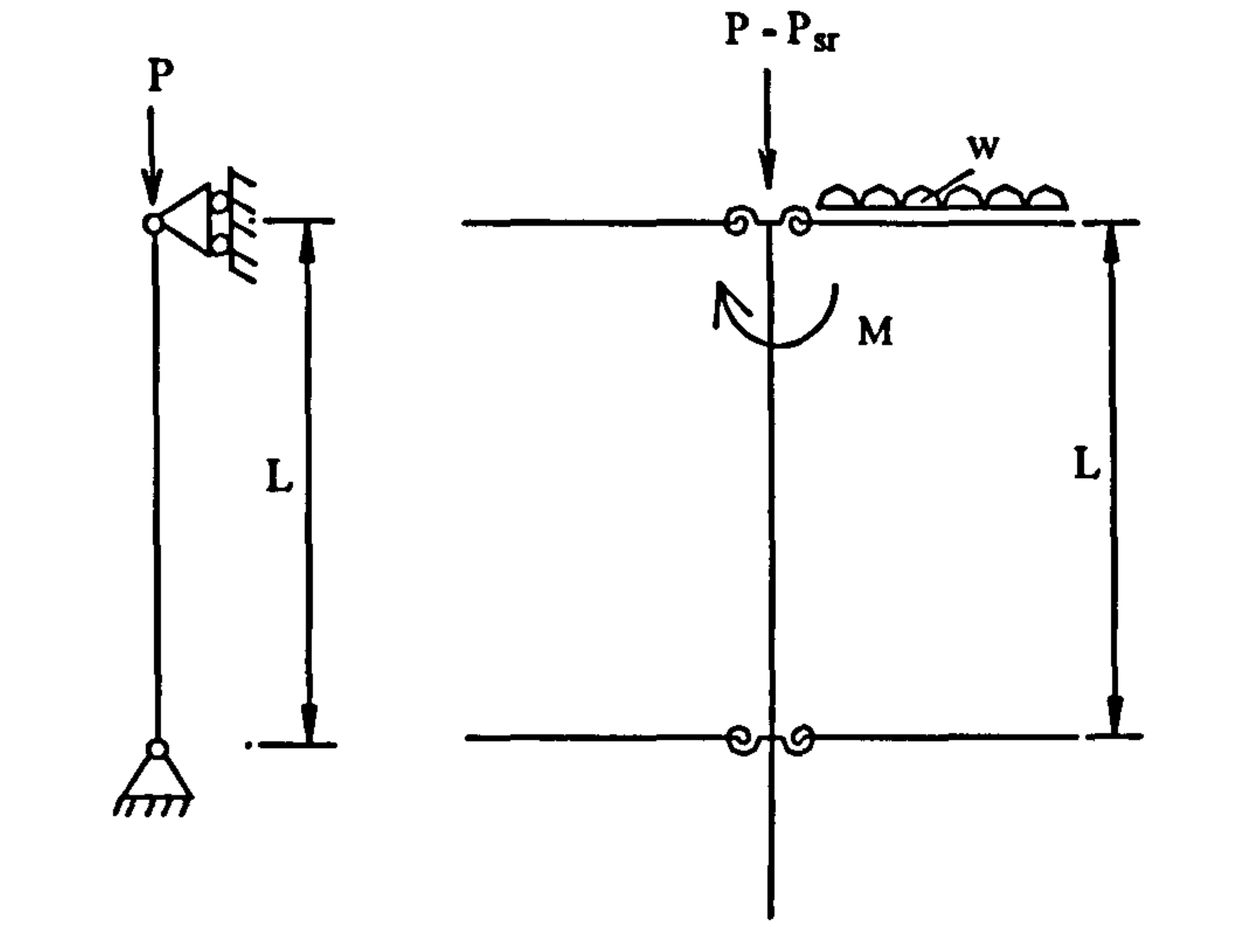

Figure 6.26 Beam-column ultimate strength curves of upper intermediate columns with various connection end types, w= 30 kN/m

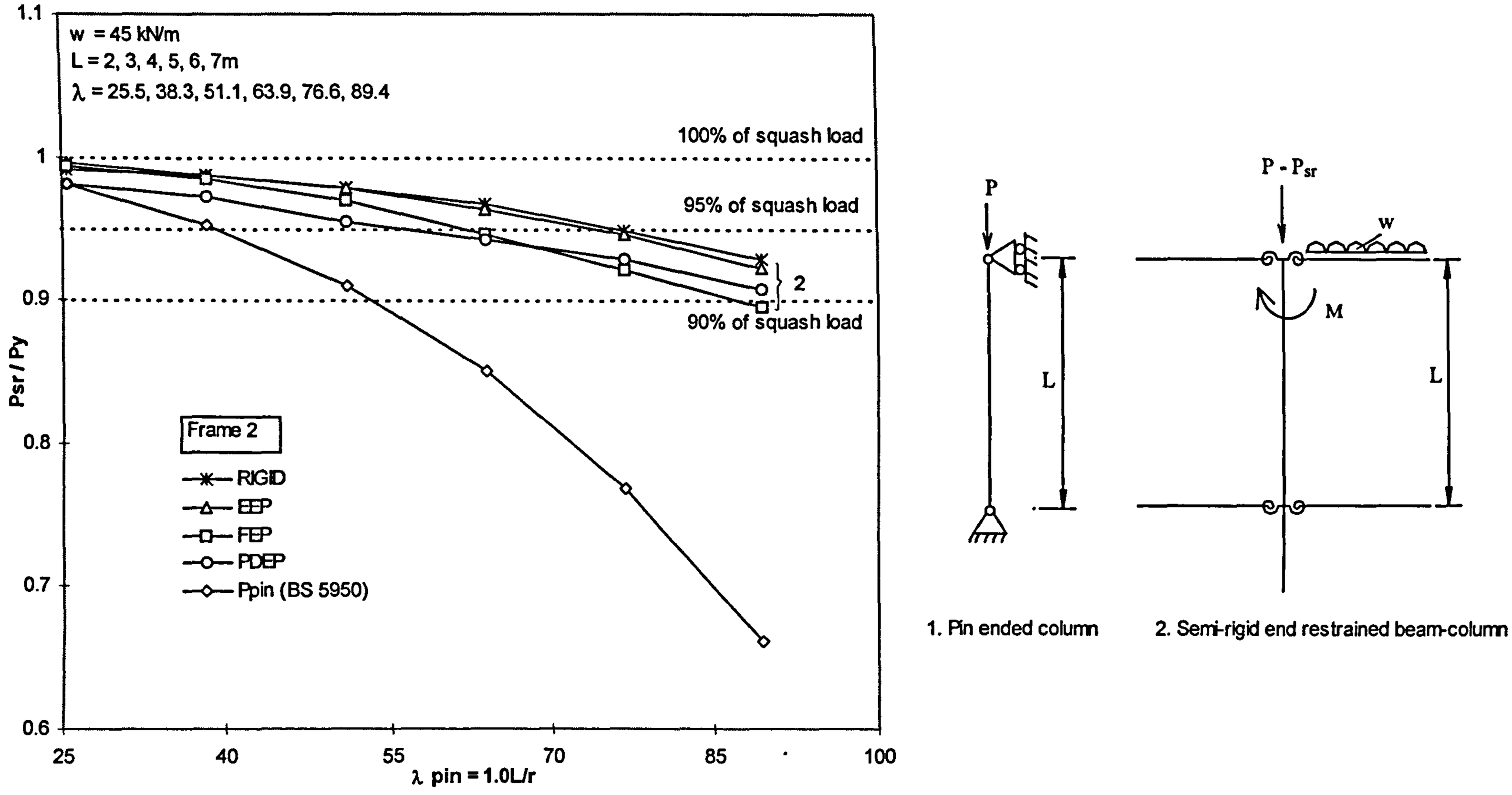

Figure 6.27 Beam-column ultimate strength curves of upper intermediate columns with various connection end types, w= 45 kN/m

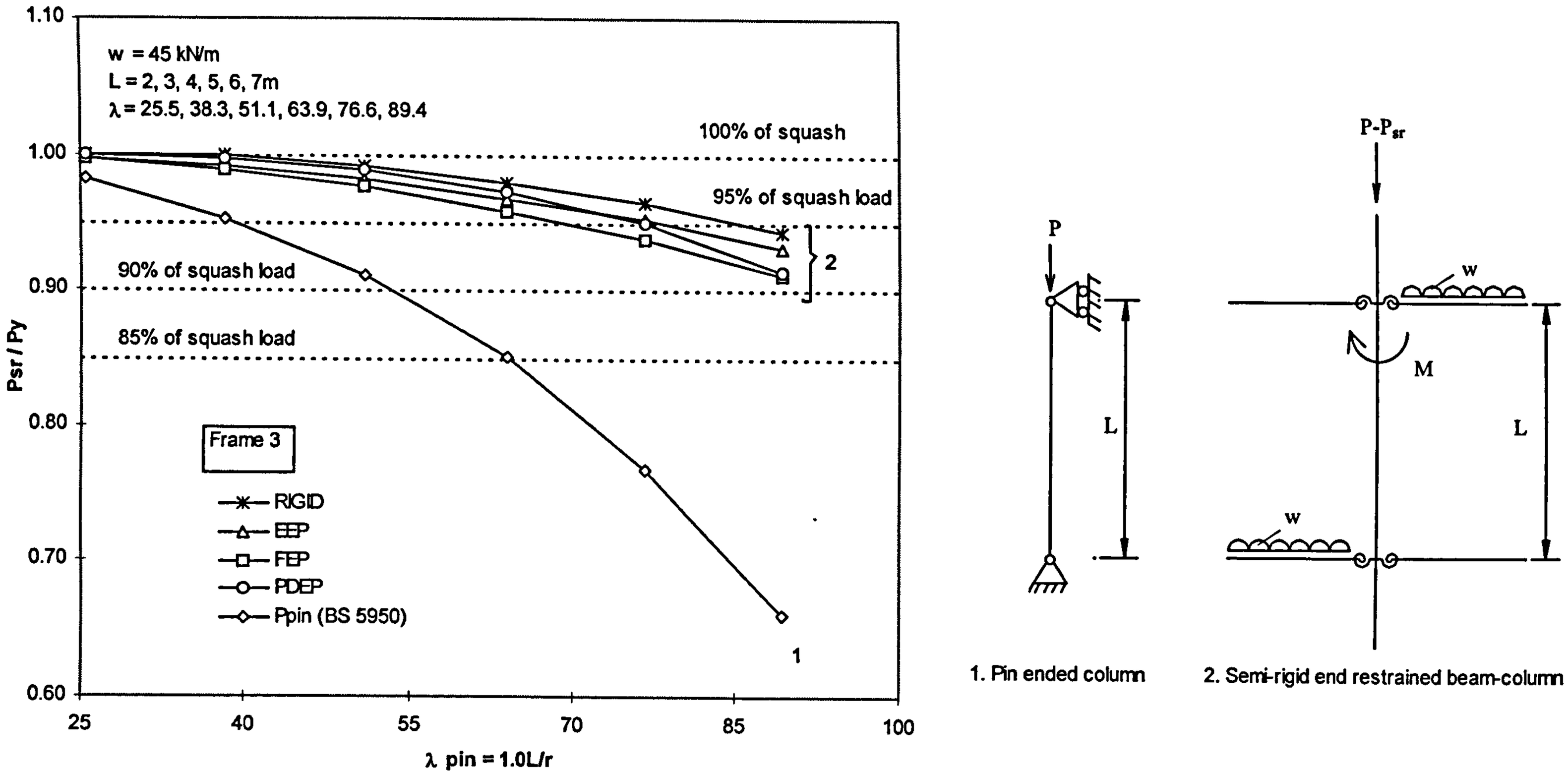

Figure 6.28 Beam-column strength curves of internal columns with 45kN/m beam load using various connection types

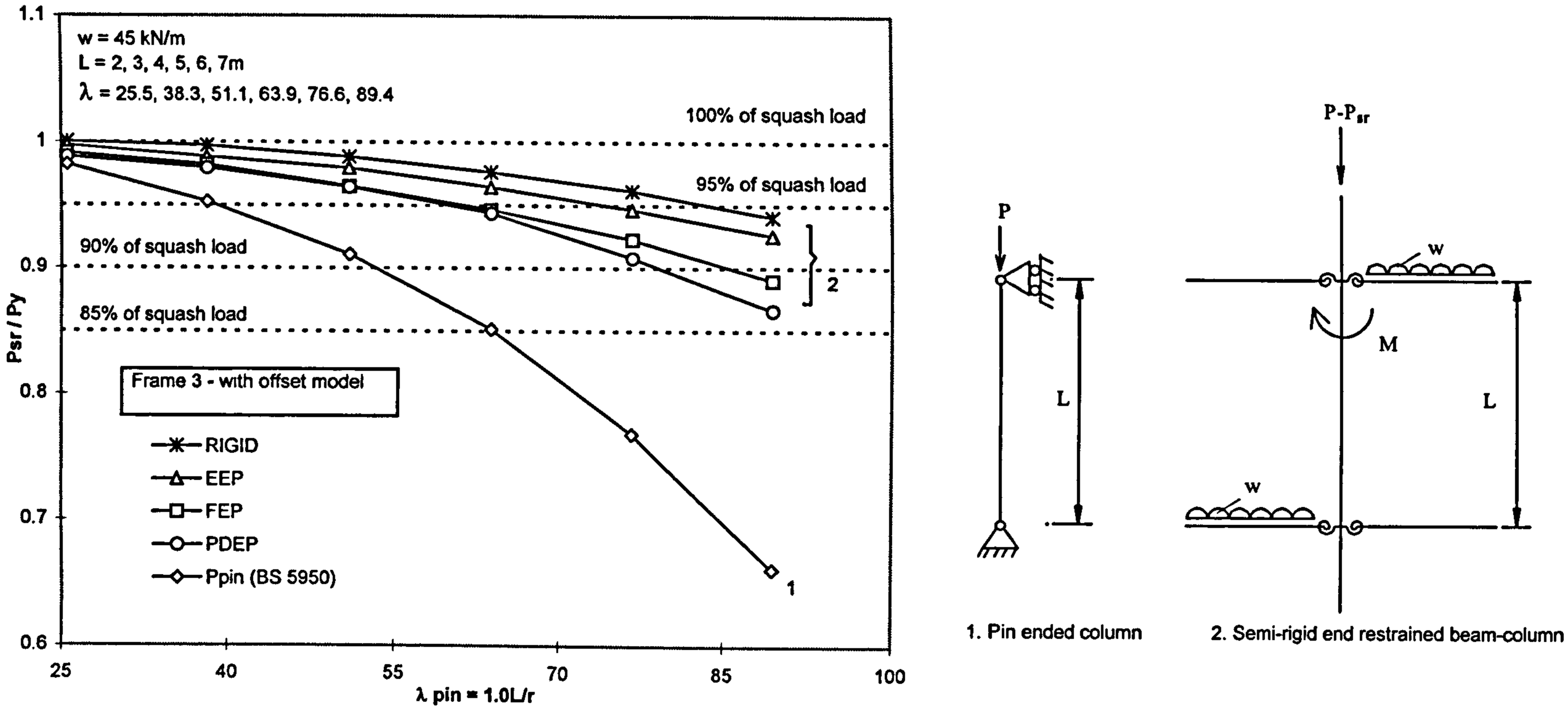

Figure 6.29 Beam-column strength curves including connection offset and beam load of 45 kN/m

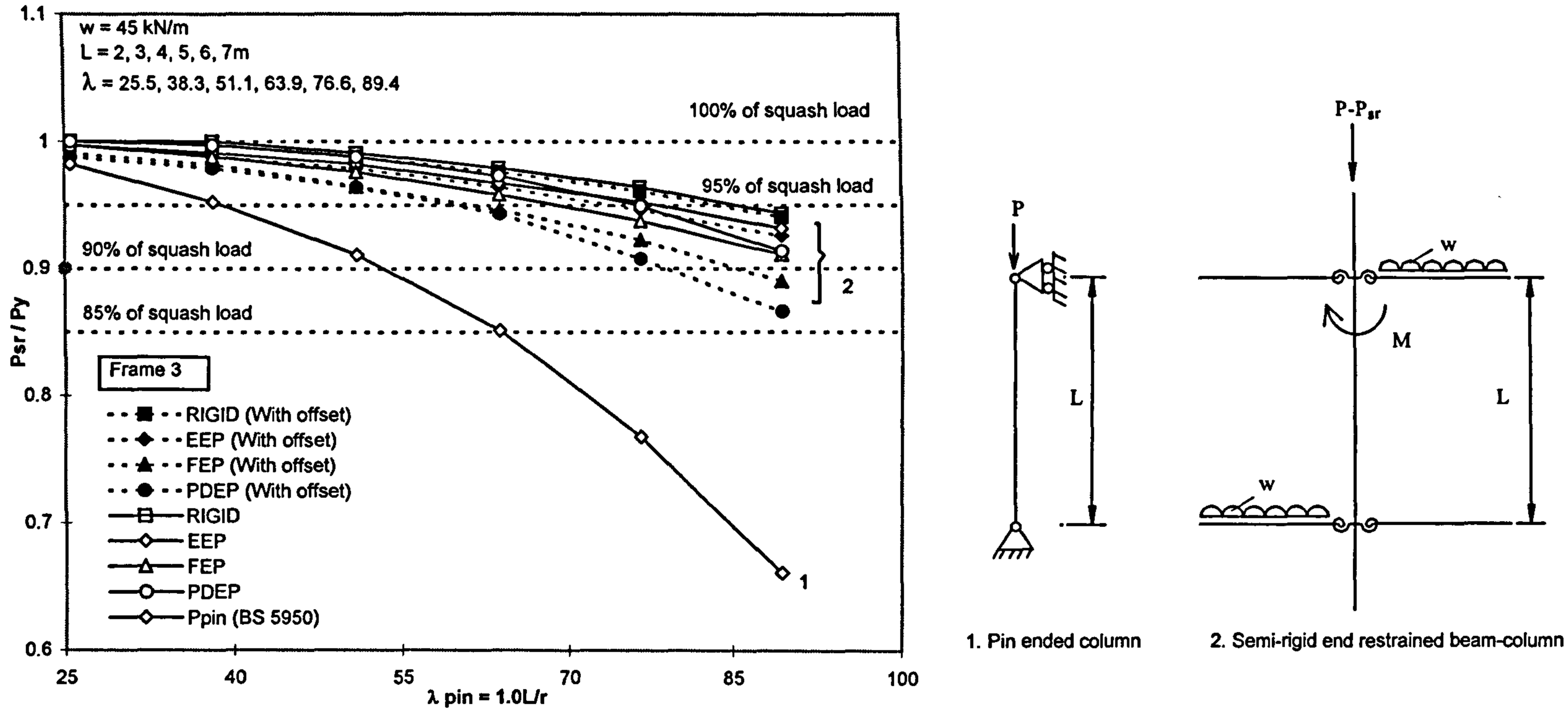

Figure 6.30 Comparison of beam-column strength curves including connection offset and not including connection offset

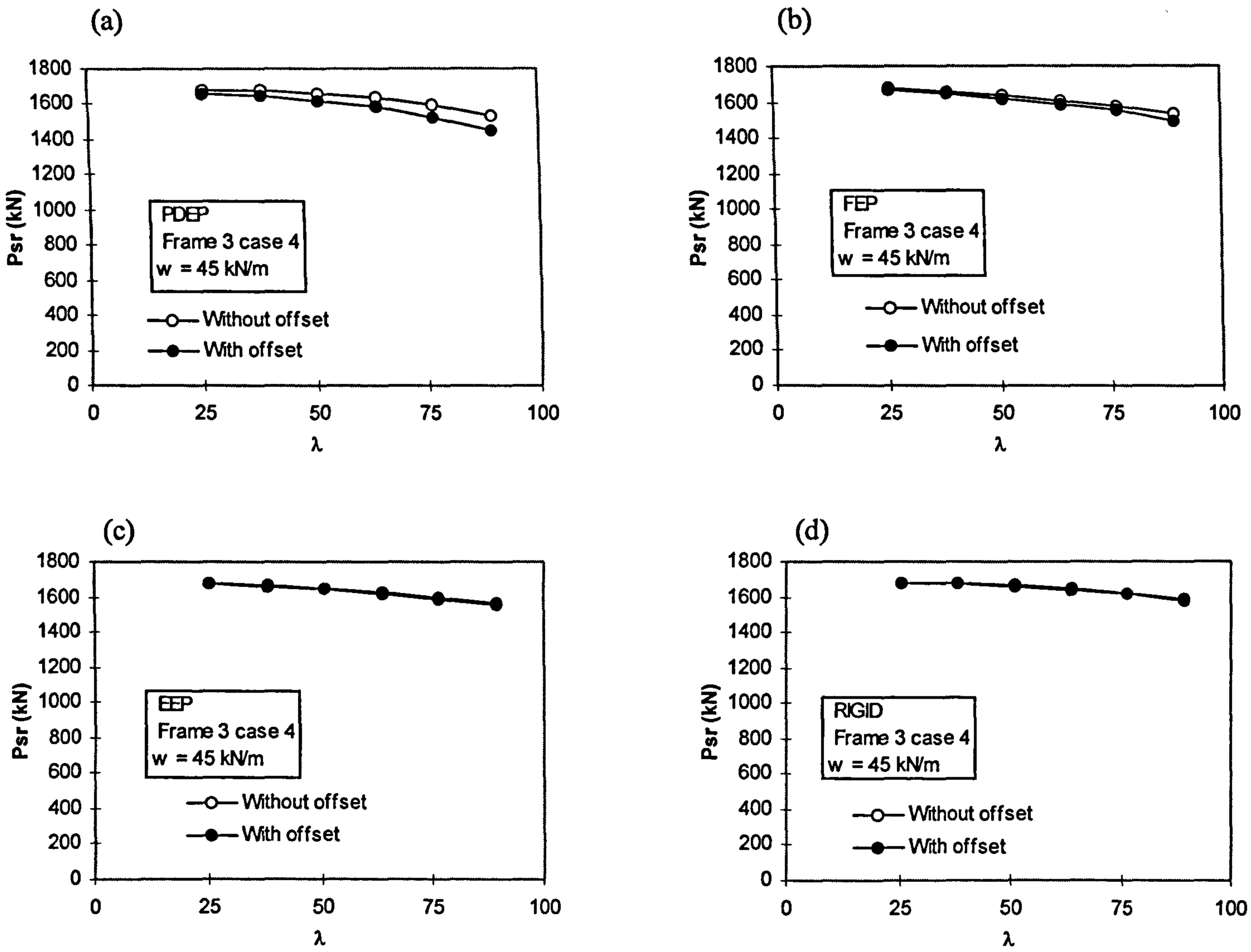

Figure 6.31 Comparison of column ultimate loads as modelled with and without connection offset for different connection types

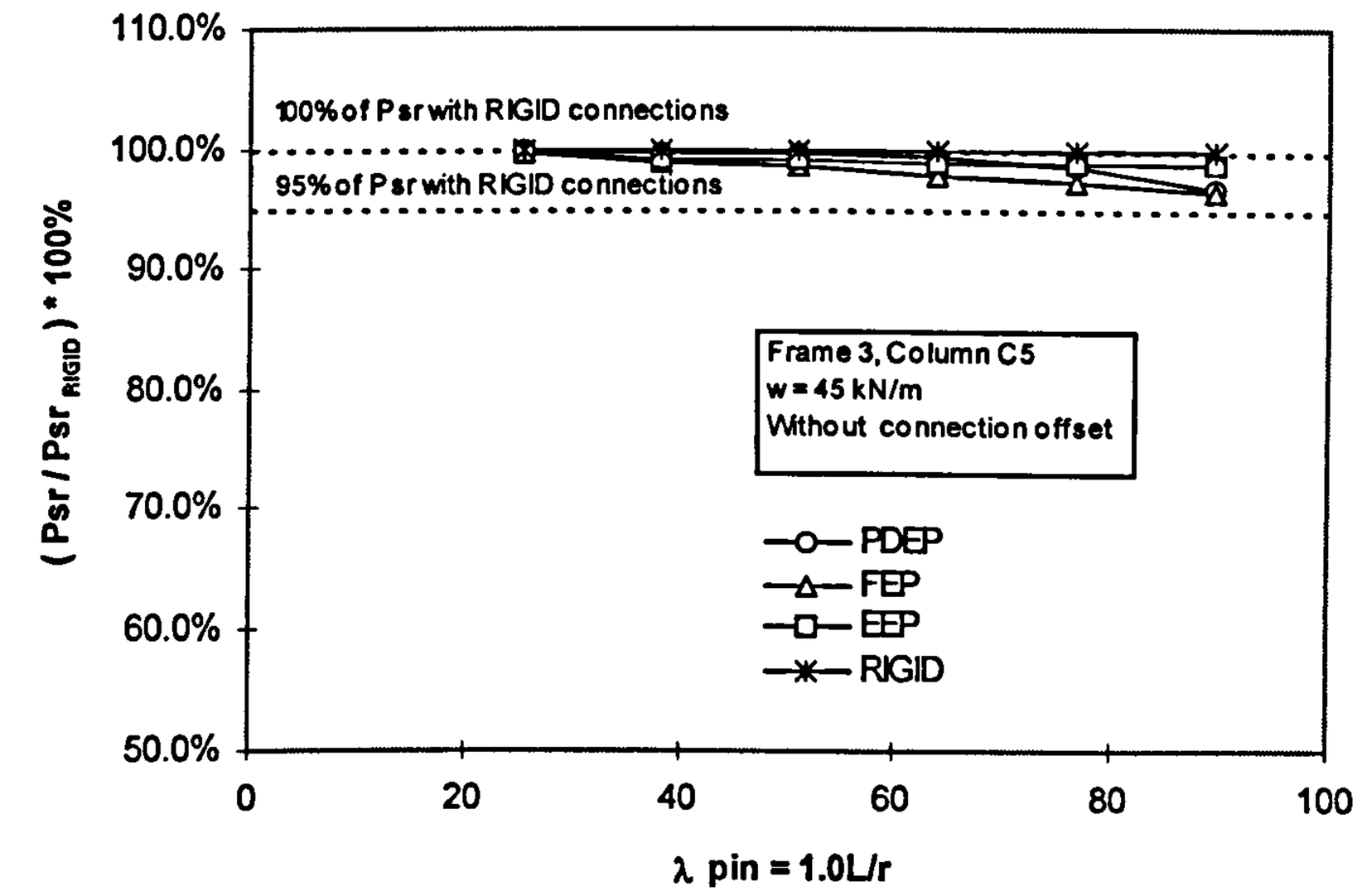

Figure 6.32 The ultimate strength of columns with less stiff connections as compared to the ultimate strength of columns using RIGID connections - without connection offset

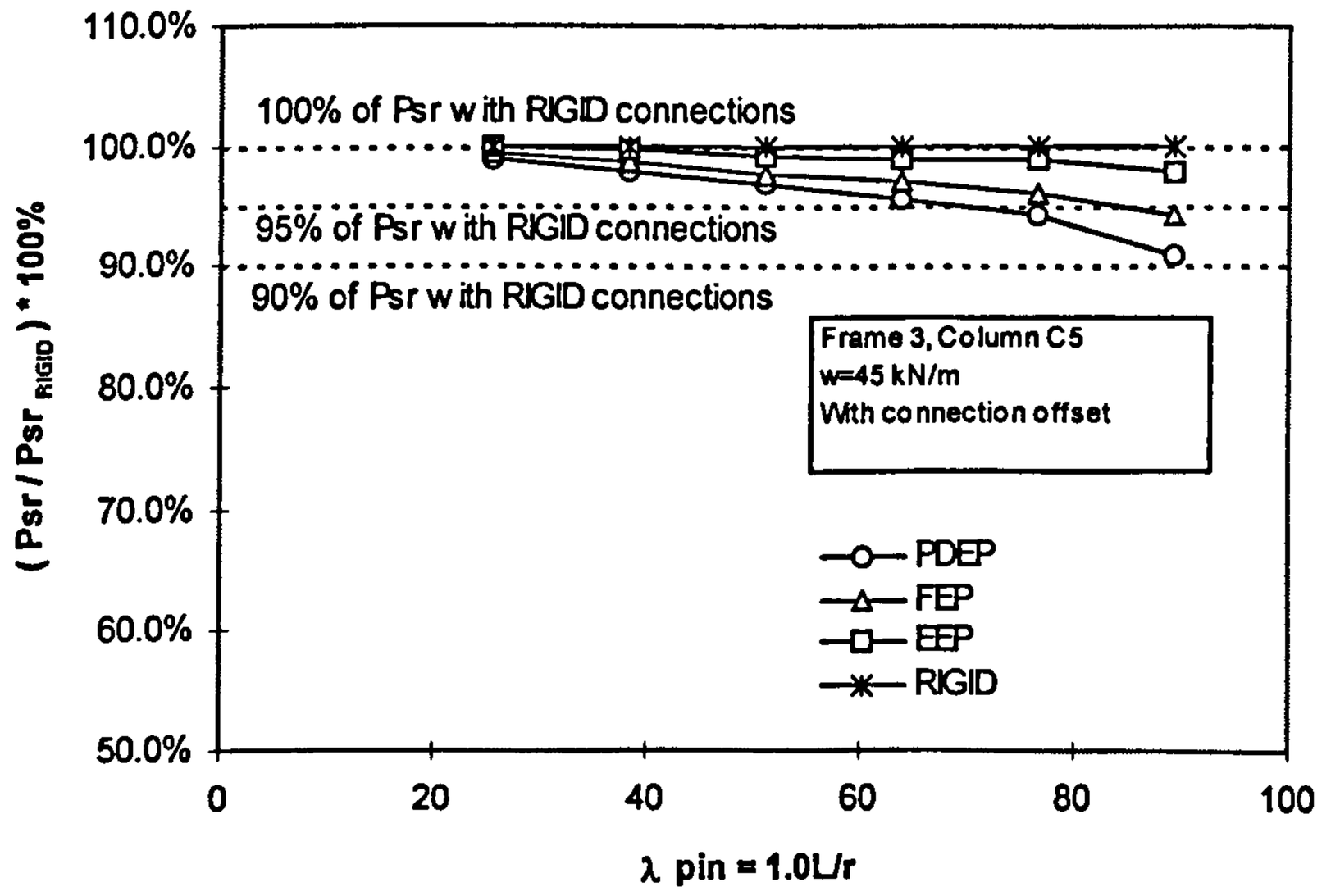

Figure 6.33 The ultimate strength of columns with less stiff connections as compared to the ultimate strength of columns using RIGID connections - with connection offset

Chapter 7

Simplified Design of

Semi-rigid Non-sway Frames

7.1 Introduction

The results of investigations carried out in Chapters 5 and 6 indicate that the behaviour of inelastic columns at higher load levels can be used as the basis for designing beam-columns in a simple manner. The results showed that the frame can be rendered as statically determinate due to the phenomenon of moment shedding. This leads to a simplified design method known as the α_{pin} approach.

In view of the above, the objectives of this chapter are:

- to demonstrate the possible use of the α_{pin} design in the daily design routine
- to extend the current α_{pin} simplified design method for simple, semi-rigid and rigid frames with tubular SHS columns
- to verify the α_{pin} design method with the experimental results

- to compare the α_{pin} design method with the current design methods.

Included in this chapter is the brief overview of the current simple, semi-rigid and rigid design methods based on BS 5950.

7.2 Current Design Method

BS 5950 [7-1] allows non-sway frames to be designed in three different methods namely; simple, semi-rigid and rigid design methods. Reference [7-2] adopts the following terminology to relate the connection types, the design methods and the frame construction types:

- *pinned connections* are used in *simple design* to produce *simple construction* frames

- *semi-rigid connections* are used in *semi-rigid design* to produce *semi-continuous construction* frames

- *rigid connections* are used in *rigid design* to produce *continuous construction* frames.

In UK practice, the most popular methods of design are the simple design and then followed by the rigid design. The simple and rigid design methods are based on the assumptions that the connections are perfectly pinned and rigid respectively. Although, the assumptions neglect the actual semi-rigid response of the connections, the two design methods still be the preferred option for designers. Some of the reasons of their popularity with respect to analysis and design are as follows:

- simplicity in the analysis and design in the case of simple design

- availability of elastic rigid programs for analysing rigid frames

- the analysis and design of the simple and rigid frames are not dependent on the M-ϕ characteristics of the connections.

Although, the research on semi-rigid connections has been conducted for more than 60 years, the implementation of the semi-rigid design is still very limited. Some of the many possible reasons of not using semi-rigid design with respect to analysis and design are:

- lack of simplified semi-rigid design methods
- the BS 5950 semi-rigid design method as specified in clause 2.1.2.4(a) [7-1] requires sufficient M-ϕ connection characteristics which must be based on experimental evidence or an involved calculation such as using Annex J of EC3 [7-3].

Current design rules, irrespective of construction systems, require the use of interaction equations which relate a combination of axial load and moments. This is due to the fact that the design procedures are formulated based on the response of beams and columns as observed at the lower load levels in which axial load and moments are present. The interaction equation is normally in the general form of

$$f\left(\frac{P}{P_u}, \frac{M_x}{M_{ux}}, \frac{M_y}{M_{uy}}\right) \leq 1.0 \qquad (7.1)$$

where

P is the axial load
P_u is the axial load capacity
M_x is the bending moment about x-x axis
M_{ux} is the bending moment capacity about x-x axis
M_y is the bending moment about y-y axis
M_{uy} is the bending moment capacity about y-y axis

The exact form of Equation (7.1) varies from code to code. In the case of BS 5950, the form of the interaction equation is discussed in the following sections.

7.2.1 Simple Design

In UK, most of the non-sway multi-storey buildings are built based on the simple construction system [7-4]. The popularity is partly attributed to the simplicity of the connections which leads to a more economical connection fabrication cost. The frames are designed based on the simple design method in which the members can be treated individually.

In this design method, beam members are designed as simply supported with perfectly pinned ends and totally neglect the effect of connection restraint although in reality, flexible connections such web cleat can possesses some amount of rotational stiffness and strength [7-5]. The columns are designed as axially loaded with the inclusion of nominal moment due to eccentricity.

Columns in a simple frame can be designed using the interaction equation as specified by clause 4.7.7 BS 5950 [7-1]

$$\frac{F_c}{A_g . p_c} + \frac{M_x}{M_{bs}} + \frac{M_y}{p_y . Z_y} \leq 1 \qquad (7.2)$$

where

F_c is the compressive force

p_c is the compressive strength

A_g is the gross cross-sectional area

M_x is the nominal moment about the major axis

M_y is the nominal moment about the minor axis

M_{bs} is the buckling resistance moment for simple columns

Z_y is the elastic modulus about the minor axis

p_y is the design strength

The connections which are employed for simple construction frames are normally web cleats or partial depth end plates. However in the past, even FEP connections with a significant amount of rotational stiffness and strength have been regarded as pinned connections in simple constructions. In fact, FEP connections are the most popular and have been used extensively. Recent guidelines from SCI, however, have discouraged the use of FEP connections in simple constructions by not including this

connection in the design manual [7-6]. This reflects that FEP connections possess significant rotational stiffness and strength which are then more suitable to be employed in semi-rigid frames.

7.2.1.1 Contradictions of the Simple Design Procedures Based on BS 5950

This section discusses some contradictions that occur in simple design procedures. The reason for this discussion is to demonstrate that the contradictions may be eliminated if the phenomenon of moment shedding is taken into consideration as the basis of the design procedures.

The procedures of the simple design method based on BS 5950 specifications [7-1] that are seen to have some contradictions are listed as follows:

- Clause 2.1.2.2 requires that the connections are assumed to be pinned and hence no adverse moment will be transmitted to the column. On the other hand, clause 4.7.7 of BS 5950, however, requires that the moment due to "partial fixity" to be included in addition to the "nominal moments" due to eccentricities. This assumption conflicts with the pin model in clause 2.1.2.2. Logically, if the connection is modelled as perfectly pinned then the "partial fixity" moment should not be present in the column (i.e. only moment due to eccentricity should be present). In fact, the requirement of the moment due "partial fixity" is in accordance with clause 2.1.2.4 which eventually resulted in the semi-rigid design method.

- Another contradiction that appears in simple construction is the treatment of loading in the column design. Clause 4.7.7 specifies that it is not necessary to consider the effect of pattern loading on columns. The clause adds further that all beams may be assumed to be fully loaded. As a result, the internal columns are normally designed as axially loaded because the eccentricity moments meeting at the joint due to the fully loaded beams are cancelled out (assuming beams of equal lengths). However according to Nethercot [7-7], if the eccentricity moment is to be

included as required in clause 4.7.6 then the effect of an unbalance loading arrangement which can induce larger unbalance moment at internal columns as shown in Figure 7.1 may need to be considered.

In view of the above, it is seen that the design procedures of simple construction as specified in BS 5950 are mainly of an empirical nature rather than on the actual behaviour of the frames. This is supported by Horne [7-8] who pointed out that the simple design method is based on the contradictory assumptions regarding the interaction between beams and columns.

However the above contradictions may no longer be present if the design procedures are based on the response of moment shedding and the inelastic column at the ultimate load level. That is, as a result of moment shedding, the acting moment on the column can be neglected. Hence, the effect of eccentricity moment and the patterned loading can be ignored in the design. As a consequence beam-columns can be designed as axially loaded. This also suggests that some assumptions made in the simple design are actually based on the response of an inelastic column at the ultimate load level.

7.2.2 Semi-rigid Design

BS 5950 provides two alternatives for designing semi-rigid frames [7-1]. The first alternative, takes account of partial continuity at the joint. The semi-rigid moment transferred from the beam to the column is evaluated based on the M-ϕ characteristics of the connections. Thus, sufficient knowledge of the connection M-ϕ characteristic is needed. The second alternative, is by adopting the simple design but in order to incorporate the effect of semi-rigid connections, a restraint moment not exceeding 10% of the free moment is assumed in the simply supported beam model. The column is then designed to resist the acting moment transmitted by the connection as well as the moment due to connection eccentricity. The basis for the design approach, however, is not given.

The beneficial aspects of semi-rigid design as compared to the simple design is that the use of semi-rigid connections reduces the beam midspan moment which consequently may lead to lighter and shallower beams.

7.2.3 Rigid Design

This design assumes full fixity between the beam and column. The column can be designed using a simplified interaction equation as specified in Clause 4.8.3.3 [7-1] which is given as follows:

$$\frac{F_c}{A_g.p_c}+\frac{mM_x}{M_b}+\frac{mM_y}{p_y.Z_y}\leq 1 \qquad (7.3)$$

where

F_c is the compressive force
p_c is the compressive strength
A_g is the gross cross-sectional area
m is the equivalent uniform moment factor
M_b is the buckling resistance moment for simple columns
Z_y is the elastic modulus about the minor axis
p_y is the design strength
M_x is the applied moment about the major axis x-x
M_y is the applied moment about the minor axis y-y

Although, it is evident that the design of rigid framing can lead to economical beam design , the use of these connections in practice is still minimal as compared to simple framing. Factors that can contribute to the unpopularity of the rigid system are the complexity in connection design and higher cost of connection fabrication which may involve extensive welding. The use of the interaction equation in the current design method has resulted in heavier columns due to larger bending moments transferred by the rigid connections from the beam to the column. This in turn increases the cost of columns.

Several attempts have been made to popularise rigid construction [7-9],[7-10] . The most significant one is the variable stiffness method proposed by Wood [7-9]. This method has resulted in lighter beams and columns as opposed to the current BS 5950 rigid design. However, the rigid connections employed in this system require column web stiffeners which again may contribute to the complexity in the design and fabrication aspects. The trend is that despite of many attempts to popularise the rigid construction many designers still prefer the simple construction types.

7.3 The Simplified Design Method (The α_{pin} Method)

A simplified design method called the α_{pin} has been developed at the University of Sheffield. The main criteria of this design method is that the effect of acting moments are taken as being outweighed by the column end restraint and hence the column can be designed as axially loaded. Previous studies on the α_{pin} method have been related to the open section columns [7-11], [7-12], [7-13], [7-14], [7-15], [7-16]. Recently, based on this study, the α_{pin} method has been adopted in the scheme design of semi-continuous braced frames published by the Steel Construction Institute, UK [7-2].

The use of the α_{pin} method is further investigated by the author for possible use in frames with tubular SHS columns. The results of the study conducted in Chapters 5 and 6 indicate that the α_{pin} design method can be used for simple, semi-rigid and rigid non-sway frames with the tubular SHS columns. As a consequence, beams can be designed as simply supported with a certain value of end restraint moment and columns can be designed as axially loaded.

7.4 Basis of the α_{pin} Method

The basis of the proposed α_{pin} method is the phenomenon of moment shedding and the response of inelastic columns at the ultimate limit state with the beams remaining elastic (see Figure 7.2). The phenomenon of moment shedding has been observed in the experimental results of both semi-rigid and rigid frames [7-4], [7-17], [7-18], [7-19]. The results of the study carried out in chapters 5 and 6 show that when the column starts to become inelastic, the column end moment is dramatically shed and relaxed to zero. This is followed by the redistribution of moments from the yielded column to the neighbouring members. This in turn resulted in a simple configuration of internal forces in the frame members. Eventually, the frame members can be rendered as statically determinate in which the columns can be treated as axially loaded and the beams as simply supported with a certain value of end restraint moment. The results show that the eccentricity moments due to beam reactions acting at the column face are also subjected to moment shedding and eventually relaxed to almost zero.

As a result of the above phenomenon, the α_{pin} design method neglects the moments resulted from the eccentric load and that transmitted by the connections.

In addition, research work on open section columns at the University of Sheffield since 1980 [7-12], [7-13], [7-14], [7-15], [7-17] discovered that the effect of column end moment can be ignored because the detrimental moment is outweighed by the beneficial effect of the connection restraint.

The idealisation of the frame for the α_{pin} design is discussed as follows:

- Figure 7.3(a) shows a semi-rigid non-sway frame carrying gravity loads. The corresponding internal moments in the frame due to working load are shown in Figure 7.3(b).

- In order to obtain the response of the inelastic column with the beam remaining elastic, a series of incremental loads is applied at the column heads of the top storey columns to cause failure of the lower columns. When the lower columns

fail as the ultimate load is reached, the corresponding internal moments of the frame that can be rendered as statically determinate are shown in Figure 7.3(c).

- At ultimate load, the column is not subjected to the acting moment as the moment is already shed to the adjoining members. As a result, the internal moment of the column is similar to the moment of axially loaded columns. Consequently, the internal moment of the beam which is affected by the failed column is in the form of the bending moment of a simply supported beam with end restraints.

Based on the above, the configuration of moments at ultimate load level is adopted as the basis of the α_{pin} design.

7.5 Verification of the α_{pin} Design Method

This section discusses the verification of the simplified design method against the results of full scale tests.

First, Table 7.1 shows the comparison of column capacity as predicted by the various design methods against the actual capacity of the columns as obtained from the two dimensional full scale test. The test frame was a non-sway frame with semi-rigid connections [7-4], [7-21]. The various design methods presented in the table are; (i). The simple design based on BS 5950 [7-1]. (ii). Moore & Nethercot design method [7-4]. (iii). The α_{pin} method based on BS 5950. It should be mentioned that the first two design methods are formulated based on the behaviour of frames at working load and hence, the interaction equations are employed. Whereas, the third design method is based on the behaviour of inelastic column at the ultimate load and the design is implemented without any interaction equation. As shown in the table, P_{design} is the column strength as predicted by the various design methods and P_{test} is the actual column strength as obtained from the test. Observation from the table shows that the values of P_{design} / P_{test} from the simple design are quite low, i.e. in the range of 0.55 to 0.69. This indicates the conservatism of the BS 5950 simple design. On the other hand, the values of P_{design} / P_{test} as obtained from Moore & Nethercot and the

α_{pin} design methods are quite close to 1.0, i.e. in the range of 0.67 to 0.89. This indicates that both design methods are safe and reasonably give accurate prediction of the actual column capacity.

Secondly, Table 7.2 shows the comparison of the predicted column capacity against the actual column capacity as obtained from the three dimensional full scale test. The test frame was a non-sway frame with semi-rigid connections [7-14]. The design methods presented in the table are; (i). The simple design based on BS 5950. (ii). The α_{β} design method as suggested by Lau [7-13]. This design method adopts the α_{pin} approach with the effective length factor, K obtained from the chart in Appendix E of BS 5950 [7-1]. The beam stiffness which is required in the chart is modified by incorporating the slip factor, β to take into account the effect of semi-rigid connections. (iii). The α_{pin} method. Similarly, as in the previous case, the results of P_{design} / P_{test} for the first design method are quite low, i.e. in the range of 0.38 to 0.61. Again, this indicates the conservatism of the simple design method based on BS 5950. Whereas, the values of P_{design} / P_{test} as obtained from the α_{β} and α_{pin} methods are quite close to 1.0, i.e. in the range of 0.75 to 0.86 and 0.64 to 0.9 respectively. This indicates that both design methods are safe and reasonably give accurate prediction of the actual column capacity. This also implies that the α_{pin} design can provide more economical column as compared to the current BS 5950 design method.

Finally, Table 7.3 shows part of Wood's extract [7-9] on the comparison of the predicted column capacity against the actual capacity of the column as obtained from the full scale test. The frame was a two dimensional non-sway frame with rigid connections [7-22], [7-23]. The design methods presented in the table are; (i). Variable stiffness method [7-9]. (ii). BS 449 rigid with the use of interaction equation [7-24]. (iii). BS 449 safe load table neglecting all the column end moments. The value of F_{design} / F_{test} is the ratio between the column capacity as predicted by the design method and the actual column capacity as obtained from the full-scale test. Column 1 of the table shows the values of F_{design} / F_{test} as obtained from the Wood's variable stiffness design method. In column 2 of the table, BS 449 rigid represents the ratio of F_{design} / F_{test} in which the F_{design} is based on the BS 449 design method using the interaction equations. The corresponding values of F_{design} / F_{test} are in the range

of 0.19 to 0.99 implying that the design is safe. Another method presented in column 3 of the table, totally neglect all the bending moments and the column capacity is predicted based on the capacity of pin ended columns as obtained from BS 449 Safe Load Tables. It can be seen that the values of F_{design} / F_{test} are in the range of 0.58 to 0.99 indicating that the design is safe and reasonably give accurate prediction of the actual column capacities. According to Wood [7-9] there is no foundation for this design approach except relying on the concept of moment shedding.

Based on the three verifications, it can be concluded that the simplified α_{pin} design approach is found to be satisfactory when compared with the actual test results.

7.6 Design for the Ultimate Limit State

7.6.1 Analysis

In order to design beams and columns, it is necessary to determine the axial forces and moments occurring in the members. Based on the response of the inelastic columns with the beams remaining elastic, the beams and columns can be analysed as isolated members and consequently can be modelled as follows:

- In the case of columns, the effect of moments transferred by the beams is ignored because of the moment shedding phenomenon at ultimate load levels. As a consequence, any pattern loading such that shown in Figure 7.1 is not required. Hence, the columns can be modelled as axially loaded compression members (see Figure 7.4(a)).

- The beams are modelled as simply supported with a certain value of end restraint moment at the beam ends. Figure 7.4(b) shows the typical bending moments of beams with pinned connections. Similarly, Figure 7.4(c) shows the typical bending moments of beams with semi-rigid and rigid connections. The corresponding values of end restraint moments at the beam ends are given in section 7.6.3.

7.6.2 Methods of Design

The design of any frame or any of its individual members may be carried out by one of the following methods:

- Simple design.
- Semi-rigid design.
- Rigid design.

All the design methods mentioned above are associated with various types of connections as utilised in the frames. The suitable connections for the above design methods, respectively, are:

- Pinned connections.
- Semi-rigid connections.
- Rigid connections.

The classification of the connections can be determined based on clause 6.9.6 of the EC3 classification [7-3]. The following sections discuss the three design methods for designing beams, columns and connections.

7.6.3 Design of Beams

The beams are designed as follows:

- *Simple design.*

  The beams are modelled as simply supported with pin ends. This in turn results in zero end restraint moments at the beam ends (see Figure 7.5).

- *Semi-rigid design.*

  The beams are modelled as simply supported with a certain percentage of end restraint moment to incorporate the effect of semi-rigid connections. The end restraint moments of the beams are suggested as follows (see Figure 7.6(a)):

  (i). 5% of M_p at the external ends of external beams.

  (ii). 10% of M_p at all internal beam ends.

It should be mentioned that the above values of end restraint moments at the beam ends are obtained based on the results of the parametric studies conducted in chapter 5 (see section 5.7) and chapter 6 (see section 6.8).

In order to simplify the analysis, the end restraint moments at both ends of the external beams are taken as 5% of M_p of the external beams (see Figure 7.6(b)). This will result in a conservative design of the external beams. Whereas, the end restraint moments at both ends of the internal beams are taken as 10% of M_p of the internal beams (see Figure 7.6(c)).

Once the beams have been designed as above, the connections at the external beam ends and at the internal beam ends located at supports B and C (see Figure 7.6(a)), should then be designed for moment which is equal to 10% of M_p of the external beam or 10% of M_p of the internal beam, whichever is the larger. This is to ensure equilibrium of moments at supports B and C. Furthermore, by choosing the larger end moment, the beam midspan moment of either the external or internal beam will not be increased. Hence, all the beams that have been designed previously are still safe.

- *Rigid design.*

  The beams are modelled as simply supported with a certain percentage of end restraint moment to incorporate the effect of rigid connections. The end restraint moments of the beams are suggested as follows (see Figure 7.6(a)):

  (i). 5% of M_p at the external ends of external beams.

  (ii). 10% of M_p at all internal beam ends.

  Similarly, the above values of end restraint moments at the beam ends are obtained based on results of the parametric studies conducted in Chapter 5 (see section 5.7) and chapter 6 (see section 6.8).

  In order to simplify the analysis, the end restraint moments at both ends of the external beams are taken as 5% of M_p of the external beams (see Figure 7.6(b)). Again, the simplification will result in a conservative design of the external beams. Whereas, the end restraint moments at both ends of the internal beams are taken as 10% of M_p of the internal beams (see Figure 7.6(c)).

Similarly, the connections at supports B and C (see Figure 7.6(a)) should be designed for 10% of M_p as explained in semi-rigid design.

7.6.4 Design of Columns

The columns are designed as follows:

- *Simple, semi-rigid and rigid design.*

  Basically, the procedures of column design are similar for all the three design types namely simple, semi-rigid and rigid design. The only difference is the value of effective length of the column which depends on the degree of the connection restraint.

  In term of design process, the advantage of this method is that the use of interaction equation is no longer employed. This is possible due to the fact that at ultimate load levels, the acting moments transferred by the connections as well as the eccentricity moments are ignored as a result of moment shedding phenomenon.

  Consequently, as the acting moments on the columns are ignored than any arrangement of pattern loadings which can induced severe unbalanced moment is not required. The most severe loading condition is due to axial loads only and can be obtained by assuming all beams to be fully loaded at all levels. Thus, the procedures of designing beam-columns follow the procedures of designing axially loaded compression members as specified in BS 5950 [7-1], EC3 [7-3] or BS 449 [7-24].

  In order to include the beneficial effect of the connection restraints at the column ends, the reduced effective length of the column (see section 7.6.4.1) is used. Figure 7.7(a) shows the beam-column model at the ultimate load level with the restraining moment. The equivalent solution of the beam-column with the reduced effective length is also shown (see Figures 7.7(b) and 7.7(c)).

The strength of beam-column with length L is evaluated as equal to the strength of pin ended column with the effective length KL. Eventually, the beam-column can be designed as a pin ended if the effective length factor K is known. It should be mentioned that, the definition of the column effective length has been discussed in section 6.6.1.1.

7.6.4.1 Column effective length factor, K

The effective length or the buckling length of a restrained column is dependent on the stiffness of the connections. However results of column failure loads presented in Chapter 6 shows that a moderate increase in the connection stiffness, e.g. from PDEP to FEP connections, does not increase the column failure load significantly. This suggest that the column buckling length is not largely affected by the moderate change in the connection restraint. In view of this, it is reasonably justified to use the simplified form of effective length as presented in Tables 7.4 and 7.5.

The effective length factor can be conservatively taken as unity [7-12]. In this study, the effective length factor of unity is taken for the following cases:

(i). The upper edge external columns (see Table 7.4(a)).

(ii).The lower external columns (see Tables 7.5(a), 7.5(b) and 7.5(c)).

The suggested effective length factors as shown in the tables which maintain the simplicity are almost identical to Table 24 of BS 5950 [7-1] and Table 5 of IStructE manual [7-25]. The suggested effective lengths can be used for the α_{pin} design based on BS 5950 [7-1] and EC3 [7-3]. The research results from Chapters 5 and 6 show that even less stiff connections such as PDEP connections can provide significant restraint to the column ends. Hence, it is acceptable to use these tables in designing beam-columns with connections that are categorised as pinned. However, these tables if used for columns with rigid connections can result in a more conservative design.

Based on the recommended effective length factors, the column design is not dependent on the relative stiffness of the connections, beams and columns. This is in

contrast with the more rigorous design practice such as clause 4.7.2 in Appendix E of BS 5950 [7-1] and the method suggested by Bjorhovde [7-26], which requires the information of connection M-ϕ curves and the relative stiffnesses of the connected members.

Basically, the main criteria of this simplified method is simplicity which can favour designers for their routine design work. Therefore, no attempt is made to evaluate the accurate effective lengths.

7.6.4.2 Design of Column Based on BS 5950

The procedures of the α_{pin} column design method based on BS 5950 follow the rules specified in clause 4.7.4 [7-1]. The formula of the axial compression resistance is given as follows:

$$\frac{P}{P_c} \leq 1 \qquad (7.4)$$

where

P is the external axial load

P_c is the column capacity

and $P_c = A_g . p_c$ (7.5)

where

A_g is the cross sectional area

p_c is the compressive strength

The value of compressive strength, p_c, depends on the column slenderness, $\lambda = KL/r$ and design strength, p_y .

7.6.4.3 Designed of Column Based on EC3

The procedures of the α_{pin} column design method based on EC3 follow the rules specified in clause 5.5 [7-3]. The formula of the axial compression resistance is given as follows:

$$\frac{N}{N_{b,Rd}} \leq 1 \qquad (7.6)$$

where

N is the external axial load

$N_{b,Rd}$ is the buckling resistance

and $N_{b,Rd} = X.\beta_A.A.f_y / \gamma_{m1}$ (7.7)

where

X is the reduction factor for the relevant buckling mode

β_A = 1.0 for class 1 section

γ_{m1} = 1.05

A is the gross sectional area of the column

f_y is the yield strength

In order to avoid local buckling, the cross section of the columns must be of plastic section classification.

7.7 Design for Serviceability Limit State

In this study, the procedures of design for serviceability limit state is suggested as follows:

1. Assume the beam as simply supported with pinned connections as suggested by Anderson and Tahir [7-27]. According to them, serviceability calculations can be simplified by retaining the assumption of pinned connections without sacrificing economy. If, however, this design check is not satisfactory then continue to step 2.

2. Incorporate the actual semi-rigid connections and use the serviceability design check as suggested by Gibbons et al. using Equation (7.8). This method, however, requires the information of connection stiffness which can be obtained from the connection M-ϕ curves.

The actual deflection of beams with semi-rigid connections as suggested by Gibbons et al. [7-28] can be determined as follows:

$$\delta_{sr} = \delta_{rigid} + (1-\mu)(\delta_{pin} - \delta_{rigid}) \tag{7.8}$$

where δ_{sr} , δ_{pin} and δ_{rigid} are beam midspan deflections with semi-rigid, pin and rigid connections respectively.

The dimensionless factor μ is defined as

$$\mu = \frac{M_{sr}}{M_{rigid}} \tag{7.9}$$

where

M_{sr} is the semi-rigid moment
M_{rigid} is the rigid moment
$\mu = 0.0$ when $M_{sr} = 0$
$\mu = 1.0$ when $M_{sr} = M_{rigid}$

The semi-rigid moment, M_{sr} can be determined by using the graphical method known as the beam line method [7-29]. An alternative is to evaluate M_{sr} based on the following equation:

$$M_{sr} = \frac{M_{rigid}}{1 + \dfrac{M_{rigid}}{\phi_{pin} . C_i}} \tag{7.10}$$

where

ϕ_{pin} is the end rotation of simply supported beam
C_i is the initial tangent stiffness of the M-ϕ curve

The values of δ_{pin} , δ_{rigid} and M_{rigid} that are required for Equations (7.9) and (7.10) can be determined by using the elastic computer program.

The author believes that it is possible to simplify further Equation (7.8) by using a suitable value of μ that is expected to occur in real frame. For example, a limited study by Lau [7-13] on frames using FEP connections (with 12mm end plates) shows that the minimum value of μ for the semi-rigid connections considered is seen to be in the vicinity of 0.3. Therefore, based on this result, it may be suggested that the conservative value of degree of fixity μ may be taken as equal to 0.3 and consequently Equation (7.8) can be simplified further. However, a more extensive study is needed to find a more reliable value of the minimum μ.

7.8 Design of Connections

In order to achieve the values of inelastic end restraint moments at beam ends as specified in section 7.6.3, the connections must satisfy the following criteria:

- *Simple design.*

  The connections must be in the category of pinned connections with the moment capacity less than $0.25M_p$ of the connected beams. Normally, PDEP connections fall into this category.

- *Semi-rigid design.*

  The connections must be in the category of semi-rigid connections and must have a minimum strength capacity of $0.25M_p$ of the connected beams. Normally, FEP and EEP connections fall in this category. However the use of FEP connections is suggested because of their wide acceptance in practice and they are less complex in terms of fabrication.

- *Rigid design.*

  The connections must be in the category of rigid connections.

The connections are classified into the three main categories namely pin, semi-rigid and rigid connections in accordance to section 6.9.6 of EC3 [7-3]. The design of the connections follows the BS 5950 code as specified in section 2.1.2.4 of paragraph (6) [7-1]. This clause states that '*the beam-to-column connections are designed to transmit the appropriate restraint moment, in addition to the end reactions assuming the beams are simply supported*'.

7.9 Discussions

This section discusses the results of designs as determined by the α_{pin} and other various methods. The calculations of all the related design examples are given in reference [7-31].

7.9.1 Comparison of the Current EC3 and the α_{pin} Design Methods for Simple Frames

Table 7.6(a) shows the results of simple design of the ECCS frame [7-30] with 54 kN/m beam load. In comparing the design results between the current EC3 simple design and the α_{pin} design methods, it is seen that both methods give similar sizes for beams and columns.

It should be mentioned that in the ECCS example, the design of the columns was carried out without the inclusion of eccentricity moments. The effective length factors of the internal and external columns were taken as unity and the connections were assumed as nominally pinned. In the case of α_{pin} design, the effective length factors for the external and internal columns were taken as 1.0 and 0.85 respectively. The eccentricity moment is not included in any column due to the moment shedding

phenomenon. The calculations of the α_{pin} design method are given in example 1 of reference [7-31].

7.9.2 Comparison of the Current EC3 and the α_{pin} Design Methods for Semi-rigid Frames

Table 7.6(b) shows the results of semi-rigid design of the ECCS with 54 kN/m beam load. In comparing the design results between the current EC3 semi-rigid design and the α_{pin} design methods, it is seen that both design methods give similar sizes of columns but not the beams.

The size of beams as designed by the α_{pin} is seen to be larger then the size of beams as obtained from the EC3 method. This is resulted from the smaller values of end restraint moments as employed in the α_{pin} design, i.e. $0.05M_p$ and $0.10M_p$ of the connected beams for the external and internal beams respectively, as compared to the ECCS design example which employed beam end restraints up to $0.26M_p$ of the connected beams. This results in the α_{pin} approach having larger span moments and hence larger beams. The design calculations are given in example 2 of reference [7-31].

7.9.3 Comparison of the Current BS 5950 and the α_{pin} Design Methods for Simple Frames

Table 7.7(a) shows the results of simple design of the ECCS frame with 60 kN/m beam load. The table shows the design results of the current BS 5950, the α_{pin} with open section columns and the α_{pin} with SHS columns.

The results show that the α_{pin} design with open section columns gives smaller external columns as compared to the current BS 5950 simple design. It is also observed that the α_{pin} design with SHS columns provides smaller columns as compared to the α_{pin} design with open section columns.

On the other hand, both the current BS 5950 and α_{pin} design methods give similar sizes of beams. This is as to be expected because in both design methods, the beams are designed as simply supported with zero end restraint moments.

The design calculations are given in example 3 of reference [7-31].

7.9.4 Comparison of the Current BS 5950 Method and the α_{pin} Design Method for Semi-rigid Frames

Table 7.7(b) shows the results of semi-rigid design of the ECCS frame with 60 kN/m beam load. The table shows the comparison of beam and column sizes as designed by the current BS 5950 semi-rigid design method, the α_{pin} with open section columns and the α_{pin} with SHS columns.

It can be seen that the α_{pin} design method gives smaller external columns as compared to the current design method. The use of SHS columns reduces the column weight quite significantly.

It is also seen that the beam sizes designed by BS 5950 and the α_{pin} are identical. The BS 5950 design employs the values of end restraint moment of $0.10M_{free}$ where M_{free} is the maximum midspan moment of a simply supported beam. However, the α_{pin} method employs $0.05M_p$ and $0.10M_p$ of the end restraint moments at the external and internal beam ends respectively. For this type of frame example, it is seen that there is no significant difference in the values of end restraint moments as calculated by the BS 5950 design and the α_{pin} method, resulting in the similar beam sizes. The calculations of semi-rigid design are given in example 4 of reference [7-31].

7.9.5 Comparison of the Variable Stiffness and the α_{pin} Design Methods for Rigid Frames

Table 7.8 shows the results of rigid design as obtained from the Wood's variable stiffness method and the α_{pin} design. The α_{pin} design is implemented based on the effective length factors suggested by the BS 449 specifications [7-24].

The reason of using the BS 449 effective length factors is to demonstrate that the use of these effective lengths can give similar results to that the Wood's variable stiffness method. If, however, the proposed effective lengths presented in Tables 7.4 and 7.5 of this thesis are employed, more conservative column sections will be obtained.

As can be seen from the table, the α_{pin} and Wood's variable stiffness methods give identical size of columns except in one case where the α_{pin} gives a slightly larger column than the Wood's variable stiffness method, i.e. 152 x 152 x 37 UC as opposed to 152 x 152 x 30 UC.

The identical results of the column sizes between the Wood's variable stiffness and the α_{pin} methods may be because of the following similarities:

- both design methods are formulated based on the phenomenon of stiffness loss and moment shedding

- both design methods are based on the response of inelastic column at ultimate load levels.

The design calculations of the α_{pin} method are given in example 5 of reference [7-31].

7.9.6 Benefits of the α_{pin} Design Method

The benefits of the α_{pin} design method as compared to the current simple design of BS 5950 are as follows:

- external and internal columns are designed as axially loaded
- beams are designed as simply supported with $0.05M_p$ and $0.10M_p$ of end restraint moments for external and internal beams respectively
- lighter or smaller external columns
- lighter or shallower beams.

Finally, Table 7.9 shows the comparison of column design at working load (lower load) and ultimate load levels.

As can be seen from the table, the design of column at working load levels requires the use of interaction equations and the sufficient knowledge of the connection M-ϕ characteristics. One of the criteria of this design is that the stiffer the connections, the larger is the acting moment at the column. This in turn resulted in larger or heavier columns, whereas, the design of columns at ultimate load levels is not subjected to acting moment and not dependent on the connection M-ϕ characteristics. As the column is designed solely due to axial load and not dependent on the acting moment then the use of pin, semi-rigid and rigid connections will result in similar size of columns (subjected that similar column effective lengths are adopted for columns with pin, semi-rigid and rigid connections). In relation to this, Figure 7.8 shows that with the α_{pin} design, the same column size can be used for either simple, semi-rigid or rigid frames.

7.10 Limitations of the Simplified Design method

Based on the limited studies carried out in this thesis, the author suggests that the simplified design method presented in this thesis is limited to low rise multi-storey frames of up to six storeys. Further investigation is needed to study the applicability of the method for portal frames particularly in the aspects of redistribution of moments and the values of end restraint moment at the ultimate load levels.

7.11 Conclusions

The α_{pin} method offers a straightforward simplified design approach which is based on the true behaviour of elastic-plastic column at ultimate load levels. As a result of the moment shedding phenomenon, the non-sway frames can be rendered as statically determinate. The beams can be designed as simply supported with a certain value of end restraint moments and the columns can be designed as axially loaded.

The configuration of internal forces at ultimate load levels in the members can be simplified as being independent of the relative stiffness of the connected members. In other words, a knowledge of stiffnesses of the beams, columns and connections are not required in the design for strength of the beams and columns. Consequently, the M-ϕ characteristics of the connections are also not essential. The stiffnesses of the connections and beams, however, may be required for the serviceability checks if the beam distorts more than is permissible assuming pinned ends.

At the ultimate load levels, the columns are not affected by the beam moments and hence consideration of pattern loading is not required.

The significant advantage of this design method is that the design calculations for beams and columns are simplified dramatically. The design method eliminates the interaction equations as normally used in the current design methods. More interestingly, the α_{pin} design method can be used to design simple, semi-rigid and rigid frames.

Further conclusions based on the limited design examples discussed in this chapter are:

1. More economical external columns can be obtained with the use of α_{pin} design.

2. In the α_{pin} method, the beam-column is designed as being dependent on axial load only and is not affected by the beam moment. As a result, the use of pinned, semi-rigid and rigid connections produces the same size of columns.

3. In the α_{pin} design method, increasing the connection restraint at the beam ends does not produce heavier columns as occurs in the current design method.

4. The increased in the degree of connection restraint increases the beam end restraint and reduces the beam midspan moment. As a result, lighter or shallower beams are sufficient to resist the smaller midspan moment. This in turn produces more economical beams.

5. It is seen that in most of the cases considered, the size of columns designed by the α_{pin} and the variable stiffness methods are almost identical. This similarity occurs may be due to the fact that both design methods are formulated based on the phenomenon of stiffness loss and moment shedding but the α_{pin} method is more straightforward in its application.

7.12 References

[7-1] BS 5950: Part 1: 1990, 'Structural use of steelwork in building', Part 1. Code of practice for design in simple and continuos construction : hot rolled sections, British Standard Institution.

[7-2] The Steel Construction Institute, 'Design of semi-continuous braced frames', Specialist Design Guides, The Steel Construction Institute, Berkshire, U.K., 1997.

[7-3] Eurocode 3, 'Design of steel structures - Part 1.1: General rules and rules for buildings', ENV 1993-1-1.

[7-4] Moore, D.B. and Nethercot, D.A., 'Testing steel frames at full scale: appraisal of results and implications for design', The Structural Engineer, Volume 71, Nos. 23 & 24, December, 1993, pp. 428-435.

[7-5] Jones, S.W., Kirby, P.A. and Nethercot, D.A., 'The analysis of frames with semi-rigid connections - A state of the art report', Journal of Constructional Steel Research, Vol. 3, No. 2, 1983, pp. 2-13.

[7-6] SCI, 'Joint in simple construction; Practical applications', Volume 2, Steel Construction Institute, Ascot, UK, 1992.

[7-7] Nethercot, D.A., 'Limit states design of structural steelwork', 2nd. edition, Chapman & Hall, London, 1991.

[7-8] Horne, M.R., 'An historical review on the interaction of plasticity and structural stability in theory and its application to design', in Frame and Slab Structures, edited by Armer, G.S.T. and Moore, D.B., Butterworth, London, 1989, pp. 1-27.

[7-9] Wood, R.H., 'A new approach to column design', Her Majesty's Stationery Office, U.K., 1974.

[7-10] Joint Committee of Institution of Structural Engineers and Welding Institute, 'Fully-rigid multi-storey welded steel frames', 2nd. Report, 1971.

[7-11] Gibbons, C., Nethercot, D.A., Kirby, P.A. and Wang, Y.C., 'An appraisal of partially restrained column behaviour in non-sway steel frames', Proceeding of Institution of Civil Engineers, Structures and Buildings, 99, February, 1993, pp. 15-28.

[7-12] Kirby, P.A., Davison, J.B. and Carr, J.F. 'A simplified approach to the design of columns in simple construction', International Colloquium in Stability of Steel Structures, Budapest, Hungary, 1995, pp. 1/41 - 1/48.

[7-13] Lau, S.M., 'The response of non-sway steel framed structures with semi-rigid connections', Ph.D. Thesis, Department of Civil and Structural Engineering, University of Sheffield, U.K., December, 1990.

[7-14] Gibbons, C., 'The strength of biaxially loaded columns in flexibly connected steel frames', Ph.D. Thesis, Department of Civil and Structural Engineering, University of Sheffield, U.K., December, 1990.

[7-15] Kirby, P.A., Bitar, S. and Gibbons, C., 'Design of columns in non-sway semi-rigidly connected frames', First World Conference on Constructional Steel Design', Acapulco, Mexico, December, 1992, pp. 54-63.

[7-16] Kirby, P.A., Davison, J.B. and Mohammad, S., 'The design of columns in simple construction under variable loadings', International Colloquium in Stability of Steel Structures, Budapest, Hungary, 1995, pp. 1/49 - 1/56.

[7-17] Gibbons, C., Kirby, P.A. and Nethercot, D.A., 'Experimental behaviour of partially restrained steel columns', Proceeding of Institution of Civil Engineers, Structures and Buildings, 99, February, 1993, pp. 29-42.

[7-18] Baker, J.F., Horne, M.R. and Heyman J., 'The steel skeleton', Cambridge University Press, Vol. 2, U.K., 1956.

[7-19] Gent, A.R. and Milner, H.R., 'The ultimate load capacity of elastically restrained H-columns under biaxial bending', Proceedings, Institution of Civil Engineers, Vol. 41, December, 1968, pp. 685-704.

[7-20] Moore, D.B., Nethercot, D.A. and Kirby, P.A., 'Steel frames. Testing steel frames at full scale', The Structural Engineer, Volume 71, Nos. 23 & 24, December, 1993, pp. 418-427.

[7-21] Springfield, J. "Discussion of 'Effects of semi-rigid connections on steel column strength' by Jones, S.W., Kirby, P.A. and Nethercot, D.A., Journal of Constructional Steel Research, Vol. 1, No, 1, September, 1980, pp. 38-46", Journal of Constructional Steel Research, Vol. 1, No. 3, May, 1981, pp. 48-51.

[7-22] Wood, R.H., 'Test of a multi-storey rigid steel frame', The Structural Engineer, No. 4, Vol. 46, April, 1968, pp. 107-119.

[7-23] Smith, R.F. and Roberts, E.H., 'Test of a fully continuous multi-storey frame of high yield steel', The Structural Engineer, No. 10, Vol. 49, October, 1971, pp. 451-466.

[7-24] BS 449: Part 1, 1970, 'The use of structural steel in building', British Standard Institution, London.

[7-25] Institution of Structural Engineers, 'Manual for the design of steelwork building structures', Institution of Structural Engineers, November, 1989.

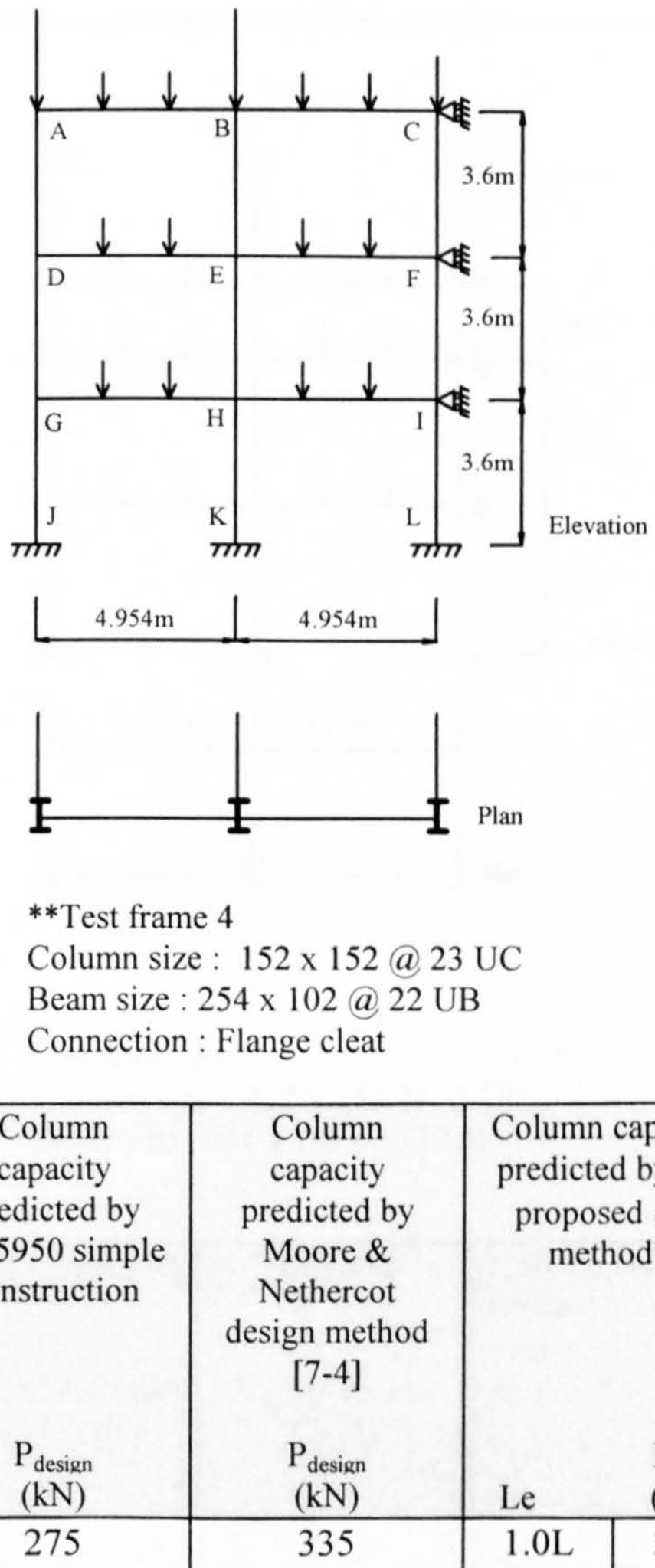

**Test frame 4
Column size : 152 x 152 @ 23 UC
Beam size : 254 x 102 @ 22 UB
Connection : Flange cleat

Column	Column capacity predicted by BS 5950 simple construction P_{design} (kN)	Column capacity predicted by Moore & Nethercot design method [7-4] P_{design} (kN)	Column capacity predicted by the proposed α_{pin} method* Le	P_{design} (kN)	Actual column capacity with the presence of beam loads obtained from full scale test** [7-4] P_{test} (kN)
External AD	275	335	1.0L	384	502
DG	334	437	1.0L	384	546
GJ	406	450	1.0L	384	627
Internal BE	361	522	0.85L	463	521
EH	361	512	0.85L	463	616
HK	478	638	0.85L	463	813
	P_{design}/P_{test}	P_{design}/P_{test}		P_{design}/P_{test}	
External AD	0.55	0.67		0.76	
DG	0.61	0.8		0.7	
GJ	0.65	0.72		0.61	
Internal BE	0.69	1.0		0.89	
EH	0.59	0.83		0.75	
HK	0.59	0.78		0.57	

* Based on BS 5950, Table 27(c) - rolled I-section in y-y axis buckling [7-1].

Table 7.1 Comparison of column capacity as predicted by the various design methods against the actual column capacity obtained from the full scale test : Frame 4/minor axis [7-4],[7-21]

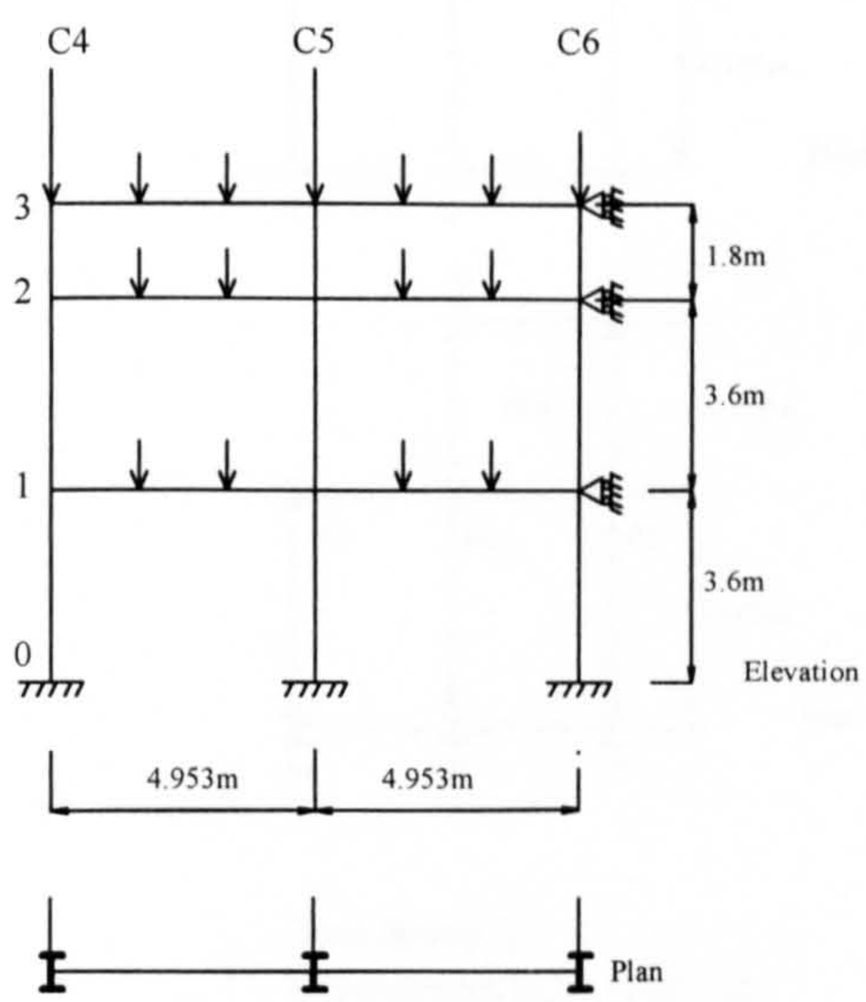

Test frame F1
Column size : 152 x 152 @ 23 UC
Beam size : 254 x 102 @ 22 UB

Column		Column capacity predicted by BS 5950 simple construction	Column capacity predicted by α_β approach [7-13]	Column capacity predicted by the proposed α_{pin} method*		Actual column capacity with the presence of beam loads obtained from Gibbon's full scale test [7-14]
		P_{design} (kN)	P_{design} (kN)	Le	P_{design} (kN)	P_{test} (kN)
Internal	C5/0-1	294	587	0.85L	702	781
	C5/1-2	406	569	0.85L	463	662
	C6/0-1	353	545	0.85L	463	719
		P_{design}/P_{test}	P_{design}/P_{test}		P_{design}/P_{test}	
Internal	C5/0-1	0.38	0.75		0.9	
	C5/1-2	0.61	0.86		0.7	
	C6/0-1	0.49	0.76		0.64	

* Based on BS 5950, Table 27(c) - rolled I-section in y-y axis buckling [7-1].

Table 7.2 Comparison of column capacity predicted by the various design methods against the actual column capacity obtained from the full scale test : Frame F1/minor axis [7-14]

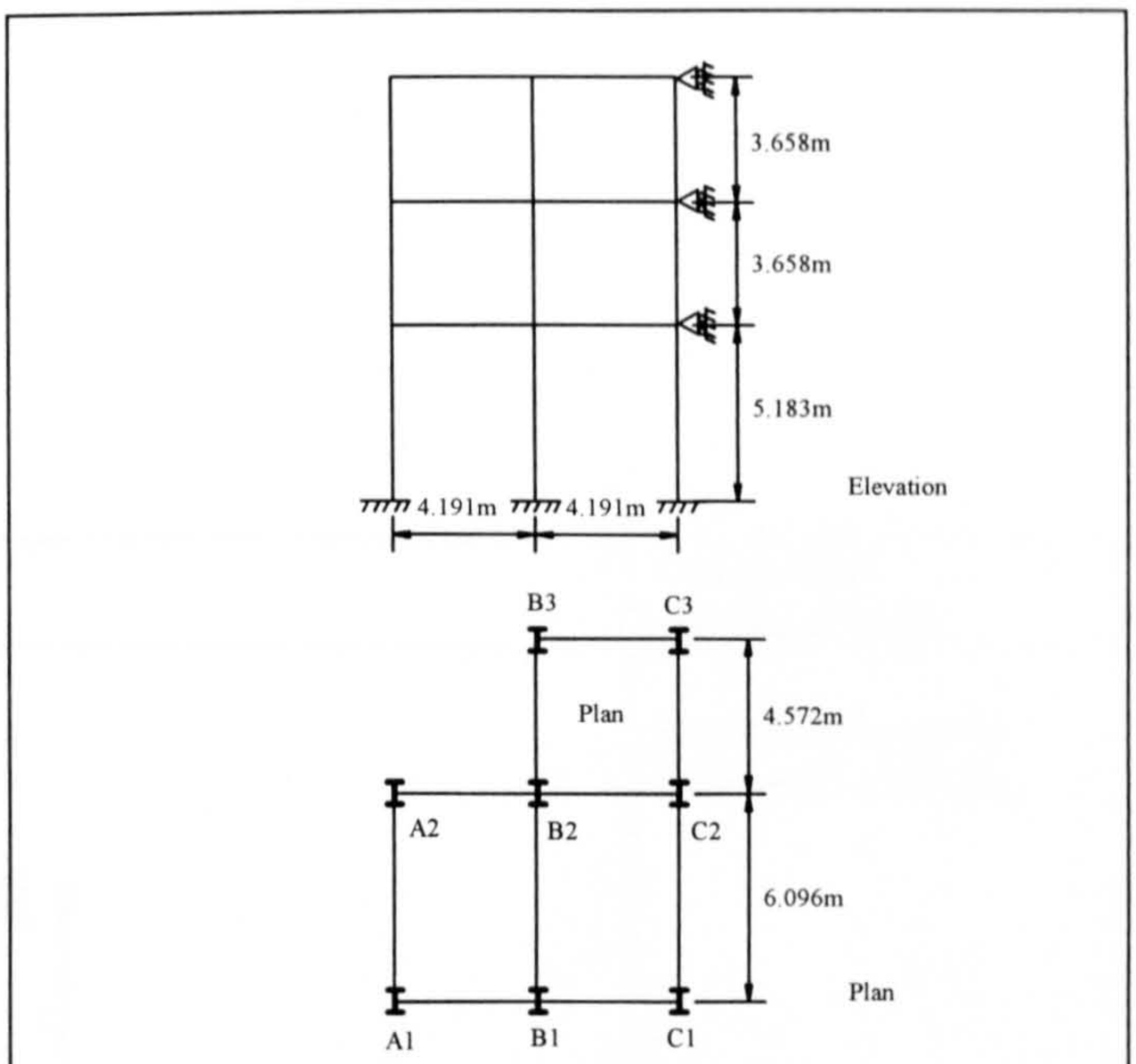

Test frame 2
Connection type : RIGID
References [7-22], [7-23]

Column code	Values of F_{design}/F_{test}		
	[1] Variable stiffness method (kN)	[2] BS 449 rigid (interaction equation) (kN)	[3] BS 449 safe load table (all column end moments are ignored) (kN)
Test frame 2:			
C3 (int)	0.79	0.59	0.78
C3 (top)	0.83	0.61	0.81
B2 (bot)	1.0	0.59	0.93
A1 (top)	0.93	0.52	0.98
C2 (bot)	0.97	0.44	0.71
B3 (int)	0.83	0.19	0.94
C1 (top)	1.05	0.99	0.99
C1 (int)	1.02	0.99	0.99
B1 (bot)	1.12	0.87	0.99
A2 (bot)	0.84	0.47	0.58
A1 (bot)	1.04	0.43	0.8
C1 (bot)	0.8	0.38	0.58
B3 (bot)	0.97	0.49	0.72

Notation:
F_{design} is the prediction of column load capacity by various design methods
F_{test} is the collapse load of the column as obtained from test frame 2
top = top storey, int = intermediate storey, bot = bottom storey

Table 7.3 Part of Wood's comparison of F_{design} / F_{test} [7-9]

Column type	Condition of restraint at ends	Effective length, L_e
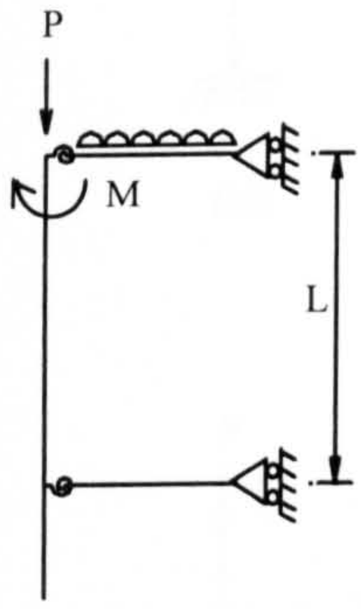 *(a).*	*(a).External column* both ends semi-rigid	*1.0L*
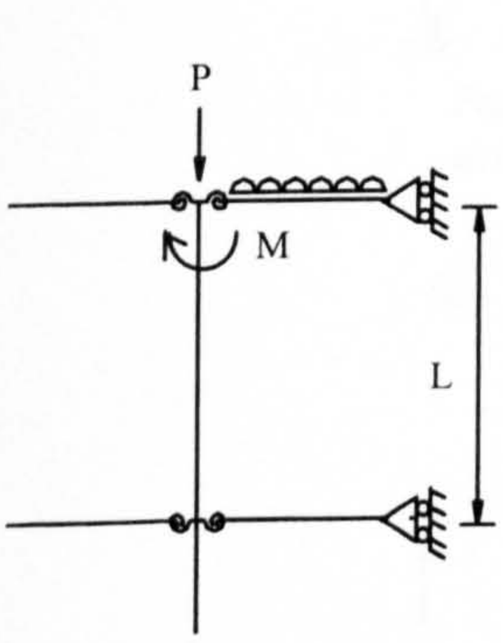 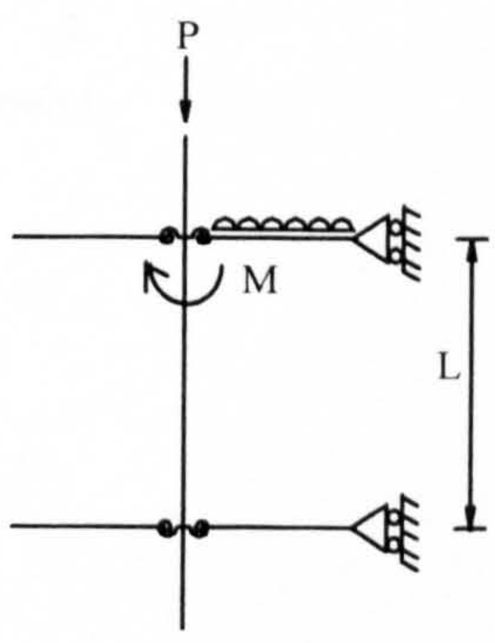 *(b)*	*(b). Internal column* both ends semi-rigid	*0.85L*

Table 7.4 Proposed effective length of beam-columns for α_{pin} design based on BS 5950 [7-1] or EC3 [7-3] : Intermediate beam-columns

Column type	Condition of restraint at ends	Effective length, L_e
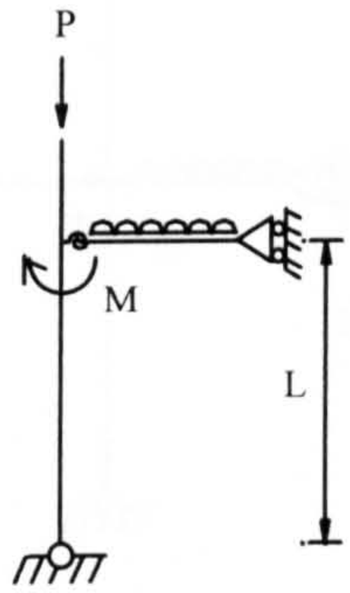 *(a).*	*External column* (a). One end semi-rigid and the other end pinned	*1.0L*
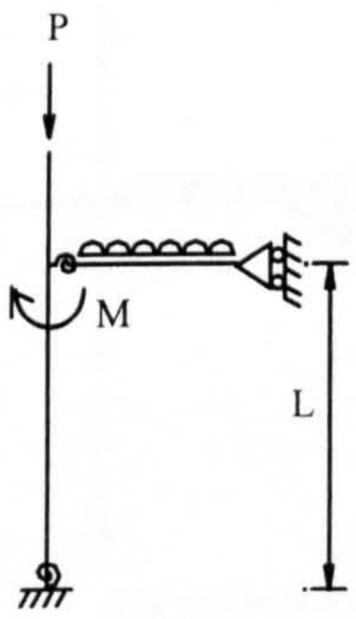 Partial restraint at base *(b).*	(b). One end semi-rigid and the other end semi-rigid	*1.0L*
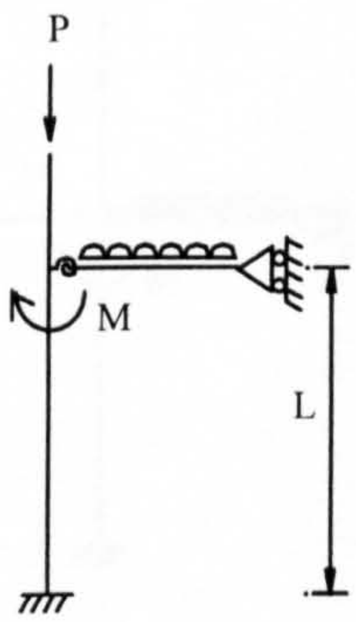 *(c).*	(c). One end semi-rigid and the other end rigid	*1.0L*

Table 7.5 Proposed effective length of beam-columns for α_{pin} design based on BS 5950 [7-1] or EC3 [7-3] : Beam-column connected to base (continue)

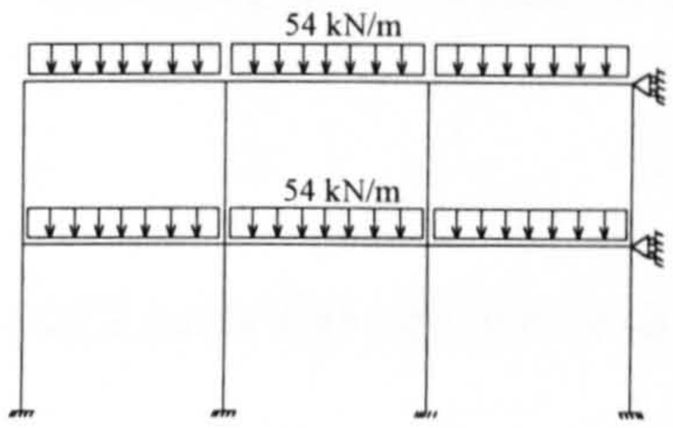

ECCS frame with 54 kN/m beam load

Member	(a). SIMPLE FRAME		(b). SEMI-RIGID FRAME	
	EC3 traditional method	α_{pin} method***	EC3 traditional method	α_{pin} method***
External column	HEA 160	HEA 160	HEA 160	HEA 160
Internal column	HEA 180	HEA 180	HEA 180	HEA 180
Exernal beams	IPE 330	IPE 330	IPE 300*	IPE 330**
Internal beams	IPE 330	IPE 330	IPE 300*	IPE 330**

Note : * Beam design is based on 26% of free moment of end restraint at beam ends.
** Beam design is based on 5% and 10% M_p of end restraints for external and internal beam ends respectively.
*** Based on EC3 [7-3].

Table 7.6 Comparison of member sizes in simple and semi-rigid frames as designed by EC3 [7-3] and α_{pin} methods

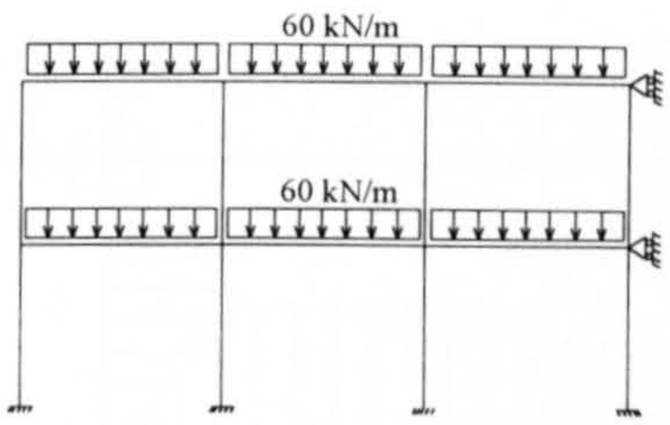

ECCS frame with 60 kN/m beam loads

Member	**(a). SIMPLE FRAME**		
	BS 5950 current method with open section column	α_{pin} method with open section column*	BS 5950 α_{pin} method with SHS column*
External column	152 x 152 UC 37	152 x 152 UC 23	120 x 120 x 6.3 SHS
Internal column	152 x 152 UC 37	152 x 152 UC 37	150 x 150 x 6.3 SHS
Exernal beams	356 x 171 UB 45	356 x 171 UB 45	356 x 171 UB 45
Internal beams	356 x 171 UB 45	356 x 171 UB 45	356 x 171 UB 45
Member	**(b). SEMI-RIGID FRAME**		
	BS 5950 current method with open section column	α_{pin} method with open section column*	α_{pin} method with SHS column*
External column	152 x 152 UC 37	152 x 152 UC 23	120 x 120 x 6.3 SHS
Internal column	152 x 152 UC 37	152 x 152 UC 37	150 x 150 x 6.3 SHS
Exernal beams	356 x 127 UB 39	356 x 127 UB 39	356 x 127 UB 39
Internal beams	356 x 127 UB 39	356 x 127 UB 39	356 x 127 UB 39

* Based on BS 5950 column strength [7-1]

Table 7.7 Comparison of member sizes in simple and semi-rigid frames as designed by BS 5950 [7-1] and α_{pin} methods

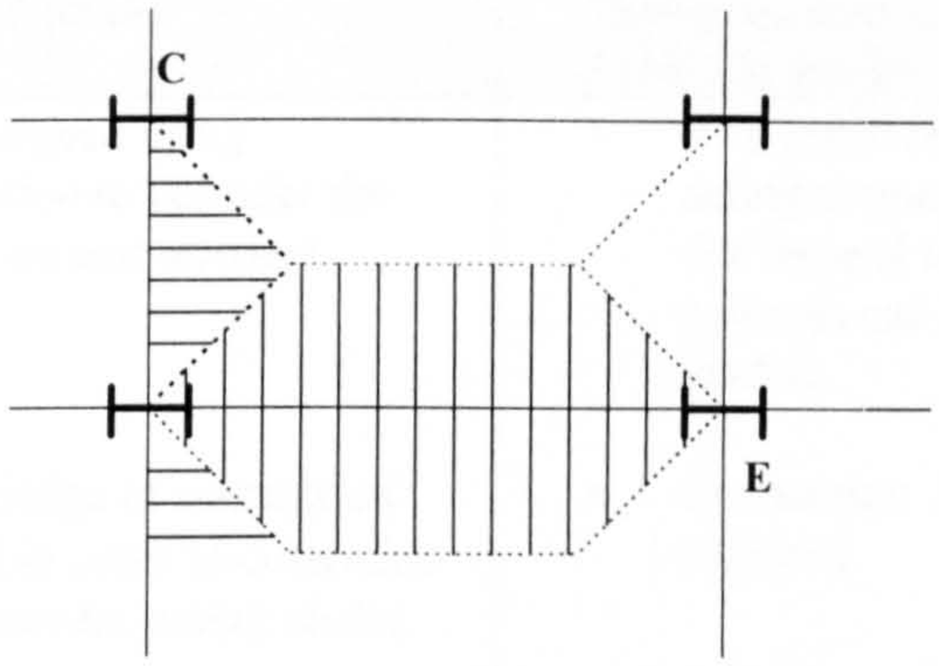

Floor-load diagram [7-9]

Member	RIGID FRAME	
	Wood's variable stiffness method	α_{pin} method with open section column*
Internal column, E	203 x 203 UC 52	203 x 203 UC 52
Corner column $C^{(1)}$	152 x 152 UC 23	152 x 152 UC 23
Corner column $C^{(2)}$	152 x 152 UC 37	152 x 152 UC 37
Edge column $E^{(3)}$	152 x 152 UC 30	152 x 152 UC 37

(1) Assume column C is a corner column.

(2) Assume column C is a corner column. The base is rigid base and the column length is 5.5m.

(3) Assume column E is an edge column with rigid base. The column orientation is changed to buckle in minor axis and the column length is 4m.

* Based on BS 449[7-24].

Table 7.8 Comparison of column sizes in rigid frame as designed by Wood's variable stiffness and α_{pin} methods

Design at lower load level / Elastic design	**Design at ultimate load level / Inelastic design**
• Columns are designed using interaction equation to consider the effect of axial load and moment.	• As a result of moment shedding, the acting moment is no longer detrimental to the column. Hence, columns can be designed as axially loaded.
• Sufficient knowledge of connection M-ϕ is required in order to determine the semi-rigid moment acting on the column.	• Connection M-ϕ curve is not required.
• Moments due to connection continuity and connection eccentricity are considered in the column design.	• Moments due to connection continuity and connection eccentricity are neglected in the column design.
• The use of stiff connections induce large moment to the column. This in turn results in larger or heavier columns.	• The use of pin, semi-rigid and rigid connections results in similar column sizes. This is due to the fact that the columns are designed as not dependent on the acting moment. This in turn results in smaller or lighter columns.

Table 7.9 Comparison of elastic and inelastic column design

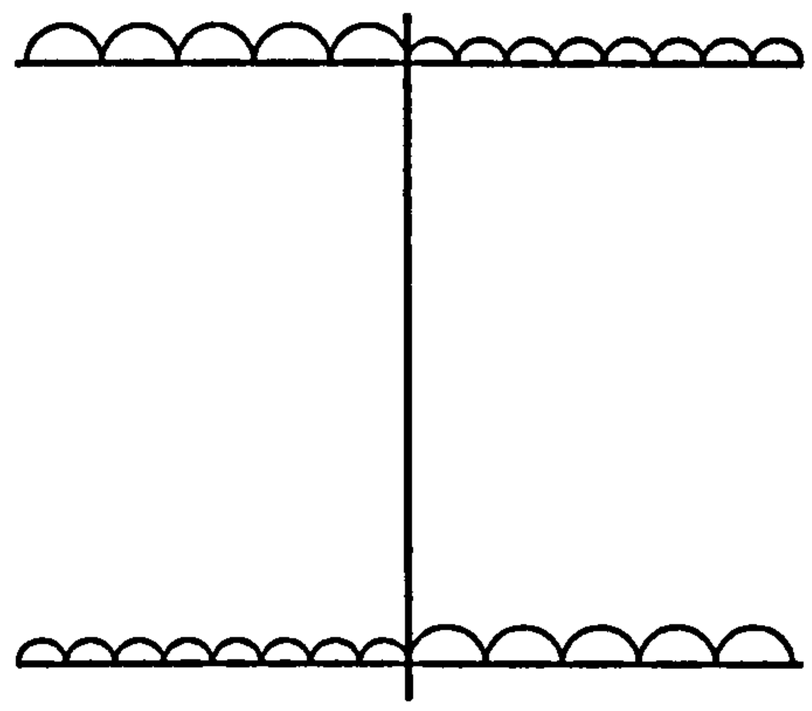

Figure 7.1 Pattern of loading to induce large moment at internal column in simple construction [7-7]

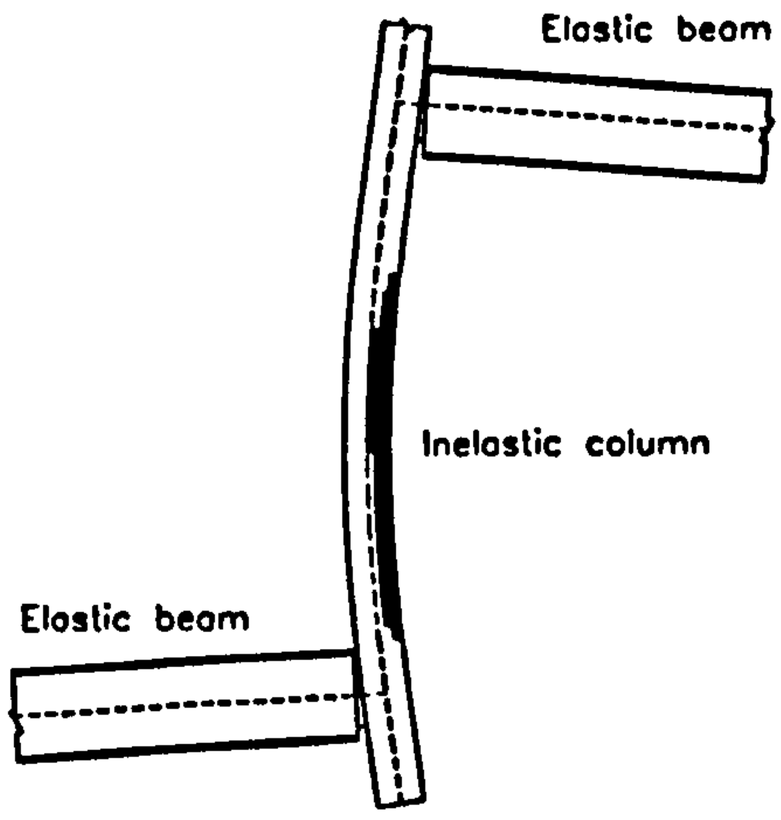

Figure 7.2 Frame design with elastic beam and inelastic column

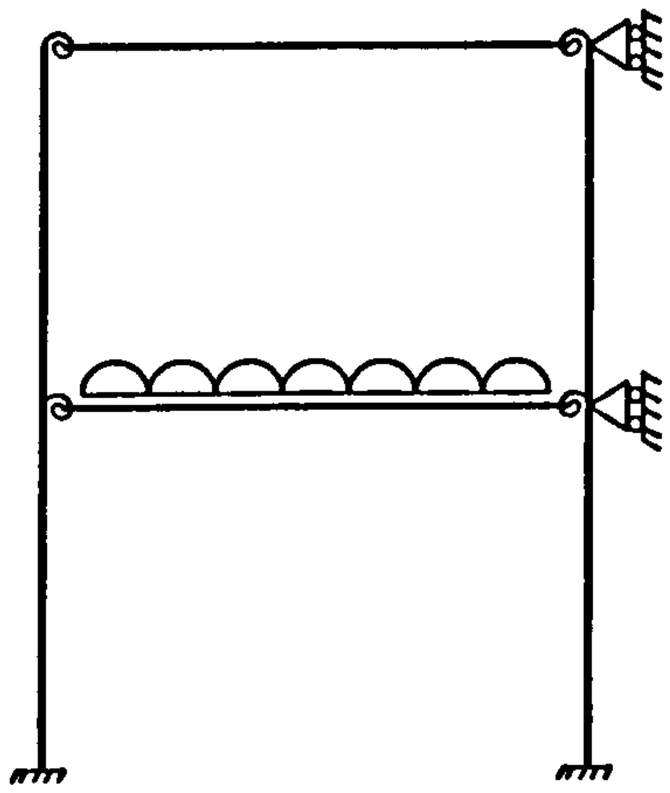

(a). Semi-rigid frome under working gravity load

Notes:

1. The failed column, Cf is used as the model for column design
2. The beam Bf affected by the failed column is used as the model for beam design

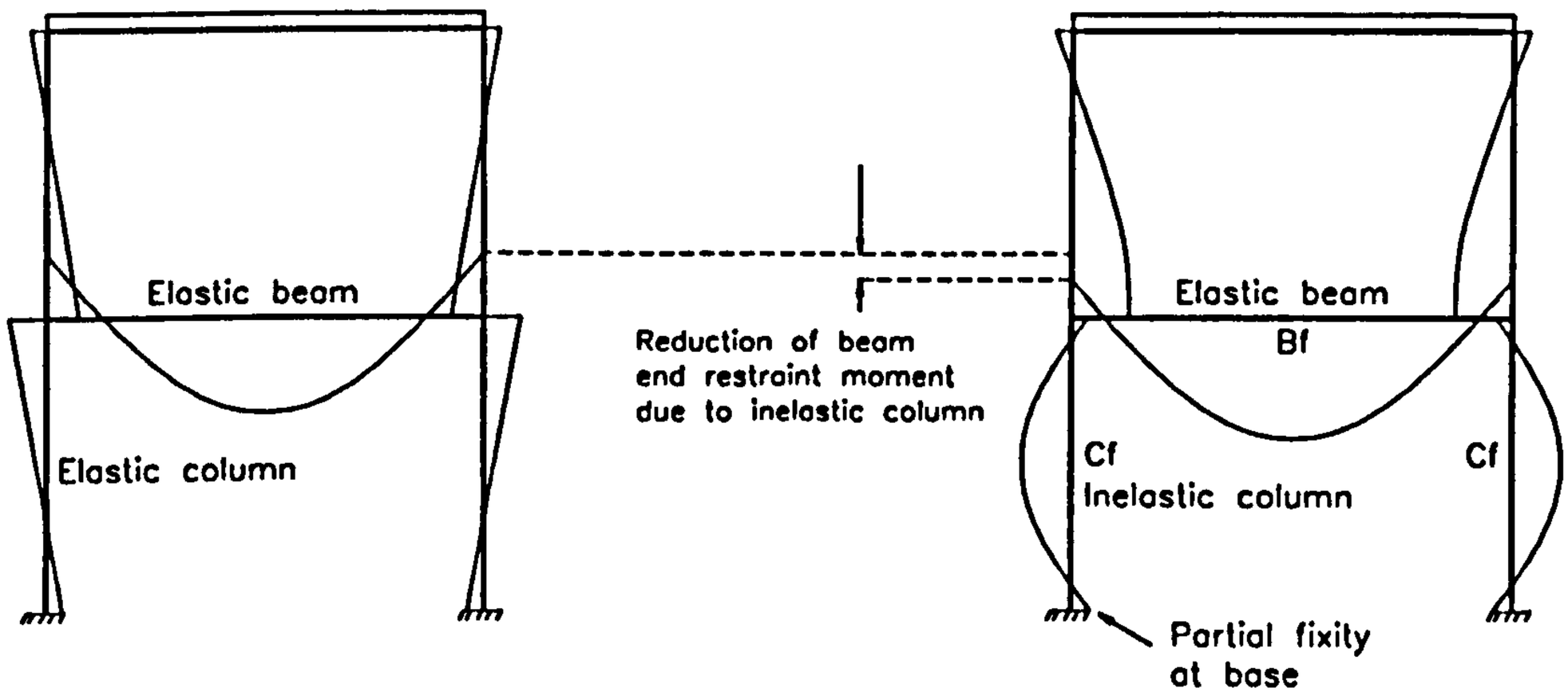

(b). Internal moment at working load (lower load level)

(c). Internal moment at ultimate load (higher load level)

Figure 7.3 Idealisation of non-sway semi-rigid frame for the alpha-pin design method

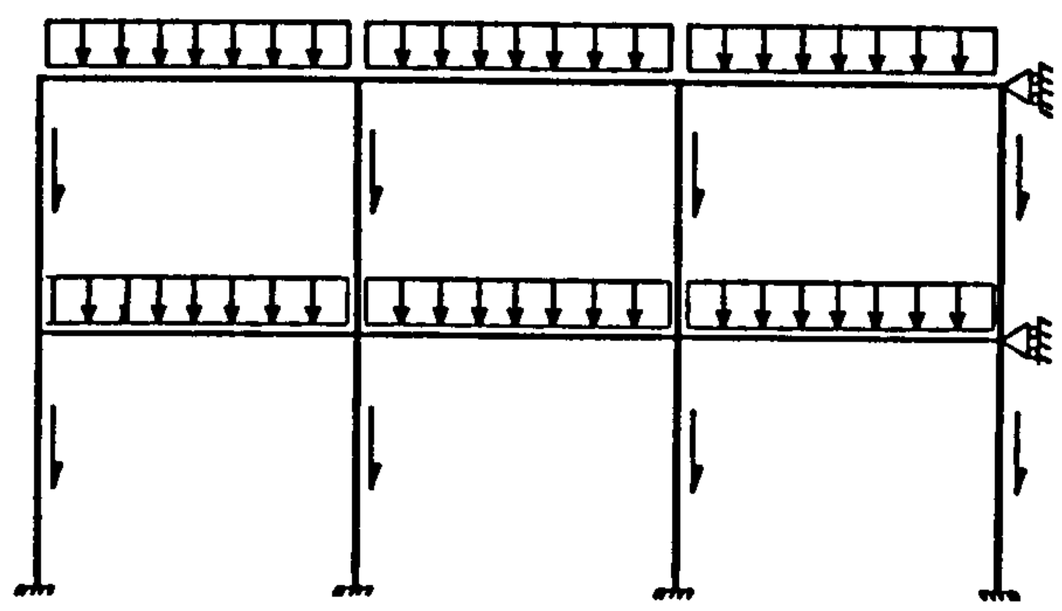

(a). Column axial loads

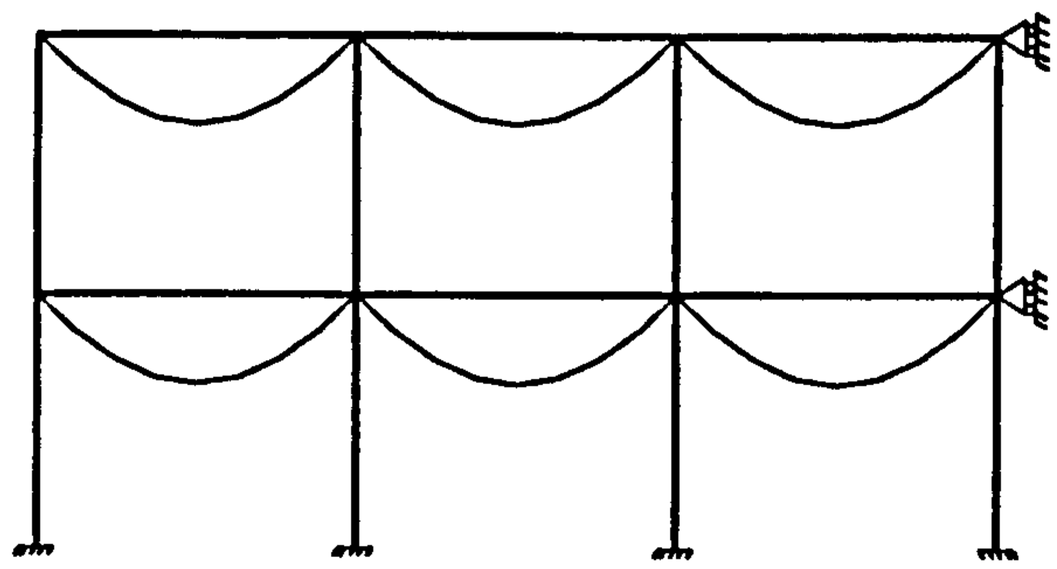

(b). Beam bending moment for simple frame

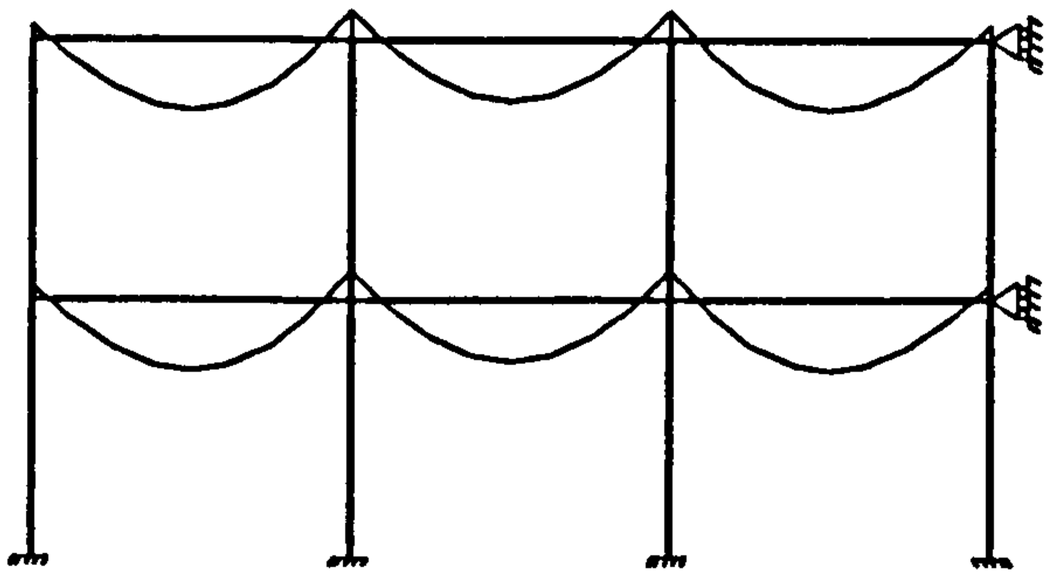

(c). Beam bending moment for semi-rigid and rigid frames

Figure 7.4 Analysis of frames for the alpha-pin approach

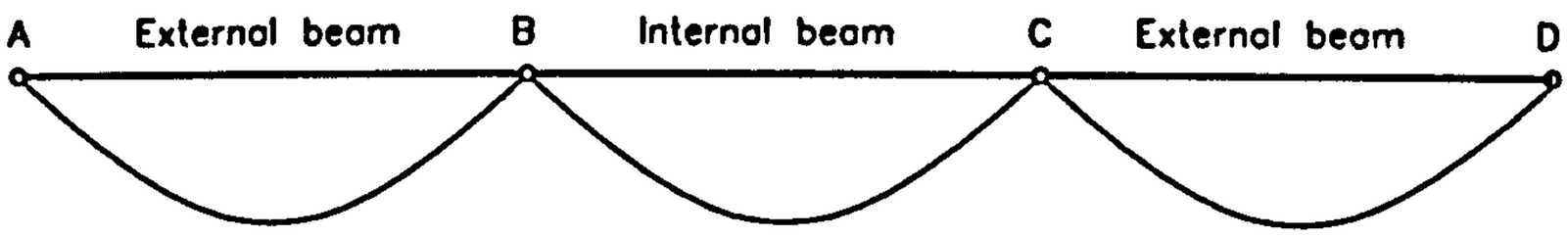

Figure 7.5 Zero end restraint moment for beams with pinned connections

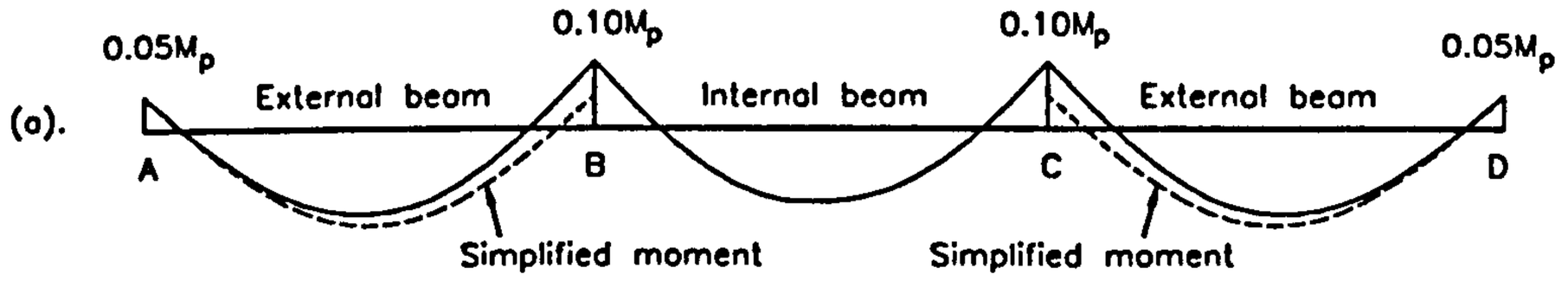

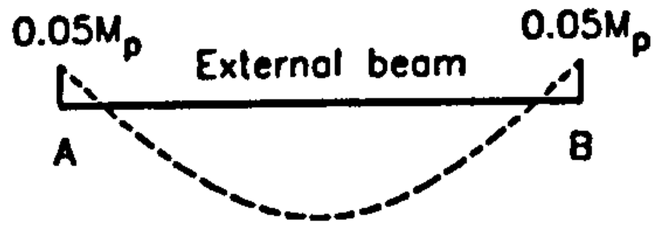

(b). Simplified end restraint moments for external beam

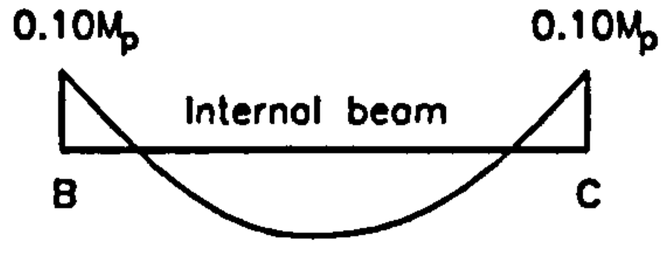

(c). End restraint moments for internal beam

Figure 7.6 Values of end restraint moments for beams with semi-rigid and rigid connections

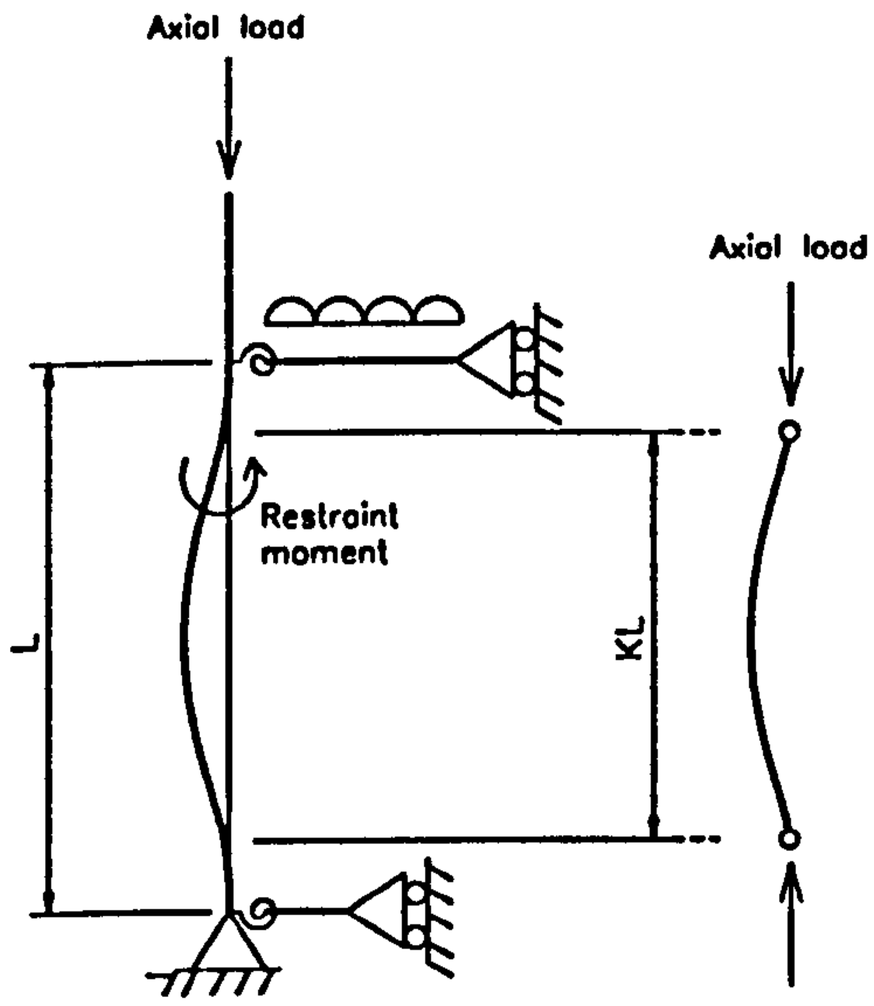

(a). Beam-column modelled as axially loaded

(b). Equivalent pin ended column with reduced effective length, KL

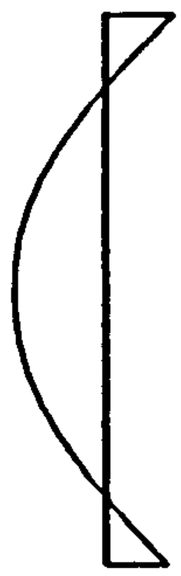

(c). Bending moment of beam-column in the form of axially loaded case

Figure 7.7 Design model of semi-rigidly restrained beam-column at ultimate load level

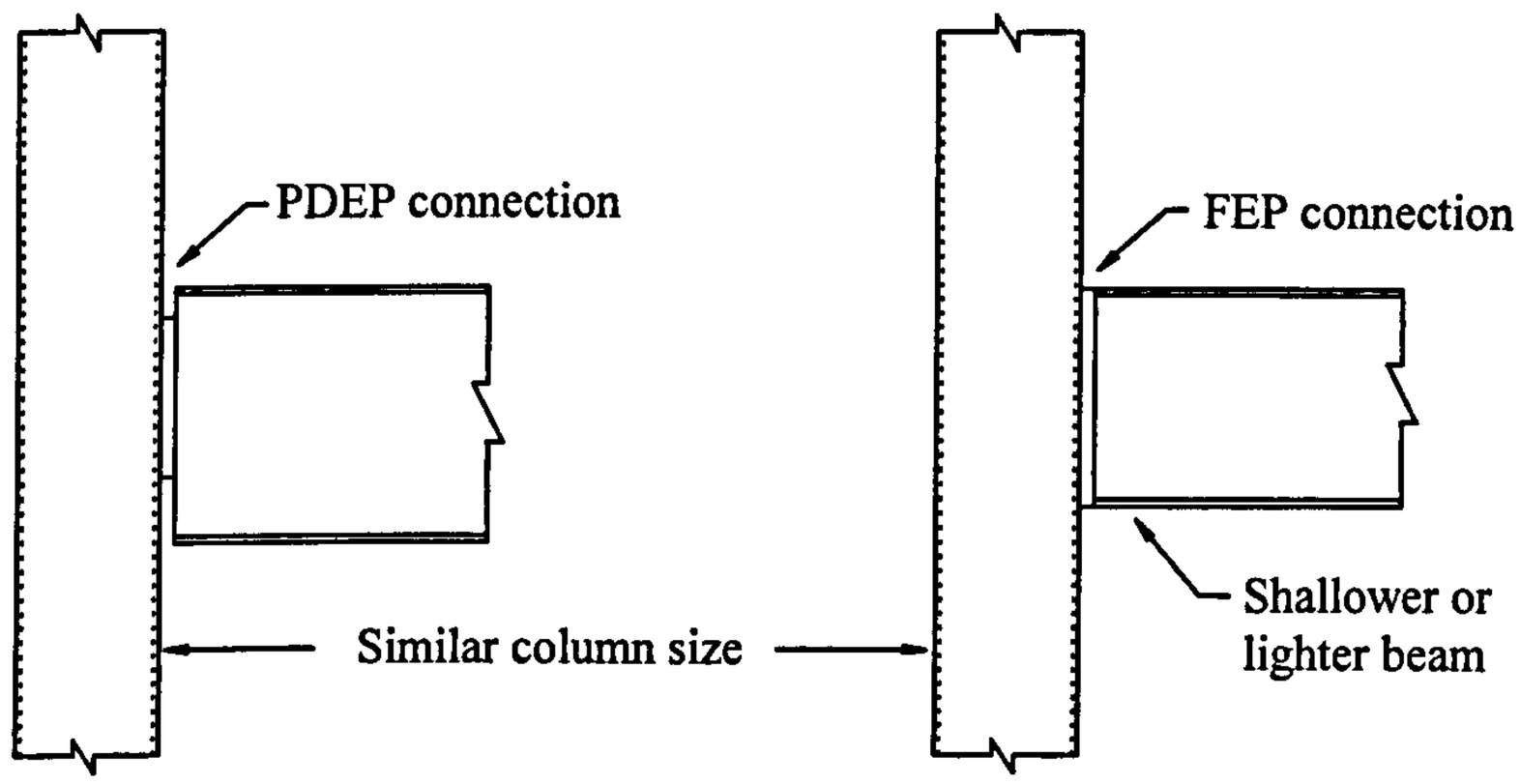

(a). Simple frame (b). Semi-rigid frame

Figure 7.8 The same column size can be employed for different frame systems with the α_{pin} design method

Chapter 8

Conclusions and Recommendations

8. 1 Summary of Work

This thesis has reported the findings of an analytical research investigation related to the behaviour of multi-storey semi-rigid non-sway frames with SHS columns. The frames utilised flowdrill connections to join the open section beams to the SHS columns. The analytical studies have been conducted by exploiting the M-ϕ curves obtained from the experimental joint tests conducted by France [8-1]. Accordingly, this section discusses the summary of research work that has been carried out.

In the early part of the thesis, the review of previous work in Chapter 2 described the experimental aspects of beam-columns at ultimate load levels. Research results show that the strength of beam-columns with end restraints are normally in excess of that predicted by the current design methods suggested by the BS 449 [8-2] and BS 5950 [8-3] codes. The high axial column load capacity is believed to be associated with the phenomenon of moment shedding. The review shows that there is a room for improvement in the design of restrained beam-columns. In view of this, it is justified to investigate further the behaviour of non-sway frames and aspects that contribute to the high ultimate strength of the beam-columns.

In order to investigate the behaviour of the frames, the finite element program discussed in Chapter 3 has been employed. The program existing at the commencement of this study has been modified to work with frames with SHS columns. The program can cater for the gradual spread of yield and hence the response of frames beyond yielding can be investigated. The program also includes the modelling of the initial geometric imperfection by incorporating the co-ordinates of the deformed shape of the columns. The program has been validated against the test results in both non-sway and sway modes. Overall, the program can reasonably predict the real behaviour of non-sway and sway frames as demonstrated in Chapter 4. Therefore, the program can be regarded as acceptable for analysing semi-rigid non-sway and sway frames.

The analytical studies conducted in Chapter 5 have contributed to a better understanding of the behaviour of inelastic columns, particularly the development of moment shedding and the redistribution of moments at the ultimate load levels. It is seen that, as a result of the redistribution of moment, the beams and columns can be treated as isolated members. The beams can be designed as simply supported with a certain degree of end restraint moment to incorporate the effects of semi-rigid connections and the beam-columns as axially loaded.

Knowing that a restrained beam-column can be treated as an axially loaded compression member, more extensive parametric studies have been carried out in Chapter 6 to investigate the ultimate strength of beam-columns with end restraints. Direct comparisons are made between the strength of restrained beam-columns against the strength of axially loaded pin ended columns based on the BS 5950 [8-3] and EC3 [8-4] codes. The results show that in all 288 cases considered, the strength of restrained beam-columns is greater than the strength of axially loaded pin ended columns as specified by the BS 5950 and EC3 codes except in three cases (where the α_{pin} values are 0.99) where the strength of restrained beam-column is very slightly lower than the strength of pin ended column. This shortfall which is related to edge columns, however, represents only 1% of all the cases considered. This implies that beam-columns can be designed safely as axially loaded compression members based on either the BS 5950 or the EC3 pin ended column curves.

The understanding of the true behaviour of inelastic columns has enabled the development of the simplified design method of semi-rigid non-sway frames. A straightforward method of designing low rise multi-storey buildings for simple, semi-rigid and rigid non-sway frames, known as the α_{pin} approach, has been presented in Chapter 7. The α_{pin} design method has been developed based on the response of loss of stiffness and the phenomenon of moment shedding occurring in the beam-columns.

The advantage of the α_{pin} design method is the simplicity with which the column can be designed. With this approach, the design of semi-rigid frames is not dependent on the stiffness M-ϕ characteristics of the connections, the stiffness of the beams and the stiffness of the columns. The α_{pin} design method eliminates the interaction equations as normally used in the current design methods. Despite of its simplicity, the design method offers economical external column design as opposed to the current BS 5950 design method. In the case of internal columns, economical column design could be achieved in cases when there is an appreciable disturbing moment due to non-symmetrical beam loads.

Additionally, the response of inelastic beam-columns as observed in this study has highlighted that the specification stated in clause 4.7.7 of BS 5950 not to consider the effect of pattern loading for the purpose of column design is actually relying on the phenomenon of moment shedding. As a result of this phenomenon, it is seen that, the column end moment diminishes and sometimes acts as restraining moment and hence the moment is no longer detrimental to the column.

The findings of the present studies, however, are based on limited parametric studies based on low rise non-sway frames. A more comprehensive study is needed to confirm the findings for high rise non-sway frames (say of more than six storeys).

8.2 Summary of Conclusions

The main observations and conclusions obtained from the limited parametric studies on low rise multi-storey non-sway frames as conducted in this thesis are:

1. At collapse load, the structure is seen to become statically determinate in which the column behaves as an axially loaded member and the beam as a simply supported member with a certain degree of end restraint moments. As a consequence, beams and columns in frames with semi-rigid connections can be treated as individual members.

2. At the ultimate load levels, the moment acting on the column diminishes as a result of moment shedding and sometime acts as a restraining moment. As a result of this phenomenon, it is not necessary to evaluate the disturbing moment transferred to the column. Hence, based on this justification, the pattern loading necessary to determine the effect of maximum detrimental moment to the columns is not required.

3. The rate of decrease (shedding) of column moment is dependent on the rate of loss of stiffness in the columns. The more rapid is the loss of stiffness, the more sudden is the moment shedding. The rapid loss of stiffness in the columns has been seen in these studies as being associated with the following parameters:

   - *The small values of second moment of area, I.* These parameters normally present in the case of columns buckle in minor axes.

   - *The more slender columns*. This parameter causes the rapid loss of stiffness in the elastic range due to the large geometrical deformation.

   - *The formation of yielding in columns*. This phenomenon causes the sudden loss of stiffness in the inelastic range as the yielded sections no longer contribute to the stiffness of the column.

4. In order to incorporate the benefit of connection restraints to the column the concept of effective length is employed. In order to avoid complexity, the

simplified effective lengths that are analogous to Table 24 of BS 5950 [8-3] are employed. This is justified based on the research conducted in Chapters 5 and 6 that showed the possibility of designing beam-columns with end restraints without the need to know precisely the M-ϕ connection characteristics, the beam stiffness and the column stiffness.

5. The amount of moment shedding redistributed from the column top end to the beams depends on the degree of connection restraint. Less stiff connections attract a small amount of the shed moment and hence permit a small amount of the moment to be redistributed back to the beams.

6. It is seen that the stiffness of the connections is more important and becomes more dominantly utilised when the column starts to undergo rapid loss of stiffness due to the attainment of first yield in the column.

7. The benefit of stiff connections is seen to be more significant in the inelastic range where it can provide large reserves of strength and largely stable deformation to the column member. Such inelastic characteristics may have important implications for the ultimate strength of steel frames with semi-rigid connections in seismic areas.

8. For columns, the effect of increasing connection stiffness is seen to be less important for columns with practical slendernesses. It is seen that the use of flexible PDEP connections can enhance the ultimate column strength to about 90% of the column load with RIGID connections. Therefore, in the practical range of column slenderness, there are no significant benefits of increasing connection restraints in order to enhance the column ultimate load.

9. The effect of increasing connection stiffness is seen to increase the restraint moments at the beam ends. This in turn reduces the maximum mid-span moment of the beams and hence resulting in shallower or lighter beam sections.

10. In the α_{pin} method, the beam-column is designed as a function of applied axial load only and not affected by the beam moment. As a result, the use of pinned, semi-rigid and rigid connections produces the same size of columns. This result is

somewhat at odds with the traditional beam-column design using the interaction equations, where the use of stiff connections induce large moment to the column and hence produce larger or heavier columns.

8.3 Recommendations for Further Studies

This section discussed several suggestions that can be extended further to:

- improve the understanding of the behaviour of semi-rigid frames
- obtain more economical beam design.

One of the interesting features of the α_{pin} design method is that the design of columns with rigid connections gives similar results to the design method based on Wood's variable stiffness method [8-5]. In view of this, comparative studies on the α_{pin} and Wood's variable stiffness methods can be undertaken. It would be interesting to know to what extent the two methods differ. On one hand, the α_{pin} column design is significantly simple to use but on the other hand, the beams as designed by Wood's variable stiffness method are seen to be more economical than the beams designed by the α_{pin} method. This is due to the fact that the proposed α_{pin} design only employs 5% and 10% of end restraint moment at the external and internal beam ends respectively; whereas, Wood's variable stiffness method employs full moment fixity which permits the beams to be designed plastically.

In view of the above, the author believes that it is possible for the α_{pin} design method to employ larger end restraint moments at the beam ends to obtain more economical beam design. The suggested studies which require the use of a three dimensional program are as follows:

- Investigate the values of beam end restraint moments at the higher load levels for three dimensional frames. In the analysis, the beams are loaded first to produce detrimental bending moment to the column, followed by loading the columns to failure. It is of interest to investigate the reduction of end restraint moments (at

higher load levels) at all beam ends with the presence of more beams connected to the column.

- Investigate the design concept known as P_xE_y that was suggested by Baker et al. [8-6] in 1950s. According to this concept, P_x and E_y , respectively, indicate that the major axis and the minor axis beams can be designed plastically and elastically. In the case of the α_{pin} approach, it is of interest to know whether the column end moment is shed to the minor axis beams only and not to the major axis beams (i.e. when the column is allowed to buckle in minor axis). As a consequence, the reduction of beam end moments only occurs at the minor axis beams and not at the major axis beams. If this behaviour is true, the design concept suggested by Baker et al. can be adopted in the α_{pin} design method, i.e. major axis beams can be designed economically using the plastic design method.

In addition, other recommendations for further studies that can be investigated by using the plane frame program are as follows:

- An investigation on the performance of frames as designed by the α_{pin} design method. This can be performed by first designing the frames with the α_{pin} design method. Then perform numerical load tests on the designed frames by applying full factored design loads on all beams followed by increasing the loads incrementally up to the frame failure. Frames that are able to carry loads larger than the factored design loads are considered safe and acceptable. Additionally, the behaviour of various frame configurations under these loading conditions can also be investigated.

- A study on the response of beam-column with the inclusion of semi-rigid connections at the base.

- A study of the α_{pin} approach in sway frames. Further extensions on the study of the α_{pin} approach can be expanded to sway frames to investigate the behaviour of inelastic columns at the ultimate load levels. Analytical studies by Zieman et al. [8-7] confirmed the response of redistribution of column moments to the neighbouring beams as the columns undergo yielding. This response gives an

indication that the phenomenon of moment shedding may also be present in sway frames. The interesting research question is that whether the understanding of the behaviour of inelastic columns with the beams remaining elastic may lead to a simplified design method that is analogous to the wind moment design method [8-8]. If so, the beams and columns could be designed individually and independent of the M-ϕ characteristics, the stiffness of the beams and the stiffness of the columns.

8.4 References

[8-1] France, J.E., 'Bolted connections between open section beams and box columns', Ph.D. Thesis, Department of Civil & Structural Engineering, University of Sheffield, U.K., January, 1997.

[8-2] BS 449: Part 1, 1970, 'The use of structural steel in building', British Standard Institution, London.

[8-3] BS 5950: Part 1: 1990, 'Structural use of steelwork in building', Part 1. Code of practice for design in simple and continuous construction : hot rolled sections, British Standard Institution.

[8-4] Eurocode 3, 'Design of steel structures - Part 1.1: General rules and rules for buildings', ENV 1993-1-1.

[8-5] Wood, R.H., 'A new approach to column design', Her Majesty's stationery Office, 1974.

[8-6] Baker, J.F., Horne, M.R. and Heyman J., 'The steel skeleton', Cambridge University Press, Vol. 2, 1956.

[8-7] Zieman, R.D., McGuire, W. and Deierlein, G.G., 'Inelastic limit states design. Part 1: Planar frame studies', Journal of Structural Engineering, Vol. 118, No. 9, September, 1992, pp. 2532-2549.

[8-8] The Steel Construction Institute, 'Wind-moment design for unbraced frames', Publication 082, 1991.

[8-9] Kirby P.A., Bitar, S.S. and Gibbons, C., 'Design of columns in non-sway semi-rigidly connected frames', First World Conference on Constructional Steel Design', Acapulco, Mexico, December, 1992, pp. 54-63.